Garik Gutman
Anni Reissell
Editors

Eurasian Arctic Land Cover and Land Use in a Changing Climate

Springer

Eurasian Arctic Land Cover and Land Use in a Changing Climate

Garik Gutman · Anni Reissell
Editors

Eurasian Arctic Land Cover and Land Use in a Changing Climate

Springer

Editors
Dr. Garik Gutman
NASA Headquarters
300 E. Street, SW
Washington, DC 20546
USA
garik.gutman@nasa.gov

Dr. Anni Reissell
Department of Physics
PO box 48 (Erik Palmenin aukio 1)
00014, University of Helsinki
Finland
anni.reissell@helsinki.fi

ISBN 978-90-481-9117-8 e-ISBN 978-90-481-9118-5
DOI 10.1007/978-90-481-9118-5
Springer Dordrecht Heidelberg London New York

Library of Congress Control Number: 2010937232

Cover illustration: A color composite of the MODIS vegetation continuous fields indicating the combination of tree and herbaceous vegetation cover and bare ground. Green hues indicate dominance of tree cover, blue hues indicate dominance of herbaceous vegetation (tundra), and red hues indicate bare ground. Land and national borders are shown and white areas represent ice, including the polar ice cap as recorded in September 2008. The figure is based on Goetz, et al. (this volume), with artwork by G. Fiske. The MODIS vegetation continuous fields product is available at http://glcf.umiacs.umd.edu/data/vcf/.

Printed on acid-free paper

Springer is part of Springer Science+Business Media (www.springer.com)

Preface

Changes in land cover and ocean ice in the Arctic are among the earliest indicators of the Earth's response to climate warming. During the last period of major climatic change – the Holocene (11,700 – ca. 2000 BP) – the changes and drivers were natural. In the Antropocene (from the late eighteenth century), the current period in the Earth's history when human activities have had a significant global impact on the Earth's ecosystems, the changes are accompanied by the added complexity of man-made anthropogenic pollutants and green house gas emissions and man-induced land-cover changes.

It is anticipated that the changes in the Arctic will be most pronounced. Also, climate change is expected to accelerate affecting both the Arctic ecosystem and the socioeconomic infrastructure. Moreover, changes in the Arctic are predicted to affect the climate and people on a global scale as the ecosystem responses to warming of the Arctic have the potential to feed back either positively or negatively to the whole climate system.

Monitoring the dynamics of the circumpolar boreal forest (taiga) and Arctic tundra boundary is important for understanding the causes and consequences of changes observed in these areas. Because of the lack of in situ data due to inaccessibility and large extent of this zone, remote sensing data play an important role. Accurate mapping of land cover and monitoring its change are fundamental requirements for global change research.

The timing of this book is very appropriate due to the recent ending of the International Polar Year (IPY). The focus is on the Arctic region of Northern Eurasia, although some comparisons are made with the results in North America. This volume contains results of vegetation-change studies, studies of the geographic patterns of fluxes of carbon dioxide and methane and their balance and changes over time, studies of changes in hydrological systems, wildlife populations and the overall habitability of the Arctic, and studies of aerosol and pollution. The articles provide pathways to strategies for adaptation to the observed and predicted changes, and facilitate assessments of the impacts and opportunities related to natural resource management of energy and transportation developments.

For sound mitigation and adaptation measures, land-use and land-cover change research should be multi- and interdisciplinary involving both natural and social scientists. In this respect, the book is a truly international, interdisciplinary effort of

a team consisting of natural and social scientists from the USA, Europe and Russia under the auspices of the Northern Eurasia Earth Science Partnership Initiative (NEESPI). NASA, US National Science Foundation, the Russian Academy of Sciences, the Academy of Finland and other European institutions supported the studies used in the book.

The book is of interest to a broad range of scientists studying recent and ongoing changes in the Arctic, be they senior or early career scientists, or graduate students. This volume is essentially the NASA Land-Cover/Land-Use Change Program's contribution to the IPY. We warmly thank all the contributors of this book and acknowledge the support from NASA and other funding agencies, the University of Helsinki and the Integrated Land Ecosystem-Atmosphere Processes Study (iLEAPS) International Project Office.

Acknowledgments

The authors and editors are grateful to Tyyne Viisanen for her technical editing and continuous, diligent work on compiling the contributions. The authors and editors also gratefully acknowledge the help and diligent editing of Alla Borisova in the final stage of this book.

The studies in this volume were supported through the grants provided as part of the following programs: the NASA Land-Cover/Land-Use Change Program, the National Science Foundation Office of Polar Programs, the NOAA Climate Program Office, Arctic System Science Program and International Polar Year programs, the NASA North American Carbon Program, the Bonanza Creek Long Term Ecological Program (funded jointly by NSF grant DEB-0423442 and USDA Forest Service, Pacific Northwest Research Station grant PNW01-JV11261952-231), the Academy of Finland through the Russia in Flux Programme to the ENSINOR project, and the Russian Academy of Science. Additional support from the Institute of Arctic Biology at the University of Alaska in Fairbanks, USA is gratefully acknowledged.

The Editors (G.G. and A.R.) acknowledge the support received by Dr. Gutman from NASA and the University of Helsinki, Finland while on detail from NASA Headquarters, during which most of the work on the compilation of this volume was accomplished. The editors also gratefully acknowledge the University of Helsinki, Department of Physics, Division of Atmospheric Sciences and Geophysics, and the Integrated Land Ecosystem-Atmosphere Processes Study (iLEAPS), a core project of the International Geosphere-Biosphere Programme (IGBP).

Thanks go to Dr. Michael S. Balshi for provision of historical fire data sets.

For Chapter 8, support was provided in part by the Research Council of Norway, Project IPY EALAT-RESEARCH: Reindeer Herders Vulnerability Network Study: Reindeer Pastoralism in a Changing Climate, grant 176078/S30. A portion of the NASA work was supported by the NASA Land Cover Land Use Change (LCLUC) Program and NASA's Radar Research Program (NASA 51-621-21-01-20). Synthetic Aperture Radar data were provided by the European Space Agency and Alaska Satellite Facility.

Authors of Chapter 8 thank Mr. Philip Burgess for his careful review and helpful comments during preparation of the article. Authors are grateful to Dr. Peter

Wasilewski, NASA GSFC History of Winter Program (HOW), for providing NASA thermochrons and Mr. Allen Lunsford for providing technical assistance for thermochron use in the EALAT snow study.

Authors of Chapter 10 acknowledge support provided by NASA IPY Radiation Program and in part by NASA Land Cover Land Use Change (LCLUC) Program.

Contents

Contributors

Jennifer C. Adam Department of Civil and Environmental Engineering, Washington State University Pullman, WA 99164-2910, USA, jcadam@wsu.edu

Domingo Alcaraz-Segura Department of Environmental Sciences, University of Virginia, Charlottesville, VA 22904-4123, USA, da6f@virginia.edu

Pieter S.A. Beck The Woods Hole Research Center, 149 Woods Hole Road, Falmouth, MA 02540-1644, USA, pbeck@whrc.org

Uma S. Bhatt Department of Atmospheric Sciences, Geophysical Institute, IARC Room 307, University of Alaska Fairbanks, 903 Koyukuk Dr, Fairbanks, AK 99775-7320, USA, bhatt@gi.alaska.edu

Theodore J. Bohn Department of Civil and Environmental Engineering, University of Washington, Seattle, WA 98195-2700, USA, tbohn@hydro.washington.edu

Andrew Bunn Department of Environmental Sciences, Huxley College, Western Washington University, Bellingham, WA 98225-9181, USA, andy.bunn@wwu.edu

Todd J. Burnside Institute of Arctic Biology, University of Alaska Fairbanks, Fairbanks, AK 99775, USA, canoebum@gmail.com

Josefino C. Comiso Cryospheric Sciences Branch, NASA Goddard Space Flight Center, Greenbelt, MD 20771, USA, josefino.c.comiso@nasa.gov

Judith Curry School of Earth and Atmospheric Sciences, Georgia Institute of Technology, Atlanta, GA 30332-0340, USA, curryja@eas.gatech.edu

John Derome[†] Rovaniemi Research Unit, Finnish Forest Research Institute, 96301 Rovaniemi, Finland, John.Derome@metla.fi

Dmitri S. Drozdov Earth Cryosphere Institute, 117982 Moscow, Russia, ds_drozdov@mail.ru

Inger Marie G. Eira Sami Allaskuvla/Sámi University College, Guovdageaidnu, Kautokeino, Norway 9520, ingermge@samiskhs.no

Vladimir Elsakov Institute of Biology, Komi Science Center, Russian Academy of Sciences, 167610 Syktyvkar, Russia, elsakov@ib.komisc.ru

Howard E. Epstein Department of Environmental Sciences, University of Virginia, PO Box 400123, Charlottesville, VA 22904-4123, USA, hee2b@virginia.edu

Vladimir Etylin Chukotka Branch of the North-Eastern Research Institute. Russian Academy of Science, Anadyr, Chukotka, Russia, etylin.vladimir@gmail.com

Bruce C. Forbes Arctic Centre, University of Lapland, 96101 Rovaniemi, Finland, bforbes@ulapland.fi

Jennifer Gebelein Department of International Relations and Geography, Florida International University, Miami, FL 33199, USA, jennifer_gebelein@hotmail.com

Scott J. Goetz The Woods Hole Research Center, 149 Woods Hole Road, Falmouth, MA 02540-1644, USA, sgoetz@whrc.org

Pavel Groisman National Climate Data Center, Ashville, NC 28801, USA, pasha.groisman@noaa.gov

Anatoly A. Gubarkov Tyumen State Oil and Gas University, 625000 Tyumen, Russia, agubarkov@gmail.com

Garik Gutman NASA Headquarters, 300, E. Street, SW Washington, DC 20546, USA, ggutman@nasa.gov

Matthew C. Hansen Geographic Information Science Center of Excellence, South Dakota State University, Brookings, SD 57007, USA, Matthew.Hansen@sdstate.edu

Tuomas Häme Technical Research Centre of Finland, 02044 Helsinki, Finland, tuomas.hame@vtt.fi

Daniel J. Hayes Institute of Arctic Biology, University of Alaska Fairbanks, Fairbanks, AK 99775, USA, Daniel.Hayes@alaska.edu

Sergey T. Im V.N. Sukachev Institute of Forest, Academgorodok, SB RAS, 660036, Krasnoyarsk, 50, Russia, stim@ksc.krasn.ru

Gensuo J. Jia START Regional Center for Temperate East Asia, Chinese Academy of Science, Institute of Atmospheric Physics, PO Box 9804, Beijing 100029, China, jiong@tea.ac.cn

Chris O. Justice Department of Geography, University of Maryland, College Park, MD 20742, USA, justice@hermes.geog.umd.edu

Elina Kaarlejärvi Ecology and Environmental Sciences, University of Umeå, 90187 Umeå, Sweden, elina.kaarlejarvi@gmail.com

Jed O. Kaplan EPFL Swiss Federal Institute of Technology, Lausanne, ENAC-ARVE, Ecole Polytechnique Fédérale de Lausanne Station 2, 1015 Lausanne, Switzerland, jed.kaplan@epfl.ch

Viatcheslav I. Kharuk V.N. Sukachev Institute of Forest, Academgorodok, SB RAS, 660036, Krasnoyarsk, 50, Russia, kharuk@forest.akadem.ru

Artem V. Khomutov Tyumen State Oil and Gas University, Volodarsky str. 38, Tyumen, 625000 Russia, akhomutov@gmail.com

David W. Kicklighter The Ecosystems Center, Marine Biological Laboratory, Woods Hole, MA 02543, USA, dkicklighter@mbl.edu

Gary P. Kofinas University of Alaska Fairbanks, Fairbanks, AK 99775, USA, ffgpk@uaf.edu

Olga N. Krankina Department of Forest Ecosystems and Society, Oregon State University, Corvallis, OR 97331, USA, krankinao@fsl.orst.edu

Timo Kumpula Department of Geographical and Historical Studies, University of Eastern Finland, 80101 Joensuu, Finland, timo.kumpula@joensuu.fi

Patrick Kuss Institute of Plant Sciences, University of Bern, Altenbergrain 21, 3013 Bern, Switzerland, patrick.kuss@ips.unibe.ch

Richard B. Lammers Water Systems Analysis Group, University of New Hampshire, Durham, NH 03824-3525, USA, richard.lammers@unh.edu

Marina O. Leibman Earth Cryosphere Institute, 117982 Moscow, Russia, ds_drozdov@mail.ru

Dennis P. Lettenmaier Department of Civil and Environmental Engineering, University of Washington, Seattle, WA 98195-2700, USA, dennisl@u.washington.edu

Heike Lischke Swiss Federal Institute for Forest Snow and Landscape Research WSL, Zürcherstr. 111, 8903 Birmensdorf, Switzerland, heike.lischke@wsl.ch

Andrea H. Lloyd Department of Biology, Middlebury College, Middlebury, VT 05443, USA, lloyd@middlebury.edu

Natalia Lukina Centre for Forest Ecology and Productivity RAS, 117997 Moscow, Russia, lukina@cepl.rssi.ru

Svein D. Mathiesen International Centre for Reindeer Husbandry, Guovdageaidnu, Kautokeino, 9520 Norway; Sami Allaskuvla/Sámi University College, Guovdageaidnu, Kautokeino, 9520 Norway; The Norwegian School of Veterinary Science, 9292 Tromso, Norway, svein.d.mathiesen@veths.no

Nancy G. Maynard Cryospheric Sciences Branch, NASA Goddard Space Flight Center, Greenbelt, MD 20771, USA, nancy.g.maynard@nasa.gov

A. David McGuire US Geological Survey, Alaska Cooperative Fish and Wildlife Research Unit, University of Alaska Fairbanks, Fairbanks, AK 99775, USA, admcguire@alaska.edu

Jerry M. Melillo The Ecosystems Center, Marine Biological Laboratory, Woods Hole, MA 02543, USA, jmelillo@mbl.edu

Nina A. Meschtyb Department of the Northern Studies, Institute of Ethnology and Anthropology, Russian Academy of Science, Leninsky pr. 32-A, 119991 Moscow, Russia, meschtyb@mail.ru

Natalia G. Moskalenko Earth Cryosphere Institute, SB RAS, 117982 Moscow, Russia, natmoskalenko@yandex.ru

Mukhtar M. Naurzbaev V.N. Sukachev Institute of Forest, Academgorodok, SB RAS, 660036, Krasnoyarsk, 50, Russia, mukhtar@forest.akadem.ru

Peder Nelson Department of Forest Ecosystems and Society, Oregon State University, Corvallis, OR 97331, USA, Peder.Nelson@oregonstate.edu

Anders Oskal International Centre for Reindeer Husbandry, Guovdageaidnu, Kautokeino, 9520 Norway, anders.oskal@reindeercentre.org

Anu Pajunen Arctic Centre, University of Lapland, 96101 Rovaniemi, Finland, anu.pajunen@oulu.fi

Dirk Pflugmacher Department of Forest Ecosystems and Society, Oregon State University, Corvallis, OR 97331, USA, Dirk.Pflugmacher@oregonstate.edu

Peter V. Potapov Geographic Information Science Center of Excellence, South Dakota State University, Brookings, SD 57007, USA, Peter.Potapov@sdstate.edu

Vladimir Radionov Arctic and Antarctic Research Institute, 199397 St. Petersburg, Russia, vradion@aari.nw.ru

Kenneth J. Ranson NASA's Goddard Space Flight Center, Greenbelt, MD 20771, USA, kenneth.j.ranson@nasa.gov

Michael A. Rawlins Department of Geosciences, University of Massachusetts, Amherst, MA, 01003, USA, rawlins@geo.umass.edu

Martha K. Raynolds Institute of Arctic Biology, Box 757000, University of Alaska Fairbanks, Fairbanks, AK 99775-7000 USA, fnmkr@uaf.edu

Anni Reissell Department of Physics, PO box 48 (Erik Palmenin aukio 1) 00014, University of Helsinki, Finland, anni.reissell@helsinki.fi

Peter Romanov NOAA World Weather Building, Camp Springs, MD 20746, USA, peter.romanov@noaa.gov

Vladimir E. Romanovsky University of Alaska Fairbanks, Fairbanks, AK 99775, USA, ffver@uaf.edu

Alexander I. Shiklomanov Water Systems Analysis Group, University of New Hampshire, Durham, NH 03824-3525, USA, alex.shiklomanov@unh.edu

Irina N. Sokolik School of Earth and Atmospheric Sciences, Georgia Institute of Technology, Atlanta, GA 30332-0340, USA, isokolik@eas.gatech.edu

Florian Stammler Arctic Centre, University of Lapland, 96101 Rovaniemi, Finland, florian.stammler@ulapland.fi

Stephen V. Stehman College of Environmental Science and Forestry, State University of New York, Syracuse, NY 13210, USA, svstehma@syr.edu

Guoqing Sun Department of Geography, University of Maryland, Greenbelt, MD 20771, USA; Biospheric Sciences Branch, NASA/GSFC, Code 923, Greenbelt, MD 20771, USA, Guoqing.Sun@nasa.gov

Johan M. Turi International Centre for Reindeer Husbandry, Guovdageaidnu, Kautokeino, 9520 Norway, johan.m.turi@reindeerworld.net

Donald A. Walker Department of Biology and Wildlife, Institute of Arctic Biology, Alaska Geobotany Center, University of Alaska Fairbanks, AK 99775-7000, USA, dawalker@alaska.edu; ffdaw@uaf.edu

Qin Yu Department of Environmental Sciences, University of Virginia, PO Box 400123, Charlottesville, VA 22904-4123, USA, qy4a@virginia.edu

Boris Yurchak Cryospheric Sciences Branch, NASA Goddard Space Flight Center, Greenbelt, MD 20771, USA, boris.s.yurchak@nasa.gov

John Richard Martin "Joonas" Derome (1947–2010): In Memoriam

John Richard Martin Derome was born on July 12 1947 in Liverpool, UK. In 1969 he received a BSc degree in England, in the same year he started his studies in forestry in Finland and in 1975 obtained a M.Sc. (For.) degree in Helsinki. Since 1969 till his dying day he worked in the Finnish Forest Research Institute (METLA). In 2000 he finished his PhD thesis: "Effects of heavy-metal and sulphur deposition on the chemical properties of forest soil in the vicinity of a Cu-Ni smelter, and means of reducing the detrimental effects of heavy metals" and got a D.Sc. (For) degree. During the past 20 years John was very active in international fora in the field of effects of environmental pollution on forest ecosystems. John Derome was a National Coordinator of ICP Forests Focal Centre in Finland. John was a wonderful man, great friend, the heart of the ICP Forests family.

Natalia Lukina

List of Abbreviations

ACIA	Arctic Climate Impact Assessment
AeroCAN	Canadian Sun-Photometer Network
AERONET	AErosol RObotic NETwork
AIRS	Atmospheric InfraRed Sounder
Al, Ca and Mg	Aluminium, calcium and magnesium
AMAP	Arctic Monitoring and Assessment Programme
AMSR-E	Advanced Microwave Scanning Radiometer-EOS
AMSU	Advanced Microwave Sounding Unit
AO	Autonomous Okrug
AO	Arctic Oscillation
AOD	Aerosol Optical Depth
AOT40	Measure of the accumulated hourly ozone levels about a threshold
ArcticRIMS	Regional, Integrated hydrological Monitoring System for the Pan-Arctic Vegetation Model
ArcVeg	Arctic Vegetation Model
ARRA	Anadyr River Research Area
ARWI	annual ring width index
ASF	Alaska Synthetic Aperture Radar (SAR) Facility
ASHT	Arctic Shrub Tundra
ASHTw	Arctic Shrub Tundra Wetlands
ASTER	Advanced Spaceborne Thermal Emission and Reflection Radiometer
AVHRR	Advanced Very High Resolution Radiometer
B.P.	Before Present
BBDF	Boreal Broadleaf Deciduous Forest
BBDFw	Boreal Broadleaf Deciduous Forest Wetlands
BC	Black Carbon
BGC	Bio-Geo-Chemical
BIOME	Global Biome Model
BNDF	Boreal Needleleaf Deciduous Forest
BNDFw	Boreal Needleleaf Deciduous Forest Wetlands
BNEF	Boreal Needleleaf Evergreen Forest

BNEFw	Boreal Needleleaf Evergreen Forest Wetlands
BRDF	Bidirectional Reflectance Distribution Function
C	Carbon
^{14}C	Carbon-14 isotope
CAFF	Conservation of Arctic Flora and Fauna
CALIPSO	Cloud-Aerosol Lidar and Infrared Pathfinder Satellite Observation
CCN	Cloud Condensation Nuclei
CD	Canopy Density
ChaO	Chukotskiy Autonomous Okrug
CO_2	Carbon dioxide
CORINE	Coordination de l'information sur l'environnement
CRU	Climate Research Unit, University of East Anglia, UK
DMS	Dimethylsulfide
DMSP	Defense Meteorological Satellite Program
DOC	Dissolved Organic Carbon
DOC_{EX}	DOC export from the terrestrial system
DVT	Dominant Vegetation Types
EALÁT	IPY Saami Project (means "good pasture" in Saami language)
ECI	Earth Cryosphere Institute
ENSINOR	Environmental and Social Impacts of Industrialization in Northern Russia
EOS	Earth Observing System
EOS Terra	Earth Observing System – Terra Platform
ESA	European Space Agency
ET	Evapotranspiration
ETM	Enhanced Thematic Mapper
ETM+	Enhanced Thematic Mapper Plus imagery in Landsat
EUROSTAT	European Statistics
EVI	Enhanced Vegetation Index
FAO	Food and Agriculture Organization
fPAR	fraction of Photosynthetically Active Radiation
FSU	Former Soviet Union
GCM	Global Climate Model
GHG	Greenhouse gases
GIMMS	Global Inventory Modeling and Mapping Studies
GIS	Geographic Information System
GISS	NASA Goddard Institute for Space Studies
GLAS	Geoscience Laser Altimeter System
GLC	Global Land Cover
GLCC	Global Land Cover Characterization
GLOBIO	Global Methodology for Mapping Human Impacts on the Biosphere
GOES	Geostationary Operational Environmental Satellites
GOSAT	Greenhouse gases Observing SATellite

GRACE	Gravity Recovery and Climate Experiment
GRAS	Grasslands / Herbaceous
GRASw	Grasslands / Herbaceous Wetlands
GSN	"Global Snowflake Network" NASA Project
HOW	"History of Winter" NASA Project
ICESat	Ice, Cloud, and land Elevation
IFL	Intact Forest Landscapes
IGBP	International Geosphere-Biosphere Programme
IGBP-DIS	International Geosphere-Biosphere Programme – Data Information System
IN	Ice-forming Nuclei
IPCC	Intergovernmental Panel on Climate Change
IPY	International Polar Year
JISAO	Joint Institute for the Study of the Atmosphere and Ocean
LAEA	Lambert Azimuthal Equal-area
LAI	Leaf Area Index
Landsat	Land Satellite
LCCS	Land Cover Classification System
LCLUC	Land-Cover/Land-Use Change NASA program
LST	Land Surface Temperature
LW	Longwave Radiation
MaxNDVI	Maximum Normalized Difference Vegetation Index
MeHg	Methyl mercury
MERIS	Medium Resolution Imaging Spectrometer
MIR	Middle Infrared
MISR	Multiangle Imaging SpectroRadiometer
MLC	Maximum-Likelihood Classifier
MODIS	Moderate Resolution Imaging Spectroradiometer
MODTRAN	MODerate spectral resolution atmospheric TRANSsmittance
MSG	Meteosat Second Generation
MSS	Multi-Spectral Sensor
MSU-SK	Multispectral Scanners with Conical Scanning
N	Nitrogen
NAM	Northern Annular Model
NAO	Nenets Autonomous Okrug
NAO	North Atlantic Oscillation
NASA	US National Aeronautics and Space Administration
NCAR	US National Center for Atmospheric Research
NCE	net C exchange between the terrestrial system and the atmosphere
NCEP	US National Center for Environmental Prediction
NDVI	Normalized Difference Vegetation Index
NECB	Net Ecosystem Carbon Balance
NEESPI	Northern Eurasia Earth Science Partnership Initiative
NELDA	Northern Eurasia Land Cover Dynamics Analysis
NGDC	US National Geophysical Data Center

NIR	Near-InfraRed
NIRR	Incident short-wave solar radiation
NMI	Norwegian Meteorological Institute
nmVOC	non-methane volatile organic compound
NOAA	National Oceanic and Atmospheric Administration
NOAA	US National Oceanic and Atmospheric Administration
NO_X	Nitrogen oxides NO and NO_2
NPI	North Pacific Index
NPP	net primary production
NRC	US National Research Council
NSF	US National Science Foundation
NSR	Northern Sea Route
O_3	Ozone
OC	Organic Carbon
OMI	Ozone Monitoring Instrument
P	Precipitation
PAH	Polycyclic aromatic hydrocarbon
PCB	Polychlorinated biphenyl
PCDD/F	Polychlorinated dibenzodioxin and dibenzofuran
PDF	Combined flux from the decay of the three post-disturbance product
PDO	Pacific Decadal Oscillation
PFT	Plant Functional Type
POP	Persistent organic pollutant
PREC	Monthly precipitation
PRISM	Passive Range-angle-angle Imaging with Spectral Measurements
PTPD	Prostrate Tundra / Polar Desert
QuikSCAT	Quick Scatterometer
RADARSAT	RADAR SATellite
RENMAN	Challenges of modernity for REiNdeer MANagement project
R_H	Heterotrophic respiration
RIM	Rapid Integrated Monitoring System
SAR	Synthetic Aperture Radar
SCE	Snow Cover Extent
SCLP	Snow and Cold Land Processes mission, NASA
SeaWiFS	Sea-viewing Wide Field-of-view Sensor, NASA
SLCR	Seasonal Land Cover Regions
SMAC	Simplified Method for Atmospheric Corrections
SMMR	Scanning Multichannel Microwave Radiometer
SO_2	Sulfur dioxide
SOM	Soil Organic Matter
SON	Soil Organic Nitrogen
SPOT	Satellite Pour l'Observation de la Terre
SSMI	Spectral Sensor Microwave Imager
SST	Sea Surface Temperature

SW	Shortwave radiation
SWE	Snow Water Equivalent
SWI	Summer Warmth Index
SWOT	Surface Water Ocean Topography mission
T_{AIR}	Monthly surface air temperature
TBDF	Temperate Broadleaf Deciduous Forest
TBDFw	Temperate Broadleaf Decid. Forest Wetlands
TCE	Total C emissions due to disturbance and land use conversion
TEM	Terrestrial Ecosystem Model
Terra	A multi-national NASA scientific research satellite in a sun-synchronous orbit around the Earth
TI-NDVI	Time-Integrated Normalized Difference Vegetation Index
TM	Thematic Mapper imagery in Landsat
TNEF	Temperate Needleleaf Evergreen Forest
TNEFw	Temperate Needleleaf Evergreen Forest Wetlands
TOA	Top-of-the-atmosphere
TRMM	Tropical Rainfall Measuring Mission
UMD	University of Maryland
UN	United Nations
UNEP	United Nations Environmental Program
UNESCO	United Nations Educational, Scientific and Cultural Organization
UN FAO	United Nations Food and Agriculture Organization
USSR	The Union of Soviet Socialist Republics
UTM	Universal Transverse Mercator
VCF	Vegetation Continuous Fields
WIFS	Wide Field-of-view Sensor
VOC	volatile organic compounds
WOOD	Xeric Woodlands
VPD	Vapor Pressure Deficit
WRH	Association of World Reindeer Herders
WRS	Worldwide Reference System
VVRA	Vaegi Village Research Area
XESH	Xeric Shrublands
YNAO	Yamal-Nenets Autonomous Okrug

Chapter 1
Introduction: Climate and Land-Cover Changes in the Arctic

Pavel Groisman, Garik Gutman, and Anni Reissell

Abstract The last 10 years have been the warmest in the Arctic during the 120-year period of instrumental observations. The global mean surface temperature during that period has increased by about 0.8°C, with stronger changes in the Arctic. Retreat of the Arctic sea ice during the past decades open an additional source of heat and water vapor in the autumn and early winter seasons. If these warming trends continue, they will significantly affect the Arctic land cover and land use, also causing impacts on the global scale. The changes will occur in the natural land cover, with perhaps the greatest effects in that part of the Arctic where the land cover has already been modified by human activities. In many Arctic areas there has been a clear shift from the land use practiced by indigenous peoples to intensive exploitation of the land for commercial and industrial uses. New navigation routes across the Arctic Ocean shelf seas are broadly discussed. If and when implemented, these routes will change the Arctic land use and the life style of the population. The International Polar Year (IPY) program involving over 200 projects with thousands of scientists from over 60 nations is coming to its final stage. This book is a compilation of the studies which have been conducted in the framework of the NASA Land-Cover/Land-Use Change Program and which have been focused on the Arctic region of Northern Eurasia, although some comparisons are made with the results in North America. The region of interest in the current book is north of 60° latitude, specifically transitional forest-tundra and tundra zones.

1.1 The Role of Northern Eurasia in the Global Climate Change

The twentieth century's climatic changes in the high latitudes of Northern Eurasia have been reflected in many atmospheric and terrestrial variables. Magnitudes of contemporary warming are higher over high latitudes than over the tropics (Fig. 1.1).

P. Groisman (✉)
National Climate Data Center, Ashville, NC 28801, USA
e-mail: pasha.groisman@noaa.gov

G. Gutman, A. Reissell (eds.), *Eurasian Arctic Land Cover and Land Use in a Changing Climate*, DOI 10.1007/978-90-481-9118-5_1,

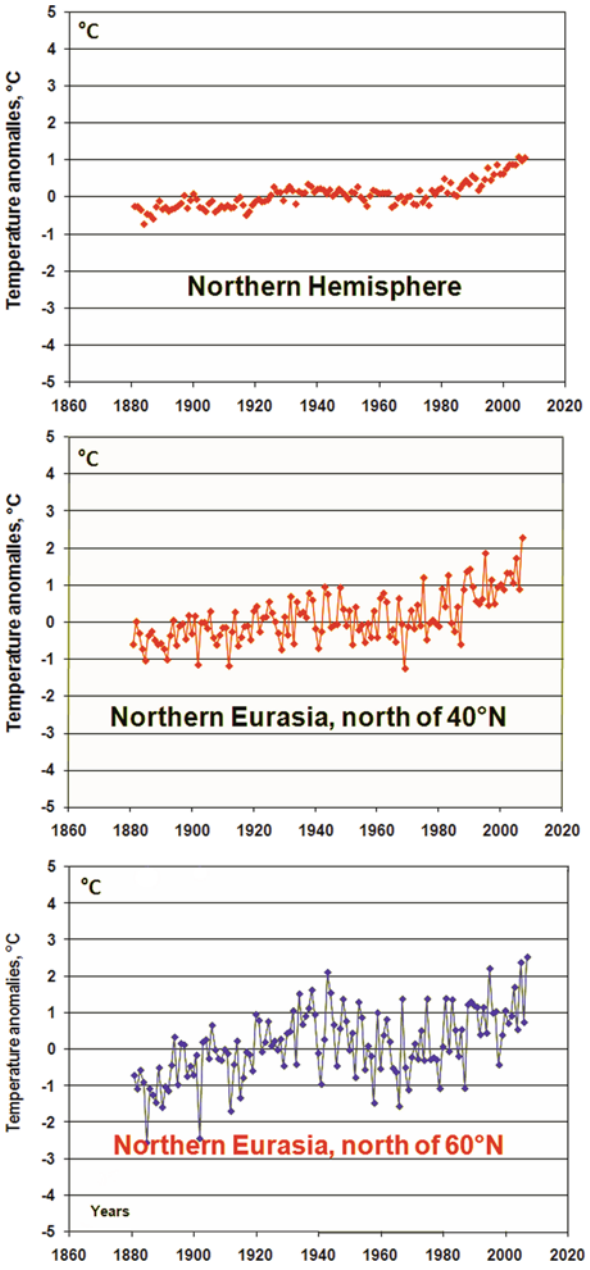

Fig. 1.1 Annual surface air temperature anomalies (°C), area averaged over the Northern Hemisphere, Northern Eurasia north of 40°N and north of 60°N for the 1881–2007 period. Anomalies were calculated from the long-term mean values for the 1951–1975 reference period. Statistically significant temperature increases (estimated by linear trends) were equal to 0.95, 1.4 and 1.7°C per 127 years respectively. Data source: Archive of Lugina et al. (2007)

They are higher over continents than over oceans and in the cold season than over the warm season (IPCC 2007). Thus, Northern Eurasia is the region where the changes are among the highest over the globe with an annual winter temperature increase by more than 2°C during the period of instrumental observations and

summer temperature in the Eurasian Arctic showing an increase by 1.35°C since 1881 (Lugina et al. 2007). The summer warming in the Eurasian Arctic has been observed during the past several decades. Summer temperatures control most of polar vegetation in the region where surface radiation balance is positive only for a short period of the year but with extremely high values.

The Eurasian Arctic Ocean coastal waters are ice-covered much of the year. Arctic sea-ice extent varied in the past, e.g., shrinking by 10% in the end of the 1930s (Fletcher 1970). During the past 3 decades a new decline in sea-ice extent and thickness has occurred and is being monitored from satellites and submarines. It appears that the Arctic Ocean is quickly moving to perennial ice-free conditions and has already lost nearly half of its end-of-summer extent since the late 1970s. This change, while causing some impact on the regional albedo, dramatically affects the cold season heat fluxes from the ocean (with temperatures around 0°C) into the atmosphere, whereas in the presence of the sea ice that insulates the "warm" ocean, the surface temperature can be –40°C.

Recent Global Climate Model (GCM) simulations (Sokolov 2008) show that the atmospheric forcing by these sea ice changes is responsible for more than half of the regional warming in high latitude land areas with a peak in December while the "causes" of the residual Arctic warming were the "global" factors that cause the global sea surface temperature warming. These simulations reproduce changes reported in land areas north of 60°N in Fig. 1.1. Thus, the Arctic Eurasia is being affected by global and regional "external" factors that are causing its change and the positive feedbacks to this forcing may further aggravate the situation (cf., Chapters 4, 5, and 6, this volume). Seasonal snow cover is observed practically over the entire Northern Eurasia for a period of 1 week–10 months controlling the energy and water balances of the region and terrestrial ecosystems. The longest data set, (from late 1960s) of snow-cover extent variations over the Northern Hemisphere (http://climate.rutgers.edu/snowcover/), was recently expanded into the past for Northern Eurasia (Brown 2000; Groisman et al. 2006). Analyses of these and the in situ snow-cover data show that during the past 40 years there were no systematic changes in winter. On the other hand, a systematic snow-cover retreat (by ~10–15%) in spring and an increase in maximum snow depth in the Eurasian Arctic have been observed (Bulygina et al. 2007a).

While changes in surface-air temperature and precipitation are most commonly addressed in the literature, changes in their derived variables (variables of economic, social and ecological interest based upon daily temperatures and precipitation) have received less attention (McBean et al. 2005). These variables (or indices) include frequency of extremes in precipitation and temperature, frequency of thaws, heating-degree days, growing season duration, sum of temperatures above/below a given threshold, number of frost-free days, day-to-day temperature variability, precipitation frequency, and precipitation-type fraction. In practice, these and other indices are often used instead of "raw" temperature and precipitation values for numerous applications that include modeling and prediction of crop yields, floods and forest fires as well as planning for pest management, plant-species development, greenhouse operations, food processing, heating oil consumption in remote locations,

heating system design, power plant construction, energy distribution, reservoir operations. These indices provide measurements for the analysis of changes that might impact agriculture, energy, and ecological aspects of high latitudes. Figure 1.2 gives examples of changes in a few temperature-derived characteristics for the former USSR and Fennoscandia. Two-digit numbers (in percentage change) indicate substantial changes during the second half of the twentieth century directly affecting the regional ecosystems and societal well-being.

Observational data show that the weather conditions in the western half of high-latitudinal Northern Eurasia during the twentieth century became more humid, while east of the Ural mountains drier weather conditions prevail (Førland and Hanssen-Bauer 2000; Groisman and Rankova 2001; Dai et al. 2004; Bulygina et al. 2007b; Groisman et al. 2005, 2007; Zolina et al. 2005). These conditions manifest themselves with an increase in frequency of intense rainfall (over most of the continent), and also with an increased potential of forest and tundra fire danger, the actual areas consumed by fires, droughts, and prolonged dry episodes (in

Characteristic trend estimates, %/54 yrs

	Former USSR	Siberia & Russian Far East south of 66.7°N
Heating-degree days	–7	–7
Degree-days below 0°C	–15	–14
Degree-days above 15°C	11	20
Duration of the growing season		
T > 10 °C	9	14
T > 5 °C	8	12
Duration of the frost-free period	8	11

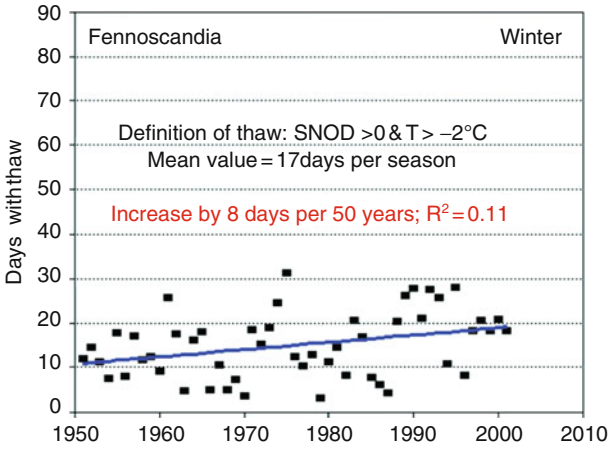

Fig. 1.2 (*top*) Changes of several temperature-derived characteristics within the former USSR boundaries during the 1951–2004 period. (*bottom*) Changes of the frequency of days with thaw over Fennoscandia (day with thaw is defined as a day with snow on the ground and daily temperature above –2°C). Archive of the Arctic Climate Impact Assessment Report (McBean et al. 2005)

the east), and with an increase of the water table and lake levels (in the west). It is worth noting that the drier atmospheric conditions over the northeastern part of Eurasia (regions with permafrost) are accompanied by an increase in streamflow to the Arctic Ocean (cf. Chapter 7, this volume), a phenomenon still requiring more in-depth explanations.

1.2 Implications of the Observed Changes

Contemporary changes in global and regional climatic variables over the high latitudes of Northern Eurasia during the past 50–100 years imply increases and decreases in risk (when the variables have economic, social and ecological implications). Whatever "implications" would be assigned to these observed changes, it is important to note that many of them have been significant enough to be noticed above the usual "weather" noise level (in particular, during the past 50 years) and thus should be further investigated in order to adapt to their impacts.

Future climate changes are expected to induce an increase in precipitation, an increase in the volume of river flow, a decline in the area with a permanent snow cover during the winter, the thawing of permafrost and, subsequently, a reduction in the area of land with frozen soil, a decrease in the incidence and coverage of lake and river ice, a retreat in the area of summer sea ice, increased melting of glaciers and the Greenland ice sheet, a rise in sea level and a decrease in ocean salinity (ACIA 2004; IPCC 2007). These changes, in turn, will affect terrestrial systems by changing the hydrology of wetlands, bringing about a northward shift in the vegetation cover, changes in biodiversity, possible increase in the outbreaks of damage caused by insects and in the incidence of both natural and man-made forest and peatland fires with the consequent loss of environmentally important old-growth forests.

1.3 Regional Contribution to the Global Carbon Cycle

Permafrost, influencing nearly 25% of the northern hemisphere land mass, shows substantial change, mostly in the form of thermal decomposition due to warming air temperatures. Permafrost degradation affects local ecology and hydrology as well as coastal and soil stability. Decomposition of permafrost will mobilize reserves of frozen carbon (C), some of which, as methane (CH_4), will increase the global greenhouse effect. A large release of carbon dioxide (CO_2) and methane from high latitude terrestrial and marine systems to the atmosphere has the potential to affect the climate system in a way that may accelerate global warming.

High latitude ecosystems are considered of crucial importance to the global carbon cycle because of their high carbon storage capacity and their vulnerability to change in climate and to natural and anthropogenic disturbances (IPCC 2007). A large, warming-induced release of carbon dioxide from arctic and boreal terrestrial systems to the atmosphere could create a positive feedback to the climate system in a way that accelerates global warming (cf., McGuire et al. 2006; Goetz et al. 2007). In recent decades, this region has experienced surface air temperature

warming (Fig. 1.1) and extensive, severe forest fires (Soja et al. 2007), along with land-use changes and changes in forest management (Forbes 2008, Chapter 5, this volume). Studies using various accounting and modeling approaches have suggested a positive terrestrial C balance (terrestrial sink) in Northern Eurasia during recent decades. However, recent process-based model estimates suggest that the large areas burned (e.g., in 2002) may be causing the region to shift toward a net CO_2 source to the atmosphere (Chapters 5 and 6, this volume). Such changes in climate, disturbance regimes and land-use and management systems have the potential to alter the balance between C uptake and release by biological processes in such a way as to weaken, or eliminate, the terrestrial sink in the high latitude ecosystems of Northern Eurasia.

Summarizing, the major mechanisms through which climate change can affect, directly or indirectly, land cover in the Arctic include changes in the reflectivity and the water cycle at the surface following melting of snow and ice cover, its replacement by a vegetation cover, and/or a changes in the underlying vegetation cover itself (e.g., due to drier/wetter weather conditions); changes in ocean circulation as the Arctic ice melts, resulting in changes in weather and climate patterns, which in turn affect vegetation cover; land-cover changes due to the permafrost thaw; and changes in the amounts of greenhouse gases emitted to the atmosphere from land, especially peatlands as warming progresses. The above processes can produce positive or negative climate feedback effects. The last two mechanisms most probably result in the further acceleration of climate change, i.e. representing a positive biogeochemical feedback.

1.4 The NASA LCLUC Program's Contribution to the International Polar Year

The Land-Cover/Land-Use Change (LCLUC) program is an interdisciplinary science program in the US National Aeronautics and Space Administration (NASA) Earth Science Research Program. LCLUC is part of the Carbon Cycle and Ecosystems Focus Area, also having strong links to the Terrestrial Hydrology program of the Water and Energy Cycle Focus Area of NASA. Relevant to the NASA LCLUC Program and aligned with the international Northern Eurasia Earth Science Partnership Initiative (NEESPI; http://neespi.org) are the following science questions:

- What has been the role of anthropogenic impacts on producing the current status of the ecosystem, both through local land-use/land-cover modifications and through global gas and aerosol inputs? What are the hemispheric scale interactions, and what are the local effects?
- How will future human actions affect Northern Eurasia and global ecosystems? How can we describe these processes using a suite of local, regional, and global models?
- What will be the consequences of global changes for regional environment, the economy, and the quality of life in Northern Eurasia?

The International Polar Year (IPY) program involving over 200 projects with thousands of scientists from over 60 nations is coming to its final stage. This volume is a compilation of the studies supported by NASA, National Science Foundation (NSF, USA), Russian Academy of Sciences, the Academy of Finland and other European and Russian agencies and institutions. The focus of the book is on the Arctic region of Northern Eurasia, although some comparisons are made with the results in North America. The region of interest is north of 60° latitude, specifically transitional forest-tundra and tundra zones. The NASA LCLUC contribution to the IPY, in general, and the NEESPI program, in particular, has been expressed through support of several projects directed at studying LCLUC interactions with climate and environment in the Arctic Eurasia, support of the NEESPI Project Scientist, and facilitation of NEESPI activities.

This volume includes results of vegetation changes studies (Chapters 2–5), studies of the geographic patterns of fluxes of carbon dioxide and methane and their balance and changes over time to improve our understanding of the processes controlling the sources and sinks of these atmospheric gases in the Earth's system (Chapter 6), studies of changes in hydrological systems (Chapter 7), wildlife populations and the overall habitability of the Arctic (Chapters 8 and 9), and studies of aerosol and pollution (Chapters 10 and 11). They use integrated geophysical, ecological and economic models to determine thresholds of critical change in various systems. These studies provide pathways to strategies for adaptation to the observed and predicted changes, and facilitate assessments of the impacts and opportunities related to natural resource management of energy and transportation developments.

References

ACIA (2004) Impacts of a warming Arctic. In: Hassol SJ (ed) Arctic climate impact assessment overview report. Cambridge University Press, Cambridge, p 144

Brown RD (2000) Northern Hemisphere snow cover variability and change, 1915–1997. J Clim 13:2339–2355

Budyko MI, Vinnikov KY (1976) Global warming. Sov Meteorol Hydrol 7:12–20

Bulygina ON, Korshunova NN, Razuvaev VN (2007a) Variations in snow characteristics over the Russian territory in the recent decades. Proc RIHMI-WDC 173:41–46 (in Russian)

Bulygina ON, Razuvaev VN, Korshunova NN, Groisman PYa (2007b) Climate variations and changes in extreme climate events in Russia. Environ Res Lett 2(4). doi:10.1088/1748-9326/2/4/045020

Dai A, Trenberth KE, Qian T (2004) A global dataset of Palmer drought severity index for 1870–2002: relationship with soil moisture and effects of surface warming. J Hydrometeorol 5:1117–1130

Fletcher JO (1970) Influence of polar sea ice on climate. Izvestiya (Proceedings) Acad Sci USSR Ser Geogr 1:24–36

Forbes BC (2008) Equity, vulnerability and resilience in social-ecological systems: a contemporary example from the Russian Arctic. Res Soc Probl Public Policy 15:203–236

Førland EJ, Hanssen-Bauer I (2000) Increased precipitation in the Norwegian Arctic: true or false? Clim Change 46:485–509

Goetz SJ, Mack MC, Gurney KR, Randerson JT, Houghton RA (2007) Ecosystem responses to recent climate change and fire disturbance at northern high latitudes: observations and

model results contrasting northern Eurasia and North America. Environ Res Lett 2(4). doi:10.1088/1748-9326/2/4/045031

Groisman PYa, Knight RW, Easterling DR, Karl TR, Hegerl GC, Razuvaev VN (2005) Trends in intense precipitation in the climate record. J Clim 18:1343–1367

Groisman PYa, Knight RW, Razuvaev VN, Bulygina ON, Karl TR (2006) State of the ground: rarely used characteristic of snow cover and frozen land: climatology and changes during the past 69 years over Northern Eurasia. J Clim 19:4933–4955

Groisman PYa, Rankova EYa (2001) Precipitation trends over the Russian permafrost-free zone: removing the artifacts of pre-processing. Int J Climatol 21:657–678

Groisman PYa, Sherstyukov BG, Razuvaev VN, Knight RW, Enloe JG, Stroumentova NS, Whifield PH, Forland E, Hannsen-Bauer I, Tuomenvirta H, Alexanderson H, Mestcherskaya AV, Karl TR (2007) Potential forest fire danger over Northern Eurasia: changes during the 20th century. Glob Planet Change 56:371–386

IPCC (2007) Climate change 2007: the physical science basis. In: Solomon S, Qin D, Manning M, Chen Z, Marquis M, Averyt KB, Tignor M, Miller HL (eds) Contribution of working group I to the 4th assessment report of the intergovernmental panel on climate change. Cambridge University Press, Cambridge, New York, p 996

Lugina KM, Groisman PYa, Vinnikov KYa, Koknaeva VV, Speranskaya NA (2007) Monthly surface air temperature time series area-averaged over the 30-degree latitudinal belts of the globe, 1881–2006. In Trends: a compendium of data on global change. Carbon Dioxide Information Analysis Center, Oak Ridge National Laboratory, US Department of Energy, Oak Ridge

McBean G, Alekseev G, Chen D, Førland E, Fyfe J, Groisman PYa, King R, Melling H, Vose R, Whitfield PH (2005) Arctic climate: past and present. Chapter 2 In: Arctic climate impact assessment – scientific report. Cambridge University Press, Cambridge, pp 21–60

McGuire AD, Chapin FS III, Walsh JE, Wirth C (2006) Integrated regional changes in arctic climate feedbacks: implications for the global climate system. Ann Rev Environ Resour 31:61–91

Robinson DA, Dewey KF, Heim R Jr (1993) Global snow cover monitoring: an update. Bull Am Meteorol Soc 74:1689–1696

Soja AJ, Tchebakova NM, French NHF, Flannigan MD, Shugart HH, Stocks BJ, Sukhinin AI, Parfenova EI, Chapin FS III, Stackhouse PW Jr (2007) Climate-induced boreal forest change: predictions versus current observations. Glob Planet Change 56:274–296

Sokolov A (2008) Impact of decreases in the Arctic sea ice on climate in high latitudinal land areas of the Northern Hemisphere. European Geosciences Union General Assembly, Vienna, 14–19 April 2008, EGU2008-A-12096

Zolina O, Simmer C, Kapala A, Gulev SK (2005) On the robustness of the estimates of centennial-scale variability in heavy precipitation from station data over Europe. Geophys Res Lett 32:L14707. doi:10.1029/2005GL023231

Chapter 2
Recent Changes in Arctic Vegetation: Satellite Observations and Simulation Model Predictions

Scott J. Goetz, Howard E. Epstein, Uma S. Bhatt, Gensuo J. Jia, Jed O. Kaplan, Heike Lischke, Qin Yu, Andrew Bunn, Andrea H. Lloyd, Domingo Alcaraz-Segura, Pieter S.A. Beck, Josefino C. Comiso, Martha K. Raynolds, and Donald A. Walker

Abstract This chapter provides an overview of observed changes in vegetation productivity in Arctic tundra and boreal forest ecosystems over the past 3 decades, based on satellite remote sensing and other observational records, and relates these to climate variables and sea ice conditions. The emerging patterns and relationships are often complex but clearly reveal a contrast in the response of the tundra and boreal biomes to recent climate change, with the tundra showing increases and undisturbed boreal forests mostly reductions in productivity. The possible reasons for this divergence are discussed and the consequences of continued climate warming for the vegetation in the Arctic region assessed using ecosystem models, both at the biome-scale and at high spatial resolution focussing on plant functional types in the tundra and the tundra-forest ecotones.

2.1 Introduction

Ecosystem responses to warming of the Arctic have the potential to feed back either positively or negatively to the climate system depending on changes in the disturbance regime, vegetation distribution and productivity (McGuire et al. 2009). The lower albedo of forest vegetation compared with tundra, for example, results in a positive feedback on temperature (Bala et al. 2007; Chapin et al. 2005; Randerson et al. 2006). Conversely, increased productivity of arctic vegetation resulting from warmer temperatures tends to result in increased carbon dioxide (CO_2) uptake by net photosynthesis, providing a negative feedback to rising temperatures (Field et al. 2007; Serreze et al. 2000). Drought can modify this feedback effect, decoupling warming and productivity, as can the balance of gross photosynthesis and plant respiration, which varies substantially by plant functional type (Chapin et al. 1996; Goetz and Prince 1999). The relative importance of these competing feedbacks, and thus the cumulative effect of changing arctic vegetation on the climate system, is still not well known. For boreal forest ecosystem (and possibly tundra as well) this

S.J. Goetz (✉)
The Woods Hole Research Center, 149 Woods Hole Road, Falmouth, MA 02540-1644, USA
e-mail: sgoetz@whrc.org

G. Gutman, A. Reissell (eds.), *Eurasian Arctic Land Cover and Land Use in a Changing Climate*, DOI 10.1007/978-90-481-9118-5_2,

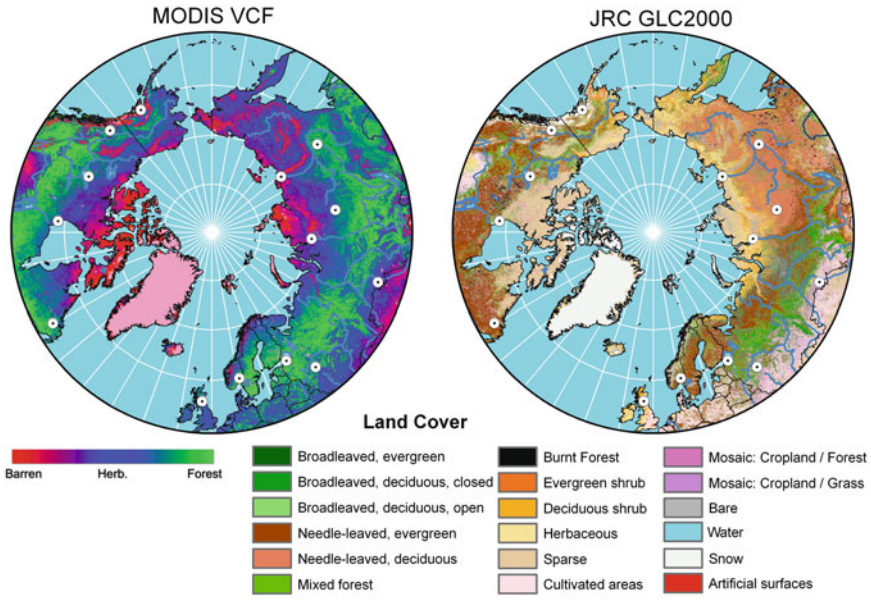

Fig. 2.1 (*left*) A color composite of the MODIS vegetation continuous fields indicating a combination of tree and herbaceous vegetation cover and bare ground. As the *circular legend* indicates, *green hues* indicate dominance of tree cover, *blue hues* indicate dominance of herbaceous vegetation (tundra), and *red hues* indicate bare ground. (*right*) A Global Land Cover 2000 map of vegetation cover types, as indicated in the legend. The *white dots* indicate major towns and are useful for referencing between the two images. Adapted from Bunn and Goetz (2006)

depends substantially upon the frequency and severity of the fire disturbance regime (Achard et al. 2008; Goetz et al. 2007; Kasischke and Stocks 2000; Mack et al. 2008; Randerson et al. 2006; Soja et al. 2007).

In this chapter, we focus primarily on changes in the productivity of arctic ecosystems in recent decades (<30 years), specifically tundra and boreal forest, as observed with a combination of satellite observations (Fig. 2.1) and field measurements, as projected by simulation modeling. We first provide an overview of changes documented in the recent literature, including our own work, and then focus on a series of case studies emphasizing more recent documented changes within Northern Eurasia. We end with a series of modeling studies that explore the likely future responses of vegetation to climate warming, focusing separately on tundra and boreal forest ecosystems.

2.2 An Overview of Recent Changes in Arctic Vegetation Productivity

Analyses of productivity metrics derived from satellite observations at high latitudes indicate that past evidence for ubiquitous “greening” trends that had been

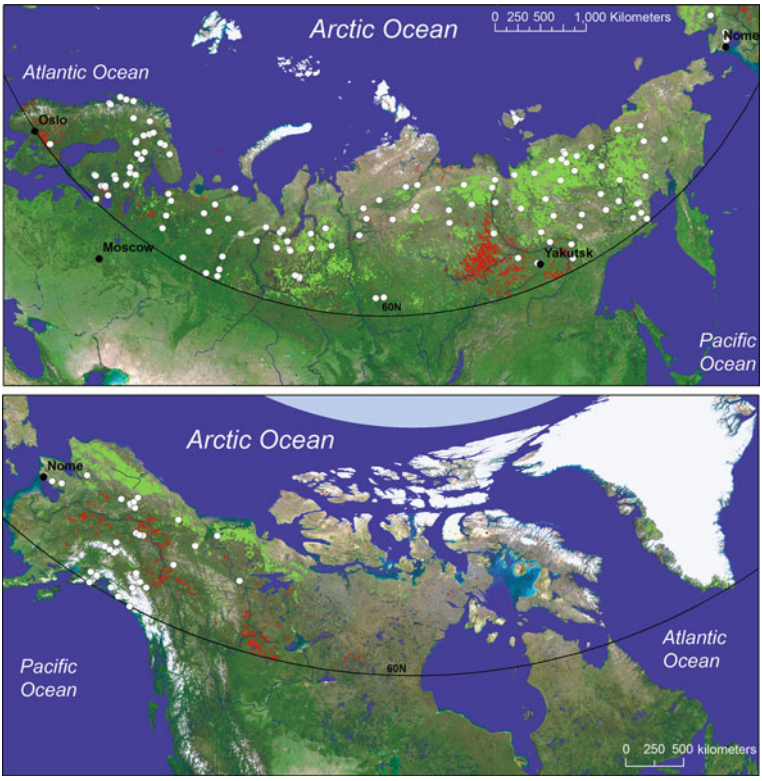

Fig. 2.2 Trends in satellite observations of vegetation productivity derived from a 1982 to 2005 time series of GIMMS-GAVHRR vegetation indices at 8-km spatial resolution, with significant positive trends shown in *bright green* and negative trends in red. Tree ring measurement sites are indicated as *white dots*. The trends map is overlaid on a 1-km resolution natural color composite of MODIS imagery. *White colors* in the MODIS image represent snow and ice. Compare these trends with tree cover and land cover maps in Fig. 2.1

widely noted (Jia et al. 2003; Myneni et al. 1997; Nemani et al. 2003; Slayback et al. 2003) did not continue after ~1990. The observed changes post-1990 were non-uniform across the broad Arctic domain, particularly after 2000 (Bunn and Goetz 2006; Goetz et al. 2005; Jia et al. 2006; Neigh et al. 2008). Arctic tundra vegetation increased both in terms of peak productivity and growing season length between 1982 and 2005 (see Fig. 2.2), and this finding is supported by a wide range of field site measurements across Northern Eurasia and the high latitudes of North America (ACIA 2004; Serreze et al. 2000; Walker et al. 2006). These dynamics include changes in the composition and density of herbaceous vegetation (Epstein et al. 2004; Shaver et al. 2007), increased woody shrub encroachment in tundra areas (Sturm et al. 2001; Tape et al. 2006), greater depths of seasonal thaw (Goulden et al. 1998; Kimball et al. 2006; Schuur et al. 2009), and associated changes in the energy regime (Chapin et al. 2005; Sturm et al. 2001).

In forested areas, by contrast, few areas not recently disturbed by fire showed any significant positive trend in productivity over the same time period, with the

exception of the West Siberian lowlands and areas with a low density of larch forest in the far east of Russia (Fig. 2.1). In North America more than 25% of undisturbed forest areas actually experienced a decline in productivity (Goetz et al. 2005). These same areas showed no systematic change in growing season length. Climatic warming occurred across the entire Arctic, but the forest response indicates that neither the intensity nor the length of the growing season changed in a way that reflected a simple relationship with increasing temperature or CO_2. The productivity trends in forested areas were most evident in the latter part of the growing season, indicating impacts of late summer drought (Vapor Pressure Deficit, VPD) on stomatal control and photosynthesis (Bunn et al. 2007; Zhang et al. 2008). Related, more densely forested areas were significantly more likely to show strong negative productivity trends (Bunn and Goetz 2006), particularly areas along the Lena River, west of Yakutsk in Siberia, and in black spruce forests of interior Alaska and central Canada (Goetz et al. 2007). These observations are supported by other recent modeling work comparing anomalies in simulated net productivity to gridded climate data, indicating that net photosynthetic gains being made in the spring months are more than offset by net photosynthetic losses later in the summer (Angert et al. 2005; Zhang et al. 2008). As noted above, these trends in productivity across unburned areas are heavily dependent on cover type and the underlying vegetation density (see Figs. 2.1 and 2.2).

2.3 Tundra Ecosystems

2.3.1 Relationships Among Sea Ice, Land Surface Temperature and Productivity

Recent dramatic reductions in summer sea-ice, particularly perennial ice, have been documented in the Arctic (Comiso 2002; Stroeve et al. 2006) and are of growing concern. Reduced sea-ice may exacerbate surface air warming, leading to increased permafrost thawing and vegetation productivity, and also potentially modifying the habitat and migration characteristics of both marine and terrestrial fauna. Our analysis documents some of these changes using ice cover derived from historical passive microwave data, surface temperature data from historical thermal infrared data, and vegetation indices (i.e. the normalized difference vegetation index [NDVI]) as a metric of vegetation productivity.

To investigate the nature of these connections, we examined the relationship between coastal ice and the adjacent land surface. The analysis employs 25-km resolution Special Sensor Microwave Imager (SSMI) estimates of sea ice concentration, based on a bootstrap algorithm (Comiso 2008), and AVHRR radiometric surface temperature (Comiso 2003, 2006), both covering the 26-year period from January 1982 to December 2007. The surface temperature data have recently been enhanced by applying more effective cloud masking techniques and an improved consistency in calibration through the utilization of in situ surface temperature data. The NASA

GIMMS NDVI data were used for the 1982–2007 summer periods. The Maximum NDVI (MaxNDVI) is the highest NDVI value obtained during the summer for each 8-km pixel and represents the peak greenness achieved during the summer. The Time-Integrated NDVI (TI-NDVI) is the sum of the biweekly NDVI values for the summer growing season. A threshold of 0.09 was used as a minimal value for green vegetation, based on an analysis of spring green-up (Jia et al. 2004). The NDVI data sets were resampled to 25-km resolution for comparisons with climate and sea-ice data sets. The NDVI analysis was limited to the area south of 72°N because of a discontinuity in the GIMMS data north of this latitude.

The spatial variations of the climate-vegetation relationships were examined for Eurasia regionally using the divisions of Treshnikov (1985) (Fig. 2.3) and for the total Eurasian domain. NDVI and summer warmth index (SWI – sum of mean monthly temperatures >0°C) time series were constructed for the tundra between treeline and 72°N (the position of the discontinuity in the NDVI data). The area south of 72° includes nearly all the Low Arctic that has more or less continuous cover of plants and peaty soil surface horizons (Walker 2005). Sea-ice indices were constructed over a corresponding 50-km ocean zone for each region. The sea-ice concentration is an average each year of the 3 weeks centered on the week of 50% climatological ice concentration, which varies by region and falls between 15 May and 22 July for the Eurasian study regions. This period was selected as it describes the transition to summer for most of the Arctic regions in our study. For correlation analyses, sea-ice concentrations were compared with SWI for 50-km seaward and landward strips along the entire Arctic coastline. For the correlations with NDVI, only the sea-ice concentrations and SWI south of 72°N were used.

The regional year-to-year variability and trends in SWI, sea-ice concentration and NDVI indices are relatively large (Fig. 2.3a–g), but there are consistent positive trends for SWI and TI-NDVI and negative trends for sea-ice concentration, albeit of varying strength, among the regions. The largest decreases in coastal sea-ice occurred in the E. Siberia and W. Chukchi seas (−49 and −47%). The largest change in summer land temperature occurred in the W. Chukchi, W. Bering, and E. Siberia Seas (+68%, +39%, +35%). More modest changes in SWI occurred elsewhere, varying from +2% in the Laptev Sea to 14% in the Barents Sea. The trends in TI-NDVI ranged from +5% in the Barents Sea to +15% in the W. Bering Sea. MaxNDVI changes varied from −1% in the Barents and W. Chukchi seas to +9% in the Laptev and W. Bering seas. For the Eurasian Arctic coast as a whole sea-ice has decreased (−29%), and SWI has increased (+16%) (Fig. 2.4a). MaxNDVI increased 4% and the TI-NDVI increased 8% (Fig. 2.4b).

The correlations between sea-ice concentration, SWI and TI-NDVI for each region are generally strong in all seas (Table 2.1), indicating that yearly variations in sea ice correspond to variations in land-surface temperatures and TI-NDVI. The exception in the West Bering region where spring sea ice and TI-NDVI are not correlated may be due to the importance of other processes, such as strong controls of NDVI by terrain and substrate variables (Raynolds 2009). For the entire Eurasia domain, sea-ice concentration and SWI were negatively correlated ($r = -0.57$, $p < 0.05$). TI-NDVI was significantly correlated with SWI ($r = 0.57$, $p < 0.05$) and

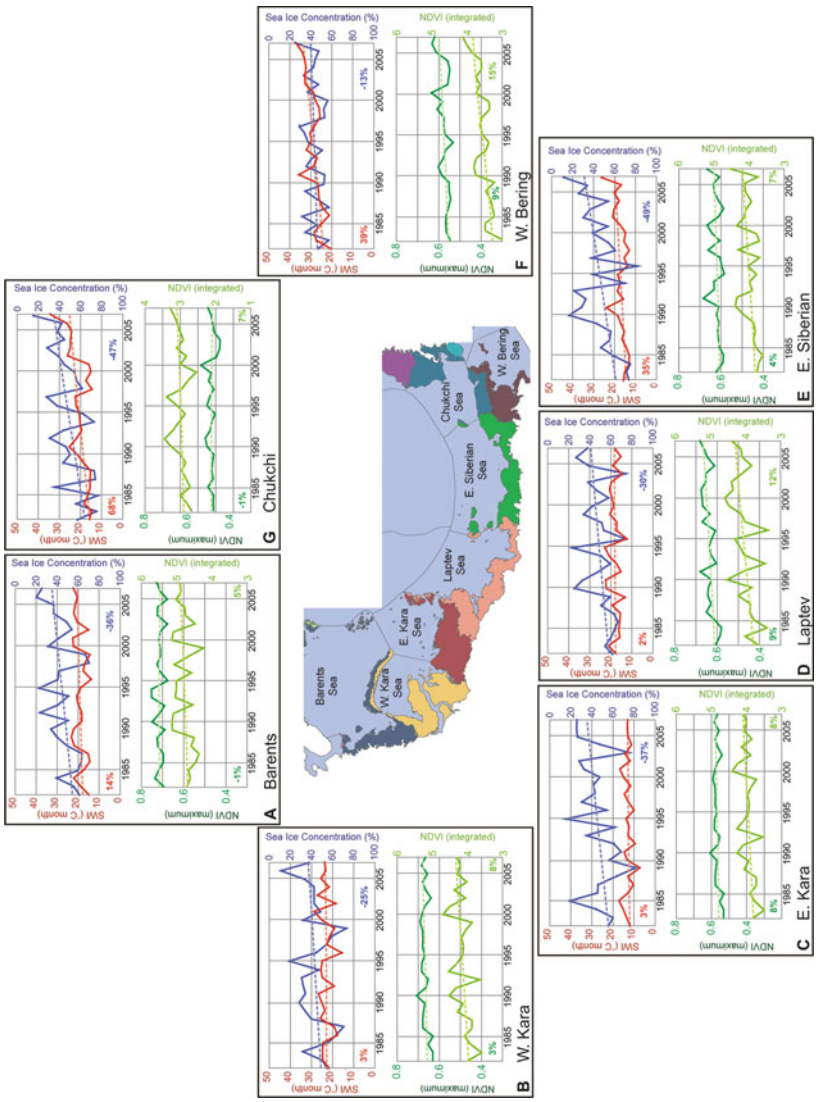

Fig. 2.3 Northern Eurasia regional (region defined by color) time series of sea-ice concentration (*blue*), summer warmth index (SWI, *red*), MaxNDVI (*dark green*), and TI-NDVI (*light green*). Sea-ice concentrations and SWI are for 50-km zones along the land and ocean. NDVI is for the tundra region south of 72°N. Decadal trends are indicated by color-coded numbers, with color corresponding to the line variable and bolded trends are significant at $p < 0.05$. All lines cover 1982–2007. Note the limits but not the scale on the TI-NDVI axis are different for the W. Chukchi. Based on Bhatt et al. (2008)

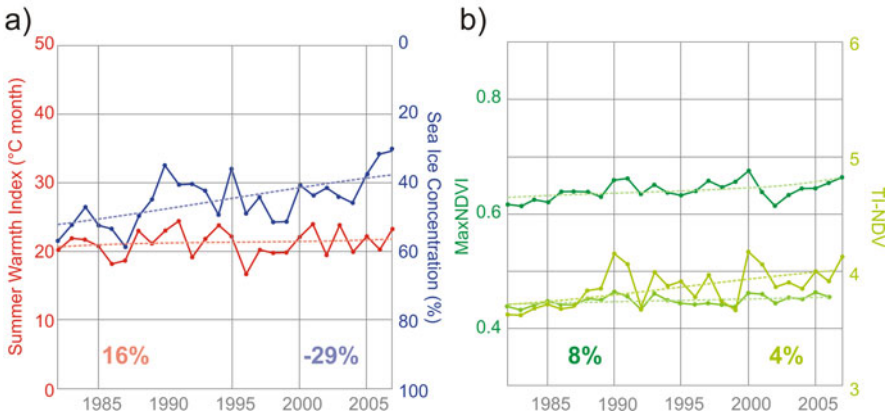

Fig. 2.4 (**a**) Northern Eurasia time series of Summer Warmth Index (*red*), 4–22 June sea-ice concentration (*blue*) in 50-km zones along the land and ocean. Note that sea ice concentration has a reversed scale. (**b**) Maximum NDVI (*dark green*) and integrated NDVI (*light green*) for the tundra region south of 72°N. Decadal trends are indicated by color coded numbers, with color corresponding to the line variable and bolded trends are significant at $p < 0.05$. All lines cover 1982–2007. Based on Bhatt et al. (2008)

Table 2.1 Correlations between SWI, sea-ice concentration, and TI-NDVI for subregions of coastal Eurasia. The sea-ice concentrations were correlated with SWI for 50-km seaward and landward strips along the entire Arctic coastline. For the correlations with TI-NDVI, only the sea-ice concentrations and SWI south of 72°N were used

Region	SWI – Sea ice	SWI – TI-NDVI	Sea-ice – TI-NDVI
Barents	−0.55*	0.60*	−0.49*
Kara-Yamal	−0.41*	0.59*	−0.31
Kara-East	−0.41*	0.62*	N/A
Laptev	−0.71*	0.74*	−0.68*
E. Siberian	−0.64*	0.49*	−0.72*
Chukchi	−0.52*	0.59*	−0.49*
W. Bering	0.0	0.54*	0

An asterisk (∗) indicates significance at the 95% level or greater. Correlations are based on linearly detrended time series. Real forest change: preditio

sea-ice concentration ($r = -0.54$, $p < 0.05$), indicating that enhanced greenness of tundra vegetation occurs with a warmer growing season and reduced sea-ice. Yearly variations in MaxNDVI, however, were not significantly correlated with sea-ice or SWI.

To examine the relationships between the large-scale climate drivers and Arctic sea-ice, SWI and NDVI, co-variability and correlations with climate indices were conducted. The climate indices used for this study include the December–March values for the North Atlantic Oscillation (NAO), Northern Annular Model (NAM or Arctic Oscillation), Pacific Decadal Oscillation (PDO) and North Pacific Index (NPI). The NAO is a measure of the north-south surface pressure gradient in

the North Atlantic, whereas the NAM is more of a hemispheric measure of this pressure gradient. The PDO describes sea-surface temperature (SST) in the North Pacific (a positive PDO index indicates cool water), and the NPI is a measure of the Aleutian Low pressure system in the North Pacific (negative index values indicate anomalously low sea level pressure). The NAO, NAM and NPI indices were provided by the National Center for Atmospheric Research (NCAR, www.cgd.ucar.edu/cas/jhurrell/). The PDO was provided by the Joint Institute for the Study of the Atmosphere and Ocean (JISAO, jisao.washington.edu/pdo/).

Relationships between Eurasian SWI, sea-ice, and TI-NDVI and climate indices are shown in Table 2.2. None of the climate indices were significantly correlated with land temperatures (SWI). The NAO, and NAM indices were significantly negatively correlated with sea-ice concentration ($r = -0.44$ and -0.53, respectively). The PDO was negatively correlated with TI-NDVI ($r = -0.50$), and the NPI and NAO were significantly positively correlated with TI-NDVI ($r = 0.44$ and 0.39, respectively). The positive phase of the NAO and NAM is generally characterized by enhanced storminess in the Arctic, increased heat transport from lower latitudes, and warmer winter temperatures. The positive phase in the NAO/NAM is consistent with decreased sea-ice, increased SWI and enhanced greenness. The negative correlation between PDO and TI-NDVI is intriguing because the interactions between the Northern Eurasia land mass and the PDO are currently not well understood (Pavelsky and Smith 2004). The significant correlations with the NPI were opposite those for the PDO (which is consistent with the inverse correlation of the NPI and PDO). Essentially the PDO increases while SWI and NDVI decrease, whereas the NPI has the opposite correlations.

This analysis indicates that there is coherent variability of SWI, sea-ice concentrations and vegetation productivity in adjacent land–ocean regions of the coastal Eurasian Arctic, where decreased sea ice is found with increased summer warmth and increased tundra productivity. This relationship holds at the continental scale and also regionally in Eurasia. There are significant correlations of sea-ice concentration, SWI and integrated NDVI with the previous winter (December–March) climate indices. This is consistent with the growth of sea-ice area during winter months and relative melting during the following spring and summer (e.g. Deser et al. 2000). While this analysis is consistent with the hypothesis that sea-ice changes are forcing vegetation changes, it is not conclusive because correlations

Table 2.2 Correlations among SWI, sea-ice concentration, and integrated NDVI in 50-km zones within subregions of coastal Eurasia

Region	SWI	Sea-ice	TI-NDVI
NAO	0.36	−0.44*	0.31
NAM	0.17	−0.53*	0.39*
PDO	−0.15	0.38	−0.50*
NPI	0.24	−0.26	0.44*

An asterisk (∗) indicates significance at the 90% level or greater

only establish co-variability and not causality. Further work is necessary to understand these relationships.

2.3.2 *Variability of Tundra Productivity Within Bioclimatic Subzones: Focus on the Yamal Peninsula*

We focused a more detailed examination of Eurasian tundra vegetation dynamics on the Yamal Peninsula, a region of northwestern Siberia that includes a relatively uninterrupted latitudinal gradient. Our analysis of inter-annual trends in tundra vegetation using satellite data encompassed all five of the arctic bioclimate subzones (Walker et al. 2005). Three of the five subzones (C–E) exist on mainland Yamal, while the other two are on islands in the Kara Sea. We combined remote-sensing, time-series data with multi-scale analyses for identifying areas of relatively pure vegetation to investigate recent changes in vegetation greenness along the latitudinal temperature and vegetation gradient of the Yamal tundra.

We again used the NASA GIMMS time series at 8-km resolution and bimonthly temporal resolution, and also included a land-cover type product derived from Moderate-Resolution Imaging Spectroradiometer (MODIS) imagery (Friedl et al. 2002) for finer scale discrimination of vegetation cover. The temporal analysis was performed with the 1982–2005 time series, stratified by bioclimate subzone. We examined changes of vegetation greenness over the 24 year record, as indicated by variations of the annual maximum NDVI, spanning High Arctic (Subzones A–C) and Low Arctic (Subzones D and E) ecosystems. Subpixel fractional vegetation cover was used to select homogenously vegetated areas of tundra throughout the Yamal region. Autoregression analysis to account for temporal autocorrelation in the data set was performed on the NDVI time series of selected, relatively homogenous areas for each subzone. Image data quality north of 70° latitude for 2004–2005 was poor due at least in part to calibration issues with AVHRR data, so only areas south of 70°N were analyzed for those years.

Linear regressions in arctic tundra vegetation greenness over the analysis period were significantly positive ($\alpha < 0.05$) for each Yamal subzone, with 82.7% of the analyzed pixels showing positive trends throughout the period 1982–2003. The average rate of change in maximum NDVI was +0.44% year^{-1} for the entire arctic Yamal ($r^2 = 0.61$, $p < 0.001$). For south of 70°N from 1982 to 2005, the average rate of change was +0.34% year^{-1} (Fig. 2.5). Vegetation productivity was expected to increase from north to south along this bioclimatic gradient; therefore, NDVI was greater in areas below 70°N relative to the full regional extent.

Changes were heterogeneous among subzones. Annual peak values of NDVI increased by 0.41–0.56% year^{-1} over the High Arctic (Subzones A–C) where prostrate dwarf shrubs, forbs, mosses and lichens dominate, and by 0.28–0.37% year^{-1} over the Low Arctic (Subzones D and E) where erect shrubs and graminoids dominate (Fig. 2.6). There was similar inter-annual variation (i.e., years of high NDVI and years of low NDVI) among the five subzones, despite the differences in NDVI

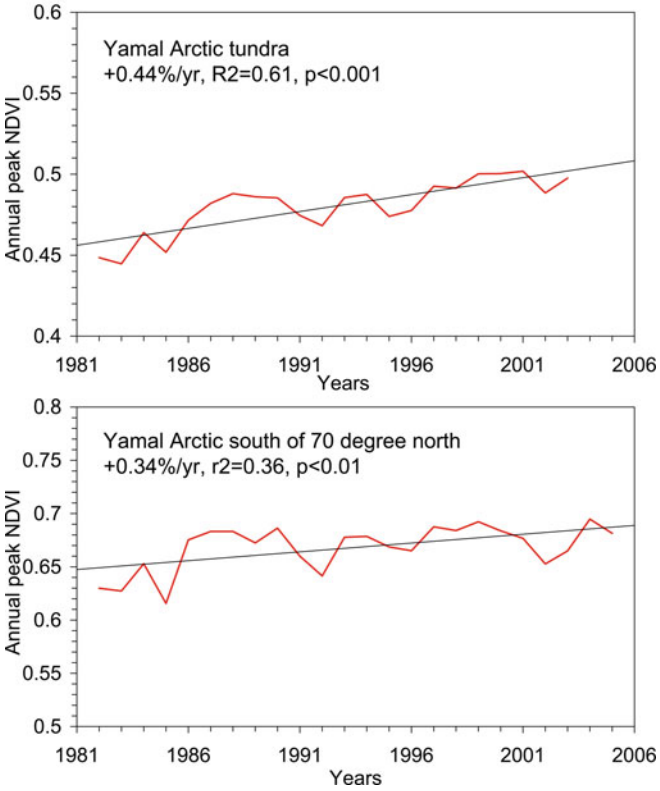

Fig. 2.5 (*top*) Changes in annual peak vegetation greenness (NDVI) over the entire Yamal region from 1982 to 2003 and (*bottom*) below 70°N from 1982 to 2005 as detected by NOAA AVHRR time series data. Annual peak NDVI represents the maximum NDVI values for each year. *Black lines* represent linear regressions. Data quality is low beyond 70°N for 2004–2005 due to calibration errors. The greening trends for the data set are +0.44% year^{-1} ($r^2 = 0.61$, $p < 0.001$) for the entire region from 1982 to 2003 and +0.34% year^{-1} ($r^2 = 0.36$, $p < 0.01$) south of 70°N from 1982 to 2005

magnitudes. Peak vegetation greenness was relatively low in the early 1980s and increased slowly over that decade. A sharp decline of greenness was observed in 1992, which is largely related to the Mt. Pinatubo eruption in late 1991. Following that decline, the trend of greening continued a gradual ascent.

The greatest rates of greening were observed for bioclimate Subzones A and B, in the northern High Arctic and polar desert (a classification specific to Subzone A). These subzones cover parts of Ostrov Belyy and Novaya Zemlya, islands located north and northwest of the Yamal Peninsula, respectively. Subzone A had the highest rate of increase of peak vegetation greenness (0.56% year^{-1}), closely followed by Subzone B (0.54% year^{-1}). Subzones A and B have very short growing seasons and low vegetation cover. Subzone A is characterized by the absence of any

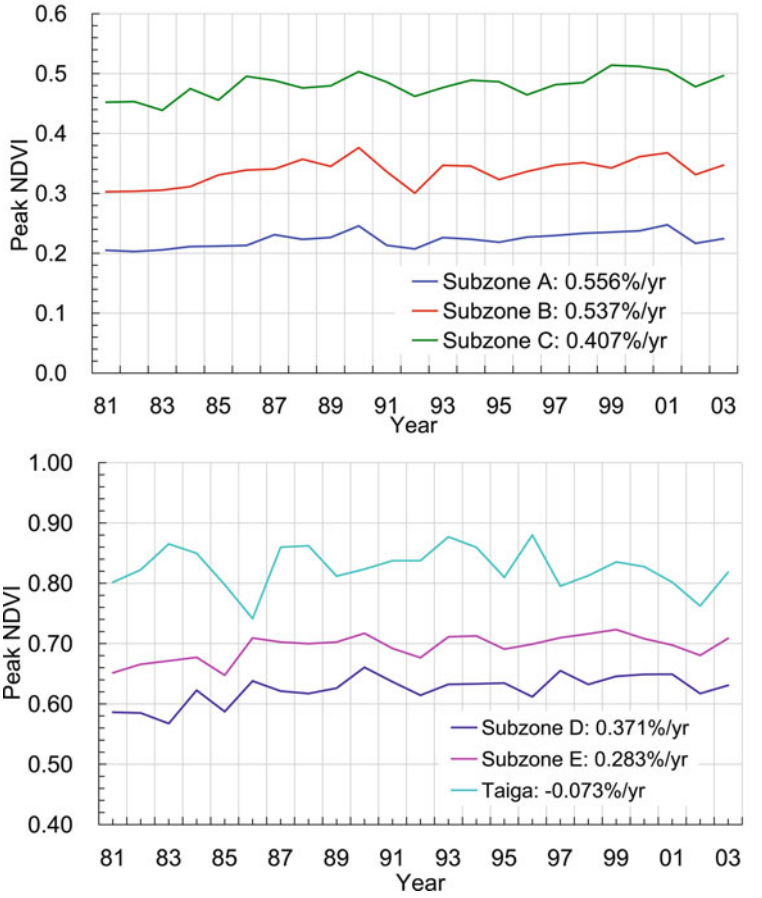

Fig. 2.6 Changes of annual peak vegetation greenness (NDVI) over each of the five arctic tundra bioclimate subzones of the Yamal, in addition to the northern taiga from 1982 to 2003 as detected by NOAA AVHRR time series data

woody plants, whereas Subzone B contains a few species of prostrate dwarf shrubs. Due to the short growing season and sparse vegetation, we were surprised to find a strong increase in peak greenness in this area. Factors that may have contributed to the greening are an increase in plant height and coverage due to warming, and possibly a more rapid earlier growth of tundra plants, as indicated by an earlier date of peak greenness (Jia et al. 2004). Mosses and lichens are persistent in these harsh environments and may respond to environmental changes more rapidly than vascular plants, enhancing their photosynthesis even during very short, favorable periods.

The lowest rate of peak greenness change was observed in Subzone E, dominated by dwarf-erect and low deciduous shrubs such as birch (e.g., *Betula nana*),

willow (*Salix spp.*) and alder (*Alnus crispa*), followed by Subzone D that is covered by sedges and erect dwarf shrubs. Located at the southern boundary of the arctic tundra biome, Subzone E has experienced an enhancement of shrub cover and the slow colonization of tree species, potentially triggered by increased surface temperatures and a deeper snow pack, which insulates the soil and increases nutrient mineralization (e.g., Shaver and Chapin 1991). Increases in fractional cover of shrubs and small trees would lead to higher NDVI values, as recently documented by Forbes et al. (2010). However, anthropogenic disturbances can be intense for mainland Yamal (Subzones C–E relative to Subzones A–B), as the arctic tundra of mainland Yamal has long been used by the Nenets people for reindeer herding. Over the past 2 decades both the Nenets population and reindeer numbers have increased substantially, putting greater pressure on the vegetation. Meanwhile, oil and natural gas exploration and extraction have increased in the region over the same time period, as new and larger fields were discovered in the 1980s and 1990s (see Forbes et al. 2009). Reindeer grazing can produce large areas of reduced vegetation, while construction of drilling platforms and service roads have created dense vehicle tracks and bare scars that are clearly detectable from higher resolution satellite data. The effects of these disturbances may have reduced the propensity for greater vegetation growth in Subzones D and E.

2.4 Boreal Forest Ecosystems

In addition to the changes documented in tundra vegetation, there have been several recent advances in understanding boreal tree responses to changing climate in the Arctic. The recent declines in productivity of many boreal forest areas, aside from recently disturbed areas, suggest that warming may not produce a negative feedback to additional warming (i.e., increased CO_2 sequestration), as had widely been expected. Moreover some positive feedbacks may result from advances of latitudinal tree-line, as has been widely documented in areas experiencing increased temperatures (e.g., Lloyd 2005), and these changes would also alter energy feedbacks associated with albedo changes. The responses of different tree species to warming vary substantially, however, as documented in the next section.

2.4.1 Tree Rings as an Integrative Measure of Growth

There are hundreds of publicly available tree growth data sets from tree rings for the northern high latitudes that are archived in the International Tree-Ring Data Bank, maintained by the National Oceanic and Atmospheric Administration's World Data Center for Paleoclimatology (http://www.ncdc.noaa.gov/paleo). A recent study by Lloyd and Bunn (2007) examined the associations between gridded climate data and tree growth for 232 sites across the northern high latitudes (see Fig. 2.1).

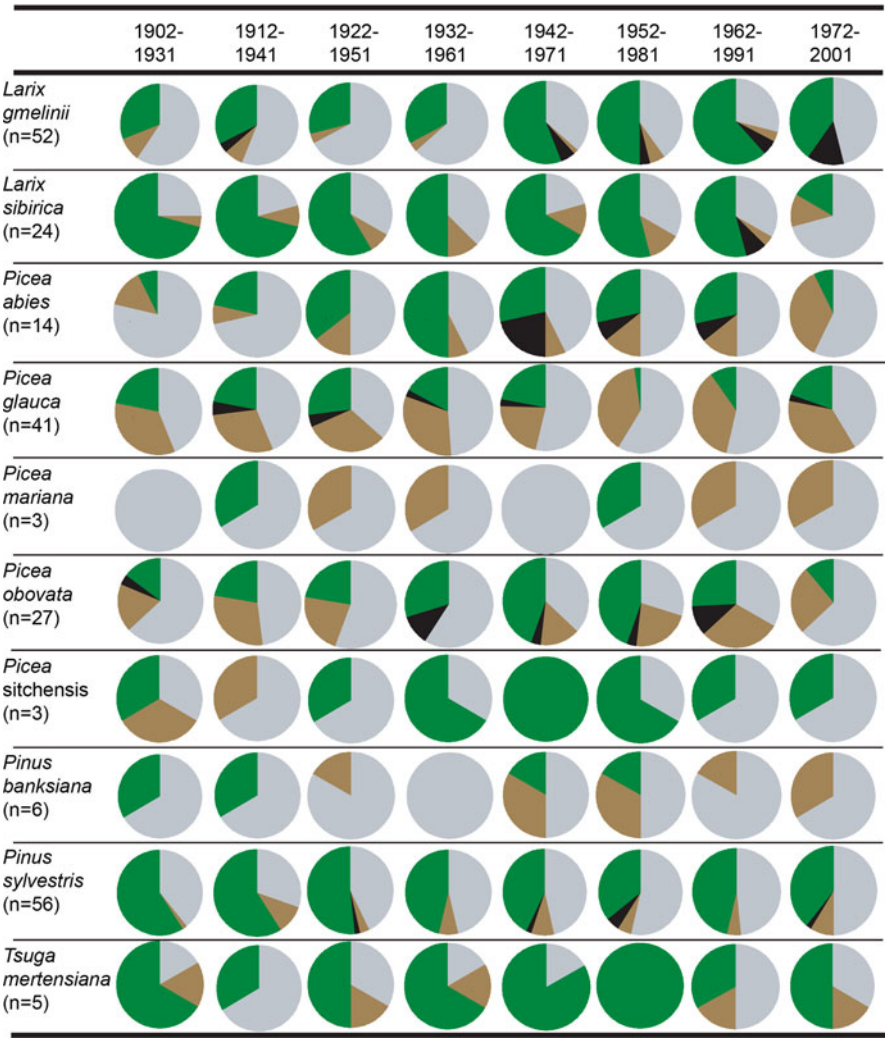

Fig. 2.7 Response to temperature of 10 boreal conifer species during eight 30-year time periods in the twentieth century. Each pie chart indicates the proportion of sites at which trees respond positively to warming (*green shading*), negatively to warming (*brown shading*), showed a mixed response to warming (positive correlations in some months, negative in others; *black shading*) or showed no response to warming (*grey shading*). Figure based on data from Lloyd and Bunn (2007)

Patterns of tree growth response to climate described in that study were idiosyncratic. Tree growth rates at many sites, particularly those occupied by the genus *Picea*, are declining in the presence of increasing temperatures (Fig. 2.7). This has been called the "divergence problem" and appears to be a widespread phenomenon in high latitude tree gowth (D'Arrigo et al. 2008). The explanation for declining

tree growth under conditions of longer and warmer growing seasons in the subarctic remains unknown, although a number of causes, including drought stress, pollution, global dimming (declining incident solar radiation), and direct temperature stress have been proposed. Although there is likely no single explanation for the phenomenon, the impact of drought on productivity (discussed earlier) is consistent with recent observations of reduced productivity in more densely forested areas. Focusing on the different responses of different species to warming may provide unique indications of change at specific locations or ecological regions. However, while tree ring data sets provide an integrative measure of growth for specific locations, they lack the complete spatial coverage afforded by productivity metrics like those derived from satellite observations. Combining these disparate data sets, therefore, would provide a useful approach to monitoring high latitude tree response to climate over large areas.

2.4.2 Correlation Between Satellite Vegetation Indices and Tree Rings

There is substantial co-variation between the tree-ring and satellite NDVI records, although defining the associations again seems to be species specific. An initial analysis shows that both spruce (*Picea* spp.) in Alaska and larch (*Larix* spp.) in Siberia are significantly positively correlated with July NDVI. Spruce growth correlated best with NDVI at a lag of 1 year, while larch, although not as strongly correlated with NDVI, had the highest correlation between current year growth and NDVI. This difference is very likely associated with the annual lifespan of needle production in larch compared with the long needle retention in spruce.

These initial correlations between tree growth from tree rings and NDVI suggest that it will be possible to merge the long records of growth from tree rings to the spatially contiguous records from satellites. There are, however, substantial challenges in determining causal links between canopy reflectance and cambial growth. The first is that the tree ring record, while extensive, is not systematically updated. In particular, the tree ring records from Russia mostly end in the mid 1990s and therefore have a smaller window that overlaps the satellite record. There are efforts underway to update these records, but the logistics for this are daunting. Given the species-specific responses seen in tree growth and climate (Fig. 2.7), it is critical that records be updated and well replicated.

Another issue affecting our ability to relate tree rings with NDVI data is that trees selected for dendroclimatic studies tend to be collected at the ecotone between forest and tundra or in sparse taiga. This causes problems when associating the relatively coarse NDVI data (8-km for the GIMMS data used here) to the individual tree ring sites. This scale mismatch is particularly problematic at latitudinal tree-line, in which much of the area within a satellite observation will primarily represent productivity of tundra rather than forest vegetation. One possible solution is to use the MODIS proportional tree cover (continuous fields) products to

weight the NDVI data proportionally by the amount of tree cover in a sampling window. This approach is being investigated by the co-authors (Beck, Bunn, Lloyd, and Goetz).

2.5 Simulation Model Projections of Arctic Vegetation Change

The observations described above demonstrate clear, albeit sometimes complex, associations between vegetation and climate variables. They also show changes in vegetation productivity that occurred across a broad geographic and ecological range of conditions in the past 20–25 years. In order to forecast how these changes will be expressed in the next few decades, however, ecosystem models are needed. In the following sections, we provide an overview of three different models that describe projected changes for different regions of the Arctic, and how these changes will vary between tundra and forest ecosystems. We first present a biome-scale model simulating broad changes across Northern Eurasia, and then describe and apply two models focused more specifically on smaller spatial domains and on the vegetation found in tundra versus the forest-tundra ecotones.

2.5.1 Changes in Distribution of Vegetation Types (BIOME4)

The BIOME4 global vegetation model has been designed to simulate patterns of land cover and the growth and decay of vegetation at relatively coarse resolution over large regions (e.g., Kaplan et al. 2002, 2003). The model is driven by basic climate and soils data and combines simplified representations of the biophysical and biochemical processes in ecosystems such as sunlight absorption by vegetation, photosynthesis, water uptake, and respiration, with ecological dynamics including establishment, succession, resource competition and migration. In order to simulate the great variety of vegetation types found globally, BIOME4 uses the concept of the Plant Functional Type (PFT). Each PFT represents a broad class of vegetation, including, e.g., temperate broadleaf deciduous trees, boreal evergreen needleleaf trees, or tropical herbaceous plants. Each PFT is defined by very broad ecoclimatic limits, and where PFT ranges overlap, they compete with each other in the model for light, water and nutrients. Vegetation models such as BIOME4 have been widely employed over the past years to explore the relationship between vegetation and climate and to make scenario calculations of the effects of future climate change on global and continental-scale land cover.

Starting with a data set of present-day observed climate (New et al. 2002) and soils (FAO 1995; Reynolds et al. 1999), we used the BIOME4 model to simulate potential natural vegetation distribution over Northern Eurasia at 10-km resolution (Fig. 2.8). Cool-temperate and cold boreal forests dominate the vegetation of eastern and Northern Eurasia, covering more than 15.6×10^6 km^2. The balance of the land cover of Northern Eurasia is occupied by a xerophytic shrublands and grasslands

at the southern boundary of boreal forest, and a sequence of tundra biomes, from high and low-shrub tundra at the polar treeline to cushion-forbs lichen and moss in the most extreme polar climate zones in the north. Biomes in Northern Eurasia are largely intact with little large-scale human impact except in the southern and westernmost boundaries of the region (see Chapter 3, this volume). Because the majority of Northern Eurasia is still occupied by potential natural vegetation, it may be particularly sensitive to future climate change and an important region for biophysical and biogeochemical feedbacks between the Earth surface and the atmosphere.

Using four future greenhouse gas emissions scenarios to run six Global Climate Models (GCMs), Kaplan and New (2006) prepared a series of future climate scenarios of the Earth under a 2°C global warming. The GCM simulations indicate that the Earth will have warmed by 2°C relative to preindustrial temperatures by 2026–2060, at which stage the area-mean annual temperature over the circumpolar Arctic (60–90°N) will have increased by 3.2–6.6°C. From the baseline land cover

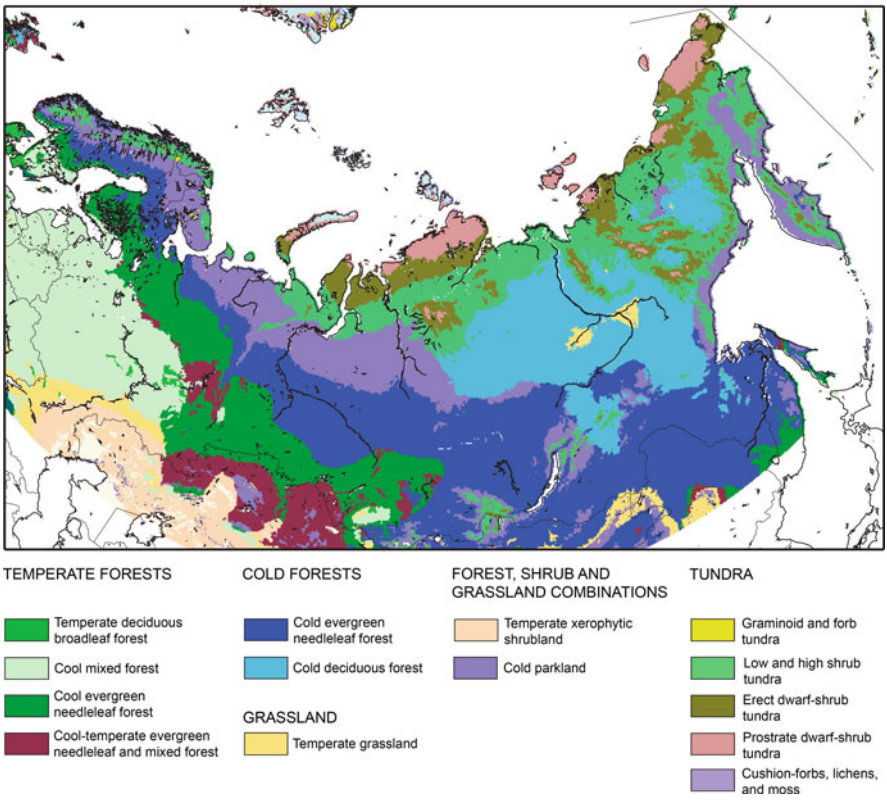

Fig. 2.8 Potential natural vegetation of the Northern Eurasia region at present-day predicted by the BIOME4 equilibrium global vegetation model (Kaplan et al. 2003), forced by late twentieth century mean CO_2 concentrations, climatology (New et al. 2002) and soils data (FAO 1995; Reynolds et al. 1999)

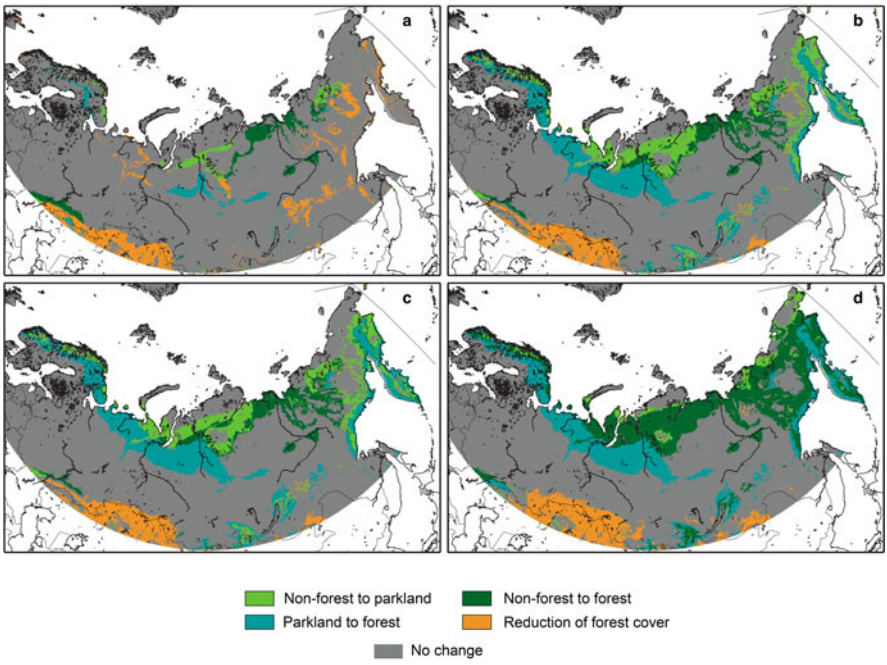

Fig. 2.9 Changes in vegetation cover relative to the potential natural state across the Northern Eurasia region predicted by BIOME4 in four scenarios of a future 2°C global warming: (**a**) 10th percentile "cool", (**b**) robust mean, (**c**) mean, and (**d**) 90th percentile "warm". For details of these climate change scenarios see Kaplan and New (2006)

illustrated in Fig. 2.8 and using these future climate scenarios, we simulated changes in the land cover of Northern Eurasia under a global 2°C warming. These future scenarios, illustrated in Fig. 2.9, indicate that forest extent could increase in Northern Eurasia on the order of 5×10^6 km^2 $\pm$ 1.8×10^6 (32%) with a corresponding 42% reduction in the tundra area. Tundra types generally shift north in the model simulations with the largest reductions in the extreme-cold tolerant dwarf-shrub tundra type, where nearly 60% of habitat is lost. Modeled shifts in the potential northern limit of trees reach up to 400 km from the present tree line, which may be limited by migration rates. Simulated physiological effects of the CO_2 increase (to ca. 475 ppm) at high latitudes were small compared with the effects of the change in climate. The increase in forest area of the Arctic could sequester 6 Pg of additional carbon, though this effect would be unlikely to be realized over next century (see Chapters 5 and 6, this volume).

The biophysical implications of these vegetation changes include increased absorption of solar radiation (decreasing albedo), which would have important feedbacks to the atmosphere, and changes in hydrological regimes because of increased snow retention (see Chapter 7, this volume). The increase in forest area in the Arctic would eventually be responsible for a large increase in carbon storage as tundra

soils are replaced by organic-rich forest soils, though this could be offset by the thawing and oxidation of organic loess (Yedoma) and peat that are currently locked in permafrost (Turetsky et al. 2007). The changes in Arctic vegetation simulated here would almost certainly have ramifications for biodiversity, effects on animal populations and human activities (Chapters 8 and 9, this volume).

2.5.2 Tundra Vegetation Dynamics (ArcVeg)

To simulate the dynamics of Northern Eurasian tundra, we used ArcVeg, a nutrient-based tundra vegetation model that projects the transient dynamics of arctic tundra plant communities (Epstein et al. 2000, 2001, 2007). ArcVeg uses a set of twelve tundra plant types including mosses, lichens, forbs, and several categories of graminoids and shrubs, and has been parameterized for the five arctic subzones described by Walker et al. (2005). Since plant-available nitrogen (N) can be strongly limiting for tundra plants (Chapin et al. 1995; Shaver and Chapin 1991), the model functions essentially by maintaining nitrogen mass balance, moving nitrogen among soil organic matter, plant-available nitrogen, and plant nitrogen pools. Plant parameters in the model include their nitrogen uptake efficiencies, biomass:N ratios, annual proportions of plant material senescing, probabilities of seedling establishment, and cold tolerances for growth. The model runs on an annual time step, however, the growing season is split into five distinct plant growth periods to capture the seasonality of vegetation growth across the full arctic climate gradient (i.e., Subzones A–E). The spatial resolution of the ArcVeg model is a 1 × 1 m grid cell, with the model simulating 100 stochastically different replicates of these grid cells (essentially a 10 × 10 m grid). The model has been validated using total and species-level biomass from field measurements throughout northern Alaska and Canada (Epstein et al. 2000, 2007). Model results and field data are relatively consistent both on the plant functional type level and for total biomass, indicating that the model is reasonable for making projections.

We simulated a 2°C warming in mean growing season temperatures, linearly ramped over a 50-year period for all five arctic subzones, which differ in their quantities of soil organic nitrogen, their rates of nitrogen mineralization, and their temperatures and growing season lengths. Model simulations were performed for 500 years in order for an equilibrium vegetation to develop, and then the model was run for an additional 500 years with the present climate. In Year 1000 a warming treatment was imposed, and the model was run for an additional 500 years (1,500 years total).

We again used the Yamal Peninsula in northwestern Siberia as the study region of interest. Due to a present lack of active layer Soil Organic Nitrogen (SON) field data from the Yamal region, we used Yamal soils data from an International Geosphere-Biosphere Programme (IGBP) global soil survey and projected active layer soil organic nitrogen using existing SON depth profiles from Alaska soils. We also assumed that for the Yamal region, reindeer would graze the tundra vegetation more frequently and intensely than the unmanaged caribou in North America.

These differences were reflected in our parameterization of the model. For the Yamal region, we assumed that Subzones C–E (southern High Arctic, and Low Arctic) are grazed more intensely than Subzones A and B (polar desert and northern High Arctic), which are off the mainland peninsula. For Subzones A and B we assumed that the system would be grazed every 10 years and that 25% of plant biomass was removed by grazing; for Subzones C, D and E, 50% of plant biomass was removed every 2 years.

In general, tundra in the Yamal region for all subzones responds to climate warming with increasing total biomass, especially for woody plants, and changes in plant community composition. For Subzones C, D and E in the Yamal region, there is less biomass compared to the same subzone in North America, due to heavy grazing by reindeer herds. Due to intense reindeer grazing and a preference for deciduous shrubs and lichens, Subzones D and E on the Yamal are dominated by evergreen shrubs and mosses.

For the Low Arctic tundra in Subzone E (Fig. 2.10a), warming led to an initial increase in dwarf-erect shrubs, and slight decreases in moss biomass due to competition with shrubs. Overall, the total biomass of Subzone E increased approximately 50% (400 g m^{-2}) dominated by the increase of evergreen shrubs (Fig. 2.10b). For Subzone D, warming increased the biomass of moss and evergreen shrubs (Fig. 2.10c). The total biomass of Subzone D also increased by approximately 50% (400 g m^{-2}, Fig. 2.10d).

For Subzone C, which is the southernmost subzone of the High Arctic, warming led to initial increases in mosses and an increase in evergreen shrubs. Total biomass of the Subzone C plant community increased by approximately 33%, (200 g m^{-2}) with warming over a period of about 50 years (Fig. 2.10f). For Subzone B, moss biomass increased substantially with warming, as did the biomass of shrubs (Fig. 2.10 g). Lichen biomass initially increased, but then dropped close to prior levels in Subzone B. Total biomass in Subzone B increased approximately 120% (600 g m^{-2}) in less than 100 years (Fig. 2.10 h). For Subzone A, the polar desert, moss and lichen biomass increased rapidly at first (Fig. 2.10i), however this was followed by increases in shrubs over a 150-year period. This increase in shrub biomass led to declines in both moss and lichen biomass, close to their original levels. Total biomass increased approximately 100% (200 g m^{-2}, Fig. 2.10j).

2.5.3 Tree-Line Dynamics (TreeMig)

Vegetation dynamics are influenced by both changing environmental conditions and anthropogenic land use. On a time scale of decades to centuries the increasing temperatures at northern high latitudes make it probable that vegetation will shift northward. Temperate species will be able to establish in regions currently too cold support them and, in the process, displace boreal species which, in turn, will migrate into tundra areas. Indications of early shifts of the arctic shrub- and tree-lines have already been observed across the arctic region, although not homogenously (Sturm

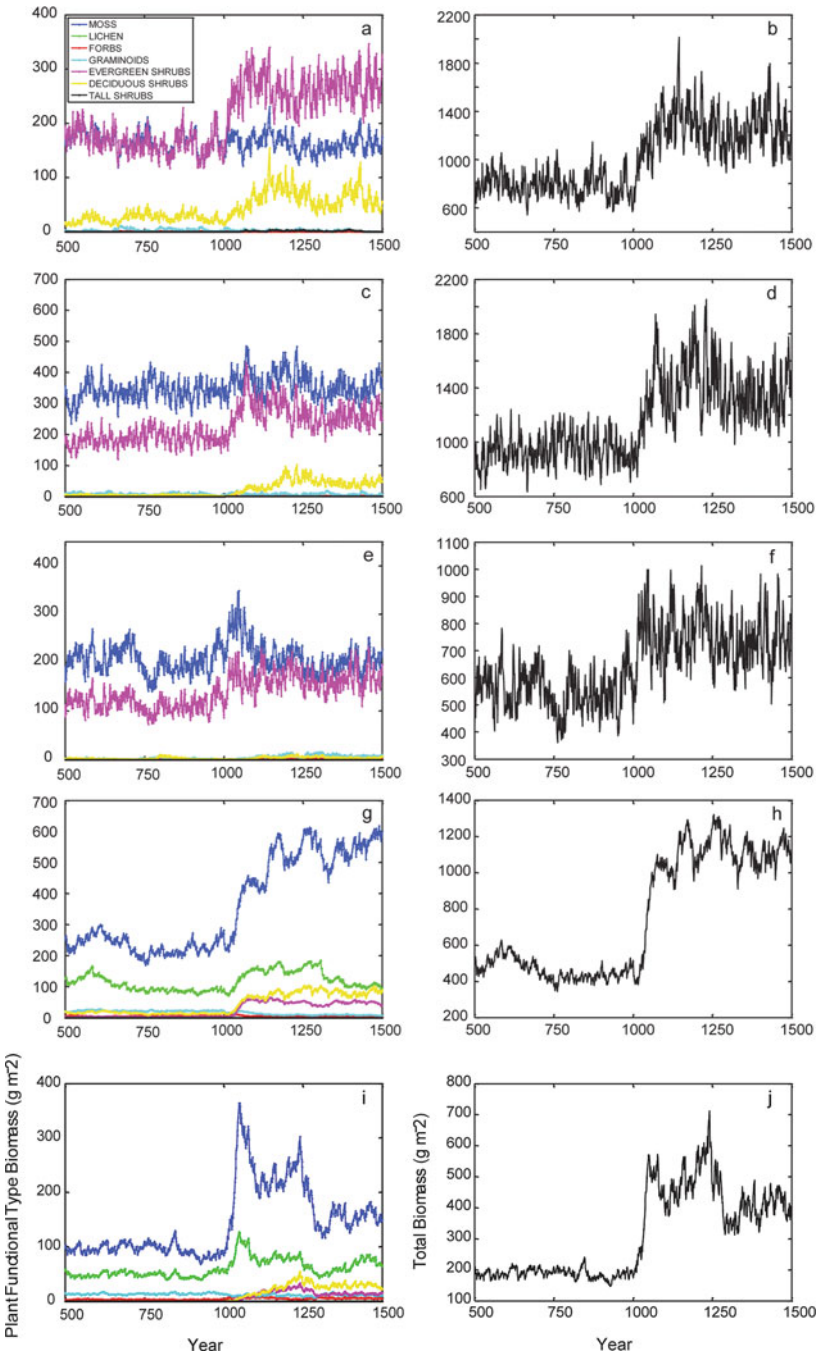

Fig. 2.10 Dynamics of above-ground biomass for seven plant functional types, and total biomass, as simulated by the ArcVeg model for arctic bioclimatic Subzones E **(a, b)**, D **(c, d)**, C **(e, f)**, B **(g, h)**, and A **(i, j)**. The model was run for each Subzone for 1,000 years with present climate, and then mean growing season temperatures were increased by 2°C, ramped linearly over a 50-year period

et al. 2001; Tape et al. 2006; Van Bogaert et al. 2007). The rate of this northward shift is bounded by the rate of climate change, i.e. the rate with which the species' fundamental niches will shift geographically. The ability of the species to migrate also limits the speed of these shifts.

Migration can be rather slow, because it involves a suite of dynamic population processes including seed production, seed dispersal, establishment, and maturation to seed production, i.e. to the next generation. In trees, maturation usually takes decades and can be prolonged by competition and adverse environmental conditions near niche limits. Thus, it is not realistic to assume an instantaneous presence of species at a location once the conditions become favorable, and assessing species' migration speed and associated shifts of their fundamental niches is not trivial.

The effects of climate change on biogeochemical cycling and species or plant functional type distributions have been examined with various coarse-scale biogeochemical models or dynamic global vegetation models. To get an impression of the order of magnitude of the lag due to migration processes, we studied the potential migration of boreal species into the tundra with a spatio-temporal dynamic forest model on an idealized transect through the boreal and tundra zone of Western Siberia. We focus on the temperature-driven population dynamics and spread of tree species, assuming other environmental factors were invariant.

We used the lattice-based, spatio-temporal dynamic tree species model TreeMig (Lischke et al. 2006). The model calculates local tree species population dynamics in each 1-km^2 grid cell, including seed bank dynamics, germination, growth, competition, mortality and seed production. The process functions depend on light and on climate variables (annual temperature sum, winter temperature, and drought). The species-specific parameters for the local dynamics had been determined previously in a study in the Ural region (unpublished). Within-cell heterogeneity is depicted by frequency distributions of tree density and consequently light intensity. Larger scale heterogeneity, e.g. a migration front within a cell, is not taken into account. Interactions between the cells occurs by seed dispersal, described by a dispersal kernel consisting of two negative exponentials, accounting for frequent short- and rare long-distance dispersal events. The mean dispersal distances (α) for species-specific wind-dispersed seeds have been estimated from sinking velocities and wind speed distributions (Lischke and Löffler 2006).

The simulation was run on a transect of 2,000 km length and 1 km width, ranging from latitude 61°N to 80°N. Climate data (monthly temperatures and monthly precipitation for 30 years) were interpolated between the latitudes from station data between longitude 74°E and 80°E along the eastern part of the Western Siberian lowlands. By adding a climate change scenario to the climate data, new means and standard deviations of yearly temperature sum, winter temperatures, and drought stress were calculated. The climate change scenario consisted of a spin-up phase of 600 years of current climate, followed by 100 years of linear temperature increase (2000–2100), according to the regional values of the A1B model mean from the Intergovernmental Panel on Climate Change (IPCC) 4th Assessment (Table 2.3, Christensen et al. 2007).

Table 2.3 Assumed temperature increases at year 2100, according to IPCC A1B scenario

Months	Temperature increase
December, January, February	7°C
March, April, May	4.4°C
June, July, August	3.5°C
September, October, November	5.7°C

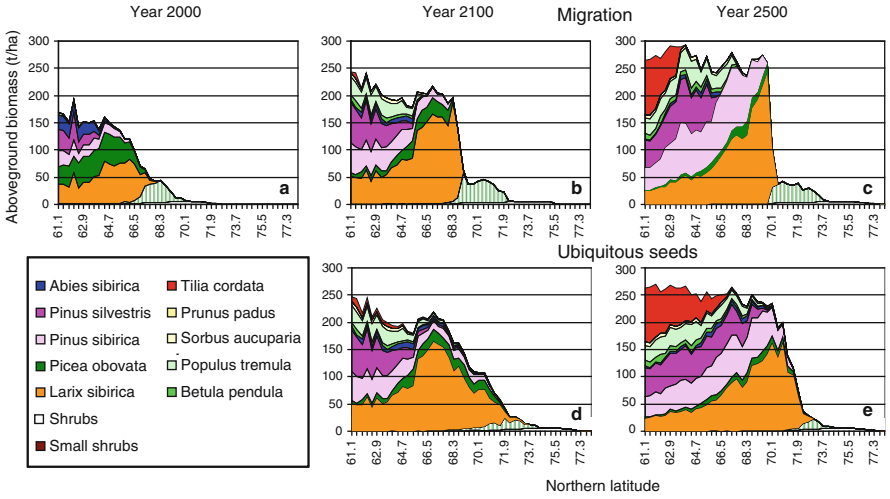

Fig. 2.11 Simulated above-ground biomass (tons per hectare) by species (y axis), with migration and seed dispersal. The x-axis is north latitude in decimal degrees

The model simulations were run in two modes: (i) seeds of all species were ubiquitously present, thus starting succession if the climatic conditions were appropriate, (ii) seeds reached a given cell only by dispersal, thus simulating migration.

In a first simulation under current conditions, we fine-tuned the species parameters for temperature dependence of growth and mortality such that the simulated tree line corresponds essentially to the position of the current observed tree line (Fig. 2.11a). Small shrubs and tundra vegetation as well as larger shrubs stretch from the tree line at about 67°N up to 72°N. Tree line is formed by larch and spruce, while other coniferous species are found more to the south. Under climate change, total above-ground biomass consistently increased (Fig. 2.11b–e), although larch and pine gained greater biomass at the expense of spruce. Broadleaf species appear in the southern part of the transect. If seeds are present, the shrubs and tree-line species reach their new range almost completely by 2100 (Fig. 2.11d), whereas within taiga, succession was finished by about 2300. With migration included (Fig. 2.11b, c), all shifts were delayed. At year 2100 none of the species has reached the same range as with seeds present, and even at year 2500, the tree species lag behind; only the shrub-line advanced to its new extent.

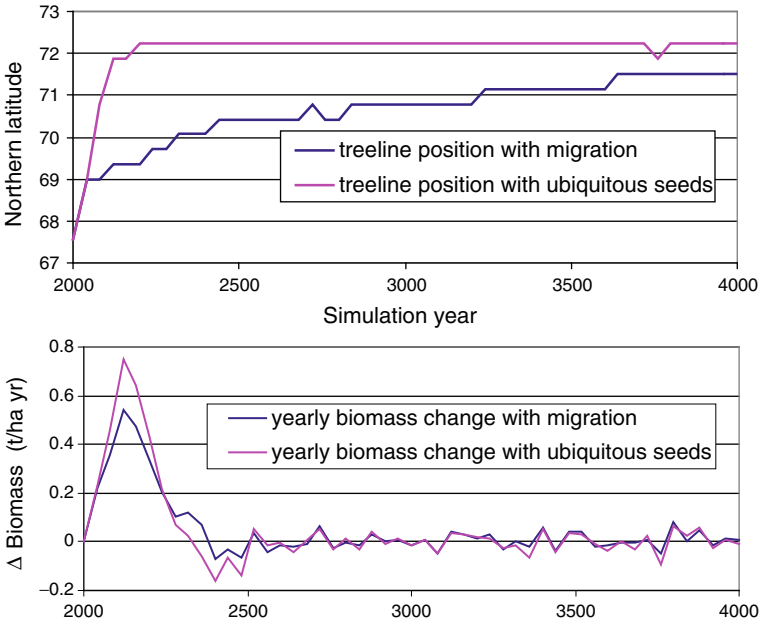

Fig. 2.12 (**a**) Simulated yearly tree-line position change (degrees north latitude) with migration and ubiquitous seeds. (**b**) Simulated yearly biomass change (tons per hectare per year) with migration and ubiquitous seeds

The comparison of tree-line position (defined as a 50 t/ha threshold) over the long term with and without ubiquitous seeds demonstrates the migrational lag of the latter case (Fig. 2.12). Even at year 4000 the tree-line of the migrating species has not yet reached the climatic distribution boundary. The rate of the tree-line shift decreased from an initial 2,000 to 150 m year^{-1} at the end of the simulation period, which corresponds well with migration speeds reconstructed from Holocene pollen data (Clark 1998). The average yearly biomass change on the transect shows the same characteristics for both modes: a strong biomass build-up from year 2000 to 2300, followed by a smaller biomass loss for about 200 years. With migration this pattern is less pronounced and delayed by about 50 years.

These simulations indicate that migration without ubiquitous seeds produces biome boundary changes much more slowly, resulting in lagged feedbacks to the climate system. For example, the treeless area is much larger for a longer period with migration than with ubiquitous seeds, potentially keeping albedo from declining. Biomass increase and associated carbon sequestration is also slower with migration included. The importance of simulating migration is supported by another similar study with two climate change scenarios and slightly different species parameters (Epstein et al. 2007). The current study agrees well in the duration of the lag and the rate of migration. The primary differences are in the representation of the shrub tundra and the nearly complete suppression of spruce after climate change.

The representation and simulations of vegetation dispersal and migration under climate change presented here are, however, limited. Many aspects of ecosystem dynamics have not been taken into account, including plant ecophysiology, soil dynamics, permafrost and its thawing, fires and their species-specific associations pest outbreaks, landscape heterogeneity, and the influences of human land use. Moreover, the model has uncertainties in the parameters relevant to dispersal and migration, e.g., wind-dispersed seeds can be uplifted to higher atmospheric layers and probably travel much farther than via near-surface winds (Nathan et al. 2002). Even more uncertain are the frequencies and distances of seed transport by animals. A thorough characterization of the spatio-temporal behavior of the model and adaptation of the parameters is required. Long-term spatial data on vegetation change are also needed. The best data source for testing simulations of long-term vegetation change is pollen assemblages. Model comparisons to pollen data are reliable only for long time periods and over broad areas. Finally, large-scale assessments of the influence of vegetation dynamics, and eventual coupling to climate models, implies computational challenges in better representing dispersal and migration speeds (Epstein et al. 2007).

2.6 Conclusions

Satellite imagery, and information derived from those observations, has become absolutely essential to monitoring remote areas across the Arctic, particularly given the extensive geographic scope and relatively few field measurements in this vast domain. The current satellite data record, particularly that from the AVHRR, is now of sufficient duration (30 years) to conduct meaningful analyses of interannual variability and trends in vegetation productivity. Further refinements in the observational data sets are needed, as are efforts to inter-calibrate sensor measurements with newer satellite platforms to ensure continuity of Earth observation data records. Nonetheless, the analyses summarized here demonstrate the utility of the satellite data for monitoring changes and trends through time, including the associations among vegetation productivity, surface temperature, and sea ice concentrations under different climate conditions.

Similarly, satellite studies of boreal forests above 60°N can be used for extending the growing tree ring database, despite the mixture of different cover types (tree versus tundra vegetation) within the satellite observations and the different responses of individual tree species to warmer temperatures. There are complementary approaches to analyzing these disparate data sets, and there is great potential for effectively extending the relatively short record from the satellites to the longer-term records of tree ring growth. Developing robust statistical models between the satellite and tree ring records also has the potential to refine process models of change in the northern high latitudes, including better estimates of the linked changes in radiation, meteorology, productivity and associated carbon exchange.

Finally, models of vegetation distribution, tree migration, and tundra vegetation responses to climate warming are currently able to capture logical transitions

and productivity changes consistent with expectations under a warming climate, but substantial refinements to the models are needed, particularly to capture dispersal mechanisms, migration rates, and changes in biogeochemical cycling (see Chapter 6, this volume). Continued collection and associated improvements to observations are also needed, not only to inform the models but also to calibrate and validate the outcomes of model simulations under the wide range of conditions that are predicted to occur across the arctic region in the next few decades. It is primarily through the combined use of field and satellite measurements that we will be able to capture the various feedbacks between terrestrial ecosystems and the physical climate system, and better predict how those changes will be expressed so that arctic communities and resource managers can plan and adapt to the inevitable changes that will follow.

References

Achard F, Eva HD, Mollicone D, Beuchle R (2008) The effect of climate anomalies and human ignition factor on wildfires in Russian boreal forests. Philos Trans R Soc Lond B. doi:10.1098/rstb.2007.2203

ACIA (2004) Impacts of a warming Arctic. In: Hassol SJ (ed) Arctic climate impact assessment overview report. Cambridge University Press, Cambridge, p 144

Angert A, Biraud S, Bonfils C, Henning CC, Buermann W, Pinzon J, Tucker CJ, Fung I (2005) Drier summers cancel out the CO2 uptake enhancement induced by warmer springs. Proc Natl Acad Sci USA. doi:10.1073/pnas.0501647102

Bala G, Caldeira K, Wickett M, Phillips TJ, Lobell DB, Delire C, Mirin A (2007) Combined climate and carbon-cycle effects of large-scale deforestation. Proc Natl Acad Sci USA. doi:10.1073/pnas.0608998104

Bhatt U, Walker D, Raynolds M, Comiso J (2008) Examining relationships between sea ice and Arctic vegetation on the Pan-Arctic regional and site scales. Eur Res Abst 10:EGU2008-A-11271

Bunn AG, Goetz SJ (2006) Trends in satellite observed circumpolar photosynthetic activity from 1982–2003: the influence of seasonality, cover type and vegetation density. Earth Interact 10:1–19

Bunn AG, Goetz SJ, Kimball JS, Zhang K (2007) Northern high latitude ecosystems respond to recent climate change. EOS 88:333–335

Chapin FS III, Bret-Harte MS, Hobbie SE, Zhong, H (1996) Plant functional types as predictors of transient responses of Arctic vegetation to global change. J Veg Sci 7:347–358

Chapin FS III, Callaghan TV, Bergeron Y, Fukuda M, Johnstone JF, Juday G, Zimov SA (2004) Global change and the boreal forest: thresholds, shifting States or gradual change? Ambio 33:361–365

Chapin FS III, Shaver GR, Giblin AE, Nadelhoffer KJ, Laundre JA (1995) Responses of Arctic Tundra to experimental and observed changes in climate. Ecology 76(3):694–711. doi:10.2307/1939337

Chapin FS III, Sturm M, Serreze MC, McFadden JP, Key JR, Lloyd AH, McGuire AD, Rupp TS, Lynch AH, Schimel JP, Beringer J, Chapman WL, Epstein HE, Euskirchen ES, Hinzman LD, Jia G, Ping CL, Tape KD, Thompson CDC, Walker DA, Welker JM (2005) Role of land-surface changes in Arctic summer warming. Science 310:657–660

Christensen JH, Hewitson B, Busuioc A, Chen A, Gao X, Held I, Jones R, Kolli RK, Kwon WT, Laprise R, Magaña Rueda V, Mearns L, Menéndez CG, Räisänen J, Rinke A, Sarr A, Whetton P (2007) Regional climate projections. In: Solomon S, Qin D, Manning M, Chen Z, Marquis M, Averyt KB, Tignor M, Miller HL (eds) Climate change 2007: the physical science

basis. Contribution of working group I to the 4th assessment report of the intergovernmental panel on climate change. Cambridge University Press, Cambridge
Clark J (1998) Why trees migrate so fast: confronting theory with dispersal biology and the paleorecord. Am Nat 152:204–224
Comiso JC (2002) A rapidly declining perennial sea ice cover in the Arctic. Geophys Res Lett 29(20):1956. doi:10.1029/2002GL015650
Comiso JC (2003) Warming trends in the Arctic from clear-sky satellite observations. J Clim 16:3498–3510
Comiso JC (2006) Arctic warming signals from satellite observations. Weather 61:70–76
Comiso JC, Nishio F (2008) Trends in the sea ice cover using enhanced and compatible AMSR-E,SSM/I, and SMMR data. J Geophys Res 113(C02S07). doi:10.1029/2007JC004257
D'Arrigo R, Wilson R, Lipert B, Cherubini P (2008) On the 'divergence problem' in northern forests: a review of the tree-ring evidence and possible causes. Glob Planet Change. doi:10.1016/j.physletb.2003.10.071
Deser C, Walsh JE, Timlin M (2000) Arctic sea ice variability in the context of recent atmospheric circulation trends. J Clim 13:617–633
Epstein HE, Calef MP, Walker MD, Chapin FS III, Starfield AM (2004) Detecting changes in arctic tundra plant communities in response to warming over decadal time scales. Glob Change Biol 10:1325–1334
Epstein HE, Chapin FS III, Walker MD, Starfield AM (2001) Analyzing the functional type concept in arctic plants using a dynamic vegetation model. Oikos 95:239–252
Epstein HE, Kaplan JO, Lischke H, Yu Q (2007) Simulating future changes in arctic tundra and sub-arctic vegetation. Comput Sci Eng 9:12–23
Epstein, HE, Walker MD, Chapin FS III, Starfield AM (2000) A transient, nutrient-based model of arctic plant community response to climatic warming. Ecol Appl 10:824–841
Field CB, Lobell DB, Peters HA, Chiariello NR (2007) Feedbacks of terrestrial ecosystems to climate change. Ann Rev Environ Resour 32:1–29
Food and Agriculture Organization (FAO) (1995) Digital soil map of the world and derived soil properties. Food and Agric Org, Rome
Forbes BC, Marc Macias F, Pentti Z (2010) Russian arctic warming and 'greening' are closely tracked by tundra shrub willows. Glob Change Biol 16(5):1542–1554
Forbes BC, Stammler F, Kumpula T, Meschtyb N, Pajunen A, Kaarlejrvi E (2009) High resilience in the Yamal-Nenets social, ecological system, West Siberian Arctic, Russia. Proc Natl Acad Sci 106(52):22041–22048
Friedl MA, McIver DK, Hodges JC, Zhang XY, Muchoney D, Strahler AH, Woodcock CE, Gopal S, Schneider A, Cooper A, Baccini A, Gao F, Schaaf C (2002) Global land cover mapping from MODIS: algorithms and early results. Remote Sens Environ 83:287–302
Goetz SJ, Bunn AG, Fiske GJ (2005) Satellite observed photosynthetic trends across boreal North America associated with climate and fire disturbance. Proc Natl Acad Sci USA. doi:10.1073/pnas.0506179102
Goetz SJ, Fiske G, Bunn A (2006) Using satellite time series data sets to analyze fire disturbance and recovery in the Canadian boreal forest. Rem Sens Environ 101:352–365
Goetz SJ, Mack MC, Gurney KR, Randerson JT, Houghton RA (2007) Ecosystem responses to recent climate change and fire disturbance at northern high latitudes: observations and model results contrasting Northern Eurasia and North America. Environ Res Lett 2(4). doi:10.1088/1748-9326/2/4/045031
Goetz SJ, Prince SD (1999) Modeling terrestrial carbon exchange and storage: evidence and implications of functional convergence in light use efficiency. Adv Ecol Res 28:57–92
Goulden ML, Wofsy SC, Harden JW, Trumbore SE, Crill PM, Gower ST, Fries T, Daube BC, Fan SM, Sutton DJ, Bazzaz A, Munger JW (1998) Sensitivity of boreal forest carbon balance to soil thaw. Science 279:214–216
Harrison SP, Prentice IC (2003) Climate and CO_2 controls on global vegetation distribution at the last glacial maximum: analysis based on paleovegetation data, biome modelling and palaeoclimate simulations. Glob Chang Biol 9:983–1004

Jia GJ, Epstein HE, Walker DA (2003) Greening of the Alaskan Arctic over the past two decades. Geophys Res Lett. doi:10.1029/2003GL018268

Jia GJ, Epstein HE, Walker DA (2004) Controls over intra-seasonal dynamics of AVHRR NDVI for the Arctic tundra in northern Alaska. Int J Rem Sens 25:1547–1564

Jia GJ, Epstein HE, Walker DA (2006) Spatial heterogeneity of tundra vegetation in response to recent temperature changes. Glob Change Biol 12:42–55

Kaplan JO, Bigelow NH, Prentice IC, Harrison SP, Bartlein PJ, Christensen TR, Cramer W, Matveyeva NV, McGuire AD, Murray DF, Razzhivin VY, Smith B, Walker DA, Anderson PM, Andreev AA, Brubaker LB, Edwards ME, Lozhkin AV (2003) Climate change and Arctic ecosystems: 2. Modeling, paleodata-model comparisons, and future projections. J Geophys Res 108(D19):8171. doi:10.1029/2002JD002559

Kaplan JO, New M (2006) Arctic climate change with a 2°C global warming: timing, climate patterns and vegetation change. Clim Change 79:213–241

Kaplan JO, Prentice IC, Buchmann N (2002) The stable carbon isotope composition of the terrestrial biosphere: modeling at scales from the leaf to the globe. Glob Biogeochem Cycles. doi:10.1029/2001GB001403

Kasischke ES, Stocks BJ (eds) (2000) Fire, climate change and carbon cycling in the boreal forest. Springer, New York

Kimball JS, McDonald KC, Zhao M (2006) Spring thaw and its effect on terrestrial vegetation productivity in the Western Arctic observed from satellite microwave and optical remote sensing. Earth Interact 10:1–22

Lischke H, Löffler T (2006) Intra-specific density dependence is required to maintain diversity in spatio-temporal forest simulations with reproduction. Ecol Model 198:341–361

Lischke H, Zimmermann NE, Bolliger J, Rickebusch S, Löffler TJ (2006) TreeMig: a forest-landscape model for simulating spatio-temporal patterns from stand to landscape scale. Ecol Model 199:409–420

Lloyd AH (2005) Ecological histories from Alaskan tree lines provide insight into future change. Ecology 86:1687–1695

Lloyd AH, Bunn AG (2007) Responses of the circumpolar boreal forest to 20th century climate variability. Environ Res Lett. doi:10.1088/1748-9326/2/4/045013

Mack M, Treseder K, Manies K, Harden J, Schuur E, Vogel J, Randerson J, Chapin FS (2008) Recovery of aboveground plant biomass and productivity after fire in mesic and dry black spruce forests of interior Alaska. Ecosystems 11(2):209–225

McGuire AD, Anderson LG, Christensen TR, Dallimore S, Guo L, Hayes DJ, Heimann M, Lorenson TD, Macdonald RW, Roulet N (2009) Sensitivity of the carbon cycle in the Arctic to climate change. Ecol Monogr 79:523–555

Myneni RB, Keeling CD, Nemani RR (1997) Increased plant growth in the northern high latitudes from 1981 to 1991. Nature 386:698–701

Nathan R, Katul GG, Horn HS, Thomas SM, Oren R, Avissar R, Pacala SW, Levin SA (2002) Mechanisms of long-distance dispersal of seeds by wind. Nature 418:409–413

Neigh CSR, Tucker CJ, Townshend JRG (2008) North American vegetation dynamics observed with multi-resolution satellite data. Rem Sens Environ 112:1749–1772

Nemani RR, Keeling CD, Hashimoto H, Jolly WM, Piper SC, Tucker CJ, Myneni RB, Running SW (2003) Climate-driven increases in global terrestrial net primary production from 1982 to 1999. Science 300:1560–1563. doi:10.1126/science.1082750

New M, Lister D, Hulme M, Makin I (2002) A high-resolution data set of surface climate over global land areas. Clim Res 21:1–25

Pavelsky TM, Smith LC (2004) Spatial and temporal patterns in Arctic river ice breakup observed with MODIS and AVHRR time series. Rem Sens Environ 93:328–338

Randerson JT, Liu H, Flanner MG, Chambers SD, Jin Y, Hess PG, Pfister G, Mack MC, Treseder KK, Welp LR, Chapin FS, Harden JW, Goulden ML, Lyons E, Neff JC, Schuur EAG, Zender CS (2006) The impact of boreal forest fire on climate warming. Science 314(5802):1130–1132. doi:10.1126/science.1132075

Raynolds MK (2009) Circumpolar Arctic NDVI and vegetation types: a spatial analysis of the distribution patterns and effects of climate and substrate. Ph.D Thesis, University of Alaska, Fairbanks.

Reynolds CA, Jackson TJ, Rawls WJ (1999) Estimating available water content by linking the FAO soil map of the World with global soil profile databases and pedo-transfer functions. AGU Spring Meeting, American Geophysical Union, Boston

Schuur EAG, Vogel JG, Crummer KG, Lee H, Sickman JO, Osterkamp TE (2009) The effect of permafrost thaw on old carbon release and net carbon exchange from tundra. Nature 459(7246):556–559

Serreze MC, Walsh JE, Chapin FS, Osterkamp T, Dyurgerov M, Romanovsky V, Oechel WC, J. Morison WC, Zhang T, Barry RG (2000) Observational evidence of recent change in the Northern high-latitude environment. Clim Change 46(1–2):159–207. doi:10.1023/A:1005504031923

Shaver GR, Chapin FS (1991) Production: biomass relationships and element cycling in contrasting arctic vegetation types. Ecol Monogr 61:1–31

Shaver GR, Street LE, Rastetter EB, van Wijk MT, Williams M (2007) Functional convergence in regulation of net CO_2 flux in heterogeneous tundra landscapes in Alaska and Sweden. J Ecol 95:802–817

Slayback DA, Pinzon JE, Los SO (2003) Northern hemisphere photosynthetic trends 1982–1999. Glob Change Biol 9:1–15

Soja AJ, Tchebakova NM, French NHF, Flannigan MD, Shugart HH, Stocks BJ, Sukhinin AI, Parfenova EI, Chapin FS III, Stackhouse PW Jr (2007) Climate-induced boreal forest change: preditions versus current observations. Glob Planet Change 56:274–296. doi:10.1016/J.GLOPLACHA.2006.07.028

Stroeve J, Markus T, Meier W, Miller J (2006) Recent changes in the Arctic melt season. Ann Glaciol 44:367–374

Sturm M, Racine C, Tape K (2001) Climate change: increasing shrub abundance in the Arctic. Nature 411:546–547

Tape K, Sturm M, Racine C (2006) The evidence for shrub expansion in Northern Alaska and the Pan-Arctic. Glob Change Biol 12:686–702

Treshnikov AF (1985) Atlas of the Arctic. Central Administrative Board of Geodesy and Cartography of the Ministereal Council of the USSR, Moscow (in Russian)

Turetsky MR, Wieder RK, Vitt DH, Evans RJ, Scott KD (2007) The disappearance of relict permafrost in boreal north America: effects on peatland carbon storage and fluxes. Glob Change Biol 13(9):1922–1934

Van Bogaert R, Walker D, Jia GJ, Grau O, Hallinger M, De Dapper M, Jonasson C, Callaghan TV (2007) Recent Changes in Vegetation. Arctic Report Card 2007. http://www.arctic.noaa.gov/reportcard/essay_vanbogaert.html. Accessed 1 June 2008

Walker DA, The CAVM Team (2005) The circumpolar arctic vegetation map. J Veg Sci 16:267–282

Walker MD, Wahren CH, Hollister RD, Henry GH, Ahlquist LE, Alatalo JM, Bret-Harte MS, Calef MP, Callaghan TV, Carroll AB, Epstein HE, Jónsdóttir IS, Klein JA, Magnússon B, Molau U, Oberbauer SF, Rewa SP, Robinson CH, Shaver GR, Suding KN, Thompson CC, Tolvanen A, Totland Ø, Turner PL, Tweedie CE, Webber PJ, Wookey PA (2006) Plant community responses to experimental warming across the tundra biome. Proc Natl Acad Sci USA. doi:10.1073/pnas.0503198103

Zhang K, Kimball JS, Hogg EH, Zhao M, Oechel WC, Cassano JJ, Running SW (2008) Satellite-based model detection of recent climate-driven changes in northern high-latitude vegetation productivity. J Geophys Res Biogeosci 113(G03033). doi:03010.01029/02007JG000621

Chapter 3
High-Latitude Forest Cover Loss in Northern Eurasia, 2000–2005

Peter V. Potapov, Matthew C. Hansen, and Stephen V. Stehman

Abstract Timely updates of large area forest cover and change facilitate studies of biogeochemical cycling and climate modeling, forest management, and ecological integrity. Our method employed an internally consistent and efficient probability-based sampling approach that integrates low and high spatial resolution satellite data sets for high-latitude gross forest cover loss estimation in Northern Eurasia. Area of forest cover loss from 2000 to 2005 within the high-latitude forest zone is estimated to be 6.6 Mha (standard error ±2.1 Mha). Estimated forest cover loss represents a 2.8% reduction in year 2000 forest area. East Siberia is shown to have the largest total forest loss area of the Northern Eurasia regions. Of the total forest cover loss area, 51.7% was attributed to wildfires. Inter-annual forest cover loss trend shows significant increases of forest loss due to wildfires for years 2002 and 2003 in East Siberia, with a subsequent decrease in forest loss. Estimated gross forest cover loss within Northern Eurasia boreal forests exceeded the humid tropics on a percentage basis for the study period and brings into question the sustainability of high-latitude forests, given the long times required to re-establish forest cover.

3.1 Introduction

Timely updates of large area forest cover and change facilitate scientific studies of biogeochemical cycling and climate modeling, forest management, and ecological integrity. A practical solution to examining trends in forest cover change at regional scales is to employ remotely sensed data. Satellite-based monitoring of forest clearing can be implemented consistently across large regions at a fraction of the cost of obtaining extensive ground inventory data. Remote sensing data are most valuable in areas where extensive and repeated in situ observations are absent. One such area is

P.V. Potapov (✉)
Geographic Information Science Center of Excellence, South Dakota State University, Brookings, SD 57007, USA
e-mail: Peter.Potapov@sdstate.edu

G. Gutman, A. Reissell (eds.), *Eurasian Arctic Land Cover and Land Use in a Changing Climate*, DOI 10.1007/978-90-481-9118-5_3,

high-latitude boreal forests. Much of this region lacks infrastructure making annual field- and aircraft-based monitoring impractical. Remotely sensed data enable the synoptic quantification of forest cover and change, providing information on where and how fast forest change is taking place. However, monitoring forest cover at these scales with remotely sensed imagery remains a challenge due to limitations concerning data quality, data access and processing capabilities.

Our method, presented here, employed an internally consistent and efficient probability-based sampling approach that integrates low and high spatial resolution satellite data sets. The method relies on high temporal, low spatial resolution MODerate Resolution Imaging Spectroradiometer (MODIS) data for mapping biome-scale forest cover loss hotspots. Low temporal, high spatial resolution Landsat data were then sampled to derive area estimates of forest cover and change within the biome from 2000 to 2005. Results for high-latitude forests presented here are a subset of a pan-boreal forest cover and change study and include assessments of the annual variation of change, a comparison of change at sub-national scale, and the attribution of forest cover change dynamic (Potapov et al. 2008a). The approach enables rapid assessments of large area forest cover change as the MODIS algorithm is used repeatedly for each time interval, and the targeted sampling of Landsat data enables precise estimation of change based on relatively few samples.

3.2 Boreal Forest Biome Boundaries and Sub-regions

The results of forest cover and forest cover loss are presented only for the Eurasian Arctic areas as defined earlier (above 60°N). The boreal forest biome boundary was

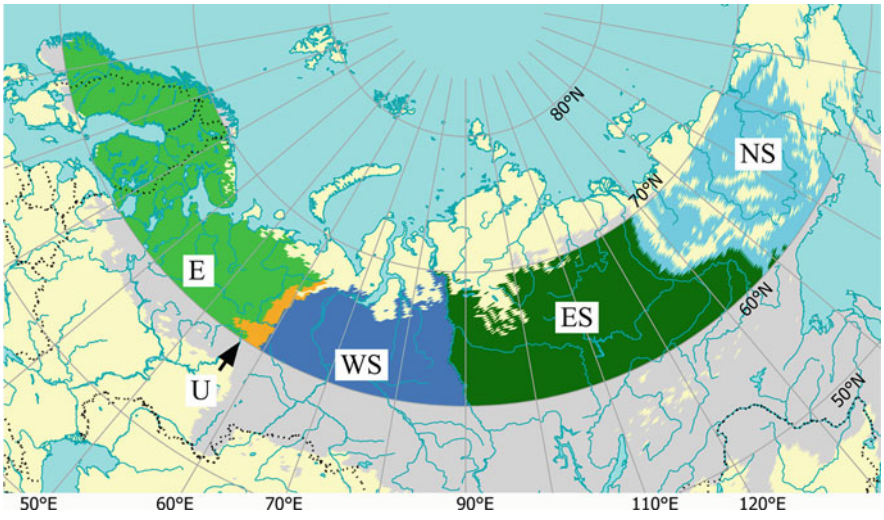

Fig. 3.1 Boreal biome and analysis regions in Northern Eurasia: Europe (E), Urals (U), West Siberia (WS), East Siberia (ES), Northeast Siberia (NS)

based on the world terrestrial ecoregion map of Olson et al. (2001). This map was modified to add forested areas of forest-tundra transitional ecoregions to the boreal biome (Fig. 3.1). Due to data limitations, a small portion of the biome greater than 70° latitude in East Siberia was excluded from the analysis.

To disaggregate change within high-latitude forests, the boreal biome was divided into regions using the ecoregion labels of Olson et al. (2001):

- Europe, consisting of European boreal and tundra ecoregions;
- Urals, consisting of Ural montane forest and tundra ecoregions;
- West Siberia, consisting of West Siberian taiga and Yamal-Gydan tundra ecoregions;
- East Siberia, consisting of East Siberian taiga and Trans-Baikal forest and mountain ecoregions;
- Northeast Siberia, consisting of Northeast Siberian taiga and mountain tundra.

3.3 Data and Methods

3.3.1 The Biome-Wide Forest Cover Loss Analysis Algorithm

The biome-based forest change analysis workflow included several steps: (I) wall-to-wall MODIS-based forest cover loss hotspot mapping; (II) stratified sampling and analysis of Landsat imagery to estimate change area; (III) analysis of disturbance factors and (IV) inter-annual change trends (Fig. 3.2). The MODIS-scale analysis was based on a set of selected annual inputs that include mean 32-day composite values and annual metrics. Two extensive training data sets, one showing forest cover loss and the second showing forest loss factors, were employed to build regression/decision tree classification models for annual and inter-annual analysis (Fig. 3.2I and IV). The final MODIS-derived result, forest loss hotspots at 500-m spatial resolution, was averaged to a biome-wide sampling frame of square blocks 18.5 km per side to stratify the biome into regions of high, medium and low likelihood of forest cover loss. Blocks were sampled within each stratum and characterized into total forest cover loss and portion of forest loss due to fire using multi-date Landsat Enhanced Thematic Mapper Plus (ETM+) imagery (Fig. 3.2II). The Landsat-derived validation/calibration data were analyzed using a separate regression estimator employing MODIS change hotspot and burnt area hotspot fraction as auxiliary variables (Fig. 3.2II and III). The additional analysis of inter-annual change trends was based on MODIS-scale annual forest loss hotspot maps (Fig. 3.2IV).

The analysis of forest cover loss was performed only for areas covered by forest in 2000, the initial year of monitoring. Forest was defined as areas with tree canopy cover greater than 25% based on the global tree canopy cover data set (part of the Vegetation Continuous Fields MODIS 500-m product, hereafter referred to as VCF) (Hansen et al. 2002, 2003). The tree canopy cover threshold was based on the ability

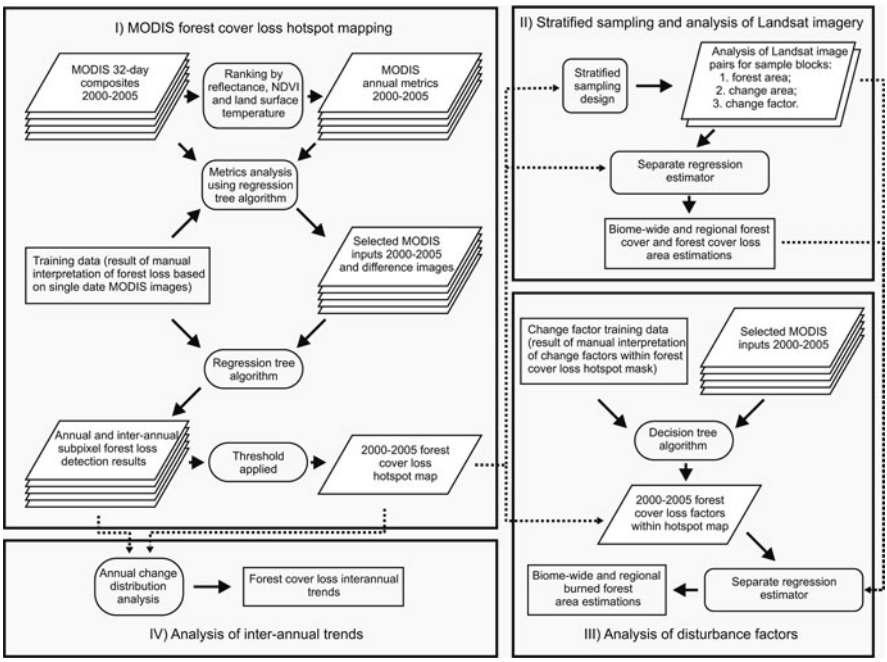

Fig. 3.2 Change analysis workflow

to consistently map forest cover given an estimated standard error for VCF tree cover of 11.5% (Hansen et al. 2005). A threshold of 25% limited the presence of forest cover commission errors (Carroll et al. 2009).

The MODIS-scale analysis and stratified sampling was conducted within the circumpolar boreal forest biome. Due to the focus of this book, results are shown only for the Eurasian high-latitude boreal and tundra ecoregions.

3.3.2 MODIS-Based Forest Cover Loss Hotspot Mapping

The MODIS/Terra visible and infrared bands (1–7) surface reflectance 8-Day L3 global 500-m (MOD09A1) composites along with Land Surface Temperature/Emissivity 8-Day L3 global 1-km product for years 2000–2005 were used as the primary inputs to our analysis. The initial 8-day composites were combined into 32-day composites that were subsequently transformed to multi-temporal annual metrics that capture the salient points of phenological variation by calculating means of spectral information from 3-, 6- and 9-month composites with highest NDVI and surface temperature values. Multi-temporal metrics have been shown to perform as well or better than time-sequential composites in mapping large areas (Hansen et al. 2005).

Our method employed a bagged regression tree algorithm (Breiman 1996) to create a wall-to-wall biome-wide forest cover loss hotspot map. Regression trees are derived using a training data set that relates spectral reflectance change signals to percent cover loss. To create training data, pairs of single date MODIS images for years 2001 and 2005 were manually classified to no-change and forest loss classes using the MODIS 250-m spatial resolution Near-infrared (NIR) reflective band. The classification results were averaged to MODIS 500-m raster cells. To build the regression tree model, percent forest cover loss from the training data set was used as the dependent variable, and annual 32-day composites and derived metrics plus their inter-annual differences were used as independent variables. The regression tree model was then applied to the biome-wide pairs of annual MODIS inputs annually and for the 2000–2005 interval. The forest cover loss results for the 2000–2005 interval were used to create the 5-year forest cover loss hotspot map, while annual change results were used for the analysis of temporal trends.

The analysis of forest cover loss factors was based on a decision tree classification. The objective was to discern the cause of the cleared forest cover per MODIS pixel. An extensive training set was manually created using available ancillary information. A sample of pixels within the final change hotspot mask was manually labeled as either burned areas or other change factors (logging, tree mortality due to insect outbreaks, windfalls). The training data related manually-assigned class information with spectral data derived from the year when change was detected. The classification results (probability of each class) thresholds were at 50% to produce two categories: burned forest areas and forest cover loss hotspots attributed to other disturbance factors.

3.3.3 Landsat Stratified Sampling Block Analysis

Landsat ETM+ (28.5-m spatial resolution) data were sampled and classified to derive area estimates of forest cover and change within the biome. Stratified sampling was implemented to enhance precision by allocating greater sampling effort to areas likely to exhibit change (Table 3.1). The strata were determined based on the MODIS-derived forest cover loss hotspot map. The biome was partitioned into a sampling frame consisting of square blocks 18.5-km per side. The 500 m forest cover loss hotspot map for 2000–2005 was aggregated per block, yielding percent change for each of the 62,625 blocks within the boreal biome. The stratum boundaries were chosen guided by the cumulative square root frequency rule and the sample size allocated to each change stratum was initially determined by optimal allocation (Cochran 1977).

A stratified random sample of 118 blocks was interpreted for forest cover, forest cover loss and forest change type using Landsat imagery from 2000 and 2005. A separate regression estimator (i.e., separate regression models and parameter estimates allowed for each stratum) was employed in the high- and medium-change strata (strata 3 and 4) to estimate Landsat-derived forest cover loss area using percent

Table 3.1 Stratified sampling design

Stratum number	MODIS-derived forest cover loss (based on change hotspot map) (%)	Standard deviation of MODIS-derived forest cover loss (%)	Number of blocks within biome	Number of blocks sampled within biome (and within Northern Eurasian)
1	0–0.25%	0.07	43,968	25(5)
2	0.25–1%	0.21	7,357	25(5)
3	1–6%	1.35	7,886	25(6)
4	>6%	11.42	3,414	43(6)
Total	–	–	62,625	118(22)

MODIS-derived change hotspots as auxiliary variable. The strata 1 and 2 estimates were constructed from the Landsat sample mean.

The same approach was used to estimate burned forest area fraction of total change area. The MODIS-derived forest cover loss hotspot area attributed to fire was used to build a regression model for burned area estimation within strata 2, 3 and 4, while the sample mean of Landsat-derived burned area was used for stratum 1 estimates.

The relationship between Landsat-based forest cover area and mean VCF tree canopy density was used to derive forest extent for the year 2000. A simple linear regression (no intercept) model was employed with mean VCF tree canopy density per block as the independent variable.

3.4 Results and Discussion

3.4.1 Forest Cover and Forest Cover Loss Area Estimates

The extent of the Northern Eurasian forest zone (above 60°N) used for the change analysis was 647.9 million ha (Mha). Using Landsat-derived forest cover classification results, forest extent within the study area was estimated to be 233.5 Mha for year 2000. The forest cover fraction of the biome area varies between the Eurasian regions (Table 3.2). Europe and the Urals have the highest forest fraction (45.7 and 59.0%, respectively) while the forest fraction in Northeast Siberia is only 15.5%.

Based on the Landsat sample blocks analysis, the area of forest cover loss from 2000 to 2005 within the high-latitude forest zone is estimated to be 1.0% (standard error 0.3%) of the total biome area. This translates to an estimated forest loss area of 6.6 Mha (s.e. ±2.1 Mha). Estimated forest cover loss represents a 2.8% reduction in year 2000 forest area, exceeding humid tropical forest loss on a percentage basis (Hansen et al. 2008).

Our estimates emphasize the significant difference in forest cover loss rates between Northern Eurasia regions (Table 3.2). The lowest change rates were detected for the Urals and West Siberia, where no major fire events happened from

Table 3.2 Sample-based forest cover and forest cover loss estimates for Northern Eurasian boreal regions

Region	Boreal biome area (Mha)	Forest fraction of biome area (%)	Area of forest cover loss (Mha)	Within-region forest cover loss area of biome land area (%)	Within-region forest cover loss area of year 2000 forest area (%)	Contribution of the region to forest cover loss area in Eurasian high-latitude forests (%)
Europe	200.2	45.7	1.92	0.96	2.10	29.3
Urals	9.3	59.0	0.05	0.53	0.90	0.8
West Siberia	108.1	40.3	0.74	0.68	1.70	11.3
East Siberia	208.8	35.6	2.92	1.40	3.94	44.6
Northeast Siberia	121.5	15.5	0.92	0.76	4.89	14.1

2000 to 2005. Northeast Siberia, while having a relatively small forest loss fraction of biome area, features the highest proportion of year 2000 forest cover cleared (4.9%). These results illustrate intensive wildfire activity within a region of sparse and fragmented forest cover. East Siberia has the largest total forest loss area (44.6% of total forest loss in Northern Eurasia) and the second highest portion of year 2000 forest loss (3.9%) of the Northern Eurasia regions. Intensive forest loss in East Siberia is associated with the extensive wildfires of 2002 and 2003. Europe is the second largest total forest cover loss region with a significant portion of forest cover cleared (2.1%), indicating high-intensity logging operations.

The Northern Eurasia study region can be divided into three sub-regions of forest cover loss intensity (Table 3.3). The "high intensity" sub-region consists of areas with a 5-year cumulative forest loss greater than 5% and largely captures the extensive burned areas within the high-latitude forest zone. Of the total forest loss area, 42% occurs in this sub-region that constitutes only 4% of the analysis area, illustrating the presence of wildfire "hotspots". East Siberia exhibits the highest portion of all forest loss allocation within the "high intensity" sub-region because of large burned forest areas. For regions with extensive forestry operations and intensive fire protection, e.g. Europe and the Urals, the area of the "high intensity" forest loss sub-region contributes little to overall forest cover change.

The "medium intensity" sub-region of 1–5% forest loss per block predominantly captures the areas of extensive logging operations. Within Europe and the Urals, this sub-region constitutes 31 and 12% of area respectively, and accounts for 55 and 35% of total forest loss. For the rest of Northern Eurasia the portion of the "medium intensity" sub-region is smaller (from 11% in Northeast Siberia to 7% in East Siberia). In these regions, the "medium intensity" sub-region mainly captures extensive burned areas within naturally fragmented forest landscapes.

Areas with less than 1% forest cover loss per block were classified in a "low intensity" sub-region that captures the extensive areas of low-intensity scattered

Table 3.3 Percent of 18.5 × 18.5-km blocks within each forest cover loss intensity sub-region (area) and percent of total change within forest cover loss intensity sub-region (change) for each Northern Eurasian region

Forest cover loss intensity sub-region	Europe		Urals		West Siberia		East Siberia		Northeast Siberia	
	Area	Change	Area	Change	Area	Change	Area	Change	Area	Change
"Low intensity" (change <1%)	67	27	88	65	88	50	86	24	86	44
"Medium intensity" (change 1–5%)	31	55	12	35	10	23	7	10	11	27
"High intensity" (change >5%)	2	18	0	0	2	27	7	66	3	29

disturbance and the majority of remaining intact forest areas. This sub-region constitutes 81% of biome area and is responsible for 31% of total high-latitude forest loss; however, the allocation of "low intensity" change within regions is highly variable. In Europe and East Siberia, this sub-region is responsible for 27 and 24% of total change respectively, while in West, Northeast Siberia and the Urals 50, 44 and 65% of all change occurs in this sub-region. Two factors could be responsible for the allocation of change within this "low intensity" sub-region: (i) oil-and-gas and mining activity, associated with extensive infrastructure development; and (ii) the effects of fire in naturally fragmented forests, such as swamp areas and forest-tundra interface. In the second case, the forest cover loss could be small even within extensive burned areas because the initial forest cover was sparse and/or fragmented.

3.4.2 Forest Cover Loss Inter-annual Trends

Inter-annual analysis of forest cover loss highlights years with increased wildfire activity and illustrates differences in change dynamics within Northern Eurasia. MODIS-derived annual forest cover loss hotspot area estimates for high-latitude forests shows significant increases of forest loss due to wildfires for 2002 and 2003 in East Siberia, with a subsequent decrease in forest loss (Fig. 3.3). A significant part of the total year 2002 forest cover loss was connected with fires in Yakutia (East Siberia) and 2003 with fires in East Siberia and in the Russian Far East (Fig. 3.4). In Northeast Siberia the major forest cover loss is connected with intensive fires for 2001 (northern part of the region) and 2003 (southern part of the region). However, because of sparse and fragmented forest cover, the majority of fire-affected areas was outside of forests and not included in the current analysis. Although wildfires are the main forest loss dynamic in West Siberia, no extreme fire seasons were observed in the region during the 2000–2005 interval. Regions where forest change is primarily related to logging activities (Europe, Urals) reflected a consistent inter-annual rate of change.

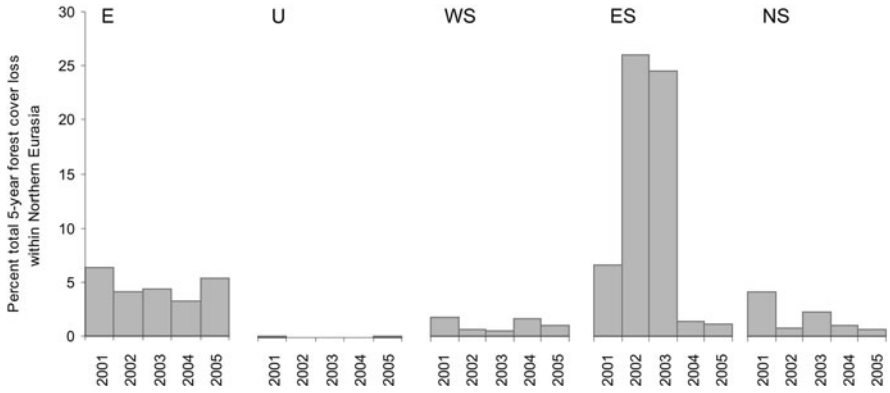

Fig. 3.3 Annual distribution of total 5-year forest cover loss hotspots within boreal biome in Northern Eurasia: Europe (E), Urals (U), West Siberia (WS), East Siberia (ES), Northeast Siberia (NS)

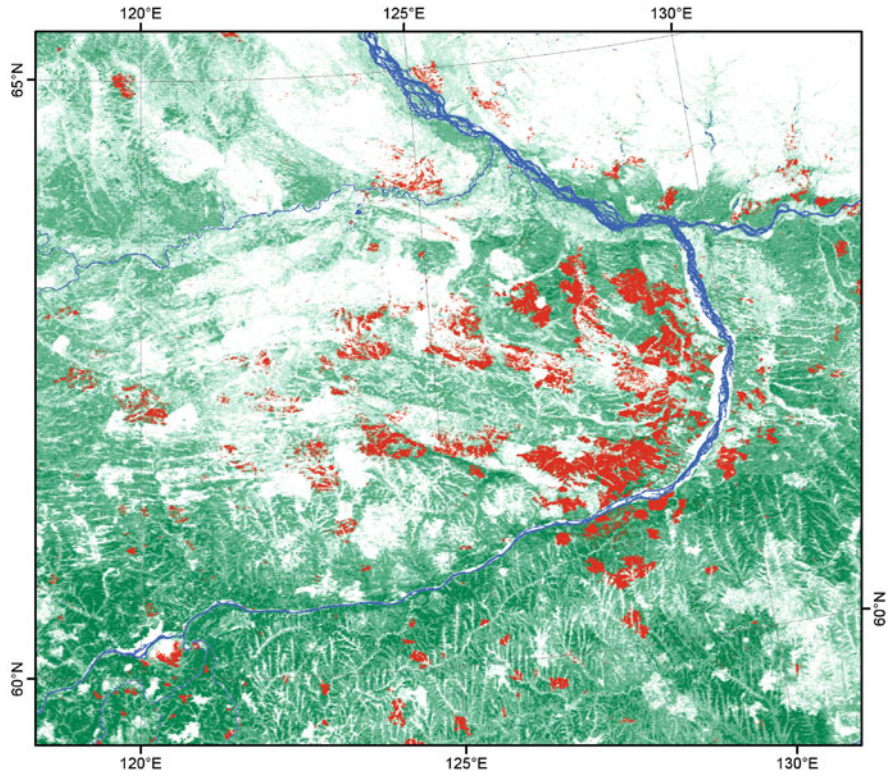

Fig. 3.4 Extensive forest burned areas in Central Yakutia, a consequence of 2002/2003 fire season: MODIS-derived forest cover loss hotspot areas 2001–2005 (*red*), tree canopy cover above 25% (*green*)

Though the presence of the 2002–2003 wildfires is confirmed by national fire statistics (Sukhinin et al. 2003; Achard et al. 2007), some remaining problems with identifying the specific year of fire events could impact our results. The main problem of fire event dating using MODIS-derived annual forest cover loss hotspot maps is connected with after-fire effects: the majority of trees that survive the fire died 1–2 years after the fire event. Fires in larch forests in Northeast and East Siberia are a special case: most of these fires occur in late autumn, during leaf fall. This factor could lead to the incorrect (1-year delay) identification of the year of the event.

3.4.3 Burned Forest Area Estimation

Fire is an integral component of boreal forest dynamics and plays a crucial role in carbon and aerosol emissions from forest ecosystems. In high latitude forests, where a large portion of the carbon is stored in soil, fire has a significantly different effect on carbon emissions when compared to other disturbances that have no immediate effect on the forest floor and soil conditions. Our analysis of change factors contributing to forest cover loss can be used for future carbon emission estimation as it disaggregates the total change area affected by fire versus all other types of disturbance (see Chapter 6, this volume).

To formally disaggregate change dynamics, a regression estimation procedure relating MODIS and Landsat forest cover loss due to fire was performed, mimicking the procedure used to derive total forest cover loss. Of the total forest cover loss area, 51.7% was attributed to wildfires and the rest, 48.3%, to other disturbances, including logging, wind and snow damage, and insect outbreaks. Among Northern Eurasia regions, Europe and the Urals have the lowest proportion of forest loss due to wildfires (Table 3.4). Logging is the predominant factor of forest cover loss in these regions. Both fires and non-fire forest cover loss factors contributed to change within West Siberia. For East and Northeast Siberia, fire is the primary forest disturbance agent. Though our results show the significant role of wildfires in forest cover loss in Northeast Siberia, it could be underestimated due to general difficulties with disturbance type recognition in sparse and fragmented forests.

Table 3.4 Sample-based forest burned areas estimates, 2000–2005

	Forest cover loss within the region attributed to fire (%)	Annual forest burned area (Mha)
Europe	19.8	0.08
Urals	22.6	0.002
West Siberia	33.0	0.05
East Siberia	78.9	0.46
Northeast Siberia	48.2	0.09

Eurasian high-latitude forest fire regimes are well studied. However, area burned estimates vary by order of magnitude depending on data sources. In general, the majority of satellite-based annual area burned estimates are an average 5–10 times higher than official Russian data (Korovin 1996; Soja et al. 2004; Goldammer et al. 2005; Achard et al. 2007). Our method of forest burned areas assessment differs from most official and remote-sensing based analyses as it was made only within forests with high (above 25%) tree canopy density and quantifies only those forested areas affected by stand-replacement fires. The difference between our forest cover loss estimations and official burned areas data could be explained by the predominance of surface fires within Northern Eurasian forests (Korovin 1996). Stand-replacement and surface fires in boreal forests have a different impact on forest cover, direct carbon emissions, albedo change and post-fire successional trajectories (Wooster and Zhang 2004; Goetz et al. 2007). Our burned forest estimates could more readily be incorporated into carbon emission and albedo change models than existing fire-affected area estimates because our analysis reflects a strict biophysical interpretation of the presence/absence of tree cover assessed using a synoptic, biome-wide approach.

Annual forest area loss attributed to wildfire within Northern Eurasian high-latitude forests for the 2000–2005 interval is estimated to be 0.7 Mha. However, two extreme fire years are responsible for more then 50% of the total 5-year burned area (e.g. in East Siberia). Our findings did not show any clear increasing inter-annual trend in fire intensity within high-latitude forests. However, there is no doubt that current and future climate changes will affect fire regimes. Moreover, the natural fire regime in all boreal regions is significantly altered by humans, including the increase of fire ignition and fire suppression activities. These changes could affect forest age composition, soil and permafrost conditions, and, as a result, carbon exchange in disturbed forest ecosystems (as discussed in Chapter 6, this volume).

3.4.4 Logging Monitoring

Our analysis highlights logging as the most important forest cover loss factor within European high-latitude forests. Two main types of intensive logging operations should be noted: intensive forestry operations within secondary forests or forest plantations, and large-scale clear-cuts along the boundary of undeveloped forest areas primarily located in northern European Russia and the Urals. The expansion of intensive forestry operations within pristine forest areas of northern European Russia increased from the 1950s to the 1990s, with a drastic decrease of logging activity in the last decade of the twentieth century due to depressed economic conditions in post-Soviet Russia. However, increasing economic activity and high profits from timber exports have led to growth in forest exploitation since 1998. The remaining intact landscapes tend to be remote, unproductive and poorly stocked in comparison to what is usually considered minimum levels for sustainable forestry (Yaroshenko et al. 2001). However, the depletion of available

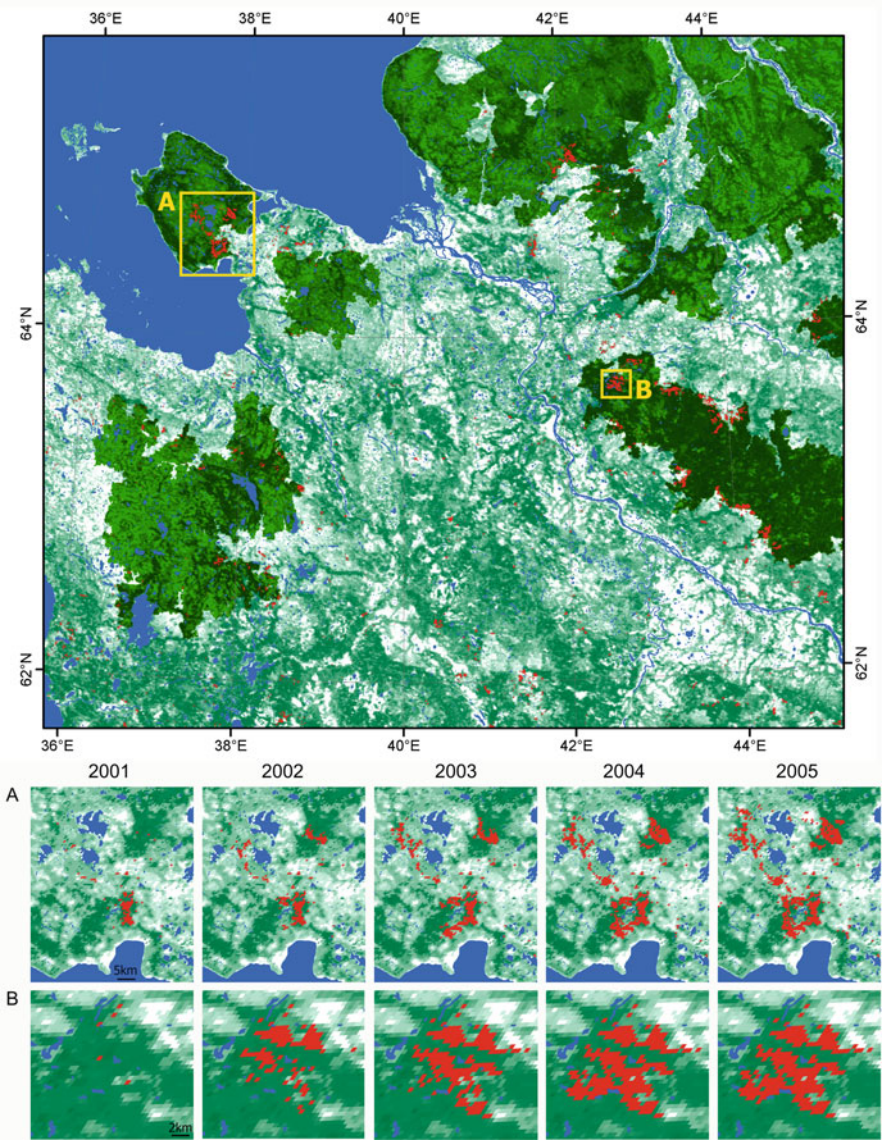

Fig. 3.5 (*Top*) Intensive logging areas located at Intact Forest Landscapes (IFL) boundaries in northern European Russia: MODIS-derived forest cover loss hotspot areas 2001–2005 (*red*), tree canopy cover above 25% (*green*), IFL (*dark green*). (*Bottom*) Time-series of cumulative forest cover loss due to clearcuts within the remaining IFL fragments in Onega peninsula (**a**) and North Dvina River basin (**b**)

timber resources within more accessible and productive forests of European Russia has led to intensive exploitation of previously undeveloped areas.

To create a baseline for logging expansion monitoring, large undeveloped forest areas were identified and mapped using a new approach for assessing human influence in forest landscapes at the global scale (Yaroshenko et al. 2001; Aksenov et al. 2002; Potapov et al. 2008b). The essence of this approach is the use of high spatial resolution satellite data (Landsat TM and ETM+) and fine-scale maps to establish a boundary of Intact Forest Landscapes (IFL). IFL were defined as an unbroken expanse of natural ecosystems within areas of current forest extent, without signs of significant human activity, and having an area of at least 500 km^2 (Potapov et al. 2008b). The map of northern European Russia IFL boundaries for the year 2000 overlapped with MODIS-derived forest cover loss 2000–2005 hotspot map shows that the majority of large-scale clear-cuts are located within the periphery of remaining IFL (Fig. 3.5, top). Logging operations are prevalent along IFL boundaries and the resulting landscape fragmentation due to clear-cutting and road building are the main cause of IFL area loss within the region (Fig. 3.5, bottom). From all MODIS-derived forest cover loss hotspots, 16% were found within the 5-km wide peripheral zone of IFL, which constitutes less then 10% of the boreal biome area within northern European Russia. The forest loss hotspot fraction within the periphery of IFL is 1.7 times higher than that within developed areas, and three times higher than in the remaining core IFL. These results reveal the increasing threat to the last remaining IFL in Europe and suggest the need to develop a comprehensive conservation strategy.

3.5 Conclusions

Gross forest cover loss within high-latitude forests is higher on a percentage basis than in the humid tropics, the most studied and reported-on forest biome (Achard 2002; FAO 2006; Hansen et al. 2008). However, like the humid tropics, great regional variation in change rates is present. Within Northern Eurasia, regional variation is significant with fire playing a primary role in areas not subject to human exploitation. Where human populations are higher and logging more readily pursued, fire is less prevalent. Extensive logging operations within the Russian portion of Northern Eurasia tend to be located along the periphery of remaining large undeveloped forest areas. Revealed variation in forest cover loss, both regionally and in terms of causation, has implications for biogeochemical and climate modeling, forest management and nature conservation, all of which benefit from the quantification of forest cover dynamics.

The overall high rates of forest cover loss need to be put into context with a longer term analysis in order to determine if they are anomalous or within the historical range. High rates of forest cover loss bring into question the sustainability of high-latitude forests, given the long times required to reestablish forest cover. Data sets such as the UNFAO Forest Resource Assessment (FAO 2005) do not enable

such determinations as they employ forestry land-use definitions in documenting change, not actual presence/absence of forest cover. Both retrospective and prospective studies using the approach detailed here will bring greater understanding on long-term trends of forest cover within high-latitude forests.

References

Achard F, Eva HD, Mollicone D, Beuchle R (2007) The effect of climate anomalies and human ignition factor on wildfires in Russian boreal forests. Philos Trans Royal Soc B. doi:10.1098/rstb.2007.2203

Achard F, Eva HD, Stibig H-J, Mayaux P, Gallego J, Richards T, Malingreau J-P (2002) Determination of deforestation rates of the world′s humid tropical forests. Science 297:999-1002

Aksenov D, Dobrynin D, Dubinin M, Egorov A, Isaev A, Karpachvskiy M, Lestadius L, Potapov P, Purekhovskiy A, Turubanova S, Yaroshenko A (2002) Atlas of Russia's intact forest landscapes. Global Forest Watch, Moscow

Breiman L (1996) Bagging predictors. Mach Learn 24:123–140

Carroll M, Townshend JRG, Hansen MC, DiMiceli C, Sohlberg R, Wurster K (2009) Vegetative cover conversion and vegetation continuous fields. In: Ramachandran B, Justice C, Abrams M (eds) Land remote sensing and global environmental change: NASA's EOS and the science of ASTER and MODIS. Springer, New York

Cochran WG (1977) Sampling techniques, 3rd edn. Wiley, New York

FAO (2005) State of the World's forests. UNFAO, Rome

FAO (2006) Global forest resources assessment 2005, FAO Forestry Paper 147. UNFAO, Rome

Goetz SJ, Mack MC, Gurney KR, Randerson JT, Houghton RA (2007) Ecosystem responses to recent climate change and fire disturbance at northern high latitudes: observations and model results contrasting Northern Eurasia and North America. Environ Res Lett 2. doi:10.1088/1748-9326/2/4/045031

Goldammer JG, Sukhinin A, Csiszar I (2005) The current fire situation in the Russian Federation: implications for enhancing international and regional cooperation in the UN framework and the global programs on fire monitoring and assessment. Int For Fire News 32:13–42

Hansen MC, DeFries RS, Townshend JRG, Carroll M, DiMiceli C, Sohlberg RA (2003) Global percent tree cover at a spatial resolution of 500 meters: first results of the MODIS vegetation continuous fields algorithm. Earth Interact. doi:10.1175/1087-3562

Hansen MC, DeFries RS, Townshend JRG, Sohlberg R, Carroll M, DiMiceli C (2002) Towards an operational MODIS continuous field of percent tree cover algorithm: examples using AVHRR and MODIS data. Rem Sens Environ 83:303–319

Hansen MC, Stehman SV, Potapov PV, Loveland TR, Townshend JRG, DeFries RS, Pittman KW, Stolle F, Steininger MK, Carroll M, DiMiceli C (2008) Humid tropical forest clearing from 2000 to 2005 quantified using multi-temporal and multi-resolution remotely sensed data. Proc Natl Acad Sci USA 105(27):9439–9444

Hansen MC, Townshend JRG, DeFries RS, Carroll M (2005) Estimation of tree cover using MODIS data at global, continental and regional/local scales. Int J Rem Sens 26:4359–4380

Korovin GN (1996) Analysis of the distribution of forest fires in Russia. In: Goldammer JG, Furyaev VV (eds) Fire in ecosystems of Boreal Eurasia. Kluwer, Dordrecht

Olson DM, Dinerstein E, Wikramanayake ED, Burgess ND, Powell GVN, Underwood EC, D'amico JA, Itoua I, Strand HE, Morrison JC, Loucks CJ, Allnutt TF, Ricketts TH, Kura Y, Lamoreux JF, Wettengel WW, Hedao P, Kassem KR (2001) Terrestrial ecoregions of the World: a new map of life on Earth. BioScience 51(10):1–6

Potapov P, Hansen MC, Stehman SV, Loveland TR, Pittman K (2008a) Combining MODIS and Landsat imagery to estimate and map boreal forest cover loss. Rem Sens Environ 112(9):3708–3719

Potapov P, Yaroshenko A, Turubanova S, Dubinin M, Laestadius L, Thies C, Aksenov D, Egorov A, Yesipova Y, Glushkov I, Karpachevskiy M, Kostikova A, Manisha A, Tsybikova E, Zhuravleva I (2008b). Mapping the World's intact forest landscapes by remote sensing. Ecol Soc 13. http://www.ecologyandsociety.org/vol13/iss2/art51/

Soja AJ, Sukhinin AI, Cahoon DR, Shugart HH, Stackhouse PW (2004) AVHRR-derived fire frequency, distribution and area burned in Siberia. Int J Rem Sens 25(10):1939–1960

Sukhinin AI, Ivanov VV, Ponomarev EI, Slinkina OA, Cherepanov AV, Pavlichenko EA, Romansko VY, Miskiv SI (2003) The 2002 fire season in the Asian part of the Russian Federation. Int For Fire News 28:1–34

Wooster MJ, Zhang YH (2004) Boreal forest fires burn less intensely in Russia than in North America. Geophys Res Lett. doi:10.1029/2004GL020805

Yaroshenko AY, Potapov PV, Turubanova SA (2001) The last intact forest landscapes of Northern European Russia. Greenpeace Russia, Moscow

Chapter 4
Characterization and Monitoring of Tundra-Taiga Transition Zone with Multi-sensor Satellite Data

Guoqing Sun, Kenneth J. Ranson, Viatcheslav I. Kharuk, Sergey T. Im, and Mukhtar M. Naurzbaev

Abstract Monitoring the dynamics of the circumpolar boreal forest (taiga) and Arctic tundra boundary is important for understanding the causes and consequences of changes observed in these areas. Because of the inaccessibility and large extent of this zone, remote sensing data can play an important role for the purposes. In this study, climate-related changes that occurred in the Ary-Mas larch forests (the world's northernmost forest range) in the last three decades of the twentieth century were analyzed. An analysis of Landsat images in 1973 and 2000 has provided evidence for an increase in the closeness of larch forest canopy by 65% and the expansion of larch to the tundra for 3–10 m per year and to areas relatively poorly protected from wind due to topographic features (elevation, azimuth, and slope). It was found that a tundra-taiga transitional area can be characterized using multi-spectral Landsat ETM+ summer images, multi-angle MISR red band reflectance images, RADARSAT images with larger incidence angle, or multitemporal and multi-spectral MODIS data. Because of different resolutions and spectral regions covered, the transition zone maps derived from different data types were not identical, but the general patterns were consistent.

4.1 Introduction

The tundra-taiga boundary stretches for more than 13,400 km around the northern hemisphere and is probably the Earth's greatest vegetation transition. This transition zone is sensitive to both climate change and human activities (Callaghan et al. 2002a, b; Knorre et al. 2006; Devi et al. 2008). The shifting of local subarctic tree lines throughout the forest-tundra biome, which is linked to ecological processes at different spatiotemporal scales, will reflect future global changes in climate (Payette

G. Sun (✉)
Department of Geography, University of Maryland, Greenbelt, MD 20771, USA; Biospheric Sciences Branch, NASA/GSFC, Code 923, Greenbelt, MD 20771, USA
e-mail: Guoqing.Sun@nasa.gov

G. Gutman, A. Reissell (eds.), *Eurasian Arctic Land Cover and Land Use in a Changing Climate*, DOI 10.1007/978-90-481-9118-5_4,

et al. 2001; Kharuk et al. 2006, 2008). Monitoring the dynamics of this tundra-taiga boundary is critical for our understanding of the causes and consequences of the changes. The high-latitude ecosystems, i.e., boreal forests and tundra, play an important role in the climate system (e.g., Bonan et al. 1995). Improved understanding of the role requires concerted research efforts to be conducted over a long enough time-period to detect and quantify ecosystem feedbacks (Chapin et al. 2000). The so-called "missing sink" in the global carbon balance emphasizes a need for satellite analysis (e.g., Myneni et al. 2001), which offers much improved information on changes in the tundra-taiga transitional zone and on forest structure in this area (Rees et al. 2002).

The tundra-taiga transition area is dynamic because it is very sensitive to human activity and climate change. During the last 6,000 years, Northern Eurasia has experienced a general cooling trend of about 2–4°C and larch and birch stands retreated 400–500 km southward during this period (Callaghan et al. 2002b). Global average surface air temperatures have risen by more than 0.5°C since the mid nineteenth century (Briffa et al. 1996) and temperatures have warmed by as much as 2°C in the past three decades in parts of the Northern Hemisphere (Hansen et al. 1999). According to recent climatic scenarios, air temperature and the amount of precipitation in the north of Siberia may increase by 4–6°C and approximately 25%, respectively, by the year 2100 (Gordon et al. 2000; IPCC 2007). If it is assumed that growth and reproduction are controlled by temperature, a rapid advance of the tree line would be predicted (Grace et al. 2002). The northward movement of tundra-taiga boundary may be the eventual outcome if climatic warming persists over centuries or millennia (Skre et al. 2002). Some studies predict that up to about one half of the tundra could be colonized by trees by 2100 (Callaghan et al. 2002b; Harding et al. 2001).

Though each taiga-tundra transition is sensitive to a unique combination of controlling factors (Epstein et al. 2004; Holtmeier and Broll 2005), there is general agreement that the temperature is of major importance in determining the northern extent of the boreal forest. Widespread degradation of permafrost has been shown in numerous studies (Osterkamp and Romanovsky 1996; Pavlov 1994). Observations by Siberian and other scientists suggest that the taiga forests are into the tundra, an indicator of climate warming (e.g., Kharuk and Fedotova 2003; Kharuk et al. 2004, 2006, 2008). In a case study conducted by Rees et al. (2002) in a portion of the West Siberian plain (66.5°N, 70.75°E) from 1968 to 1997, seven of their 20 test sites showed colonization by advancing forests, one showed an inconclusive shift in the treeline, and one test site, surrounded by water and wetlands, showed evidence of forest retreat. The remaining 11 sites showed no appreciable forest advance but four of these sites had developed denser forest cover. In studies of the Polar Ural mountains, Kharuk et al. (2003) found that during the period between 1968 and 1989 the crown closure of stands increased considerably (4–5 times), and the tree line boundary moved 100–300 m into tundra zone. The tree invasion into tundra area is a slow process and is limited by low larch seeds fertility (about 5–7%) and the radius of the seeds dispersion. Those changes were attributed to the vegetation growth period and precipitation increase. These observations are consistent with those in northern Canada, where the primary effect of climate warming has been on

tree density, and there have been only minor changes in the advance of the tree line (Payette and Gagnon 1985). Research on this subject has revealed that during the past 100–150 years white spruce density increased in forest tundra ecotone stands in western, central and eastern Canada, but without any significant displacements of the arctic tree line (Payette et al. 2001). A study of the forest-tundra boundaries in two areas of northern Canada using Landsat imagery has also confirmed that the boreal forest extents in the areas remain basically stable (Masek 2001).

In response to global warming, the directions of vegetation change may take place at the site level depending on local species and environmental conditions. The situation is further complicated by human activities that have led to ecosystem degradation in this area. In some case studies (Virtanen et al. 2002; Vlassova 2002; Toutoubalina and Rees 1999; Rees et al. 2003; Hagner and Rigina 1998), southward displacement of the tundra-taiga boundary was reported due to human disturbance and increasing water-logging, which led to paludification and the death of treeline trees. Local variations in climate and human activities require continued monitoring and research. The transition from taiga to tundra is characterized by a change in tree-cover density and is determined by forest gradients related to the presence of the landscape such as rivers, bogs, and uplands. The tundra-taiga boundary is not a distinct edge but a transition area where patches of tundra and forest are mixed. Because the boundary is not clearly defined, it is obvious that the change of this transition zone is also difficult to quantify. Rees et al. (2002) presented several case studies for characterization and monitoring of tundra-taiga interface in Russia using Landsat and Synthetic Aperture Radar (SAR) data and the potential and limitations of the remote sensing technology. While optical remote sensing technology has been reasonably well established for delineation of different vegetation types, rapid phenological change is still a source of confusion when comparing images collected at different dates. Furthermore, the frequency of cloud cover at high latitudes makes the acquisition of visual and infrared images difficult. It is generally accepted that at a regional scale, in order to get images within a week of the peak of the growing season each year for monitoring the transition zone, we are limited to the instruments with wide swaths such as Advanced Very High Resolution Radiometer (AVHRR), SPOT VEGETATION, Medium Resolution Imaging Spectrometer (MERIS), Moderate Resolution Imaging Spectroradiometer (MODIS), Multiangle Imaging SpectroRadiometer (MISR), Wide Field-of-view Sensor (WIFS), etc. Radar, due to its all-weather capability and sensitivity to forests, provides an alternative to optical technology. However, the image speckle and the sensitivity of radar image to terrain, surface roughness and moisture may cause confusion between forests and rough surfaces, especially at short wavelengths (Bourgeau-Chavez et al. 2002). Stow et al. (2004) gave an overview of multitemporal remote sensing and the special challenges and opportunities for land-cover change applications in the Arctic, and presented a series of case studies with a range of spatial resolution from 1 m to 10 km, spatial extents from 100 m to circumpolar, and time duration from months to 20 years. These studies have showed that the climatically induced changes in vegetation cover and composition in Arctic need to be monitored at different spatial scales.

There is an increasing amount of evidence for the expansion of trees to the tundra at both latitudinal and altitudinal limits of tree growth and for an increase in the canopy density and radial tree increment in sub-tundra forests in the last decades of the twentieth century (Vaganov et al. 1999; Suarez et al. 1999; Skre et al. 2002; Lloyd and Fastie 2002; Kharuk and Fedotova 2003; Kharuk et al. 2004; 2006; Shiyatov et al. 2005; Gamache and Payette 2005). The response of trees to climatic changes should be more distinct in the zone where temperature is the limiting factor, i.e., in the forest-tundra ecotone at the northern boundary of tree growth. In Asia, this boundary is formed by larch stands, which include the world's northernmost forest range in the Ary-Mas area (72°28′N, 101°40′E). Tracing the influence of climatic trends on the dynamics of vegetation involves an analysis of long-term series of observations on test plots combined with dendrochronological data (Shiyatov et al. 2005). Time series of satellite images offer additional opportunities for such an analysis. They allow specialists to reveal changes in plant cover and use the results of on-ground observations for extrapolations at regional and sub-global levels (Myneni et al. 1997; Kharuk et al. 2004).

Ground studies and remote sensing analysis are required to develop techniques to identify the establishment of taiga species in traditional tundra areas. The response of forest-tundra larch forests (exemplified by the Ary-Mas forest range) to climatic trends using the data of on-ground surveys and satellite images were analyzed in this study. We have examined the capabilities of several types of remote sensing data for identifying the existing tundra-taiga transition zone (Ranson et al. 2004a). A Landsat-7 Enhanced Thematic Mapper Plus (ETM+) image and IKONOS image both acquired on July 17, 2002, were used to develop a base map of the study area and other remote sensing data (SAR, MISR and MODIS) were compared to this base map.

4.2 Study Area and Data

4.2.1 Study Site

The study area extends from 72°02′ to 72°40′N and from 101°15′ to 102°06′E including the Ary-Mas forest itself and larch forests on southeastern slopes descending to the Khatanga River. Figure 4.1 is a map of the area showing the study site location and general cover types from 1990 Russian forest survey. Ary-Mas area is a reserve and is recognized as the farthest north known area that supports tree growth (Kharuk et al. 2004). The local elevation and hydrology affect the tree distribution, including dendritic patterns along the river valleys. There is usually no abrupt change between forest and tundra since trees often colonize an area and slowly increase in crown cover.

The Ary-Mas forest occupies terraces on the right bank of the Novaya River at elevations of up to 80 m a.s.l. This unique "forest island" was described for the first time by Tyulina (1937). It extends along the river for about 20 km (Fig. 4.2) and is

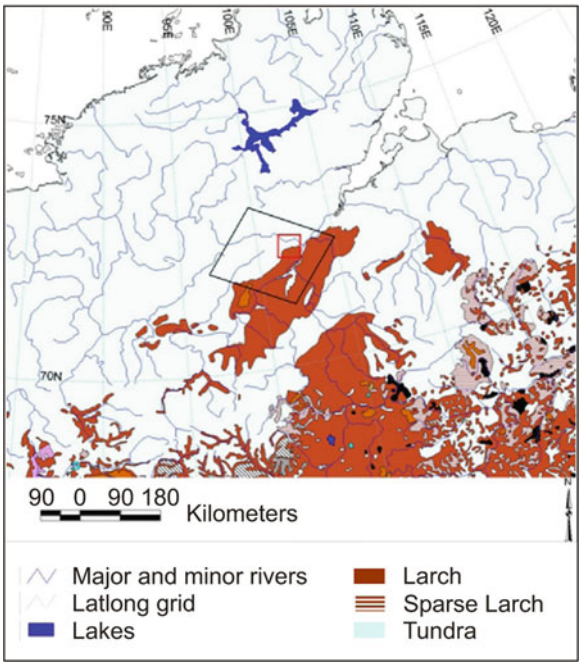

Fig. 4.1 1990 forest-cover map of the Ary-Mas area. The *square* indicates the study area location

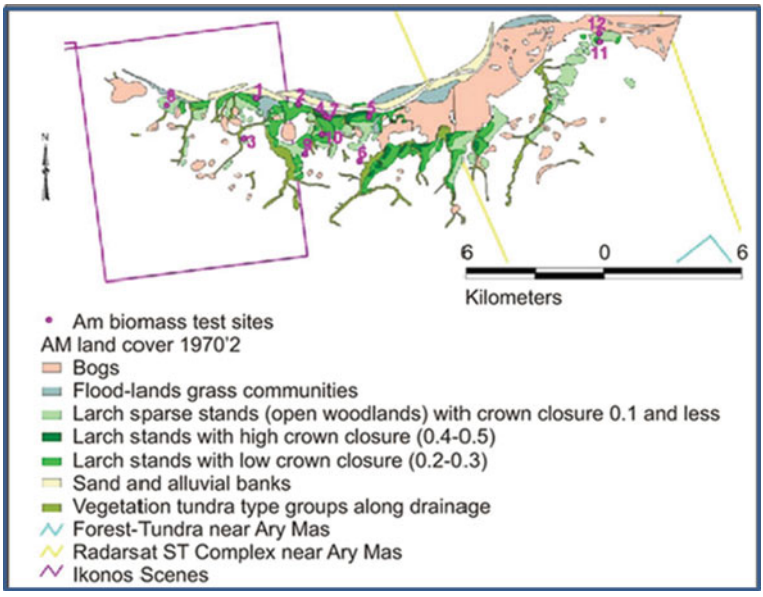

Fig. 4.2 Ary-Mas land cover in 1970s and field samplings in 1969–1971, 1989–1991 and 2000

0.5–1.5 km wide, with sparse trees spreading away from the river, along the valleys of streams, for 3–4 km. On the left bank, tree stands occupy a narrow strip along the river. In the swamp lowland lying on the north, small clusters of larch trees (mainly prostrate forms) occur in sites protected from wind, such as depressions near lakes, at a distance of up to 50–70 km from the Ary-Mas area. Larch (*Larix gmelinii*) is the frontier species in this region. The crown cover of established stands can reach 0.5, while the tree height and diameter average at 5–8 m and 10–14 cm, reaching 10–12 m and 25 cm, respectively. Tree ages can be 50–700 years. Fructification begins when tree age reaches 30 years; and cones are abundant and small (1.5–2 cm) and seed germination rate is relatively low. The density of young tree growth varies from 100 to 2,000 trees ha^{-1}, and the overall average is 200 trees ha^{-1}. The study region has a sharply continental climate with the annual precipitation, evaporation, and average air temperature being approximately 250 mm, 50–100 mm, and −15°C, respectively. The greater part of precipitation falls in summer, with a peak in August. Relative air humidity in summer is 78%. Fogs are rare, because most days are windy. Approximately one-third of the annual precipitation falls in the winter period, with snow cover lasting for approximately 250 days. Snow appears in late September, and melts on elevated areas in the first 10-day period of June, but is often preserved throughout summer on northern slopes and in depressions. Snow depth reaches a peak in April, being 30–50 cm in open areas and 60–70 cm in sites protected from wind. Air temperature in June may reach +29°C, and its monthly average value is +5°C. The period with above-zero temperatures is about 100 days, but subzero temperatures and snow may occur throughout summer. The depth of the ground layer that freezes in winter and thaws in summer is 50–70 cm in mineralized areas (up to 1 m on steep slopes under open forests or sparse trees) and 10–30 cm under the moss cover. In winter, low temperatures combined with strong winds place the Ary-Mas range among Asia's areas with the severest climate. February is the coldest month, with a monthly average air temperature of −31°C and an absolute minimum of −59°C. The average wind velocity in winter is about 5 m s^{-1}. The number of days with blizzards reaches 50 on an approximately average of 20 days per year (Norin 1978).

4.2.2 Remote Sensing Data

Table 4.1 lists the satellite data used in this study. Landsat-7 ETM+ data was acquired on July 17, 2002. Figure 4.3a is the Landsat-7 image with Bands 4 (0.75–0.90 μm), 3 (0.63–0.69 μm), and 2 (0.525–0.605 μm) displayed as red, green and blue, respectively. Taiga appears as red on the right side of the image and is dominated by larch and the left portion of the image is tundra. RADARSAT standard beam data at various incidence angles were acquired in August 2001 (see Table 4.1). Because of the higher backscattering from trees at larger incidence angles (ST5 and ST6), these forested areas appear bright in the image shown in Fig. 4.3b (beam ST6).

MISR (Multi-angle Imaging Spectral Radiometer) is a four spectral band instrument with nine cameras positioned for fore-, aft and nadir Earth viewing. MISR

Table 4.1 List of remote sensing data used in the study

Data	Acquisition date	Characteristics
Landsat-1 MSS	07-26-1973	4 bands: Bands 4–7
Landsat-7 ETM+	07-17-2002	7 bands: Bands 1–7
RADARSAT ST2	08-02-2001	27.74° incidence angle
RADARSAT ST3	08-05-2001	34.10° incidence angle
RADARSAT ST4	08-15-2001	36.56° incidence angle
RADARSAT ST5	08-08-2001	39.22° incidence angle
RADARSAT ST6	08-11-2001	44.14° incidence angle
IKONOS	07-17-2002	B,G,R.NIR, pan
MISR	07-17-2002	MISR reflectance in B,G,R,NIR bands, 9 look angles: DF = 70.5°, CF = 60.0°, BF = 45.6°, AF = 26.1°, AN = 0°, AA = 26.1°, BA = 45.6°, CA = 60.0°, DA = 70.5°
MOD13A1	05-25-2001–10-16-2001	MODIS 500 m 16-day composite NDVI, Red and MIR reflectance products

B – blue band, G – green band, R – red band, NIR – near infrared band, MIR – middle infrared

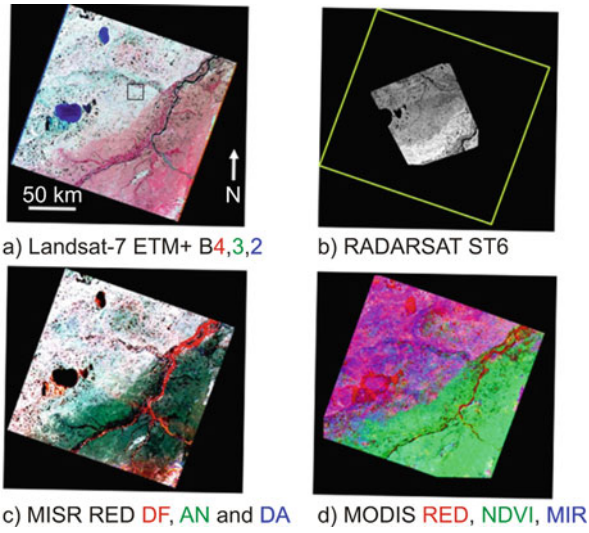

Fig. 4.3 Satellite images of Ary-Mas study site. (**a**) Landsat-7 ETM+ image 17 July 2002: Band 4 (*red*), Band 3 (*green*), Band 2 (*blue*). (**b**) RADARSAT data 11 August 2001: ST 6 (incidence angles 44°). (**c**) MISR *Red channel image* 17 July 2002: DF camera (*red*), AN camera (*green*), and DA camera (*blue*). (**d**) MODIS 500-m 16-day composite 25 May–16 October 2001: spring maximum of *red band reflectance* (*red*), mean of NDVI (*green*), and mean of MIR band reflectance (*blue*)

flies along with MODIS (Moderate Resolution Imaging Spectroradiometer) on the NASA EOS Terra spacecraft (Diner et al. 2002). The MISR data used in this study were acquired on July 17, 2002, a few minutes after the Landsat-7 ETM+ data were acquired. The MISR data were processed using the HDF-EOS Data Format

Converter (HEG) (Raytheon System Co. 2003). Figure 4.3c shows a false color composite image of MISR Red band data acquired at different angles. The forward-looking camera at 70.5° (DF) data is displayed as red, AN (nadir-looking) as green and DA (70.5° backward-looking) as blue. The effect of the composite of three angle images is a clear difference between tundra and taiga in the MISR image.

The multi-temporal MODIS data from the Terra spacecraft (http://terra.nasa.gov/About/) were utilized. The 500-m, 16-day composite data (MOD13A1 product) were acquired from the NASA Earth Observing System (EOS) Land Processes Distributed Active Archive Center. Because the 2002 MODIS data were not yet available processed to Collection 4 at the time this study was conducted, the 2001 data were used. The winter time data were affected by snow cover and low illumination so only data from early spring to fall (March–October) were used. Several statistical indices, such as minimum, maximum, mean and standard deviation was calculated for the spring, summer and fall time series. Figure 4.3d is a false color composite of the MODIS data with spring maximum red reflectance coded as red, Normalized Vegetation Index (NDVI) summer maximum as green, and summer mean MIR reflectance as blue.

The Geoscience Laser Altimeter System (GLAS) data across the taiga-tundra transition zone were also acquired. GLAS instrument aboard the Ice, Cloud, and land Elevation (ICESat) satellite, launched on 12 January 2003 (Zwally et al. 2002). Because of the reduced lifetime of the laser system, GLAS started to use a 91-day repeat orbit, and each time when the laser was turned on, a 33-day sub-cycle data were acquired. From early October to November 19, 2003, GLAS completed the first 33-day sub-cycle using laser 2 (L2A). Since then, several 33-day sub-cycle data sets have been acquired in February–March (L2B), May–June (L2C), October–November (L3A) in 2004, and February–March (L3B), and May–June (L3C) in 2005, and so on. These 33-day sub-cycles are nearly the repeat-passes of the October–November 2003 data (L2A), providing a capability for seasonal and inter-annual change monitoring. The October–November, 2003 data are the best data acquired using the second laser on ICESat. Lidar data provide direct measurements of canopy height, and may be used to characterize various forest structure and disturbances (Ranson et al. 2004b, c; Lefsky et al. 2005; Carabajal and Harding 2005; Simard et al. 2008; Sun et al. 2008; Rees 2007). The waveform vertical height indices from GLAS data acquired in the fall of 2003 from the second laser (L2A) were used to show the changes across the transition zone.

4.2.3 Map and Field Observations

An early land-cover map (Knorre 1972) near Ary-Mas was available along with the field data from sampling plots recorded in 1969–1971, 1989–1991 (see Fig. 4.2). The cover map was generated based on the ground tests plots data and of the 35,000 black/white airborne photography interpretation. In the year 2000 the repeated sampling data were acquired by Sukachev Institute of Forest personnel. However, these data cover only a small part of the area and were used for training and testing

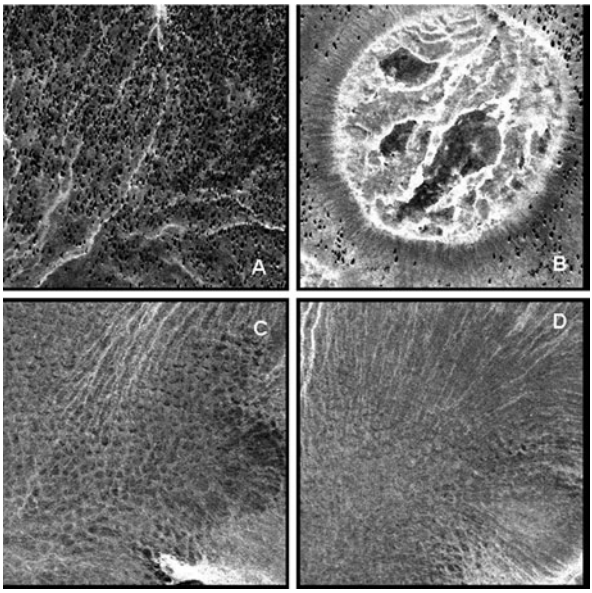

Fig. 4.4 IKONOS 1-m pan images of typical targets in the area. The area imaged by IKONOS is marked by the *black square* on ETM+ images in Fig. 4.3a

purposes. One IKONOS image acquired the same day as the Landsat7 ETM+ data within the area was also used as ground truth. Figure 4.4 shows IKONOS panchromatic images of several typical targets in the area. The densest taiga in the study area was located mainly to the south of this imaged area and is not represented on the IKONOS image. The surface of the tundra is mostly covered by lichen, which has relatively high reflectance. Larch is the only tree species in this area. Because of the low Sun angle in this area, the shadows of trees are elongated and make the area significantly darker than the surroundings. The taiga area presented in Fig. 4.4a is relatively low density (estimated to be ~20% cover using dot-grid counting of the image) and clearly shows the shadows on the tundra background. Bogs have more complex structure and reflectance properties (Fig. 4.4b). Tundra areas (Fig. 4.4c, d) have various surface conditions. The images used as training and testing data in the study also included a panchromatic image made by the Corona system on February 28, 1965 (pixel size 7 × 7 m); and panchromatic aerial photographs made on July 31, 1970, (scale 1:35,000) and on July 27, 1984 (scale 1:15,000). The Corona KH-4A system operated from August 1963 to October 1969, scanning a strip 19.6-km wide and 267-km long with a resolution of 2.7 m.

The earliest data with geo-botanical, pedological, and taxonometric descriptions were obtained in 1969–1971, including the map of the Ary-Mas range, and characteristics of 12 test plots 0.25–1.0 ha in size (Norin 1978). Subsequent taxonometric surveys were made in 1989–1991 and 2000. Core samples taken in ten test plots were used to construct tree-ring chronologies covering the period from

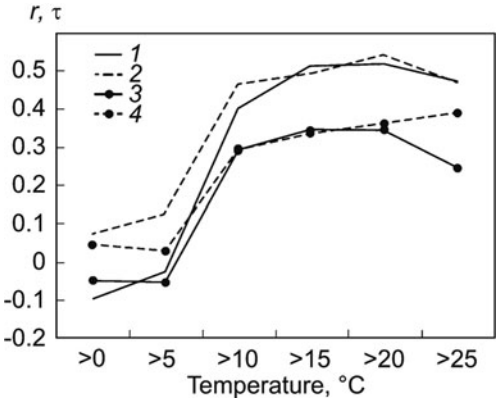

Fig. 4.5 Dependence of the annual ring width index (ARWI) on the number of days with air temperature above the values shown on the abscissa

1900 to 1990. The trend of radial increment was determined as the tangent of the angle between the abscissa and the regression line of the Annual Ring Width Index (ARWI). Data on air temperature and precipitation were obtained from the Khatanga weather station located at a distance of approximately 45 km from the study area. The summer period was assumed to be 3 months, from June to August; the remaining 9 months were conventionally regarded as the winter period. The spring and autumn were not distinguished because of their short duration and variation in the dates of the onset and end of the growing period.

To select a measurement for characterizing the length of the growing period, the following parameters were considered: (1) the number of days with air temperatures exceeding 0, 5, 10, 15, 20, or 25°C; and (2) the sum of temperatures accumulated on the days when air temperature exceeded these values. According to the results of our analysis, ARWI most strongly correlated with the number of days with temperatures above 15°C (Fig. 4.5), and the same was true for the sum of temperatures exceeding this threshold. Hence, the number of days on which temperature rose above 15°C was chosen as a measure of the length of the growing period. As a criterion of the onset of the growing period, we considered the date on which air temperature first rose above 0, 5, or 10°C and the date on which the sum of above-zero temperatures exceeded 100 or 300°C. The response of tree plants (with respect to ARWI and the density of young growth) was observed when the latter parameter exceeded 300°C.

4.3 Methods

4.3.1 Landsat Image Classification and Change Detection

The L-MSS and L-7 images were converted into the same projection and referred to control topographic points, and re-sampled to the same resolution (60 × 60 m) and classified using supervised maximum likelihood method. The position of the forest-tundra boundary was determined from the image made by the Corona system, in which trees stood out against the background of snow due to the shadow they cast,

especially at a low sun angle. A matrix of elevations was used to exclude from analysis the areas lying beyond the altitudinal limits of larch growth (below 5 m and above 80 m a.s.l.).

To generate learning and control samples, we used the map of larch forest types in the Ary-Mas range and aerial photographs. Because of uncertainty in determining the "forest boundary" in the forest-tundra ecotone (Hustich 1953), we classified forest areas by the index of canopy density (CD): (1) sparse stands (L_1, CD < 0.1), (2) open stands (L_2, 0.1 < CD < 0.3), and (3) "normal" stands (L_3, CD > 0.3). Larch stands of the Ary-Mas range are typologically diverse. According to the results of on-ground surveys, they belong to 18 different classes represented on the initial map by 88 categories, each with taxonometric and geobotanical descriptions. In addition to larch stands, eight classes of tundra, four types of bogs, and five classes of dwarf-birch and willow coppice were distinguished in this range. However, as the total area of tundra and bogs on this map was relatively small, the learning samples of the corresponding classes were generated using topographic maps (scale 1:100,000), on which tundra and bogs were better represented. On the whole, we initially distinguished 35 classes, which were subsequently generalized. The resultant classes were as follows: (1) sparse larch stands (L_1); (2) open larch stands (L_2); (3) normal larch stands (L_3); (4) background areas usually devoid of trees, such as tundra, bogs, and open woodland; (5) sand or pebble banks; and (6) water areas. Images were analyzed with regard to both spectral channels and layers corresponding to the slope (α), elevation (h), and azimuth (az) of different elements of relief. The slope proved to be the most informative parameter.

The accuracy of classification was estimated on the basis of a matrix of errors and K-statistics (Rosenfield and Fitzpatric-Lins 1986). In addition to regression analysis, we used Kendall's nonparametric **x** parameter (Nonparametric Statistics 2003). The **x** parameter may assume values from the interval [−1, +1] and is calculated as **x** = (the number of coincidences – the number of non-coincidences)/(the total number of pairs compared). The zero value of **x** indicates the absence of correlation, and values of +1 and −1 correspond to a complete synchrony and asynchrony of the series compared, respectively.

4.3.2 Signatures Across the Taiga-Tundra Transition Zone

The treeless tundra and taiga forest can be visually identified on almost all the channels of the data used, except the RADARSAT data at the steepest angle (ST2). A transect running north to south across the transition zone was used to show the differences in spectral information from various instruments. To zoom into the transition region and compare the changes in images of different sensors, the profiles of the most sensitive channels were registered in space and plotted in the same plot as shown on Fig. 4.6. A vertical line on the plot identifies the center of the tundra-taiga boundary. For each channel, the image value was normalized by the maximum value. The normalized data will range between 0 and 1. These profiles

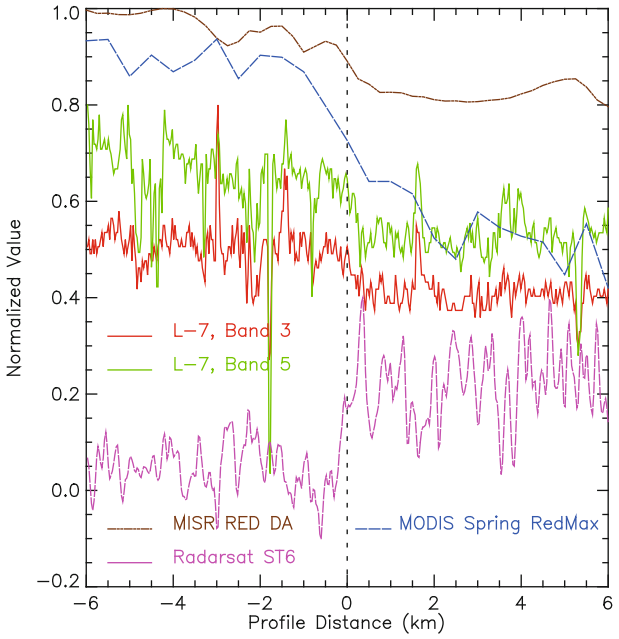

Fig. 4.6 Signature profiles of ETM+, RADARSAT, MISR and MODIS data across a tundra-taiga transition boundary

will be crowded near 1.0 if they were plotted on single plot as they were. The two Landsat-7 curves (bands 3 and 5) were then adjusted down by 0.2, the RADARSAT curves were lowered by 0.6, and the MODIS profile was lowered by 0.1 so these normalized curves can be compared more easily on the plot. Figure 4.7 shows a

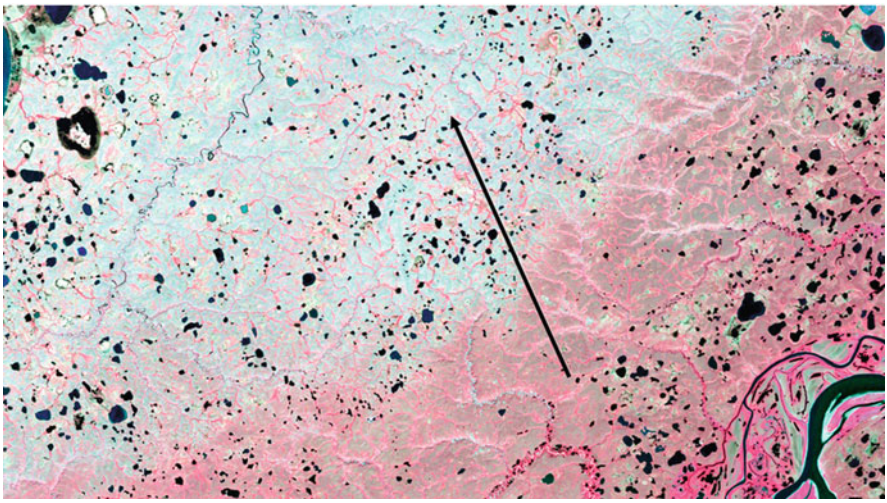

Fig. 4.7 GLAS orbit across the taiga-tundra boundary

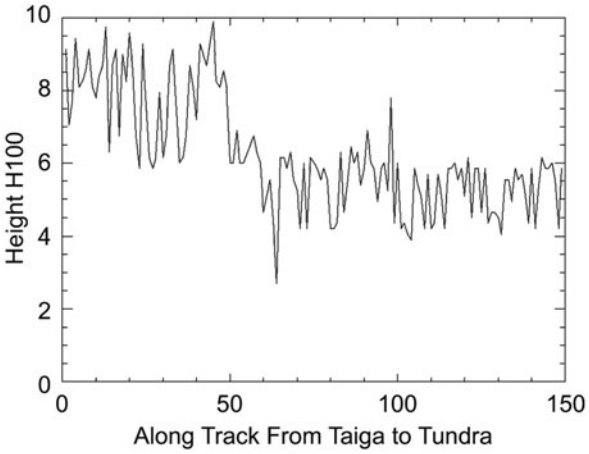

Fig. 4.8 Change of the height of the waveform beginning point above ground surface across the boundary

GLAS orbit passing across the taiga-tundra transition zone. The data was acquired on October 30, 2003. Ground should be covered by snow, but leafless larch trees were above the snow surface. The height from the signal beginning to the surface of GLAS footprints along this ascending orbit plotted in Fig. 4.8 clearly show the changes across the transition zone.

4.3.3 Taiga-Tundra Transition Area Mapping from Landsat ETM+

As we have mentioned in the introduction, the tundra-taiga transition is a gradual change from dense taiga to taiga with patches of tundra, then to tundra with patches of taiga, and finally to pure treeless tundra. The tree stem density also gradually changes across the transitional zone. Characterizing this zone requires information on tree density of the taiga stands and on the spatial patterns of the tundra-taiga mosaic structure. Because of the spatial resolution limitation of remote sensing data used in this study, spectral linear unmixing was used.

Figure 4.4a illustrates that a taiga forest stand may be considered as trees (mainly the shadows) over the tundra background. Even for the dense stands in this area, the crown closure is relatively low. Therefore the crown shadow is always a significant factor in determining the target signature. Two end members, i.e., the dense forest stand and treeless tundra will be used in the unmixing. However, areas of not typically tundra and taiga land cover types need to be identified and excluded from the spectral unmixing.

The Landsat 7 ETM+ image was classified into categories found in this area using a supervised classifier (Maximum-Likelihood Classifier, MLC). These classes include water bodies (lakes and rivers), taiga (larch forest), tundra, bogs (shrubs and

grass cover), riparian vegetation, and sand bars. IKONOS data and a land-cover map were used in locating training sites. A mask image, which excludes all non-forest and non-tundra pixels, was developed from the ETM+ classification. This mask image was later used in processing of RADARSAT, MISR and MODIS data. The taiga and tundra end-members were located in the Landsat 7 ETM+ image based on the classification and image tones, and linear spectral unmixing technique was applied to all pixels of the 7-band ETM+ selected by the mask image.

Linear spectral unmixing methods have been increasingly applied in the remote sensing community to resolve the sub-pixel mixture information (Sabol et al. 2002). An important step in spectral unmixing is to identify the end-member and obtain the spectra of these end-members. Common practice is to obtain the end-member spectra manually from certain small regions in remote-sensing imagery, and then use the least-squares method to estimate the cover class proportion for each pixel (Hu et al. 1999). Researchers have found that the most uncertainty of the unmixing results arose from the end-member creation, not from the least-square method (Sohn and McRoy 1997). The end-member selection is the crucial step in the spectral unmixing, and some techniques such as the selection scheme by Saghri et al. (2000) have been developed to ensure the quality of end-members.

The number of the end-members should be less than (or equal) the data channels. The limiting number of useful channels for the sensors used here was three for RADARSAT. In order to study the tundra-taiga boundary by identifying the changes of tree coverage across the transition zone, two end-members, i.e., tundra and taiga were used. All the pixels, which do not belong to tundra or taiga based on the MLC classification discussed above were excluded from analysis. The taiga end-member represents the targets with densest trees in the study area. The abundance of taiga, therefore, does not necessarily mean the actual percentage of tree crown cover.

Both category types were selected from homogeneous area, avoiding river valleys. Because the unit sum constraint was applied, the sum of the abundances of tundra and taiga should be 1.0. The abundance should be in the range of 0–1.0 in ideal situations. Actually, these values could also be negative, or larger than 1.0 because of errors in the solutions of the linear equations. The linear spectral unmixing determines the relative abundance of the end. Only the abundance of taiga was used in the analysis. The linear spectral unmixing routine available from Research Systems Inc. (2002) was used for this analysis.

4.3.4 Mapping of the Transition Zone Using Other Satellite Data

4.3.4.1 RADARSAT Data

The RADARSAT standard beam data (beams 2, 3, 4, 5 and 6) were received in a complex format from the Alaska Science Facility. At the Goddard Space Flight Center, the data were converted from complex format to power, multi-looked by 6×6 pixels using the ENVI software. Then, the data were converted from slant to ground range using the altitude of the platform and the near slant range distance. Finally, data were filtered using a 5×5 gamma filter, which reduces speckle

while preserving edges in radar images (Shi and Fung 1994). Since the Ary Mas area does not have a strong topographic gradient, no ortho-rectification was performed. The ground range SAR data then were registered to Landsat-7 ETM+ image manually with accuracy within two pixels. Since the radar images have been co-registered with ETM+ image, the tundra-taiga mask image, and the locations of the two end-members were directly used in linear spectral unmixing of the RADARSAT image data.

4.3.4.2 MISR and MODIS Data

MISR (Diner et al. 2002) red band data (9 cameras) were re-sampled into 30-m pixels size and the overlapping area with the Landsat-7 ETM+ image was extracted. Only the red band data were used for further analysis for the following reasons: (1) the purpose of using MISR data was mainly to investigate the capability of multi-angle data for tundra-taiga zone mapping, (2) most cameras at the other bands have images with pixel size of 1.1 km instead of 275 m, and (3) the red band is useful to show the differences between taiga and tundra. The Terra MODIS science products received included a time series of Normalized Vegetation Index (NDVI), Enhanced Vegetation Index (EVI), and spectral reflectance of blue (channel 4), red (channel 1), Near Infrared (NIR), (channel 2) and Middle Infrared, (MIR channel 7). Only the NDVI, red and MIR data were used. For each time series, the minimum, maximum, mean and standard deviation in spring, summer and fall were calculated. By checking these channels (a total of 12 for each series), six channels, which showed promise in discrimination between tundra and taiga, were selected. They were summer minimum and mean of NDVI, summer mean and spring maximum of red reflectance, summer maximum and mean of MIR reflectance. These data were also re-sampled to 30 m and the overlapping area with ETM+ data was extracted. The tundra-taiga mask image and the two end-members were used in the linear spectral unmixing of the MISR and MODIS image data. Figure 4.6 presents the relative abundance of taiga resulting from linear spectral unmixing.

4.4 Spatial Patterns of the Transition Zone

To reveal the patterns of tundra-taiga composition in the transitional zone, the percentage of taiga was calculated within a moving window. The relative abundance images of taiga generated by linear spectral unmixing (Fig. 4.6) have a 30-m pixel size. The original data has different pixel sizes (i.e., 25 m for RADARSAT SAR data, 30 m for ETM+, 275 m for MISR and 500 m for MODIS data), these results were difficult to compare directly. We used a window of 33 by 33 pixels, and calculated the abundance of taiga within the window. If the center pixel was masked out during the process, the new pixel value was set to the value representing the background. The linear spectral unmixing process produced about 0.5% pixels with negative values for the abundance of the taiga. These values were set to zero (tundra) when calculating the average abundance in the moving window. Therefore the

average abundance will be the sum of all positive values in the window and divided by the number of pixels that was not masked out during the linear spectral unmixing. The resulting images still have a pixel size of 30 m, but represent the information in a 1-km (990-m) window. These results are more comparable since the information they show is at a similar spatial scale. Figure 4.7 shows the relative abundance of taiga from ETM+, SAR, MISR and MODIS at the 1-km scale. The abundance profiles were also calculated across the boundary using various windows.

4.5 Results

4.5.1 Landsat Image Classification and Change Detection

The accuracy of classification could be regarded as satisfactory: 60% ($\mathbf{K} = 0.47$) for the L-MSS image (1973) and 66% ($\mathbf{K} = 0.49$) for the L-7 image (2000). The numerical indices in Tables 4.2 and 4.3 show the characterization of the dynamics of classes L_1–L_3 during the same period. The most significant changes were observed in the class of normal larch stands (CD > 0.3): their area increased by 66% (Table 4.2). The areas of open and sparse forests ($0.1 < CD < 0.3$ and $CD < 0.1$) increased by 16 and 8%, respectively, whereas the background area became 19% smaller.

Table 4.3 shows a matrix of transitions between the classes for the period between 1973 and 2000, with their areas in the 2000 map shown as percentages of those in the 1973 map. For example, the area of class "normal stands" in the 2000 map consists of the following classes delimited in the 1973 map: normal stands, 44.4%; open stands, 17.2%; sparse stands, 5.4%; and background areas, 36.9%. This is indicative of a transition to stands with increasing density (from sparse to open and from open to normal stands), with background areas turning into sparse stands. However, a considerable proportion of class "normal stands" in the 2000 map (36.9%) originated from the background class of the 1973 map. This could not be attributed to a classification error alone, as the background class in the 2000 map included only 2% of the normal stand class delimited on the 1973 map. Apparently, the background class (tundra, bogs, and open woodland) also included areas with the presence of larch. According to the results of on-ground surveys, individual trees may occur at

Table 4.2 Dynamics of land classes in the Ary-Mas range from 1973 to 2000

Class	S_1 (ha) (t_1, 1973)	S_2 (ha) (t_2, 2000)	A_1 (ha) (S_2-S_1)	A_2 (%) $(S_2-S_1)/S_1$	A_2 (%/year) (t_2-t_1)
Sparse (L_1)	17,883	19,264	1,381	+8	0.29
Open (L_2)	13,887	16,133	2,245	+16	0.60
Normal (L_3)	9,415	15,601	6,186	+66	2.43
Background	51,654	41,842	−9,812	−19	−1.12

Table 4.3 Dynamics of transitions between land classes in the Ary-Mas range from 1973 to 2000

	Areas of classes in 2000 relative to those in 1973, %			
Class in 1973 (MS composite)	Normal stands (L3)	Open stands (L2)	Sparse stands (L1)	Background
Normal stands (L3)	40.4	11.5	2.1	2.0
Open stands (L2)	17.2	34.4	12.5	7.7
Sparse stands (L1)	5.4	16.5	29.1	21.0
	36.9	37.6	56.3	69.3
Background Total	100	100	100	100

considerable distances (over 500 m) from the zone of open forests. In the zone of transition from sparse stands to the tundra, fructifying prostrate forms of larch prevail. Such plants may have up to 10–20 stems aged more than 100 years, with the root system being older than the above-ground plant parts. Under favorable conditions, prostrate larch plants can form large clusters, and this fact may account for the transition of some areas from the background class to larch stand classes.

We estimated change in the area of larch stands (classes L_1, L_2, and L_3) and the rate of displacement of their boundaries (i.e., the velocity of expansion v) over the period between 1973 and 2000. Data on the average annual change in stand areas are shown in Table 4.2. The greatest and smallest changes were characteristic of denser (normal) and sparse stands (2.43 and 0.29%), with open stands occupying an intermediate position (0.6% per year). The average rate of larch expansion was estimated by approximating the area of each class (L_1–L_3) as a rectangle with one side oriented along the direction of expansion and the side perpendicular to it being equal to the size of the tundra ecotone (approximated by a straight line). This approximation is adequate, as the Ary-Mas range is an elevation with gentle slopes that is shaped like a truncated polyhedron.

Strong winds and a vertical temperature gradient provided for the formation of a relative uniform, linear boundary of larch growth across the slope. As noted above, larch expands up the altitudinal gradient. The length of altitudinal boundary (estimated from the Landsat image at approximately 93 km) was assumed to be equal for all three classes of stands, as they were similarly arranged on the slope after one another. The other (shorter) side of the rectangle was calculated from its area. The difference between these sides showed the displacement of the boundary of larch growth over the period from 1973 to 2000. The rates of this displacement (expansion) for sparse, open, and normal stands were estimated at 3, 9, and 11 m per year, respectively. In all cases, normal larch stands expanded at the highest rate, and sparse stands expanded at the lowest rate. As sparse stands (L_1) are at the forefront of advancement to the tundra, the rate for this class (approximately 3 m per year) should be regarded as the rate of larch expansion in general. It should be noted that the above rates reflect not only the expansion of trees to the tundra, but also an increase in the density of sparse and open stands.

4.5.2 Spectral Signatures Across the Transition Zone

The spectral response from the tundra-taiga ecotone was found to vary with surface and satellite type. The spectral composite images shown in Fig. 4.3 highlight some of these differences. Landsat-7 ETM+ false-color band 4,3,2 combination shows increasing vegetation response from tundra to taiga (diagonally up-left to bottom-right in Fig. 4.3a). Radar backscattering is mostly controlled by plant water content and the surface roughness, therefore the lack of trees makes the tundra appear smoother and thus darker than the taiga (Fig. 4.3b). At a steeper incidence angle (ST2), backscattering from all surfaces is relatively high. When the incidence angle increases (i.e., ST5 and ST6) the backscattering from smoother surfaces, i.e. tundra, decreases. The multi-angle red band image from MISR also shows differences across the transition zone. Here the tundra is relatively bright in all bands, but the forest areas appear darker because of absorption by the larch needles and shadows cast by the trees. Because of Terra's descending orbit and because the solar illumination was coming from the south (~40° elevation, ~180° azimuth), the DF camera received high reflectance from glint off the water surface (seen as red lakes in Fig. 4.3c) while the DA camera was near the hot-spot position. The MODIS data clearly shows the taiga areas against the tundra (lower NDVI and higher red and MIR reflectance).

The profiles of normalized signatures for a set of selected channels in Fig. 4.4 show the capabilities of each sensor for discriminating between forest and non-forest areas. For example, the red and middle-infrared bands of Landsat-7 ETM+ show obvious transition from tundra to taiga. The MISR red band data (especially the AN and the afterward cameras) show a difference between tundra and taiga. Statistical parameters (such as minimum and maximum, mean and standard deviation) of the temporal MODIS data were also found to be useful for tundra-taiga transition zone mapping. The RADARSAT ST6 data shows that the backscattering is lower for smoother tundra surface and higher for the taiga. The ST6 data also shows a great deal of change across the boundary region. In addition to vegetation change, other factors such as elevation, ground surface roughness and hydrological conditions may also play a role here. For the MISR red band, signatures from both forward (DF, not shown) and backward (DA, shown in Fig. 4.6) cameras exhibited more change than the nadir looking image (not shown). Among the nadir looking MISR (275-m resolution) images, the red band shows the most significant change, consistent with Landsat-7 ETM+ data. The change patterns of ETM+ band 3 (red curve) and MISR red band DA image (black curve) are similar. The MODIS maximum red-band reflectance during spring time shows higher values for tundra areas with a sharp decrease across the boundary into the taiga. All the sensor channels shown in Fig. 4.4 recorded a change across the transition zone.

4.5.3 Transition Zone Mapping from Remote Sensing Data

The linear spectral unmixing determines the relative abundance of the end-member within a pixel. The linear spectral unmixing results for ETM+ are shown in Fig. 4.9a.

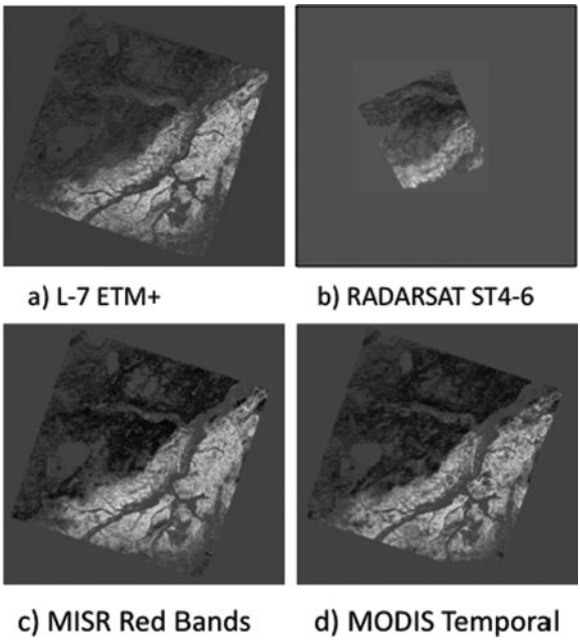

Fig. 4.9 Relative abundance of taiga (0–1.0, *black* to *white*) from linear spectral unmixing of (**a**) Landsat-7 ETM+, (**b**) RADARSAT, (**c**) MISR red band, and (**d**) MODIS temporal data

In this case the results are shown as grey levels of taiga abundance from 0.0 (black) to 1.0 (white). The RADARSAT ST4-6 data, the MISR Red band data for all 9 cameras, and the six MODIS time series data indices were also linearly unmixed to calculate the abundance of taiga forest. These images were re-sampled to 30 m, and the Landsat-7 mask was used to process the same pixels in the overlapped area. These results are shown in Fig. 4.9. The results from the MISR and the MODIS

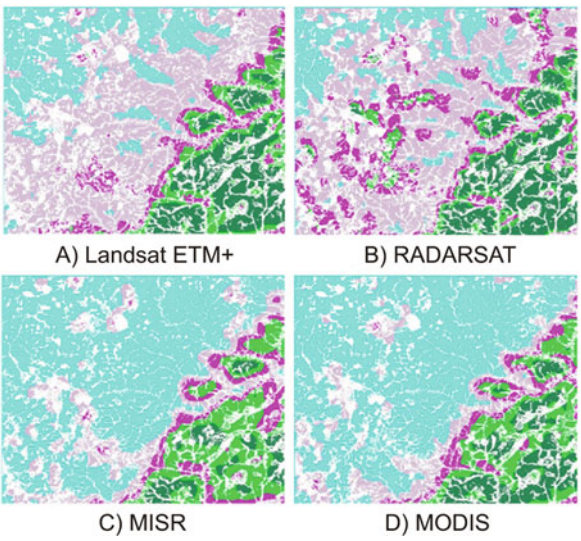

Fig. 4.10 Comparisons of mapped current tundra-taiga transition zone from (**a**) Landsat-7 ETM+, (**b**) RADARSAT multi-beam data, (**c**) MISR red band, and (**d**) MODIS temporal NDVI, *red* and MIR reflectance. Taiga abundance was calculated using a 1-km moving window and color density sliced: ≤ 0.0 (*cyan*), 0.0–0.25 (*thistle*), 0.25–0.5 (*magenta*), 0.5–0.75 (*light green*), and > 0.75 (*dark green*)

data closely resemble the results from the Landsat-7 ETM+ data. Even though the gamma filter has been used to smooth the radar data, the results show more variance, and may include terrain and surface roughness effects.

The taiga abundance calculated using a 1-km moving window and the resulting image was color-density sliced into five classes as shown in Fig. 4.10. The results from both MISR and MODIS data have a similar pattern for the transition zone. This is shown with magenta and thistle colorings in Fig. 4.10.

A comparison of classification results for MODIS, MISR and RADARSAT and Landsat-7 is shown in Tables 4.4, 4.5, and 4.6. The classes used were the density-sliced categories in Fig. 4.10. The L-7 ETM+ results were used as "true" classes. The tundra was accurately identified by MODIS (96.5%) and MISR (96.6%), but not by the SAR (42.7%). This indicates that the treeless tundra area was quite homogeneous in terms of surface reflectance, so the sensor's spatial

Table 4.4 Results of MODIS taiga abundance classification relative to Landsat

Classified as	Class Tundra	0–0.25	0.25–0.5	0.5–0.75	Taiga
Tundra	96.5	82.1	21.4	1.1	0.0
0–0.25	3.47	17.2	35.1	5.1	0.5
0.25–0.5	0.0	0.7	35.7	26.1	2.1
0.5–0.75	0.0	0.0	7.7	54.8	37.0
Taiga	0.0	0.0	0.1	12.9	60.4
Unclassified	0.0	0.0	0.0	0.0	0.0

Table 4.5 Results of MISR taiga abundance classification relative to Landsat

Classified as	Class Tundra	0–0.25	0.25–0.5	0.5–0.75	Taiga
Tundra	96.6	81.9	9.5	0.0	0.0
0–0.25	3.4	17.5	52.7	8.1	0.0
0.25–0.5	0.0	0.6	35.6	44.3	7.0
0.5–0.75	0.0	0.0	2.3	45.8	62.5
Taiga	0.0	0.0	0.0	1.8	30.5
Unclassified	0.0	0.0	0.0	0.0	0.0

Table 4.6 Results of RADARSAT taiga abundance classification relative to Landsat results

Classified as	Class Tundra	0–0.25	0.25–0.5	0.5–0.75	Taiga
Tundra	42.7	7.8	1.2	0.0	0.0
0–0.25	53.0	67.6	39.8	0.9	0.0
0.25–0.5	0.6	21.1	44.7	23.5	0.5
0.5–0.75	0.0	3.1	13.1	37.1	6.2
Taiga	0.0	0.4	1.2	38.4	93.32
Unclassified	3.7	0.0	0.0	0.0	0.0

resolution doesn't matter much. But due to the possible heterogeneity of the surface roughness and moisture contents, and the SAR speckle, many tundra pixels appeared to have some trees, so more than half (53%) of the tundra pixels went to the class with 0−25% taiga. On the other hand, SAR identified most of the taiga pixels (93.3%), but MODIS and MISR did poorly (60.4 and 30.5%, respectively). The rest of the taiga pixels were assigned to the category with taiga abundance of 0.5–0.75. This indicates that at the 1-km scale, the taiga was not very dense and homogeneous, but with patches of tundra or other types of gaps. The accuracy of other classes between tundra and taiga varies. But mostly, they were confused

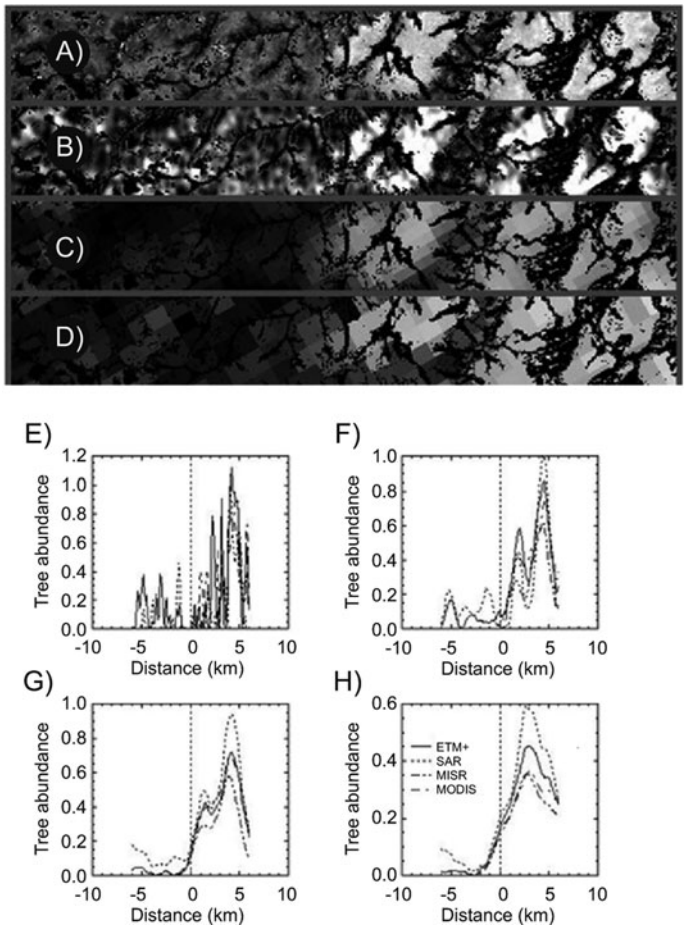

Fig. 4.11 Images (**a**–**d**) show taiga abundances calculated for a transect crossing the tundra-taiga transition from ETM+, RADASAT, MISR and MODIS data, respectively. Taiga abundances are plotted for each data type using various window sizes: (**e**) using a 90-m moving window, (**f**) 510-m window, (**g**) 990-m window, and (**h**) 2,010-m window. The *vertical lines* in images (**a**–**d**) correspond to the *dashed vertical line* in graphs

with the neighboring classes, likely because the class definition between them were arbitrarily selected.

The abundance profiles were also calculated across the boundary using various window sizes. Figure 4.11 shows four of these profiles using window sizes of 90, 510, 990 and 2,010 m, respectively. When the window is small (90 m), both Landsat and SAR show the details of the change, which were not shown in the low-resolution MISR and MODIS data. When the window size is above 500 m, the transition patterns from Landsat, MISR and MODIS were similar.

4.6 Conclusions

This study has shown that data from Landsat-7 ETM+, MISR red band multi-angle data, MODIS time series data, and RADARSAT large-incidence angle images are all sensitive to the surface and vegetation structure change in tundra-taiga transition zone in our study area. The location of the transition zone from images with very different spatial resolutions was consistent. Global coverage available from RADARSAT may be used to analyze where high resolution is required and cloud cover or low illumination precludes the use of Landsat-like data. Current Landsat-7 coverage problems caused by the scan line corrector malfunction make this option especially useful. For MISR, the utility may be limited by frequent cloud cover and the infrequent coverage of MISR. The results suggest that MODIS may be an appropriate tool for longer term monitoring of the ecotone when Landsat data or other high or moderate resolution data is available for training purposes. The 500-m data sets used in this study provided useful information, but more work is needed. Further studies will reveal the effectiveness of 250-m two-channel MODIS data sets. Our future studies will include mapping and characterization of other parts of this transition zone from these remotely sensed data.

In Ary-Mas, the world's northernmost forest range, an increase in the density of larch stands (by approximately 65%) and the expansion of larch to the tundra (for 3–10 m per year) were recorded in the late twentieth century. This effect, being induced by climatic trends, depends on orographic features of the study area. Larch is now expanding to areas poorly protected from winds due to their topographic features (elevation, azimuth, and slope). According to the present-day scenarios of climate change (IPCC 2007), this process will result in the expansion of larch to the Arctic coast, the phenomenon that took place in the Holocene. On the other hand, the zone dominated by larch is invaded by dark coniferous species (Siberian stone pine, spruce, and fir) entering from the south and west (Kharuk et al. 2005).

References

Bonan GB, Chapin FS, Thompson SL (1995) Boreal forest and tundra ecosystems as components of the climate system. Clim Change 29(2):145–167

Bourgeau-Chavez LL, Kasischke ES, Brunzell S, Mudd JP, Tukman M (2002) Mapping fire scars in global boreal forests using imaging radar data. Int J Rem Sens 23(20):4211–4234

Briffa KR, Jones PD, Schweingruber FH, Karlen W, Shiyatov SG (1996) Tree-ring variables as a proxy-climate indicators: problems with low-frequency signals. In: Jones PD, Bradley RS, Jouzal J (eds) Climate variations and forcing mechanisms of the last 2000 years. NATO ASI Series, I, Global Environmental Change, vol 41. Springer, Berlin, p 649

Callaghan TV, Crawford RMM, Eronen M, Hofgaard A, Payette S, Rees WG, Skre O, Sveinbjornsson B, Vlassova TK, Werkman BR (2002b) The dynamics of the tundra-taiga boundary: an overview and suggested coordinated and integrated approach to research. AMBIO Spec Rep 12:3–5

Callaghan TV, Werkman BR, Crawford RMM (2002a) The tundra-taiga interface and its dynamics: concepts and applications. AMBIO Spec Rep 12:6–14

Carabajal CC, Harding DJ (2005) ICESat validation of SRTM C-Band digital elevation models. Geophys Res Lett 33:L22S01

Chapin FS III, McGuire AD, Randerson J, Pielke R, Baldocchi D, Hobbie SE, Roulet N, Eugster W, Kasischke E, Rastetter EB, Zimov SA, Running SW (2000) Arctic and boreal ecosystems of western North America as components of the climate system. Glob Change Biol 6: 211–223

Devi N, Hagedorn F, Moiseev P, Bugmann H, Shiyatov S, Mazepa V, Rigling A (2008) Expanding forests and changing growth forms of Siberia larch at Polar Urals treeline during the 20th century. Glob Chang Biol 14(7):1581–1591

Diner DJ, Beckert JC, Bothwell GW, Rodriguez JI (2002) Performance of the MISR instrument during its first 20 months in Earth orbit. Trans Geosci Rem Sens 40(7):1449–1466

Epstein HE, Beringer J, Gould WA, Lloyd AH, Thompson CD, Chapin FS, Michaelson GJ, Ping CL, Rupp TS, Walker DA (2004) The nature of spatial transitions in Arctic. J Biogeogr 31(12):1917–1933

Gamache I, Payette S (2005) Latitudinal response of subarctic tree lines to recent climate change in eastern Canada. J Biogeogr 32(5):849–862

Gordon C, Cooper C, Senior C, Banks H, Gregory JM, Johns TC, Mitchell JFB, Wood RA (2000) The simulation of SST, sea-ice extents, and ocean heat transport in a version of the Hadley Centre Coupled Model without flux adjustments. Clim Dyn 16:147–168

Grace J, Berninger F, Nagy L (2002) Impacts of climate change on the tree line. Ann Bot 90(4):537–544

Hagner O, Rigina O (1998) Detection of forest decline in Monchegorsk area. Rem Sens Environ 63(1):11–23

Hansen J, Ruedy R, Glascoe J, Sato M (1999) GISS analysis of surface temperature change. J Geophys Res 104:30997–31022

Harding R, Kuhry P, Christensen TR, Sykes MT, Dankers R (2001) Climate feedbacks at the taiga/tundra interface. AMBIO Spec Rep 12:47–55

Holtmeier FK, Broll G (2005) Sensitivity and response of northern hemisphere altitudinal and polar treelines to environmental change at landscape and local scales. Glob Ecol Biogeogr 14(5):395–410

Hu YH, Lee HB, Scarpace FL (1999) Optimal linear spectral unmixing. Trans Geosci Remote Sens 37(1):639–644

Hustich I (1953) The boreal limits of conifers. Arctic 6:149–62

IPCC (2007) Climate change 2007: synthesis report. Valencia, 12–17 November 2007

Kharuk VI, Dvinskaya ML, Im ST, Ranson KJ (2008) Tree vegetation of the forest-tundra ecotone in the Western Sayan Mountains and climate trends. Russian J Ecol 39(1):8–13

Kharuk VI, Dvinskaya ML, Ranson KJ, Im ST (2005) Expansion of evergreen conifers to the larch-dominated zone and climatic trends. Russian J Ecol 3:186–193

Kharuk VI, Fedotova EV (2003) Forest-Tundra ecotone dynamics. In: Bobylev LP, Kondratyev KY, Johannessen OM (eds) Arctic environment variability in the context of global change. Springer, Heidelberg, pp 281–299

Kharuk VI, Im ST, Ranson KJ, Naurzbaev MM (2004) Temporal dynamics of larch in the forest-tundra ecotone. Dokl Earth Sci 398(7):1020–1023

Kharuk VI, Ranson KJ, Im ST, Naurzbaev MM (2006) Forest-tundra larch forests and climate trends. Russian J Ecol 37(5):291–298

Knorre AA, Kirdyanov AV, Vaganov EA (2006) Climatically induced interannual variability in aboveground production in forest-tundra and northern taiga of central Siberia. Oecologia 147(1):86–95

Knorre AV (1972) The generalized sketch-map of the Ary-Mas larch forest. In: Report on the geobotany, forests, climate and dendrochronology investigations in the Ary-Mas area. The Central Committee on the Reserves at Russian Federation Government, and the Botany Institute of Russian Academy of Sciences, Leningrad, p 99

Lefsky MA, Hudak AT, Cohen WB, Acker SA (2005) Geographic variability in lidar predictions of forest stand structure in the Pacific Northwest. Remote Sens Environ 95(4):532–548

Lloyd A, Fastie C (2002) Spatial and temporal variability in the growth and climate response of treeline trees in Alaska. Clim Change 52:481–509

Masek JG (2001) Stability of boreal forest stands during recent climate change: evidence from Landsat satellite imagery. J Biogeogr 28(8):967–976

Myneni RB, Dong J, Tucker CJ, Kaufmann RK, Kauppi PE, Liski J, Zhou L, Alexeyev V, Hughes MK (2001) A large carbon sink in the woody biomass of northern forests. Proc Natl Acad Sci USA 98(26):14784–14789

Myneni RB, Keeling CD, Tucker CJ, Asrar G, Nemani RR (1997) Increase in plant growth in the Northern High Latitudes from 1981– 1991. Nature 386:698–702

Norin BN (ed) (1978) Ary-Mas: environment conditions, flora and vegetation of the most northern forest area in the world. Nauka, Leningrad, p 192

Osterkamp TE, Romanovsky VE (1996) Impacts of thawing permafrost as a result of climatic warming. EOS Trans AGU 77(46):F188

Pavlov AV (1994) Current changes of climate and permafrost in the Arctic and Sub-Arctic of Russia. Permafrost and Periglacial Process 5:101–110

Payette S, Fortin M, Gamache I (2001) The subarctic forest-tundra: the structure of a biome in a changing climate. BioScience 51(9):709–718

Payette S, Gagnon R (1985) Late Holocene deforestation and tree regeneration in the forest–tundra of Quebec. Nature 313:570–572

Ranson KJ, Sun G, Kovacs K, VI Kharuk VI (2004a) Assessing tundra-taiga boundary with multi-sensor satellite data. Remote Sens Environ 93:283–295

Ranson KJ, Sun G, Kovacs K, Kharuk VI (2004b) Landcover attributes from ICESat GLAs data in central Siberia. IGARSS 2004 Proceedings, Anchorage, 20–24 September 2004

Ranson KJ, Sun G, Kovacs K, Kharuk VI (2004c) Use of ICESat GLAS data for forest disturbance studies in central Siberia. IGARSS 2004 Proceedings, Anchorage, 20–24 September 2004

Raytheon System Co (2003) HDF-EOS data format converter (HEG) users guide, v 1.0, Technical Paper 170-TP-013-001

Research Systems Inc (2002) ENVI user's guide, version 3.4. Boulder, p 930

Rees WG (2007) Characterization of Arctic treelines by LiDAR and multispectral imagery. Polar Rec 43(227):345–352

Rees WG, Brown I, Mikkola K, Virtanen T, Werkman B (2002) How can the dynamics of the tundra-taiga boundary be remotely monitored? AMBIO Spec Rep 12:56–62

Rees WG, Williams M, Vitebsky P (2003) Mapping land cover change in a reindeer herding area of the Russian Arctic using Landsat TM and ETM+ imagery and indigenous knowledge. Remote Sens Environ 85(4):441–452

Rosenfield GH, Fitzpatric-Lins K (1986) A coefficient of agreement as a measure of thematic classification accuracy. Photogramm Eng Remote Sens 52(2):223–227

Sabol DE, Gillespie AR, Adams JB, Smith MO, Tucker CJ (2002) Structural stage in Pacific Northwest forests estimated using simple mixing models of multispectral images. Remote Sens Environ 80(1):1–16

Saghri JA, Tescher AG, Jaradi F, Omran M (2000) A viable end-member selection scheme for spectral unmixing of multispectral satellite imagery data. J Imag Sci Technol 44(3):196–203

Shi Z, Fung KB (1994) A comparison of digital speckle filters. Proceedings of IGARSS'94, New York, pp 2129–2133

Shiyatov SG, Terentjev MM, Fomin VV (2005) Spatiotemporal dynamics of Forest-Tundra communities in the Polar Urals. Russian J Ecol 36(2):83–90

Simard M, Rivera-Monroy VH, Mancera-Pineda JE, Castaneda-Moya E, Twilley RR (2008) A systematic method for 3D mapping of mangrove forests based on Shuttle Radar Topography Mission elevation data, ICEsat/GLAS waveforms and field data: application to Cienaga Grande de Santa Marta, Colombia. Remote Sens Environ 112(5):2131–2144

Skre O, Baxter R, Crawford RMM, Callaghan TV, Fedorkov A (2002) How will the tundra-taiga interface respond to Climate Change? AMBIO Spec Rep 12:37–46

Sohn YS, McCoy RM (1997) Mapping desert shrub rangeland using spectral unmixing and modeling spectral mixture with TM data. Photogramm Eng Remote Sens 63(6):707–716

Stow DA, Hope A, McGuire D, Verbyla D, Gamon J, Huemmrich F, Houston S, Racine C, Sturm M, Tape K, Hinzman L, Yoshikawa K, Tweedie C, Noyle B, Silapaswan C, Douglas D, Griffith B, Jia G, Epstein H, Walker D, Daeschner S, Patersen A, Zhou L, Myneni R (2004) Remote sensing of vegetation and land-cover change in Arctic tundra ecosystems. Remote Sens Environ 89(3):281–308

Suarez F, Binkley D, Kaye MW, Stottlemyer R (1999) Expansion of forest stands into Tundra in the Noatak National Preserve, Northwest Alaska. Ecoscience 6(3):465–470

Sun G, Ranson KJ, Kimes DS, Blair JB, Kovacs K (2008) Forest vertical structure from GLAS: an evaluation using LVIS and SRTM data. Remote Sens Environ 112(1):107–117

Toutoubalina OV, Rees WG (1999) Remote sensing of industrial impact on Arctic vegetation around Noril'sk, northern Siberia: preliminary results. Int J Remote Sens 20(15–16):2979–2990

Tyulina LN (1937) Forest vegetation near its Northern limit in the Khatanga region. Trudy Arkticheskogo instituta (Proc Arctic Inst) 63(Geobotanika):83–180

Vaganov EA, Hughes MK, Kirdyanov AV, Schweingruber FH, Silkin PP (1999) Influence of snowfall and melt timing on tree growth in Subarctic Eurasia. Nature 400:149–151

Virtanen T, Mikkola K, Patova E, Nikula A (2002) Satellite image analysis of human caused changes in the tundra vegetation around the city of Vorkuta, north-European Russia. Environ Pollut 120:647–658

Vlassova TK (2002) Human impacts on the tundra-taiga zone dynamics: the case of the Russian lesotundra. AMBIO Spec Rep 12:30–36

Wolfe RE, Nishihama M, Fleig AJ, Kuyper JA, Roy D, Storey JC, Patt FS (2002) Achieving sub-pixel geolocation accuracy in support of MODIS land science. Remote Sens Environ 83:31–49

Zwally HJ, Schutz B, Abdalati W, Abshire J, Bentley C, Brenner A, Bufton J, Dezio J, Hancock D, Harding D, Herring T, Minster B, Quinn K, Palm S, Spinhirne J, Thomas R (2002) ICESat's laser measurements of polar ice, atmosphere, ocean, and land. J Geodyn 34(3–4):405–445

Chapter 5
Vegetation Cover in the Eurasian Arctic: Distribution, Monitoring, and Role in Carbon Cycling

Olga N. Krankina, Dirk Pflugmacher, Daniel J. Hayes, A. David McGuire, Matthew C. Hansen, Tuomas Häme, Vladimir Elsakov, and Peder Nelson

Abstract Comparison of several recent, publicly available and widely used land-cover products for the Eurasian Arctic revealed important differences in their representations of vegetation distribution. Such disparities have important implications for models that use these products as driving data sets to monitor vegetation and its role in carbon dynamics. The differences between GLC-2000 and MODIS.PFT are concentrated at borders between biomes, as well as in parts of the region where a significant presence of open-canopy vegetation is expected. In these two maps, tree cover is represented more consistently than shrub or herbaceous cover, and the MODIS.VCF product corroborates the general pattern of tree-cover distribution. The comparison of the MODIS.VCF and AVHRR.VCF maps over northeastern Europe indicates good agreement in the south with increasing disagreement further north primarily due to differences in definitions of the mapped variables. The analysis of land-cover maps at two Landsat validation sites showed different patterns of agreement and disagreement. At the forest dominated St. Petersburg site, the GLC-2000 and MODIS.PFT classifications both exaggerated tree cover and under-reported shrub and herbaceous vegetation. At the tundra site (Komi), the over-reporting of tree cover by GLC-2000 and the failure of MODIS.PFT to separate shrub and herbaceous vegetation were the major issues in representing the overall land cover. A simple analysis that extrapolated results of biogeochemical modeling showed that a very different picture of the regional carbon balance emerges when different vegetation maps are used as model inputs.

5.1 Introduction

Accurate mapping of land cover and monitoring its change are fundamental requirements for global change research. These are especially important in the Arctic zone, which has experienced rapid rates of warming in recent years and the evidence of

O.N. Krankina (✉)
Department of Forest Ecosystems and Society, Oregon State University, Corvallis, OR 97331, USA
e-mail: krankinao@fsl.orst.edu

G. Gutman, A. Reissell (eds.), *Eurasian Arctic Land Cover and Land Use in a Changing Climate*, DOI 10.1007/978-90-481-9118-5_5,

regional impacts of warmer climate is mounting (Anisimov et al. 2007). Vegetation cover is expected to generate potentially critical, but not fully understood, feedbacks to a changing climate as a function of surface energy balance and the patterns of sources and sinks of atmospheric carbon dioxide (CO_2) and other greenhouse gases (Chapin et al. 2005; Field et al. 2007; Houghton 2003). In addition to direct climate forcings, natural disturbances and human activities can substantially alter the patterns and processes that create and transform these terrestrial sources and sinks (Houghton et al. 2004; Schimel et al. 2001).

The terrestrial ecosystems of the Arctic cover approximately 25% of the Earth's vegetated land surface (McGuire et al. 1997) and contain about one third of the total global terrestrial ecosystem carbon (C) pool (Schlesinger 1991). The large land area of boreal and arctic ecosystems across Northern Eurasia represents a key component in both the high latitude and global C budgets. In recent decades, this region has experienced extensive and severe forest fires (Sukhinin et al. 2004), along with changes in land use and forest management (Krankina et al. 2005). Studies using various accounting and modeling approaches, including top-down atmospheric inversions (Gurney et al. 2004) and bottom-up inventory-based estimates (Shvidenko and Nilsson 2003; Myneni et al. 2001) have suggested a positive terrestrial C balance (terrestrial sink) in Northern Eurasia during recent decades. More recent process-based model estimates by Balshi et al. (2007), which include the 2002 fire year, suggest that the large area burned may be causing the region to shift toward a net CO_2 source to the atmosphere. The combined effects of the recent changes in climate (Polyakov et al. 2002), disturbance (Sukhinin et al. 2004) and land management (Krankina et al. 2005) on the contemporary C budget of this region are examined in Chapter 6, this volume.

The models that are being used to investigate the role of arctic vegetation in the global climate system require complete coverage with accurate and repeated measures of vegetation and land cover attributes as key driving variables. Several moderate and coarse resolution land-cover datasets are available for the Eurasian Arctic region (Hansen et al. 2000; Loveland et al. 2000; Friedl et al. 2002; Bartalev et al. 2003; Fritz et al. 2003; Hansen et al. 2003a, b), and more are being developed. However, there is a significant disagreement among these datasets and high latitudes appear particularly problematic for land-cover mapping (Giri et al. 2005; Fritz and Lee 2005; Herold et al. 2008; Krankina et al. 2008). This is not surprising because all of these datasets rely on spectral satellite imagery. The high level of cloudiness, in combination with low sun angle and the shortness of the growing season in the Arctic, reduces data availability from passive sensors.

The accuracy of land-cover products for Arctic regions and the product utility for various applications remains largely uncertain. This is because the validation of coarse resolution maps is a persistent challenge, particularly for Northern Eurasia where validation sites are sparse, several land-cover types are unique, and processes of ecosystem disturbance and land-cover change are widespread, including fire, timber harvest, insect outbreaks, agricultural conversion and abandonment, forest regrowth, and melting permafrost. The lack of independent validation makes it often impossible to ascertain which products perform better in specific geographic

domains, for specific land-cover types, or in specific applications. Detailed examination of available global land-cover products showed that the classification legends are not well suited for parameterizations of C cycling models, which is among the major applications of global and continental land-cover maps (Jung et al. 2006).

Changes in land cover are among the principal indicators of the impact of global change on terrestrial ecosystems. While some aspects of Earth surface cover (e.g., sea ice) have been carefully monitored and, in fact, show significant change (e.g., Stroeve et al. 2006), change in land cover has not received the same level of attention (see review of recent studies in Chapter 2 by Goetz et al., this volume). The shortness of the satellite data record relative to the temporal scale of vegetation succession is an inherent difficulty in monitoring vegetation change and this problem is particularly significant in the Arctic. At present, coarse resolution sensors such as MODIS are investigated for their potential to track many forms of vegetation change. The MODIS record is now long enough to support monitoring of forest ecosystem disturbance and recovery (Hansen et al. 2010; Potapov et al. 2008; Chapter 3, this volume). In the future, the growing length of the data record will further expand opportunities for monitoring land-cover change. However, the disagreement among the maps of current vegetation cover results in uncertainty as to which land-cover type undergoes change and indicating an urgent need for improved land-cover mapping.

This study examines recent, publicly available and widely used land-cover products representing two principal approaches to mapping vegetation cover in the Eurasian Arctic: categorical maps and continuous field maps. First, we cross-compare the regional datasets and then we validate them in two locations using detailed, Landsat-based maps derived from local ground data and knowledge of land cover. Finally, we assess the significance of the current uncertainty in vegetation cover for estimating C stores, sources and sinks in terrestrial ecosystems of the region and outline approaches for improved regional representation of land cover.

5.2 Representation of Vegetation Cover in Coarse Resolution Maps

Knowledge about the distribution and dynamics of arctic vegetation has improved in the last two decades through the development of coarse resolution satellite-based land-cover maps. The first global land-cover map based on remote sensing was developed by DeFries and Townshend (1994) with data from the Advanced Very High Resolution Radiometer (AVHRR) sensor at one-degree spatial resolution. Later, maps with finer resolution (1-km) were developed using AVHRR data acquired between April 1992 and March 1993: the Global Land Cover Characterization (GLCC) data base (Loveland et al. 2000) and the University of Maryland (UMD) Global Land Cover (GLC) data set (Hansen et al. 2000). Although the two maps utilized the same sensor data, the mapping methodologies differed

considerably, which led to disagreements between the two maps (Hansen et al. 2000). In addition to land-cover maps based on satellite observations, regional maps are also produced based on legacy geobotanical data sets with remotely sensed data used primarily for georeferencing of polygons that represent various landscape types and delineating areas of high shrub within some provinces (Walker et al. 2005). Because of the large size of polygons on geobotanical maps a direct comparison with satellite-based land-cover products appears problematic.

5.2.1 Comparison of Categorical Maps

The two major recent global land-cover mapping activities are the Global Land Cover 2000 (GLC-2000) (Fritz et al. 2003) and the Moderate Resolution Imaging Spectroradiometer (MODIS) land-cover product (Friedl et al. 2002). The GLC-2000 mapping was lead by the Joint Research Center of the European Commission in partnership with more than 30 institutions around the world (Fritz et al. 2003), and MODIS land cover product was prepared by scientists from Boston University for US National Aeronautics and Space Administration's (NASA) Earth Observing System (EOS) MODIS land science team (Friedl et al. 2002). The two maps have a 1-km spatial resolution, but they were created using different satellite data, methodologies and classification schemes. For example, the global GLC-2000 map was derived from 19 regional subsets with regionally specific classification schemes. In comparison, the MODIS team used a global classification approach involving training sites distributed across the globe.

We assessed the agreement between these two maps, GLC-2000 and MODIS land cover, in representing the Dominant Vegetation Types (DVTs) which we defined as trees, shrubs, herbaceous vegetation, and barren with sparse vegetation. MODIS land cover (MOD12Q1) is available in five classification schemes (IGBP, UMD, LAI/fPAR, BGC and PFT). We obtained the PFT (Plant Functional Types) layer for Eurasia for the year 2001 (V004) in Lambert Azimuthal Equal-area (LAEA) projection (http://duckwater.bu.edu/lc/mod12q1.html; last accessed 20 February 2008). The MODIS.PFT classification consists of 12 classes and was developed for the National Center for Atmospheric Research (NCAR) land surface model (Bonan et al. 2002).

The GLC-2000 map is based on Satellite Pour l'Observation de la Terre (SPOT) VEGETATION data acquired daily between November 1999 and December 2000. The GLC-2000 uses a legend based on the hierarchical Land Cover Classification System (LCCS, Di Gregorio 2005). Both, the regional products (e.g., Bartalev et al. 2003 for Northern Eurasia) and a global mosaic of the regional products with a harmonized legend are available. We downloaded the global data set (v1.1) from (http://www-gvm.jrc.it/glc2000/; last accessed 20 January 2008) in geographic coordinate space, and reprojected it to LAEA, the geographic reference system of the MODIS map.

To assess the spatial agreement between GLC-2000 and MODIS.PFT, we cross-referenced the LCCS and PFT legends using the DVT logic (Table 5.1). While

Table 5.1 Agreement/disagreement matrix for GLC-2000 and MODIS.PFT land cover

	GLC-2000.LCCS (rows) MODIS.PFT (columns)	1 Needleleaf evergreen tree	2 Broadleaf evergreen tree	3 Needleleaf deciduous tree	4 Broadleaf deciduous tree	5 Shrub	6 Grass	7 Cereal crop	8 Broadleaf crop	9 Urban and built-up	10 Snow and ice	11 Barren or sparsely vegetated	0 Water
1	Tree cover, broadleaved, evergreen	T	T	T	T	ts	th	th	th	tb	tb	tb	lw
2	Tree cover, broadleaved, deciduous, closed	T	T	T	T	ts	th	th	th	tb	tb	tb	lw
3	Tree cover, broadleaved, deciduous, open	T	T	T	T	ts	th	th	th	tb	tb	tb	lw
4	Tree cover, needle-leaved, evergreen	T	T	T	T	ts	th	th	th	tb	tb	tb	lw
5	Tree cover, needle-leaved, deciduous	T	T	T	T	ts	th	th	th	tb	tb	tb	lw
6	Tree cover, mixed leaf type	T	T	T	T	ts	th	th	th	tb	tb	tb	lw
7	Tree cover, regularly flooded, fresh water	T	T	T	T	ts	th	th	th	tb	tb	tb	lw
8	Tree cover, regularly flooded, saline water	T	T	T	T	ts	th	th	th	tb	tb	tb	lw
9	Mosaic: Tree cover/other natural vegetation	T	T	T	T	S	H	th	th	tb	tb	tb	lw
10	Tree cover, burnt	T	T	T	T	ts	th	th	th	tb	tb	tb	lw
11	Shrub cover, closed-open, evergreen	ts	ts	ts	ts	S	sh	sh	sh	sb	sb	sb	lw
12	Shrub cover, closed-open, deciduous	ts	ts	ts	ts	S	sh	sh	sh	sb	sb	sb	lw
13	Herbaceous cover, closed-open	th	th	th	th	sh	H	H	H	hb	hb	hb	lw
14	Sparse herbaceous or sparse shrub cover	tb	tb	tb	tb	sb	hb	hb	hb	B	B	B	lw
15	Regularly flooded shrub and/or herbaceous cover	ts	ts	ts	ts	S	H	H	H	hb	hb	hb	lw
16	Cultivated and managed areas	th	th	th	th	sh	H	H	H	hb	hb	hb	lw
17	Mosaic: cropland / Tree cover / other natural vegetation	T	T	T	T	S	H	H	H	hb	hb	hb	lw
18	Mosaic: cropland / shrub and/or herbaceous cover	th	th	th	th	S	H	H	H	hb	hb	hb	lw
19	Bare areas	tb	tb	tb	tb	sb	hb	hb	hb	B	B	B	lw
20	Water bodies (natural & artificial)	lw	lw	lw	lw	lw	lw	lw	lw	lw	lw	lw	W
21	Snow and ice (natural & artificial)	tb	tb	tb	tb	sb	hb	hb	hb	B	B	B	lw
22	Artificial surfaces and associated areas	tb	tb	tb	tb	sb	hb	hb	hb	B	B	B	lw

Agreement: T=tree, S=shrub, H=herbaceous, B=barren/sparse vegetation, W=water; Disagreement: ts=tree-shrub, th=tree-herbaceous, tb=tree-barren, sh=shrub-herbaceous, sb=shrub-barren, hb=herbaceous-barren, lw=land-water

the MODIS.PFT classification translates directly into the four DVT classes, the GLC-2000 classification featured four out of 22 classes with no unique dominant vegetation type (three mosaic classes and a "regularly flooded shrub and/or herbaceous cover" class; Table 5.1). In these four cases multiple types of agreement were possible. For example, if GLC-2000 mapped a pixel as "Mosaic: Cropland, Tree cover and other natural vegetation," this pixel was considered in agreement with MODIS tree, shrub or herbaceous classes, but in disagreement with MODIS barren and sparsely vegetated classes (including "Urban and built-up", "Snow and ice" and "water"). Land cover mosaics and "regularly flooded shrub and/or herbaceous cover" class occupy 330×10^3 km^2 (3.7%) and 688×10^3 km^2 (7.6%), respectively, on GLC-2000 map.

The comparison of the GLC-2000 and MODIS.PFT land-cover maps showed significant differences between the two maps in representing dominant vegetation types, mainly tree and shrub vegetation. According to GLC-2000, 50% of the Eurasian land area between 60° and 74° N fall into tree dominated vegetation types, followed by 26% shrub types, 14% barren or sparse vegetation and 10% herbaceous vegetation. These percentages include the area of land cover mosaics and regularly flooded shrub and/or herbaceous vegetation, which we assigned to a DVT class after cross-referencing and overlaying the MODIS.PFT map (Table 5.1). In comparison, MODIS.PFT mapped only 30% of the area as tree-dominated, while the majority (60%) was identified as shrub-dominated vegetation types. The MODIS.PFT estimate of herbaceous vegetation cover was similar (8%), but the area defined as barren/sparse vegetation was much smaller than on GLC-2000 map (3%).

The overall spatial agreement between GLC-2000 and MODIS.PFT on a pixel-by-pixel basis was fairly low at 53% (Table 5.2, Fig. 5.1). Most of the disagreement occurred between tree and shrub vegetation (21% of land area), the majority of which is in regions where MODIS.PFT mapped shrub and GLC-2000 mapped tree vegetation (19% of land area). This area of disagreement is consistent with the overall higher representation of tree-dominated cover in the GLC-2000 map (20% higher than MODIS.PFT). In comparison, the 30% of the land area that are mapped as tree vegetation by MODIS.PFT are in good agreement with the GLC-2000 map (91% agreement, Table 5.2). The confusion between GLC-2000 tree and MODIS.PFT shrub vegetation marks the transition zone from boreal forest to shrub tundra and is mostly concentrated on permafrost lands in northeastern Siberia and parts of the Far East (Fig. 5.1) where low-stature open-canopy trees can be difficult to distinguish from shrubs. The second most common disagreement is between MODIS shrub and GLC-2000 barren (11%) and herbaceous vegetation (8%) and it is concentrated primarily in the tundra zone. While 85% of the shrub pixels in the GLC-2000 map were confirmed by MODIS.PFT, only 36% of the pixels identified as shrub by MODIS.PFT were confirmed by GLC-2000 (Table 5.2). The fact that the vegetation types that are mapped conservatively on one map have high level of agreement with the other map (e.g., trees on MODIS.PFT and shrub on GLC-2000) suggests that the mapping results are robust in these cases. Large areas of agreement are concentrated in the western part of the Eurasian Arctic where the availability of ground data for training the mapping algorithms is better (Fig. 5.1).

Table 5.2 Area of agreement and disagreement (in 1,000 km^2) for GLC-2000 and MODIS.PFT dominant vegetation types in the Eurasian Arctic (excluding water)

	MODIS.PFT					
GLC-2000	Tree	Shrub	Herbaceous	Barren	Total	Agreement (%)
Tree	2.395	1.697	351	7	4.450	54
Shrub	200	1.922	105	31	2.258	85
Herbaceous	24	698	160	34	916	17
Barren	12	973	64	183	1.232	15
Total	2.630	5.290	680	255	8.855	
Agreement (%)	91	36	23	72		53

Herbaceous vegetation appears to be the most problematic type for finding agreement between the two maps. Even though the total area estimates for herbaceous vegetation are not dramatically different in the two maps, the spatial agreement is very low (<25%, Table 5.2). The confusion of herbaceous vegetation with other vegetation types may stem from the fact that in the Arctic many areas with herbaceous vegetation are in fact wetlands, often with significant presence of *Sphagnum* spp. and other mosses and lichens. This vegetation type has a substantially different spectral reflectance compared to vascular herbaceous plants (Vogelman and Moss 1993; Bubier et al. 1997; Krankina et al. 2008). The test of available global and regional wetland and peatland datasets against detailed land-cover maps for the St. Petersburg region showed that peatlands were correctly classified as such in coarse-resolution datasets but a large proportion (74–99%) was overlooked (Krankina et al. 2008). The under-reporting of the actual extent of wetlands on this scale is especially problematic for estimating carbon stores and flux in the Arctic (McGuire et al. 2007). Even though the potential of MODIS to capture the distribution of boreal wetlands was demonstrated (Pflugmacher et al. 2007), this potential has not been exploited for improving wetland mapping across the Eurasian Arctic and the inconsistent representation of herbaceous vegetation on continental maps may be in part attributable to that.

5.2.2 Vegetation Continuous Field Maps

Unlike categorical maps, Vegetation Continuous Field (VCF) maps provide subpixel proportional estimates of land cover. Continuously varying maps of cover provide improved spatial detail when compared to categorical maps that by definition discretize landscapes. Areas undergoing disturbance are more accurately characterized at sub-pixel scales, resulting in map products that more fully exploit the inherent variability found in imagery (Hansen et al. 2002). Unlike classifications, continuous cover maps enable users to define their own thresholds for land-cover classes and can also be used consecutively to identify areas undergoing land-cover change. VCF maps for forest cover have been developed for different regions in

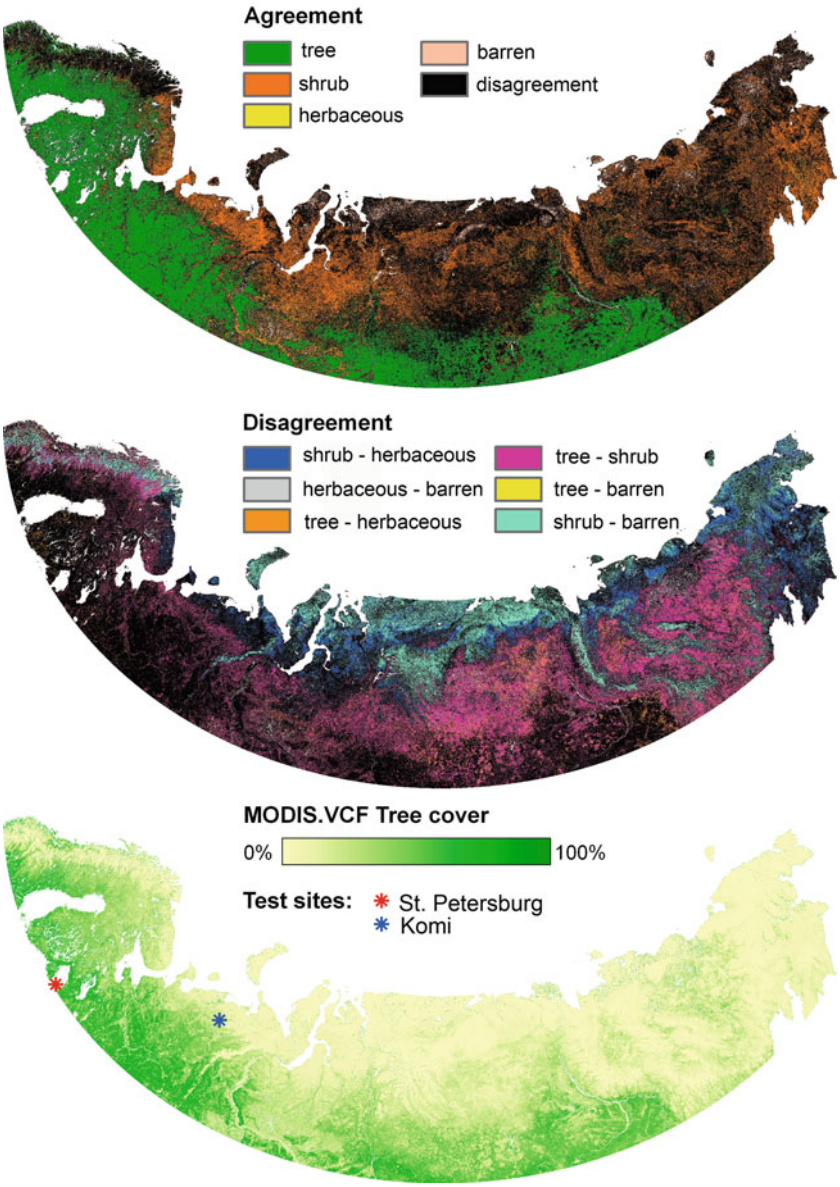

Fig. 5.1 (*Top*) Maps agreement and (*middle*) disagreement in dominant vegetation cover for GLC-2000 and MODIS.PFT, and (*bottom*) MODIS.VCF tree-cover map in the Eurasian Arctic

the world and from different sensor types, e.g., AVHRR (Zhu and Evans 1994; DeFries et al. 1997; Häme et al. 2000 and 2001) and MODIS (Hansen et al. 2005). In this study, we analyze a MODIS-based VCF product for Northern Eurasia and an AVHRR-based VCF product for the pan-European region.

The MODIS.VCF tree canopy cover data set was developed by MODIS land science team members from the University of Maryland at a spatial resolution of 500 m (Hansen et al. 2003a, b). The MODIS.VCF of tree-cover estimates sub-pixel percent tree-canopy cover for the entire globe. Percent tree-canopy cover refers to the amount of skylight orthogonal to the surface that is obstructed by tree canopies equal to or greater than 5 m in height and is different than percent crown cover, which includes both the canopy cover and the within-crown skylight/gaps. Current VCF percent tree-cover products are generated using sub-pixel training data derived from Landsat imagery. Each Landsat pixel is classified as one of four tree-cover strata and assigned a mean canopy-cover value. These values are then averaged to MODIS scale (500 m) and used as reference training data. The training labels are related to annual metrics (Hansen et al. 2002) that are generated from 32-day composites of Terra MODIS data. MODIS bands 1–7, derived Normalized Difference Vegetation Index and Land Surface Temperature are used as inputs (Wolfe et al. 1998; Wan et al. 2002). Annual metrics are time-integrated means, amplitudes, and ranks of annual composite imagery that represent salient features of vegetation phenology without reference to specific time of year, and have been shown to perform as well or better than time-sequential composites in mapping large areas (Hansen et al. 2005). A regression-tree bagging algorithm (Breiman 1996) is used to relate the percent tree-canopy cover training data to the annual metrics in creating the VCF tree-cover product.

Annual VCF tree-cover products are available for 2000–2005 and free for download through the Land Processes Distributed Active Archive Center (http://edcdaac.usgs.gov) and through the Global Land Cover Facility at the University of Maryland (http://glcf.umiacs.umd.edu). We downloaded a MODIS Tree canopy cover data set for year 2001 (V003) from the latter site (last accessed 20 February 2008) with a geographic coordinate system and reprojected it to LAEA (Fig. 5.1).

The distribution of VCF tree cover across the region (Fig. 5.1) provides additional corroboration for the presence of trees in the areas where GLC-2000 and MODIS.PFT both identify tree-dominated cover: these are the areas with high values of VCF tree cover. The areas of disagreement between the two compared categorical maps tend to be those with low tree cover on the MODIS.VCF map (Fig. 5.1). Overall, the open-canopy forests dominate the region with 42% of the total land area having tree canopy cover between 10 and 40% while only 7% of the land area has tree-canopy cover of 65% and higher (Fig. 5.2). The total area of tree-canopy cover derived from MODIS.VCF product for lands north of 60° is 1977 thousand km^2 (Fig. 5.3).

Another VCF-type product relies on the probability method which was originally developed for mapping forest extent in the pan-European region (i.e., all Europe up to the Ural Mountains) using the AVHRR instrument data of the NOAA series satellites (Häme et al. 2000, 2001; Paivinen et al. 2001; Schuck et al. 2002). The target variables, including proportions of coniferous, broadleaved and mixed forest were estimated within 1-km^2 units. Forty eight (48) AVHRR images were collected from summer 1996 and one image from 1997. The images were calibrated into

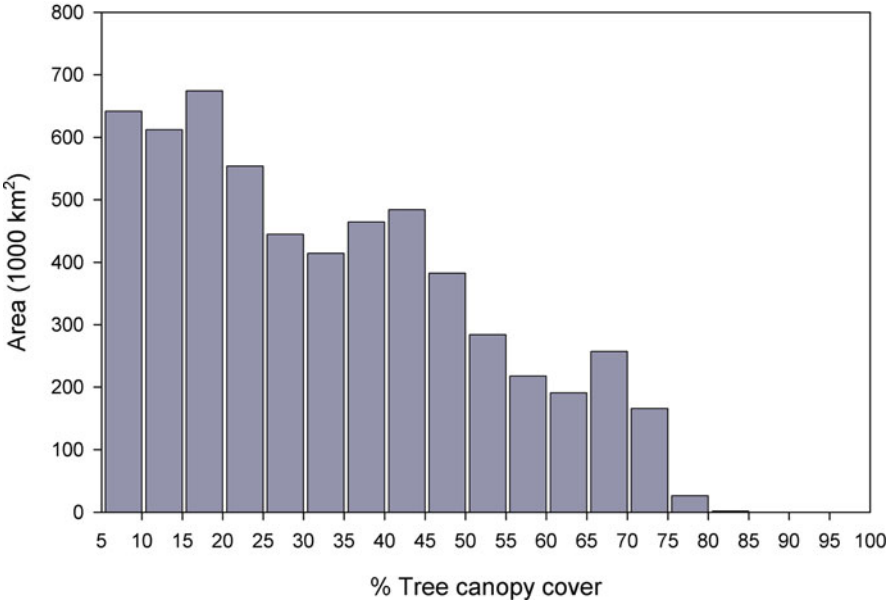

Fig. 5.2 Histogram of tree-canopy cover in the Eurasian Arctic from MODIS.VCF for canopy cover greater than 5%

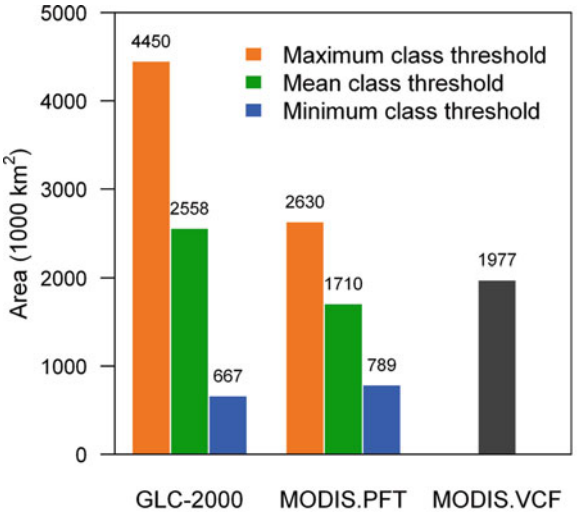

Fig. 5.3 Representation of the total tree-covered area on GLC-2000, MODIS.PFT, and MODIS.VCF

spectral reflectance values by applying the SMAC atmospheric correction (Rahman and Dedieu 1994) and a BRDF correction using Roujean model (Wu et al. 1995). A mosaic was compiled using the radiometrically and geometrically corrected images. The average reflectance of overlapping pixels was computed after applying an automatic cloud screening algorithm.

The probability method includes an unsupervised image classification as a preliminary step. For the classes of unsupervised clustering a reference data sample was selected from the European CORINE land cover data base that was available from the central and southern European region (CORINE 1993). The sample comprised squares of 500 m by 500 m within which the tree species proportions were computed. The sampling was done using three strata: Mediterranean region, Atlantic region, and continental temperate region. No CORINE reference data was available from the boreal or arctic region.

The multi-normal density functions of the spectral classes from unsupervised clustering and the reference data values for the same classes were combined using the probability algorithm (Häme et al. 2000, 2001). The estimated values of the forest area were compared with the official EUROSTAT (1998) forestry statistics and with the national-level forest inventory statistics in selected countries. They also were calibrated to match district-wise with those statistics (Päivinen et al. 2001). Based on calibrated map, the total area of conifer-dominated forest north of 60° in Europe is 995,013 km^2 and broadleaf-dominated forest is 190,191 km^2. At country level in the boreal zone (most of Sweden belongs to the boreal vegetation zone) the AVHRR-based forest area estimation matched with the statistical data well (Fig. 5.4). Also at sub-national level within Finland agreement was relatively good (Fig. 5.5). At a sub-district level, the AVHRR map underestimated the coniferous and broadleaved forest areas in Finland (Fig. 5.6). The likely reason for this was the different nomenclatures in the Finnish national forest inventory and CORINE.

The comparison of MODIS.VCF and AVHRR.VCF map indicates reasonably good agreement in the southern part of northeastern Europe and increasing disagreement further north (Fig. 5.7a). The abrupt northern boundary on AVHRR.VCF

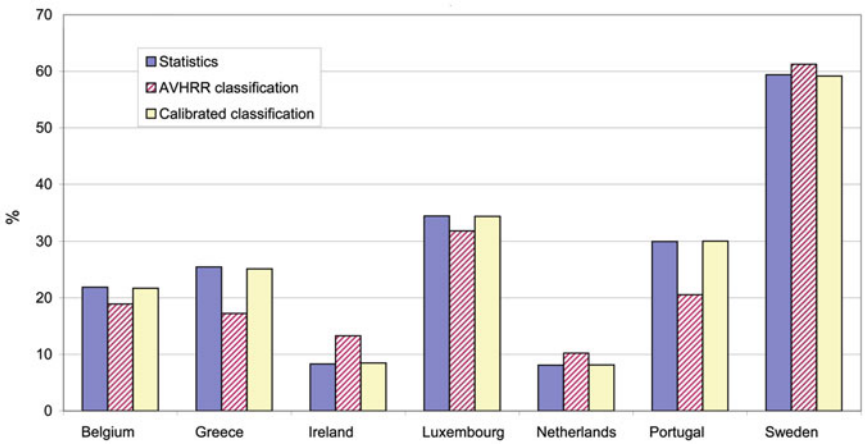

Fig. 5.4 Comparison of EUROSTAT forest statistics and calibrated and uncalibrated AVHRR.VCF forest cover estimates in some European countries (from Paivinen et al. 2001). Reproduced by permission of European Forest Institute

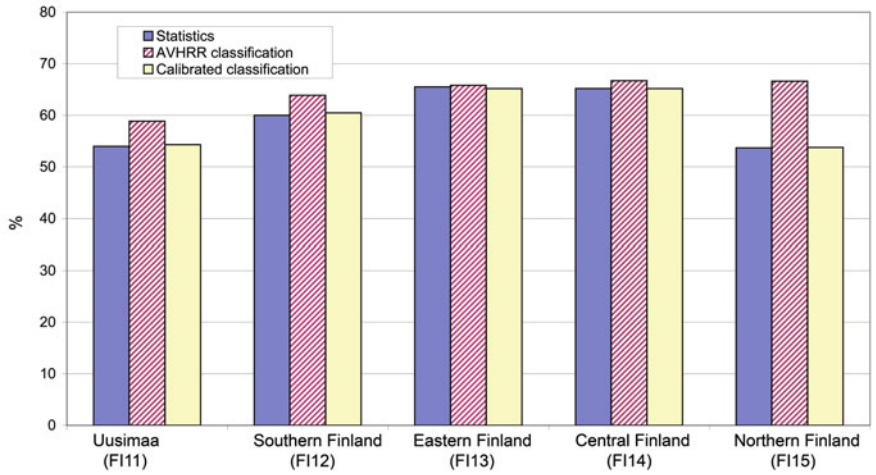

Fig. 5.5 Comparison of EUROSTAT forest statistics and calibrated and uncalibrated AVHRR.VCF forest cover estimates within districts in Finland (virtually the entire territory of Finland is above 60°N; from Paivinen et al. 2001). Reproduced by permission of European Forest Institute

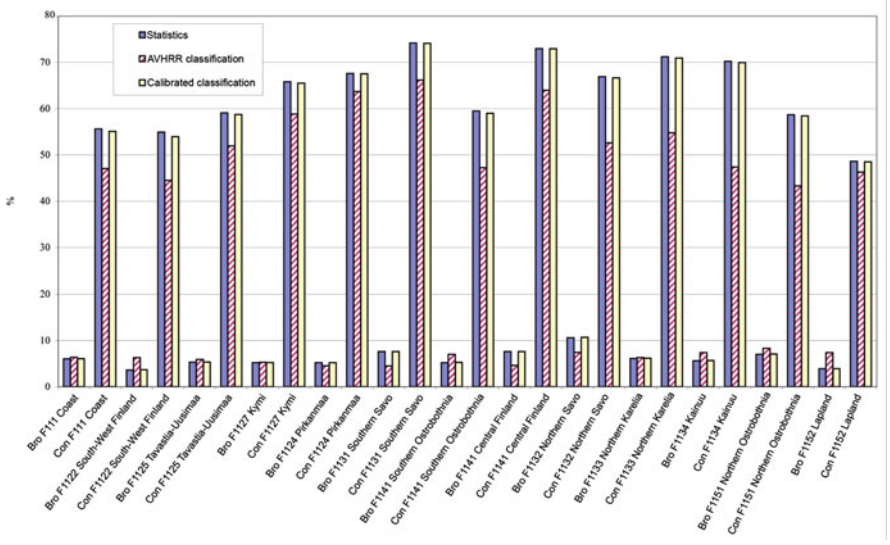

Fig. 5.6 Comparison of Finnish National Forest Inventory statistics within sub-districts and calibrated and uncalibrated AVHRR.VCF estimates of the proportion of conifer and broadleaf tree-cover (mixed forest class excluded from AVHRR classification values; split between broadleaved and conifer types in calibrated classification values to match inventory statistics; from Paivinen et al. 2001). Reproduced by permission of European Forest Institute

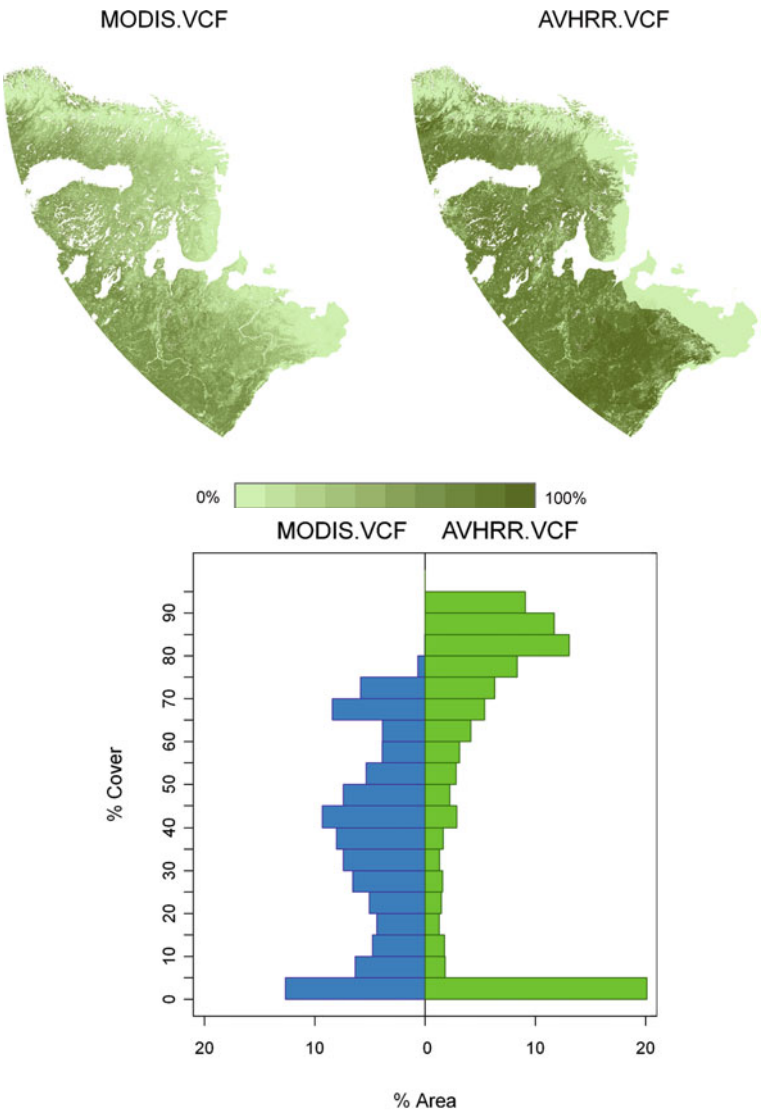

Fig. 5.7 Continuous field products for North-Eastern Europe: (*top*) Distribution of percent tree-canopy cover on MODIS.VCF map and percent forest cover on AVHRR.VCF map; (*bottom*) histogram for MODIS.VCF and AVHRR.VCF

map reflects the northern tree line that was extracted from the literature and applied before calibrating the continuous estimates using the Eurostat statistics. The total area of tree crown cover is projected to occupy 36% by MODIS.VCF whereas percent forest cover based on AVHRR.VCF is 55%. Differences in definitions of the mapped variable appear to account for most of the difference in the results. The percent tree crown cover approximately corresponds to 0.8 of percent canopy cover

(Hansen et al. 2003a); taking this adjustment into account the MODIS.VCF estimate of crown cover is approximately 45%, which is still lower than AVHRR.VCF estimate. Furthermore, CORINE definition of "forest" includes lands with >15% tree-canopy cover (Heiskanen 2008); thus pixels with as low as 15% tree cover would be classified as "100% forest" if this tree cover is distributed evenly across the pixel. The more open tree canopies tend to be, the greater the disagreement between the two products can be expected due to differences in definition of the continuously mapped variable. This explains the increasing disagreement as one moves further north, the overall higher area estimate, and the greater proportion of pixels with high percent tree cover on AVHRR.VCF (Fig. 5.7b). The comparison of MODIS.VCF maps with a detailed biotype map in northern Finland indicated that the MODIS.VCF map underestimated in areas with high forest cover and overestimated in areas with low tree cover, particularly on mires (Heiskanen 2008).

5.2.3 Comparison of Tree Cover Representation on Coarse Resolution Maps

Certain characteristics of tree cover in Arctic Eurasia make the categorical mapping challenging, including large areas occupied by open low-stature trees with heights close to the lower boundary of the "tree" definition (3–5 m) and the significant presence of other (non-tree dominated) land-cover types within 1-km pixels. However, the estimates of the total tree-canopy cover for the Arctic region of Eurasia agree better among the examined land-cover products than the results of per-pixel spatial disagreement may suggest (Table 5.2). The MODIS.VCF estimate of regional total tree-canopy cover (22% of the total land area) is lower than the tree-dominated area estimate from GLC-2000 (50%) or MODIS.PFT (30%), although it is closer to the MODIS.PFT estimate. However, the three estimates are not directly comparable. While the total VCF tree cover is an estimate of the area of tree-canopy cover, the tree-dominated area estimates from the categorical maps include land surface not covered by tree canopies. This is especially significant in regions with open forests because land with canopy cover as low as 15% is still defined as tree-dominated by legends of categorical maps. The tree-cover estimate derived from MODIS.VCF is consistent with this difference in definitions and suggests that categorical maps may over-represent tree cover for the region primarily as a result of their inability to capture the sub-pixel scale variations in tree cover. In the GLC-2000 data set, tree-dominated pixels are defined to have tree-canopy cover between 15 and 100% (57.5% mid-range). In the MODIS.PFT classification, forests are defined as pixels where tree cover dominates over shrub, herbaceous or non vegetated land cover, which could be as low as 30% or as high as 100% (65% mid-range). Therefore, estimates of tree canopy cover derived from the categorical maps could theoretically range anywhere between the minimum and maximum thresholds of the class definitions (Fig. 5.3). Canopy cover estimates using the mid-range value of tree class from the categorical data sets compare well with the MODIS.VCF tree cover estimate. Note however, that the actual distribution of tree cover within the classes is

unknown, so the actual mean tree cover might be lower or higher than the class mid-range. Considering the known prevalence of open-canopy tree stands in the region (Fig. 5.2), the actual mean value of tree cover in tree-dominated pixels is likely to be lower than the mid-range values. If we translated MODIS.VCF dataset to discrete classes and estimated the total tree-dominated area following GLC-2000 definition (i.e., counted all pixels with VCF tree cover >15% as tree-dominated) it would be 5,174 thousand km^2 compared to 4,550 thousand km^2 actually mapped by GLC-2000; for MODIS.PFT the relevant values are 3,334 and 2,630 thousand km^2, respectively. Thus when class definitions are aligned, the MODIS.VCF product suggests greater area with tree cover than either of the two examined categorical maps; the difference is 13% for GLC-2000 and 27% for MODIS.PFT and indicates either an omission of low-canopy cover forests from GLC-2000 and MODIS.PFT or commission (overestimation) in the VCF map.

Open-canopy tree cover is very common not only in Northern Eurasia but in the entire Arctic. Interestingly, the global and regional GLC-2000 legends separate closed and open broadleaf deciduous trees, thus allowing representation of tropical savannas but not the open-canopy needle-leaf tree cover in the Arctic region. This may indicate the lack of attention from map developers to the Arctic region and to a vegetation type that has an important control over feedback mechanisms to climate change, including albedo and carbon cycling (McGuire et al. 2007). In selecting the suitable map for the region the availability of open-canopy needle-leaf tree class can be an important feature which is available on some maps (e.g., MODIS.IGBP). The open-canopy needle-leaf tree cover class would be important to include in future mapping programs aimed at improving the utility of land-cover maps for global change research in the Arctic.

5.3 Comparison of Coarse Resolution Maps with Landsat-Based Land Cover

The cross-comparison of the GLC-2000 and MODIS.PFT map revealed areas of uncertainty, geographically and thematically. However, analyses of agreement and disagreement between coarse resolution maps provide only an indirect measure of class confidence. Independent validation and accuracy assessment has long been recognized as an important challenge for all land-cover products (Morisette et al. 2002; Stahler et al. 2006). Since there is a paucity of validation data in the Arctic, this challenge will likely persist. To obtain some indication of the products' performance in Northern Eurasia we compared the coarse resolution maps with Landsat-based land-cover maps at two validation sites. The two site maps were developed as part of an ongoing, broader effort to validate land-cover maps within the region (Northern Eurasia Land Cover Dynamics Analysis (NELDA) project http://www.fsl.orst.edu/nelda/index.html). Dominant vegetation cover data from GLC-2000 and MODIS.PFT were compared with medium resolution (28.5 m) land-cover maps developed for two sites: Komi (66°55′ N, 55°35′ E) and St. Petersburg (59°45′ N, 31° 11′ E). Land-cover maps for the two sites were produced from ground inventory

data and Landsat Enhanced Thematic Mapper Plus (ETM+) data. The imagery was first orthorectified using an automated procedure (Kennedy and Cohen 2003) and then radiometrically corrected to remove atmospheric scattering effects (Chavez Jr 1996; Canty et al. 2004). The legends for the two maps followed the LCCS classification scheme (Di Gregorio 2005) and were recoded into the DVT classes: tree, shrub, herbaceous vegetation, and barren or sparse vegetation (Fig. 5.8). The LCCS classification defines "tree dominated" cover as land with greater than 15% tree cover, where trees are woody vegetation taller than 5 m or trees taller than 3 m. Similarly, shrub and herbaceous dominated vegetation types have a minimum of 15% plant cover, respectively. However, the dominance of a life form is defined hierarchically by the height of the canopy layer, which ranges from trees to shrubs to herbaceous plants. Thus, a landscape with a top canopy layer represented by trees with canopy cover >15% (for example 20%) and a sub layer represented by shrubs with a canopy cover of 40% will be classified as "tree dominated". Lands with less than 15% vegetation cover are labeled as "bare land and sparse vegetation".

5.3.1 Komi Site

The Komi test site is located in the subarctic climate zone in the northeast of European Russia. The climate is continental with brief summers, long winters and a daily average temperature below 0°C during 227 days a year. Mean annual temperature varies between −3 and −5°C. The mean temperature in July is 12.3°C, in January it is −18.9°C. The snow cover lasts on average for 225 days (3 Oct–1 Jun); the annual precipitation is 430–436 mm year^{-1}; 30% is snow. Severe climate, excessive moisture, relatively flat terrain and seasonally-frozen ground (and permafrost) determine the high degree of soil water saturation and presence of many wetlands. The site is located in the forest-tundra zone. Tundra communities are dominated by dwarf-birch (*Betula nana* L.) and willow species (*Salix glauca, S. lanata* and *S. phylicifolia*). Further south, forest-tundra and northern taiga communities mainly consist of Siberian spruce *(Picea obovata* Ledeb.) and birch species (*B. tortuosa* or *B. pubescens*). The density of human population is low. The traditional land use is reindeer herding and in recent years the extraction of vast resources of carbohydrates from terrestrial and shelf deposits of the Timano-Pechorsk oil-gas province became the second major human impact. Wild fire is also a significant factor in vegetation dynamics.

The analysis of vegetation distribution was based on a Landsat ETM+ image from June 8, 2000 (WRS-2 path 172, row 13, UTM projection, zone 40). Twelve vegetation cover classes (plus water) were identified using supervised classification and these were aggregated to the dominant vegetation types used in this study (Fig. 5.8). Map accuracy was assessed using forest inventory and other ground truth data. The overall agreement with of DVT map with the ground data is 84.3% (kappa = 68.6%).

At the Komi site, the overall agreement between GLC-2000 and MODIS.PFT is 65%. The spatial distribution of tree-dominated vegetation mapped on all

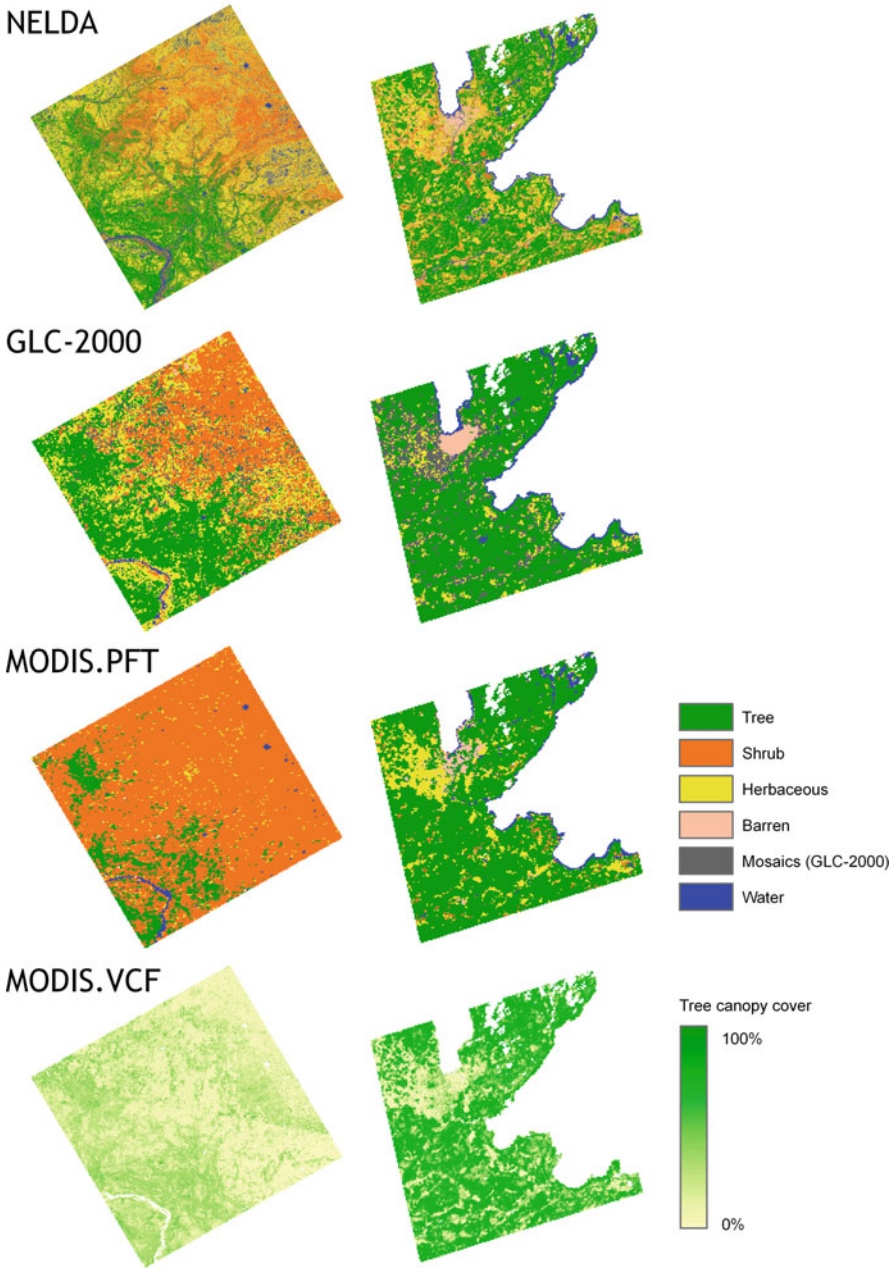

Fig. 5.8 (*Left* column) Dominant vegetation types at Komi site and (*right* column) St. Petersburg site mapped by NELDA, GLC-2000, MODIS.PFT, and MODIS.VCF

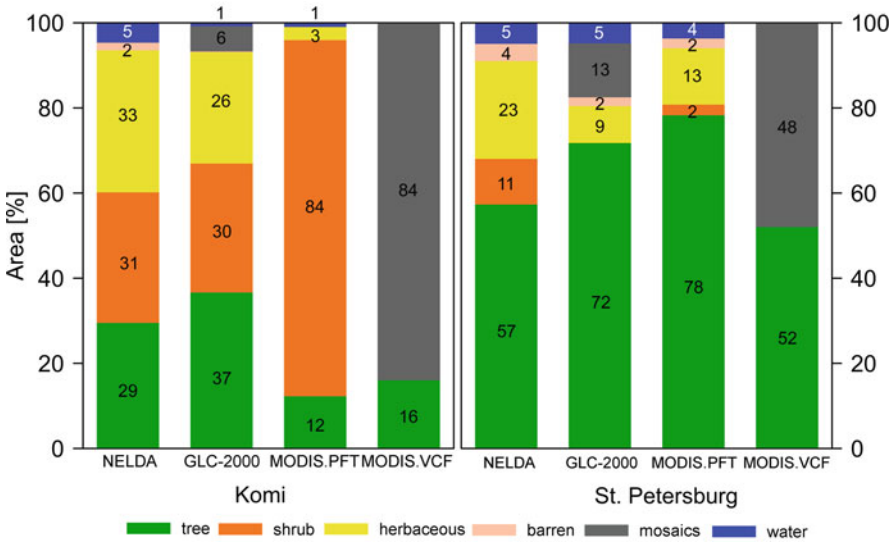

Fig. 5.9 (*Left*) Composition of dominant vegetation types at Komi site and (*right*) St. Petersburg site as mapped by NELDA, GLC-2000, MODIS.PFT, and MODIS.VCF

coarse-resolution products is in general agreement (Fig. 5.8) but the area proportion of tree-dominated vegetation mapped by MODIS.PFT (12%) and MODIS.VCF (16%) is lower than the NELDA reference map (29%, Fig. 5.9). In comparison, the area occupied by tree vegetation on GLC-2000 map is higher (37%). Furthermore, with 84% of the area mapped as shrubs, MODIS.PFT fails to distinguish between shrub and herbaceous vegetation. The confusion between tree and shrub is the most common disagreement at the Komi site, and it occupies 27% of the total mapped area. The second most common type of confusion is between shrub and herbaceous vegetation (6% of total area). Both MODIS.PFT and GLC-2000 underestimate the area occupied by water bodies (1% compared to 5% mapped by NELDA). While water covers only a small fraction of the land surface, it is very important ecologically as changes in arctic lakes are an important indicator of permafrost dynamics (e.g., Frohn et al. 2005). Improved region-wide mapping of terrestrial water bodies is clearly important.

5.3.2 St. Petersburg Site

The St. Petersburg test site is located in northwestern Russia at the southern boundary of the study region. The site has a maritime climate, with cool wet summers and long cold winters. Mean temperature ranges from 16 to 18°C in July and −7 to −11°C in January. The mean daily temperatures are below zero from

November until March. Annual precipitation is 600–800 mm. The natural vegetation of the area is southern taiga: major dominant conifer species include Scots pine (*Pinus sylvestris L.*) and Norway spruce (*Picea abies* (L.) Karst.), growing in both pure and mixed stands. After disturbance, these species are often replaced by northern hardwoods, including birch (*Betula pendula* Roth.) and aspen (*Populus tremula* L.). The site is part of the East-European Plain; the terrain is flat and consists of ancient sea sediments covered by a layer of moraine deposits. Toward the northwest, glacial features dominate the landscape and bedrock topology is more prominent. Soils are mostly podzols on deep loamy to sandy sediments. The site has a long history of agricultural and forest management dating from the eighteenth century. The human population of the region is close to 7 million, with over 5 million people living in the city of St. Petersburg (Krankina et al. 1998).

Land cover was mapped using a nearly cloud-free Landsat ETM+ image from June 2, 2002 (WRS-2 path 184, row 18, UTM Zone 36 N, WGS84). After geometric and radiometric correction, the image was transformed into Tasseled Cap indices of brightness, greenness, and wetness (Crist 1985). Using an iterative unsupervised classification of the Tasseled Cap image, maps of land cover were created at different hierarchical classification levels starting with the 5 DVT classes that were then broken up into 17 more detailed classes. Forest inventory data (Kukuev et al. 1997) and expert-classified reference polygons were used for accuracy assessment. For 17 classes the agreement with reference data was 66.6% (kappa = 61.4%). At the level of dominant vegetation type the agreement with reference data is near-perfect 98.5% (kappa = 95.6%).

At the St. Petersburg site, the overall agreement between GLC-2000 and MODIS.PFT is high at 83%. The landscape is very fragmented and GLC-2000 mapped 13% of the site as mosaics of tree, shrub and herbaceous (including croplands) vegetation possibly inflating the calculated percent agreement with MODIS.PFT (Table 5.1, Fig. 5.8). The tree cover is overestimated by the GLC-2000 map (72%) and MODIS.PFT map (78%) when compared to NELDA (57%; Fig. 5.9). In comparison, the MODIS-VCF estimate of 52% tree cover is in good agreement with NELDA, but as explained in the regional analysis (see 5.2.3), the results for categorical maps and VCF are not directly comparable. By far the most common confusion type at the St. Petersburg site is between trees and herbaceous vegetation (8% of total area). One likely cause for this confusion is the significant presence of peatlands and other wetlands at the St. Petersburg site, with their characteristic mix of open canopy trees, low shrubs, and a moss-dominated herbaceous layer (Krankina et al. 2008). These complex plant assemblages fit poorly in class definitions of land-cover maps (Frey and Smith 2007). Both GLC-2000 and MODIS.PFT underestimate the extent of shrubs and herbaceous vegetation in the overall land cover of the St. Petersburg site (Fig. 5.9).

5.4 Effects of Vegetation on Carbon Stores in Terrestrial Ecosystems of Arctic Eurasia: Major Controlling Factors and Sources of Uncertainty

Information on land cover is among the principal inputs for simulation modeling, which is a fundamental tool for understanding ecosystem responses to climate and disturbance and extrapolating these processes over time and space. Here, we discuss the results of a re-analysis of the terrestrial C budget for Arctic Eurasia over the last decade (1997–2006) for different vegetation types of the region. The Terrestrial Ecosystem Model (TEM; Raich et al. 1991) was driven by spatially- and temporally-explicit climatology, disturbance, and land-cover/land-use data sets with the objective of determining the role that different vegetation and ecosystem types play in the regional terrestrial C balance in response to changing atmospheric CO_2 concentration, climate variability, ecosystem type, fire, forest management and agricultural land use.

We simulated 1,000+ years of C dynamics for potential vegetation over Arctic Eurasia with CO_2 fertilization effects, variable climate and transient disturbance and land use. The TEM is calibrated to site-specific vegetation parameters and extrapolated across the study area based on a 0.5° latitude x 0.5° longitude grid matching the input climate data sets (Climate Research Unit, University of East Anglia, UK; Mitchell and Jones 2005). The model was run on a monthly time-step at sub-grid resolution based on a non-spatial mosaic of "cohorts" representing unique vegetation types and disturbance histories within each grid cell. Additional methodological details on TEM, the input data sets, and the simulation framework are given in Chapter 6 (this volume).

The input potential vegetation data set was derived from the Global Land Cover Characterization (GLCC; Loveland et al. 2000) version 2 Seasonal Land Cover Regions (SLCR) Eurasia data set at 1-km (equal-area) resolution. Among the various vegetation data sets available for this region (see Section 5.2, above), the GLCC.SLCR map was chosen for its detail in classification (200+ categories) and its description of vegetation mosaics, thereby allowing flexibility in translating for the arctic conditions, boreal and temperate ecosystem types for which the TEM is calibrated. The translated vegetation map, which included 10 upland categories, was aggregated to the 0.5º grid, but retaining the area represented by each unique vegetation type within a grid cell as an individual, non-spatial cohort. Wetland cohort areas were assigned to each grid cell based on a 1° × 1° grid cell fraction inundated database (Matthews and Fung 1987), where wetland area equals the product of fraction inundated and total cell area. The final classification, then, contained 17 categories (in addition to water, ice, and barren; Table 5.3) of upland and associated wetland vegetation types (some ecosystem types, such as polar desert and xeric shrublands, were not allowed to have wetland associates). Although at a relatively coarse resolution (0.5°), the cohortized potential vegetation map was designed to capture upland vegetation community type mosaics and their transitions across spatial gradients, along with spatially-explicit data on wetland extent and type.

Table 5.3 Classification scheme and areas represented by the ecological zones for Eurasian Arctic (north of 60°N) as input data for the TEM simulations. In parenthesis is the four-letter code for each ecozone; it is followed, in quotations, by its assigned dominant vegetation type (DVT) for comparison with the other vegetation maps considered in Chapter 5

	Ecological zone	Area (km^2)
	Inland water	372,877
	Ice, rock, "Barren"	2,337,878
1	Prostrate Tundra / Polar Desert (PTPD), "Herbaceous"	1,782,272
2	Arctic Shrub Tundra (ASHT), "Shrub"	1,638,383
3	Arctic Shrub Tundra Wetlands (ASHTw), "Shrub"	678,759
4	Boreal Needleleaf Evergreen Forest (BNEF), "Tree"	1,128,228
5	Boreal Needleleaf Evergreen For. Wetlands (BNEFw), "Tree"	530,967
6	Boreal Needleleaf Deciduous Forest (BNDF), "Tree"	1,229,673
7	Boreal Needleleaf Deciduous For. Wetlands (BNDFw), "Tree"	489,069
8	Boreal Broadleaf Deciduous Forest (BBDF), "Tree"	740,583
9	Boreal Broadleaf Deciduous Forest Wetlands (BBDFw), "Tree"	67,061
10	Temperate Needleleaf Evergreen Forest (TNEF), "Tree"	469,347
11	Temperate Needleleaf Evergr. Forest Wetlands (TNEFw), "Tree"	65,643
12	Temperate Broadleaf Deciduous Forest (TBDF), "Tree"	60,732
13	Temperate Broadleaf Decid. For. Wetlands (TBDFw), "Tree"	2,724
14	Xeric Woodlands (WOOD), "Tree"	4,291
15	Xeric Shrublands (XESH), "Shrub"	155,577
16	Grasslands (GRAS), "Herbaceous"	163,691
17	Grasslands / Herbaceous Wetlands (GRASw), "Herbaceous"	11,310
	Total inland area	11,929,065

The location and timing of disturbances are determined from data sets on fire occurrence, area burned, fire severity, and fire return interval, as well as modeled data for rates of forest harvest and crop and pasture establishment and abandonment. The annual area burned data set for Eurasia was based on AVHRR satellite-derived fire scars data from 1996–2002 (Sukhinin et al. 2004) and backcasted to the year 1000 based on 0.5° resolution fire return intervals. For a complete description of the historical fire data set, fire return interval calculation, and backcasting approach, see Balshi et al. (2007). That study's fire database was extended from 2002 to 2006 for Northern Eurasia using the Global Fire Emission Database version 2 (van der Werf et al. 2006). The data set provides monthly burn fraction by 1° × 1° grid cell, which was converted to annual burn area and extracted from cohorts based on a priority list of burnable ecosystem types, thereby creating a new, secondary cohort of age zero for that year. In the same way, forest harvest and land use (crops or pasture) cohorts were created in the input data set, derived from 1° × 1° gridded, annual land use transitions data for years 1700 through 2000, modeled by Hurtt et al. (2006).

The model produced monthly estimates of C stocks in vegetation, soil and product pools for each cohort over the length of the simulation, which we report as average annual total ecosystem C stocks across all cohorts within each ecozone, and average these values over the 10-year analysis period (1997–2006). The average annual change in C stocks reported here represents the Net Ecosystem C Balance

(NECB) of the system (see Chapin et al. 2006). NECB includes both the C flux from the terrestrial system to the atmosphere through the initial conversion flux (e.g. from fire) and subsequent decomposition of reactive soil organic matter and decay of post-harvest product pools as well as the lateral leaching flux of dissolved organic C via stream export.

We summarized the disturbance data and their effects (along with CO_2 and climate) on total ecosystem C stores and average annual balance by ecozone across the study area for the 1997–2006 time period (Table 5.4). The simulation shows that the study area as a whole is losing C from terrestrial ecosystems on an average rate of 44 Tg C year^{-1} from 1997–2006. The system is estimated to contain total ecosystem C stocks (in vegetation, soils, and product pools) on the order of 266 Pg C. More than 167,000 km^2 were burned over this decade (about 2% of the total study area), with another 119,000 km^2 of forest harvested (~2.5% of forest area) and 72,000 km^2 (less than 1% of the total study area) in agricultural land use (crops and pastures). The majority of area burned occurred in larch-dominated forests of eastern Siberia (Boreal Needleleaf Deciduous Forest, BNDF, ecozone), with an average 0.6% of its area burned annually during this time period. The results show this ecozone as having the majority contribution toward the overall C loss in the study area. The BNDF ecozone alone is losing more C than the study area as a whole, suggesting that the rest of the ecozones combined acted as a net C sink (of about 21 Tg C year^{-1}) over this decade. Most of the strength of that sink is found in the tundra types (Prostrate Tundra/Polar Desert, PTPD, and Arctic Shrub

Table 5.4 Disturbance area and C stocks for each ecozone and land use type in the Eurasian Arctic for the period 1996–2006. Wetland types were merged with their upland counterparts to present these data by ecozones

Ecozones	Area[a](km^2)	Area harvested[b] (km^2)	Area burned[b] (km^2)	Total (Tg C)	Density (kg C m^{-2})	Change in stocks[c](Tg C year^{-1})
PTPD	1,774,437	0	1,788	30,255	17.05	8.75
ASHT	2,312,690	0	5,338	63,991	27.67	17.93
BNEF	1,654,928	41,778	25,379	26,556	16.05	−16.81
BNDF	1,717,593	12,726	104,436	123,271	71.77	−65.03
BBDF	797,853	7,918	14,336	11,275	14.13	3.57
TNEF	517,291	47,148	1,478	3,755	7.26	7.55
TBDF	49,802	9,551	18	972	19.51	−0.06
WOOD	3,369	0	77	66	19.73	0.01
XESH	153,642	0	7,628	3,581	23.31	−0.33
GRAS	164,299	0	7,167	1,439	8.76	−1.25
CROP	41,489	0	0	522	12.54	1.09
PAST	30,917	0	0	146	4.73	0.09
Total	9,218,310	119,121	167,645	265,828	28.84	−44.49

[a]Area represented by each ecozone or land use in year 2006.
[b]Area harvested or burned for each ecozone during the period 1996–2006.
[c]All C values are given as the 10-year average between 1996 and 2006.

Tundra, ASHT). The majority of the forest harvest area occurred in temperate and boreal pine and spruce forests (Temperate Needleleaf Evergreen Forest, TNEF, and Boreal Needleleaf Evergreen Forest, BNEF, ecozones). With relatively small area burned, the temperate part (TNEF) located primarily in the western portion of the study region is estimated to be sequestering C at a rate of 7.6 Tg C $year^{-1}$, while the boreal part (BNEF), with higher rates of fire, is losing C at nearly 17 Tg C $year^{-1}$.

The C budget for the ecozones of Northern Eurasia over the past decade assembled here, when compared with the disturbance data, suggests some of the potential controlling factors on the sources and sinks of C in this region. The ecozones losing the most C over the time period also had the largest burned area, thus fire appears to have a substantial effect on C loss from the system. The very large area burned in the larch-dominated forests (BNDF ecozone) combined with its high C density (more C available to be released during and after fire) to produce the vast majority of the C source for the study area. The tundra ecozones (PTPD and ASHT) represent a large and mostly undisturbed area that may be responding to changes in climate in producing a net C sink.

5.5 Significance of the Current Uncertainty in Vegetation Cover for Estimating Carbon Stores, Sources, and Sinks in Terrestrial Ecosystems

The analysis in Section 5.4 shows that the different ecozones have large variation in their C stocks and fluxes, indicating that the underlying vegetation map used to drive model simulations can have important consequences for regional C budget estimates. To assess the effect of different input vegetation data sets on the modeled estimates of regional C balance, we performed a simple analysis in which we produced estimates of live vegetation and total ecosystem C density and mean estimates of per-area change in C stores for each ecozone from our simulations (Table 5.4). The density and change estimates incorporate the "average" effects of CO_2, climate, and disturbance at the ecozone level. We then aggregated the ecozones to the broader DVT categories (see Table 5.3) and used the per-area stock and flux estimates to extrapolate across each DVT category according to the area represented by these categories in the ecozone classification used in this study (Table 5.3) as well as in the GLC-2000 and MODIS.PFT maps (Table 5.2). This "bookkeeping" type approach to regional C budget analysis assumes average, constant effects of climate and disturbance within each DVT. While this is admittedly a very simplistic approach, it does provide the first approximation of the effect of input vegetation data sets on the modeled estimates of regional C balance.

The GLCC-based vegetation classification (Loveland et al. 2000) used in C modeling for this study agrees more closely with the GLC-2000 than the MODIS.PFT in terms of the total areas represented by the DVT categories, particularly with the tree and shrub estimates (Table 5.5). Note also that C simulation considered a larger

Table 5.5 Comparison of the effect on regional C balance estimates of extrapolating simulated C stock and flux density across the different area estimates of the dominant vegetation type categories (DVT) from the classifications discussed in this chapter (A – live vegetation C, B – total ecosystem C)

	Simulated averages		GLCC			GLC-2000			MODIS.PFT		
A	Density	Density Δ	Area	Total	Δ in Stocks	Area	Total	Δ in Stocks	Area	Total	Δ in Stocks
Tree	5.043	0.032	4,741	24	0.15	4,450	22	0.14	2,630	13	0.08
Shrub	0.651	0.022	2,466	2	0.05	2,258	1	0.05	5,290	3	0.12
Herb.	0.387	0.003	2,011	1	0.01	916	0	0	680	0	0
Barren	0	0	2,338	0	0	1,232	0	0	255	0	0
Total	2.832	0.023	11,556	26	0.21	8,856	24	0.2	8,855	17	0.2
B											
Tree	34.992	−0.149	4,741	166	−0.7	4,450	156	−0.66	2,630	92	−0.39
Shrub	27.398	0.071	2,466	68	0.18	2,258	62	0.16	5,290	145	0.38
Herb.	16.091	0.042	2,011	32	0.09	916	15	0.04	680	11	0.03
Barren	0	0	2,338	0	0	1,232	0	0	255	0	0
Total	28.783	−0.05	11,556	266	−0.44	8,856	232	−0.46	8,855	248	0.02

Units: Density (kg C m^{-2}); density Δ (kg C m^{-2} $year^{-1}$); Area (103 m^{-2}); Total C stocks (Pg C); Δ in stocks (Pg C $year^{-1}$).

overall study area than the map analysis from Section 5.2 (11.8 million km^2 in C simulation compared to 8.9 million m^2 in the two maps). However, the difference is primarily in areas of the Herbaceous and Barren DVT types because GLCC-based map included all areas above 60ºN latitude whereas the GLC-2000 and MODIS.PFT maps did not include areas above 74ºN – most of which is dominated by herbaceous vegetation (PTPD) and Ice, Rock (Barren) types.

While all three C budgets produce similar estimates of total ecosystem C stocks for the region, the estimated average annual change in C stocks (i.e. terrestrial C balance) over the last decade differs substantially for the MODIS.PFT classification as compared with the other two (Table 5.5). Extrapolations based on the vegetation data used in C simulation and the GLC-2000 actually produced very similar estimates of regional C balance (-0.44 and -0.46 Pg C $year^{-1}$, respectively), primarily because of the similarity in areas of the tree and shrub categories. While these two estimates suggest a substantial loss of C from this region during the 1997–2006 time period, the extrapolation based on the MODIS.PFT classification resulted in a more neutral C balance estimate (a small net sink of 20 Tg C $year^{-1}$). This result is due to the higher estimate of shrub area, which acts as a C sink in our simulations and offsets the lesser area of C loss from the tree cover category.

The impact of the input vegetation data appears even more significant when live vegetation C is examined separately (Table 5.5b). The estimate of C stock in live vegetation based on the GLC-2000 map (24 Pg C) is 40% higher than the estimate based on the MODIS.PFT map (17 Pg C). While the estimates of the overall change in live vegetation C stocks are very similar for both maps (0.2 Pg C sink), the attribution of the projected C sink is quite different depending on the map used: based on GLC-2000 map most of the C accumulation occurs in tree-dominated ecosystems while MODIS.PFT map would attribute most of the C sink to shrub vegetation.

This extrapolation provides only a general sense of the effect that different input vegetation data sets will have on estimates of C stocks and flux. A more comprehensive, quantifiable estimation of these effects would require new simulations in which the different vegetation maps were incorporated into the spatially-explicit data sets used to drive the model. In this analysis, for example, the near-neutral C balance estimate based on the MODIS.PFT classification does not fully capture the effects of fire because of the lower estimate of tree-cover area in this map. More explicitly connecting this data set with the fire data would more realistically distribute area burned across the study region, including fires in shrub-dominated area. This may alter the overall MODIS.PFT-based estimate of NECB for the region.

5.6 Summary and Conclusions

Significant differences exist between land-cover maps of Arctic Eurasia even at relatively coarse resolution and at the level of broad plant functional and dominant vegetation types. Thus, the choice of a specific land-cover product can have a major impact on the results of many research projects in the region and this source of uncertainty is often overlooked. The distinct geographic patterns of differences

indicate the areas where the effects of map selection can be the greatest and where further improvements in mapping are needed. The discrepancies in categorical maps are concentrated at borders between biomes and in parts of the region where significant presence of open canopies of woody plants (trees and shrubs) or herbaceous vegetation is expected.

Overall, the extent of disagreement between the compared categorical maps is greater in Siberia and Far East than in the western part of Arctic Eurasia. The paucity of ground data and the presence of larch (deciduous conifer) in the eastern part of the study region may be responsible. However, the high level of confusion between the two compared land-cover maps at the treeline and further north is prevalent throughout the region. This geographic distribution of disagreement may reflect the limitation of coarse resolution categorical maps in representing open vegetation covers and mixed or fragmented landscapes. Vegetation continuous field maps of dominant vegetation types are a promising alternative to categorical maps.

The agreement among the compared maps is highest for tree-dominated vegetation, which is represented more consistently than other vegetation-cover types in the categorical maps. Tree-cover representation in the MODIS.VCF product corroborates the general pattern of agreement in tree-cover distribution between the two categorical maps. Furthermore, the estimates of the total area of tree-dominated vegetation cover in the study region agree reasonably well among the three maps (GLC-2000, MODIS.PFT, and MODIS.VCF). The degree of spatial agreement is the lowest for herbaceous vegetation. One of the reasons for that may be the misclassification of herbaceous wetlands, which cover a significant proportion of the land mass in Eurasian Arctic. Mosses (especially *Sphagnum* mosses) and lichens on herbaceous wetlands exhibit distinct spectral signatures and a seasonal pattern of change that is substantially different from other plants in the "herbaceous" group.

The analysis of land-cover maps at two test sites highlighted specific strengths and weaknesses of the examined land-cover products in these two locations. At the St. Petersburg site both categorical maps agreed well, but both exaggerated tree cover and under-reported shrub and herbaceous vegetation. At the Komi site, the over-reporting of tree cover by GLC-2000 and failure of MODIS.PFT to separate shrub and herbaceous vegetation were the major issues in representing the overall land cover. Depending on specific application of the map other features may be significant, such as under-reporting of small but abundant water bodies in the arctic region on categorical coarse-resolution maps.

Different vegetation maps used in biogeochemical modeling could produce substantially different estimates of the regional C balance. A simple analysis in which we extrapolated simulated C stock and flux density for dominant vegetation types across the area estimates of these types in different land-cover products showed that a very different picture of the regional C balance emerges when changing the ratio of tree cover (an estimated C source) to shrub cover (C sink). A separate examination of live vegetation C indicated that the use of GLC-2000 map could lead to substantially higher estimate of C stock in forest biomass and greater role of trees as C sink than MODIS.PFT map. While simplified calculations provide a

general idea of how the underlying vegetation data can change regional C balance estimates, a more detailed comparison of its effects would require additional, spatially-explicit simulations using each of the different land-cover maps to drive the model.

References

Anisimov OA, Vaughan DG, Callaghan TV, Furgal C, Marchant H, Prowse TD, Vilhjálmsson H, Walsh JE (2007) Polar regions (Arctic and Antarctic) In: Parry ML, Canziani OF, Palutikof JP, van der Linden PJ, Hanson CE (eds) Climate change 2007: impacts, adaptation and vulnerability, contribution of working group II to the fourth assessment report of the intergovernmental panel on climate change, Cambridge University Press, Cambridge, pp 653–685

Balshi MS, McGuire AD, Zhuang Q, Melillo J, Kicklighter DW, Kasischke E, Wirth C, Flannigan M, Harden J, Clein JS, Burnside TJ, McAllister J, Kurz WA, Apps M, Shvidenko A (2007) The role of historical fire disturbance in the carbon dynamics of the pan-boreal region: a process-based analysis. J Geophys Res 112. doi:10.1029/2006JG000380

Bartalev SA, Belward AS, Erchov DV, Isaev AS (2003) A new Spot4-Vegetation Derived Land Cover Map of Northern Eurasia. Int J Rem Sens 24:1977–1982

Bonan GB, Levis S, Kergoat L, Oleson KW (2002) Landscapes as patches of plant functional types: an integrating concept for climate and ecosystem models. Glob Biogeochem Cycles 16. doi:10.1029/2000GB001360

Breiman L (1996) Bagging predictors. Mach Learn 26:123–140

Bubier JL, Rock BN, Crill PM (1997) Spectral reflectance measurements of boreal wetland and forest mosses. J Geophys Res-Atmos 102:29483–29494

Canty MJ, Nielsen AA, Schmidt M (2004) Automatic radiometric normalization of multispectral imagery. Rem Sens Environ 91:441–451

Chapin FS III, Sturm M, Serreze MC, McFadden JP, Key JR, Lloyd AH, McGuire AD, Rupp TS, Lynch AH, Schimel JP, Beringer J, Chapman WL, Epstein HE, Euskirchen ES, Hinzman LD, Jia G, Ping CL, Tape KD, Thompson CDC, Walker DA, Welker JM (2005) Role of land-surface changes in Arctic summer warming. Science 310:657–660

Chapin FS III, Woodwell GM, Randerson JT, Rastetter EB, Lovett GM, Baldocchi DD, Clark DA, Harmon ME, Schimel DS, Valentini R, Wirth C, Aber JD, Cole JJ, Goulden ML, Harden JW, Heimann M, Howarth RW, Matson PA, McGuire AD, Melillo JM, Mooney HA, Neff JC, Houghton RA, Pace ML, Ryan MG, Running SW, Sala OE, Schlesinger WH, Schulze ED (2006) Reconciling carbon-cycle concepts, terminology, and methods. Ecosystems 9:1041–1050. doi:10.1007/s10021-005-0105-7

Chavez PS Jr (1996) Image-based atmospheric corrections – revisited and improved. Photogramm Eng Rem Sens 62:1025–1036

Commission of the European Communities (1993) CORINE land cover: guide technique. Brussels, Belgium

Crist EP (1985) A TM tasseled cap equivalent transformation for reflectance factor data. Rem Sens Environ 17:301–306

DeFries RS, Townshend JRG (1994) NDVI derived land cover classifications at a global scale. Int J Rem Sens 15:3567–3586

DeFries RS, Hansen M, Steininger M, Dubayah R, Sohlberg R, Townshend JRG (1997) Subpixel forest cover in central Africa from multisensor, multitemporal data. Rem Sens Environ 60:228–246

Di Gregorio A (2005) Land cover classification system: classification concepts and user manual for software – version 2, Rome

EUROSTAT (1998) Forestry statistics 1992–1996, Luxembourg

Field CB, Lobell DB, Peters HA, Chiariello NR (2007) Feedbacks of terrestrial ecosystems to climate change. Ann Rev Environ Res 32:1–29

Frey KE, Smith LC (2007) How well do we know northern land cover: Comparison of four global vegetation and wetland products with a new ground-truth database for West Siberia. Glob Biogeochem Cycles 21. doi:10.1029/2006GB002706

Friedl MA, McIver DK, Hodges JCF, Zhang XY, Muchoney D, Strahler AH, Woodcock CE, Gopal S, Schneider A, Cooper A, Baccini A, Gao F, Schaaf CB (2002) Global land cover mapping from MODIS: algorithms and early results. Rem Sens Environ 83:287–302

Fritz S, Bartholome E, Belward A, Hartley A, Stibig HJ, Eva H, Mayaux P, Bartalev SA, Latifovic R, Kolmert S, Roy PS, Agrawal S, Bingfanf W, Wenting X, Ledwith M, Pekel JF, Giri C, Mucher S, de Badts E, Tateishi R, Champeaux JL, Defourny P (2003) Harmonisation, mosaicing and production of the Global Land Cover 2000 database, Ispra

Fritz S, Lee L (2005). Comparison of land cover maps using fuzzy agreement. Int J Geogr Inf Sci 19:787–807

Frohn RC, Hinkel KM, Eisner WR (2005) Satellite remote sensing classification of thaw lakes and drained thaw lake basins on the North Slope of Alaska. Rem Sens Environ 97:116–126

Giri C, Zhu ZL, Reed B (2005) A comparative analysis of the Global Land Cover 2000 and MODIS land cover data sets. Rem Sens Environ 94:123–132

Gurney KR, Scott Denning A, Rayner P, Pak B, Baker D, Bousquet P, Bruhwiler L, Chen YH, Ciais P, Fung IY, Heimann M, Higuchi K, John J, Maki T, Maksyutov S, Peylin P, Prather M, Taguchi S (2004) Transcom 3 inversion intercomparison: Model mean results for the estimation of seasonal carbon sources and sinks. Glob Biogeochem Cycles 18:GB1010. doi:10.1029/2003GB002111

Häme T, Stenberg P, Rauste Y (2000) A methodology to estimate forest variables at sub-pixel level. In: Zawila-Niedzwiecki T, Brach M (eds) Proceedings of conference on remote sensing and forest monitoring, Rogow

Häme T, Stenberg P, Andersson K, Rauste Y, Kennedy P, Folving S, Sarkeala J (2001) AVHRR-based forest proportion map of the Pan-European area. Rem Sens Environ 77:76–91

Hansen MC, DeFries RS, Townshend JRG, Sohlberg R (2000) Global land cover classification at 1 km resolution using a decision tree classifier. Int J Rem Sens 21:1331–1365

Hansen MC, DeFries, RS, Townshend J, Sohlberg R, Carroll M, Dimiceli C (2002) Towards an operational MODIS continuous field of percent tree cover algorithm: examples using AVHRR and MODIS data. Rem Sens Environ 83(1–2):303–319

Hansen MC, DeFries RS, Townshend JRG, Carroll M, Dimiceli C, Sohlberg RA (2003a) Global percent tree cover at a spatial resolution of 500 meters: First results of the MODIS vegetation continuous fields algorithm. Earth Interact 7:1–15

Hansen MC, DeFries RS, Townshend JRG, Carroll M, Dimiceli C, Sohlberg R (2003b) Vegetation continuous fields MOD44B, 2001 percent tree cover – collection 3, College Park

Hansen MC, Townshend JRG, DeFries RS, Carroll M (2005) Estimation of tree cover using MODIS data at global, continental and regional/local scales. Int J Rem Sens 26:4359–4380

Hansen MC, Stehman SV, Potapov PV, Loveland TR, Townshend JRG, DeFries RS, Pittman KW, Stolle F, Steininger MK, Carroll M, Dimiceli C (2010) Humid tropical forest clearing from 2000 to 2005 quantified using multi-temporal and multi-resolution remotely sensed data. Proceedings of the national academy of sciences of USA 107(19):8650–8655

Heiskanen J (2008) Evaluation of global land cover data sets over the tundra-taiga transition zone in northernmost Finland. Int J Rem Sens 29:3727–3751

Herold M, Mayaux P, Woodcock CE, Baccini A, Schmullius C (2008) Some challenges in global land cover mapping: An assessment of agreement and accuracy in existing 1 km datasets. Rem Sens Environ 112(5). doi:10.1016/j.rse.2007.11.013

Houghton RA (2003) Why are estimates of the terrestrial carbon balance so different. Glob Chang Biol 9:500–509

Houghton RA, Joos F, Asner GP (2004) The effects of land use and management on the global carbon cycle. In: Gutman G, Janetos AC, Justice CO, Moran EF, Mustard JF, Rindfuss RR, Skole D, Turner BL II, Cochrane MA (eds) Land change science: Observing, monitoring, and understanding trajectories of change on the Earth's surface. Kluwer Academic Publishers, Dordrecht

Hurtt GC, Frolking S, Fearon MG, Moore B III, Shevliakova E, Malyshev S, Pacala S, Houghton RA (2006) The underpinnings of land-use history: Three centuries of global gridded land-use transitions, wood harvest activity, and resulting secondary lands. Glob Chang Biol 12:1–22

Jung M, Henkel K, Herold M, Churkina G (2006) Exploiting synergies of global land cover products for carbon cycle modeling. Rem Sens Environ 101:534–553

Kennedy RE, Cohen WB (2003) Automated designation of tie-points for image-to-image coregistration. Int J Rem Sens 24:3467–3490

Krankina ON, Fiorella M, Cohen W, Treyfeld RF (1998) The use of Russian forest inventory data for carbon budgeting and for developing carbon offset strategies. World Res Rev 10:52–66

Krankina ON, Houghton RA, Harmon ME, Hogg EH, Butman D, Yatskov M, Huso M, Treyfeld RF, Razuvaev VN, Spycher G (2005) Effects of climate and disturbance on forest biomass across Russia. Can J For Rese 35:2281–2293

Krankina ON, Pflugmacher D, Friedl M, Cohen WB, Nelson P, Baccini A (2008) Meeting the challenge of mapping peatlands with remotely sensed data. Biogeosci Discuss 5:1–26

Kukuev YA, Krankina ON, Harmon ME (1997) The forest inventory system in Russia. J Forest 95:15–20

Loveland TR, Reed BC, Brown JF, Ohlen DO, Zhu Z, Yang L, Merchant JW (2000) Development of a global land cover characteristics database and IGBP DISCover from 1 km AVHRR data. Int J Rem Sens 21:1303–1330

Matthews E, Fung I (1987) Methane emission from natural wetlands: Global distribution, area, and environmental characteristics of sources. Glob Biogeochem Cycles 1:61–86

McGuire AD, Melillo JM, Kicklighter DW, Pan Y, Xiao X, Helfrich J, Moore B III, Vorosmarty CJ, Schloss AL (1997) Equilibrium responses of global net primary production and carbon storage to doubled atmospheric carbon dioxide: Sensitivity to changes in vegetation nitrogen concentration. Glob Biogeochem Cycles 11:173–189

McGuire AD, Chapin F S III, Wirth C, Apps M, Bhatti J, Callaghan T, Christensen T R, Clein J S, Fukuda M, Maximov T, Onuchin A, Shvidenko A, Vaganov E (2007) Responses of high latitude ecosystems to global change: Potential consequences for the climate system In: Canadell JG, Pataki DE, Pitelka LF (eds.) Terrestrial Ecosystems in a Changing World. The IGBP Series. Springer, Berlin, pp 297–310

Mitchell TD, Jones PD (2005) An improved method of constructing a database of monthly climate observations and associated high-resolution grids. Int J Climatol 25(6):693–712

Morisette JT, Privette JL, Justice CO (2002) A framework for the validation of MODIS Land products. Rem Sens Environ 83:77–96

Myneni RB, Dong J, Tucker CJ, Kaufmann RK, Kauppi PE, Liski J, Zhou L, Alexeyev V, Hughes MK (2001) A large carbon sink in the woody biomass of northern forests. Proc Natl Acad Sci of USA 98:14784–14789

Päivinen R, Lehikoinen M, Schuck A, Häme T, Väätäinen S, Kennedy P, Folving S (2001) Combining earth observation data and forest statistics. European Forest Institute, Joint Research Centre – European Commission, EFI Research Report 14, Joensuu, Finland and Ispra

Pflugmacher D, Krankina ON, Cohen WB (2007) Satellite-based peatland mapping: Potential of the MODIS sensor. Glob Planet Change 56:248–257

Polyakov ID, Alekseev GV, Bekryaev RV, Bhatt U, Colony R, Johnson MA, Karklin VP, Makshtas AP, Walsh D Yulin AV (2002) Observationally based assessment of polar amplification of global warming. Geophys Res Lett 29. doi:10.1029/2001GL011111

Potapov P, Hansen MC, Stehman SV, Loveland TR, Pittman K (2008) Combining MODIS and Landsat imagery to estimate and map boreal forest cover loss. Rem Sens Environ 112: 3708–3719

Rahman H, Dedieu G (1994) SMAC: A simplified method for the atmospheric correction of satellite measurements in the solar spectrum. Int J Rem Sens 15:123–143

Raich JW, Rastetter EB, Melillo JM, Kicklighter DW, Steudler DA, Peterson BJ, Grace AL, Moore B III, Vörösmarty CJ (1991) Potential net primary productivity in South America: Application of a global model. Ecol Appl 1:399–429

Schimel DS, House JI, Hibbard KA, Bousquet P, Ciais P, Peylin P, Braswell BH, Apps MJ, Baker D, Bondeau A, Canadell J, Churkina G, Cramer W, Denning AS, Field CB, Friedlingstein P, Goodale C, Heimann M, Houghton RA, Melillo JM, Moore B III, Murdiyarso D, Noble I, Pacala SW, Prentice IC, Raupach MR, Rayner PJ, Scholes RJ, Steffen WL, Wirth C (2001) Recent patterns and mechanisms of carbon exchange by terrestrial ecosystems. Nature 414:169–172. doi:10.1038/35102500

Schlesinger WH (1991) Biogeochemistry: An analysis of global change. San Diego, New York

Schuck A, Van Brusselen J, Päivinen R, Häme T, Kennedy P, Folving S (2002) Compilation of a calibrated European forest map derived from NOAA-AVHRR data. European Forest Institute. EFI Internal Report 13, 44 pp plus Annexes

Shvidenko A, Nilsson S (2003) A synthesis of the impact of Russian forests on the global carbon budget for 1961–1998. Tellus 55B:391–415

Sukhinin AI, French NHF, Kasischke ES, Hewson JH, Soja AJ, Csiszar IA, Hyer EJ, Loboda T, Conrad SG, Romasko VI, Pavlichenko EA, Miskiv SI, Slinkina OA (2004) AVHRR-based mapping of fires in Russia: New products for fire management and carbon cycle studies. Rem Sens Environ 93(4):546–564

Stahler AH, Boschetti L, Foody GM, Friedl MA, Hansen MC, Herold M, Mayaux P, Morisette JT, Stehman SV, Woodcock CE (2006) Global land cover validation: Recommendations for evaluation and accuracy assessment of global land cover maps. Luxembourg: Office for Official Publications of the European Communities, 60 pp

Stroeve J, Markus T, Meier W, Miller J (2006) Recent changes in the Arctic melt season. Ann Glaciol 44(1):367–374. doi:10.3189/172756406781811583

van der Werf GR, Randerson JT, Giglio L, Collatz GJ, Kasibhatla PS, Arellano Jr. AF (2006) Interannual variability in global biomass burning emissions from 1997 to 2004. Atmos Chem Phys 6:3423–3441

Vogelmann JE, Moss DM (1993) Spectral reflectance measurements in the Genus Sphagnum. Rem Sens Environ 45:273–279

Walker DA, Raynolds MK, Daniels FJA, Einarsson E, Elvebakk A, Gould WA, Katenin AE, Kholod SS, Markon CJ, Melnikov ES, Moskalenko NG, Talbot SS, Yurtsev BA, Team C. (2005) The circumpolar Arctic vegetation map. J Veg Sci 16:267–282

Wan Z, Zhang Y, Zhang Q, Li ZL (2002) Validation of the land surface temperature products retrieved from Terra Moderate Resolution Imaging Spectroradiometer data. Rem Sens Environ 83:163–180

Wolfe RE, Roy DP, Vermote EF (1998) MODIS land data storage, gridding, and compositing methodology: Level 2 grid. IEEE Trans Geosci Rem Sens 36(4):1324–1338

Wu A, Li Z, Cihlar J (1995) Effects of land cover type and greenness on AVHRR bidirectional reflectances. J Geophys Res 100:9179–9192

Zhu Z, Evans DL (1994) US forest types and predicted percent forest cover from AVHRR data. Photogramm Eng Rem Sens 60:525–531

Chapter 6
The Effects of Land Cover and Land Use Change on the Contemporary Carbon Balance of the Arctic and Boreal Terrestrial Ecosystems of Northern Eurasia

Daniel J. Hayes, A. David McGuire, David W. Kicklighter, Todd J. Burnside, and Jerry M. Melillo

Abstract Recent changes in climate, disturbance regimes and land use and management systems in Northern Eurasia have the potential to disrupt the terrestrial sink of atmospheric CO_2 in a way that accelerates global climate change. To determine the recent trends in the carbon balance of the arctic and boreal ecosystems of this region, we performed a retrospective analysis of terrestrial carbon dynamics across northern Eurasia over a recent 10-year period using a terrestrial biogeochemical process model. The results of the simulations suggest a shift in direction of the net flux from the terrestrial sink of earlier decades to a net source on the order of 45 Tg C year^{-1} between 1997 and 2006. The simulation framework and subsequent analyses presented in this study attribute this shift to a large loss of carbon from boreal forest ecosystems, which experienced a trend of decreasing precipitation and a large area burned during this time period.

6.1 Introduction

Carbon dioxide concentrations in the atmosphere have been rapidly increasing over the last century and an increase in global surface air temperature (Jones and Moberg 2003; Hansen et al. 2006), particularly since the 1980s (Alley et al. 2003; Johannessen et al. 2004), has been attributed to this increase in radiatively active gases (IPCC 2007). Terrestrial ecosystems have potentially critical, but not fully known, feedbacks with a changing climate as a function of surface energy balance and the patterns of sources and sinks of atmospheric carbon dioxide (CO_2) and other greenhouse gases (Chapin et al. 2008; Field et al. 2007; Houghton 2003). In addition to climate forcings, natural disturbances and human activities can substantially alter the patterns and affect the underlying processes that create and transform these terrestrial sources and sinks (Houghton et al. 2004; Schimel et al. 2001).

D.J. Hayes (✉)
Institute of Arctic Biology, University of Alaska Fairbanks, Fairbanks, AK 99775, USA
e-mail: Daniel.Hayes@alaska.edu

G. Gutman, A. Reissell (eds.), *Eurasian Arctic Land Cover and Land Use in a Changing Climate*, DOI 10.1007/978-90-481-9118-5_6,

Recent studies have revealed surface air temperature increases on average of 0.35°C per decade from 1970 to 2000 for terrestrial regions between 50 and 70°N (Euskirchen et al. 2007; Serreze and Francis 2006). Elevated CO_2 levels and warmer temperatures may create a negative feedback to climate through expansion of higher productivity ecosystems into arctic regions (Tape et al. 2006; Sturm et al. 2001) and increased carbon (C) uptake by vegetation (Kimball et al. 2007). These processes are potentially offset, or even overtaken, by positive feedbacks through changes in surface energy balance (Chapin et al. 2005; Brovkin et al. 2006) and increased CO_2 respiration and methane (CH_4) release from arctic tundra and boreal forest soils (Zhuang et al. 2007). Further, evidence suggests that changes in climate are increasing the frequency and severity of forest fires (Kasischke and Turetsky 2006; Soja et al. 2007) and insect outbreaks (Kurz et al. 2008), creating a large source of CO_2 to the atmosphere from boreal forest regions. Potential longer-term mitigation of this source (i.e., negative feedbacks on climate forcing) by changes in energy balance following disturbance is not completely understood (Randerson et al. 2006a; Goetz et al. 2007).

6.1.1 Scope and Objectives of the Analysis

The objective of this analysis is to determine the recent trends in the terrestrial C balance of Eurasian arctic and boreal ecosystems, with a focus on the role of land-cover and land-use change processes in these dynamics. Studies based on inversion modeling or forest inventory data are able to provide estimates of net C exchange between the land and the atmosphere as well as the total terrestrial C budget, respectively. While such approaches can be used to generate overall estimates of terrestrial C exchange, they do not individually consider the effects of particular controlling factors (i.e., land-cover/land-use and other environmental changes) and thus do not allow for explicit valuation of the underlying mechanisms that drive these exchanges. Furthermore, these studies that have been conducted to date are not sufficiently current as to ascertain the latest trends in the terrestrial C dynamics or their response to recent changes in disturbance, land use and environmental conditions.

Process-based simulation modeling is a fundamental tool for understanding and reducing uncertainty with respect to ecosystem responses to climate and disturbance, and for extrapolating these processes over time and space – the key step in predicting the future response of climate and ecosystem function. Simulation frameworks can be designed to assess the influence of various controlling factors on C dynamics and quantify their effects (e.g., McGuire et al. 2001). To understand the role of land cover and land use change on regional C balance, it is necessary to evaluate their effects in the context of other climatic and environmental changes. An approach based on ecosystem process simulation modeling, then, can be used to extrapolate estimates of C exchange beyond the spatial and temporal extents of the inverse modeling and inventory data studies described above, as well as to

investigate hypotheses relating to the attribution of mechanisms and controlling factors in determining C balance.

For this study, we employ a terrestrial ecosystem biogeochemistry model, driven by spatially- and temporally-explicit climatology, ecological data, disturbance, and land-cover/land-use data sets, to perform a retrospective analysis of terrestrial C dynamics across Northern Eurasia over the last decade (1997–2006). To drive these simulations, we used updated and contemporary input data sets to generate more up-to-date (through 2006) estimates of C balance than previous studies, incorporating recent changes in climate, disturbance and land use across the region. The simulation framework was designed to investigate the individual effects of changing atmospheric CO_2, atmospheric chemistry and climate variability, fire, forest management and agricultural land use. This study design provided the opportunity to evaluate the effect of the recent trends in land cover and land use change, in the context of other factors, on the contemporary C balance of the region. The goal of the analysis was to detect any recent changes in the C balance of Northern Eurasian ecosystems, with respect to earlier studies, and to identify the factors driving these changes.

6.2 Methods

6.2.1 Overview

To evaluate the relative importance of land-cover/land-use change (LCLUC) factors and non-LCLUC factors on terrestrial C dynamics in Northern Eurasia, we conducted five model simulations using different combinations of factors (see Section 6.2.4) as driving variables into the Terrestrial Ecosystem Model (TEM). For non-LCLUC factors, we considered CO_2 fertilization, and the combined effects of climate variability, ozone pollution and atmospheric nitrogen (N) deposition on terrestrial C balance. For LCLUC factors, we considered disturbance by wildfire, and the land uses of agriculture (row crops and pastures) and timber harvest. Here, we report on the comparison of model estimates of C stocks and fluxes among the simulations for the analysis time period of 1997 to 2006. To initialize the C, N and water pools for the beginning of the analysis period (i.e. January 1997), we simulated C dynamics since the year 1000 in each model run. The methods used to generate comprehensive and continuous driving variables for year 1000–2006 were specific to each input data set, and are described below.

6.2.2 The Terrestrial Ecosystem Model

The Terrestrial Ecosystem Model (TEM) is a process-based ecosystem model that uses spatially referenced information on atmospheric chemistry, climate, elevation, soils, and land cover to estimate monthly terrestrial C, N, and water fluxes and pool

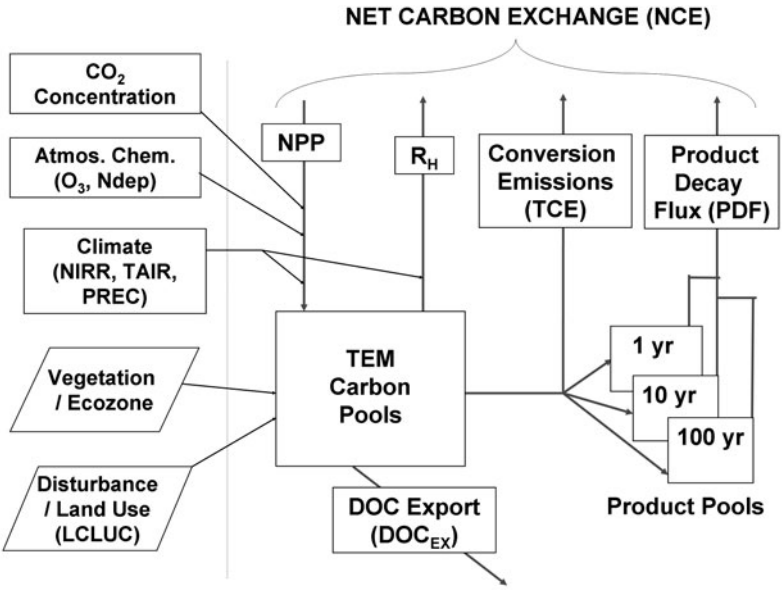

Fig. 6.1 A conceptual illustration of the effects of CO_2 fertilization, atmospheric chemistry, climate variability, vegetation type, land use and multiple disturbances on terrestrial C dynamics, as simulated by the Terrestrial Ecosystem Model (TEM). This diagram depicts Net Carbon Exchange (NCE) of the terrestrial system with the atmosphere as the balance between C inputs via net primary production (NPP) and C losses to the atmosphere through heterotrophic respiration (R_H), the direct emissions due to disturbance and land use conversion (TCE) and the combined flux from the decay of the three post-disturbance product pools (PDF). For this study, TEM calculates the overall C balance for the system as Net Ecosystem Carbon Balance (NECB), which includes NCE plus additional C losses from the terrestrial system through the leaching flux of dissolved organic C via stream export (DOC_{EX})

sizes. Driven by these various input data sets, TEM can be set up to incorporate the effects of both LCLUC and non-LCLUC factors on terrestrial C dynamics (Fig. 6.1). TEM is well-documented and has been used to examine patterns of terrestrial C dynamics across the globe, including how they are influenced by multiple factors such as CO_2 fertilization, climate change and variability, row-crop agriculture, wildfire and ozone pollution (Melillo et al. 1993; McGuire et al. 1997, 2000a,b, 2001, 2004; Tian et al. 1998, 1999, 2000, 2003; Xiao et al. 1998; Prinn et al. 1999; Reilly et al. 1999, 2007; Clein et al. 2000, 2002; Webster et al. 2003; Zhuang et al. 2003, 2006, 2007; Felzer et al. 2004, 2005, 2007; Brovkin et al. 2006; Euskirchen et al. 2006; Balshi et al. 2007; Sokolov et al. 2008).

For this study, we used a version of TEM that has been modified from Felzer et al. (2004), which simulated ozone pollution effects, to also include the influence of permafrost dynamics (Zhuang et al. 2003; Euskirchen et al. 2006), atmospheric N deposition, dissolved organic carbon (DOC) leaching, wildfire, pastures and timber harvest on terrestrial C dynamics. To simulate the effects of N deposition, NH_x

and NO_y from prescribed atmospheric sources are added to the available N pool within TEM for potential uptake by microbes and vegetation. DOC is assumed to be produced by the incomplete decomposition of soil organic matter (SOM) and DOC leaching losses are associated with water yield from the ecosystem. The treatment of permafrost dynamics, and their influence on the availability of SOM for decomposition, has also been modified in this new version of TEM. Instead of a fixed rooting depth, the amount of SOM available for decomposition in a particular month is determined by the proportion of the SOM found within a varying active layer depth. As the permafrost thaws and the active layer depth increases, the relative amount of SOM available to decompose increases.

The TEM is calibrated to site-specific vegetation parameters (Raich et al. 1991; McGuire et al. 1992; Clein et al. 2000; 2002, 2007; Euskirchen et al. 2006) and extrapolated across the study area based on spatially-explicit time-series data organized on a 0.5° latitude by 0.5° longitude grid. The model uses a monthly time-step to simulate ecosystem dynamics for each "cohort" in a non-spatial mosaic of cohorts representing unique vegetation types and disturbance histories within each grid cell. In this study, we simulate terrestrial C dynamics under four different land uses (natural, row-crop agriculture, pasture, timber harverst) along with the influence of wildfire and the conversion of land from one use to another on these dynamics. The simulation of these LCLUC dynamics by TEM have been described previously for natural ecosystems (e.g., Melillo et al. 1993; Tian et al. 1999), row-crop agriculture (Felzer et al. 2004), wildfire (Balshi et al. 2007), and the conversion and abandonment of land to/from row-crop agriculture (McGuire et al. 2001; Felzer et al. 2004).

6.2.3 Driving Data Sets

To extrapolate TEM across Northern Eurasia, we incorporated driving data sets that have (1) spatial variability, but no temporal variability (elevation and soil texture); (2) temporal variability, but no spatial variability (atmospheric CO_2 concentration); and (3) temporal and spatial variability (air temperature, precipitation, solar radiation, AOT40 ozone (O_3) index (a measure of the accumulated hourly ozone levels about a threshold), atmospheric N deposition, and land cover including fire disturbance. The non-temporal-varying spatial datasets were aggregated to 0.5° spatial resolution, with elevation based on the TerrainBase v1.1 data set from the National Geophysical Data Center, Boulder, CO (NGDC 1994) and soil texture from the Global Gridded Surfaces of Selected Soil Characteristics data set (Global Soil Data Task Group 2000).

Most of the temporally varying datasets have been used in previous studies, but needed to be extended from 2000 or 2002 to 2006, as well as "backcasted" to year 1000 of the model initialization period, for use in this study. Global annual atmospheric CO_2 data are from the Mauna Loa station (Keeling and Whorf 2005). Atmospheric CO_2 concentration for the time period of years 1000–1900 was held

constant at the year 1901 level (296.3 ppm). Monthly surface air temperature (TAIR, ^{o}C), precipitation (PREC, mm), and incident short-wave solar radiation (NIRR, W m^{-2}) data derived from observations for the period 1901–2002, gridded at 0.5° resolution, were obtained from the Climate Research Unit (CRU; University of East Anglia, UK; Mitchell and Jones 2005). The CRU climate variables were extended to 2006 with National Centers for Environmental Prediction/National Center for Atmospheric Research (NCEP/NCAR) Reanalysis one data sets (NOAA-ESRL Physical Sciences Division, Boulder, CO, USA) using a regression procedure based on data anomalies from a 10-year (1993–2002) mean for each variable (see Drobot et al. 2006). These data sets were back-casted to year 1000 by a repeating 30-year cycle of the 1901–1930 monthly data to initialize the C pools with climate variability (except for the simulation without climate variability, where 1901–1930 monthly means were used to drive the model for each year). The ozone (O_3) pollution data set used in this study, represented by the AOT40 index, is based on Felzer et al. (2005) and covers the time period from 1860 to 2006. Before 1860, the ozone level in each 0.5° grid cell was assumed to equal the AOT40 of 1860 (which is equal to zero). The atmospheric N deposition data were based on Van Drecht et al. (2003), extended from 2000 to 2006 by adding the difference in annual N deposition rate from 1999 to 2000 to succeeding years, for each 0.5° grid cell (e.g., 2001 N deposition rate = 2000 + (2000–1999), etc.). For years 1000–1859, annual N deposition was assumed to equal the per grid cell rates in 1860.

To enable the evaluation of different LCLUC activities, we have developed a number of spatially explicit LCLUC time series data sets to prescribe the timing, area and distribution of historical LCLUC, including wildfire, over Northern Eurasia. The distribution of vegetation types was derived from the 1-km Global Land Cover Characterization (GLCC; Loveland et al. 2000) data set, which was translated to the upland arctic, boreal and temperate ecosystem types for which the TEM is calibrated. The translated vegetation map was aggregated to the 0.5° grid matching the input climate data sets, but the area represented by each unique vegetation type within a grid cell was retained as an individual, non-spatial cohort. A more detailed description of the creation of this vegetation data set is given in Krankina et al. (see Chapter 5, this volume).

To represent the influence of land-use change on terrestrial carbon dynamics, TEM now uses a dynamic cohort approach. In this approach, TEM initially assumes a grid cell is covered by undisturbed natural vegetation, or "potential vegetation", which is represented by initial cohorts that collectively sum to the entire land area of the grid cell. When a disturbance occurs, a new cohort is formed and a certain amount of land area within the grid cell is then subtracted from the potential vegetation cohort and assigned to the new disturbed cohort. As time progresses in the TEM simulation and more disturbances occur, more cohorts are added to the grid cell. As each disturbance and its effects are tracked separately within TEM, different types of disturbances within a grid cell can be considered simultaneously and allows TEM to consider the impacts of multiple disturbances on terrestrial C and N dynamics (details for the input data on vegetation disturbances are given in Chapter 5, this volume).

For Eurasia, the land use transitions data set was backcasted to the start of the initialization period by linearly "ramping-up" the transitions rates from 0% per year (for each $1° \times 1°$ grid cell) in year 1000 to the year 1700 rates. The data were extended by simply using the 2000 rates for year 2001–2006.

6.2.4 Simulation Framework

To quantify the effects of the various controlling factors considered in this study on terrestrial C dynamics in Northern Eurasia, we conducted a series of five model simulations. The simulation framework was designed to allow an analysis of the relative contribution of LCLUC and non-LCLUC factors to the overall C balance of the system over the recent 10-year period (Table 6.1). Each simulation, labeled S1 through S5, builds upon the potential vegetation data set by incorporating an additional transient data set at each successive model run. The first simulation (S1) was driven by interannually non-varying climate and atmospheric data sets (with each year represented by mean monthly data calculated from the 1901–1930 time period), where land cover is assumed to be potential vegetation throughout the model run (i.e., no disturbance or land use), and with the global annual atmospheric CO_2 level being the only transient data set. The transient climate and atmospheric chemistry data sets (O_3 pollution and N deposition) were added to varying CO_2 level to drive all subsequent simulations, with the second (S2) based on undisturbed potential vegetation. In each successive model run, a new disturbance data set was imposed on potential

Table 6.1 The framework for the multiple TEM simulations conducted and data sets used to analyze different LCLUC and non-LCLUC controlling factors on C balance over the study area. The input data sets are added sequentially in each successive simulation, so that the S5 simulation includes all effects (total), and each effect is isolated by subtracting the results from the previous simulation

Simulation	Effects	Variables and data sets
Non-LCLUC Factors		
S1	Vegetation type	Potential vegetation (Loveland et al. 2000)
	+ CO_2	Global annual CO_2 (Keeling and Whorf 2005)
S2	+ Climate variability	TAIR, PREC, NIRR (CRU and NCEP data sets)
	+ Atmospheric chemistry	O_3 (Felzer et al. 2005), N dep (Van Drecht et al. 2003)
LCLUC Factors		
S3	+ Fire	Area Burned (Sukhinin et al. 2004; Balshi et al. 2007; Randerson et al. 2006b)
S4	+ Agriculture	Crop/pasture establishment and abandonment (Hurtt et al. 2006)
S5	+ Forest harvest (Total effect)	Area harvested (Hurtt et al. 2006)

vegetation and, along with transient CO_2 and climate, was used to drive the S3 (area burned), S4 (land use) and S5 (forest harvest) simulations. To distinguish the effects of wildfire, agriculture and timber harvest, essentially three unique LCLUC data sets were developed for this study: one that includes only the occurrence of wildfire, a second that prescribes fire and agricultural (crops and pastures) establishment and abandonment, and a third that incorporates fire, agriculture and timber harvest.

Since the transient data sets were individually added in each successive run, the effects of each on C stocks and change were determined by subtracting the results of a simulation from those of the subsequent run. Specifically, climate and atmospheric chemistry effects were determined by subtracting S1 results from the S2, fire by S2 from S3, agriculture by S3 from S4 and forest harvest by S4 from S5. In addition, we report the effect of CO_2 fertilization from the S1 results, the combined disturbance and land use effect (LCLUC effect) as S5 minus S2, and the total effect of all controlling factors considered here as the S5 results. Note that with this simulation framework being built in an "additive" fashion, as opposed to a full factorial analysis, any effects reported contain both the direct effects of the factor being considered plus any interactions with the factors included in the preceding simulations.

6.2.5 Data Analysis

The model produces monthly estimates of C stocks from vegetation, reactive SOM, non-reactive SOM, DOC, and three harvest product pools (1-, 10- and 100-year; see McGuire et al. 2001) for each cohort over the length of the simulation. We report the sum of these C stocks as annual total ecosystem C. Annual changes in C stocks are calculated as the difference of the December standing stocks of successive years. Total changes in C stocks for our analysis period are determined as the difference in standing stocks between December 1996 and December 2006 and are reported as an average annual change in teragrams (Tg) of C $year^{-1}$ (10^{12} g C $year^{-1}$). This average annual change in C stocks reported here represents the net ecosystem C balance (NECB) of the system (see Chapin et al. 2006), the sum of all fluxes into and out of the terrestrial system (Fig. 6.1):

$$\mathrm{NECB} = \mathrm{NPP} - (\mathrm{R_H} + \mathrm{TCE} + \mathrm{PDF} + \mathrm{DOC_{EX}}) \tag{6.1}$$

where NPP is net primary production, R_H is heterotrophic respiration, TCE represents the total C emissions due to disturbance and land use conversion, PDF corresponds to the combined flux from the decay of the three post-disturbance product pools, and DOC_{EX} is DOC export from the terrestrial system. The vertical flux, or net C exchange between the terrestrial system and the atmosphere (NCE), is determined by the difference between NPP input and the sum of C emissions from R_H, TCE and PDF. As such, NECB does not equate exactly to NCE, because it also includes the lateral leaching flux of DOC via stream export.

We compared the modeled C balance responses to climate, disturbance and land use effects with temporally- and spatially-explicit climatology and LCLUC data for

the Northern Eurasia study area over the 1997–2006 analysis period. In this analysis, we report the cohort-level results aggregated to broad vegetation categories, as well as for the total study area, to illustrate the differences in C balance responses among the major ecological zones ("ecozones") of the region. These ecozones, based on the input potential vegetation layer, include arctic tundra (prostrate and shrub vegetation), boreal forest (needleleaf evergreen and deciduous and broadleaf), temperate forest (evergreen and deciduous) and other non-forest types (xeric wood and shrub lands, grasslands, croplands and pastures). LCLUC effects on C balance within and across ecozones were compared with area burned, forest area harvested, and the area in crops and pastures.

Climate effects were compared with trends in average annual surface air temperature (TAIR, °C) and total annual precipitation (PREC, mm) over the time period, with the trend defined as the slope of the regression relationship of the climate variable on year. The overall trends for the 1997–2006 time period are reported as the annual trends aggregated to the 10-year time period (decade^{-1}). Anomalies in the climate variables for each year in the analysis period were calculated as the deviation from long-term means for TAIR and PREC from a previous 30-year time period, 1961–1990. To report climate trends and anomalies separately for an individual ecozone, we used in the calculation only those grid cells that had a majority area coverage (>50%) by that ecozone.

6.3 Results

6.3.1 General Trends

Overall, our study suggests that the Northern Eurasia region as a whole is losing C from terrestrial ecosystems on average of 44.5 Tg C year^{-1} from 1997 to 2006 (Table 6.2). Both climate and LCLUC variability had negative (source) effects on

Table 6.2 The quantitative effects, of the controlling factors considered amongst the various simulations in this study, on total ecosystem C balance (Tg C year^{-1}) for the major ecozones of the study area, for the 1997 to 2006 analysis period

	Ecozones				
Effects	Tundra	Boreal forest	Temperate forest	Other	Total study area
CO_2 (S1)	13.0	44.0	3.02	0.40	60.5
Climate (S2−S1)	13.0	−32.2	3.06	−0.92	−17.1
Non-LCLUC (S2)	26.0	11.8	6.08	−0.52	43.4
Fire (S3–S2)	4.25	−80.0	1.0	−1.0	−75.8
Agriculture (S4–S3)	−3.64	−1.04	−0.27	1.17	−3.78
Harvest (S5–S4)	0.00	−8.97	0.64	0.00	−8.33
LCLUC (S5–S2)	0.61	−90.0	1.40	0.12	−87.9
Total (S5)	26.7	−78.2	7.48	−0.40	−44.5

regional C balance, with disturbance and land use having the largest magnitude effect on the total study area of the controlling factors considered here. The combined negative (source) effect of about 105 Tg C $year^{-1}$ on the regional C balance from climate, atmospheric chemistry and disturbance responses is partially offset by a nearly 61 Tg C $year^{-1}$ positive effect (sink) from CO_2 fertilization. The study area as a whole lost an estimated 17 Tg C $year^{-1}$ from the terrestrial ecosystems in response to variability in climate and atmospheric chemistry (S2−S1 simulation results). The model simulations estimate that the region all together lost 88 Tg C $year^{-1}$ over the time period in response to the combined effect of disturbance, forest management and land use (S5−S2 simulations). Fire, agriculture and forest harvest each individually produced negative (source) effects on the C balance for the study area, with fire by far contributing the majority of the LCLUC-driven source (76 Tg C $year^{-1}$).

While the study area as a whole was estimated to be acting as a source of C during the time period of analysis, closer inspection of the broad ecozone categories demonstrates that these ecosystems have considerable variation in C balance with respect to the effects of the controlling factors of the simulations (Table 6.2). In terms of the total effects (S5 simulation), the majority of the C source across the study area was found in the boreal forest ecozone. The 78 Tg C $year^{-1}$ loss of total ecosystem C from the boreal zone was partially offset, however, by net C accumulation in the other ecozones, primarily corresponding with the nearly 27 Tg C $year^{-1}$ net sink in the arctic tundra ecozone. The C accumulation over the 10-year period in the tundra and temperate forest ecosystems was largely driven by the positive (sink) effects of CO_2, atmospheric chemistry and climate (S1 and S2 simulations), while the majority of the C release (source) from the boreal forest ecozone was due to the LCLUC effect (S5−S2 simulation results).

6.3.2 Non-LCLUC Effects

The global annual CO_2 concentration in the atmosphere increased by 14.9 ppm over the 10-year period, up to 378.7 ppm in 2006. The 60.5 Tg C $year^{-1}$ sink estimate from the S1 simulation (Table 6.2) equates to an overall effect of 6.4 g C m^{-2} $year^{-1}$ across the study area from CO_2 fertilization. Comparing the per-area effects of the different major ecozones illustrates the variability in the strength of this effect across the region. Among ecozones, the effect of CO_2 on total ecosystem C stocks was strongest in the boreal forest, at 10.6 g C m^{-2} $year^{-1}$ averaged over the 1997–2006 time period. A substantially smaller sink effect of 3.2 g C m^{-2} $year^{-1}$ was estimated for the tundra ecozone. Within each ecozone, the positive CO_2 effect was generally of similar magnitude to the climate effect. While CO_2 fertilization enhanced the climate sink in arctic tundra and temperate forests, the negative climate effects observed for the boreal forest and non-forest ecozones mostly or completely offset the positive CO_2 effect.

The study area as a whole was warmer and wetter during the analysis period (1997–2006) relative to the reference period (1961–1990), with an overall average TAIR anomaly of 0.7°C year^{-1} and PREC anomaly of 10 mm year^{-1}. An examination of the variation in C balance of the individual ecozones in the study area suggests that they may be responding differently to changes in climate and atmospheric chemistry over the time period (Table 6.2). The climate-driven sink (positive effect) of 13 Tg C year^{-1} in the arctic tundra ecozone was in response to increases in TAIR and PREC during the analysis period (1997–2006) of 0.7°C year^{-1} and 1.4 mm year^{-1}, respectively, relative to the reference period (1961–1990), while the boreal zone, in contrast, showed a negative (source) climate effect of about 32 Tg C year^{-1} over the 10-year period with a similar increase in TAIR (0.7°C year^{-1}) and a larger average PREC anomaly (13 mm year^{-1}). Similarly, but to a lesser degree, warmer and wetter climate changes produced a slight positive effect in the temperate zone and a small negative effect in the non-forest zone. The net result was an overall negative climate effect on the study area as a whole in response to general increases in TAIR and PREC during the analysis period, which could be mostly attributed to the climate-driven C source corresponding to the boreal forest.

Arctic tundra and boreal forest comprise the two major ecozones in the region in terms of area coverage and ecosystem C stocks (Chapter 5, this volume), and this analysis indicates that these ecozones have experienced markedly different overall trends in climate during the 1996–2006 time period. The temporal patterns in the climate data suggests that C stocks among the individual ecozones may not necessarily be responding to observed differences in climate relative to the reference period, but rather to variation in TAIR and PREC trends during the analysis period. Figure 6.2 illustrates the responses of vegetation and soil C stocks for each of these ecozones to trends in TAIR and PREC over this time period. The climate effects (S2−S1 simulation results) on the cumulative change in total ecosystem C stocks follow the general climate trends, with tundra C stocks accumulating in response to strong, increasing trends in both TAIR and PREC, and C loss from the boreal zone corresponding to a strong decreasing PREC trend (with a relatively weak trend in TAIR). In the tundra ecozone, C was accumulated in both the vegetation and soil pools at rates of similar magnitude (7.1 and 5.9 Tg C year^{-1}, respectively), contributing more-or-less equally to the overall climate-driven sink in tundra ecosystems over the analysis period. While vegetation C stocks increased in the boreal ecozone over this time period (19.7 Tg C year^{-1}), this accumulation was overwhelmed by a substantial loss of soil C in response to climate effects (−51.9 Tg C year^{-1}).

6.3.3 LCLUC Effects

The large, negative effect of LCLUC on the total ecosystem C balance of the region was almost entirely a consequence of the −90 Tg C year^{-1} effect in the boreal forest ecozone, which was the largest magnitude effect of any of the controlling factors considered in this study (Table 6.2). The boreal ecozone had the largest area

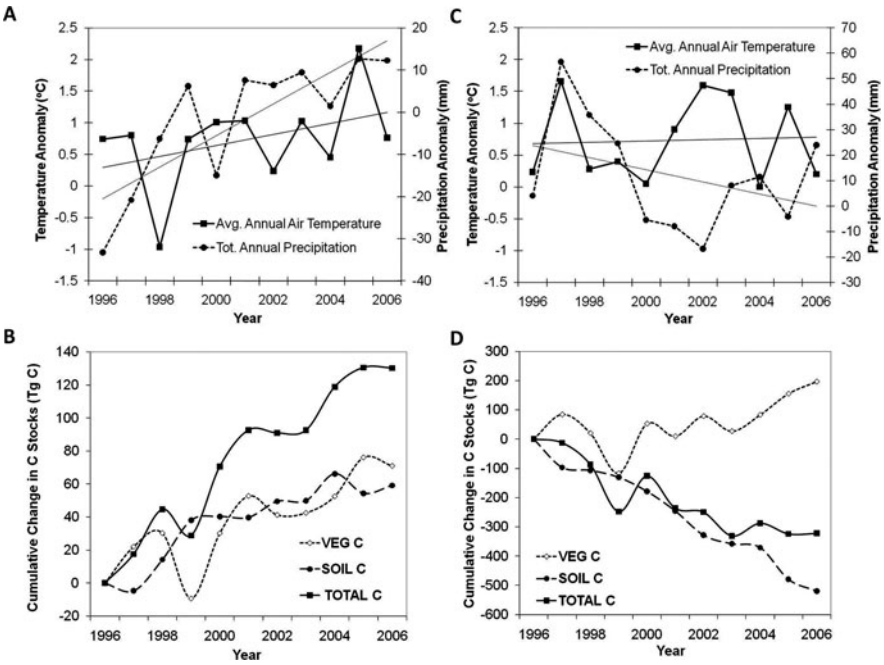

Fig. 6.2 The temporal trends in air temperature and precipitation data and the climate effects on C stocks in vegetation and soil of arctic tundra and boreal forest ecosystems. **Panel A** plots the annual anomalies (as compared to the 1961–1990 reference period) in average annual surface air temperature and total annual precipitation over the tundra ecozone for the analysis period, with the trend lines for each variable superimposed on the annual data. Climate data points from 1996 are also shown for comparison with the C stock plots (cumulative since December 1996) below. **Panel B** shows the response of tundra C stocks according to the climate effects (S2–S1 simulation results), with cumulative change in vegetation, soil stocks and total ecosystem C stocks since December 1996 shown for the analysis period. The same climate anomalies and changes in C stocks are shown for the boreal forest ecozone in **panels C** and **D**, respectively

affected by fire and forest harvest, with 52% of the forest harvest and 86% of the area burned in the total study area contained in this ecozone. Relative to the area of each ecozone, the temperate forest had the highest percentage of area affected by LCLUC, with 10% harvested over the 10-year period. Combined with low levels of fire, this resulted in a small positive (sink) LCLUC effect in the temperate forest ecozone. The non-forest ecozone also had a small positive LCLUC effect, with an area burned that, although less in total, was a slightly greater percentage of its area than that of the boreal zone (3.9−3.5%, respectively). In addition to area burned, this ecozone includes agricultural areas (crop and pasture lands) in its results. There was also a small positive LCLUC effect for the arctic tundra ecozone, which had less than 0.2% of its area burned over the time period. The combined positive LCLUC effect of less than 4 Tg C year^{-1} from the three other ecozones did little toward offsetting the large negative effect in the boreal zone.

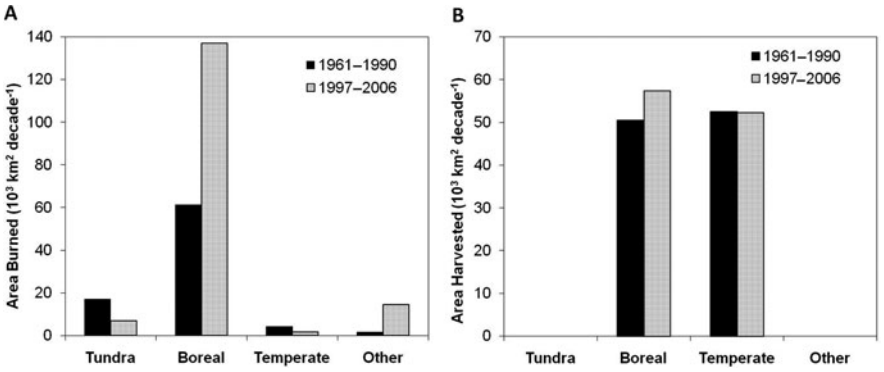

Fig. 6.3 (**panel A**) Comparison of the area burned and (**panel B**) area harvested by ecozone during the analysis period (1997–2006) relative to the average per decade area affected during the reference period (1961–1990)

To understand the role that LCLUC processes play in the contemporary C budget of Northern Eurasian terrestrial ecosystems, the magnitudes of fire and forest harvest during the 1997 to 2006 analysis period, for each of the major ecozones, are reported and compared to the longer-term average data from the 1961–1990 reference period (Fig. 6.3). Nearly 160×10^3 km^2 were burned over this decade (about 2% of the total study area), the majority of which occurred in the boreal forest ecozone (Fig. 6.3a). The total area burned during the analysis period represented a 76×10^3 km^2 increase over the per-decade average area burned estimated by the fire return interval backcasting approach (Balshi et al. 2007) for the 1961–1990 reference period. Approximately 110×10^3 km^2 of forest were harvested during the analysis period (~2.5% of the combined boreal and temperate forest area), a 6% increase in area according to the modeled data (Hurtt et al. 2006) from the reference period (Fig. 6.3b). The total area of forest harvested was more-or-less evenly distributed between boreal and temperate forests in both the analysis period (57×10^3 km^2 and 52×10^3 km^2, respectively) and the reference period (51×10^3 km^2 and 53×10^3 km^2, respectively). The methodology used in this study whereby the coarse resolution ($1^\circ\times1^\circ$) modeled forest-harvest transition data (Hurtt et al. 2006) was allocated to individual cohorts in our LCLUC data sets based on a priority toward forest types resulted in no harvest area simulated in non-forest ecosystems during either the analysis or reference periods.

The transitions to and from agricultural use over the full study area, including row-crop agriculture and pasture land uses, were also compared between the analysis period and the per decade area averages for the reference period (Fig. 6.4). Approximately 62×10^3 km^2 (less than 1% of the total area) was in agricultural land use, of which 32×10^3 km^2 was represented by row-crop agriculture and 32×10^3 km^2 by pastures. This actually represents a net loss of total agricultural area (from about 71×10^3 km^2 in 1997), as the modeled land use upon which we based our LCLUC data set (Hurtt et al. 2006) suggests that the rates of agricultural abandonment outpaced those of establishment over the analysis period for this study area.

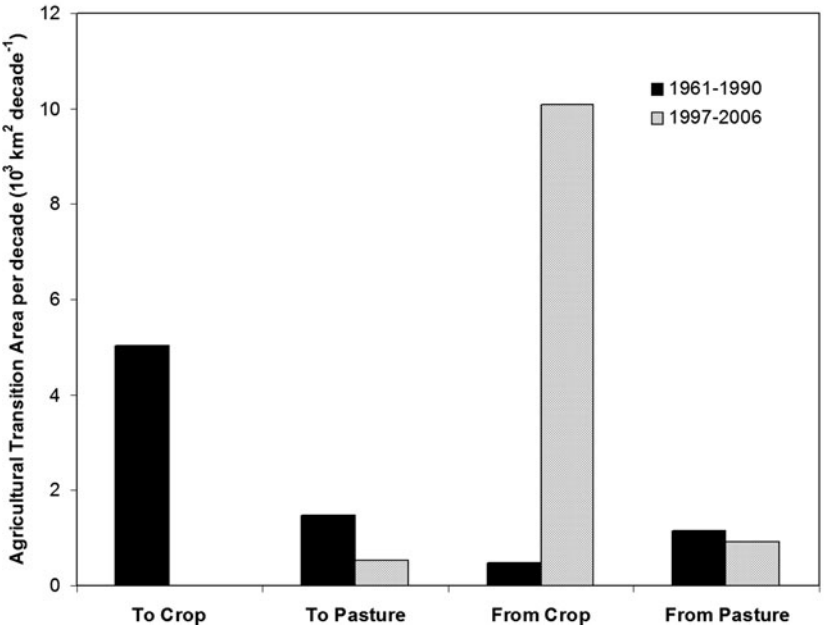

Fig. 6.4 A comparison of the area converted to and from agricultural use over the full study area, including row-crop agriculture and pasture land uses, during the analysis period (1997–2006) relative to the average per decade area affected during the reference period (1961–1990)

Between 1997 and 2006, there was only a slight reduction in the area in pasture land use (0.4×10^3 km^2), while vast majority (96%) of the abandonment was from row-crop agriculture. This 10.5×10^3-km^2 net loss of agricultural area during the analysis period was a reversal in trend from an average net gain in agricultural area of 1.6×10^3 km^2 per decade over the reference period.

The interannual variability in disturbance and land-use change over the region as a whole was analyzed to get a sense for the trends in LCLUC within the analysis period, which was then compared with annual dynamics in C balance during this time period (Fig. 6.5). The areas affected by forest harvest and pasture land use were estimated to remain steady over the analysis period, while the decline in modeled row-crop agricultural use, described above, is apparent (Fig. 6.5a). The largest variability in LCLUC during this time period is found with the fire data set, with area burned increasing to great heights in years 2001–2003 from the relatively low levels of the other years. The average of 33.5×10^3 km^2 year^{-1} burned in years 2001–2003 is almost 400% higher than the average area burned during the other years in the analysis period. The vast majority of area burned during the 10-year period was located in the boreal forest (Fig. 6.3a), and the large fire years from 2001 to 2003 correspond to comparatively warm and dry conditions in this ecozone (Fig. 6.2c).

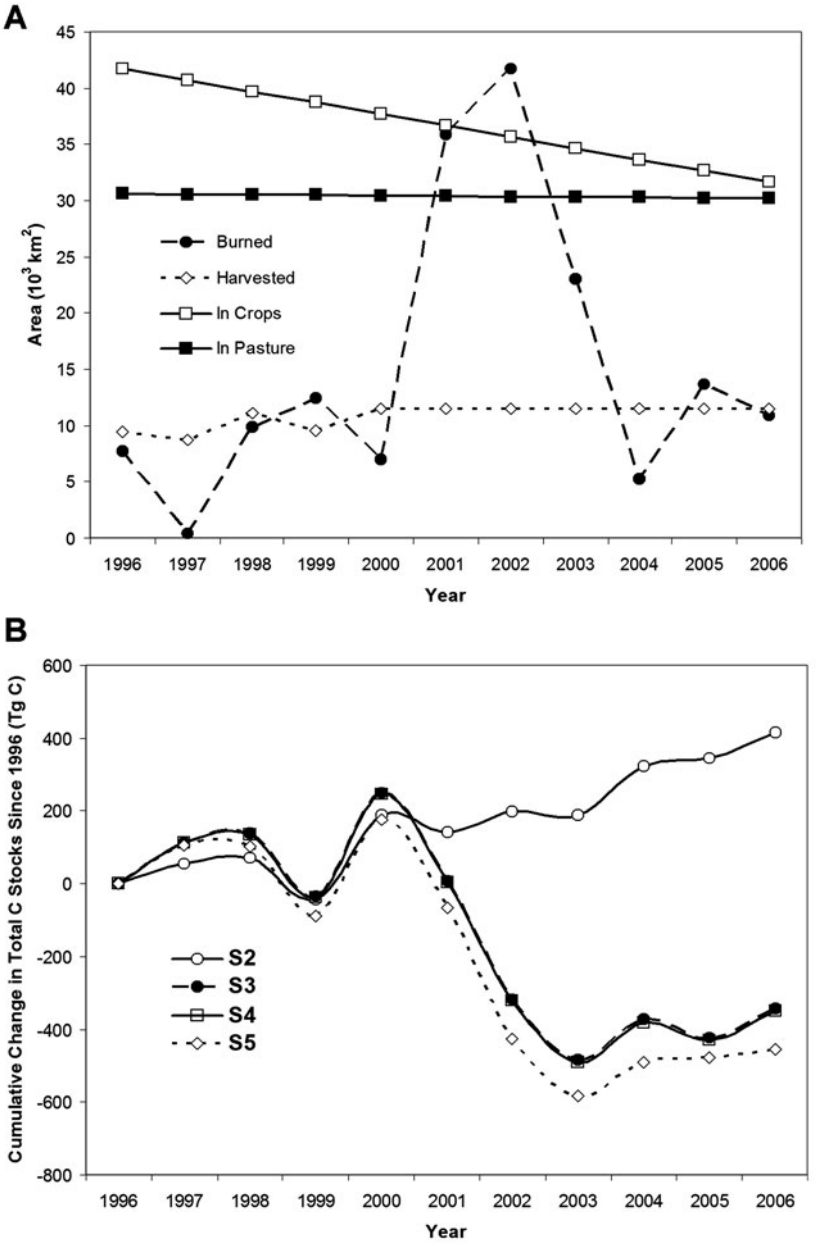

Fig. 6.5 The annual variability in area burned, harvested and in agricultural use over the study area as a whole from 1996 to 2006 (**panel A**) in relation to the trends in the cumulative change in total ecosystem C stocks since 1996 for the full study area (**panel B**), according to the results of the different simulations analyzed in this study (see Section 6.2.3)

The effects of these recent trends in LCLUC on C dynamics are reflected in the change in total ecosystem C stocks across each year in the analysis period (Fig. 6.5b). The cumulative change in C stocks for the LCLUC simulations (S3, S4 and S5) follows that of the simulated CO_2 and climate effects (S2) for the first 4 years in the analysis period. This suggests that only small LCLUC effects were found at low levels of fire and forest harvest. At low levels of area burned in 1997, 1998 and 2000, the simulations resulted in small positive fire effects (S3−S2). Beginning in 2001, however, the added fire effects on CO_2 and climate (S3 simulation) launch a divergence in C stocks toward a large negative effect corresponding to the large area burned from 2001 through 2003. By December 2003, the study area had lost approximately 730 Tg C as a result of the fire effect since December 2000, just prior to the onset of the large fire years. After 2003, the C stocks began to recover according to the pattern of the CO_2 and climate effects but retained the large deficit in cumulative C stocks as a legacy of the large fire years. By the end of the analysis period (2006), the fire effect on total C stocks was cumulatively about −760 Tg C.

The cumulative loss of total ecosystem C from the fire effect (S3−S2 simulation results) constituted about 87% of the overall LCLUC effect for the study area over the 10-year period (S5−S2). The simulation results in which area burned was added to CO_2 and climate effects (S3) resulted in a large negative effect on total C stocks after 2001, as compared to the simulation without fire (S2). Adding land use (crops and pastures) to the fire, CO_2 and climate simulation (S4) had little effect on total C stocks over the time period. Adding forest harvest in the simulations resulted in a cumulative loss of 108 Tg C over the 10-year period, all of which was accounted for in the boreal and temperate ecozones. The magnitude of this negative harvest effect accounted for 12% of the overall LCLUC source effect.

6.3.4 Landscape Analysis

Figure 6.6 presents the spatial patterns of C balance across the study area from 1996 to 2006 in relation to those of some of the controlling factors (i.e., vegetation, climate and LCLUC) considered in this analysis. The map of the base-line potential vegetation data set (Panel A) depicts the distribution of arctic tundra, boreal forest and temperate and non-forest types across the study area. The input potential vegetation map portrays upland vegetation community type mosaics and their transitions across spatial gradients by describing the area represented by each vegetation type within a half-degree cell as individual cohorts. The resulting map captures the transition zones between vegetation types, including boreal forest and tundra in central Siberia, and the boreal and temperate/other zones in Northern Europe.

Average air temperature anomalies (Panel B) show that increases in TAIR relative to the reference period were nearly ubiquitous in grid cells across the region during the analysis period, with stronger warming observed over Scandinavia and other, localized areas in the artic tundra and boreal forest regions. While the region as

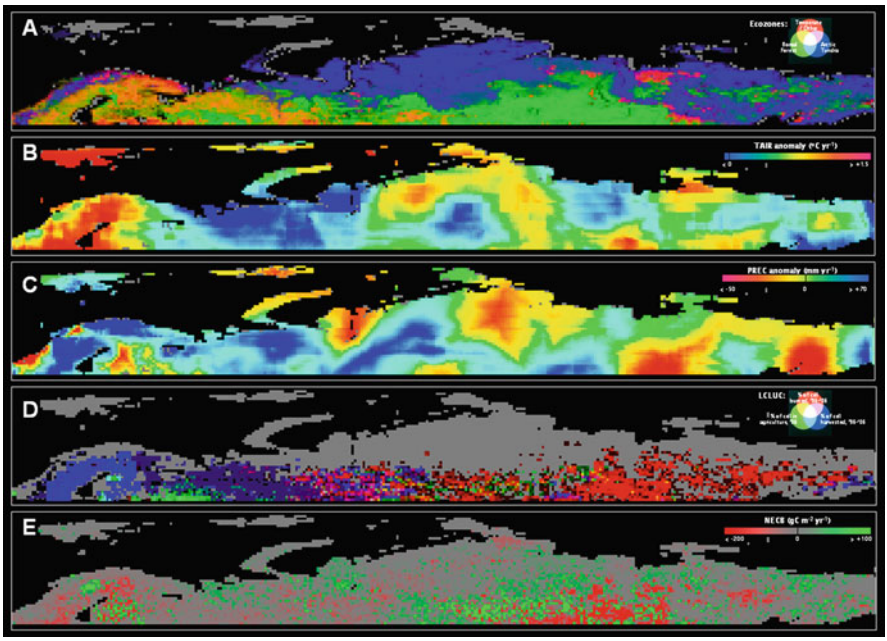

Fig. 6.6 The spatial patterns of the ecozone mosaics according to the input vegetation map (**panel A**), the anomalies in average annual surface air temperature (**panel B**) and total annual precipitation (**panel C**), and the disturbance data sets (area burned, harvested and in agriculture) (**panel D**), in relation to the net ecosystem C balance of the study area (**panel E**). Each map shows the variable summarized for each 0.5° grid cell over the 1997–2006 analysis period

a whole was generally wetter during the analysis period than during the reference period, the spatial pattern of PREC anomalies illustrates high variability across the region (Panel C). The strongest increases in precipitation were located in the mixed ecozones of Scandinavia and western Russia, while large areas of the tundra and boreal forest zones in central Siberia and the Far East show substantial negative PREC anomalies during the analysis period.

The majority of disturbance and land use activity (Panel D) was located outside of the arctic tundra ecozone, but covered much of the southern and inland portions of the study area. A large band of burned area during this time period stretched across the boreal forest of Siberia, and included a portion of the tundra/boreal transition zone in the Far East. Most of the harvest area, on the other hand, was concentrated in the mixed boreal and temperate forests further to the west, especially in Scandinavia. Agricultural land use was found primarily toward the southern extent of the study area, in eastern Europe and central Siberia. A subset of the region in western and central Siberia represented a mixed mosaic of fire, forest harvest and agricultural land use.

The spatial patterns of vegetation types, climate anomalies, and LCLUC combine in part to produce the variation observed in C balance across the region (Panel E).

The strongest fluxes both into and out of the terrestrial system during the analysis period occurred in central and eastern Siberia, as well as over northern Scandinavia. These fluxes correspond to areas of high LCLUC activity in the boreal and temperate forest ecozones. The large C source (negative NECB) in eastern Siberia clearly matches the area of high fire activity in the boreal forest during this time period. This large area burned was mostly linked to the patterns of increased TAIR and decreased PREC, according to the climate anomaly maps. A mix of both source and sink activity was found in the boreal/temperate forest mosaic of the Scandinavian region, where the highest rates of forest harvest activity were found. The results of the simulations also suggest a strong C sink in the boreal forest of central Siberia, where the data sets show mixed LCLUC activity and a mostly warmer, wetter climate compared to the reference period. Much of the arctic tundra ecozone was represented by a lesser, dispersed positive C balance, particularly in areas where TAIR anomalies were not as strongly positive.

6.4 Discussion

A large amount of political, social and scientific attention over the last decade has been directed to the measured increases of CO_2 concentrations in the atmosphere, and attempts to balance the global C budget have consistently shown that accumulation in the atmosphere is proceeding at a slower pace than suggested by the overall rate of emissions from anthropogenic sources (i.e., cement production and the burning of fossil fuels). This 'drawdown' of atmospheric CO_2 levels has long been of interest to global change scientists, and studies have produced convincing evidence that global ocean and land ecosystems have been approximately equally responsible for the uptake of this residual C (Prentice at el. 2001; Sabine et al. 2004). Recent estimates place the residual terrestrial sink at about 2.6 Pg C year^{-1} from 2000 to 2005 (IPCC, 2007), or roughly one-third of the 7.2 $\pm$ 0.3 Pg C year^{-1} from anthropogenic emissions (Marland et al. 2006). Studies using *top–down* approaches (i.e. atmospheric inversion models) for estimating global C budgets have shown that the majority of this land-based sink can be attributed to northern extratropical regions, with a generally accepted flux estimate of about 2 Pg C year^{-1} into the terrestrial ecosystems over these regions (Tans et al. 1990; Kaminiski et al. 1999; Myneni et al. 2001; Gurney et al. 2002).

6.4.1 The High-Latitude Terrestrial Sink

While inverse modeling calculations are poorly constrained at continental and regional scales, other estimates based on *bottom-up* approaches (process-based modeling and inventory methods) suggest that high latitude terrestrial ecosystems have been responsible for a significant portion of the extratropical land-based sink.

Inventory-based studies on the C balance of boreal forest and arctic tundra ecosystems suggests a net uptake of CO_2 on the order of 0.3–0.6 Pg C year^{-1} over the late twentieth Century in these regions (McGuire et al. 2009). More specific to the region analyzed in this study, estimates from both *top–down* and *bottom–up* studies suggest that the terrestrial ecosystems of Eurasia have been responsible for a majority of this sink activity. Gurney et al. (2004) estimated a 0.36 ± 0.56 Pg C year^{-1} net sink over boreal Asia from 1992 to 1996 using inverse modeling calculations. Inventory-based methods have estimated the terrestrial CO_2 sink in recent decades at 0.32 Pg C year^{-1} for Russian forests (Shvidenko and Nilsson 2003) and 0.47 Pg C year^{-1} over Eurasia (Myneni et al., 2001). Process-based model estimates from Balshi et al. (2007), which include the effects of CO_2 fertilization and fire on C dynamics, are reported as 0.22 Pg C year^{-1} for Russia and 0.31 Pg C year^{-1} for the larger Eurasia region. Taking the range of these estimates, the high latitude terrestrial ecosystems of Eurasia have been responsible for somewhere between 16 and 24% of the overall northern extratropical 2 Pg C year^{-1} land-based sink.

Given the role of this region as a significant terrestrial CO_2 sink in recent decades, any changes to the strength of this sink will have important consequences for the global C cycle. The current and future directions of the C balance in high latitudes remain uncertain, but are critical for understanding the role of these ecosystems with respect to feedbacks to future changes in climate. While models generally estimate that boreal regions were a sink in the late twentieth Century, several studies have suggested that the sink strength is decreasing, and possibly changing to a source, as a result of increased disturbance and changes in climate (Kurz and Apps 1999; Goetz et al. 2005; Balshi et al. 2007; Kurz et al. 2008). At the global scale, Canadell et al. (2007) offer a discussion on the potential for 'sink saturation', in which they review evidence that the balance between C uptake by biological processes and the emission of CO_2 from terrestrial ecosystems may be changing in such a way as to cause a decrease, or even disappearance, of the terrestrial sink.

6.4.2 Saturation of the Sink in Northern Eurasia Ecosystems

The results from our retrospective analysis of the C balance of Northern Eurasian terrestrial ecosystems over a recent 10-year period lend credence to further consideration of the near-term prospect of terrestrial sink saturation, at least in the context of high latitude ecosystems. While the studies mentioned above show the larger Eurasia region, and the pan-Arctic as a whole, acting as a C sink in earlier time periods, our analysis of the terrestrial Eurasian ecosystems north of 60°N shows a net source of nearly 45 Tg C year^{-1} from 1997 to 2006. The results from the model simulations reported in this study, when viewed in a longer-term historical perspective of total effects on C balance, show that indeed the terrestrial C source in recent years marked a switch in C balance from a sink in earlier decades (Fig. 6.7). Our simulations show the total effect of all controlling factors considered as a net C sink of

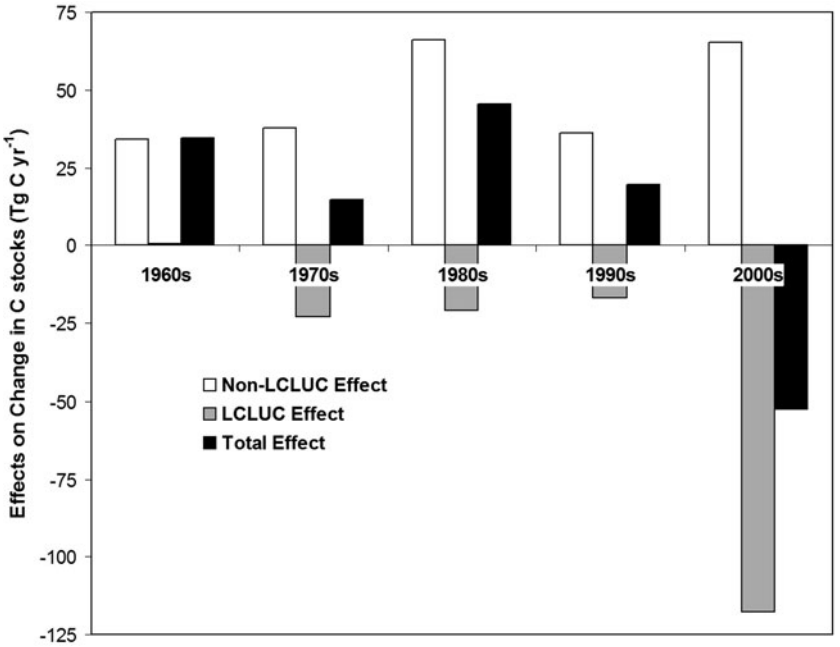

Fig. 6.7 The non-LCLUC (CO_2 concentration, atmospheric chemistry and climate variability), LCLUC (fire, forest harvest, and agricultural land use), and combined total effects on the simulated net ecosystem carbon balance for the Northern Eurasia study area during each decade from the 1960s through the 2000s. The change in carbon stocks is given as the annual average over each 10-year period, except for the 2000s decade, which is the 7-year average from 2000 to 2006.

28.5 Tg C year^{-1} from the 1960s through the 1990s, with a dramatic shift to a 52.5 Tg C year^{-1} source from 2000 to 2006. It should be noted that the latter estimate is nearly an order of magnitude lower than those from the studies mentioned earlier (although within the range of uncertainty of some of these studies), but for various reasons it is problematic to directly compare these different results. The smaller spatial extent of our analysis may be responsible in part for the lower estimate, along with the different controlling factors considered in this study. For example, most previous studies do not include the full effects of atmospheric chemistry changes, which can have a significant effect on C balance estimates (Felzer et al. 2005). Additionally, the version of TEM employed here more explicitly considers the effect of increasing active layer depth on the decomposition of SOM than previous versions (see Section 6.2.2). The effect of recent climate trends on the melting of near-surface permafrost remains a source of uncertainty and debate in the scientific literature (Yi et al. 2007; Euskirchen et al. 2006; Burn and Nelson 2006; Lawerence and Slater 2005). A better understanding of this issue will be required for current and future C balance estimates of arctic regions (see also Chapter 7, this volume).

6.4.3 Mechanisms Leading to the Shift in C Balance

Canadell et al. (2007) describe several mechanisms that control the dynamics of the terrestrial C sink and could contribute to its saturation, including both non-LCLUC (CO_2 fertilization, atmospheric chemistry effects, and climate variability) and LCLUC (disturbances and land use change and management) controlling factors. The framework of simulations used to produce the analyses reported in this study allow for consideration of the relative contribution of these different effects toward creating the net source of C observed in our results. The longer-term effects of these controlling factors on the simulation results (Fig. 6.7) suggest that the regional C balance during the 1960s though the 1990s was driven primarily by the positive effects of CO_2 fertilization and atmospheric chemistry and climate responses. Any negative effects from the LCLUC factors were small (-15.1 Tg C year^{-1}) relative to the non-LCLUC response (43.6 Tg C year^{-1}), and did not substantially impact the overall sink activity of the region. The nature of this balance between negative LCLUC and positive non-LCLUC effects has been shifted substantially in the current decade, however, according to our simulations. While the non-LCLUC effect remains positive in this decade (65.2 Tg C year^{-1}), this response has been overwhelmed by a much larger negative LCLUC effect from 2000 to 2006 (-118 Tg C year^{-1}) than was found in earlier decades.

Of the non-LCLUC factors considered in this study, they combine to produce a 43.4 Tg C year^{-1} net sink effect on the C balance of the total study area for the 10-year analysis period (1997–2006). However, the atmospheric chemistry and climate effects alone (without the CO_2 effect) were estimated to be a net source of 17.1 Tg C year^{-1} for the study area. While we did not explicitly separate the effects of atmospheric chemistry from climate variability for this study, past results with TEM simulations that considered these factors have shown that the positive effects of CO_2 fertlization are mostly cancelled out by the negative effects of atmospheric pollution (i.e. O_3) on overall C balance (Felzer et al. 2004). Felzer et al. (2005) noted that consideration of ozone pollution caused the carbon balance of some regions to change from a positive balance to a negative balance, including eastern Europe, which is a "hot spot" of ozone pollution according to that analysis.

Amongst the major ecozones in the study area, our results suggest that arctic tundra has been responding differently to climate effects than the boreal forest ecozone (Table 6.2). The positive C balance (sink) in tundra ecosystems may be explained in part by observations, described in several other studies, of enhanced productivity in the Arctic due to increased CO_2 uptake, longer-growing seasons, increasing active layer depth and the expansion of woody vegetation (see Goetz et al. 2005). The overall negative climate effect, however, is largely driven by that of the boreal forest ecozone. Subsequent analysis showed that the loss of C from the boreal forest due to the climate effect generally followed the trend toward decreasing annual precipitation in this ecozone (Fig. 6.2). This result is consistent with growing evidence of a declining trend in productivity in undisturbed boreal forests, both in North America and Asia, which has been attributed to increasing drought stress in these ecosystems (Bunn et al. 2007; Zhang et al. 2007; Goetz et al. 2005).

Changes in land cover and land use are known to play an important, but uncertain, role in the operation of the terrestrial C sink, globally and within high latitude ecosystems (McGuire et al. 2001; Houghton 2003). In addition to the drought-induced reduction of productivity in boreal forests, other studies have discussed the potential for shifts in disturbance and land use regimes to alter the strength of the C sink in these ecosystems (Randerson et al. 2006a; Goetz et al. 2007). Despite only small effects in earlier decades (Fig. 6.7), LCLUC processes combined to produce a large, negative (source) effect on the C balance of Northern Eurasia during the last decade, an effect that overwhelmed all other factors considered in this study and was primarily responsible for the overall loss of C during this time period. Our results show that the negative effect of fire in the boreal forest ecozone was responsible for most of this C loss simulated for the analysis period. Over the longer-term, the data used in these model simulations indicate that harvest levels have remained constant since the 1960s, and the simulations suggest that agricultural land use has had only small effects on C balance. On the other hand, the data show a large increase in area burned across the study area in recent years, which coincides with the shift from an overall net C sink to a net source for this region.

6.5 Conclusions

An ecosystem biogeochemistry model driven by spatially- and temporally-explicit data sets on vegetation, climate, fire, forest management and land use was used to simulate a retrospective C budget analysis for the past decade (1997–2006) over the Northern Eurasia terrestrial region. The results of the simulations indicate the study area as a whole was losing C on the order of 45 Tg year^{-1} from terrestrial ecosystems over this recent time period in response to the total effect of the controlling factors included in this study. The overall C source during the past decade, according to this analysis, marks a shift in direction of the net flux from the terrestrial sink of earlier decades that has been identified in this and other studies of Northern Eurasian ecosystems. The simulation framework and subsequent analyses presented in this study allow for attribution of mechanisms responsible for the shift in C balance for this region over the recent 10-year analysis period. Our results show that the estimated positive effect on regional C balance from CO_2 fertilization was offset by negative responses to climate, disturbance and land use change. The current trend toward a warmer and wetter climate over arctic tundra regions appears to be enhancing C storage in this ecozone, while the loss of C stocks due to climate effects in the boreal forest follows the strong decreasing trend in precipitation over this ecozone. The current trend toward warmer, drier conditions in the boreal forest may also be leading to increased area burned and therefore a large, additional negative LCLUC effect. Indeed, our analysis shows this correlated climate and fire effect in boreal forests to be the largest signal in the negative C balance response of the Northern Eurasian region during the 10-year time period.

Our model simulations suggest that a shift in terrestrial ecosystem C balance from a sink to source may be occurring in the boreal forests of Northern Eurasia as

a result of changes in climate and an increase in fire activity in recent years over the region. These results do include several important sources of uncertainty, however, as well as bring to light other issues to prioritize for future research. Overall, it will be important to compare these results to other studies of regional C balance, particularly those using other methods (e.g., inversion models and inventory-based estimates). While our simulations agree with previous studies demonstrating that the high latitude regions of Eurasia acted as a C sink during earlier decades (through the 1990s), we are not aware of any studies that have made more current estimates of C balance, especially considering the recent large fire years in this region.

The results presented here, which suggest that LCLUC plays a key role in this shift in C balance, are also based on modeled data that could be corroborated and/or improved with more detailed, regional-level data on forest harvest statistics and agricultural land use data sets. The ability of the model to estimate C dynamics in earlier time periods, and to simulate the stand age distribution of the boreal forest landscape, is limited primarily by the length of the historical fire record. It is also important to note that the LCLUC data sets used to drive the model simulations presented here do not include any data on insect disturbance, which has been suggested to emit C in peak outbreak years on a magnitude comparable to that of fires (Kurz et al. 2008). Finally, while it is difficult to reduce the uncertainty of estimates of contemporary C dynamics, especially with respect to the effects of LCLUC, it is even more of a challenge to produce projections of C balance according to future scenarios. All of these issues are important to consider in lieu of a potential weakening, or disappearance, of the terrestrial C sink in high latitude ecosystems having serious consequences for the global C budget, creating a positive feedback to climate change by effectively accelerating the build-up of CO_2 in the atmosphere.

References

Alley RB, Marotzke J, Nordhaus WD, Overpeck JT, Peteet DM, Pielke RA Jr, Pierrehumbert RT, Rhines PB, Stocker TF, Talley LD, Wallace JM (2003) Abrupt climate change. Science 299:2005–2010. doi:10.1126/science.1081056

Balshi MS, McGuire AD, Zhuang Q, Melillo J, Kicklighter DW, Kasischke E, Wirth C, Flannigan M, Harden J, Clein JS, Burnside TJ, McAllister J, Kurz WA, Apps M, Shvidenko A (2007) The role of historical fire disturbance in the carbon dynamics of the pan-boreal region: a process-based analysis. J Geophys Res 112:G02029. doi:10.1029/2006JG000380

Brovkin V, Claussen M, Driesschaert E, Fichefet T, Kicklighter D, Loutre MF, Matthews HD, Ramankutty N, Schaeffer M, Sokolov A (2006) Biogeophysical effects of historical land cover changes simulated by six earth system models of intermediate complexity. Clim Dynam 26(6):587–600. doi:10.1007/s00382-005-0092-6

Bunn AG, Goetz SJ, Kimball JS, Zhang K (2007) Northern high latitude ecosystems respond to recent climate change. Eos 88(34):333–335 doi:10.1029/2007EO340001

Burn CR, Nelson FE (2006) Comment on "A projection of severe near-surface permafrost degradation during the 21st century" by Lawrence DM, Slater AG. Geophys Res Lett 33:L21503. doi:10.1029/2006GL027077

Canadell JG, Gifford R, Houghton R., Lou Y, Pataki D, Raupach M, Smith P, Steffen W (2007) Saturation of the terrestrial carbon sink. In: Canadell JG, Pataki D, Pitelka L (eds) Terrestrial ecosystems in a changing world, The IGBP series. Springer, Berlin, pp 59–78

Chapin FS III, Sturm M, Serreze MC, McFadden JP, Key JR, Lloyd AH, McGuire AD, Rupp TS, Lynch AH, Schimel JP, Beringer J, Chapman WL, Epstein HE, Euskirchen ES, Hinzman LD, Jia G, Ping CL, Tape KD, Thompson CDC, Walker DA, Welker JM (2005) Role of land-surface changes in Arctic summer warming. Science 310:657–660

Chapin III FS, Woodwell GM, Randerson JT, Rastetter EB, Lovett GM, Baldocchi DD, Clark DA, Harmon ME, Schimel DS, Valentini R, Wirth C, Aber JD, Cole JJ, Goulden ML, Harden JW, Heimann M, Howarth RW, Matson PA, McGuire AD, Melillo JM, Mooney HA, Neff JC, Houghton RA, Pace ML, Ryan MG, Running SW, Sala OE, Schlesinger WH, Schulze ED (2006) Reconciling carbon-cycle concepts, terminology, and methodology. Ecosystems 9:1041–1050

Chapin III FS, Randerson JT, McGuire AD, Foley JA, Field CB (2008) Changing feedbacks in the climate-biosphere system. Front Ecol Environ 6(6):313–320. doi:10.1890/080005

Clein JS, Kwiatkowski BL, McGuire AD, Hobbie JE, Rastetter EB, Melillo JM, Kicklighter DW (2000) Modeling carbon responses of moist tundra ecosystems to historical and projected climate: a comparison of fine- and coarse-scale ecosystem models for identification of process-based uncertainties. Glob Chang Biol 6 (Suppl. 1):127–140

Clein JS, McGuire AD, Zhang X, Kicklighter DW, Melillo JM, Wofsy SC, Jarvis PG. Massheder JM (2002) Historical and projected carbon balance of mature black spruce ecosystems across North America: the role of carbon-nitrogen interactions. Plant Soil 242(1):15–32

Clein JS, McGuire AD, Euskirchen ES, Calef MP (2007) The effects of different climate input data sets on simulated carbon dynamics in the Western Arctic. Earth Interact 11(12):1–24. doi:10.1175/EI229.1

Drobot S, Maslanik J, Herzfeld UC, Fowler C, Wu W (2006) Uncertainty in temperature and precipitation datasets over terrestrial regions of the Western Arctic. Earth Interact 10(23):1–17. doi:10.1175/EI191.1

Euskirchen ES, McGuire AD, Kicklighter DW, Zhuang Q, Clein JS, Dargaville RJ, Dye DG, Kimball JS, McDonald KC, Melillo JM, Romanovsky VE, Smith NV (2006) Importance of recent shifts in soil thermal dynamics on growing season length, productivity and carbon sequestration in terrestrial high-latitude ecosystems. Glob Chang Biol 12(4):731–750. doi:10.1111/j.1365-2486.2006.01113.x

Euskirchen SE, McGuire AD, Chapin FS III (2007) Energy feedbacks of northern high-latitude ecosystems to the climate system due to reduced snow cover during 20th century warming. Glob Chang Biol 13:2425–2438. doi:10.1111/j.1365-2486.2007.01450.x

Felzer B, Kicklighter D, Melillo J, Wang C, Zhuang Q, Prinn R (2004) Effects of ozone on net primary production and carbon sequestration in the conterminous United States using a biogeochemistry model. Tellus 56B:230–248

Felzer B, Reilly J, Melillo J, Kicklighter D, Sarofim M, Wang C, Prinn R, Zhuang Q (2005) Future effects of ozone on carbon sequestration and climate change policy using a global biogeochemical model. Clim Change 73:345–373. doi:10.1007/s10584-005-6776-4

Felzer BS, Cronin T, Reilly JM, Melillo JM, Wang X (2007) Impacts of ozone on trees and crops. Comptes Rendus Geosci 339:784–798

Field CB, Lobell DB, Peters HA, Chiariello NR (2007) Feedbacks of terrestrial ecosystems to climate change. Ann Rev Environ Res 32. doi:10.1146/annurev.energy.1132.053006.141119

Global Soil Data Task Group (2000) Global gridded surfaces of selected soil characteristics (International geosphere-biosphere programme – data and information system), Oak Ridge National Laboratory Distributed Active Archive Center, Oak Ridge

Goetz SJ, Bunn A, Fiske G, Houghton RA (2005) Satellite observed photosynthetic trends across boreal North America associated with climate and fire disturbance. Proc Natl Acad Sci USA 102:13521–13525

Goetz SJ, Mack MC, Gurney KR, Randerson JT, Houghton RA (2007) Ecosystem responses to recent climate change and fire disturbance at northern high latitudes: observations and model results contrasting Northern Eurasia and North America. Environ Res Lett 2(4). doi:10.1088/1748-9326/2/4/045031

Gurney KR, Law RM, Denning AS, Rayner PJ, Pak BC, Baker D, Bousquet P, Bruhwiler L, Chen Y, Ciasis P, Fung IY, Heimann M, John J, Maki T, Maksyutov S, Peylin P, Prather M, Taguchi S (2004) Transcom 3 inversion intercomparison: model mean results for the estimation of seasonal carbon sources and sinks. Glob Biogeochem Cycles 18:GB1010. doi:10.1029/2003GB002111

Gurney KR, Law RM, Denning AS, Rayner PJ, Baker D, Bousquet P, Brhwiler L, Chen Y-H, Ciais P, Fan S, Fung IY, Gloor M, Heimann M, Higuchi K, John J, Maki T, Kaksyutov S, Masarie K, Peylin P, Prather M, Pak BC, Randerson J, Sarmiento J, Toguchi S, Takahashi T, Yuen C-W (2002) Towards robust regional estimates of CO2 sources and sinks using atmospheric transport models. Science 415:626–630

Hansen J, Sato M, Ruedy R, Lo K, Lea DW, Medina-Elizade M (2006) Global temperature change. Proc Natl Acad Sci USA 103:14288–14293

Houghton RA (2003) Why are estimates of the terrestrial carbon balance so different? Glob Chang Biol 9:500–509. doi:10.1046/j.1365-2486.2003.00620.x

Houghton, RA, Joos F, Asner GP (2004) The effects of land use and management on the global carbon cycle. In: Gutman G, Janetos AC, Justice CO, Moran EF, Mustard JF, Rindfuss RR, Skole D, Turner BL II, Cochrane MA (eds) Land change science: observing, monitoring, and understanding trajectories of change on the earth's surface. Kluwer, Dordrecht, pp 237–256

Hurtt GC, Frolking S, Fearon MG, Moore B, Shevliakovas E, Malyshev S, Pacala SW, Houghton RA (2006) The underpinnings of land-use history: three centuries of global gridded land-use transitions, wood-harvest activity and resulting secondary lands. Glob Chang Biol 12: 1208–1229

IPCC (2007) Climate change 2007: the physical science basis. Contribution of working group I to the fourth assessment report of the intergovernmental panel on climate change. In: Solomon S, Qin D, Manning M, Chen Z, Marquis M, Averyt KB, Tignor M, Miller HL (eds). Cambridge University Press, Cambridge; New York, 996 p

Johannessen OM, Bengtsson L, Miles MW, Kuzima SI, Semenov VA, Alekseev GV, Nagurnyi AP, Zakarov VF, Bobylev LP, Pettersson LH, Hasselmann K, Cattle HP (2004) Arctic climate change: observed and modelled temperature and sea-ice variability. Tellus 56A:328–341

Jones PD, Mogberg A (2003) Hemispheric and large scale air temperature variations: an extensive revision and an update to 2001. J Clim 16:206–223

Kaminski T, Heimann M, Giering R (1999) A coarse grid three-dimensional global inverse model of the atmospheric transport 1. Adjoint model and Jacobian matrix. J Geophys Res Atmos 104:18535–18553

Kasischke ES, Turetsky MR (2006) Recent changes in the fire regime across the North American boreal region. Geophys Res Lett 33:L09703. doi:10.1029/2006GL025677

Keeling CD, Whorf TP (2005) Atmospheric CO_2 records from sites in the SIO air sampling network. In Trends: A Compendium of Data on Global Change, Carbon Dioxide Information Analysis Center, Oak Ridge National Laboratory, US Department of Energy, Oak Ridge

Kimball JS, Zhao M, McGuire AD, Heinsch FA, Clein J, Calef M, Jolly WM, Kang S, Euskirchen SE, McDonald KC, Running SW (2007) Recent climate driven increases in vegetation productivity for the western Arctic: Evidence of an acceleration of the northern terrestrial carbon cycle. Earth Interact 11(4):1–30

Kovacs K, Ranson KJ, Sun G, Kharuk VI (2004) The relationship of the Terra MODIS fire product and anthropogenic features in the central Siberian landscape. Earth Interact 8:1–25

Krankina ON, Houghton RA, Harmon ME, Hogg EH, Butman D, Yatskov M, Huso M, Treyfeld RF, Razuvaev VN, Spycher G (2005) Effects of climate and disturbance on Forest Biomass across Russia. Can J For Res 35:2281–2293

Kurz WA, Dymond CC, Stinson G, Rampley GJ, Neilson ET, Carroll AL, Ebata T, Safranyik L (2008) Mountain pine beetle impacts on forest carbon: feedback to climate change. Nature 452:987–990. doi:10.1038/nature06777

Kurz WA, Apps MJ (1999) A 70-year retrospective analysis of carbon fluxes in the Canadian forest sector. Ecol Appl 9:526–547

Lawrence DM, Slater AG (2005) A projection of severe near-surface permafrost degradation during the 21st century. Geophys Res Lett 32. doi:10.1029/2005GL025080

Loveland TR, Reed BC, Brown JF, Ohlen DO, Zhu Z, Yang L, Merchant JW (2000) Development of a global land cover characteristics database and IGBP DISCover from 1 km AVHRR data. Int J Rem Sens 21(6&7):1303–1330

Marland G, Boden TA, Andres RJ (2006) Global, regional, and national CO2 emissions. In Trends: a compendium of data on global change, Carbon Dioxide Information Analysis Center, Oak Ridge National Laboratory, US Department of Energy, Oak Ridge

McGuire AD, Chapin FS III, Walsh JE, Wirth C (2006) Integrated regional changes in arctic climate feedbacks: implications for the global climate system. Ann Rev Environ Res 31: 61–91

McGuire AD, Melillo JM, Joyce LA, Kicklighter DW, Grace AL, Moore B III, Vorosmarty CJ (1992) Interactions between carbon and nitrogen dynamics in estimating net primary productivity for potential vegetation in North America. Glob Biogeochem Cycles 6:101–124

McGuire AD, Melillo JM, Kicklighter DW, Joyce LA (1995) Equilibrium responses of soil carbon to climate change: empirical and process-based estimates. J Biogeogr 22:785–796

McGuire AD, Melillo JM, Kicklighter DW, Pan Y, Xiao X, Helfrich J, Moore B III, Vorosmarty CJ, Schloss AL (1997) Equilibrium responses of global net primary production and carbon storage to doubled atmospheric carbon dioxide: Sensitivity to changes in vegetation nitrogen concentration. Glob Biogeochem Cycles 11:173–189

McGuire AD, Clein JS, Melillo JM, Kicklighter DW, Meier RA, Vorosmarty CJ, Serreze MC (2000a) Modeling carbon responses of tundra ecosystems to historical and projected climate: sensitivity of pan-arctic carbon storage to temporal and spatial variation in climate. Glob Chang Biol 6(1):141–159. doi:10.1046/j.1365-2486.2000.06017.x

McGuire AD, Melillo JM, Randerson JT, Parton WJ, Heimann M, Meier RA, Clein JS, Kicklighter DW, Sauf W (2000b) Modeling the effects of snowpack on heterotrophic respiration across northern temperate and high latitude regions: comparison with measurements of atmospheric carbon dioxide in high latitudes. Biogeochemistry 48:91–114

McGuire AD, Apps M, Chapin FS III, Dargaville R, Flannigan MD, Kasischke ES, Kicklighter D, Kimball J, Kurz W, McCrae DJ, McDonald K, Melillo JM, Myneni R, Stocks BJ, Verbyla DL, Zhuang Q (2004) Land cover disturbances and feedbacks to the climate system in Canada and Alaska. In: Gutman G, Janetos AC, Justice CO, Moran EF, Mustard JF, Rindfuss RR, Skole D, Turner II BL, Cochrane MA (eds) Land change science: observing, monitoring, and understanding trajectories of change on the earth′s surface. Kluwer, Dordrecht, pp 139–161

McGuire AD, Sitch S, Clein JS, Dargaville R, Esser G, Foley J, Heimann M, Joos F, Kaplan J, Kicklighter DW, Meier RA, Melillo JM, Moore III B, Prentice IC, Ramankutty N, Reichenau T, Schloss A, Tian H, Williams LJ, Wittenberg U (2001). Carbon balance of the terrestrial biosphere in the twentieth century: analyses of CO_2, climate and land-use effects with four process-based ecosystem models. Glob Biogeochem Cycles 15:183–206

McGuire AD, Anderson L, Christensen TR, Dallimore S, Guo L, Hayes DJ, Heimann M, Lorenson T, Macdonald R, Roulet N (2009) Sensitivity of the carbon cycle in the Arctic to climate change. Ecol Monogr 79:523–555

Melillo JM, McGuire AD, Kicklighter DW, Moore III B, Vorosmarty CJ, Schloss AL (1993) Global climate change and terrestrial net primary production. Nature 363:234–240

Mitchell TD, Jones PD (2005) An improved method of constructing a database of monthly climate observations and associated high-resolution grids. Int J Climatol 25(6):693–712

Myneni RB, Dong J, Tucker CJ, Kaufmann RK, Kauppi PE, Liski J, Zhou L, Alexeyev V, Hughes MK (2001) A large carbon sink in the woody biomass of northern forests. Proc Natl Acad Sci 98:14784–14789

National Geophysical Data Center (NGDC) (1994), TerrainBase v. 1.1, 5-min digital terrain model data. Boulder

Prentice IC, Farquhar GD, Fasham MJR, Goulden ML, Heimann M, Jaramillo VJ, Kheshgi HS, Quéré CL, Scholes RJ, Wallace DWR (2001) The carbon cycle and atmospheric carbon dioxide.

In: Houghton JT et al. (eds) Climate change 2001: the scientific basis. Cambridge University Press, Cambridge, pp 183–237

Prinn R, Jacoby H, Sokolov A, Wang C, Xiao X, Yang Z, Eckaus R, Stone P, Ellerman D, Melillo J, Fitzmaurice J, Kicklighter D, Holian G, Liu Y (1999) Integrated global system model for climate policy assessment: feedbacks and sensitivity studies. Clim Change 41(3/4): 469–546

Polyakov ID, Alekseev GV, Bekryaev RV, Bhatt U, Colony R, Johnson MA, Karklin VP, Makshtas AP, Walsh D, Yulin AV (2002) Observationally based assessment of polar amplification of global warming. Geophys Res Lett 29:1878. doi:10.1029/2001GL011111

Raich JW, Rastetter EB, Melillo JM, Kicklighter DW, Steudler PA, Peterson BJ, Grace AL, Moore B III, Vorosmarty CJ (1991) Potential net primary productivity in South America: application of a global model. Ecol Appl 1, pp 399–429

Randerson JT, Liu H, Flanner MG, Chambers SD, Jin Y, Hess PG, Pfister G, Mack MC, Treseder KK, Welp LR, Chapin FS, Harden JW, Goulden ML, Lyons E, Neff JC, E. Schuur AG, Zender CS (2006a) The impact of boreal forest fire on climate warming. Science, 314: 1130–1132

Randerson JT, van der Werf GR, Giglio L, Collatz GJ, Kasibhatla PS (2006b) Global Fire Emissions Database, Version 2 (GFEDv2.1). Data set. Available on-line [http://daac.ornl.gov/] from Oak Ridge National Laboratory Distributed Active Archive Center, Oak Ridge. doi:10.3334/ORNLDAAC/849

Reilly J, Prinn R, Harnisch J, Fitzmaurice J, Jacoby H, Kicklighter D, Melillo J, Stone P, Sokolov A, Wang C (1999) Multi-gas assessment of the Kyoto Protocol. Nature 401: 549–555

Reilly J, Paltsev S, Felzer B, Wang X, Kicklighter D, Melillo J, Prinn R, Sarofim M, Sokolov A, Wang C (2007) Global economic effects of changes in crops, pasture and forests due to changing climate, carbon dioxide and ozone. Energy Policy 35:5370–5383

Sabine CL, Heimann M, Artaxo P, Bakker DCE, Chen C-TA, Field CB, Gruber N, Le Quere C, Prinn RG, Richey JE, Romero P, Sathaye JA, Valentini R (2004) Current status of past trends of the global carbon cycle. In: Field C, Raupach M (eds) Global carbon cycle, integrating humans, climate and the natural world. Island Press, Washington DC, pp 17–44

Schimel DS, House JI, Hibbard KA, Bousquet P, Ciais P, Peylin P, Braswell BH, Apps MJ, Baker D, Bondeau A, Canadell J, Churkina G, Cramer W, Denning AS, Field CB, Friedlingstein P, Goodale C, Heimann M, Houghton RA, Melillo JM, Moore B III, Murdiyarso D, Noble I, Pacala SW, Prentice IC, Raupach MR, Rayner PJ, Scholes RJ, Steffen WL, Wirth C (2001) Recent patterns and mechanisms of carbon exchange by terrestrial ecosystems. Nature 414:169–172

Schlesinger WH (1991) Biogeochemistry: an analysis of global change. Academic Press, New York

Serreze MC, Francis JA (2006) The Arctic amplification debate. Clim Change 76:241–264

Shvidenko A, Nilsson S (2003) A synthesis of the impact of Russian forests on the global carbon budget for 1961–1998. Tellus 55B:391–415

Soja AJ, Tchebakova NM, French NHF, Flannigan MD, Shugart HH, Stocks BJ, Sukhinin AI, Parfenova EI, Chapin FS, Stackhouse PW (2007) Climate-induced boreal forest change: predictions versus current observations. Glob Planet Change 56:274–296

Sokolov AP, Kicklighter DW, Melillo JM, Felzer B, Schlosser CA, Cronin TW (2008) Consequences of considering carbon/nitrogen interactions on the feedbacks between climate and the terrestrial carbon cycle. J Clim 21:3776–3796

Sturm M, Racine C, Tape K (2001) Climate change: increasing shrub abundance in the Arctic. Nature 411:546–547

Sukhinin AI, French NHF, Kasischke ES, Hewson JH, Soja AJ, Csiszar IA, Hyer EJ, Loboda T, Conrad SG, Romasko VI, Pavlichenko EA, Miskiv SI, Slinkina OA (2004) AVHRR-based mapping of fires in Russia: New products for fire management and carbon cycle studies. Rem Sens Environ 93(4):546–564

Tans PP, Fung IY, Takahashi T (1990) Observational constraints on the global CO_2 budget. Science 247:1431–1438

Tape K, Sturm M, Racine C (2006) The evidence for shrub expansion in northern Alaska and the pan-Arctic. Glob Chang Biol 12:686–702

Tian H, Melillo JM, Kicklighter DW, McGuire AD, Helfrich JVK III, Moore B III, Vörösmarty CJ (1998) Effect of interannual climate variability on carbon storage in Amazonian ecosystems. Nature 396:664–667

Tian H, Melillo JM, Kicklighter DW, McGuire AD, Helfrich J (1999) The sensitivity of terrestrial carbon storage to historical climate variability and atmospheric CO_2 in the United States. Tellus 51B:414–452

Tian H, Melillo JM, Kicklighter DW, McGuire AD, Helfrich JVK III, Moore B III, Vörösmarty CJ (2000) Climatic and biotic controls on annual carbon storage in Amazonian ecosystems. Glob Ecol Biogeogr 9:315–336

Tian H, Melillo JM, Kicklighter DW, Pan S, Liu J, McGuire AD, Moore B III (2003) Regional carbon dynamics in monsoon Asia and its implications for the global carbon cycle. Glob Planet Change 37:201–217. doi:10.1016/S0921-8181(02)00205-9

Van Drecht G, Bouwman AF, Knoop JM, Beusen AHW, Meinardi CR (2003) Global modeling of the fate of nitrogen from point and nonpoint sources in soils, groundwater, and surface water. Glob Biogeochem Cycles 17(4):1115. doi:10.1029/2003GB002060

Webster M, Forest C, Reilly J, Babiker M, Kicklighter D, Mayer M, Prinn R, Sarofim M, Sokolov A, Stone P, Wang C (2003) Uncertainty analysis of climate change and policy response. Clim Change 61(3):295–320

Xiao X, Melillo JM, Kicklighter DW, McGuire AD, Prinn RG, Wang C, Stone PH, Sokolov A (1998) Transient climate change and net ecosystem production of the terrestrial biosphere. Glob Biogeochem Cycles 12:345–360

Yi SH, Woo MK, Arain MA (2007) Impacts of peat and vegetation on permafrost degradation under climate warming. Geophys Res Lett 34:L16504. doi:10.1029/2007GL030550

Zhang K, Kimball JS, Zhao M, Oechel WC, Cassano J, Running SW (2007) Sensitivity of pan-Arctic terrestrial net primary productivity simulations to daily surface meteorology from NCEP-NCAR and ERA-40 reanalyses. J Geophys Res 112:G01011. doi:10.1029/2006JG000249

Zhuang Q, McGuire AD, Melillo JM, Clein JS, Dargaville RJ, Kicklighter DW, Myneni RB, Dong J, Romanovsky VE, Harden J, Hobbie JE (2003) Carbon cycling in extratropical terrestrial ecosystems of the Northern Hemisphere during the 20th century: a modeling analysis of the influences of soil thermal dynamics. Tellus 55(B):751–776

Zhuang Q, Melillo JM, Sarofim MC, Kicklighter DW, McGuire AD, Felzer BS, Sokolov A, Prinn RG, Steudler PA, Hu S (2006) CO_2 and CH_4 exchanges between land ecosystems and the atmosphere in northern high latitudes over the 21st century. Geophys Res Lett 33:L17403. doi:10.1029/2006GL026972

Zhuang Q, Melillo JM, McGuire AD, Kicklighter DW, Prinn RG, Steudler PA, Felzer BS, Hu S (2007) Net emissions of CH4 and CO2 in Alaska: Implications for the region's greenhouse gas budget. Ecol Appl 17:203–202

Chapter 7
Interactions Between Land Cover/Use Change and Hydrology

Alexander I. Shiklomanov, Theodore J. Bohn, Dennis P. Lettenmaier, Richard B. Lammers, Peter Romanov, Michael A. Rawlins, and Jennifer C. Adam

Abstract The water cycle is a vital component of the North Eurasian environment and plays a central role in the region's climate, biology, biogeochemistry and in human interactions with the natural environment. The Northern Eurasian arctic drainage covers more than 2/3 of the pan-arctic land mass. Substantial changes in land cover and land use have occurred over the region in recent decades, as a result of changes in climate, permafrost, and water management, among other factors. These changes are likely to affect large-scale linkages between the regional and global climate system, but the nature of these interactions is not well understood. In this chapter, we analyze changes in the dominant hydrological components and explore the interaction of the terrestrial and atmospheric water cycles, with particular attention to key regional cryospheric processes and linkages between the water and carbon cycles. The monitoring of the water cycle from observational networks and remote sensing along with strategies for improving hydrological change detection are discussed in the context of changes in land cover and land use.

7.1 The Water Cycle of Northern Eurasia

The water cycle is a vital component of the Northern Eurasian environment and plays a central role in the region's climate, biology, biogeochemistry and in human interactions with the natural environment. The Northern Eurasian arctic drainage covers more than 2/3 of the pan-arctic land mass. Substantial changes in land cover and land use have occurred over the region in recent decades, as a result in changes in the dynamics of fire, permafrost, climate, and water management, among other factors. These changes are likely to interact in the larger scale linkages of regional to global climate, but the nature of these changes are not well understood. In this chapter, we explore the interaction of the terrestrial, atmospheric, and oceanic water

A.I. Shiklomanov (✉)
Water Systems Analysis Group, University of New Hampshire, Durham, NH 03824-3525, USA
e-mail: alex.shiklomanov@unh.edu

G. Gutman, A. Reissell (eds.), *Eurasian Arctic Land Cover and Land Use in a Changing Climate*, DOI 10.1007/978-90-481-9118-5_7,

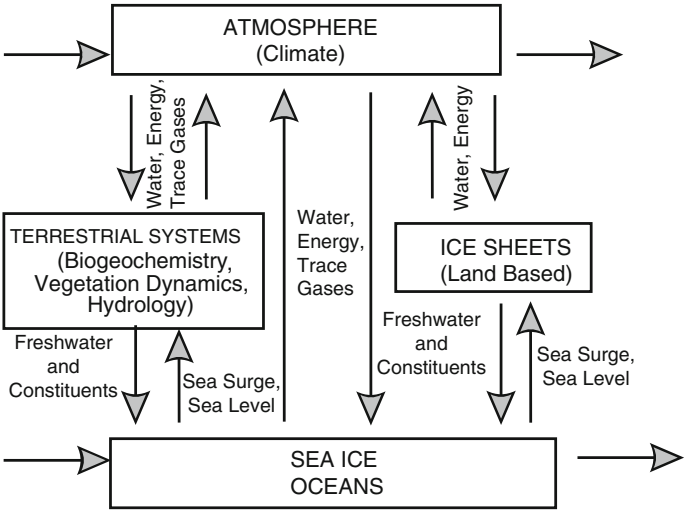

Fig. 7.1 Conceptual diagram of the arctic system, showing linkages among the atmosphere, land surface, and ocean systems. Links within the arctic region as well as the larger earth system must be considered to achieve an integrated view of the hydrological cycle. From Walsh et al. (2001)

cycles, with particular attention to the unique role that the cryosphere plays in the region (Fig. 7.1).

Atmospheric circulation is a major source of variability in the regional terrestrial water cycle. Advective processes are the source of most of the water (both liquid and solid) that reaches the interior of the continent and substantially modify the climate of the region. Most of the precipitable water that initially comes from outside the region may be recycled several times via the precipitation/evaporation processes (Drozdov and Grigorieva 1963; Trenberth 1999) until the moisture ultimately leaves the region by atmospheric transport. Thus the terrestrial water cycle processes that regulate evaporation, runoff, and changes in hydrological storage are directly linked with atmospheric processes.

The export of freshwater from the Eurasian land mass is of special importance to the Arctic Ocean since it contains only 1% of the world's ocean water, yet receives 11% of global river runoff (Shiklomanov et al. 2000). It is, therefore, the most river-influenced ocean on the planet. About three-quarters of Arctic Ocean riverine freshwater input derives from the Eurasian part of the drainage basin. Sea surface salinity distribution and sea ice formation are strongly affected by continental runoff (Steele and Boyd 1998). Changes in the freshwater flux to the Arctic Ocean may exert significant control over the North Atlantic meridional overturning (thermohaline) circulation and therefore the global ocean circulation by controlling the volume of North Atlantic Deep Water formation (Broecker 1997; Peterson et al. 2002). However, it now appears that potential changes in Arctic freshwater discharge would not be sufficient to interrupt the thermohaline circulation (see Rennermalm et al. 2007), as had once been feared.

Terrestrial ecosystems, and hence the terrestrial branch of the carbon cycle, strongly interact with the water cycle. As just one example, water levels in the region's wetlands determine whether and under what conditions methane (CH_4) and/or carbon dioxide (CO_2) are produced. The region's rivers, lakes, and reservoirs play an important role in environmental sustainability and are a link between global and regional cycles of carbon and other biogenic elements. Due to low water temperatures in this high latitude region, the processes of self-purification in the majority of rivers and water bodies of Northern Eurasian pan-Arctic are slow and fresh water systems in the region are therefore especially vulnerable to pollution. The biotic component of fresh water systems is also very vulnerable to external anthropogenic impacts. At the same time, its functions are extremely important for regulation of the fresh water systems state, their self-purification, and self-recovery. Biogeochemical riverine export of carbon from terrestrial ecosystems to coastal and ocean ecosystems, estimated for Russian rivers at 60 Tg C per a year (Nilsson et al. 2003), is another important link between terrestrial ecosystems, freshwater aquatic systems and the global carbon cycle.

Human activity causes direct (land cover change, water withdrawal, impoundments, and regulation) and indirect (feedbacks through changing atmospheric composition and water quality) impacts on numerous processes in the biosphere, hydrosphere, cryosphere, and atmosphere. The impact of such disturbances on the land surface processes is the most direct and among the strongest in fragile arctic environments.

Hydrological processes in the region are closely related to land cover and land use changes such as permafrost and glacier degradation, deforestation, forest fires, drying-out of wetlands, cultivation, and irrigation. Land cover (natural vegetation or disturbed conditions) modifies surface energy and water exchanges depending upon its physical (albedo, heat conductivity), mechanical (surface roughness, plant surface area density), and biological (leaf area index, stomatal conductance, photosynthesis, root depth) properties. Some characteristics of land cover (vegetation, snow, ice, frozen soil, and soil itself) change during surface heat and water exchanges, feed back to them and, therefore, have become integral components of the surface processes.

The role of the regional water cycle is linked closely with growing evidence of environmental change in the region. Various changes in terrestrial hydrologic variables have been detected across the Northern Eurasian Arctic drainage, including increases in air temperature and runoff, changing magnitudes and timing of precipitation and the freeze/thaw cycle, melting of glaciers, thawing of permafrost and increasing vegetation productivity (Smith et al. 2007; Shiklomanov et al. 2007; Rawlins et al. 2006, and Chapter 6 in ACIA 2005). Knowledge of causes, interactions and feedbacks among these regional changes is especially important because of their possible global effect through direct linkages to ocean and atmosphere processes therefore we need to understand the dynamics of the processes occurring throughout the Northern Eurasian Earth Science Partnership Initiative (NEESPI) region.

7.2 Hydrological Changes

7.2.1 River Runoff

River runoff is an important integrator of hydrological behavior across large regions (watersheds). It also plays a significant role in the fresh-water budget of the Arctic Ocean. Ocean salinity and sea ice formation are critically affected by river input. Changes in the fresh water flux to the Arctic Ocean can exert significant control over global ocean circulation by affecting North Atlantic deep water formation (Manabe and Stouffer 1994; Rahmstorf and Alley 2002). Eurasia contributes 75% of the total terrestrial runoff to the Arctic Ocean (Shiklomanov et al. 2000) and has three of the four major arctic rivers. Observations of combined river discharge from the six largest Russian arctic rivers (N.Dvina, Pechora, Ob, Yenisei, Lena and Kolyma) have shown an increase of 7% over the period 1936–1999 (Peterson et al. 2002). More recent estimates have shown this increase has continued into the twenty-first Century (Richter-Menge et al. 2006). The mean annual 2000–2006 discharge from the six largest Eurasian rivers was 127 km^3 (7%) higher than the long-term mean over 1936–1999 (Fig. 7.2). Preliminary projections of the river discharge for 2007, based on near-real time data from the ArcticRIMS (Rapid Integrated Monitoring System) data repository (http://RIMS.unh.edu), show a new historical maximum of the annual discharge to the Arctic Ocean from Eurasia.

The physical mechanisms driving the observed runoff changes are not yet completely understood. Analysis of changes in monthly discharge for the six largest Russian rivers showed that changes in winter discharge (November–April) are responsible for most of the observed changes in annual discharge (Richter-Menge et al. 2006). This is likely related at least in part to within-year redistribution of

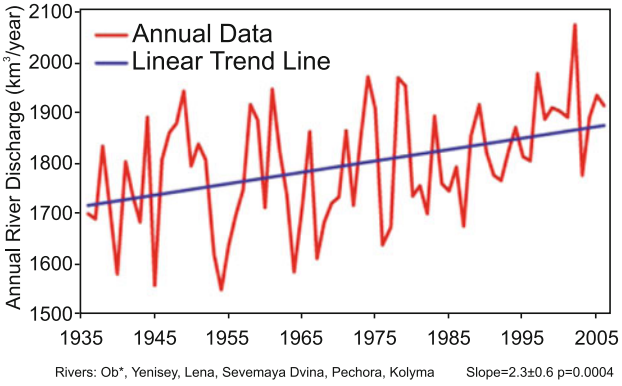

Fig. 7.2 Total annual discharge to the Arctic Ocean from the six largest rivers in the Eurasian pan-Arctic for the observational period 1936–2004. Updated from Peterson et al. (2002). Reprinted with permission from the American Association for the Advancement of Science

streamflow due to reservoir regulation and earlier snowmelt runoff, however, natural causes, such as permafrost change, increasing number and magnitude of winter snowmelt events, less frozen ground and an increase in the ground water table may also be factors. Terrestrial runoff is ultimately determined (at least on average) by the difference between precipitation (P) and evapotranspiration (ET) and it follows that any processes and feedbacks affecting P or ET will impact the freshwater discharge to the Arctic Ocean. It should be also recognized that changes in different climate-related hydrologic variables may have opposing influences on river discharge. A pervasive problem in assessing individual and net impacts is that key time series (precipitation, evapotranspiration and permafrost active later thickness) are often short, spatially sparse, and/or of questionable quality. It is also important to differentiate climate-related effects on the terrestrial hydrologic budget from direct anthropogenic impacts, such as water diversions, impoundments, and land cover change. We discuss below direct anthropogenic effects (specifically, water management) on streamflow, and follow with a summary of current understanding of climate and land cover-related changes.

Numerous large reservoirs were constructed on arctic rivers during the twentieth century, including eleven large reservoirs on the rivers Lena, Yenisei, and Ob between 1950 and 1990 (ICOLD 2003). Adam et al. (2007) applied a physically-based reservoir model to investigate the effects of reservoirs on the discharge of the Lena, Yenisei, and Ob river basins between 1937 and 1998. Their analysis included the effects of initial reservoir filling, reservoir operations, and reservoir evaporation. The results showed that while the reservoirs have had little effect on long-term ($\geq$30 years) changes in annual discharge, they have had large effects on seasonal streamflow, especially in winter. Figure 7.3 shows the reservoir signatures at the outlets of each of these basins using the results of four studies (Adam et al. 2007; McClelland et al. 2004; Yang et al. 2004; Ye et al. 2003), where the reservoir signature is defined as the change in the mean monthly hydrograph due to reservoirs. In terms of absolute discharge, the largest impact of the reservoirs was the reduction of early summer flows; a secondary effect was a small increase in late winter and spring flows. However, when expressed as a percentage of monthly discharge, the late winter and spring flows increased by as much as 80% (Fig. 7.3, right column), which far overshadows the much smaller relative reduction in summer flows. This increase in flow accounts for between 60 and 100% of observed long-term observed winter trends at the outlets of the major Eurasian river basins (Adam et al. 2007).

Reservoir management cannot explain all of the observed trends in runoff, however. Analysis of changes in seasonal runoff for 97 Russian watersheds with insignificant human influence on the hydrological regime showed that from the late 1970s to the present winter river runoff increased over most of Northern Eurasia (Georgievsky 2002). Significant increases (10–30%) in winter and summer-autumn runoff occurred on rivers located on the north slope of European Russia. Even greater changes occurred in Siberia. Winter runoff has increased by up to 60% in the Irtysh basin (a southern Ob tributary) and in southeastern Siberia, and up to 15–35% in northern Siberia (Shiklomanov et al. 2007; ACIA 2005).

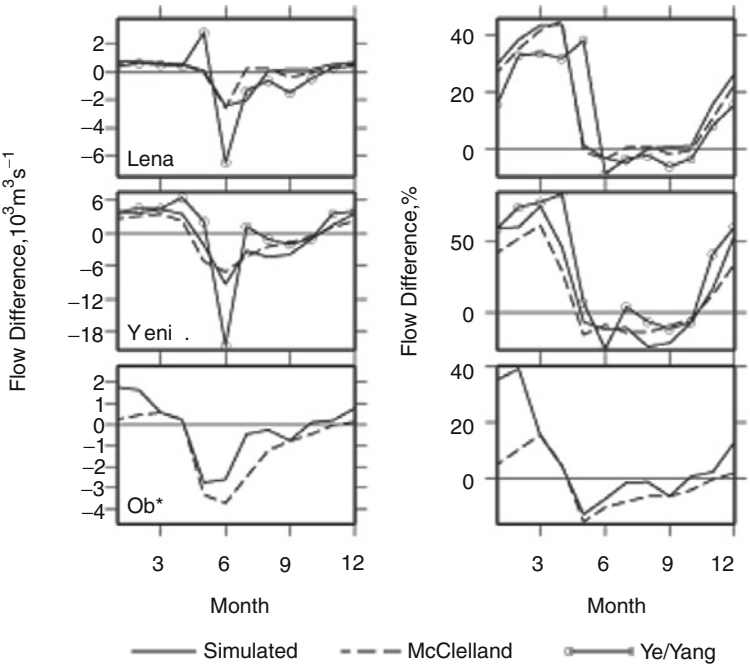

Fig. 7.3 Comparison of the Adam et al. (2007) simulated monthly reservoir signatures to the reservoir signatures inferred from three reconstructed streamflow products (McClelland et al. 2004) for the Lena (Ye et al. 2003), and for the Yenisei (Yang et al. 2004) at the outlets of the Lena, Yenisei, and Ob' River basins. Reservoir signatures are defined as the change in the mean monthly hydrograph due to reservoirs, over the period 1937–1998. From Adam et al. (2007)

It has been well documented that surface air temperatures across the Eurasian pan-Arctic have risen (Hansen et al. 2006) and are expected to continue to increase (ACIA 2005). There are many indications that the temperature increases have led to significant changes in land cover which may, in turn, alter river discharge. Thawing of permafrost (Brown and Romanovsky 2008), a changing freeze-thaw cycle in soils (McDonald et al. 2004), reductions in and disappearance of wetland/natural lake numbers, areas and volumes (Smith et al. 2005), glacier retreat (ACIA 2005), deforestation and change in vegetation structure (Zhou et al. 2003) may provide part of the explanation.

7.2.2 Precipitation

Analysis of seasonal (snowfall and rainfall) precipitation across the Eurasian pan-Arctic using several observational data sets has helped to better understand the role of precipitation in the river discharge changes (Rawlins et al. 2006). Annual snowfall across Eurasian pan-Arctic exhibits a strongly significant increase from 1936

to the late 1950s and moderately significant decrease thereafter. A strongly significant decline in derived rainfall was noted. Spatially, snowfall increases are noted primarily across north-central Eurasia, an area where rainfall decreases are most prominent (Rawlins et al. 2006). As a result of these spatial variations, an integration across the northern drainage basins yielded no significant changes in annual precipitation. A similar conclusion about the general inconsistency between runoff and several precipitation datasets was drawn by Berezovskaya et al. (2004), who suggested that either the existing precipitation products are unable to capture high-latitude precipitation changes, or some other processes are responsible. Adam and Lettenmaier (2008) examined the discrepancies between annual precipitation and streamflow trends for various permafrost regimes and time periods. They found that streamflow trends generally exceeded precipitation trends in continuous permafrost regions (suggesting an additional source of water, speculated to be from permafrost melt), while precipitation trends generally exceeded streamflow trends outside of permafrost regions (an indication that ET is increasing). In regions of discontinuous or isolated permafrost, no consistent discrepancy existed.

The changes in spring maximum discharge across the Eurasian pan-Arctic are consistent with precipitation changes during the cold period, except for the Lena basin, where increasing spring peak discharge occurs even though cold season precipitation has decreased (Shiklomanov et al. 2007). However, the hypothesis that reported increases in extreme rainfall across Russia (Groisman et al. 2005) has resulted in higher extreme discharge risk, was not confirmed because no significant changes were found in the magnitude of summer-fall floods (Shiklomanov et al. 2007). The conclusion of heavy precipitation increases in these publications was mostly made by taking into account the increasing frequency of intense rains rather than their magnitude. Arguably, for maximum monthly discharge, the magnitude of extreme rains is more important.

7.2.3 Snow Cover

Snow cover is effectively an integrated response to both temperature and winter-time precipitation. A warming climate is expected to bring substantial changes in the distribution and dynamics of snow at high and mid latitudes (e.g., Van Blarcum et al. 1995; Raisanen 2008; Dery and Wood 2006). However, high spatial and temporal variability of snow cover properties makes detection and quantitative evaluation of these changes challenging. Most studies of historic surface observations of snow depth and satellite-based snow maps support the results of model simulations and agree on the decreasing trend over the last 30–50 years in the yearly average snow extent and in the length of the snow season in the northern hemisphere and in Eurasia in particular (Dery and Brown 2007; Brown 2000; Brown 1997; Serreze et al. 2000; Groisman et al. 2005). There is also a general consensus as to trends towards earlier time of spring snowmelt and snow retreat. At the same time estimates of the magnitude of these trends vary substantially from one region to another and depend strongly on the particular time period used in the analysis.

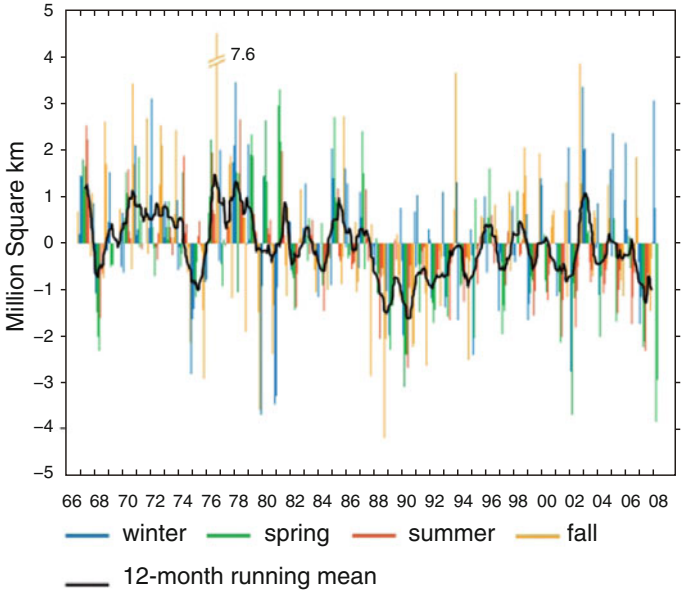

Fig. 7.4 Monthly anomalies in Eurasia Snow Cover Extent, November 1966–April 2008, derived from NOAA interactive snow cover charts. Courtesy of D. Robinson at the Global Snow Laboratory of Rutgers University (http://climate.rutgers.edu/snowcover)

Weekly National Oceanic and Atmospheric Administration (NOAA) northern hemisphere charts of snow cover derived from visual analysis of satellite imagery are available since late 1960s (Robinson et al. 1993)**.** Estimates of the Eurasia snow extent derived from these charts demonstrate an above average coverage in the middle of 1970s and a substantial decline in the yearly average snow-covered area during 1980s and beginning of 1990s (see Fig. 7.4). Later in the second half of 1990s the continental-scale snow extent recovered and remained close to its average values from late 1990s into the beginning of the twenty-first century. Despite this recovery, the overall trend in the satellite-derived snow extent since the early 1970s remains negative. Recent estimates by Dery and Brown (2007) show that over the last 35 years, 1972–2006, the yearly average snow extent has decreased by 0.48×10^6 km^2 or 3% of the yearly average snow cover. The most pronounced decline occurred during spring and early summer months March to June (1×10^6 to 2×10^6 km^2 in 35 years) whereas in November and December the continental-scale snow extent has slightly increased. A smaller spring-time decreasing trend of $1 \times 10^6 - 2 \times 10^6$ km^2 per 100 years was reported by Brown (2000). The latter study covered a longer time period of 1922–1997 and used snow extent time series reconstructed from combined satellite and surface observations. Similar to Dery and Brown (2007), a positive trend of snow extent during the month of October was found.

Not all studies agree on a strictly declining snow cover in Eurasia. Furthermore, there is some evidence of regional peculiarities in the long-term change of snow

cover properties. Ye and Ellison (2003) have shown that during 1936–1995 the length of snow season in eastern Siberia decreased by 2 days per decade, whereas in the European Russia it increased by 1–2 days per decade. Another finding of this work was an increase of up to 6 days per decade in the length of transitional seasons in spring and fall across Eurasia. Similar to Ye and Ellison (2003, regional peculiarities in the snow cover change, i.e., shorter by 2–5 days snow season in northeastern Siberia and longer by up to 2 days season in the northeastern Russia were reported by Groisman et al. (2005). The latter estimates were made from 49-year long time series (1956–2004) of ground-based observations of the state of land surface.

Lugina et al. (2006) also draw attention to a nonlinear change of the surface temperature and, hence of the snow extent in the northern hemisphere and in Eurasia in the last century. Warmer temperatures in the 1930s and 1940s probably caused a considerable reduction in the snow extent and therefore affect the trend estimates based on pre-1950s data. Observations made in Russia in 1956–2004 indicate that the snow season has shortened by about 2 days during that time. In the same time the same trend estimated over the period of 1936–2004 becomes strongly positive with a more than 5 days overall increase in the length of the snow season. On the other hand, a decrease of more than 4 days in the length of the snow season over Former Soviet Union (FSU) was found when observations made during the fastest decline in the snow extent (1956–1991) were only included in the analyses.

Analyses of historical in situ data on snow depth offer some support to model predictions of increased snow accumulation due to increasing wintertime precipitation in the middle and high latitudes of the northern hemisphere. Fallot et al. (1997) have examined snow depth data from FSU snow depth dataset during 1881–1981 and found that snow depth has increased in the Northern European Russia (north of 63°N) after 1945–1950 and in western Siberia after 1960–1970. At the same time consistently decreasing trends in the snow depth during 1921–1981 were found in the southern regions of Russia. This finding supports simulation results of Raisanen (2008) who predicted an increasing wintertime snow accumulation in the coldest areas (north of the −20°C isotherm) and its decrease in warmer climates.

7.2.4 Permafrost and Seasonally Frozen Ground

Permafrost and seasonally frozen ground play important roles in defining the unique character of arctic hydrology, both because of their prevalence and because their extent and behavior are sensitive to climate change. The presence of frozen soils inhibits subsurface water flow and groundwater connectivity, promotes the formation of lakes and wetlands, and imposes narrow limits on the length of the growing season. The extent of frozen soils has changed substantially in recent decades and likely will continue to change in the foreseeable future if temperatures continue to rise as predicted by most climate models. These changes will have important consequences to both arctic hydrology and global climate.

Permafrost is defined as soil or rock whose temperature has remained below 0°C for two or more consecutive years (ACIA 2005). As shown in Fig. 7.5, permafrost

Fig. 7.5 Distribution of permafrost in the northern hemisphere. Image courtesy of Hugo Ahlenius, UNEP/GRID-Arendal. Original data source: Brown et al. (1997). From UNEP/GRID-Arendal (2007)

underlies approximately 22.8×10^6 km^2 or 24% of the exposed land area of the northern hemisphere, the vast majority of which falls within the Arctic (Zhang et al. 1999). The distribution of permafrost is classified into three main zones: continuous, in which all land is underlain by permafrost (with the exception of river channels and lake basins), discontinuous, in which 10–90% of the land surface is underlain by permafrost, and sporadic, in which permafrost underlays less than 10% of the surface (ACIA 2005). An enormous amount of frozen water is contained within permafrost globally, both in soil pore spaces and in pockets of solid ice in excess of soil porosity; estimates of the total volume range from 54,000 to 177,000 km^3 (Zhang et al. 1999). Thawing of even a small fraction of this reservoir could have a significant impact on arctic hydrology.

Permafrost has exhibited a pronounced response to recent climate change. Over the last few decades of the twentieth century, borehole temperatures increased 1–2°C at depths between 6 and 30 m throughout the continuous permafrost zone (ACIA 2005, and references contained therein). Where longer records are available, these temperature increases have been occurring over longer time periods but at slower rates; for example, permafrost temperatures in northern Alaska have increased by 4–7°C over the twentieth century, with 2–3°C of this increase in the last 20 years (Lachenbruch and Marshall 1986; Osterkamp 2005). Zhang (2005) showed that differences in air temperature trends alone cannot explain these trends, and postulated that changes in snow cover (which insulates the underlying permafrost) may be a factor. Temperatures in discontinuous and sporadic permafrost have exhibited fewer and smaller trends (e.g., Alaska interior, Osterkamp 2005; central and southern MacKenzie valley, Smith et al. 2005; European Russia, Oberman and Mazhitova 2001), which may be due to the permafrost in those regions being closer to the melting point; in some locations, absorbed heat may be causing a phase change rather than raising the temperature.

Accompanying these increases in permafrost temperatures at depth have been changes in the timing, duration, and thickness of the active layer (the portion of permafrost at the surface subject to seasonal thawing). Increases in summer air temperature and winter snow depth have been responsible for an increase in active layer thickness across the Russian Arctic of more than 20 cm over the period 1956–1990, based on soil temperature measurements (Zhang 2005; Frauenfeld et al. 2004). Freezing and thawing indices based on monthly average temperatures imply similar deepening of the active layer in the North American Arctic as well (Frauenfeld et al. 2007). Non-permafrost regions are also experiencing change. Across parts of Russia the thickness of seasonally frozen ground has decreased by over 0.34 m from 1956 to 1990 (Frauenfeld et al. 2004).

Together the changes in soil freeze-thaw processes are a significant driver in the seasonal cycle of CO_2 exchange, vegetation greening and productivity, and land surface hydrology. Using passive microwave remote sensing data, McDonald et al. (2004) found that the growing season in early spring has advanced by approximately 7 days from 1988 to 2001 across the Northern Eurasian pan-arctic basin (Fig. 7.6). Other regional studies also show a 6–8 day advance in growing season across the Arctic (Myneni et al. 1997; Zhou et al. 2001).

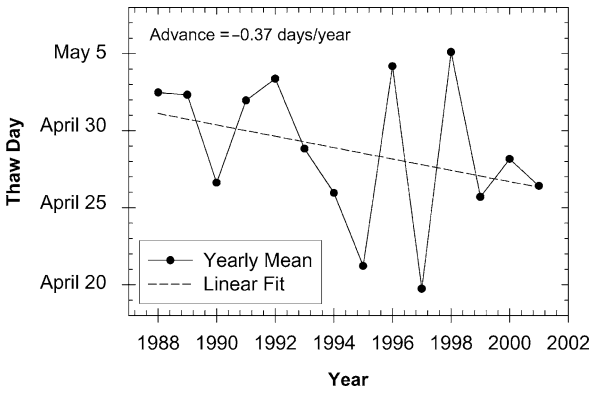

Fig. 7.6 Timing and trend in timing of spring thaw derived from SSM/I. These data sets have shown a correspondence between thaw and regional anomalies in annual NPP derived from MODIS and AVHRR. From McDonald et al. (2004)

Other consequences of permafrost warming include the formation of thermokarst, the growth of taliks, changes in lake and wetland extent (see Section 7.2.5 "Lakes and wetlands", below), the release of ancient carbon to the atmosphere in the form of greenhouse gases (see Sections 7.3 "Links to the Carbon Cycle", below), and possible changes in runoff and streamflow regimes.

While the warming of permafrost certainly causes dramatic changes in the hydrologic characteristics of the soil, its impact on streamflow is not fully understood. The thicker active layer resulting from permafrost thawing has more ground water storage which tends to increase infiltration and reduce surface runoff. Melt water of the excess ground-ice near the permafrost surface can contribute to an increase in river runoff. The deeper active layer delays its freeze-up date in winter. The late active layer freeze-up and increased ground water storage result in greater contribution of subsurface water to the river system, and hence to the winter runoff. Smith et al. (2007) documented a significant increase in minimum daily discharge across the Russian pan-arctic. These minimum-flow changes are most noticeable (and more statistically evident) during winter (Fig. 7.7). They indicate a broad-scale mobilization of subsurface water activity during last 50–60 years and indirectly confirm the idea of additional water release to streams due to thawing permafrost and associated melting of ground ice. However, based on simple volumetric calculations using plausible thaw depths, McClelland et al. (2004) argue that unreasonably deep (and unobserved) permafrost thaw is required to explain the observed river discharge increases and this cause cannot on its own explain the large increases in Russian river discharge.

7.2.5 Lakes and Wetlands

The latitudes north of 50° N account for approximately half of the total global lake and wetland area (Lehner and Döll 2004; Matthews and Fung 1987). In many areas

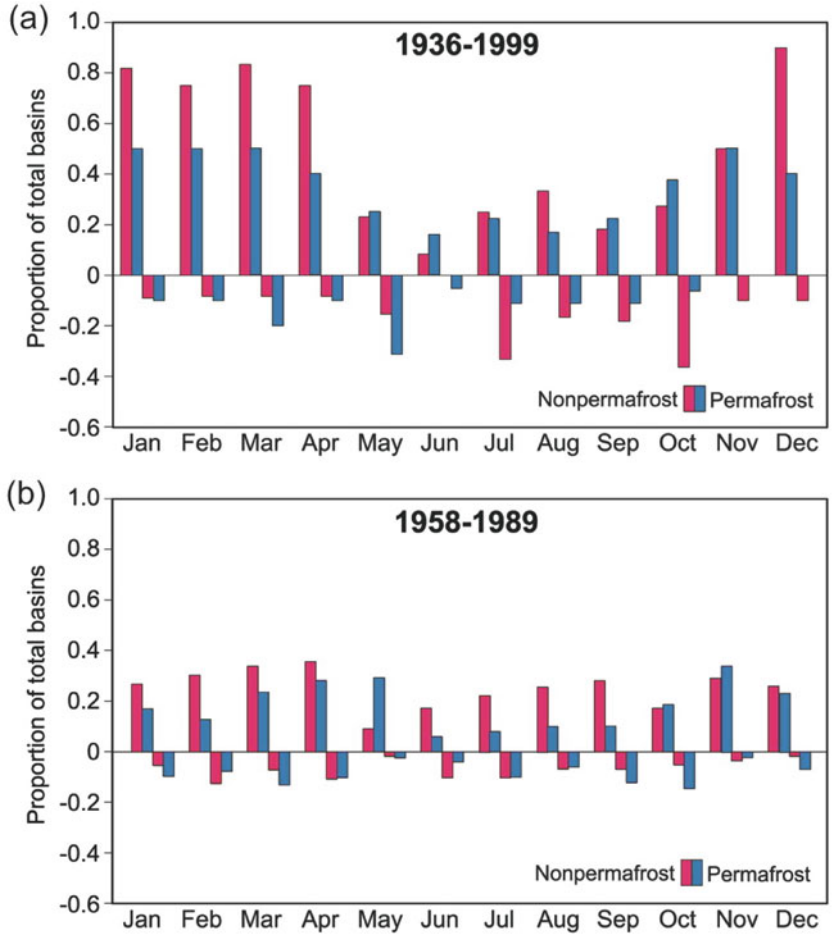

Fig. 7.7 Relative proportions of permafrost-free (*magenta*) and permafrost-influenced (*cyan*) basins with statistically significant increases and decreases in minimum daily discharge, (**a**) 1936–1999 and (**b**) 1958–1989. Note that the absolute values or (**a**) are higher than (**b**) because statistical significance is more difficult to achieve over the shorter record length. For both study periods, more rivers experienced positive statistically significant trends than negative trends, particularly in winter. The proportion of non-permafrost rivers with statistically significant flow increases generally equaled or exceeded those for permafrost rivers. From Smith et al. (2007)

of the arctic coastal plains and the West Siberian lowlands, lakes and wetlands dominate the landscape (Gorham 1991; Bowling et al. 2003). These lakes and wetlands exert unique and important influences on the boreal and arctic hydrologic cycle, and also play important roles in the regional carbon cycle. Yet there are indications that the climatic and hydrologic factors on which these lakes and wetlands depend are changing, giving rise to possible feedbacks to climate change.

Most boreal and arctic lakes and wetlands owe their existence to a combination of poor drainage, as a result of either extremely low topographic gradients or underlying permafrost, and a short growing season, in which cumulative evaporation cannot completely consume the stored water (e.g., Gorham 1991; Bowling et al. 2003). While deep peat layers can impede drainage in peatlands, lakes are more dependent on an impermeable layer of permafrost. In areas underlain by permafrost, and along the Arctic coastal plains of Alaska and Siberia in particular, where there are many lakes, the spring snowmelt first fills up the lake basins until a certain critical connectivity is reached, at which time further meltwater runs off into the local channel network (Bowling et al. 2003). Once the melt is over, runoff declines and drainage network becomes fragmented again, delaying the response to precipitation events. Evaporation continues to draw down the lake level, until the end of the growing season when soil freezes and snow falls again. Thus river discharge in these areas exhibits strong snowmelt peak in spring, followed by decreasing flows until the following year's snow melt. A larger portion of the available energy is spent on evaporation of liquid water in summer, rather than warming or thawing the active layer.

To the extent that the widespread extent of arctic lakes and wetlands results from the drainage impedance of permafrost, there is concern that changing dynamics and patterns of permafrost could affect lake and wetland characteristics in the region. In particular, as climate warms and permafrost degrades, drainage may improve and these lakes and wetlands may disappear, causing major alterations to the local hydrologic cycle and possibly to the global carbon cycle as well. Smith et al. (2005) and Walter et al. (2006) observed increases in lake extent between 1973 and 1997 in those portions of West and East Siberia underlain by continuous permafrost, based on analysis of Landsat TM imagery. During the same time period, lake extent decreased in the portion of West Siberia underlain by discontinuous permafrost (Smith et al. 2005) (Fig. 7.8). The main explanation offered was that climate warming has increased the rate at which lakes thaw the permafrost underneath them

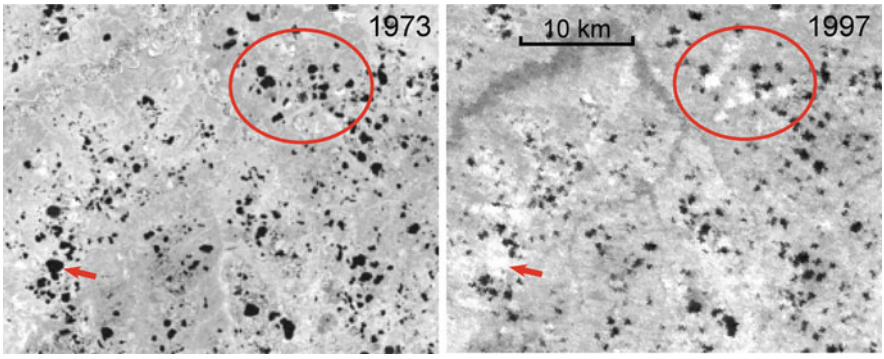

Fig. 7.8 "Change-detection" figure illustrating disappearing lakes in the western Siberia from 1974 (Landsat image to the *left*) to 1997 (RESURS image to the *right*). From Smith et al. (2005). Reprinted with permission from AAAS

and around their perimeters. In areas of continuous permafrost, this process results in lake expansion. In areas of discontinuous permafrost, this process results in the thaw bulbs beneath these lakes eventually connecting with other patches of unfrozen ground, leading to the draining and disappearance of these lakes.

7.2.6 Glaciers

Arctic land ice, in the form of mountain glaciers, ice caps, and the Greenland ice sheet, represents a vast reservoir of freshwater (>3 million km^3, Parkinson 2006). Of this area, the Greenland ice sheet accounts for over half, occupying about 1.6 million km^2 (Parkinson 2006); mountain glaciers and ice caps occupy roughly 275,000 km^2 (Dowdeswell et al. 1997). However, due to their greater sensitivity to climate change, mountain glaciers and ice caps have played a disproportionately significant role in recent changes in the arctic hydrologic cycle (Parkinson 2006; Barry 2006). Recent reductions in the extent of arctic mountain glaciers have received considerable attention because they provide dramatic evidence of climate change (Barry 2006). More importantly, in terms of the hydrologic cycle, these reductions have exerted a major influence on both the freshening of the Arctic Ocean and global sea level rise (Dyurgerov and Carter 2004).

Like most other mountain glaciers, arctic mountain glaciers have displayed a predominantly negative average annual mass balance over the last few decades (Barry 2006; Dowdeswell et al. 1997). Mass balances vary widely in both time and space (Fig. 7.9). Based on observations of glacier length, Hoelzle et al. (2003) found mass loss rates ranging from -0.3 m w.e. $year^{-1}$ (annual water equivalent over the area of the glacier) in maritime regions to -0.1 m w.e. $year^{-1}$ in continental interiors, with Scandinavia having the highest loss rate and the Altai region in the southern Siberia having the lowest loss rate. For most sites (both in the Arctic and around the globe) where long enough records are available, it appears that while glaciers have exhibited negative mass balances since at least 1961, annual loss rates generally increased starting in the mid-1970s (Dyurgerov and Meier 2000). Using a combination of Passive Range-angle-angle Imaging with Spectral Measurements (PRISM), Corona, Landsat Enhanced Thematic Mapper Plus (ETM+), and Advanced Spaceborne Thermal Emission and Reflection Radiometer (ASTER) imagery, Surazakov et al. (2007) found a 7.2% decline in glacier extent in the Altai region between 1956 and 2006; the rate of decline from 1976 to 2006 was 1.8 times that from 1956 to 1976. Arendt et al. (2002) found a similar near-doubling in mass loss rates among Alaskan glaciers when comparing glacier reductions over an "early" period (mid-1950s to mid-1990s) to those over a "recent" period (mid-1990s to 2001).

Not all trends have been negative, however. Mass balances of glaciers in Norway (where mass balances are the most negative) have actually become less negative in recent decades (Dowdeswell et al. 1997). Some of these differences may be a function of regional climate; summer temperatures influence ablation and winter precipitation influences accumulation (Dowdeswell et al. 1997). Braithwaite (2005) found that glaciers in maritime (warm and wet) regions exhibited much larger

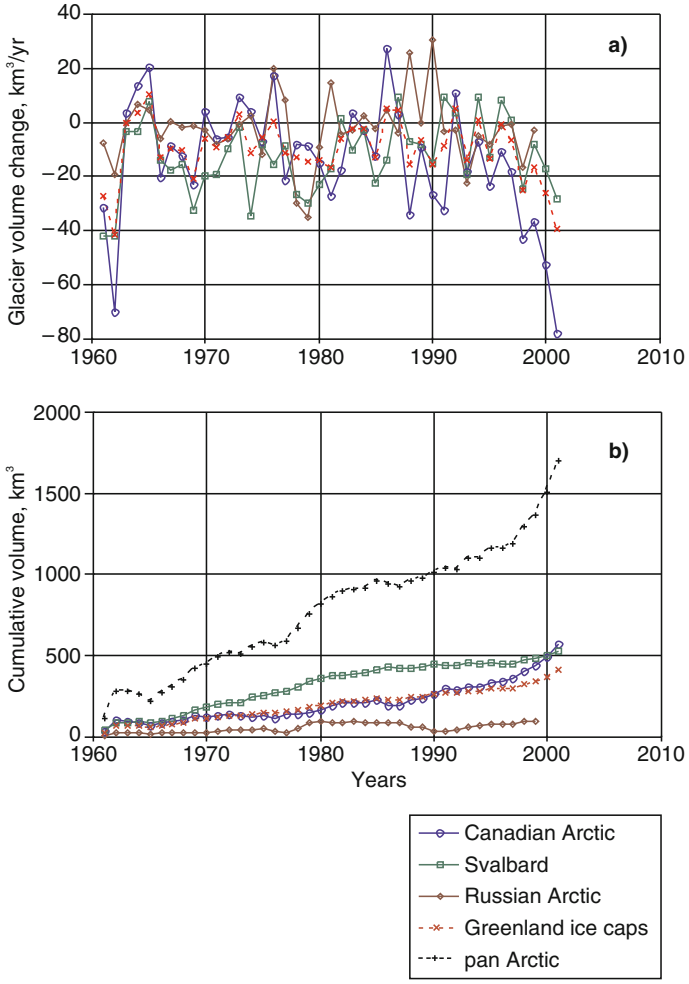

Fig. 7.9 (*above*) Net annual mass balances and (below) cumulative mass balances for various sub-regions of the Arctic, for the period 1961–1998. From Dyurgerov and Carter (2004)

seasonal and inter-annual variability in mass balances, and greater sensitivity to temperature, than those in continental (cold and dry) regions. Noting that most of the glaciers in the Canadian and Russian archipelagos fell into the continental climate category, due to their being surrounded by sea ice, Braithwaite (2005) speculated that a retreat of sea ice from these islands could cause them to become more variable and sensitive to climate.

Another factor in glacier ablation rates is the lowering of albedo caused by the deposition of aerosols, often produced by forest fires some distance away

(e.g., observed in Spitzbergen by Stohl et al. 2007). While this effect has not yet been fully quantified in the Arctic, Sicart and Arnaud (2007) observed a 10–20% reduction in albedo on a Bolivian glacier during the week following a fresh snow fall, due to aerosol deposition. Atmospheric transport simulations indicate that boreal forest fires in central Alaska could potentially deposit 20% of their aerosol particles on glaciers in southern Alaska (Kim et al. 2005). Given the indications of increasing forest fire frequencies across much of the boreal zone over the last several decades (e.g., Groisman et al. 2007), aerosol deposition may be playing an increasing role in accelerating glacier mass losses.

These reductions in glacier size have very real and immediate consequences for both the Arctic and the globe. One immediate impact is the rise in sea level. The melting of land ice worldwide contributes roughly 1.8 mm year^{-1} to sea level rise, the only other major source being warming of the oceans (Meier et al. 2007). 60% of this amount comes from mountain glaciers and ice caps. For example, Arendt et al. (2002) estimated that glaciers in southern Alaska were contributing approximately 0.27 mm year^{-1} to sea level rise. If the recent observed accelerations in loss rates were to continue, mountain glaciers and ice caps could contribute roughly 25 cm of sea level rise by the year 2100 (Meier et al. 2007).

Another impact of glacier mass loss is the export of fresh water to the Arctic Ocean. While seasonal glacier ablation likely constitutes a small portion of the total annual fresh water influx to the Arctic Ocean, its contribution to the total has grown much more quickly than non-glacial contributions to river discharge. Dyurgerov and Carter (2004) found that glacial melt accounted for approximately 75% of the cumulative increases in the combined discharge to the Arctic Ocean of the nine largest Arctic river basins over the period 1961–1998 (Fig. 7.10). At first glance, this may seem to contradict the trend observed in river discharge by Richter-Menge et al. (2006) (Fig. 7.2). However, the results of Richter-Menge et al. (2006) cover a longer period (1936–2006) and include discharge from only the six major Eurasian basins. The much larger inter-annual variability seen in non-glacial discharge compared to glacial melt obscures any longer-term trends when viewed over the 39-year period analyzed by Dyugerov and Carter (2004). Nevertheless, the fact that glacial melt showed a much stronger trend than non-glacial sources of discharge belies the different climate responses of glaciers and non-glacial river basins: while increases in glacial melt were likely due to warmer summer temperatures during this period (Dyugerov and Carter 2004), non-glacial river basins are subject to a variety of factors, including changes in annual precipitation and evapotranspiration, changes in snow pack volume and melt timing, permafrost thaw, water management, and land cover change (see Section 7.2.1). These two discharge sources also have different seasonal fingerprints. Because glacial melt occurs later in the year (summer) than the snow melt frechet (late spring), these increases may explain some, but not all, of the increasing low flows observed in Northern Eurasian rivers by Smith et al. (2007). Given the role of the Arctic Ocean's salinity on the global thermohaline circulation (IPCC 2007), it is important to take glacial mass losses into account when predicting future changes in arctic river discharge.

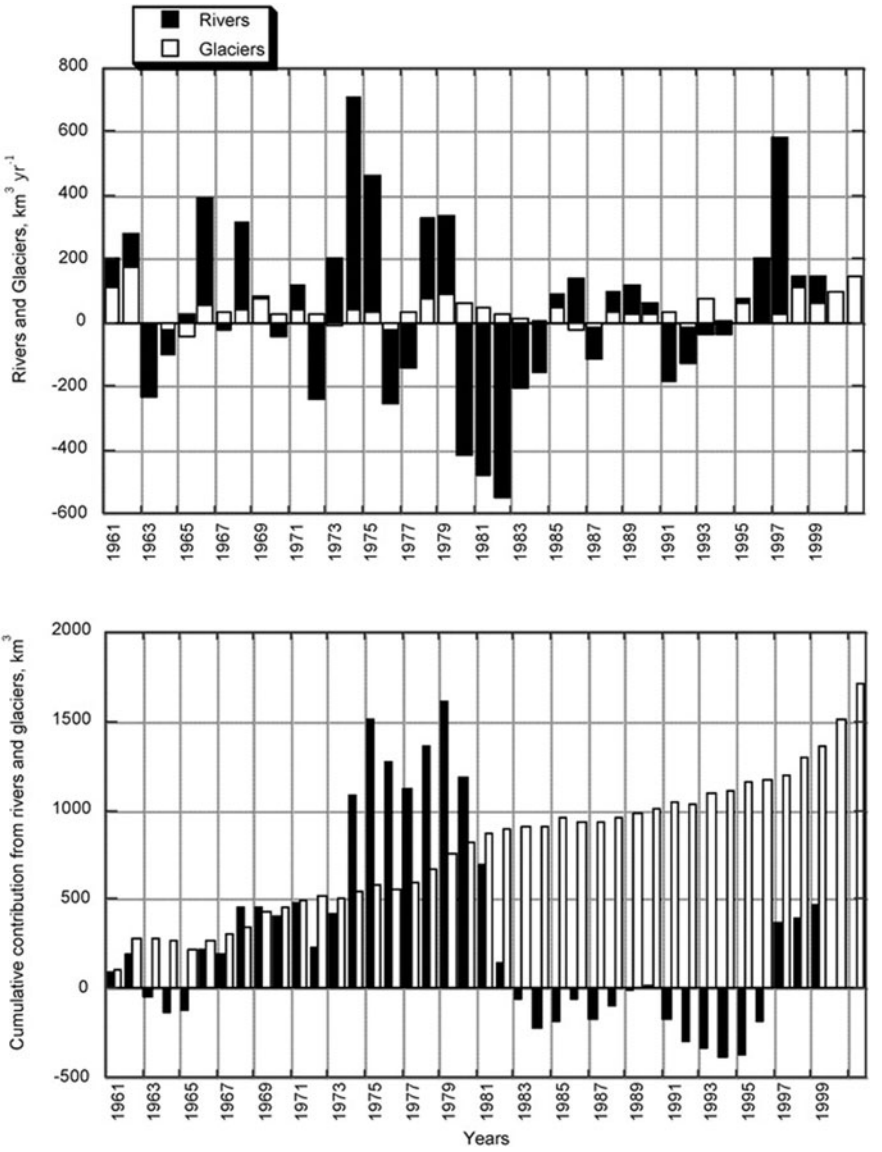

Fig. 7.10 (*above*) Annual and (*below*) cumulative anomalies in discharge to the Arctic Ocean, over the period 1961–1998, due to glacial melt and non-glacial runoff. From Dyurgerov and Carter (2004)

7.3 Links to Carbon Cycle

The water and carbon cycles are closely linked, both globally and at high latitudes. Similar to the journey of water in the hydrologic cycle, the carbon cycle involves carbon's passage from the atmosphere to the landscape (including aquatic systems),

its temporary residence in a variety of forms of storage within the landscape or oceans, and its eventual return to the atmosphere. During all of these stages, water plays several important roles, acting as a transport mechanism and a control on the physical, chemical, and biological pathways that carbon can follow. For example, soil moisture and its movement modulates plant photosynthetic activity, leaching carbon and nutrients from soils, and determining the dominant vegetative cover across the landscape. In boreal and arctic regions in particular, hydrology has a strong influence over carbon fluxes in lakes, streams, and wetlands, providing potentially significant feedbacks to climate change.

7.3.1 Lakes, Permafrost, and Methane

Ongoing changes in lake extent in regions underlain by permafrost, described above, have serious implications for the carbon budget of Northern Eurasia. For instance, much of East Siberia's permafrost contains a vast reservoir of carbon-rich soil called *yedoma* (Walter et al. 2007, 2006; Zimov et al. 1997). The carbon in yedoma soils is still labile, having been frozen before microbial activity could break it down completely. Laboratory tests show that, upon thawing, this carbon is readily respired anaerobically to produce methane at high rates (Zimov et al. 1997). Large methane fluxes have been observed recently in some of the lakes underlain by frozen yedoma soil, with the largest fluxes occurring along the lake margins where active thawing of the permafrost is taking place (Walter et al. 2006).

While these lakes likely have been actively thawing the permafrost and emitting methane to the atmosphere since the last Ice Age, there are signs that future emissions may be much larger than in the past. Evidence from radiocarbon dates (Walter et al. 2007) indicates that the rates of thermokarst lake initiation, and presumably methane emissions, varied with climate since the last Ice Age, reaching a maximum during between 11 and 9 kyr BP, corresponding to the warmest temperatures of the current interglacial in West Siberia. This is corroborated by a modeling study by West and Plug (2007), which indicated that thaw lake growth rates are correlated with soil temperature, lake size, and ground ice content. Walter et al. (2006) estimated that if all the carbon stored in yedoma soils were respired anaerobically at the active margins of expanding lakes, the methane concentration of the atmosphere could double. This has led to concerns that these lakes may provide a substantial positive feedback to climate change.

7.3.2 Frozen Soil and DOC Export

Another link between changes in the hydrologic and carbon cycles is related to trends in river discharge and export of dissolved organic carbon (DOC). Increases in the riverine fluxes of DOC have been observed in boreal and arctic streams in North America, Europe, and Asia over the last 2–3 decades (e.g., Worrall and Burt 2007). The vast majority of this riverine DOC originates in terrestrial ecosystems (e.g., Kling et al. 1991; Cole et al. 1994) and is transported to lakes and streams via

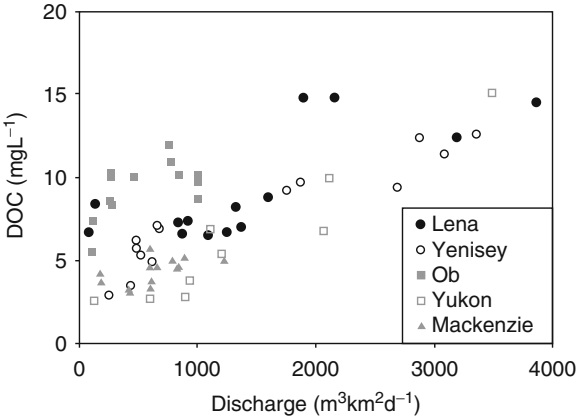

Fig. 7.11 Dissolved organic carbon (DOC) concentrations vs. daily discharge at the mouths of major Arctic rivers. From Raymond et al. (2007)

groundwater (e.g., Billett et al. 2004). The leaching of DOC from soils to streams via groundwater has recently been recognized as a significant loss term in terrestrial carbon budgets and is thought to be responsible for the observed losses of substantial amounts of carbon from soils (e.g., Bellamy et al. 2005).

Globally, it has been difficult to attribute observed increases in DOC fluxes to any single factor (Worrall and Burt 2007). However, in the Arctic, Holmes et al. (2008) and Raymond et al. (2007), among others, have found strong correlations between daily river discharge and DOC concentrations (Fig. 7.11). In this context, the increase in the annual discharge of the six major rivers of the Russian Arctic (Peterson et al. 2002), and especially the recently discovered increase in minimum flows across Northern Eurasian pan-Arctic (Smith et al. 2007) discussed above, may have important consequences for the carbon cycle. Because minimum flows generally reflect the influence of groundwater, Smith et al. (2007) speculated that cause of these trends is a reduction in the intensity of seasonal soil freezing, allowing more connectivity in subsurface drainage networks. If this process is indeed occurring, it is conceivable that the increased flushing of the soils by groundwater, accompanied by longer growing seasons and greater microbial activity during seasons in which the soils historically have been frozen, could lead to greater mobility and loss of soil carbon. Establishing a link between these phenomena will require further research.

The loss of DOC from terrestrial soils may be greatest and most sensitive to climate in the zones of discontinuous permafrost in Siberia, Canada, and Alaska (Frey and Smith 2005). Not only do these areas contain large areal coverage of peatlands, but it appears that permafrost in these areas has stabilized much of the soil carbon in the watersheds. Frey and Smith (2005) found that streams draining watersheds south of the −2°C isotherm of mean annual air temperature had much higher DOC concentrations than streams draining watersheds north of this isotherm. This isotherm corresponds roughly to the southern edge of the discontinuous permafrost zone. Most climate models forecast that this isotherm will shift northward in the next century. The implication is that permafrost will thaw and large amounts of DOC

will be leached from soils in these areas. DOC in streams and in the oceans is at risk of being respired and released to the atmosphere as CO_2 (Kling et al. 1991). Since many arctic ecosystems are only marginally sinks of carbon, these ongoing changes have the potential to tip the regional balance from a sink to a source of carbon.

7.3.3 Peatlands, Water Table, and Greenhouse Gases

Globally, wetlands play a dual role in the carbon cycle, as both a net carbon sink (76 Tg C $year^{-1}$ for high-latitude peatlands alone, Gorham 1991) and the largest natural source of methane (115 Tg CH_4 $year^{-1}$, Matthews and Fung 1987). Both the extent of wetlands and the balance between their methane emissions and carbon sequestration depend on climatological and hydrological factors, leading to potentially significant feedbacks to the global climate system. This is especially true in the northern high latitudes, which are home to approximately 50% of the world's wetlands (Matthews and Fung 1987), and where ongoing and projected climate change is most pronounced (Serreze et al. 2000; IPCC 2007). While few records of greenhouse gas emissions in wetlands are long enough to establish trends, the responses of these emissions to seasonal and inter-annual changes in climate can provide insights into their possible response to climate change.

The vast majority of high-latitude wetlands are *peatlands*, characterized by shallow water tables and carbon-rich soils (Matthews and Fung 1987). Peatland soils become enriched in carbon as waterlogged, anoxic soils, cold winters, and tannic acids secreted by sphagnum mosses combine to inhibit soil respiration. As a result, annual respiration tends to be less than annual production, and carbon-rich organic matter (peat) accumulates in the soil (Gorham 1991), often reaching depths of 3 m or more (e.g., Sheng et al. 2004). Peatlands tend to form in flat areas with poor drainage, with vast concentrations in the West Siberian lowlands (between the Ob and Yenisei rivers) and the Hudson/James Bay lowland of Canada. Boreal and subarctic peatlands cover approximately 3.5 million km^2, and store approximately 455 Pg C in their soils (Gorham 1991). There is some concern that, if a warming climate were to cause peatland water tables to drop, this vast reservoir of carbon could be rapidly released to the atmosphere as carbon dioxide.

The same hydrologic conditions in peatlands that promote the accumulation of carbon in the soil also lead to the production of methane (CH_4), which is a much stronger greenhouse gas than carbon dioxide (by a factor of 23 on a 100-year time scale, IPCC 2007). Several studies (e.g., Moore and Roulet 1993; Dise et al. 1993) have shown that, below the water table, anoxic conditions promote anaerobic respiration, whose end product is methane. Above the water table, aerobic respiration predominates, producing carbon dioxide. Less is known about the relationship of CO_2 emissions to water table depth, and their relationship to CH_4 emissions. Recent studies have begun to focus on this issue (e.g., Friborg et al. 2003; Strack and Waddington 2007). Nevertheless, the position of the water table appears to have some influence over the partitioning the end-products of soil respiration into CO_2 and CH_4.

Climate factors also play major roles in greenhouse gas emissions from peatlands, both directly and indirectly via their influence on the water table. An increase in precipitation tends to raise the water table, increasing the total soil volume producing CH_4. Soil temperature plays two roles. On one hand, an increase in soil temperature tends to lower the water table, through increased evapotranspiration, decreasing the total soil volume producing CH_4. On the other hand, an increase in soil temperature leads to an increase in production of both CO_2 and CH_4 per unit soil volume, by increasing metabolic rates (e.g. Lloyd and Taylor 1994; Moore and Roulet 1993; Dise et al. 1993; Frolking and Crill 1994). Simulations of future climate suggest that, by the end of the twenty-first century, the northern latitudes will experience warming of between 1 and 5°C and possible increases or decreases in precipitation of up to 15% (IPCC 2007). Due to the opposing influences of temperature and precipitation on water table depth, as well as the opposing effects on CO_2 and CH_4 emissions, it is not immediately clear what the net response of peatlands will be.

Complicating matters further are small-scale variations in water table depth and vegetation across the landscape. The depth to the water table and extent of inundation within peatlands varies both on scales of several kilometers, due to position in the landscape (e.g. raised bogs vs. fens, Kremenetski et al. 2003; Vitt et al. 2000), and on scales of meters, due to microtopographic variations in the moss cover (e.g., Saarnio et al. 1997; Vitt et al. 2000; Panikov et al. 2001; Kremenetski et al. 2003; Friborg et al. 2003). The nonlinear response of methane emissions to water table depth makes estimation of emissions using some average water table depth somewhat inaccurate.

Additionally, methane emissions have shown some dependence on local vegetation cover, and have been found to vary considerably along transects of only a few hundred meters (e.g., Panikov et al. 2001; Saarnio et al. 1997). Vegetation cover also responds to changes in climate and land use (e.g., draining of peatlands for agriculture); the coupled changes in water table and vegetation cover have been found to influence emissions of both CH_4 and CO_2 (Strack and Waddington 2007).

Finally, the physical pathways taken by emissions vary in time and space as a function of hydrology, meteorology, and vegetation cover. Pathways include moisture-dependent diffusion through the soil (Crill 1991; Bartlett and Harriss 1993), vegetation-dependent transport through plant tissues (Shannon and White 1994; Bubier et al. 1995), and sporadic large ebullition events (Baird et al. 2004), often triggered by drops in atmospheric pressure. Thus, the current set of sparse point measurements of methane emissions may be unrepresentative of emissions across the domain.

Despite the difficulties inherent in estimating the greenhouse gas emissions from peatlands across large areas as a function of climate, several attempts have been made using large-scale models (e.g., Bohn et al. 2007; Zhuang et al. 2006; Gedney et al. 2004; Shindell et al. 2004). To date, large-scale investigations have focused on methane emissions under likely climate scenarios for the end of the twenty-first century. These models take a variety of approaches, but the consensus is that methane emissions from northern peatlands will likely double relative to current emissions,

providing a significant feedback to the climate system. While large uncertainties remain, it is clear that hydrology plays a key role in the carbon cycle of high-latitude peatlands.

7.4 Monitoring of the Water Cycle in the Context of LCLUC

7.4.1 Ground Observational Networks

Our understanding of large-scale climate and hydrology has traditionally been derived from station networks positioned throughout the landscape. Among the major elements of surface water budget only precipitation and streamflow are observed at relatively dense and well-established monitoring sites. Measurements of evaporation and soil moisture were made in the USSR over very sparse networks mostly located outside of the arctic drainage basin (e.g. Valdai located at the midpoint between St. Petersburg and Moscow).

The total number and distribution of stations changed significantly over the twentieth century, particularly across the high latitudes of the northern hemisphere. This has been a concern as biases have been shown to arise when interpolating from spatially heterogeneous networks (Willmott et al. 1994). For most continents, traditional interpolation from early station networks tends to overestimate spatial precipitation, as meteorological observations were more prevalent in regions with higher precipitation (e.g. western Russia) and gradually expanded into drier ones over time. As a result, station networks across Eurasia tended to overestimate annual precipitation during the 1940s and 1950s when the total number of gauges was low (Rawlins et al. 2006, Fig. 7.12). The figure shows that early networks in the high latitudes of the north originated in the warmer and wetter southerly zones and gradually expanded northward and into the continental interiors, where the continental climates are colder and drier. Any interrogation of commonly available gridded data sets for trends in spatially-averaged precipitation is at risk of being contaminated by the effects of these changing station network configurations. Given that early networks were biased to wetter regions, it is possible that any positive temporal trends in precipitation would tend to be underestimated. Additionally, given other uncertainties in historical arctic precipitation records such as gauge under catch (Groisman et al. 1991; Goodison et al. 1998) any trend estimates for the latter half of the 20th century should be interpreted with caution.

River discharge is one of the most accurately measured components of the water cycle. Recent assessments of river discharge accuracy for large Russian rivers showed the uncertainty of annual discharge for individual gauges to be ± 2–7% (Shiklomanov et al. 2006). Despite the value of discharge information, ungauged or poorly monitored areas dominate many parts of the Eurasian Arctic (Fig. 7.13). Over the last 10 years the accessibility of river discharge data for the pan-Arctic has been significantly expanded by the release and regular updates of the University of New Hampshire's R-ArcticNet database (http://www.R-ArcticNet.sr.unh.edu,

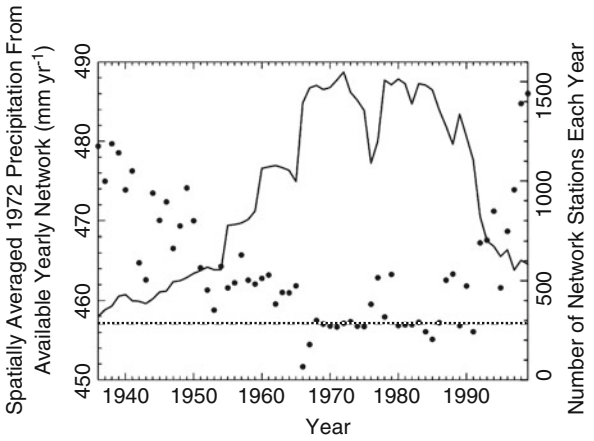

Fig. 7.12 Annual Eurasian pan-arctic precipitation interpolated from station data. The number of stations is shown on the *right* axis. Potential biases induced when gridding from irregular station networks was estimated by attempting to recreate total precipitation in 1972 (when the station network was most dense) using the available station networks each year from 1936 to 1999. Starting from the 1972 network, annual precipitation was sampled at only those stations in operation each year for 1936, 1937,. . ., 1999. Those subsets were then interpolated prior to spatial averaging. A similar bias was observed when alternate base years were used. From Rawlins et al. (2006)

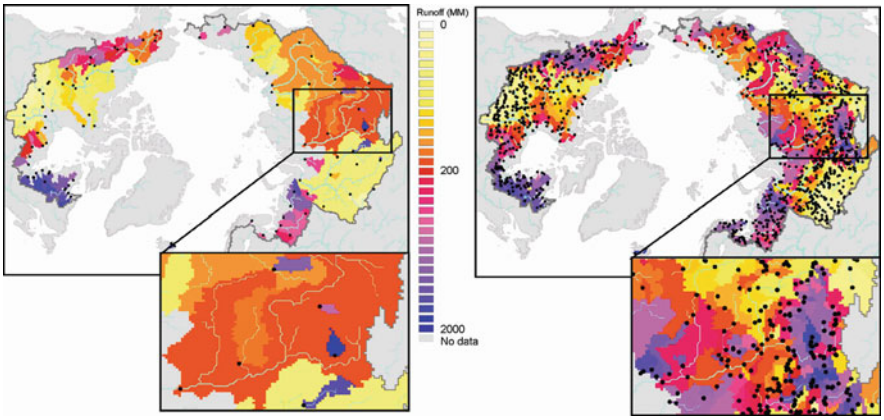

Fig. 7.13 Long-term mean annual runoff in the pan-Arctic based on observational data from data available in 1998 (Vörösmarty et al. 1996, 1998): Global River Discharge Database (RivDis v1.0) and from data available in 2006 (UNH R-ArcticNET v4.0 (2005). A Regional, Hydrometeorological Data Network For the pan-Arctic Region. Shown only gauges and watersheds larger 5,000 km^2)

Fig. 7.13), however recent sharp declines in Russian hydrometric gauging networks (Shiklomanov et al. 2002) and delays in data reporting, especially for Russia (Vörösmarty et al. 2001), hamper the research progress.

Sparse monitoring networks in the northern, remote regions are experiencing the most dramatic changes in both climate and land cover and this is precisely the area where there is the most significant gap in existing ground observation networks. The density of river discharge and precipitation gauges throughout the Russian pan-arctic region for land cover classes and permafrost regions are shown in Table 7.1. The classes with the highest density of gauges are steppe/shrub and taiga forest for land cover and non-permafrost. The lowest gauging station density is in the tundra and continuous permafrost areas. These high and low gauge density areas tend to be associated with population (Lammers et al. 2001). Ideally, monitoring would be stratified according to the likelihood and/or evidence of ongoing change; i.e., transitional land-cover classes. If one considers the transitional classes to be forest/tundra and discontinuous permafrost, the existing densities of long term gauges are 124 and 87 per 10^6 km^2 for river discharge, and 21 and 19 per 10^6 km^2 for precipitation over Northern Eurasia (see Table 7.1). Whether or not this is sufficient for change detection purposes is not clear at present.

Table 7.1 Gauges and gauge density by land cover type and permafrost type for the Russian pan-arctic drainage system

	Percent	All river gauges		Long term river gauges		Large river gauges		Precipitation	
Class	Area	Count	Density	Count	Density	Count	Density	Count	Density
Land cover									
Polar desert	8.0	75	74	49	48	17	17	10	10
Tundra	9.7	66	54	52	42	24	20	20	16
Forest/tundra	29.4	571	153	464	124	178	48	80	21
Taiga forest	41.1	1,166	223	994	190	389	74	236	45
Steppe/shrub	11.9	429	284	348	231	136	90	168	111
Total	100.0	2,307		1,907		744		514	
Permafrost									
Continuous	48.5	507	81	391	62	169	27	102	16
Discontinuous	7.2	103	111	81	87	41	44	18	19
Intermittent	8.9	203	176	176	152	80	69	46	40
Sparodic	8.1	194	184	164	155	78	74	42	40
No permafrost	27.2	1,300	368	1,095	310	376	106	306	87
Total	100.0	2,307		1,907		744		514	

Density: Gauges per 1,000,000 km^2 of class
Total domain area: 1,2970,000 km^2

Sources: TEMVeg land cover map, IPA permafrost map, R-ArcticNet river discharge data, TD9813 precipitation dataset; Long term gauges: $\geq$ 10 years of records; Large gauges: Drainage area $\geq$ 5,000 km^2.

7.4.2 Remote Sensing Monitoring of Water Cycle

Remote sensing provides an important alternative to in situ monitoring for purposes of environmental change detection. In addition to providing data for areas that are difficult to access on the ground (a common characteristic of much of Northern Eurasia and the Arctic in general), remote sensing products can reveal complex spatial variations that cannot be readily elucidated by traditional in situ observations. Remote sensing techniques have been used to monitor key components of the hydrologic cycle, including precipitation, snow cover extent and snow depth, water storage in lakes and reservoirs, river stage, glacial extent, soil moisture, and even ground water storage. However, remote sensing is not without its limitations, especially at high latitudes. Two such limitations are the difficulty of measuring solid precipitation from satellites, and the fact that many well-known satellite missions, such as the Tropical Rainfall Measuring Mission (TRMM), have used inclined orbits, designed to provide greater coverage at low latitudes at the expense of high latitude coverage. We discuss the various remote sensing methods for studying components of the hydrologic cycle below.

7.4.2.1 Snow Water Equivalent

At high latitudes, the most important water budget term is arguably the snow pack water equivalent (SWE). Microwave frequencies have been the spectral range of choice for monitoring SWE, owing to their sensitivity to snow depth, insensitivity to cloud cover, and ability to make observations at night (Derksen et al. 2003). Since 1978, global observations of snow cover extent have been performed using microwave measurements beginning with the Nimbus-7 Scanning Multichannel Microwave Radiometer (SMMR) and later, since 1987, with the Special Sensor Microwave Imager (SSM/I flown by the Defense Meteorological Satellite Program (DMSP) (e.g., Grody and Basist 1996). Snow cover products have also been generated from the Advanced Microwave Sounding Unit (AMSU) onboard NOAA polar orbiting satellites since 1998 (Kongoli et al. 2004) and from the Advanced Microwave Sounding Radiometer (AMSR-E) onboard the NASA Aqua satellite since 2002 (Kelly et al. 2003). These products range in resolution from 10 to 50 km.

Yet, despite the importance of monitoring SWE, the reliability of satellite retrieval methods remains problematic. Microwave observations of snow water equivalent suffer from several limitations. Primary among them is that retrieval algorithms tend to saturate at SWE values greater than 100–200 mm, due to the limited penetration of the 37 Hz band beyond 0.8 m within the snow pack (e.g., Foster et al. 2005; Kelly et al. 2003). Furthermore, other factors besides snow depth, such as grain size, density, and stratification, can also influence the microwave scattering signature of the pack (Rosenfeld and Grody 2000). The presence of liquid water in the pack inhibits scattering and can also interfere with the microwave signatures observed by satellites (Grody and Basist 1996). Forest cover presents another problem, particularly for passive microwave sensors, as the microwave emissions from the vegetation tend to overwhelm the snow emission signature (Derksen et al. 2003;

Kelly et al. 2003; Singh and Gan 2000; Pulliainen et al. 1999; Tait 1998). Kelly et al. (2003) estimated uncertainties of 50–70% in SWE retrievals from forested areas. Thus, useful satellite observations of SWE are currently limited to relatively thin, dry snow in sparsely vegetated areas such as tundra and the Canadian prairies. Planned missions like NASA's Snow and Cold Land Processes mission (SCLP), which will combine passive and active sensors, are expected to provide substantially better estimates of SWE at high latitudes.

7.4.2.2 Snow Cover Extent

In contrast with SWE, snow cover extent (SCE) has proven much more amenable to satellite observation. While techniques have been developed to monitor SCE in the microwave, visible and infrared spectral bands, visible and infrared products tend to perform better than microwave products, both in terms of spatial resolution and accuracy. Because of a tendency to miss shallow and melting snow, microwave products typically underestimate the snow extent. Armstrong and Brodzik (2001) found that the SSM/I and SMMR data-based algorithm maps consistently less snow over the northern hemisphere as compared to NOAA interactive snow charts. The difference in the estimated snow-covered area ranges from 2% in early spring to 25% in late fall. At the same time, anomalies in the yearly average in the snow extent derived from SSM/I demonstrate a noticeable correlation with NOAA interactive charts (Fig. 7.14).

Visible-range SCE products tend to perform better and have higher resolution than microwave products. Daily global snow maps at a spatial resolution from 500 m to 5 km are derived from the Moderate Resolution Imaging Spectrometer (MODIS) onboard Terra (since 2000) and Aqua (since 2002) satellites (Hall et al. 2002). Since 2006 observations of the Advanced Very High Resolution Radiometer (AVHRR) onboard NOAA satellites have been used to routinely generate daily snow maps over Eurasia at 4 km. resolution (http://www.star.nesdis.noaa.gov/smcd/emb/snow/HTML/eurasia_snow.html).

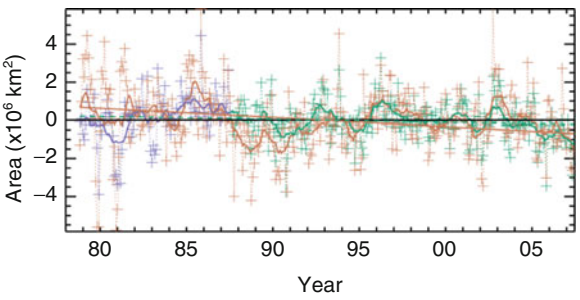

Fig. 7.14 Northern hemisphere snow-covered area departures from monthly means, 1978–2007, from NOAA snow charts (*orange*) and microwave satellite (*purple*/*green*) data sets. Image courtesy of R. L. Armstrong and M. J. Brodzik, National Snow and Ice Data Center, CIRES/University of Colorado at Boulder

Maps of snow cover distribution are also produced from a number of other instruments onboard polar orbiting satellites (e.g., Xiao et al. 2004; Dozier and Painter 2004). Estimates of the relative accuracies of snow maps derived from visible-band sensors, compared to surface observations, range from 80 to 100% for MODIS (Simic et al. 2004; Hall and Riggs 2007) and 88% for Geostationary Operational Environmental Satellites (GOES; Romanov et al. 2000), although forest cover and clouds can adversely affect performance (Maurer et al. 2002).

The need for cloud-free scenes and for illumination from the sun (which is rare in winter in the high latitudes) are major limitations for visible sensors. To compensate for these limitations, blended algorithms involving multiple sensors have been developed. Examples of multisensor snow products include an 8-day snow cover/snow depth product generated from MODIS and AMSR-E snow maps (Armstrong et al. 2003) and a blended daily snow cover map derived from AMSR-E, MODIS and QuikSCAT scatterometer data (Foster et al. 2008). Since 1999 an automated algorithm using combined observations from GOES and SSM/I have been routinely generating 4-km resolution snow maps over North America (Romanov et al. 2000). In 2006 this algorithm was complemented with observations from NOAA AVHRR and Meteosat Second Generation (MSG) and the snow mapping domain was expanded to the whole globe (http://www.star.nesdis.noaa.gov/smcd/emb/snow/HTML/multisensor_global_snow_ice.html). The common approach in these algorithms consists of the use of snow cover estimates in the visible and infrared over clear-sky portions of the map, whereas in cloudy conditions the map is complemented with snow retrievals in the microwave.

7.4.2.3 Surface Water Extent

As outlined in Prigent et al. (2007), a variety of remote sensing techniques have been used to monitor inundation and open water extent, including visible, infrared, and passive and active microwave observations. Each type has advantages and disadvantages, which often involve trade-offs between spatial and temporal resolution. Visible sensors have proven useful for monitoring open water extent, due to their high resolution and frequent return periods. For example, Smith et al. (2005) and Walter et al. (2006) used LANDSAT Multispectral Scanner (MSS), RESURS-1 Multispectral Scanners with Conical Scanning (MSU-SK) and LANDSAT ETM+ imagery to quantify the dramatic changes in lake extent in West and East Siberia over the last few decades. Passive microwave sensors have long been popular in monitoring inundation, due to their sensitivity to the presence of water, ability to detect surface water obscured by vegetation canopies, and daily return periods. For example, Grippa et al. (2007) used SSM/I imagery to estimate trends in annual open water extent in the West Siberian lowlands. However, passive microwave imagery typically has spatial resolutions of 25–50 km, and thus cannot give precise estimates of the extent of inundation. Active microwave techniques such as Synthetic Aperture Radar (SAR) have much higher spatial resolution (10–50 m), but infrequent overpasses. Approaches using a combination of observation types (e.g., Prigent et al.

2007) hold some promise for optimizing the spatial and temporal resolution of monitoring efforts.

7.4.2.4 Surface and Sub-surface Water Storage

Satellite altimetry over lakes and reservoirs, started in the early 1990s, provides critical information for tracking changes in water level/storage of medium and large water bodies and is an important complement to ground based stations, which are sparse or nonexistent at high latitudes (Birkett 1998). The proposed Surface Water Ocean Topography mission (SWOT) (http://bprc.osu.edu/water/) using wide-swath altimetry technology as a means of completely covering the world's oceans and freshwater bodies with repeated elevation measurements will result in substantial improvements in the ability to track freshwater storage and movement at high latitudes. Currently, knowledge of the global dynamics of terrestrial surface waters as well as their interactions with coastal oceanic waters is poor, and SWOT should help to extend our understanding of these processes. Another technique that may prove useful in monitoring both surface and sub-surface water storage is satellite gravimetry. The twin satellites of the Gravity Recovery and Climate Experiment (GRACE) have been monitoring monthly global geoid height with an accuracy of 2–3 mm and spatial resolution of 400 km since 2002 (Tapley et al. 2004). Large scale hydrological budget closure estimates using GRACE have been carried out over the major Russian drainage basins and indicate the actual discharge of water from the basins may be much higher than current river discharge measurements (Syed et al. 2007).

7.4.2.5 Glaciers and Soil Freeze/Thaw

Other hydrologic components that can be monitored remotely include glacier volume and extent, and soil freeze/thaw status. Arendt et al. (2002) used airborne laser altimetry to monitor the surface elevation (and thus the volume) of glaciers in southern Alaska. Changes in glacier extent have been observed primarily through visible sensors such as LANDSAT ETM+, ASTER, PRISM and Corona (e.g. Surazakov et al. 2007). To monitor growing season onset in Northern Eurasia, McDonald et al. (2004) used SSM/I passive microwave observations of soil thaw (Fig. 7.6). Their estimates compared favorably to the onset of productivity derived from MODIS and AVHRR.

7.4.3 Hydrologic Monitoring and the Carbon Cycle

The main challenge in monitoring carbon fluxes at high latitudes is how to represent the vast, sparsely-populated, and relatively inaccessible areas that are typical of most of the region. In situ measurements can measure carbon fluxes more or less directly but can represent an extremely small portion of the landscape. Extrapolating such heterogeneous phenomena as water table depth and greenhouse gas emissions from these isolated points leads to substantial inaccuracies in estimates of regional

fluxes. Flux tower networks have been implemented in recent years but while these measurements represent average conditions over a larger area (up to several hundred meters radius from most towers, although taller towers are being constructed that can sample larger areas), they too are sparsely spaced, separated by hundreds of kilometers. In contrast, remote sensing offers a way to monitor large, otherwise inaccessible areas such as the interiors of Siberia and Canada, with spatial resolutions ranging from 25–50 km to 10–50 m and return periods as short as one day.

Some satellite-based sensors, such as Atmospheric Infrared Sounder (AIRS) and Greenhouse gases Observing Satellite (GOSAT; to begin operation in 2008) can measure vertically-integrated atmospheric concentrations of greenhouse gases such as methane on daily time scales (Toptygin et al. 2005). To attribute these concentrations to sources and sinks at specific locations on the ground requires inverse modeling using atmospheric transport models. Although development of these techniques is ongoing, they have already been employed to analyze observed atmospheric CO_2 concentrations and CO_2 emissions measured at flux towers (e.g., Pacala et al. 2001). Other available remote sensing techniques (such as those mentioned in the previous section) cannot directly measure carbon fluxes at the land surface. Instead, we can monitor those hydrological processes that influence carbon fluxes and use them as proxies. The most relevant hydrological observations for this purpose are inundation and open water extent, as they are closely related to local water table depth. As mentioned above, soils can emit methane without water being present at the surface. Therefore, the inundated area necessarily represents a lower bound on the extent of methane-emitting land surface. However, because the largest emissions occur when the water table is within 10 cm of the surface, and drops off rapidly with depth below 10 cm (Christensen et al. 2003), estimates of methane emissions based on remotely-sensed inundated extent may capture the bulk of the emissions. The satellite-derived inundated extent could be used directly as an input into a methane emissions model, or used to constrain a more sophisticated model of the distribution of water table depth across the landscape, which then could be used to drive a methane emissions model.

7.4.4 A Strategy for Improving Hydrological Change Detection

One goal of NEESPI is to detect emerging changes in the hydrological system over Northern Eurasia. Effective change detection requires anticipation of where and when they are expected to take place. This requires identifying (i) the natural variability of the system as well as ii) new sources of variability from climate change and direct human-induced changes (e.g., land cover land use change, engineering structures).

A coordinated plan might consist of the following elements: multi-faceted observation networks, detailed process studies, integrated data and modeling information system.

Each of these elements is discussed briefly below.

(1) Observation networks: Observation networks are the backbone for all other components of a change detection strategy. Observations include in situ point measurements (e.g., river discharge, precipitation, active layer depth), remotely sensed products (e.g., snow cover, laser altimetry, GRACE) and the incorporation of human dimensions data (land use, population). Detailed observations are the product of process studies and/or monitoring systems, but also contribute as the inputs, parameterizations, and testing and evaluation procedures for the models that of necessity must be used for upscaling to the regional level. Observations must be harmonized and integrated into the information system for archiving, analysis and dissemination. An important component of the observation network is a near real-time data capability to allow for rapid response in a changing environment.
(2) Process studies: Process studies provide a detailed look at specific components of the hydrological system and typically focus on a narrow spatial domain (fine scale) in order to understand the processes relevant to that domain. Focusing on particular time periods (e.g. spring snowmelt) is also vital. Such studies are most often carried out with experimental investigations in the field and therefore have a limited spatial and temporal scope. However, these studies need to be cast within a coordinated, wider multi-scale approach to allow up-scaling to the full NEESPI domain.
(3) Integrated data and modeling information system: Modeling and data information systems are best treated as an integrated system for maximum effect. This allows for the seamless harmonization of data streams into the modeling environment with a user interface for easy accessibility by researchers and others with a variety of disciplinary backgrounds. Models serve two roles. First, they can be used to perform scientific experiments, and second they provide a means of operational data processing to satisfy the needs of scientists as well as managers, policy makers and other stakeholders. An important part of each of these building blocks is the need to embrace new technologies to generate innovative uses of existing data and to create novel data streams to improve process studies as well as performing synthesis activities across the system.

7.5 Conclusions

The hydrologic cycle of Northern Eurasia (and the Arctic in general) has undergone dramatic changes in the last few decades. Although the changes have not been uniform, some general trends have emerged. These include:

- increasing river discharge, especially in winter
- warming and degrading permafrost
- deepening permafrost active layer thickness
- retreating glaciers
- changes in lake distribution

At present, the reasons for these changes are only partially understood. In many cases, several climatological and anthropogenic factors could produce similar effects, and no single factor appears dominant throughout the region. For instance, several hypotheses have been proposed for the observed increases in river discharge: increases in annual precipitation, permafrost thaw, glacial retreat, and reservoir management.

Thus, the hydrologic effects of land-cover change are intertwined with the effects of climate change over last 50 years. Unfortunately, existing observations are too sparse or cover too short a time period to allow us to unravel these competing effects entirely. The harsh climate found in much of the region has inhibited intensive in situ measurements of hydrologic variables such as precipitation, discharge, and soil moisture. Not only are the measurements sparse, but their spatial distributions are skewed towards the warmer parts of the domain where population density is highest.

Satellite imagery can help overcome the sparseness of in situ observations, and the role of satellite data sets will continue to grow. Remote sensing has proven extremely useful in monitoring changes in lake extent, glacier retreat, and soil freeze/thaw conditions. However, while satellite-derived snow cover extent (SCE) products show some degree of reliability, at present high quality satellite-based methods of monitoring snow water equivalent (SWE) are still lacking. Since SWE is the most important term in the high-latitude hydrologic cycle, it is crucial that these methods improve.

Another shortcoming of remote sensing is that there are often trade-offs between spatial and temporal resolution. For example, synthetic aperture radar (SAR) sensors have sufficient spatial resolution to accurately capture the extent of "minority" land cover classes such as lakes and wetlands, but have low temporal frequency, making it difficult to capture the seasonal evolution of lake and wetland extent. Meanwhile, passive microwave sensors provide daily overpasses but at low spatial resolution. Blended, or multi-sensor products, may help solve this problem. The proposed SWOT mission, with its high spatial and temporal resolution, will also solve this problem in the context of monitoring surface water storage with altimetry.

While remote sensing can expand the scale of our monitoring efforts, it will always have limits in resolution and penetration. To draw conclusions about subsurface processes, inferences must be drawn from large-scale hydrologic models that incorporate the remotely-sensed data, i.e., via data assimilation. These models present another set of challenges, simulating some processes poorly or not at all (e.g., the lack of glacier dynamics in most large-scale hydrologic models). Improvements in these models, in turn, ultimately depend on better in situ and remotely-sensed observations.

Thus, to fully understand the hydrologic cycle of Northern Eurasia and to predict how it might respond to future changes in climate and land use, it will be necessary to combine in situ and remotely-sensed observations, modeling, and process studies into a more coherent system. Certainly each of these components can be improved individually. In situ networks can be extended, satellite sensors can begin emphasizing some of those hydrologic components that are under-sampled (e.g., permafrost), and model formulations of certain hydrologic processes can be improved. But the

usefulness of each of these components depends in part on the quality of the others. Therefore future observation missions should be designed from a systems perspective that specifically anticipates the merging of in situ and satellite data and their use in large-scale models, and prioritizes development of these components accordingly.

References

ACIA (2005) Arctic climate impact assessment scientific report. Cambridge University Press, New York, 1042 p

Adam JC, Haddeland I, Su F, Lettenmaier DP (2007) Simulation of reservoir influences on annual and seasonal streamflow changes for the Lena, Yenisei and Ob′ Rivers. J Geophys Res 112:D24114. doi:10.1029/2007JD008525

Adam JC, Lettenmaier DP (2008) Application of new precipitation and reconstructed streamflow products to streamflow trend attribution in Northern Eurasia. J Climate 21(8):1807–1828

Arendt AA, Echelmeyer KA, Harrison WD, Lingle CS, Valentine VB (2002) Rapid wastage of Alaska glaciers and their contribution to rising sea level. Science 297:382–386. doi:10.1126/science.1072497

Armstrong RL, Brodzik MJ (2001) Recent Northern Hemisphere snow extent: a comparison of data derived from visible and microwave satellite sensors. Geophys Res Lett 28:3673–3676

Armstrong RL, Brodzik MJ, Savoie M, Knowles K (2003) Enhanced hemispheric-scale snow mapping through the blending of optical and microwave satellite data. EGS-AGU-EUG Joint Assembly, Nice, 6–11 Apr 2003, abstract 12824

Baird AJ, Beckwith CW, Waldron S, Waddington JM (2004) Ebullition of methane-containing gas bubbles from near-surface Sphagnum peat. Geophys Res Lett 31(21):L21505. doi:10.1029/2004GL21157

Barry RG (2006) The status of research on glaciers and global glacier recession: a review. Prog Phys Geog 30(3):285–306. doi:10.1191/0309133306

Bartlett KB, Harriss RC (1993) Review and assessment of methane emissions from wetlands. Chemosphere 26:261–320

Bellamy PH, Loveland PJ, Bradley RI, Lark RM, Kirk GJD (2005) Carbon losses from all soils across England and Wales 1978–2003. Nature 437. doi:10.1038/nature04038

Berezovskaya S, Yang D, Kane DL (2004) Compatability analysis of precipitation and runoff trends over the large Siberian watersheds. Geophys Res Lett 31:L21502. doi:10.1029/2004GL021277

Billett MF, Palmer SM, Hope D, Deacon C, Storeton-West R, Hargreaves KJ, Flechard C, Fowler D (2004) Linking land-atmosphere carbon fluxes in a lowland peatland system. Global Biogeochem Cycles 18(1). doi:10.1029/2003GB002058

Birkett CM (1998) Contribution of the TOPEX NASA radar altimeter to the global monitoring of large rivers and wetlands. Water Resour Res 34:1223–1239

Bohn TJ, Lettenmaier DP, Sathulur K, Bowling LC, Podest E, McDonald KC, Friborg T (2007) Methane emissions from Western Siberian wetlands: heterogeneity and sensitivity to climate change. Environ Res Lett 2. doi:10.1088/1748-9326/2/4/045015

Bowling LC, Lettenmaier DP, Nijssen B, Polcher J, Koster RD, Lohmann D (2003) Simulation of high latitude hydrological processes in the Torne-Kalix basin: PILPS Phase 2(e) 3: equivalent model representation and sensitivity experiment. J Glob Planet Change 38(1–2):55–71

Braithwaite RJ (2005) Mass balance characteristics of arctic glaciers. Ann Geol 42:225–229

Broecker WS (1997) Thermohaline circulation, the Achilles Heel of our climate system: will man-made CO_2 upset the current balance? Science 278:1582–1588

Brown RD (1997) Historical variability in Northern Hemisphere spring snow covered area. Ann Glaciol 25:340–346

Brown RD (2000) Northern Hemisphere snow cover variability and change, 1915–97. J Climate 13:2339–2355

Brown J, Ferrians OJJ, Heginbottom JA, Melnikov ES (1997) International Permafrost Association Circum-Arctic Map of Permafrost and Ground Ice Conditions, Scale 1:10,000,000. U.S. Geological Survey

Brown J, Romanovsky VE (2008) Report from the International Permafrost Association: state of permafrost in the first decade of the 21st century. Permafrost Periglac Process 19(2):255–260

Bubier JL, Moore TR, Bellisario L, Comer NT, Crill PM (1995) Ecological controls on methane emissions from a northern peatland complex in the zone of discontinuous permafrost, Manitoba, Canada. Global Biogeochem Cycles 9(4):455–470

Christensen TR, Ekberg A, Ström L, Mastepanov M, Panikov NS, Öquist M, Svensson BH, Nykänen H, Martikainen PJ, Oskarsson H (2003) Factors controlling large-scale variations in methane emissions from wetlands. Geophys Res Lett 30(7). doi:10.1029/2002GL016848

Cole JJ, Caraco NF, Kling GW, Kratz TK (1994) Carbon-dioxide supersaturation in the surface waters of lakes. Science 265(5178):1568–1570

Crill PM (1991) Seasonal patterns of methane uptake and carbon dioxide release by a temperate woodland soil. Global Biogeochem Cycles 5:319–334

Derksen CA, Walker A, LeDrew E, Goodison B (2003) Combining SMMR and SMM/I data for time series analysis of central North American snow water equivalent. J Hydrometeorol 4: 304–316

Dery SJ, Brown RD (2007) Recent Northern Hemisphere snow cover extent trends and implications for the snow-albedo feedback. Geophys Res Lett 34:l22504. doi:10.1029/2007gl031474

Dery SJ, Wood EF (2006) Analysis of snow in the 20th and the 21st century Geophysical Fluid Dynamics Laboratory coupled climate model simulations. J Geophys Res 111:D19113. doi:10.1029/2005JD006920

Dise NB, Gorham E, Verry S (1993) Environmental factors controlling methane emissions from peatlands in Northern Minnesota. J Geophys Res 98(D6):10583–10594

Dowdeswell JA, Hagen JO, Björnsson H, Glazovsky AF, Harrison WD, Holmlund P, Jania J, Koerner RM, Lefauconnier B, Ommanney CSL, Thomas RH (1997) The mass balance of circum-Arctic glaciers and recent climate change. Quat Res 48:1–14

Dozier J, Painter TH (2004) Multispectral and hyperspectral remote sensing of alpine snow properties. Ann Rev Earth Planet Sci 32:465–494

Drozdov OA, AS Grigorieva (1963) Water cycle in the atmosphere. Leningrad, Gidrometeoizdat, 156 p (in Russian)

Dyurgerov MB, Carter CL (2004) Observational evidence of increases in freshwater inflow to the Arctic Ocean. Arct Antarct Alp Res 36(1):117–122

Dyurgerov MB, Meier MF (2000) Twentieth century climate change: evidence from small glaciers. Proc Natl Acad Sci USA 97(4):1406–1411

Fallot JM, Barry RG, Hoogstrate D (1997) Variations of mean cold season temperature precipitation and snow depths during the last 100 years in the former Soviet Union. Hydrol Sci J 42:301–327

Foster JL, Hall DK, Eylander JB, Riggs GA, Kim EJ, Tedesco M, Nghiem SV, Kelly REJ, Choudhury BJ (2008) A new blended global snow product using visible, passive microwave, and scatterometer satellite data. Proceedings of the 88th annual meeting of American meteorological society, 20–24 Jan 2008, New Orleans. http://ams.confex.com/ams/pdfpapers/130069.pdf

Foster JL, Sun C, Walker JP, Kelly R, Chang A, Dong J, Powell H (2005) Quantifying the uncertainty in passive microwave snow water equivalent observations. Rem Sens Environ 94:187–203. doi:10.1016/j.rse.2004.09.012

Frauenfeld OW, Zhang T, Barry RG, Gilichinsky D (2004) Interdecadal changes in seasonal freeze and thaw depths in Russia. J Geophys Res 109:D5101. doi:10.1029/2003JD 004245

Frauenfeld OW, Zhang TJ, McCreight JL (2007) Northern hemisphere freezing/thawing index variations over the twentieth century. Int J Climatol 27:47–63. doi:10.1002/joc.1372

Frey KE, Smith LC (2005) Amplified carbon release from vast West Siberian peatlands by 2100. Geophys Res Lett 32:L09401. doi:10.1029/2004GL022025

Friborg T, Soegaard H, Christensen TR, Lloyd CR, Panikov NS (2003) Siberian wetlands: where a sink is a source. Geophys Res Lett 30(21). doi:10.1029/2003GL017797

Frolking S, Crill P (1994) Climate controls on temporal variability of methane flux from a poor fen in southeastern New Hampshire: measurement and modeling. Glob Biogeochem Cycles 8(4):385–397

Gedney N, Cox PM, Huntingford C (2004) Climate feedback from wetland methane emissions. Geophys Res Lett 31:L20503. doi:10.1029/2004GL020919

Georgievsky VYu (2002) Changes of the Russian river runoff. Report of the State Hydrological Institute, St. Petersburg, 85 p (in Russian)

Goodison B, Louie P, Yang D (1998) WMO solid precipitation measurement intercomparison, final report. WMO/TD-872, Instruments and observing methods report 67

Gorham E (1991) Northern peatlands: role in the carbon cycle and probable responses to climate warming. Ecol Appl 1(2):182–195

Grippa M, Mognard NM, Le Toan T, Biancamaria S (2007) Observations of changes in surface water over the western Siberia lowland. Geophys Res Lett 34:L15403. doi:10.1029/2007GL030165

Grody NC, Basist AN (1996) Global identification of snow cover using SSM/I measurements. Trans Geosci Rem Sens, 34:237–249

Groisman PYa, Knight RW, Easterling DR, Karl TR, Hegerl GC, Razuvaev VN (2005) Trends in intense precipitation in the climate record. J Climate 18:1343–1367

Groisman PYa, Koknaeva VV, Belokrylova TA, Karl TR (1991) Overcoming biases of precipitation measurement: a history of the USSR experience. Bull Am Meteorol Soc 72:1725–1733

Groisman PYa, Sherstyukov BG, Razuvaev VN, Knight RW, Enloe JG, Stroumentova NS, Whitfield PH, Førland E, Hannsen-Bauer I, Tuomenvirta H, Aleksandersson H, Mscherskaya AV, Karl TR (2007) Potential forest fire danger over Northern Eurasia: changes during the 20th century. Glob Planet Change 56:371–386. doi: 10.1016/j.gloplacha.2006.07.029

Hall DK, Riggs GA (2007) Accuracy assessment of the MODIS snow products. Hydrol Process, 21:1534–1547

Hall DK, Riggs G, Salomonson V, DiGirolamo NE, Bayr KJ (2002) MODIS snow cover products. Rem Sens Environ 83:181–194

Hansen J, Sato Mki, Ruedy R, Lo K, Lea DW, Medina-Elizade M (2006) Global temperature change. Proc Natl Acad Sci USA 103:14288–14293. doi:10.1073/pnas.0606291103

Hoelzle M, Haeberli W, Dishl M, Peschke W (2003) Secular glacier mass balances derived from cumulative glacier length changes. Glob Planet Change 36:295–306

Holmes RM, McClelland JW, Raymond PA, Frazer BB, Peterson BJ, Stieglitz M (2008) Lability of DOC transported by Alaskan rivers to the arctic ocean. Geophys Res Lett 35(3). doi:10.1029/2007GL032837

ICOLD (2003) World register of dams, Paris, 340 p

IPCC (2007) Climate change 2007: the physical science basis. Contribution of working group I to the 4th assessment report of the intergovernmental panel on climate change. In: Solomon S, Qin D, Manning M, Chen Z, Marquis M, Averyt KB, Tignor M, Miller HL (eds). Cambridge University Press, Cambridge, 996 p

Kelly RE, Chang AT, Tsang L, Foster JL (2003) A prototype AMSR-E global snow area and snow depth algorithm. Trans Geosci Rem Sens 41:230–242

Kim Y, Hatsushika H, Muskett RR, Yamazaki K (2005) Possible effect of boreal wildfire soot on Arctic sea ice and Alaska glaciers. Atmos Environ 39:3513–3520

Kling GW, Kipphut GW, Miller MC (1991) Arctic lakes and streams as gas conduits to the atmosphere: implications for tundra carbon budgets. Science 251:298–301

Kongoli C, Grody NC, Ferraro RR (2004) Interpretation of AMSU microwave measurements for the retrievals of snow water equivalent and snow depth. J Geophys Res 109:D24111. doi:10.1029/2004JD004836

Kremenetski KV, Velichko AA, Borisova OK, MacDonald GM, Smith LC, Frey KE, Orlova LA (2003) Peatlands of the Western Siberian lowlands: current knowledge on zonation, carbon content and late quaternary history. Quat Sci Rev 22:703–723

Lachenbruch AH, Marshall BV (1986) Changing climate: geothermal evidence from permafrost in the Alaskan Arctic. Science 234, 689–696

Lammers RB, Shiklomanov AI, Vörösmarty CJ, Fekete BM, Peterson BJ (2001), Assessment of contemporary Arctic river runoff based on observational discharge Records. J Geophys Res-Atmos 106(D4):3321–3334

Lehner B, Döll P (2004) Development and validation of a global database of lakes, reservoirs, and wetlands. J Hydrometeorol 296:1–22

Lloyd J, Taylor JA (1994) On the temperature dependence of soil respiration. Funct Ecol 8:315–323

Lugina KM, Groisman PYa, Vinnikov KYa, Koknaeva VV, Speranskaya NA (2006) Monthly surface air temperature time series area-averaged over the 30-degree latitudinal belts of the globe, 1881–2005. In trends: a compendium of data on global change. Carbon Dioxide Information Analysis Center, Oak Ridge National Laboratory, US Department of Energy, Oak Ridge. doi:10.3334/CDIAC/cli.003

Manabe S, Stouffer RJ (1994) Multiple-century response of a coupled ocean-atmosphere model to an increase of atmospheric carbon dioxide. J Climate 7: 5–23

Matthews E, Fung I (1987) Methane emission from natural wetlands: global distribution, area, and environmental characteristics of sources. Glob Biogeochem Cycles 1(1):61–86

Maurer E, Rhoads JD, Dubayah RO, Lettenmaier DP (2002) Evaluation of the snow-covered area data product from MODIS. Hydrol Process 17(1):59–71

McClelland JW, Holmes RM, Peterson BJ, Stieglitz M (2004) Increasing river discharge in the Eurasian Arctic: consideration of dams, permafrost thaw, and fires as potential agents of change. J Geophys Res 109:D18102. doi:10.1029/2004JD004583

McDonald KC, Kimball JS, Njoku E, Zimmermann R, Zhao M (2004) Variability in springtime thaw in the terrestrial high latitudes: monitoring a major control on the biospheric assimilation of atmospheric CO_2 with spaceborne microwave remote sensing. Earth Interact 8(20):1–23

Meier MF, Dyurgerov MB, Rick UK, O'Neel S, Pfeffer WT, Anderson RS, Anderson SP, Glazovsky AF (2007) Glaciers dominate eustatic sea-level rise in the 21st century. Science 317:1064-1067. doi: 10.1126/science.1142906

Moore TR, Roulet NT (1993) Methane flux: water table relations in northern wetlands. Geophys Res Lett 20(7):587–590

Myneni RB, Keeling CD, Tucker CJ, Asrar G, Nemani RR (1997) Increased plant growth in the northern high latitudes from 1981–1991. Nature 386:698–702

Nilsson S, Vaganov E, Shvidenko A, Stolbovoi V, Rozhkov V, McCallum I., Jonas M (2003) Carbon budget of vegetation ecosystems of Russia. Doklady Earth Sci 393A(9):1281–1283

Oberman NG, Mazhitova GG (2001) Permafrost dynamics in the northeast of European Russia at the end of the 20th century. Norwegian J Geogr 55:241–244

Osterkamp TE (2005) The recent warming of permafrost in Alaska. Glob Planet Change 49:187–202. doi:10.1016/j.glopjacha.2005.09.001

Pacala SW, Hurtt GC, Baker D, Peylin P, Houghton RA, Birdsey RA, Heath L, Sundquist ET, Stallard RF, Ciais P, Moorcroft P, Caspersen JP, Shevliakova E, Moore B, Kohlmaier G, Holland E, Gloor M, Harmon ME, Fan SM, Sarmiento JL, Goodale CL, Schimel D, Field CB (2001) Consistent land- and atmosphere-based US carbon sink estimates. Science 292:2316–2320. doi:10.1126/science.1057320

Panikov NS, Dedysh SN, Kolesnikov OM, Mardini AI, Sizova MV (2001) Metabolic and environmental control on methane emission from soils: mechanistic studies of mesotrophic fen in West Siberia. Water Air Soil Pollut: Focus 1(2–6):415–428

Parkinson CL (2006) Earth's cryosphere: current state and recent changes. Ann Rev Environ Res 31:33–60. doi:10.1146/annrev.energy.31.041105.095552

Peterson BJ, Holmes RM, McClelland JW, Vörösmarty CJ, Lammers RB, Shiklomanov IA, Rahmstorf S (2002) Increasing river discharge to the Arctic Ocean. Science 298:2171–2173

Prigent C, Papa F, Aires F, Russow WB, Matthews E (2007) Global inundation dynamics inferred from multiple satellite observations. J Geophys Res 112:D12107. doi:10.1029/2006JD007847

Pulliainen JT, Grandell J, Hallikainen M (1999) HUT snow emission model and its applicability for snow water equivalent retrieval. Trans Geosci Rem Sens 37:1378–1390

Rahmstorf S, Alley RB (2002) Stochastic resonance in glacial climate, Eos, Trans Am Geophys Union 83(12):129–135

Raisanen J (2008) Warmer climate: less or more snow? Climate Dynamics 30:307–319

Rawlins MA, Willmott CJ, Shiklomanov A, Frolking S, Vörösmarty CJ (2006) Evaluation of trends in derived snowfall and rainfall across Eurasia and linkages with discharge to the Arctic Ocean. Geophys Res Lett 33:L07403. doi: 10.1029/2005GL025231

Raymond PA, McClelland JW, Holmes RM, Zhulidov AV, Mull K, Peterson BJ, Striegl RG, Aiken GR, Gurtovaya TY (2007) Flux and age of dissolved organic carbon exported to the Arctic Ocean: a carbon isotopic study of the five largest arctic rivers. Glob Biogeochem Cycles 21(4). doi:10.1029/2007GB002934

Rennermalm AK, Wood EF, Weaver AJ, Eby M, Dery SJ (2007) Relative sensitivity of the Atlantic meridional overturning circulation to river discharge into Hudson Bay and the Arctic Ocean. J Geophys Res 112:G04S48. doi:10.1029/2006JG000330

Richter-Menge J, Overland J, Proshutinsky A, Romanovsky V, Gascard JC, Karcher M, Maslanik J, Perovich D, Shiklomanov A, Walker D (2006). Arctic, Chapter 5b. In: Shein KA (ed) State of the climate in 2005, Bull Am Meteorol Soc 87(6)

Robinson DA, Dewey KF, Heim RR (1993) Global snow cover monitoring: an update. Bull Am Meteorol Soc 74:1689–1696

Romanov P, Gutman G, Csiszar I (2000) Automated monitoring of snow cover over North America with multispectral satellite data. J Appl Meteorol 39:1866–1880

Rosenfeld S, Grody N (2000) Anomalous microwave spectra of snow covered observed from special sensor microwave/imager measurements. J Geophys Res 105(D11):14913–14925

Saarnio S, Alm J, Silvola J, Lohila A, Nykänen H, Martikainen PJ (1997) Seasonal variation in CH4 emissions and production and oxidation potentials at microsites of an oligotrophic pine fen.Oecologia 110:414–422

Serreze MC, Walsh JE, Chapin FS, Osterkamp T, Dyurgerov M, Romanovsky V, Oechel WC, Morison J, Zhang T, Barry RG (2000) Observational evidence of recent change in the northern high-latitude environment. Clim Change 46:159–207

Shannon RD, White JR (1994) A three-year study of controls on methane emissions from two Michigan peatlands. J Ecol 84(2):239–246

Sheng Y, Smith LC, MacDonald GM, Kremenetski KV, Frey KE, Velichko AA, Lee M, Beilman DW, Dubinin P (2004) A high-resolution GIS-based inventory of the west Siberian peat carbon pool. Glob Biogeochem Cycles 18:GB3004. doi:10.1029/2003GB002190

Shiklomanov AI, Lammers RB, Rawlins MA, Smith LC, Pavelsky TM (2007) Temporal and spatial variations in maximum river discharge from a new Russian data set. J Geophys Res 112:G04S53. doi:10.1029/2006JG000352

Shiklomanov AI, Lammers RB, Vörösmarty CJ (2002) Widespread decline in hydrological monitoring threatens pan-Arctic research, EOS, Trans Am Geophys Union, 83:16–17

Shiklomanov IA, Shiklomanov AI, Lammers RB, Peterson BJ, Vörösmarty CJ (2000) The dynamics of river water inflow to the Arctic Ocean. In: Lewis EL (ed.) The freshwater budget of the arctic ocean. Kluwer Academic Press, Dordrecht, pp 281–296

Shiklomanov AI, Yakovleva TI, Lammers RB, Karasev IPh, Vörösmarty CJ, Linder E (2006) Cold region river discharge uncertainty – estimates from large Russian rivers. J Hydrol 326: 231–256

Shindell DT, Walter BP, Faluvegi G (2004) Impacts of climate change on methane emissions from wetlands. Geophys Res Lett 331:L21202. doi:10.1029/2004GL021009

Sicart JE, Arnaud Y (2007) Preliminary spectral characterization of snow in a high altitude tropical glacier and potential effects of impurities in snow on albedo of tropical glaciers. Hydrol Process 21:3642–3644. doi: 10.1002/hyp.6741

Simic A, Fernandes R, Brown R, Romanov P, Park W (2004) Validation of VEGETATION, MODIS, and GOES + SSM/I snow-cover products over Canada based on surface snow depth observations. Hydrol Process 18|:1089–1104

Singh P, Gan TY (2000) Retrieval of snow water equivalent using passive microwave brightness temperature data. Rem Sens Environ 74:275–286

Smith SL, Burgess MM, Riseborough D, Nixon FM (2005) Recent trends from Canadian permafrost monitoring network sites. Permafr Perigl Process 16:19–30

Smith LC, Pavelsky TM, MacDonald GM, Shiklomanov AI, Lammers RB (2007) Rising minimum daily flows in Northern Eurasian rivers: a growing influence of groundwater in the high-latitude hydrologic cycle. J Geophys Res 112:G04S47. doi:10.1029/2006JG000327

Smith LC, Sheng Y, MacDonald GM, Hinzman LD (2005) Disappearing Arctic lakes. Science 308:1429

Steele M, Boyd T (1998) Retreat of the cold halocline layer in the Arctic Ocean. J Geophys Res 103(C5):10419–10435

Strack M, Waddington JM (2007) Response of peatland carbon dioxide and methane fluxes to a water table drawdown experiment. Glob Biogeochem Cycles 21:GB1007. doi:10.1029/2006GB002715

Stohl A, Berg T, Burkhart JF, Fjæraa AM, Forster C, Herber A, Hov Ø, Lunder C, McMillan WW, Oltmans S, Shiobara M, Simpson D, Solberg S, Stebel K, Ström J, Tørseth K, Treffeisen R, Virkkunen K, Yttri KE (2007) Arctic smoke – record high air pollution levels in the European Arctic due to agricultural fires in Eastern Europe in spring 2006. Atmos Chem Phys 7:511–534

Surazakov AB, Aizen VB, Aizen EM, Nikitin SA (2007) Glacier changes in the Siberian Altai Mountains, Ob river basin, (1952–2006) estimated with high resolution imagery. Environ Res Lett 2. doi: 10.1088/1748-9326/2/4/045017

Syed TH, Famiglietti JS, Zlotnicki V, Rodell M (2007) Contemporary estimates of Pan-Arctic freshwater discharge from GRACE and reanalysis. Geophys Res Lett 34. L19404. doi:10.1029/2007GL031254

Tait AB (1998). Estimation of snow water equivalent using passive microwave radiation data. Rem Sens Environ 64:286–291

Tapley BD, Bettadpur S, Ries JC, Thompson PF, Watkins MM (2004) GRACE measurements of mass variability in the Earth system. Science 305:503–505. doi:10.1126/science.1099192

Toptygin AY, Gribanov KG, Imasu R, Bleuten W, Zakharov VI (2005) Seasonal methane content in atmosphere of the permafrost boundary zone in Western Siberia determined from IMG/ADEOS and AIRS/AQUA data. Proc SPIE 5655:508–514. doi:10.1117/12.579494

Trenberth KE (1999) Short-term climate variations. Recent accomplishments and issues for future progress. Storms vol 1. Pielke RSr, Pielke RJr (Eds). Routledge Press, London, pp 126–141

UNEP/GRID-Arendal (2007) Permafrost extent in the Northern Hemisphere, UNEP/GRID-Arendal maps and graphics library, Accessed 27 July 2010. http://maps.grida.no/go/graphic/permafrost-extent-in-the-northern-hemisphere

Van Blarcum SC, Miller JC, Russel GL (1995) High latitude runoff in a doubled CO_2 climate. Clim Change 30:7–26

Vörösmarty CJ, Fekete B, Tucker BA (1996) River Discharge Database, Version 1.0 (RivDis v1.0), Volumes 0 through 6. A contribution to IHP-V Theme 1. Technical Documents in Hydrology Series. UNESCO, Paris

Vörösmarty CJ, Fekete B, Tucker BA (1998) River Discharge Database, Version 1.1 (RivDis v1.0 supplement). Available through the Institute for the Study of Earth, Oceans, and Space / University of New Hampshire, Durham, NH (USA)

Vörösmarty CJ, Hinzman LD, Peterson BJ, Bromwich DH, Hamilton LC, Morison J, Romanovsky VE, Sturm M, Webb RS (2001) The hydrologic cycle and its role in arctic and global environmental change: a rationale and strategy for synthesis study. Arctic Research Consortium of the US (ARCUS), Fairbanks, 84 p

Vitt DH, Halsey LA, Bauer IE, Campbell C (2000) Spatial and temporal trends in carbon storage of peatlands of continental western Canada through the Holocene. Can J Earth Sci 37: 683–693

Walsh J, Curry J, Fahnestock M, Kennicutt M, McGuire D, Rossow W, Steele M, Vorosmarty C, Wharton R (2001) Enhancing NASA's contribution to polar science: A review of polar geophysical data sets. Commision on geosciences, environment and resources, National Research Council, National Academy Press, Washington DC, 124 p

Walter KM, Edwards ME, Grosse G, Zimov SA, Chapin FS III (2007) Thermokarst lakes as a source of atmospheric CH4 during the last deglaciation. Science 318:633–636. doi:10.1126/science.114.2924

Walter KM, Zimov SA, Chanton JP, Verblya D, Chapin FS III (2006) Methane bubbling from Siberian thaw lakes as a positive feedback to climate warming. Nature 443:71–75

West JJ, Plug LJ (2007) Time-dependent morphology of thaw lakes and taliks in deep and shallow ground ice. J Geophys Res 113(F1). doi:10.1029/2006JF000696

Willmott CJ, Robeson SM, Feddema JJ (1994) Estimating continental and terrestrial precipitation averages from raingauge networks. Int J Climatol 14:403–414

Worrall F, Burt TP (2007) Trends in DOC concentration in Great Britain. J Hydrol 346:81–92

Xiao X, Zhang Q, Boles S, Rawlings M, Moore III B (2004) Mapping snow cover in the Pan-Arctic zone, using multi-year (1998–2001) Images from optical VEGETATION and SPOT sensor. Int J Rem Sens 25:5731–5744

Yang DQ, Ye BS, Kane DL (2004) Streamflow changes over Siberian Yenisei river basin. J Hydrol 296:59–80

Ye H, Ellison M (2003) Changes in transitional snowfall season length in Northern Eurasia. Geophys Res Lett 30. doi:10.1029/2003GL016873

Ye BS, Yang DQ, Kane DL (2003) Changes in Lena river streamflow hydrology: human impacts versus natural variations. Water Resourc Res 39:1200–1213

Zhang T (2005) Influence of the seasonal snow cover on the ground thermal regime: An overview. Rev Geophys 43:RG4002. doi:10.1029/2004RG000157

Zhang T, Barry RG, Knowles K, Heginbottom JA, Brown J (1999) Statistics and characteristics of permafrost and ground ice distribution in the Northern Hemisphere. Polar Geogr 23(2): 147–169

Zhou L, Kaufmann RK, Tian Y, Myneni RB, Tucker CJ (2003) Relation between interannual variations in satellite measures of northern forest greenness and climate between 1982 and 1999. J Geophys Res 108(D1):4004. doi:10.1029/2002JD002510

Zhou L, Tucker CJ, Kaufmann RK, Slayback D, Shabanov NV, Myneni RB (2001) Variations in northern vegetation activity inferred from satellite data of vegetation index during 1981 to 1999. J Geophys Res 106(D17):20069–20083

Zhuang Q, Melillo JM, Sarofim MC, Kicklighter DW, McGuire AD, Felzer BS, Sokolov A, Prinn RG, Steudler PA, Hu S (2006) CO_2 and CH4 exchanges between land ecosystems and the atmosphere in northern high latitudes over the 21st century. Geophys Res Lett 33:L17403. doi:10.1029/2006GL026972

Zimov SA, Schuur EAG, Chapin FS (2006) Permafrost and the global carbon budget. Science 312:1612–1613

Zimov SA, Voropaev YV, Semiletov IP, Davidov SP, Prosiannikov SF, Chapin FS, Chapin MC, Trumbore S, Tyler S (1997) North Siberian lakes: a methane source fueled by Pleistocene carbon. Science 277:800–802

Chapter 8
Impacts of Arctic Climate and Land Use Changes on Reindeer Pastoralism: Indigenous Knowledge and Remote Sensing

Nancy G. Maynard, Anders Oskal, Johan M. Turi, Svein D. Mathiesen, Inger Marie G. Eira, Boris Yurchak, Vladimir Etylin, and Jennifer Gebelein

Abstract Eurasian indigenous reindeer herders have developed an important initiative to study the impacts of climate change and to develop local adaptation strategies based upon their traditional knowledge of the land and its uses – in an international, interdisciplinary partnership with the science community – involving extensive collaborations and co-production of knowledge to minimize the impacts of the various changes. This unprecedented reindeer herder-led initiative is the IPY EALAT Project, "EALAT, Reindeer Pastoralism in a Changing Climate". This chapter provides an overview of the EALAT initiative, with an emphasis on how remote sensing, Geographic Information Systems (GIS), and other scientific data are being combined with indigenous knowledge to "co-produce" datasets to improve decision-making and herd management; some early results; and a description of the EALAT/Monitoring data integration and sharing system and portal being developed for reindeer pastoralism to integrate traditional indigenous knowledge together with remote sensing and other scientific data to enhance early warning and management for change responses and adaptation.

8.1 Introduction

8.1.1 Reindeer Pastoralism and Arctic Changes

The Arctic is home to many indigenous peoples, including those who depend on reindeer herding for their livelihood, in one of the harshest environments in the world. For the largely nomadic peoples, reindeer not only form a substantial part of the arctic food base and economy, but they are also culturally important, shaping their way of life, mythologies, festivals and ceremonies. Reindeer pastoralism

N.G. Maynard (✉)
Cryospheric Sciences Branch, NASA Goddard Space Flight Center, Greenbelt, MD 20771, USA
e-mail: nancy.g.maynard@nasa.gov

G. Gutman, A. Reissell (eds.), *Eurasian Arctic Land Cover and Land Use in a Changing Climate*, DOI 10.1007/978-90-481-9118-5_8,

or husbandry has been practiced by numerous peoples all across Eurasia for thousands of years and involves moving herds of reindeer, which are very docile animals, from pasture to pasture depending on the season. This means herders lead either a nomadic life living in a tent on the arctic tundra year-round as a family unit, or a semi-nomadic life, having permanent residences for parts of the year and having fewer family members herding on a daily basis. Thus, herders must adapt on a daily basis to find optimal conditions for their herds according to the constantly changing conditions.

Having learned over generations to live with uncertainties in an arctic environment, indigenous societies that practice traditional reindeer husbandry are good examples of sustainable human communities that are highly interconnected with the ecosystems in which they live, also reflecting the American Indian concept of the "power of place" described by Deloria and Wildcat (2001). Climate change and variability plus rapid development are increasingly creating major changes in the physical environment, ecology, and cultures of these indigenous reindeer herder communities in the north, and climate changes are occurring significantly faster in the Arctic than the rest of the globe, with correspondingly dramatic impacts (Oskal 2008).

In response to these changes, Eurasian reindeer herders have created the EALÁT project, a comprehensive new initiative to study these impacts and to develop local adaptation strategies based upon their traditional knowledge of the land and its uses – in targeted partnership with the science and remote sensing community – involving extensive collaborations and co-production of knowledge to minimize the impacts of the various changes. This unprecedented new reindeer herder-led initiative has resulted in the development of an international, interdisciplinary collaboration with scientists through the International Polar Year (IPY) EALÁT Consortium (IPY Project # 399 "EALÁT, Reindeer Pastoralism in a Changing Climate") that directly addresses the herders' need for additional data and information for responding to the global and environmental changes through a variety of different projects.

The EALÁT initiative is considered unique because the study was conceived and implemented by indigenous reindeer herders who continue to lead a large multidisciplinary group of invited scientists and other collaborators in this complex study of the multiple challenges facing arctic reindeer herding communities. In addition, the EALÁT study sites are located in areas where reindeer pastoralism has been practiced over thousands of years, and, thus, this wealth of traditional knowledge provides a special perspective similar to that articulated by Deloria for American Indians, who stated that "Traditional knowledge enables us to see our place and our responsibility within the movement of history as it is experienced by the community" (Deloria 2001).

This Chapter provides background on climate and development challenges to reindeer husbandry across the Arctic and an overview of the EALÁT initiative, with an emphasis on indigenous knowledge, remote sensing, Geographic Information Systems (GIS), and other scientific data to "co-produce" data sets for use by herders for improved decision-making and herd management. It also provides a description

of the EALÁT monitoring data integration and sharing system and portal being developed for reindeer pastoralism. In addition, this Chapter provides some preliminary results from the EALÁT project, including some early remote sensing research results.

8.1.2 Reindeer Pastoralism Across the Arctic – Background and Challenges

Reindeer husbandry has a long history in the Arctic. There are more than 20 different indigenous peoples in the Arctic who are reindeer herders. Reindeer husbandry is practiced in Norway, Sweden, Finland, Russia, Mongolia, China, Alaska, Canada and Greenland. This livelihood involves some 100,000 herders and approximately 2.5 million semi-domesticated reindeer, which graze approximately 4 million km^2 in Eurasia (Fig. 8.1). While reindeer husbandry is spread across the Arctic and across many cultures, its organization is remarkably similar everywhere, consisting of a nomadic livelihood with family-based working communities and a typical indigenous way of life. For hundreds of years, reindeer herders have managed vast barren circumpolar areas of land that hold little value for others. Herding represents a model for sustainable management of these areas that has developed through generations. In recent years, however, as noted earlier, arctic reindeer herders increasingly face major challenges, such as climate change, loss of grazing land due to development by humans, and effects of global change in their local societies (Oskal 2008).

Reindeer/caribou are the very base of the traditional economy for many indigenous northern peoples across the Arctic. *Rangifer tarandus*, called reindeer or caribou, is the most common large land mammal of the Arctic and sub-Arctic, gathering in large herds of tens to hundreds of thousands of animals on their calving grounds during the arctic summer, and scattering widely in smaller groups for the remainder of the year (Hall 1989). In Russia, the total number of domesticated reindeer in the region has decreased significantly within the last 100 years with particularly marked change from approximately 2.5 million in 1969 to 1.2 million in 2000 (Jernsletten and Klokov 2002). This decline in numbers of reindeer in northern Russia, which has by far the largest share of pasture lands (87%) and about 67% of all reindeer, is causing a serious decline in the reindeer husbandry industry, and, in turn is directly affecting the health and well-being of the indigenous peoples associated with reindeer husbandry (Jernsletten and Klokov 2002; Nuttal et al. 2005). This decline is not only causing poverty in the Russian indigenous communities associated with reindeer herding, but also, because reindeer husbandry is the very core of their traditional way of life, the decline is causing serious damage to the ethnic traditions and to the families of nomadic reindeer herders (Abrjutina 2003; Jernsletten and Klokov 2002; Glazovsky et al. 2004; Nuttal et al. 2005; Klokov 2000).

In Norway, reindeer husbandry is one industry in which the number of people involved has increased over the past 50 years (Eira 2001). However, while approximately 40% of mainland Norway is designated reindeer pastureland, there

Fig. 8.1 Reindeer peoples of Eurasia. Location of Eurasian indigenous peoples who are reindeer herders, involving approximately 100,000 herders and 2.5 million semi-domesticated reindeer, which graze about 4 million km^2 in Eurasia. Adapted from and reproduced by permission of the International Centre for Reindeer Husbandry

are serious threats to those lands from not only climate changes, but also loss of pastures by increasing encroachment from development, tourism, damming of rivers, cultivation, oil and gas development, and roads and power lines, accompanied by similar impacts as are observed in Russia (Eira 2001). In Finnmark, which is the northernmost, largest and least populated county in Norway (Fig. 8.2), there are approximately 2,000 registered reindeer owners which represent 73 and 75% of semi-domesticated reindeer and Sami reindeer owners in Norway, respectively (Tyler et al. 2007).

In recent years, a number of studies have been published on historical and future challenges which relate directly to reindeer herding in Eurasia including, as a few examples, Eira et al. (2008), Nuttal et al. (2008, 2005), and Klein et al. (2005), a diverse collection of multidisciplinary articles summarizing results from the RENMAN Project ("The challenges of modernity for REiNdeer MANagement: integration and sustainable development in Europe's subarctic and boreal regions" by Forbes et al. 2006), the ENSINOR Project (Stammler and Burgess 2007;

Fig. 8.2 Saami reindeer herd near Kautokeino, Norway (photo by I.M.G. Eira)

Chapter 9, this volume, Jia et al. 2003; Tommervik et al. 2004; Hinzman et al. 2005; Kitti et al. 2006; Kumpula et al. 2006; Tape et al. 2006).

8.1.3 Reindeer, Climate Change and Development

As mentioned in Chapter 1, this volume, in the Arctic climate change is happening faster than in any other region of the world. The changes in snow and ice cover and increases in temperature have already impacted reindeer husbandry and will continue to do so both directly, for example through changes in food availability, and indirectly such as through changes in human land use (Oskal 2008). Temperature changes have begun to cause some rivers to freeze later in the autumn and melt earlier in the spring, resulting in challenges for the annual migration of reindeer between different seasonal pastures. Warming-induced changes in freeze-thaw cycles are also creating problems. For example, as river and lake ice thaws earlier in the spring along migration routes, newborn calves can no longer cross the ice surface, but have to attempt crossing open waters, and large numbers of calves have been swept away by currents (Klein et al. 2005, Nuttal et al. 2005). Another change that has already been observed is increasing climate variability at a local level (Fig. 8.3). This is especially true during the critical wintertime, where, increasingly, periods of mild weather accompanied by rain will be followed by colder periods, form ice layers in the snow and block the reindeers' access to food on the ground. As reindeer live only on natural pastures, this often represents a "worst-case scenario" from the reindeer herders' perspective. Increasing precipitation in the

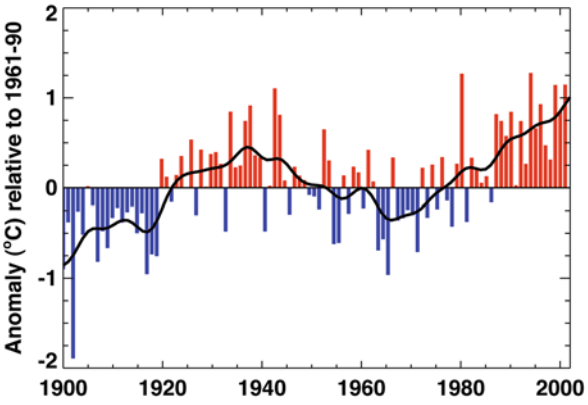

Fig. 8.3 Climate variability in the Arctic. Annual anomalies of land-surface air temperature variations in the Arctic (60–90° N) for the period 1900–2003. Data sets document a statistically significant warming trend during this period and, while general features of the arctic time series are similar to those of the global time series, decadal trends and interannual variability are greater in the Arctic. Reproduced by permission of Arctic Climate Impact Assessment Team (ACIA 2004)

form of snow can add to these challenges, while warming would shorten the period of snow cover in any particular year (Oskal 2008).

A deeper snow pack in winter can also make the reindeer more vulnerable to predator attacks (e.g., wolves) because the lighter wolves can travel on thinner snow crusts where reindeer sink through (Brotton and Wall 1997). Increased insect harassment, accompanying warmer temperatures, is a second major factor shown to interfere with foraging (Kitti et al. 2006). The outcome of this harassment is increased energy requirements, and results in a significant decline in body fat and lactation, and decrease in calving success (Walsh et al. 1992, Brotton and Wall 1997, Gunn and Skogland 1997). One example of recent climate impact is the unusually warm winter of 1996–1997, which was associated with a deep snow pack and icing, and which caused about 10,000 reindeer to die of starvation on Russia's far northeast Chukotsk Peninsula (Malcolm 1996, Nuttal et al. 2005).

Reindeer herders have also observed major changes in biodiversity. A significant example of this is repeated occurrences of certain species replacing others, such as the spreading of shrubs into the barren tundra-areas (Jia et al. 2003, Hinzman et al. 2005, Tape et al. 2006). Shrubs contribute to a hard packing of snow during the tough winter months, thus making access to food a challenge for reindeer. In addition, important food resources for the reindeer, such as lichens and reindeer preferred species of grasses, in time may disappear partially if not fully due to this shrub encroachment. Changes and/or increases in insect populations could also change reindeer behaviour during the summer by not allowing them to feed long enough in summer pastures due to increased harassment (Oskal 2008; Kitti et al. 2006).

Indirect effects of climate change are also being observed, with major implications for reindeer pasture availability and migration routes (Kitti et al. 2006). Due to the sea ice melting and longer summers, increased accessibility of the Arctic regions for human activities is a growing threat to reindeer herders. Human development and activities represent disturbances with negative effects for the semi-domesticated reindeer herds (Kitti et al. 2006) and irreversible loss of marginal pasture resources – a serious challenge for reindeer husbandry. In particular, female reindeer and calves will stay away from humans, physical installations and general human activity. In the last 50 years, for example, approximately 25% of the reindeer pastures of the Euro-Arctic Barents region have in effect been lost due to human development (Tyler et al. 2007).

Of particular relevance today is the fact that the Arctic is estimated to contain approximately 25% of the world's remaining undeveloped petroleum resources. For instance, Yamal in western Siberia holds about 90% of Russia's gas reserves, while also being the largest reindeer herding area of the world. Activities to access these resources would reduce the grazing lands, and are viewed as another human activity in the Arctic contributing to the reduction of the "available room for adaptation" for reindeer husbandry (Nuttal et al. 2005). In fact, industrial development (e.g., pipelines, oil and gas infrastructure) has increased across reindeer migration routes in northern Russia, blocking pathways to summer pasturelands (Forbes et al. 2006; see also Chapter 9, this volume).

It is also expected that there will be a sharp increase in the near future in oil and gas development, mining, and other forms of development in northern Russia – accompanied by infrastructure, pollution, and other manifestations of human presence – which will increase future pressure on available pasturelands for the reindeer and the indigenous communities associated with them (Forbes et al. 2006; Jernsletten and Klokov 2002, see Chapter 11, this volume). Furthermore, future reductions in sea ice from global warming recently projected are very likely to increase the amount of marine traffic and general access to the Arctic and, as a result, significantly increase development as well as serious problems related to sovereignty, social, cultural and other environmental issues, which will directly impact the indigenous reindeer herding community (McCarthy et al. 2005).

8.1.4 Socioeconomic, Political and Other Pressures

Parts of the Arctic are unique in terms of the political settlements and land claims that have been achieved over the last 30 years or so. The extent of vulnerability and resilience to climate change not only depends on cultural aspects and ecosystem diversity, but on the political, legal, and institutional rules which govern social-economic systems and social-ecological systems (Nuttal et al. 2005, 2008). On the one hand, climate change has the potential to enhance economic development, but with further climate change (Fig. 8.4), the climate in the Arctic is predicted to become more variable and extreme weather events more frequent and severe,

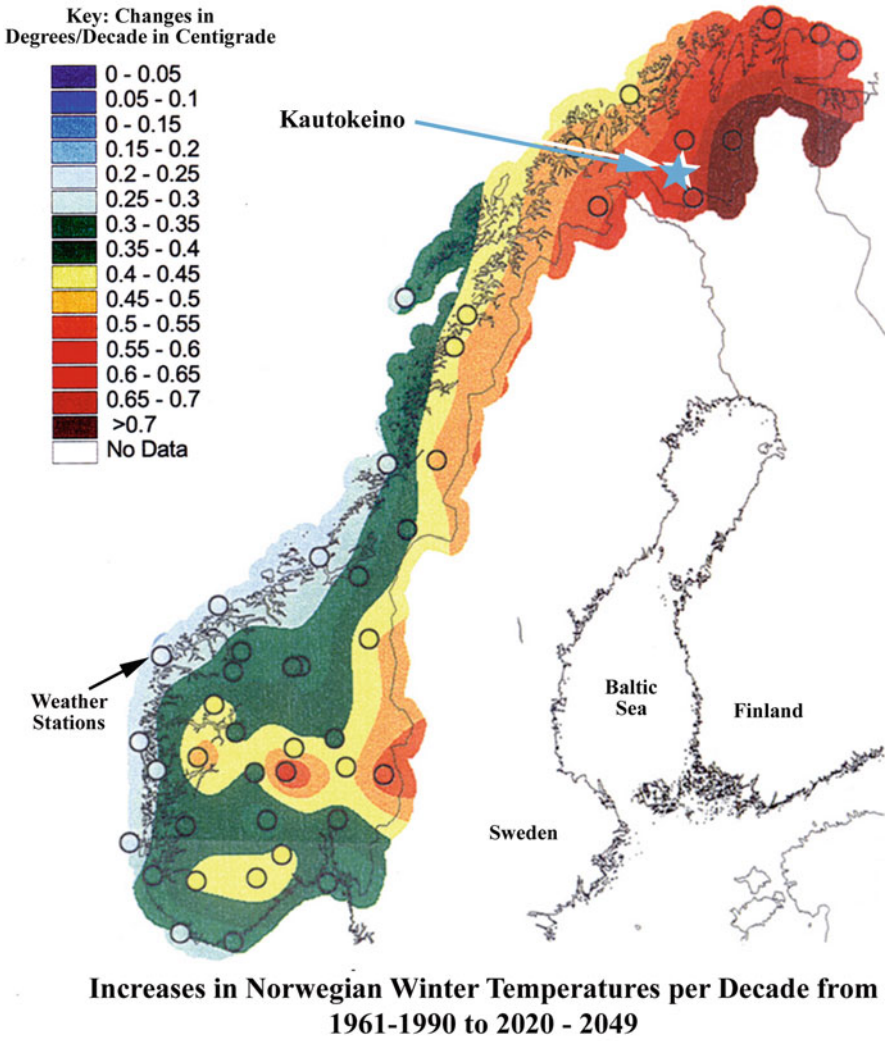

Fig. 8.4 Future warming in Norway showing increased future temperatures in the north and east in regions important for reindeer grazing in winter. Reproduced by permission of Arctic Climate Impact Assessment Team Hanssen-Bauer et al. 2003

which, on the other hand, can undermine economic activities. Thus, it seems particularly important that attention be given to the management of resources and to the effectiveness of governance institutions, and critical questions must be asked as to whether they can create additional opportunities to increase resilience, flexibility and the ability to deal with change (Nuttal et al. 2005).

Compounding the problem for the reindeer herding community in Russia, the transition of Russia to a market economy has, over the past few years, resulted in

considerable disorder in many parts of the supply and transport systems in remote northern areas. This has resulted in serious disruption of any system of goods, services, and health care to northern Russian indigenous peoples (Nuttal et al. 2005; Abrjutina 2003; Jernsletten and Klokov 2002; Klokov 2000). Basic commodities such as paraffin lighting, fabrics, and vegetables or other foods are no longer easily available. The reindeer herders have also been cut off from any health care services at all, and, as a result of these factors combined, health and living conditions are rapidly deteriorating in the reindeer herder communities, with growing death rates and serious health impacts (Nuttal et al. 2005; Abrjutina 2003; Jernsletten and Klokov 2002; Klokov 2000).

For all of these reasons, the Arctic Council has called for the full attention of the international community to the situation in the reindeer herding industry and the critical state of the indigenous peoples of the north in Russia. The 2nd World Reindeer Herders' Congress (2003) reported that there is a "real threat of the complete loss of reindeer husbandry in large parts of eastern Russia" and "indigenous peoples connected with reindeer husbandry here face an ethnic disaster". These concerns were echoed once again at the 3rd World Reindeer Herders' Congress in March 2005. Since that time, the reindeer herding communities have increasingly continued to develop new partnerships and organizations to improve their collective abilities to respond to the challenges of climate change and development. Indeed, as a result, the interdisciplinary multiparty EALÁT Project was successfully launched by the Association of World Reindeer Herders in partnership with the Russian Union of Reindeer Herders, the Sami Reindeer Herders Association of Norway, and the Sami Council. The project was established to address these numerous threats to reindeer herding through collaborative efforts to help prepare reindeer herders in Eurasia, their societies, institutions, and management for change, and accordingly, begin to reduce their vulnerability to these changes.

8.2 IPY EALÁT Project: "Reindeer Pastoralism in a Changing Climate"

8.2.1 EALÁT Overview

Developed under the leadership of indigenous reindeer herders, the IPY EALÁT Project ("Reindeer Pastoralism in a Changing Climate") is an inter-disciplinary, inter-cultural study that is assessing the vulnerability of reindeer herding – a coupled human-ecological system – to changes in key aspects of the natural and human environments, actively involving reindeer herders, linguists, remote sensing scientists, meteorologists, lawyers, anthropologists, biologists, geographers, philosophers (the ethical dimension) as well as indigenous institutions and organizations, relevant industrial enterprises and management authorities. The name of the project, EALÁT, which comes from the word "pasture" in the Sámi language, reflects the emphasis of the project on the close connection these cultures have to the environment

in which they live. It focuses on the adaptive capacity of reindeer pastoralism to climate variability and change and, in particular, on the integration of reindeer herders' knowledge with scientific research and analysis of their ability to adapt to environmental variability and change (http://www.EALAT.org).

The IPY EALÁT Project was initiated by the Association of World Reindeer Herders (WRH), a circumpolar indigenous peoples' organization with observer status in the Arctic Council. The project leaders believe that valuing traditional and scientific knowledge equally and, hence, integrating herders' experience and competence within the scientific method will enable it to contribute towards reducing the vulnerability of reindeer husbandry to the effects of climate change, which are likely to be pronounced over reindeer pastures in the north (Fig. 8.5). *The EALÁT-Network* study has adopted a multi-cultural approach in a multi-disciplinary field that includes monitoring, research, outreach and communication.

To accomplish the goals of the EALÁT Project, there are seven core "Work Packages", which are self-contained areas of research and investigation that cover the wide range of issues that EALÁT addresses. They are:

1. dentification of local climate conditions important for reindeer herding and development of basic climate scenarios
2. Customization of pasture conditions for reindeer pastoralism
3. Reindeer herders' knowledge: codifying and communicating coping mechanisms
4. Social and economic adaptation – institutions and governance as constraints and opportunities
5. Reindeer: consequences of climate variability and change
6. Reindeer welfare and nutrition: herders' observations and scientific data
7. Synthesis: assessing vulnerability

Fig. 8.5 Saami reindeer husbandry activity (photo by I.M.G. Eira)

EALÁT-Outreach has as its objective to communicate Arctic reindeer herders' traditional knowledge and scientific knowledge related to climate change to herders and the mainstream society in the Arctic. *The Reindeer Portal* (http://www.reindeerportal.org) is a multiplatform web portal into the world of reindeer husbandry. Developed by the International Centre for Reindeer Husbandry in Kautokeino, the goal of the Reindeer Portal is to be a one-stop-shop information site for reindeer herders, students, administrators, politicians, indigenous people, business interest, the general public and anyone that is remotely interested in reindeer and the peoples that herd them.

In the IPY EALÁT Consortium, *EALÁT-Monitoring* is already endorsed as a future expert monitoring network in the Circumpolar Biodiversity Monitoring Program of the CAFF (Conservation of Arctic Flora and Fauna) Working Group of the Arctic Council. The data collected in IPY will be the start of a future place-based monitoring system of reindeer herders' pastures and societies, while at the same time representing a unique opportunity for validation of satellite imagery in cooperation with the US National Aeronautics and Space Administration (NASA) Land Cover Land Use Change (LCLUC) program.

The legacy of IPY EALÁT will be continued through a UArctic Institute for Reindeer Husbandry (UArctic EALÁT) hosted in Kautokeino, Norway, as a pilot institute for research, outreach and education. For detailed information on EALÁT, the reader is referred to http://www.EALAT.org.

8.2.2 EALÁT Goals

The primary goals of the IPY EALÁT Project are to assess the vulnerability of reindeer herding – a coupled human-ecological system – to climate and other changes in key aspects of the natural and human environments and to build optimal adaptive strategies through the integration of indigenous reindeer herder knowledge with scientific data and analyses. The IPY EALÁT project partners believe that it is critical to empower indigenous peoples in Eurasia with the best technologies available to combine with indigenous knowledge for achieving a truly sustainable development of the Arctic. The EALÁT team also believes it is important that indigenous peoples' traditional knowledge must be a critical component of the future management and monitoring of the reindeer pastures and their societies. Therefore, another important goal of EALÁT is to build competence locally about land cover/land use change, including tools such as remote sensing observations and GIS as one important factor which could increase future adaptive capacity locally in Eurasian reindeer herding societies. Thus, developing training programs as well as EALÁT monitoring systems for Eurasian reindeer herders, which will extend well beyond the duration of the IPY are a high priority.

For adaptation questions, *EALÁT-Research* uses a vulnerability framework to assess the degree to which reindeer pastoralism is likely to experience harm as a result of exposure to multiple and interacting forces of change. The goal of the *EALÁT-Outreach* component of the project is to communicate arctic reindeer

herders' traditional knowledge and scientific knowledge related to climate change to herders and the mainstream society in the Arctic.

In recent years, traditional knowledge has increasingly become an integral part of scientific studies and a number of projects have included indigenous scientists and reindeer herders as full participants in project planning, implementation and dissemination of studies based on indigenous knowledge of modern reindeer management (Kitti et al. 2006; Magga 2005). However, the EALÁT project is considered unique because indigenous reindeer herders have organized and are leading this complex, interdisciplinary, intercultural study, inviting scientists and other colleagues to collaborate. In this effort to inform the Arctic nations both about the changes to which they are subjected and give some concrete examples how herders' traditional knowledge relates to adaptation to changing conditions, another important goal of the study includes the challenge of taking reindeer herders' knowledge into action for sustainable development of the Arctic.

8.2.3 EALÁT Study Sites

The IPY EALÁT project has research, information, and outreach activities in five different reindeer herding societies across Eurasia: Nenets, Yamal-Nenets and Chukotka Autonomous Areas and Republic of Sakha (Yakutia) in Russia, as well as Saami in Northern Europe (Fig. 8.6). Researchers will concentrate initially

Fig. 8.6 Map of five EALÁT study sites. The five primary IPY EALÁT sites include: (*1*) Saami area of Norway, Finland, Sweden, Russia (initial emphasis on Norway), (*2*) Nenets Autonomous Area, (*3*) Yamal-Nenets Autonomous Area, (*4*) Republic of Sahka (Yakutia), and East Chukotka Autonomous Area. EALÁT researchers are concentrating initially on site 1 in the Norwegian county of Finnmark and site 3 in Yamal-Nenets Autonomous Area in Russia. Adapted from http://www.EALAT-information.org. Reproduced by permission of the International Centre for Reindeer Husbandry

on the two largest reindeer herding cultures in the world: the Sámi, who inhabit Northern Europe and the Kola Peninsula in northwestern Russia, with a focus on the Norwegian county of Finnmark, and the Nenets, focusing in particular on herders in the Yamal-Nenets Autonomous Okrug in Russia. Future research in the other regions where IPY EALÁT has carried out information activities, will be implemented as part of the IPY EALÁT legacy.

8.3 EALÁT Studies

8.3.1 EALÁT Results from Early Studies: SAR Studies for Pasture Quality

This section describes some results from Reindeer Mapper, an early EALÁT pilot project of the NASA Land Cover Land Use Change Program, to investigate the possible use of SAR (Synthetic Aperture Radar) for characterizing pasture quality as an alternative to sensors relying on the visible part of the electromagnetic spectrum and the resulting problems due to low illumination and cloud cover in the Arctic (Maynard et al. 2005; Yurchak and Maynard 2005). This work, part of a larger study called Reindeer Mapper, preceded the EALÁT program as a pilot for the EALÁT project to study remote sensing technologies for reducing the threats to reindeer husbandry from climate and land changes by creating a source of usable, timely satellite data that could be combined with traditional, local and other data and information for improved decision-making (Maynard et al. 2003, Maynard and Yurchak 2003, Maynard et al. 2004). Based upon discussions among Reindeer Mapper team members from within the reindeer husbandry community, including discussions and publications such as the Yakutsk Declaration from the Third World Reindeer Herders' Congress in March 2005, a preliminary list of the highest priority environmental measurements for remotely sensed data was generated. These requirements constituted the primary elements determining pasture quality and state, the most important overall set of parameters for reindeer herders (Fig. 8.7).

This preliminary study of the use of SAR for characterizing the quality of reindeer pasture was initiated because SAR does not rely on the visible part of the spectrum and, therefore, has the ability to provide data regardless of weather or light conditions (Yurchak and Maynard 2005). These early studies focused initially on the highest priority measurements/data products identified by the reindeer herders on the team. The applications of SAR for characterization of vegetation and measuring snow parameters are not as well-developed as optical sensors. Initial studies of seasonal changes in SAR backscatter from different kinds of land features in two locations, Anadyr River Research Area (ARRA) and Vaegi Village Research Area (VVRA) in Chukotka, Russia, were carried out for the four seasons of the period between the years 2000 and 2004. Site selection was done based on data availability from the Alaska Satellite Facility (ASF) and on the location of typical tundra

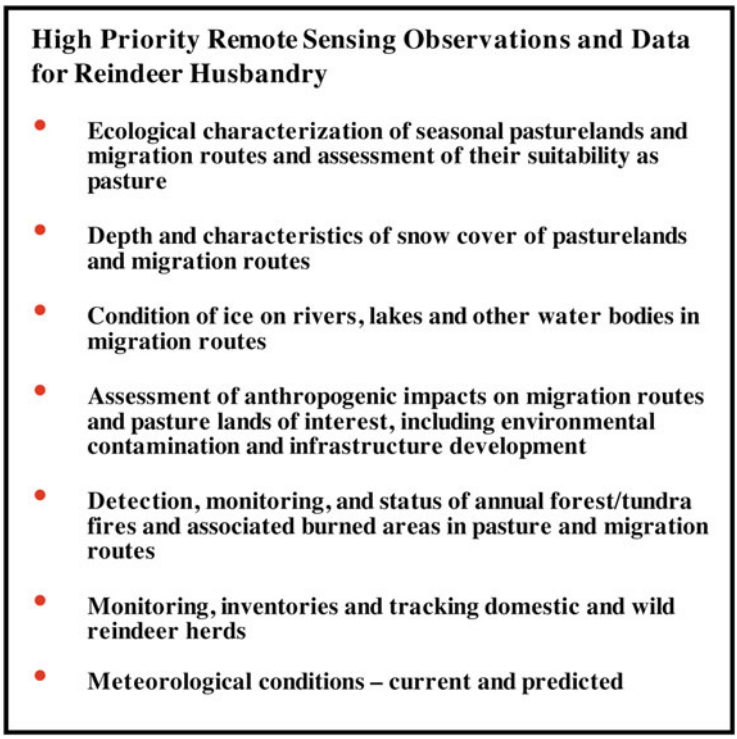

Fig. 8.7 Highest priority remote sensing measurements/data products identified by EALÁT reindeer herders during NASA LCLUC Reindeer Mapper study for characterization of pasture quality for pastures and migration routes. Reproduced from Maynard et al. (2005)

landscapes on reindeer pasture areas. Based on these criteria, two sites within the Anadyr district of Chukotskiy Autonomous Okrug (ChAO) were selected. The first site is a nature conservation area north of "Krasnoe" lake along the Anadyr river (Anadyr river research area – ARRA); the second site, a fire risk area south of Vaegi Village (Vaegi Village research area – VVRA) (Maynard et al. 2005, Yurchak and Maynard 2005).

Results from the study showed that the SAR data detect fire scars very well and could be used for fire scar inventory mapping in conjunction with other systems such as the Moderate Resolution Imaging Spectroradiometer (MODIS) Rapid Response System. An analysis of tundra lakes' radar properties suggested the possibility for remote assessment of the depth of lakes (Yurchak and Maynard 2005). It was also possible to observe the snow masking effect (Ulaby et al. 1984) and wet snow (Bagdadi et al. 1997). Studies showed the capability of SAR to delineate different types of tundra species as well as demonstrate seasonal changes in radar backscatter from tussock and mountain tundra in time series studies. The sensitivity of SAR

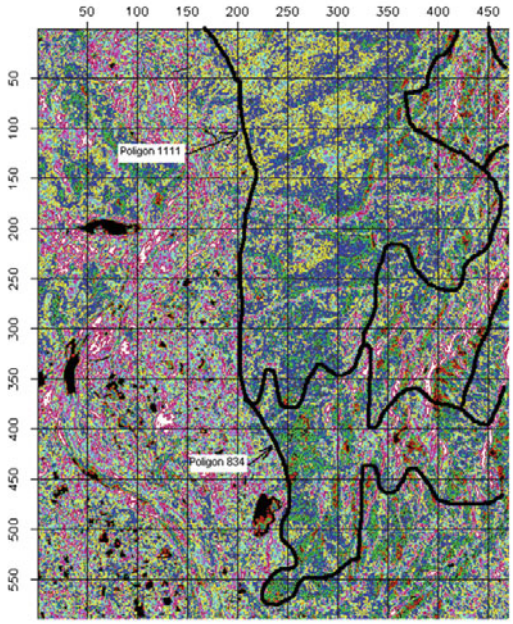

Fig. 8.8 A classified part of a SAR low resolution image of the Anadyr River Research Area (ARRA), Russia, based on comparison with geobotanical map (courtesy of A. Polezhaev). 28 July 2003. Image center: 65° 35′ N, 174° 08′ E. Reproduced from Maynard et al. (2005)

data to vegetation and snow cover over plains and mountain tundra is demonstrated in a time series study of a selected area in the north of ARRA (Figs. 8.8 and 8.9a, b).

The results showed clear seasonal changes in tundra radar backscatter. For tussock tundra the backscatter was higher in summer months and dropped to the lowest value in the fall due to decrease of soil (vegetation) moisture because of freezing. The subsequent backscatter increase in the winter could be related to snow cover impact. For mountain tundra, summer backscatter behavior is opposite to that of tussock: it is the lowest. Also, the range of winter-summer decrease is rather high: ~60 Digital Numbers. The reason for such behavior, probably, is different local incidence angles for tussock tundra (~ 23°) and for the mountain slope (~0°). Further field validation work was planned for this study. In addition, SAR data were shown to be capable of delineating detailed geobotanic polygons. SAR data were compared with ground-based geobotanic maps and were found to provide a higher resolution set of polygons than aerial surveys. These preliminary results suggested that further development of the methodology as well as its validation and calibration may result in a reliable method for SAR applications to these important environmental parameters.

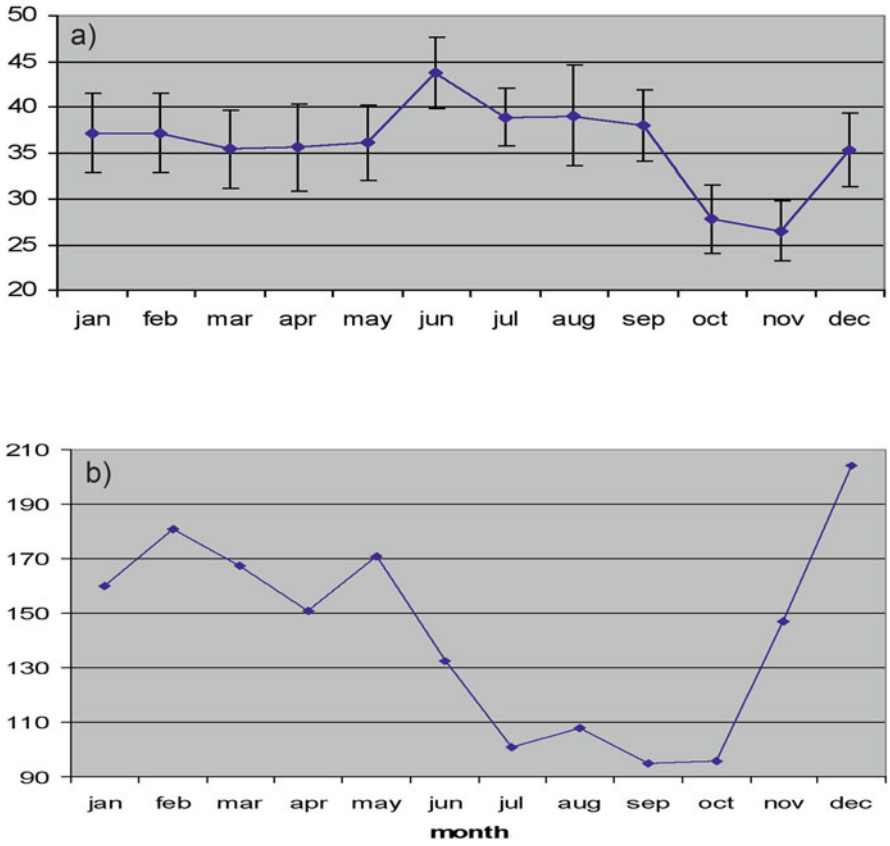

Fig. 8.9 Time series of SAR backscatter from (**a**) plains tussock tundra and (**b**) mountain tundra within Anadyr River Research Area, Russia (ARRA). Reproduced from Maynard et al. (2005)

In summary, the study showed that SAR data can detect fire scars very well and could be used for fire scar inventory mapping in conjunction with other systems such as the MODIS Rapid Response System. Studies showed the capability of SAR to delineate different types of tundra species as well as demonstrate seasonal changes in radar backscatter from tussock and mountain tundra in time series studies. In addition, SAR data were shown to be capable of delineating detailed geobotanic polygons. SAR data were compared with ground-based geobotanic maps and were found to provide an even higher resolution set of polygons than aerial surveys. An analysis of tundra lakes' radar properties suggests that SAR may provide a useful means of remotely assessing the state of lakes. As temperature increases cause earlier melting of lakes along migration routes in springtime, this technique for lake assessment could prove to be very valuable for herders on a real-time basis.

8.3.2 EALÁT On-Going Studies

8.3.2.1 Indigenous Linguistics Studies of Reindeer Herding Language

One of the main objectives within the IPY EALÁT project is documenting indigenous knowledge about snow conditions and indigenous perceptions about how they are adapting to changing conditions. A great deal of insight can be gained from centuries-old knowledge within reindeer herding societies such as the Sáami and the Nenets. With the declining numbers of those from traditional reindeer herding communities following more traditional ways of life, it is important to document this knowledge as much as possible while it still exists. The study of the language itself is important because it is through language that traditional knowledge becomes available and, particularly, through specific terminology.

Some early results from an EALÁT project on the language of reindeer husbandry have recently been summarized by Eira et al. (2008) and they demonstrate the importance and the richness of the use of all kinds of information and knowledge to address the dramatic changes occurring in the Arctic today. This EALÁT study is focusing on how to empower indigenous reindeer herders with the best information – indigenous knowledge as well as scientific/technical knowledge – for addressing the increasing challenges from climate change and loss of grazing lands. Language is a very important part of this and one of the main objectives of the overall EALÁT project is to document indigenous knowledge about reindeer herding, with the traditional language of reindeer herders in the key role structuring their knowledge and knowledge-sharing.

In the EALÁT linguistics study, one of the key early investigations has been the collection and analysis of the existing linguistic concepts that are used in Saami reindeer herding language. There are, for example, in the dialect of Guovdageaidnu/Kautokeino over 1,000 individual terms describing reindeer and especially their appearance, including 50 words describing the shape of the antlers (Magga 2005, Eira et al. 2008). This early investigation has been studying techniques for the use of language in communicating traditional knowledge about reindeer herding among reindeer herders as well as to non-indigenous scientific and the broader world communities. Results are being documented and publications prepared at this time (Eira et al. 2008).

8.3.2.2 Indigenous and Scientific Snow Studies

A joint indigenous and scientific snow project now underway addresses a key EALÁT objective to document knowledge about snow conditions and how reindeer herders are adapting to the changing conditions in relation to snow and pasture availability and mobility of the herds. As noted earlier, for indigenous peoples of the north, a clear understanding of real-time snow, precipitation, and ice in their area has been critical to their survival. Current EALÁT studies are focusing on Saami snow terminology and herding strategies during the winter to find the best forage

for the herd. Section 8.3.2.1 describes a key EALÁT indigenous linguistics study of reindeer herding language, which highlights centuries-old knowledge from herder societies. In addition, historical observations are being documented which include oral histories and stories from parents, grandparents and other elders about extreme snow events and other phenomena.

The study described in this section is a joint observational study by EALÁT and NASA indigenous and scientific collaborators, which is a data collection project with a focus on climate and development changes (snow and vegetation especially). The study is being led by a reindeer herder and PhD student at the Sami University College and Co-PI of EALÁT (Eira et al. 2008). She is coordinating the collection of a comprehensive set of observations in northern Norway, by six reindeer herders over several years, each of whom provide a detailed set of observations of snow, vegetation, meteorological conditions, herd behavior, and other data as they traverse their seasonal migration routes throughout complete seasons. The study area is located across the Saami migration pastures of northern Norway in EALÁT Study area #1 (Fig. 8.10).

This project includes continued data collection with the EALÁT-NASA thermochrons which was initiated in 2007 (see Section 8.3.2.3). Each reindeer herder is recording on special data log sheets the GPS location/time/date of their daily observations data on eleven weather parameters (e.g., wind, cloud cover, precipitation, temperatures), Saami snow terms, physical measurements of snow depth, type, and description, herd behavior, snow conditions as they pertain to the ability of the reindeer to reach the lichens beneath the snow, and thermochron location data.

The herder observations will also be supported by remote sensing and meteorological data from the same time period wherever possible. Remote sensing data to be combined with the herder archives are presently being inventoried for land cover/land use change assessment information including Landsat, MODIS,

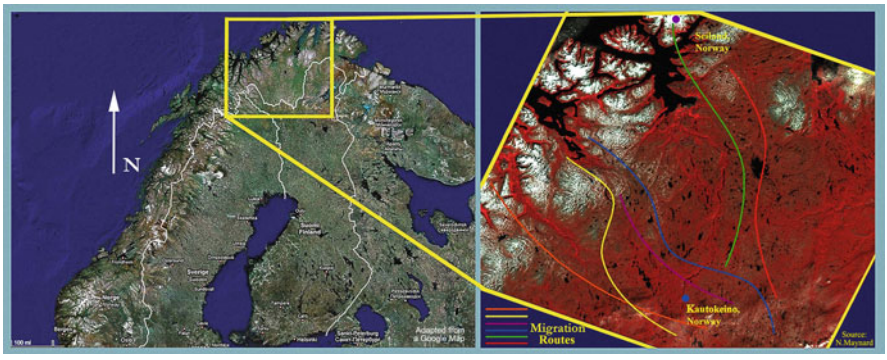

Fig. 8.10 Location of EALÁT-NASA Project Site 1 in Northern Norway and approximate locations of Saami reindeer migration routes where reindeer herders are collecting multi-year, detailed data on snow, vegetation, meteorology, traditional Saami observations of snow and herd behavior and forage availability for reindeer vulnerability studies to be combined with NASA and other data. Source: N.G. Maynard, I.M.G Eira

Advanced Microwave Scanning Radiometer-EOS (AMSR-E), and high resolution commercial satellite imagery. A series of cloud-free Landsat scenes between 1972 and 2007 over the field areas of interest have been obtained and these will be combined with Eurasian GIS data layers, meteorological data, in situ field data, and indigenous knowledge described in other sections of this chapter.

8.3.2.3 Indigenous and Scientific Studies of Pasture Icing or "Lock-Out"

The increasing temperature variations which are accompanying climate change in the Arctic are causing more freeze-thaw-freeze cycles, resulting in icing of the lichens or ice layers within and on the snow pack in reindeer pastures and pasture "lock-out". EALÁT Project members are carrying out field research to obtain indigenous and scientific data that can improve the capability of reindeer herders to predict and adapt to these adverse weather conditions and climate changes, especially with climate change making weather conditions more variable and less predictable than before.

For example, the traditional practice of the Sáami reindeer herders in northern Scandinavia was to allow their reindeer to graze on the tundra in coastal areas during the summer months, where they can graze on abundant grasses, bushes, mushrooms and daffodils. However, these traditional practices have been disrupted somewhat due to the presence of modern national borders, development, and climate changes. After the annual slaughter and the first snowfall, the herders bring their reindeer to over-wintering pastures in the mountains and tundra in the interior part of upper Scandinavia, where reindeer dig through the snow to get to lichens, the primary staple of the winter diet of reindeer (Fig. 8.11).

However certain meteorological conditions can sometimes create conditions that "lock out" winter grazing pastures. If a warm period that partially melts the snow

Fig. 8.11 Reindeer in over-wintering pastures of Scandinavia digging through snow to reach lichens, the primary staple of the winter diet. Increasing temperature variations which are accompanying climate change in the Arctic are causing more freeze-thaw cycles, resulting in icing of the lichens or ice layers within and on the snow pack, making it impossible for reindeer to access their primary food source (called pasture "lock-out") (photo by I.M.G. Eira)

is followed by rain and then the temperature drops below freezing, this can create a thick coating of ice in the winter pastures that makes it impossible for reindeer to access their primary food source. This can lead to illness and starvation for the reindeer, which translates into serious losses for herders.

Accordingly, the IPY EALÁT project is developing a new adaptive strategy for "lock out" prediction to avoid this increasingly difficult problem. Researchers are using indigenous knowledge together with scientific data to better predict when and where adverse winter grazing conditions might occur so that eventually a service could be set up that would help herders know where winter pastures with bad grazing conditions are so they can avoid them. Meteorologists from the Norwegian Meteorological Institute in Oslo are providing data for models that try to predict snow conditions in Finnmark by looking at temperature gradients throughout the snow pack.

These models are being combined with real-time field observations by herders to verify the predictions the models make, including, the use of some NASA technologies. Starting in October 2007, a team of researchers from the Sámi University College placed NASA thermochrons (small data recorders that take temperature readings at regular intervals) along several reindeer migration routes at various depths between the ground and the top of the snow pack (Fig. 8.12). In May 2008, the team removed the first set of thermochrons and temperature data is being analyzed and compared with Norwegian Meteorological Institute (NMI) model predictions. Observations are being compared with remote sensing data from NASA and the European Space Agency (ESA) and data shared with collaborators in the NASA Global Snowflake Network (GSN) and History of Winter (HOW; http://education.gsfc.nasa.gov/how/). This process is being repeated for four successive winters in order to get an adequate data set to compare with the model.

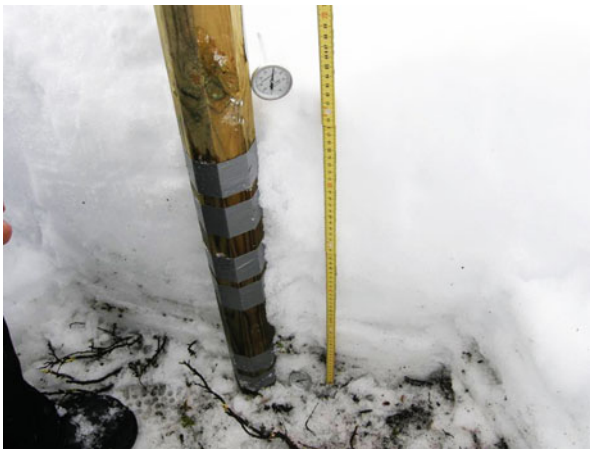

Fig. 8.12 NASA thermochrons at Saami snow station (photo by I.M.G. Eira)

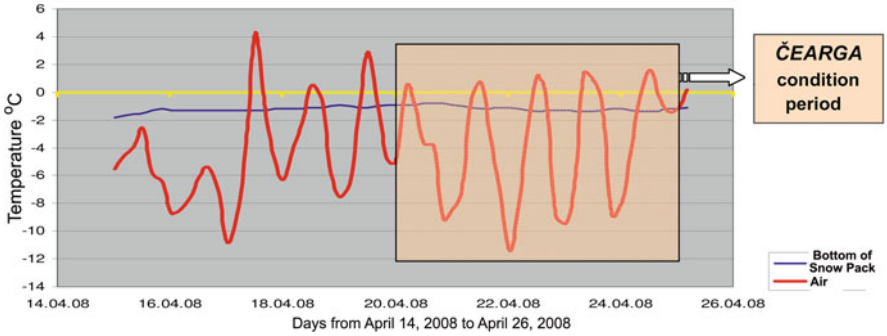

Fig. 8.13 Thermochron temperature measurements. Temperatures (ºC) measured by EALÁT-NASA thermochrons at one of the reindeer herder observation stations in April 2008, during formation of *Cearga* conditions (creating pasture "lock-out"). Temperatures were measured on the ground (at the bottom of the snowpack) and in the air (at 1.5 m above ground). *Cearga* in Saami means snow pack which is so hard that it bears the weight of the reindeer. Source: I.M.G. Eira

Figure 8.13 shows the temperatures (°C) measured by NASA thermochrons in one of the reindeer observations stations. The temperatures were measured on the ground (at the bottom of the snowpack) and in the air (at 1.5 m above ground). The thermochron data show rapid changes in temperature during this period. According to daily observations recorded by the reindeer herders, the snow conditions became worse and *cearga* conditions were formed from April 20 (*Cearga* in Saami means snowdrift which is so hard that it bears the weight of the reindeer, i.e., a very hard snow pack). Prior to April 15, cold temperatures and strong winds developed the conditions conducive to formation of the *cearga*. On April 18, frequent temperatures above 0°C created even worse grazing conditions during this period. This snow condition could be characterized as a kind of "lock-out" condition because it prevents the reindeers' access through the snow to the vegetation.

New data sets will be produced for snow type and distribution as a result of the thermochron study, which include NASA remote sensing data such as MODIS and AMSR-E as well as in situ data from the Norwegian Meteorological Institute and US National Oceanic and Atmospheric Administration/National Center for Environmental Prediction (NOAA/NCEP) and integrated into indigenous knowledge and observations for that area.

The Polar View Consortium, which runs a variety of Earth-observation services for its end-users all over the world, will also be contributing to the study by providing researchers with snow maps created using satellite data. These maps help in giving an overview of the amount of snow cover and snow cover type in the regions being studied in the EALÁT project. These observations will provide useful information on the snow temperature from the ground to the surface of the snow pack because the influence of the temperature of the ground on the snow above is not fully-understood. Researchers are also examining historical meteorological

data taken over the past several decades as well as satellite data, concentrating in particular on years when many pastures were "locked out" due to ice cover.

The combined set of observations will help to better understand what happens to the snow above if warming occurs on the ground. Will the snow get wetter or will it get drier? The answers to these questions will aide in understanding how the energy exchange occurs between the ground and the snow above.

Data from the snow study will be integrated by Saami reindeer herders into a system which will become part of a special service to be produced by the combination of all observations and a model to predict whether certain pastures will be locked out due to ice in the snow pack, so that herders can avoid these areas. This information will constitute a unique data set for the land-use and land-cover studies for this part of Eurasia and the first "adaptation early warning system" created by and for reindeer herders. All data such as these will be distributed through the International Centre for Reindeer Husbandry as part of this special service to reindeer herders.

8.3.2.4 Indigenous and Remote Sensing/GIS Pasture Studies

A remote sensing/GIS pasture study, based upon earlier EALÁT and Reindeer Mapper studies, has recently been initiated. NASA and university colleagues are starting to obtain and process satellite and GIS data and information to combine with indigenous knowledge to document changes in vegetation and infrastructure. The team has obtained Landsat and GIS data for two sites, including EALÁT study sites #1 and #2, set priorities for data requirements, and have begun analyzing and classifying data sets. The team is creating a specific qualitative and quantitative assessment of multi-spectral information from remote sensing combined with indigenous data into a GIS environment where impacts of global warming, climate change and infrastructure development can be shown and mapped as it directly impacts reindeer pastures and migration routes in these areas of northern Norway and Russia. These direct observations and data will be integrated with indigenous historical knowledge and recent observations from herder's daily data logs. Higher resolution imagery will be obtained and processed as funding becomes available. Emphasis of the study is on spatial and temporal changes in vegetation, water bodies, and infrastructure together with variations/changes in weather and climate. One of the issues of interest mentioned earlier is the identification of possible shrub area increase from 1987 to 2007. An increase of shrub land area in reindeer grazing lands makes food access increasingly difficult, so classification of changes in precise locations of these shrub land areas is planned. Other GIS data layers including roads, oil and gas infrastructure, railways, drainage areas, utility lines, urban development, dwellings, water bodies are being obtained and will be validated with GPS ground-truthed field data from reindeer herder data sets. Discussions are under way among EALÁT team members to establish joint data analyses through student/faculty exchanges and data exchange programs between the UArctic Institute, Saami University College and US university students and NASA. Data products will be distributed through web sites, locally-appropriate means, and the International Centre for Reindeer Husbandry.

8.4 EALÁT Monitoring and Information Integration System – Adaptation and Planning for the Future

To achieve optimal adaptation strategies for reindeer husbandry, it is imperative that governments, local reindeer herders, management, policy, and decision-makers include reindeer herders and their traditional local and scientific knowledge in future decision-making which impacts the herding community. To enable the efficient, timely collection and integration of their data into these decision- and policy-making processes, EALÁT Project reindeer herders are developing their own system to monitor changes based upon traditional knowledge and modern technologies. This new system is based on the principles of the United Nations (UN) Convention of Biological Diversity Art 8, UN Agenda 21 Declaration Ch 26, ILO-169 Convention on Rights of Indigenous Peoples, UN Declaration concerning the rights of Indigenous Peoples 2007, the United Nations Educational, Scientific and Cultural Organization (UNESCO) Convention on Protection and Development of Cultural Diversity, and the Yakutsk Declaration from Third World Reindeer Herders Congress in 2005. In fact, the Yakutsk Declaration explicitly stated that reindeer herders should develop their own system to monitor changes of the arctic natural resources, based on traditional knowledge and modern technology.

EALÁT-Monitoring is developing an observation program or monitoring system for reindeer pastoralism in place-based studies in the Saami area (Norway, Sweden, Finland, and northwestern Russia) and Yamal-Nenets Autonomous Area, and, later possibly, Nenets Autonomous Area, the Republic of Sakha (Yakutia), and Chukotka Autonomous Area. The EALÁT/Reindeer Mapper System, being developed at the International Center for Reindeer Husbandry, is a data integration and sharing system to integrate traditional indigenous knowledge together with physical, scientific, and technical data into a common GIS database for improved decision-making and herd management. An early EALÁT pilot project of the NASA Land Cover Land Use Change Program called Reindeer Mapper developed a preliminary concept for this type of system (Fig. 8.14), designed to bring remote sensing, ground measurements, and information technologies together with indigenous traditional and local knowledge for herder use in management of Northern Eurasian reindeer herds (Maynard et al. 2003, Maynard and Yurchak 2003b, Maynard et al. 2004, 2005).

This EALÁT georeferenced data sharing system will use secure Intranet connections for data collection, management, transmission, analysis, access, and dissemination. The system will function as a portal to link data from a variety of sources and provide that information to multiple herders. Observations and information are being integrated into a central GIS data base so that data from all sources such as NASA products, reindeer herder knowledge, observations and maps, ground-based measurements and observations, herd movements can all be put in, managed, transmitted, accessed, and disseminated in real time for herd management. The EALÁT-Reindeer Mapper Information System will assist in the ongoing analysis of trends and detection of emerging events and conditions, which affect humans, agriculture, and the environment to enhance early warning and management of responses and adaptation.

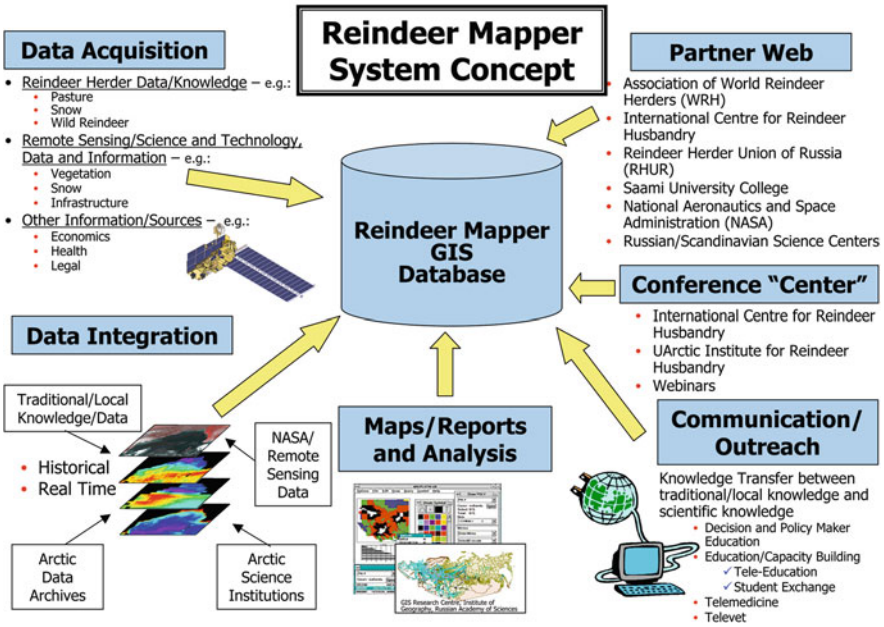

Fig. 8.14 Reindeer Mapper System concept. Reindeer Mapper concept was originally developed to bring remote sensing, ground measurements, and information technologies together with indigenous traditional and local knowledge for herder use in decision-making and management of Northern Eurasian reindeer herds (Maynard et al. 2003)

It is intended that EALÁT will be able to provide reindeer herders with an efficient tool for managing the real-time movements and migrations of their herds. This is accomplished through improved efficiency in linking different members of the herder settlements or communities and by providing real-time local, satellite or other data (e.g., ice melt in lakes and rivers, weather events), thus enabling realtime adjustments to herd movements to avoid problems such as changing weather/climate conditions, freeze-thaw "lock-out" problems, or to take advantage of availability of better pasturelands along migration routes (Fig. 8.15). The system is being designed to incorporate local data to allow users to bring their own data into the system for analysis, in addition to the data provided by the system itself. With the local information of the population, up-to-date environmental data and habitat characteristics, the system could generate maps depicting important features of interest for reindeer managers.

One of the products derived from the planned system will be a web-based graphic display that allows analysts to quickly pinpoint areas of interest such as those with large concentrations of reindeer, and provide surrounding environmental information. The system could be automatically updated with near-real-time information such as hourly precipitation and snowfall rate and accumulation, daily surface and air temperatures, and vegetation cover conditions. The system could bring attention

Fig. 8.15 Dangers of early ice melt (photo by S.D. Mathiessen)

to the proximity of human and animal populations as part of the need for control response. A local GIS will bring these many layers together with several supporting models, showing only a straightforward graphic of the real-time situation in the field. Because the proposed system will be operating in the Internet environment, it should be virtually accessible from any network computers and wireless remote access from the field. The International Center for Reindeer Husbandry in Kautokeino, Norway, is providing regional and international coordination of and access to data sets and expertise, and will act as overall clearinghouse for EALÁT information.

8.5 Reindeer Pastoralism and the Future: UArctic International Institute for Reindeer Husbandry

For a sustainable future, reindeer herders themselves are now have to define and anticipate risks related to rapid change in their local communities and plan for optimal adaptation strategies. Reindeer herders in Eurasia from the Bering Strait in the east to the Atlantic Ocean in the west will face many challenges related to changes in their grazing lands and their societies due to climate variability and change, and arctic industrial development. Reindeer herders therefore have to prepare themselves, their societies, and management authorities to reduce their vulnerability to change, including empowering themselves with new technologies to monitor their local communities based on the best knowledge available.

The most recent development in direct response to these needs is the initiative from the Association of the World Reindeer Herders (WRH) and the International Centre for Reindeer Husbandry in collaboration with Saami University College to the establishment of the UArctic Institute for Reindeer Husbandry ("UArctic EALÁT") to ensure EALÁT has a legacy after the IPY years. As stated by the International Centre for Reindeer Husbandry:

> The new UArctic Institute will be hosted in Kautokeino, Norway, as a pilot institute for research, outreach and education within the objectives of the UArctic Strategic Plan 2008–2013, in accordance with the Yakutsk Declaration (2005) from the Third Congress of World Reindeer Herders and in agreement with the Fairbanks Declaration from the Eighth conference of Parliamentarians of the Arctic Region, Fairbanks, the United States of America, 12–14 Aug 2008.

The Fairbanks Declaration states:

> Further build capacity in Arctic communities to adapt to climate change, including the development of new education programmes and skills training initiatives, to allow. Encourage the University of the Arctic to build practical capacity in the north to address the challenges of adaptation to climate change, and to solve the Arctic's needs for energy, from technical, cultural, economic as well as environmental perspectives, and to provide further education of health care personnel with special focus on Arctic conditions.

The UArctic EALÁT Institute will provide a unique opportunity in building competence locally in reindeer herders' society not presently available in the UArctic. The EALÁT network is today responsible for the UArctic thematic network: Adaptation to globalization of the Arctic. The EALÁT network is based on the unique cooperative network established by the Association of World Reindeer Herders (WRH) through the Eurasian North.

The institute is a very significant vehicle for building the capacity of arctic countries and, in particular, indigenous peoples, to adapt to climate change, industrial development, and globalization across the Arctic as well as to reduce their vulnerabilities through empowerment with the best indigenous, scientific and technological knowledge available – including, remote sensing.

References

Abrjutina LI (2003) State policy and health of small nationalities of the north of Russia. Presented at the meeting of the Organizing Committee of the Association of Radical Small Native Nationalities of the North, Siberia and the Far East of the Russian Federation. Moscow, Russia, 28 January 2003

ACIA (2004) Impacts of a warming Arctic. Arctic climate impact assessment overview report. In: Hassol SJ (ed) Cambridge University Press, Cambridge, 144 p

Bagdadi N, Gauthier Y, Bernier M (1997) Capability of multitemporal ERS-1 SAR data for wet-snow mapping. Rem Sens Environ 60:174–186

Brotton J, Wall G (1997) Climate change and the Bathurst Caribou Herd in the Northwest Territories, Canada. Clim Change 35:35–52

Deloria V (2001) Knowing and understanding. In: Deloria V Jr, Wildcat D (eds.) Power and place: Indian education in America. American Indian Graduate Center and Fulcrum Resources, Golden, pp 41–46

Deloria V Jr, Wildcat D (2001) Power and place: Indian education in America. American Indian Graduate Center and Fulcrum Resources, Golden, 168 p

Eira AJ (2001) Reindeer husbandry in Norway. In: The 2nd World Reindeer Herders Ćongress. Arctic Centre Reports 36, University of Lapland, Rovaniemi, 42–43

Eira IMG, Magga OH, Bongo MP, Sara MN, Mathiesen SD, Anders O (2008) The challenges of Arctic reindeer herding: the interface between reindeer herders traditional knowledge and modern understanding of the ecology, economy, sociology and management of Sami Reindeer

Herding. Presented at governing shared resources: connecting local experience to global challenges, 12th Biennial conference of the International Association for the Study of Commons, Cheltenham, 14–18 July, 2008

Forbes BC, Bolter M, Muller-Wille L, Hukkinen J, Muller F, Gunslay N, Konstantinov Y (2006) Reindeer management in northernmost Europe: linking practical and scientific knowledge in social-ecological systems. Ecological Studies 184. Springer, Berlin

George TH, Stringer WJ, Baldridge JN (1977) Reindeer range in western Alaska from computer-aided digital classification of Landsat data. Proceedings of the 11th international symposium on remote sensing of environment, 25–29 Apr 1977, 1671–1682

Glazovsky NG, Ojima DS, Maynard NG, Bergen KM, Chubarova N, Davaasuren N, Fisher G, Genikhovich EL, Goisman PY, Kalaabin GV, Kotlyakov VM, Kust G, Osipov V, Romanovsky V, Rosenzweig C, Seto K, Chibilev A, Tubiello F, Vandysheva N, Walker R. (2004) Land use interactions: societal-ecosystem linkages. NEESPI science plan, Chapter 3.4, NOAA, Ashville

Gunn A, Skogland T (1997) Responses of caribou and reindeer to global warming. In: Oechl WC, Callaghan T, Gilmanov T, Holten JI, Maxwell B, Molau U, Sveinbjörsson B (eds.) Global change and arctic terrestial ecosystems. Springer, New York

Hall ED (1989) People and Caribou in the northwest territories. Government of the Northwest Territories, Yellowknife

Hall DK, Fagre DB, Klasner F, Linebaugh G, Liston GE (1994) Analysis of ERS-1 synthetic aperture radar data of frozen lakes in northern Montana and implications for climate studies. J Geophys Res 99(C11):22473–22482

Hanssen-Bauer I, Forland EJ, Haugen JE, Tveito OE (2003) Temperature and precipitation scenarios for Norway: comparison of results from dynamical and empirical downscaling. Climate Research 25:17–27

Hinzman L, Bettez N, Bolton WR, Chapin FS III, Dyurgerov M, Fastie C, Griffith B, Hollister RD, Hope A, Huntington HP, Jensen A, Jia GJ, Jorgenson T, Kane DL, Klein DR, Kofinas G, Lynch AH, Lloyd AH, McGuire AD, Nelson F, Oechel WC, Osterkamp TE, Racine C, Romanovsky VE, Stone R, Stow D, Sturm M, Tweedie CE, Vourlitis G, Walker MD, Walker DA, Webber PJ, Welker JE, Winker K, Yoshikawa K (2005) Evidence and implications of recent climate change in northern Alaska and other Arctic regions. Clim Change 73:251–298

Jernsletten JL, Klokov KB (2002) Sustainable reindeer husbandry. Arctic council. University of Tromso, Tromsø, 157 p

Johansen B, Karlsen SR (2002) Finnmarksvidda – changes in lichen cover 1987–2000. Proceedings of the 12-th Nordic conference on reindeer research in Kiruna, Sweden, 11–13 Mar 2002

Justice CO, Korontzi S (2001) A review of satellite fire monitoring and the requirements for global environmental change research. In: Ahern F, Goldammer G, Justice CO (eds) Global and regional vegetation fire monitoring from space: planning a coordinated international effort. SPB Academic Publishing, The Hague, pp 1–18

Justice CO, Townshend JRG, Vermote EF, Masuoka E, Wolfe RE, El N Saleous, Roy DP, Morisette JT (2002) An overview of MODIS Land data processing and product status. Rem Sens Environ 83(1–2):3–15

Kelly REJ, Chang ATC, Foster JL, Hall DK (2004) Using remote sensing and spatial models to monitor snow depth and snow water equivalent. In: Kelly REJ, Drake NA, Barr S (eds) Spatial modelling of the terrestrial environment, Chichester, Wiley, Chichester

Kitti H, Gunslay N, Forbes BC (2006) Defining the quality of reindeer pastures: the 2 perspectives of Sámi reindeer herders. Ecol Stud 184:141–165

Kitti H, Kumpula T (2002) Classification of reindeer pastures: mapping based on traditional ecological knowledge (TEK) and remote sensing based mapping. Proceedings of the 12th Nordic conference on reindeer research in Kiruna, Sweden, 11–13 Mar 2002

Klein DR, Baskin LM, Bogoslovskaya LS, Danell K, Gunn A, Irons D, Kofinas G, Kovacs K, Magomedova M, Meehan R, Russell D, Valkenburg P (2005) Management and conservation of

wildlife in a changing Arctic climate. In: Arctic climate impact assessment, ACIA. Cambridge University Press, Cambridge, pp 597–648
Klokov K (2000) Nenets reindeer herders on the lower Yenisei River: traditional economy under current conditions and responses to economic change. Polar Res 19(1):39–47
Kumpula T, Manderscheild A, Colpaert A (2002) Evidence of different pasture use from satellite images: cases from Lapland and the Tibetan plateau. Proceedings of the 12-th Nordic conference on reindeer research in Kiruna, Sweden, 11–13 Mar 2002
Levine JS, Bobbe T, Ray N, Singh A, Witt RG (1999) Wildland Fires and the environment: a global synthesis. UNEP/DEIAEW/TR.99-l
Li S, Guritz R, Logan T, Shindle M, Groves J, Olmsted C, Carsey F, Macmahon J (1999) Summer environmental mapping potential of a large-scale ERS-1 SAR mosaic of the state of Alaska. Int J Rem Sens 20(2):387–401
Liew SC, Kwoh LK, Lim OK, Lim H (2001) Remote sensing of fire and haze. In: Eaton P, Radojevic M (eds) Forest fires and regional haze in Sourtheast Asia. Nova Science Publishers, New York, Chapter 5, pp 67–89
Magga OH (2005) Reindriftsnaeringen I partnerskap med forskningen. In: Seminar manuscript: Reinkjott 2005-en positive framtid for reinkjott med fodus pa kvalitet, 25–26 May 2005. Saami University College, Guovdageaidnu, Norway
Malcolm JR (1996) The demise of an ecosystem: Arctic wildlife in a changing climate. World Wildlife Fund Report, Washington DC
Maynard NG, Yurchak BS (2003) Integrated scientific, local and indigenous knowledge for management and decision-making on environment, climate and health issues. Open meeting human dimensions of global environmental change, Montreal, 16–18 Oct 2003
Maynard NG, Yurchak BS, Turi JM (2003) Shared knowledge for decision-making on environment and health issues in the Arctic. SEARCH (A Study of environmental arctic change) Open Science Meeting, Seattle, 27 Oct 2003
Maynard NG, Yurchak BS, Sleptsov YA, Turi JM, Mathiesen S (2005) Space technologies for enhancing the resilience and sustainability of Indigenous Reindeer Husbandry in the Russian Arctic. Proceeding of the 31st international symposium on remote sensing of environment, global monitoring for sustainability and security, Saint Petersburg, 20–24 Jun 2005
Maynard NG, Yurchak BS, Turi JM, Mathiesen SD, Aissi-Wespi RL (2004) Integrating indigenous traditional, local and scientific knowledge for improved management, policy and decision-making in Reindeer husbandry in the Russian Arctic. IASSA 5th international congress of arctic social scences (ICASS V), Fairbanks, 19–23 May 2004
McCarthy JJ, Martello ML, Corell RW, Eckley N, Fox S, Hovelsrud-Broda GK, Mathiesen SD, Polsky C, Selin H, Tyler NJC, Strøm Bull K, Siegel-Causey D, Eira IG, Eira NI, Eriksen S, Hanssen-Bauer I, Kalstad JK, Nellemann C, Oskal N, Reinert E, Storeheier PV, Turi JM (2005) Climate change in the context of multiple stressors and resilience Arctic. Arctic climate impact assessment scientific report, Cambridge University Press, Cambridge, 945–988
Mironenko O (2000) The ways of optimizing of land use and organization systems in reindeer trade-husbandry economies. Novosti Olenevodstva (Reindeer Husbandry News, in Russian)
Nieminen M, Kumpula J, Colpaert A (2002) Winter pasture resources of wild forest reindeer (Rangifer tarandus fennicus) in Salamajarvi area in central Finland. Proceedings of the 12-th nordic conference on Reindeer Research in Kiruna, Sweden, 11–13 Mar 2002
Nuttal M, Berkes F, Forbes B, Kofinas G, Vlassova T, Wenzel G (2005) Hunting, herding, fishing, and gathering: iondigenous peoples and renewable resource use in the Arctic. In: Arctic climate impact assessment, ACIA. Cambridge University Press, Cambridge, pp 649–690
Nuttal M, Forest PA, Mathiesen SD (2008) Background paper on adaptation to climate change in the Arctic. In: Snellmann O, Kullerud L, Lindstrom G, Ropstad BW (eds) Proceedings of the joint seminar uarctic rectors forum and the standing committee of parliamentarians of the Arctic regions. UArctic Publications Series 2. International Centre for Reindeer Husbandry. 17–21

Oskal A (2008) Old livelihoods in new weather: Arctic indigenous reindeer herders face the challenges of climate change. Development Outreach, World Bank Institute Special Paper, 22–25

Rees WG, Williams M, Vitebsky P (2003) Mapping land cover change in a reindeer herding area of the Russian Arctic using Landsat TM and ETM+ imagery and indigenous knowledge. Rem Sens Environ 85:441–452

Sandstrom P, Pahlen T, Edenius L, Tommervik H, Hagner O, Remberg L, Bisson H, Baer K, Stenlund T, Brandt L, Egberth M (2003) Conflict resolution by participatory management: remote sensing and gis as tools for communicating land-use needs for reindeer herding in Northern Sweden. Ambio 32(8):557–567

Tait AB, Hall DK, Foster JL, Armstrong RL (2000) Utilizing multiple datasets for snow-cover mapping. Rem Sens Environ 72:111–126

Tamstorf MK, Aastrup P (2002) Vegetation mapping of Westgreenland caribou ranges. Proceedings of the 12-th nordic conference on reindeer research in Kiruna, Sweden

Tape K, Sturm M, Racine C (2006) The evidence for shrub expansion in Northern Alaska and the Pan-Arctic. Glob Chang Biol 12:686–702

Tyler NJC, Turi JM, Sundset MA, Strøm Bull K, Sara MN, Reinert E, Oskal N, Nellemann C, McCarthy JJ, Mathiesen SD, Martello ML, Magga OH, Hovelsrud GK, Hanssen-Bauer I, Eira NI, Eira IMG, Corell RW (2007) Saami reindeer herding under climate change: applying a generalized framework for vulnerability studies to a sub-arctic social-ecological system. Glob Environ Change 17(2):191–206

Ulaby FT, Stiles EH, Abdelrazik MA (1984) Snowcover influence on backscattering from terrain. Trans Geosci Rem Sens GE-22:126–133

Vistnes I, Nellemann C, Jordhøy P, Strand O (2002) Infrastructure as barriers to wild reindeer migration. Proceedings of the 12-th Nordic conference on reindeer research in Kiruna, Sweden, 11–13 Mar 2002

Walsh NE, Fancy SG, McCabe TR, Pank LF (1992) Habitat use by the Porcupine caribou herd during predicted insect harassment. J Wildlife Manage 56(3):465–473

Wang C, Qi J, Moran S, Marsett R (2004) Soil moisture estimation in a semiarid rangeland using ERS-2 and TM imagery. Rem Sens Environ 90:178–189

Yurchak BS, Maynard NG (2005) Time-series SAR observations of Chukotka Sub-Arctic Lakes and Forest-Tundra Fire Scars. Proceedings of the 31st international symposium on remote sensing of environment, global monitoring for sustainability and security, Saint Petersburg, 20–24 Jun 2005

Chapter 9
Cumulative Effects of Rapid Land-Cover and Land-Use Changes on the Yamal Peninsula, Russia

Donald A. Walker, Bruce C. Forbes, Marina O. Leibman, Howard E. Epstein, Uma S. Bhatt, Josefino C. Comiso, Dmitri S. Drozdov, Anatoly A. Gubarkov, Gensuo J. Jia, Elina Kaarlejärvi, Jed O. Kaplan, Artem V. Khomutov, Gary P. Kofinas, Timo Kumpula, Patrick Kuss, Natalia G. Moskalenko, Nina A. Meschtyb, Anu Pajunen, Martha K. Raynolds, Vladimir E. Romanovsky, Florian Stammler, and Qin Yu

Abstract The Yamal Peninsula in northwest Siberia is undergoing some of the most rapid land-cover and land-use changes in the Arctic due to a combination of gas development, reindeer herding, and climate change. Unusual geological conditions (nutrient-poor sands, massive ground ice and extensive landslides) exacerbate the impacts. These changes will likely increase markedly as transportation corridors are built to transport the gas to market. Understanding the nature, extent, causes and consequences (i.e., the cumulative effects) of the past and ongoing rapid changes on the Yamal is important for effective, long-term decision-making and planning. The cumulative effects to vegetation are the focus of this chapter because the plants are a critical component of the Yamal landscape that support the indigenous Nenets people and their reindeer and also protect the underlying ice-rich permafrost from melting. We are using a combination of ground-based studies (a transect of five locations across the Yamal), remote-sensing studies, and analyses of Nenets land-use activities to develop vegetation-change models that can be used to help anticipate future states of the tundra and how those changes might affect traditional reindeer herding practices and the thermal state of the permafrost. This chapter provides an overview of the approach, some early results, and recommendations for expanding the concept of cumulative-effects analysis to include examining the simultaneous and interactive effects of multiple drivers of change.

D.A. Walker (✉)
Department of Biology and Wildlife, Institute of Arctic Biology, Alaska Geobotany Center, University of Alaska Fairbanks, AK 99775-7000, USA
e-mail: dawalker@alaska.edu; ffdaw@uaf.edu

G. Gutman, A. Reissell (eds.), *Eurasian Arctic Land Cover and Land Use in a Changing Climate*, DOI 10.1007/978-90-481-9118-5_9,

9.1 Introduction

9.1.1 Impending Changes to the Yamal Peninsula

Although the Yamal Peninsula is currently one of the most remote regions on the planet with few roads, no major cities, largely intact natural ecosystems, and indigenous people who still live a nomadic lifestyle, it is poised for some of the most dramatic changes in any area of the Arctic (Fig. 9.1). Four major forces are combining to make this a "hot spot" of rapid change: an impending gas-development boom, rapid climate change, an unusually sensitive permafrost environment, and the rapid growth of the populations of gas workers, the indigenous Nenets and their reindeer herds. We address each of these separately in this report, but we are most interested in the combined effect of all four. This chapter focuses on the Yamal, but the approach should be of wide value in many other areas of the Arctic where similar forces of change are occurring (for example see Chapter 8, this volume). The goal is to develop predictive models and tools that can be used to help the indigenous people and other stakeholders in the Arctic to plan for and adapt to future change.

Fig. 9.1 Nenets reindeer herder passing a gas derrick in the Bovanenkovo gas field, Yamal Peninsula, Russia. The presence of the gas field provides both economic opportunities for the Nentsy and a source of conflict because of competition for land and barriers created by roads and pipelines during the annual migrations. Climate change could enhance the growth of shrubs, also shown in the figure, and change the character of the reindeer pasture lands (Copyright and reproduced by permission of Bryan and Cherry Alexander)

9.1.2 Description of the Yamal

Yamal is a Nenets term for the "end of the land", which is fitting for this long tundra-covered finger of land that juts into the Arctic Ocean (Fig. 9.2); the peninsula stretches roughly 700 km from the Arctic Circle (66° 33.5′ N) in the south to Ostrov

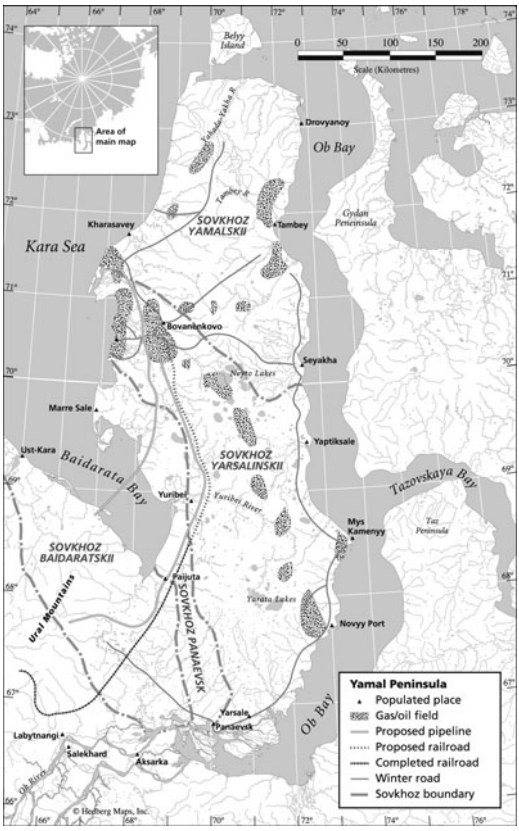

Fig. 9.2 Yamal Peninsula and associated gas and oil fields, with existing planned transportation corridors. The main existing gas field is at Bovanenkovo (From Forbes 1999a with permission of the editors of *Polar Research*)

Belyy (White Island, 73° 20′ N) at the tip of the peninsula. It is bounded on the west and north by the Kara Sea and on the east by the embayment of the Ob River. The peninsula is about 150 km wide with an area of 122,000 km^2 (somewhat larger than Pennsylvania or North Korea). This flat to gently rolling plain consists of a series of mainly marine, lacustrine, and alluvial deposits; the oldest deposits are in the interior parts of the peninsula at elevations between 45 and 90 m and were deposited more than 130,000 years ago; most of the peninsula consists of younger sediments deposited during and following the last glacial maximum (ca. 30,000–12,000 years ago). The deposits are sandy to clayey, most are saline within the permafrost, and some are saline in the active layer (the layer of soil above the permafrost that melts annually). Hilltops in sandy areas are often windblown with sand hollows, some covering large areas. Low areas between the hills are often occupied by polygonal peatlands. The peninsula was unglaciated during the last glaciation and supported Pleistocene (from 2.588 million to 12,000 years BP covering the world's recent period of repeated glaciations) plants mammals and humans throughout the glaciation and into the Holocene (ca. 12,000 years ago to the present) (Forman et al. 1999).

Politically, the peninsula is the northern part of the Yamal-Nenets Autonomous Okrug (YNAO), a high-level administrative district within Russia. The YNAO is situated east of the Ural Mountains and the northern part of the geographic border between Europe and Asia. The YNAO is 730,300 km^2 or about 1.5 times the size of France, and has a population of only about half a million people most of which are concentrated in cities in the southern part of the okrug that have grown rapidly in response to the discovery of oil and gas in the region, starting in the 1960s. The Yamal Peninsula itself is entirely within the Yamal'skii Raion (district), one of seven administrative districts within the YNAO, and is very sparsely populated; most of the population consists of nomadic Nentsy (see Section 9.4), who use the peninsula as pasturelands for their large reindeer herds (Stammler 2005).

9.2 Study Goals and Approach

This study is intended to contribute to the large questions regarding the future of the Nentsy and their reindeer. How will the indigenous people and their herds be affected by the simultaneous major changes associated with climate warming, industrialization, and the growth of their own herds (Forbes 1999a, 2008)? The major foci of our study are the linkages between the vegetation, natural and anthropogenic disturbance factors, climate, sea-ice concentrations, land-surface temperatures, and other landscape variables. A principal goal is to develop better, more far-looking tools to project the cumulative effects of resource development, climate-change, and traditional land use by combining scientific and traditional knowledge of the landscapes, socio-economic analyses, remote sensing, climate change analyses, and vegetation-change models.

9.2.1 Information from Previous Studies

The project is a collaboration of investigators from three primary groups: (1) the Earth Cryosphere Institute (ECI), Moscow, (2) members of the Environmental and Social Impacts of Industrialization in Northern Russia (ENSINOR) project at the Arctic Centre in Rovaniemi, Finland, and (3) US investigators who are part of this NASA-funded Land-Cover Land-Use Change project.

The Russian and Finnish investigators have worked in the Yamal region for many years; they are providing key background information and are collaborating in all aspects of this ongoing research. Our aim is the co-production of knowledge, in concert with the Yamal-Nentsy to assess the overall cumulative effects – both positive and negative – from past resource exploration, reindeer herding, and climate change.

9.2.1.1 ECI Baseline Studies

Researchers from the Earth Cryosphere Institute have been studying permafrost, vegetation and land processes on the Yamal Peninsula since the early hydrocarbon

exploration in the region in the 1970s. In the process, they have developed extensive climate and geocryological spatial data bases for much of West Siberia and northern Russia (Melnikov 1998; Minikin et al. 2001; Drozdov et al. 2005), and considerable field knowledge about the key sites along the Yamal transect. The ECI studies are coordinated with numerous international IPY programs and other Russian integrative and regional programs that are aimed at assessing changing permafrost conditions in Russia. The ECI colleagues are the principal collaborators for the field research in this project involving analysis of climate, vegetation, permafrost, and environmental variation along the Yamal climate transect (see Section 9.5). This knowledge foundation is essential to these cumulative effects studies.

9.2.1.2 ENSINOR Project

The ENSINOR project was funded by the Academy of Finland in 2004–2007 to make comparative case studies of oil and gas activities in two key federal districts – the Nenets Autonomous Okrug (NAO) and the Yamalo-Nenets Autonomous Okrug (YNAO) (Stammler et al. 2009). The ENSINOR project is providing key background information on the Nentsy, their reindeer and historical vegetation and landscape changes that have occurred in the Bovanenkovo gas field and elsewhere on the Yamal (Forbes 1999b, 2008; Forbes and Stammler 2009). These districts contain Russia's most productive proven energy sources for the present and the foreseeable future and so are particularly important to the energy security of Europe. As major clients and/or partners of Russian oil and gas companies, Finland, Norway and other Western European countries have responsibilities to see that the developments proceed in a manner that minimizes negative impacts to the landscapes and indigenous people in the affected areas. The ENSINOR project, conducted mainly by the Arctic Centre at the University of Lapland in Rovaniemi, Finland, undertook a thorough multidisciplinary analysis of the social and environmental consequences of energy development in the study region. This study incorporates knowledge that stems from different traditions among both scientists and herders and their respective ways of knowing about contemporary social-ecological systems.

9.2.2 Field Research

One objective of the project is to quantify variations in the natural zonal vegetation and associated biophysical properties across the bioclimate gradient on the Yamal Peninsula, which has vegetation representative of four of the five circumpolar tundra bioclimate subzones[1] contained on the Circumpolar Arctic Vegetation Map

[1]The Arctic bioclimate subzones are defined by key plant growth forms, species limits and mean July temperatures (MJT): Subzone A: cushion-forb, *Saxifraga oppositifolia*, MJT <3°C. Subzone B: prostrate-dwarf-shrub, *Dryas integrifoli*a, 3°C < MJT <5°C. Subzone C: hemiprostrate-dwarf-shrub, *Cassiope tetragona*, 5°C < MJT <7°C. Subzone D: erect-dwarf-shrub, *Betula nana/exilis*, 7°C < MJT <9°C. Subzone E: low-shrub, *Alnus viridis,* 9°C < MJT <12ºC (Walker et al. 2005).

(Walker et al. 2005, 2008b) plus the northern boreal forest. Ground observations are being conducted at five locations representative of the subzones during field campaigns in 2007–2009. The locations were chosen to be representative of the zonal soils and vegetation, but also include variation regarding substrate (clayey vs. sandy soils) at each location. Usually this means sampling sites of different geologic age at each location. From north to south, the locations for the ground observations are Ostrov Belyy (subzone B, Kharasavey (subzone C), Vaskiny Dachi (near Bovanenkovo, subzone D), Laborovaya (subzone E), and Nadym (northern boreal forest)) (Fig. 9.2).

A data report summarizing the 2007 field information includes general descriptions of each locality and sample sites with photographs, maps of the study plots, and transects, summaries of sampling methods used, vegetation data (species lists, species cover), leaf-area index (LAI), Normalized Difference Vegetation Index (NDVI), soil data (profile descriptions and chemical and physical soil properties), and active-layer depth (Walker et al. 2008a).

9.2.3 Modeling Studies

The modeling approaches are highlighted in another chapter in this book (Chapter 2, this volume) and are only described briefly here. At the global scale, we use the BIOME4 iteration of the BIOME series of models to examine projected shifts of tundra types in the tundra biome as a result of climate change (Prentice et al. 1992; Kaplan et al. 2003). The BIOME models incorporate biogeography and biogeochemistry into a mechanistically-based equilibrium approach that essentially redistributes vegetation types geographically based on a new environment. BIOME4 adds three arctic plant functional types to the nine plant functional types simulated in BIOME3. Driven by General Circulation Model (GCM) output, the BIOME4 model projects a northward migration of the boreal evergreen forest at the expense of arctic tundra, as well as the expansion of erect shrubs to displace prostrate shrubs. A more comprehensive analysis using BIOME4 predicts that the boreal forest extent will increase by 55% and that the arctic tundra extent will decrease by 42%, with a 60% loss of prostrate dwarf-shrub tundra (Kaplan and New 2006).

Another model, ArcVeg (Epstein et al. 2000), uses the results from the Yamal field studies and a comparable transect in North America to predict the long-term dynamic changes in biomass for plant functional types growing within five bioclimate subzones of the Arctic. A modified version of ArcVeg (Epstein et al. 2007) is being used to model the effects of changes in summer temperature, different reindeer foraging regimes, rate of succession following denuding of the land, and responses on different soil types. The model uses a set of twelve plant functional types for five arctic subzones that range from the coldest areas at high latitudes to the relatively warm Low Arctic near tree line. We also assume that for the Yamal region, the managed reindeer graze and trample the range more intensely and more frequently than do caribou of North America. Frequent grazing also increases the interannual

variability in tundra primary productivity. In the final year of the project, we will incorporate the soil data from the Yamal into the model, improve the reality of the grazing subroutine, add a component that will examine succession on barren mineral soils, and conduct a rigorous sensitivity analysis of the effect of grazing on tundra productivity and functional type composition.

9.3 Gas Development

9.3.1 Overview

Oil and gas development is having large positive and negative economic, social, and environmental consequences in localized areas of Arctic North America, Russia, and Scandinavia, and these consequences will grow in the near future as resource extraction in these regions accelerates (Vilchek 1997; Walker 1997; NRC 2003; Forbes 2004). A 2050 scenario developed by the United Nations Environment Program (UNEP) Global Methodology for Mapping Human Impacts on the Biosphere (GLOBIO) project estimated that with the same growth rates of industrial development that occurred between 1940 and 1990, 50–80% of the Arctic will be accessible by expanding road networks and infrastructure by 2050 (UNEP 2001).

The Yamal Peninsula contains the largest known untapped gas reserves in Russia; several major hydrocarbon deposits were discovered on the Yamal Peninsula in the 1980s, and there are now 200 known gas fields (Gubarkov 2008) – the largest ones are shown in Fig. 9.2. Yamal gas deposits contain 13.5 trillion m^3 of proven gas reserves on land, and an estimated 50 trillion m^3 with additional deposits on the Kara Sea shelf. The deposits near Bovanenkovo, Kharasavey and Novy Port are estimated to contain 5.8 trillion m^3 of gas, 100.2 million metric tons of gas condensate, and 227 million metric tons of oil. The gas deposits of Yamal will contribute considerably to the World production. Proven Yamal reserves are close to the combined reserves of North America (7.5 trillion m^3) and South America (7.1 trillion m^3) (Gubarkov 2008).

The YNAO is Russia's top gas producing region – as of 2003 it accounted for about 25% of the total world gas production and one-fifth of the total revenue of the Russian government; however, the gas deposits of the Yamal Peninsula itself have remained untapped because infrastructure development was blocked due to unsolved ecologic problems in the 1980s and proceeded slowly during the time of political upheaval in Russia in the 1990s. During this time, the Russian government developed oil resources in more southerly parts of West Siberia, such as the Khanty-Mansiisky Okrug of Tyumen Oblast (Stammler 1998, 2005; Starobin 2008). To date, most of the major infrastructure on the Yamal Peninsula is in the giant Bovanenkovo gas field, where there is an extensive network of drilling sites, construction pads, and roads that began in 1987 (Vilchek 1997; Forbes 1999a, 2004). Russia is currently on the verge of approving development schemes on the Yamal Peninsula costing

billions of dollars. The Gazprom gas consortium has accepted the Yamal hydrocarbons transportation scheme of a main pipeline across the Baidarata Bay of the Kara Sea (Fig. 9.2). Four pipelines will transport 50–60 billion m^3 of gas each. A new road to the south and the Obskaya-Bovanenkovo Railway are under construction now. A cargo train operation is planned for in 2009 and passenger train service by 2011. There are plans to build an airport and river port in Bovanenkovo settlement. The seaport and fleet of vehicles are expanding in Kharasavey settlement as well. A network of winter roads between the various gas fields is estimated to be finished by 2020 (Gubarkov 2008).

Industrial activities and infrastructure on the Yamal Peninusula are currently concentrated in relatively small areas around the major gas deposits and along the railway/road corridor being constructed from Obskaya, near Labytnangi, to the Bovanenkovo Gas Field (70°17′ N, 68°54′ E). Outside these areas of relatively focused activity, there are many off-road vehicle trails and scattered signs of the exploration activities (Vilchek 1997; Forbes et al. 2001).

9.3.2 Land-Cover and Land-Cover Changes Within the Bovanenkovo Gas Field

Remote sensing and geographic-information-system (GIS) technology are being used to characterize the present-day distribution of vegetation and plant biomass and to catalog the changes to the landscape within the Bovanenkovo gas field and elsewhere on the peninsula. A combination of Advanced Very High Resolution Radiometer (AVHRR), Landsat Multi-Spectral Sensor (MSS), Landsat Thematic Mapper (TM), Satellite Pour l′Observation de la Terre (SPOT), Advanced Spaceborne Thermal Emission and Reflection (ASTER) TERRA, Quickbird-2, Corona and aerial-photo imagery are being used. A digital elevation model of the gas field was prepared from 1:100,000-scale topographic maps of the region. Details of the infrastructure (road network, pipeline network, off-road vehicle trails, construction pads, and quarries) were delineated on the remotely sensed images (Fig. 9.3). Comparison of the information that could be identified on each type of imagery showed that Quickbird multispectral imagery with 63-cm resolution gave results that were comparable and sometimes better than ground surveys (Table 9.1) (Kumpula et al. 2010; Kumpula 2008). For example, off-road tracks were easier to detect on the Quickbird imagery. All infrastructure pads, roads, pipelines, quarries and detectable off-road-vehicle trails were digitized and entered into a GIS of the region.

The total area covered by direct impacts including the footprint of the roads, pipelines and construction pads totals 9.3 km^2 (Table 9.2). The total perimeter of the gas field where there is restricted access to traditional pasturelands of the Nentsy is 448 km^2, or about 48 times the area of the planned impacts.

The extent direct impacts of the Bovanenkovo field can be compared to similar data from the North Slope of Alaska, where the giant Prudhoe Bay and Kuparuk oil fields are situated (NRC 2003) (Table 9.2). The total direct impacts of the North

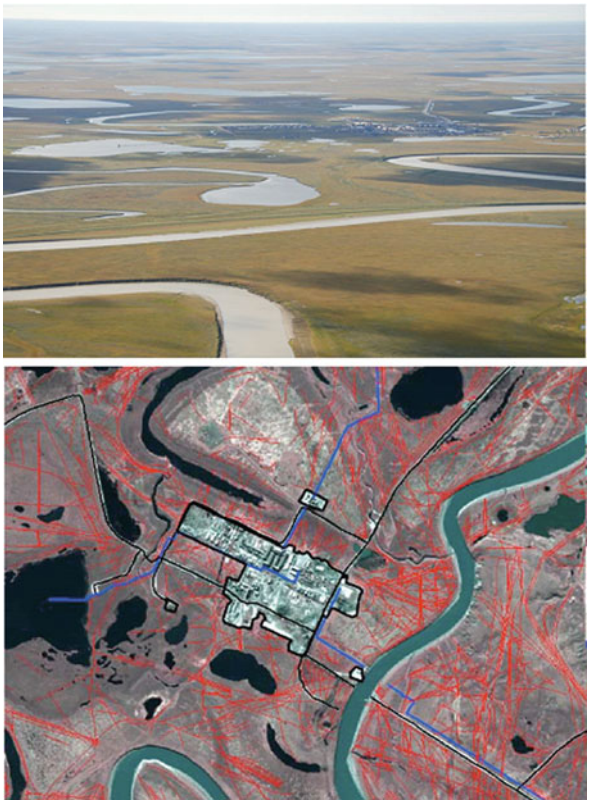

Fig. 9.3 (*top*) Landscape and main developed area in the Bovanenkovo gas field. Reproduced by permission of D.A. Walker. (*bottom*) Quickbird image of the main developed area. *Colored lines* were digitized for GIS analysis and show construction pads for buildings and storage and roads (*black*), pipelines (*blue*), and off-road vehicle trails (*red*). Reproduced by permission of Timo Kumpula

Slope cover about 6.7 times as much area as the Bovanenkovo impacts. The total extent of the areas affected by the North Slope development (defined by the perimeter of the field) is about 2,600 km^2, or about 5.8 times the extent of the Bovanenkovo field. There are about twelve times as many roads, ten times as much area covered by gravel pads, and six times as much area affected by quarries on the North Slope compared to the Bovanenkovo field.

Some indirect terrestrial ecological impacts associated with seismic surveys, off-road vehicle trails, pollution of pastures by trash and petrochemicals, road dust and disturbance from the roads and quarries can be assessed from the aerial images (Forbes 1995, 2004; Vilchek 1997). Additional related social impacts that are not visible on the images include exposure of herders to alcohol, feral dogs which can harass and kill reindeer, plus the spiritual and energetic toll from altered migration routes, driving herds across roads/railways, and the degradation of sacred sites, key fishing lakes and streams, and traditional camp sites (Forbes 2008; Forbes et al. 2009).

The available data indicate that the indirect impacts that are detectable on the available images at Bovanenkovo cover 8.8 times the area of the direct impacts

Table 9.1 Analysis of relative detectibility of disturbance features using different sensor methods. Reproduced with permission of Timo Kumpula

Impact type	Field survey	Quickbird-2 panchromatic	Quickbird-2 multi-spectral	ASTER TERRA VNIR	Landsat TM	Landsat MSS
Soil contamination, oil & chemicals	x	–	–	–	–	–
Removal of topsoil and vegetation	xxx	xxx	xxx	xx	x	x
Quarries	xxx	xxx	xxx	xxx	xx	x
Garbage						
– Metal	xx	–	–	–	–	–
– Glass	x	–	–	–	–	–
– Concrete	xxx	x	x	–	–	–
– Wood	xxx	x	–	–	–	–
Pipelines	xxx	xx	x	–	–	–
Powerlines	xxx	xx	x	–	–	–
Roads	xxx	xxx	xxx	xxx	x	x
Offroad tracks	xx	xxx	xx	xx	x	x
Winter roads	xx	xx	xx	xx	x	–
Drill towers	xxx	xxx	xx	x	–	–
Barracks	xxx	xxx	xx	x	–	–
Trucks/vehicles	xx	xx	x	–	–	–
Changes in hydrology	xxx	xxx	xx	xx	x	x

(direct: indirect = 7.1: 62.4 km^2; Table 9.2). On Alaska's North Slope, the documented indirect impacts cover about a third of the area of the direct impacts (24: 9.3 km^2; Table 9.2). However, the data sets are not totally comparable because different methods were used to determine indirect impacts – high-resolution Quickbird satellite images were used in the Bovanenkovo field, whereas historical

Table 9.2 Extent of Bovanenkovo gas field impacts (modified from Kumpula 2010) compared to extent of the North Slope, Alaska oil development (NRC 2003)

	Area (Length) km^2 (km)	
Impact type	Bovanenkovo	North Slope
Direct impacts:		
Roads	2.9 (79)	12.0 (954)
Airstrips	0	1.1
Gravel pads	2.1	23.5
Quarries	4.3	25.8
Off-shore gravel placement	–	0.6
Total direct impacts	9.3	62.4
Other affected area (includes peat roads, disturbed areas around pads, tractor trails, major off-road vehicle trails)	24	7.1
Total extent of field (perimeter, including currently enclosed unimpacted areas)	448	2,600

high-altitude aerial photographs were used on the North Slope (see also Forbes et al. 2009, Table S1). Also, the nature of the off-road-vehicle trails are different in both areas – in northern Alaska, specially designed vehicles with low-pressure tires have created extensive networks of off-road trails that are difficult to detect on the available images and were not quantified in the US National Research Council data (NRC 2003). Despite these differences, ground observations in both areas indicate that there is a relatively relaxed regulatory environment on the Yamal compared to that in northern Alaska. Transport on the Yamal tundra has legally not been allowed in summer since 1989, but this restriction is routinely ignored, resulting in extensive surface disturbance. More recent construction methods have reduced but not eliminated the extent of these types of disturbance.

The extent of developed areas on the Yamal Peninsula will rapidly increase as the Bovanenkovo field is brought into production and additional gas fields are developed. Big questions remain regarding how to minimize disturbance and remediate impacts when they do occur.

9.3.3 Geological Factors Contributing to Landscape Sensitivity

9.3.3.1 Sand Deposits

Two major geological factors add to the sensitivity of the Yamal landscapes to disturbance. First, much of the region is covered by eolian and alluvial sand deposits that have been dated to 30,000–12,000 years ^{14}C B.P. in the vicinity of Marresale (Forman et al. 2002). Although peat accumulation has occurred throughout most of the Holocene, there has been considerable recent reactivation of these sands starting about 1,000 years ^{14}C B.P., that is thought to reflect abundant sand from denuded hilltops associated with heavy reindeer grazing starting at about that time (Forman et al. 2002). Generally areas of active eolian activity are concentrated in the windier environments near the coast and where reindeer are most frequent. The animals focus on hilltop areas where lichen cover is the greatest and snow cover is at minimum.

Once exposed by disturbance, the nutrient-poor sands are difficult to re-vegetate (Forbes and McKendrick 2002). This has implications for both infrastructure construction and reindeer-herding activities. Large sand quarries are mined for construction and these are difficult to stabilize and re-vegetate (Fig. 9.4, top). The sands are also exceedingly poor material for constructing roads, which require constant maintenance, especially each spring after many sections of the roads wash away when the snow melts. As reindeer populations increase and the area available for forage is reduced by expanding infrastructure networks, this type of disturbance is likely to increase.

9.3.3.2 Massive Ground Ice and Landslides

Another important geological factor is the massive tabular ground ice that is common throughout the region. Ice deposits from <1 to >20 m thick are found in

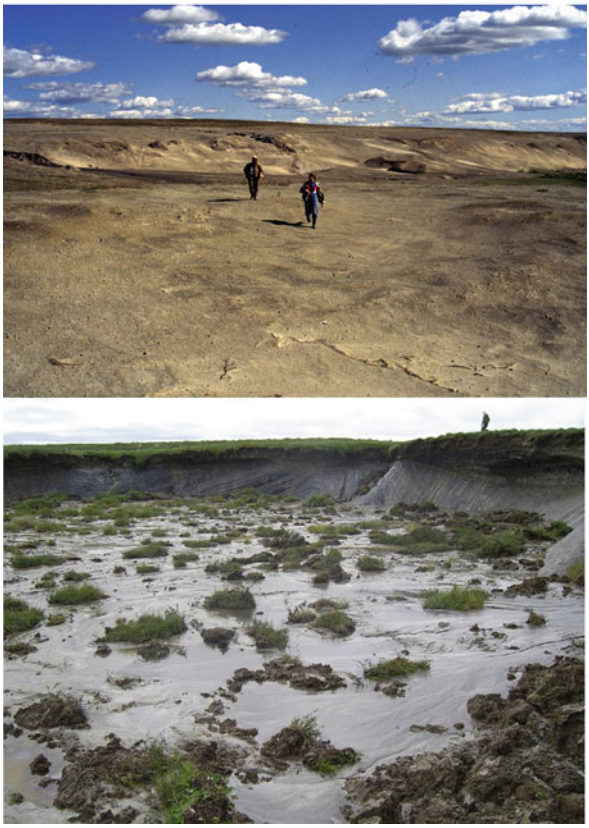

Fig. 9.4 Landscape factors that add to the sensitivity of the Yamal to disturbance. (*top*) Barren sand quarry, near Obskaya. The sandy nutrient-poor soils are common in the region and are difficult to revegetate, especially in the more northern bioclimate subzones. Photo by Bruce Forbes. (*bottom*) Thawing permafrost and earth flow in Central Yamal within the designated corridor of the pipeline. Note tabular ice beneath organic soils along the headwall of the slide area. Reproduced by permission of Marina Leibman.

thousands of boreholes at various depths from a few to dozens of meters (Dubikov 2002). This ice occurs at the interface between salty marine clay and overlying sandy sediments (Streletskay and Leibman, 2003). The origin of this ice is not entirely clear (Leibman 1996). If the overlying deposits are removed or thermal and hydrologic conditions are changed sufficiently, the ice-rich sediments are liquefied and landslides occur, exposing underlying clay-rich and salty marine sediments that are within and beneath the ice (Leibman and Kizyakov 2007). Slope failures resulting from thawing of ice-rich permafrost often occur, forming earth flows consisting of meltwater mixed with mineral and organic material (Fig. 9.4, bottom). The landslides resulting from thawing of tabular ground ice is hazardous for infrastructure construction.

Landslide disturbances are so common on the Yamal Peninsula that they dominate the landscape in many areas. In August 1989, 400 new landslides occurred within an area of 10 km^2, where previously there were only three modern landslides (but hundreds of ancient landslides). This was in response to an abnormally wet year. During the last two warm summers (2006–2007) several new areas of tabular

ground ice were exposed by landslide activity. So both abnormally wet and abnormally warm years can trigger major landslide events. Five of the older landslides near Bovanenkovo were dated to be 300–2,000 years old (Leibman and Kizyakov 2007).

The landslides totally change the substrates available for plants. A striking aspect of the vegetation of the central Yamal region is the abundance of willow thickets (*Salix lanata* and *S. glauca*) that cover many hill slopes and valley bottoms (Ukraintseva 1998) (Fig. 9.5). Climatically, Bovanenkovo is in bioclimate subzone D where the typical zonal vegetation is low-growing sedges, dwarf shrubs, and mosses (including *Carex bigelowii, Vaccinium vitis-idaea, Salix polaris, S. phylicifolia, Betula nana, Hylocomium splendens, Aulacomnium turgidum*). Normally in subzone D dense shrublands are found mostly along streams and in association with anthropogenically disturbed sites, places where there are abundant nutrients and warmer soils.

Studies of the willow communities in relationship to landslides have included: (a) vegetation succession, (b) ash chemistry of each vegetation group, (c) ground water chemistry, and (d) plant and soil chemistry using water extraction and X-ray–fluorescent analyses of air-dry and homogenized plants (Ukraintseva 1997, 1998; Ukraintseva and Leibman 2000, 2007; Ukraintseva et al. 2000, 2002, 2003). There is a strong correlation between disturbance age, soil fertility, and willow growth. The soil of stable hilltops is characterized by low acidity (pH 5.5–5.8), very low base saturation (4.5%), low nitrogen content (0.08–0.18%), and rather high organic carbon (1.5–2.3%); whereas, recent landslide surfaces have high soil pH (7.5–8.0), much higher base saturation (50–100%), and low organic carbon content (0.2–0.7%). Desalination of old marine sediments after the landslide events leads to soil enrichment with water-soluble salts, which supply plants with nutrition, provide

Fig. 9.5 Shrubby vegetation (*Salix lanata* and *S. glauca*) occurs on an old landslide surface that flowed from the foreground into the right middle background. A more recent 1989 landslide occurred behind the standing figure and is being naturally revegetated mainly by grasses and forbs (e.g., *Deschampsia* sp., *Poa alpigena*, *Puccinellia sibirica*, *Phippsia concinna*, *Tripleurospermum hookeri*). Reproduced by permission of D.A. Walker

active re-vegetation of herbs, and re-formation of soils, followed by willow-shrub expansion.

Tall willow thickets occupy old landslide surfaces due to additional nutrients and especially where there is enhanced (but not the deepest) winter snow cover. On 1,000–2,000-year old landslides, soils showed gradual reduction in pH (down to 6.5) and base saturation (down to 24.5%) that indicate continuing desalination of the active layer deposits towards the background conditions. Organic carbon and nitrogen concentrations in the older soils were double those of recent landslide surfaces. The chemical composition of the plants is also related to the age of the landslide surface. The plants growing on the landslide surfaces had higher nutrient content. Concentrations of carbon (C) and nitrogen (N) increase with age of the landslides, and trace elements in willow branches essentially follow an age sequence with the highest values in the modern slides, followed by old and then ancient landslides and finally willows growing on stable surfaces (Ukraintseva and Leibman 2000). The nutrient content of plants growing on landslides is also an important consideration for forage quality for reindeer.

9.4 Reindeer Herding

Amidst the ongoing rapid industrial expansion at the dawn of the twenty-first century, the Yamal Nenets continue to migrate with their reindeer much as they have for countless generations, cued by – among other things – the cyclic greening and senescing of tundra vegetation, the melting and re-freezing of ancient rivers, and the appearance and disappearance of biting insects. There is archaeological evidence that these migrations have been taking place for at least 1,000 years, perhaps significantly longer (Stammler 2005). Some of the Nentsy travel over linear migration routes from the forests south of peninsula to the summer pastures on Kara Sea coast and back – up to 1,200 km (Fig. 9.6). These remarkable migrations occur annually between the beginning of April and the end of December and are described by Florian Stammler, who in 2000–2001 lived and traveled with a group of herders and their families (Stammler 2005). Other groups of Yamal Nentsy, mainly in the northern part of the Yamal, have shorter more circular migration routes and stay year round on the tundra (Fig. 9.6).

The Yamal region is currently the top reindeer herding area in Russia. Approximately 5,000 nomadic indigenous Yamal Nentsy live on the Yamal migrating with about 290,000 reindeer. The proposed massive new development schemes would significantly affect the social-ecological systems of the Nentsy (Forbes et al. 2004, 2009; Stammler and Wilson 2006; Forbes 2008; Forbes and Stammler 2009). The steady increase of reindeer as well as humans living on the tundra, mainly gas workers but also Nenets, is exceptional. This has resulted in increased use of natural resources, such as heavy spring to autumn grazing over most of the reindeer pastures and unsustainable fishing practices in lakes and rivers accessible to gas workers.

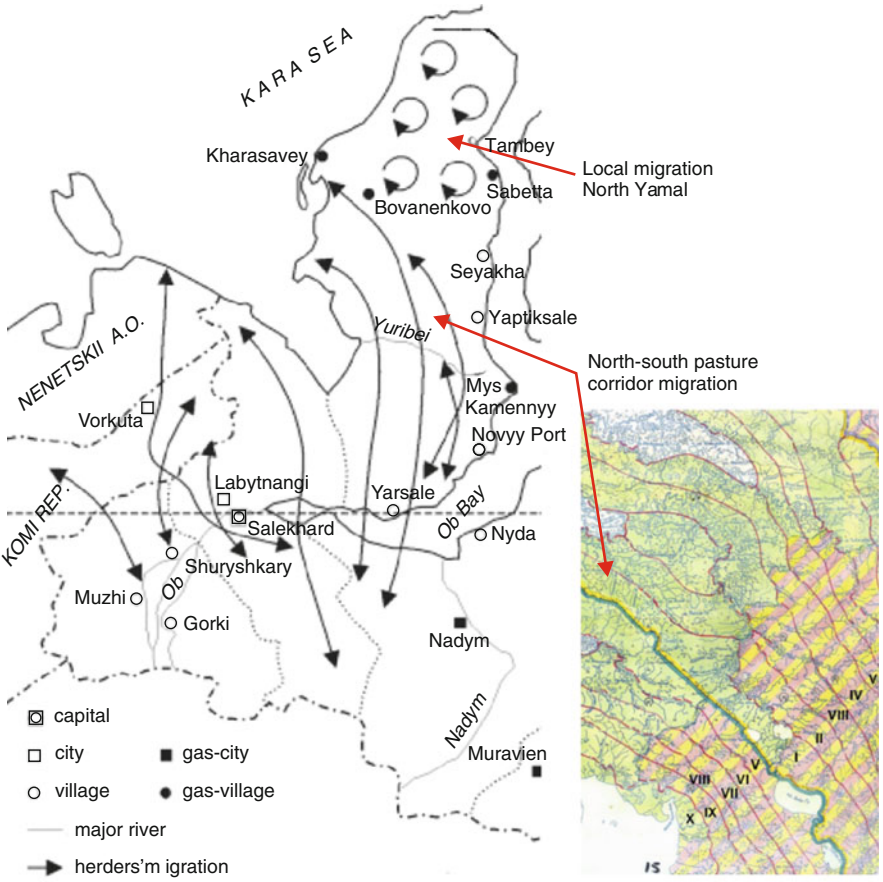

Fig. 9.6 (*left*) Current land-use patterns for Nentsy who use corridor (linear) migration routes in the southern and western part of the Yamal region (two headed *arrows*) and local (*circular*) migration patterns in the northern part of the Yamal Peninsula (*circular arrows*). (*right*) *Red lines* delineate corridors for brigades. Brigade numbers in each corridor are shown by Roman numerals. Brigade corridors IV and VIII pass through the Bovanenkovo gas field. Reproduced by permission of Florian Stammler

Many regions across Russia experienced a near total collapse of reindeer herding after the demise of the Soviet Union. Yet, within the North and Far East, there is a general sense that Yamal has faired quite well compared to other regions (Stammler 2005; Forbes 2008). There are many positive social and economic effects of development, including access to health care, extensive support for urban-based populations, jobs, and the possibility to barter or pay cash for goods on the tundra during migrations. Helicopter transport and relations between oil and gas workers and reindeer herders are central aspects of life on the tundra. Overall, reindeer herders continue to be mostly in favor of the ongoing gas development, although as the development accelerates they wish to be more carefully consulted about plans for

new infrastructure and to receive appropriate compensation for lost pastures and access for migrations (Stammler et al. 2009; Forbes et al. 2009). For example, two brigades that traditionally used the Bovanenkovo region for their summer pasturelands now avoid these areas and have lost 22 and 25% of their total summer pasturelands due to the presence of the gas development (Kumpula et al. 2010). It is predicted that 165 families of nomadic Nenets people will move to live in the settlements as a result of reduction of the pastures, and 286 families will have to change the pasture routes for the same reason. Experts estimate that expenses exceeding several billion dollars are needed to minimize negative impact of development on the human life and disturbed environments by 2011. Both herders and scientists have cited the ongoing gas field infrastructure development and destruction of vast areas of pastures as extremely important issues for the future of reindeer herding in the region.

Nenets reindeer herders whose migration routes intersect the most intensive areas of infrastructure development participated in a study pertaining to land-cover changes that have occurred over the past 30+ years. Their participation in the earlier ENSINOR project was through group and individual interviews with members of three herding brigades to document local knowledge of plant-animal-climate interactions in the vicinity of Bovanenkovo, where both hydrocarbon-related activities and reindeer grazing/trampling exert important controls over vegetation (Fig. 9.7). Herders participated in interviews along the course of the Yamal migration. The interviews included presentation of a set of "what if" scenarios of projected changes, leading to discussions of the implications of these changes to land-cover and land-use changes, reindeer herding and traditional ways of life for the Nentsy.

Fig. 9.7 Florian Stammler interviewing a Nenets family. In addition to taking part in the daily life and experiencing how the reindeer and fishing resources were managed, the combined anthropology and ecology research teams conducted semi-structured interviews that were recorded on digital media or film. Very high-resolution satellite imagery of the areas helped to focus the discussions on specific places and features that the herders recognized easily. Photo by Bruce C. Forbes

Fig. 9.8 Reindeer herding and effects: (**a**) Nenets brigadier and children playing volleyball in front of herded reindeer. Animals are often concentrated in small areas for selection of animals for sled teams and other purposes. (**b**) Barren area due to trampling caused by concentrated reindeer activity. (**c**) Grassification – replacement of typical shrub tundra vegetation with grassland (foreground) following heavy grazing and trampling. The Nenets camp in the background is that of a brigade. Four to 12 herders with their families travel together in a brigade, usually moving camp every 2–3 days. Each tepee-like structure (chum) houses 1–2 families. (**d**) Wind erosion in sandy areas aggravated by heavy trampling by reindeer. Photos by Bruce C. Forbes

The reindeer exert important controls over the structure and function of the Yamal tundra. When the animals are concentrated in small circumscribed areas on organic substrates, dense graminoid swards can develop (grassification) (Fig. 9.8a–c). These can be seen in and around campsites and along migration routes. On well-drained, sandy substrates with minimal organic content, concentrated trampling can thin and eventually break through the otherwise closed vegetation mat, leading to erosion via deflation (Fig. 9.8d). Perhaps most significant to the vegetation is the projected simultaneous reduction in available pasturelands due to infrastructure expansion and the increases in the Nenets and reindeer populations that will make heavy demands on the pasturelands in the future. Between 1981 and 2004, the number of nomadic households on the Yamal Peninsula increased from 693 to 964, and the number of private reindeer (excludes state-owned collectives) has increased about three fold from about 54,000–158,000 (Stammler 2005 77–78).

9.5 Climate-Vegetation Relationships

Climate change is another factor affecting ecosystems across the Arctic (ACIA 2004). The very extensive retreat of the summer sea-ice in 2007 alerted scientists to the possibility of a summer-ice free Arctic within this century (Stroeve et al. 2007; Nghiem et al. 2007; Comiso et al. 2008). More open water during the summer in the Arctic will very likely lead to increased flow of heat to the land (Lawrence et al. 2008). The expected changes include changes in vegetation, thawing permafrost, changes in soil characteristics, and changes in the habitat and migration characteristics of the fauna. It is hypothesized that an earlier ice-melt forces atmospheric and land-surface temperatures changes, leading to increased summer warmth and enhanced greenness of vegetation. Increased vegetation greenness has been noted in some areas of the Arctic such as northern Alaska and is attributed to warmer summer temperatures and the expansion of shrub vegetation (Jia et al. 2003; Chapter 2, this volume; Tape et al. 2006; Walker et al. 2009; Forbes et al. 2010). The warming temperatures are also affecting permafrost temperatures leading to local thaw, subsidence, and altered hydrological regimes (Romanovsky and Osterkamp 2001; Hinzman et al. 2005).

Some of the critical questions related to climate change involve how are the changing sea-ice regimes related to changes in vegetation and permafrost regimes. For example, if winds become stronger or precipitation decreases or temperatures increase, wind erosion of sandy surface deposits would become more common. On the other hand if summer precipitation increases, landslides may become more frequent, and shrubby tundra would probably cover larger areas of the peninsula. Shrubs also would likely generally increase if the climate warms. The increased cover and height of shrubs would likely trap more snow in the landscape. Perhaps most critical to the Nentsy is the possibility of increased frequency and severity of winter thaws when melt water in the snowpack refreezes at the soil surface to form a hard "ice shield" that acts as a barrier to reindeer seeking the underlying vegetation (Stammler 2005; Bartsch et al. 2010).

9.5.1 Spatial Distribution of Vegetation Productivity (NDVI)

A question in the present analysis is how would a warming climate contribute to the expected changes in plant production as manifested by NDVI? In most of the Arctic, NDVI is strongly related to the amount of summer warmth available for plant growth (Raynolds et al., 2006, 2008a). We were interested in how the present distribution of NDVI on the Yamal Peninsula conforms to the general circumpolar pattern of decreasing NDVI with latitude (and decreasing summer warmth). Information for this analysis was extracted from a circumpolar GIS database containing a variety of landscape variables including dominant vegetation, elevation, landscape type, substrate type, land-surface temperatures, and percent lake cover. Much of the information came from the Earth Cryosphere Institute (Drozdov et al. 2005; Melnikov

and Minkin 1998; Minkin et al. 2001), and the Circumpolar Arctic Vegetation Map (Walker et al. 2005). The methods used in constructing the maps of land-surface temperature and maximum NDVI are described in Raynolds et al. (2008a).

Global tundra land-surface temperatures were calculated from AVHRR thermal data compiled from 1982 to 2003, providing the longest satellite temperature record available (Raynolds et al. 2008a). Daily differencing and moving window techniques were used to eliminate cloud-contaminated pixels (Comiso 2000, 2003). A constant emissivity value of 0.94 was used to calculate temperature from the thermal infrared channels.

As in Chapter 2, we used a Summer Warmth Index (SWI) to characterize the amount of warmth available for plant growth at the ground surface. This index combines the effect of both the length and the warmth of summer temperatures, and is the climate variable found to correlate well with variations in arctic plant diversity and biomass trends within the Arctic (Young 1971; Rannie 1986; Edlund 1990; Walker et al. 2005). This index characterizes the plant growing season by summing monthly mean temperatures that are greater than 0°C. The units of SWI are˚C mo, or thawing degree months.

Across most of the Arctic, from north to south, NDVI increases as summer land-surface temperatures increase. A regression of NDVI vs. the summer warmth index explains about 58% of the total variation in circumpolar NDVI values (Raynolds et al. 2008a). Given the rather strong north–south temperature gradient (Fig. 9.9a), the presence of four of the five Arctic bioclimate subzones along the Yamal Peninsula and the strong circumpolar correlation between NDVI with summer temperatures we would expect to see a similar strong trend in NDVI related to temperature on the Yamal (Fig. 9.9b). In fact the correspondence between NDVI and surface temperatures is rather weak on the Yamal (Fig. 9.10). Using the same data set as for the circumpolar analysis, surface temperature explains only about 22% of the spatial variation in NDVI on the Yamal Peninsula (Raynolds et al. 2008b). Most of the peninsula has higher NDVI values than would be expected from the global trends of NDVI-temperature relationships (Fig. 9.9c).

A General Linear Model analysis using data from a regional GIS (Fig. 9.11) revealed that temperature explains less than 2% of the total deviance in a data set containing many more variables than the simple NDVI-SWI regression (Raynolds et al. 2008b) (Table 9.3); 49% of the NDVI deviance is explained by a combination of elevation and landscape type (e.g., low plains with marine deposits, low plains with alluvial and lacustrine deposits, high plains with fluvial and lacustrine deposits, foothills, and mountains); another 9% is explained by substrate type (peat, clay, silt, sand) and broad vegetation categories from the Circumpolar Arctic Vegetation Map. The rather paradoxical positive correlation between NDVI and elevation (normally NDVI decreases with elevation in the mountains) is due to the geography of the Yamal Peninsula, where elevations increase toward the warmer southern part of the peninsula, and the uplands have dense dwarf-birch (*Betula nana*) plant communities with high NDVI values. The pattern of landslides and shrubs is undoubtedly a major control on the high NDVI patterns over much of the peninsula. Although individual landslides cannot be resolved at the scale of the maps, the areas of

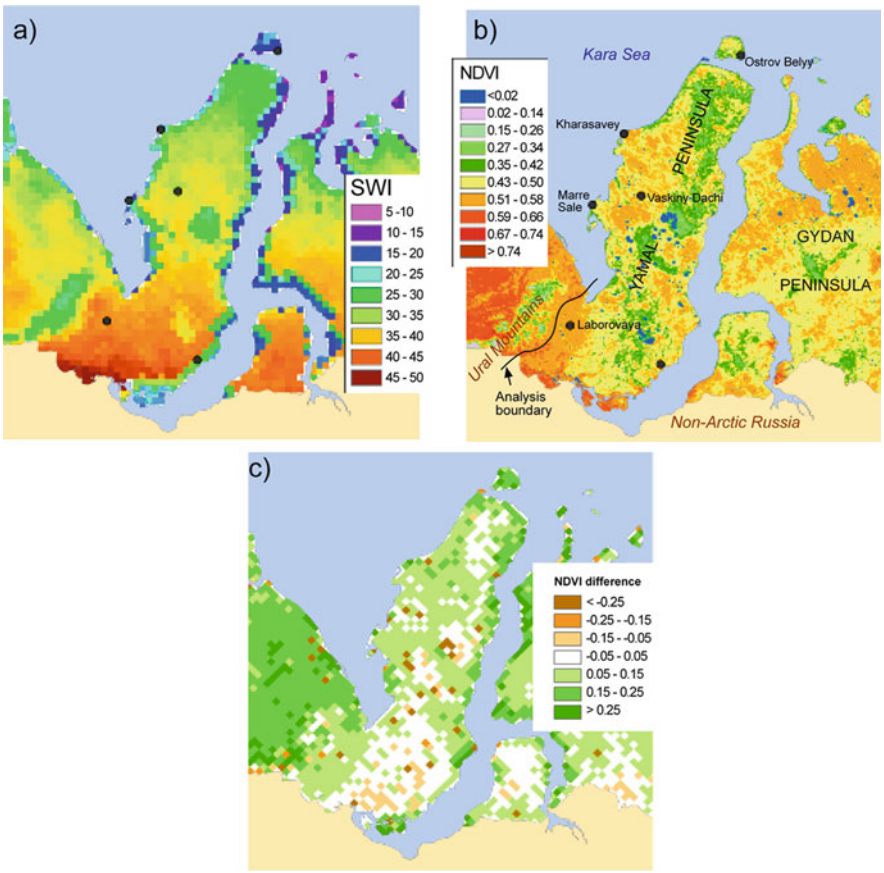

Fig. 9.9 Land-surface temperatures, NDVI, and NDVI on the Yamal compared to expected values from a global arctic land-surface temperature – NDVI relationship (Raynolds et al. 2008a). (**a**) Summer Warmth Index (SWI) is the sum of the mean monthly land-surface temperatures above freezing (1982–2003) as measured with the AVHRR thermal infrared bands. (**b**) Maximum NDVI of the Yamal region. (**c**) NDVI on Yamal compared with expected values based on global NDVI-surface-temperature relationship. Green areas are warmer than predicted by the regression model (Fig. 9.10) and brown areas are cooler. The southern boundary of the colored maps corresponds to tree line. Reproduced by permission of Martha Raynolds

higher-than-expected NDVI values tend to be concentrated on low marine plains and alluvial valleys that have been eroded into the sandy upland deposits. These areas have abundant cover of low-shrub vegetation that has developed on ancient landslides.

In summary, the NDVI on the Yamal Peninsula increases with warmer summer land-surface temperatures, but the relationship is not as strong as in the Arctic as a whole. Broad valleys with concentrations of marine clays have higher NDVI than upland areas dominated by sands. These trends are related to the distribution of ancient landslides and valley floors where willow thickets dominate.

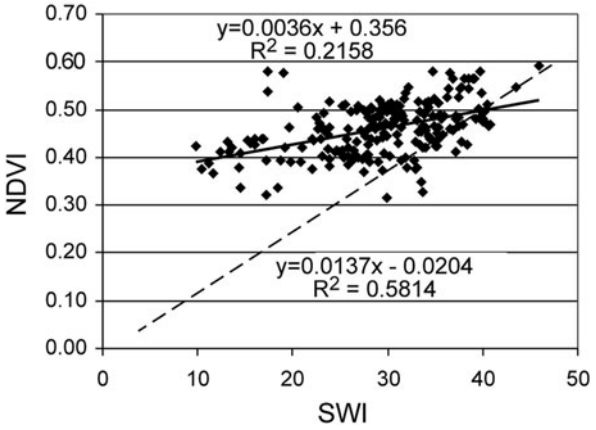

Fig. 9.10 Regression between NDVI and ground-surface temperatures as measured using the summer warmth index (SWI). *Solid line* and *dots* show the data from the Yamal region. *Dashed line* is the regression for the entire circumpolar region. Data points for the circumpolar regression line are not shown. Reproduced by permission of Martha Raynolds

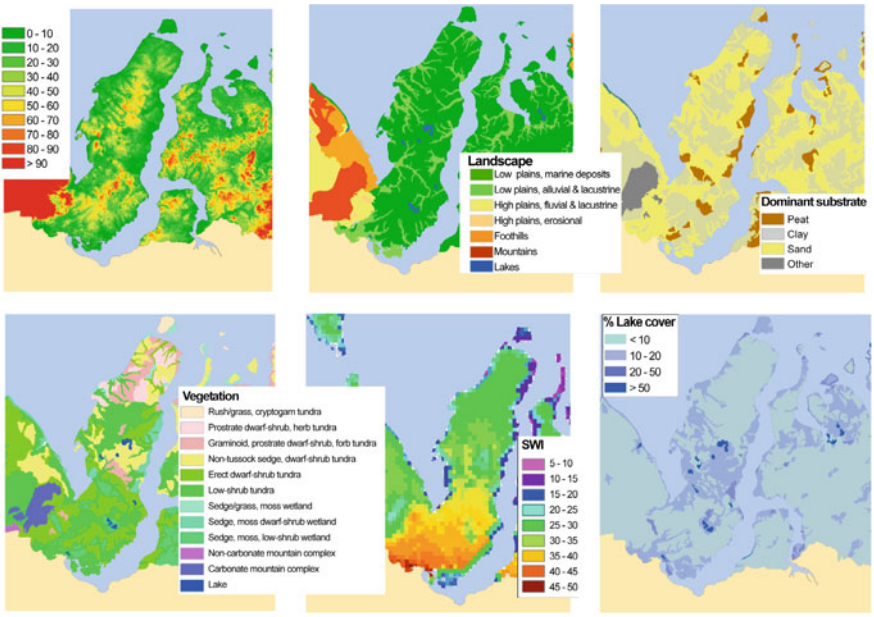

Fig. 9.11 Variables used in the general linear model to examine the NDVI relationships. Reproduced by permission of Martha Raynolds

Table 9.3 Results of general linear model analysis of NDVI compared to other variables in a geographic information system (Raynolds et al. 2008b)

GIS variable	Deviance	Residual deviance	Deviance accounted for (%)	Significance
Null		2.065		
Elevation	0.603	1.462	29.21	< 0.000000
Landscape	0.407	1.055	19.72	< 0.000000
Substrate	0.101	0.954	4.88	< 0.000000
Vegetation	0.088	0.865	4.29	0.000004
Land temp	0.039	0.827	1.87	0.000012
Lake area	0.032	0.794	1.57	0.000934
Total			61.55	

9.5.2 Temporal Changes in Sea-Ice Concentration, Land-Surface Temperatures, and NDVI

This portion of the study utilizes satellite-derived data to examine the recent trends in sea-ice distribution, land-surface temperatures (LST), and patterns of vegetation greening as indicated by the NDVI (Bhatt et al. 2007). We use ice-cover data derived from historical 25-km resolution Spectral Sensor Microwave Imager (SSMI) passive microwave data (Comiso 1999), AVHRR surface temperature data (Comiso 2006, 2003), and 8-km AVHRR-NDVI data (Tucker et al. 2005). The analysis employs data covering the 26-year period from January 1982 to December 2007. The sea-ice, LST, and NDVI trends were examined in a 50-km terrestrial region seaward and landward of the Arctic coastline in the Yamal/Kara Sea region. These relationships are compared and contrasted with other sub-basins within the Arctic Ocean as defined in the Russian *Arctic Atlas* (Treshnikov 1985). Here we compare the trends in the Yamal/Kara Sea area with those in the Beaufort Sea area, where the land warming and NDVI trends have been described previously (Jia et al. 2003). Patterns for the Northern Eurasia region are described in Chapter 2 of this volume (Goetz et al.). Climate analysis techniques were applied to evaluate the direct relationship between the trends of sea-ice, LST and NDVI and various climate indices such as the North Atlantic Oscillation (NAO), Arctic Oscillation (AO), and the Pacific Decadal Oscillation (PDO). The NCEP/NCAR Reanalysis provided climate information for the analysis (http://dss.ucar.edu/pub/reanalysis/index.html).

Between 1982 and 2007, sea-ice in the 50-km coastal strip of the Yamal/Kara Sea area during the period 18 June–22 July decreased −4.5%/decade (Fig. 9.12). The time period (18 June–22 July) was selected because this is the time of transition to summer-ice conditions across most of the Arctic and is the time when sea-ice concentrations have the most variability. Land-surface temperatures (as indicated by the summer warmth index (SWI), showed a slight increase (0.2°C mo). This was less of a response than for the Eurasian area as a whole, where sea-ice decreased −5.8%/decade, and SWI increased +1.2°C mo/decade. The greening response of the vegetation (as indicated by the summer maximum NDVI and the total integrated NDVI) increased modestly 0.01 and 0.13 NDVI units per decade, respectively. This

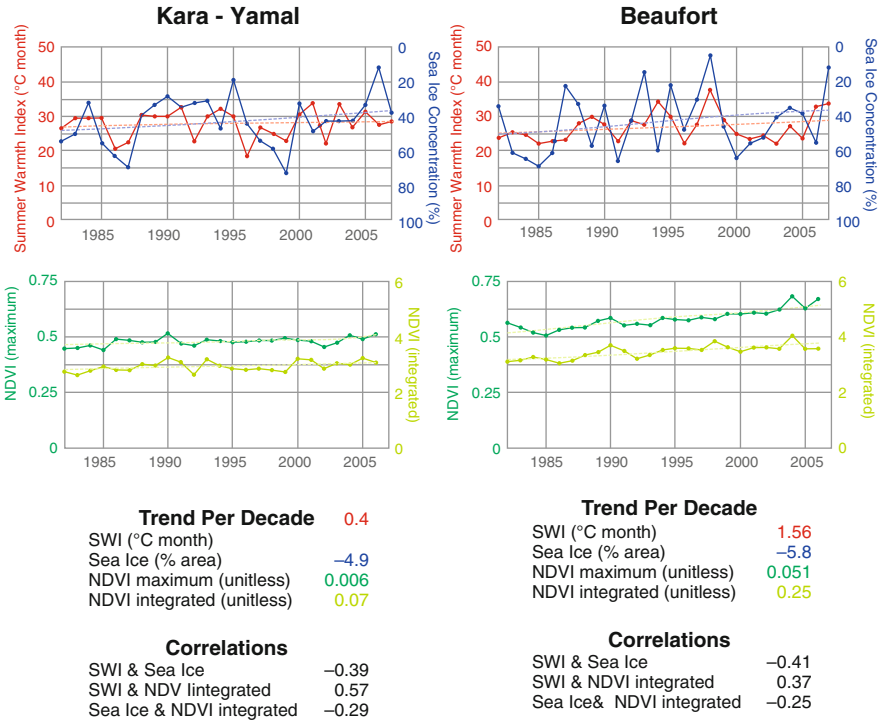

Fig. 9.12 Trends and correlations of sea-ice concentration, land-surface temperature (SWI) and maximum and integrated NDVI for (*left*) the Kara/Yamal region and (*right*) the Beaufort Sea region. Reproduced by permission of Uma Bhatt

was somewhat more than for Eurasia as a whole (0.006 and 0.06/decade, respectively), and much less than in the Beaufort Sea of North America region where SWI increased 1.6°C mo and the integrated-NDVI increased 0.33/decade (Bhatt et al. 2007, 2008, 2010) (Fig. 9.12). In the Kara/Yamal region, sea-ice concentrations and SWI were negatively correlated ($r = 0.41$, $p > 0.05$) and the SWI and integrated NDVI were positively correlated ($r = 0.65$, $p > 0.05$) (see Chapter 2, this volume) for a more full discussion of the analysis of the sea-ice, SWI, and NDVI trends and climate correlations for the seven seas in the Northern Eurasia region). These trends are consistent with all other coastal areas studied in the Arctic – i.e., periods of lower sea-ice concentration are correlated with warmer land-surface temperatures and higher NDVI values. Compared to areas that are contiguous with the North Atlantic and the North Pacific, the Kara/Yamal is more continental and displayed relatively large decreases in sea-ice (−3.7 to −7.3%/decade) and modest increases in SWI (+0.2C mo/decade). The sea-ice and land-surface trends are much stronger in the E. Siberian and Chukchi sectors of the Russian Arctic (< −10%/decade respectively and > 2.2°C/decade).

Sea-ice concentrations trends in the Kara/Yamal region showed a significant negative correlation with the NAO during the December to March period of the preceding winter ($r = 0.41$, $p > 0.05$) and summer warmth index had a weak positive correlation ($r = 0.28$) with the NAO. The NAO is a measure of the north-south surface pressure gradient in the North Atlantic. The positive phase of the NAO is generally characterized by enhanced storminess in the Arctic, increased heat transport from lower latitudes, and warmer winter temperatures. This would be consistent with the negative correlation between the NAO and sea-ice concentrations in the Kara Sea region.

In summary, sea-ice has retreated somewhat earlier over the past 24 years in the Kara/Yamal region but not as strongly as in the E. Siberian and Chukchi Seas. Land surface temperatures on the Yamal have increased slightly, but nowhere near as strong an increase as in the E. Siberia, Chukchi and Bering Sea regions. Greenness has increased, but not as strongly as it has it has in other areas of Northern Eurasia (e.g., W. Bering and Chukchi seas regions) and in the Beaufort Sea.

9.6 Cumulative Effects

Resource development often proceeds in a piecemeal fashion – a process called "nibbling" (Horak et al. 1983; Beanlands et al. 1986; Lee and Gosselink 1988). The US Regulatory definition of cumulative impacts is:

> an impact on the environment which results from the incremental impact of the action when added to other past, present, and reasonably foreseeable-future actions regardless of what agency (Federal or non-Federal) or person undertakes such actions. Cumulative impacts can result from individually minor but collectively significant actions taking place over a period of time (CEQ 1978).

The approach used here expands the concept of cumulative impacts to include the simultaneous and interactive effects of developing many gas fields and other ongoing social and ecological factors such as population growth and climate change. The aim is to look further into the future and anticipate the combined effects from several agents of change.

Some of the most critically needed models are ones that will anticipate the structure of future networks of pipelines and roads. Such models are being developed in Canada (Holroyd and Retzer 2005). These models can help predict the length and density of road and pipeline networks based on assumptions about the geological structure of the gas fields and gas-field technology. Best practices scenarios can be developed if the assumptions in the models are accurate and based on the latest and best information from all sides – including petroleum geologists, oil-field engineers, and land-use planners. If reasonable assessments of road and pipeline densities can be made, then the implications for wildlife habitat can be made (Weller et al. 2002), as well as the consequences to resident populations of people.

A comparison with cumulative effects of developments in other Arctic areas could lead to better international understanding of the unique constraints imposed on

the development of arctic gas fields with different environmental, political, social, regulatory, and economic systems. The data presented in Table 9.2 of this analysis compares the available information from the Bovanenkovo field with data in northern Alaska, that was obtained by the National Research Council during a large publicly funded assessment of the cumulative effects of oil and gas activities on Alaska's North Slope (NRC 2003). The 18-member committee responsible for writing the report included experts in geology, permafrost, economics, anthropology, marine and terrestrial mammals, birds, fish, vegetation, contaminants, arctic ecology, and the native people, and included members of government agencies, private consultants, university professors, and non-governmental agencies. The North Slope oil fields began development in 1968 and oil was flowing through the trans-Alaska pipeline by 1977; this 30-year history provides much valuable insight to ecologically sound development of arctic oil and gas resources. The cumulative effects issues being faced on the Yamal are in many ways similar to those being faced in Alaska (Walker et al. 1987), the Mackenzie River delta region of Canada (Holroyd and Retzer 2005) and the Barents Sea region of northern Norway (Mathiessen 2008, also see Chapter 7, this volume), and are a precursor to much more extensive changes that are sure to come in northern Russia, including the Nenets Autonomous Okrug, and elsewhere.

9.7 Conclusions

The multiple effects of rapid resource development, climate change, and population growth make the Yamal Peninsula one of the most rapidly changing areas in the Arctic. New tools are needed for the various stakeholders in the region to envision the cumulative effects of these and other influences. Here we have enumerated the effects of industrial activities, climate change, and the expanding populations of gas workers, Nenets and reindeer. We have shown that the direct (planned) impacts of industrial activities are currently relatively local and limited in extent, but this is changing fast as extensive gas fields are developed and land and sea transportation corridors are developed to transport the gas to market. Indirect impacts, such as those from blowing sand and dust, are much more extensive than the direct impacts. Industrial development (mainly roads and pipelines) is creating serious barriers to migration corridors and limiting the areas of summer pasture. As well, fishing is threatened from poaching and as rivers and lakes are damaged during road and pipeline construction (Forbes 2008; Forbes et al. 2009). Herders generally view the threats from industrial development to be much greater than threats from climate change (Forbes and Stammler 2009). Land withdrawals by industry, increasing populations of gas workers and Nenets, and larger reindeer herds are increasing pressure on the rangelands as well as fishing resources. However, despite the negative impacts, the Nentsy have an overall positive view of gas development because of increased economic and social advantages (Stammler 2005; Forbes 2008; Forbes and Stammler 2009).

Satellite data suggest that there has been a modest summer land-surface warming and only slight greening across the Yamal during the past 24 years. The trend is not as strong as in other parts of the Arctic, such as the Beaufort Sea. The trend in land-surface temperatures has co-varied with the trend in sea-ice – low sea-ice in the preceding December–March period is correlated to warmer land temperature the following summer. Climate analysis indicates that the trends of sea-ice and land temperatures in the Kara Sea-Yamal region are tied to variation in the North Atlantic Oscillation index. The small greening response to warming is partially due to a generally lower than normal correspondence between vegetation production and local climate. This is due to the high level of natural disturbance (landslides) that is responsible for abundant willow growth across much of the peninsula, which gives the region higher than expected NDVI values. The actual effects of climate-change on vegetation are currently hard to document at the ground level because of lack of baseline and long-term ground observations and difficulty of excluding reindeer in these studies. Ground-based baseline studies, are important for documenting future changes in plant species composition, biomass, NDVI, active layer depths and soils properties.

There is high potential for extensive landscape effects due to unstable sandy soils, and extremely ice-rich permafrost near the surface on slopes. If exposed by natural or anthropogenic causes the ice-rich permafrost is highly susceptible to catastrophic failures. Over large areas of the Yamal, landslides have transformed the zonal sedge, dwarf-shrub tundra to the low-shrub tundra that is typically found on disturbed sites in this subzone. Present evidence indicates that the landslides are triggered most abundantly in wet years, as in 1989, and in warm years, as in the recent years since 2005.

Vegetation change models such as ArcVeg will help predict the changes that will occur to the vegetation from the combined influence of climate change, industrial development, and changes in reindeer foraging impact (see Goetz et al., Chapter 2). Additional modeling efforts are needed to predict the effects of new road and pipeline networks. Also needed are more wide-ranging assessments that include air and water quality, and biodiversity of terrestrial and aquatic organisms. Comprehensive assessments and models that can anticipate numerous development scenarios and draw on other international experiences are needed to plan for the cumulative effects of resource development, climate change, and demographic changes that are occurring on the Yamal and other Arctic regions.

References

ACIA (2004) Impacts of a warming arctic: arctic climate impact assessment. Cambridge University Press, Cambridge, 144p

Bartsch A, Kumpula T, Forbes BC, Stammler F (2010) Detection of snow surface thawing and refreezing in the Eurasian Arctic with QuikSCAT: implications for reindeer herding. Ecol Appl (in press)

Beanlands GE, Erckmann WJ, Orians GH, O'Riordan J, Policansky D, Sadar MH, Sadler B (1986) Cumulative environmental effects: a binational perspective. Canadian Environmental Assessment Research Council/US National Research Council, Ottawa and Washington DC

Bhatt US, Walker DA, Raynolds M, Comiso J (2007) The relationship between sea ice variability and arctic tundra on the pan-Arctic, regional, and site scales. Eos, Transact Am Geophys Union 88(52), Fall Meet. Suppl. Abstract U41C-0612

Bhatt US, Walker DA, Raynolds MK, Comiso J (2008) Circumpolar and regional analysis of the relationship between sea-ice variability, summer land-surface temperatures, Arctic tundra greenness and large-scale climate drivers. Talk given at the LCLUC science team meeting, NASA carbon cycle and ecosystems joint science workshop, Adelphi, 1–2 May 2008, Abstract 363. http://cce.nasa.gov/cgi-bin/meeting_2008/mtg2008_ab_search.pl

Bhatt US, Walker DA, Raynolds MK, Comiso JC, Epstein HE, Jia GJ, Gens R, Pinzon JE, Tucker CJ, Tweedie CE, Webber PJ (2010) Circumpolar Arctic tundra vegetation change is linked to sea-ice decline. Earth Interactions 14. doi: 10.1175/2010EI1315.1171

CEQ (1978) National Environmental Policy Act: implementation of procedural provisions; final regulations. Federal Register, 559900

Comiso J (1999) Bootstrap sea ice concentrations for NIMBUS-7SMMR and DMSP SSM/I, June to September 2001. National Snow and Ice Data Center, Digital Media, Boulder

Comiso JC (2000) Variability and trends in Antarctic surface temperatures from in situ and satellite infrared. J Climate 13:1674

Comiso JC (2003) Warming trends in the Arctic from clear sky satellite observations. J Climate 16:3498–3510

Comiso JC (2006) Arctic warming signals from satellite observations. Weather 61:70–76

Comiso JC, Parkinson CL, Gersten R, Stock L (2008) Accelerated decline in the Arctic sea ice cover. Geophys Res Lett 35(L01703). doi:01710.01029/02007GL031972

Drozdov DS, Rivkin FM, Rachold V, Malkova GVA, Ivanova NV, Chehina IV, Koreisha MM, Korostelev YV, Melnikov ES (2005) Electronic atlas of the Russian Arctic coastal zone. Geo-Marine Lett 25:81–88

Dubikov GI (2002) Composition and cryogenic construction of the frozen rocks of West Siberia. GEOS Publisher, Moscow, 246 p (in Russian)

Edlund S (1990) Bioclimate zones in the Canadian Archipelago. In: Harrington CR (ed) Canada's missing dimension: science and history in the Canadian Arctic islands. Canadian Museum of Nature, Ottawa, pp 421–441

Epstein HE, Walker MD, Chapin FS III, Starfield AM (2000) A transient, nutrient-based model of arctic plant community response to climate warming. Ecol Appl 10:824–841

Epstein HE, Walker DA, Raynolds MK, Jia GJ, Kelley AM (2008) Phytomass patterns across a temperature gradient of the North American arctic tundra. J Geophys Res-Biogeosci, 113:G03S02

Epstein HE, Yu Q, Kaplan JO, Lischke H (2007) Simulating future changes in arctic and subarctic vegetation. Comput Sci Eng 9(4):12–23

Forbes BC (1995) Tundra disturbance studies, III: short-term effects of Aeolian sand and dust, Yamal Region, Northwest Siberia. Environ Conserv 22:335–371

Forbes BC (1999a) Land use and climate change on the Yamal Peninsula of north-west Siberia: some ecological and socio-economic implications. Polar Res 18:367–373

Forbes BC (1999b) Reindeer herding and petroleum development on Poluostrov Yamal: sustainable or mutually incompatible uses? Polar Rec 35:317–322

Forbes BC (2004) Impacts of energy development in polar regions. In: Cleveland CJ (ed) Encyclopedia of energy. Academic Press, San Diego, pp 93–105

Forbes BC (2008) Equity, vulnerability and resilience in social-ecological systems: a contemporary example from the Russian Arctic. Research in Social Problems and Public Policy 15:203–236

Forbes BC, Ebersole JJ, Strandberg B (2001) Anthropogenic disturbance and patch dynamics in circumpolar arctic ecosystems. Conserv Biol 15:954–969

Forbes BC, Fresco N, Shvidenko A, Danell K, Chapin FS III (2004) Geographic variations in anthropogenic drivers that influence the vulnerability and resilience of social-ecological systems. Ambio 33:377–382

Forbes BC, Macias Fauria M, Zetterberg P (2010) Russian Arctic warming and "greening" are closely tracked by tundra shrub willows. Glob Chang Biol 16:1542–1554

Forbes BC, McKendrick JD (2002) Polar tundra. In: Perrow M, Davy AJ (eds) Handbook of ecological restoration. Cambridge University Press, Cambridge, pp 355–375

Forbes BC, Stammler F (2009) Arctic climate change discourse: the contrasting politics of research agendas in the West and Russia. Polar Research 28:28–42

Forbes B, Stammler F, Kumpula T, Meschtyb N, Pajunen A, Kaarlejärvi E (2009) High resilience in the Yamal-Nenets social-ecological system, West Siberian Arctic, Russia. Proc Natl Acad Sci 106:22041–22048

Forman SL, Ingólfsson O, Gataullin V, Manley WF, Lokrantz H (1999) Late Quaternary stratigraphy of western Yamal Peninsula, Russia: New constraints on the configuration of the eurasian ice sheet. Geology 27:807–810

Forman SL, Ingólfsson O, Gataullin V, Manley WF, Lokrantz H (2002) Late Quaternary stratigraphy, glacial limits, and paleoenvironments of the Marresale area, western Yamal Peninsula, Russia. Quat Res 57:355–370

Gubarkov A (2008) Overview of gas and oil development on the Yamal Peninsula. Yamal land-cover land-use change workshop, Moscow, 28–30 January 2008. http://www.geobotany.uaf.edu/library/ptFiles/gubarkov_2008_yamal.pdf

Hinzman L, Bettez N, Bolton WR, Chapin FS III, Dyurgerov M, Fastie C, Griffith B, Hollister RD, Hope A, Huntington HP, Jensen A, Jia GJ, Jorgenson T, Kane DL, Klein DR, Kofinas G, Lynch AH, Lloyd AH, McGuire AD, Nelson F, Oechel WC, Osterkamp TE, Racine C, Romanovsky VE, Stone R, Stow D, Sturm M, Tweedie CE, Vourlitis G, Walker MD, Walker DA, Webber PJ, Welker JE, Winker K, Yoshikawa K (2005) Evidence and implications of recent climate change in northern Alaska and other Arctic regions. Clim Change 73:251–298

Holroyd P, Retzer H (2005) A peak into the future: potential landscape impacts of gas development in northern Canada. The Pembina Institute, Drayton Valley, Alberta

Horak GC, Vlachos EC, Cline EW (1983) Fish and wildlife and cumulative impacts: is there a problem? Office of Biological Services, Fish and Wildlife Service, Albuquerque

Jia GJ, Epstein HE, Walker DA (2003) Greening of arctic Alaska, 1981–2001. Geophys Res Lett 30:2067. doi:2010.1029/2003GL018268

Kaplan JO, Bigelow NH, Prentice IC, Harrison SP, Bartlein PJ, Christensen TR, Cramer W, Matveyeva NV, McGuire AD, Murray DF, Razzhivin VY, Smith B, Walker DA, Anderson PM, Andreev AA, Brubaker LB, Edwards ME, Lozhkin LV (2003) Climate change and Arctic ecosystems: 2. Modeling, paleodata-model comparisons, and future projections. J Geophys Res 108(D198171). doi:1029/2002DJ002559

Kaplan JO, New M (2006) Arctic climate change with a 2°C global warming: timing, climate patterns and vegetation change. Clim Change 79:213–241

Kumpula T, Forbes BC, Stammler F (2010) Remote sensing and local knowledge of hydrocarbon exploitation: the case of Bovanenkovo, Yamal, West Siberia. Arctic 63:65–178

Lawrence DM, Slater AG, Tomas RA, Holland MM, Deser C (2008) Accelerated Arctic land warming and permafrost degration during rapid sea ice loss. Geophys Res Lett 35(L11506). doi:11510.11029/12008GL033985

Lee LC, Gosselink JG (1988) Cumulative impacts on wetlands: linking scientific assessments and regulatory alternatives. Environ Manage 12:591–602

Leibman MO (1996) Results of chemical testing for various types of water and ice, Yamal Peninsula, Russia. Permafr Perigl Process 7:287–296

Leibman MO, Kizyakov AI (2007) Cryogenic landslides of the Yamal and Yugorsky Peninsulas. Earth Cryosphere Institute SB RAS Press, Moscow, p 206 (In Russian).

Mathiessen S (2008) Climate adaptation in relation to reindeer herding. Talk given at the LCLUC Sience Team Meeting, NASA Carbon Cycle and Ecosystems Joint Science Workshop, Adelphi, 1–2 May 2008

Melnikov ES (1998) Uniting basis for creation of ecological maps for the Russian cryolithozone. Procedings of the 7th International Conference on Permafrost, Yellowknife, 719–722

Melnikov ES, Minkin MA (1998) About strategy of development of electronic geoinformation systems (GIS) and databases in geocryology. Earth Cryosphere II:70–76 (in Russian)

Minkin MA, Melnikov ES, Leibman MO (2001) Russian national geocryological database and a strategy for its development. In: Raepe R, Melnikov V (eds) Permafrost response on economic development, environmental security and natural resources. Kluwer Academic Publishers, Netherlands

Nghiem SV, Rigor IG, Perovich DK, Clemente-Colón P, Weatherly JW (2007) Rapid reduction of Arctic perennial sea ice. Geophys Res Lett 34. doi:10.1029/2007GL031138

NRC (2003) Cumulative environmental effecs of oil and gas activities on Alaska's North Slope. National Academies Press, Washington DC

Prentice IC, Cramer W, Harrison SP, Leemans R, Monserud RA, Solomon AM (1992) A global biome model based on plant physiology and dominance, soil properties and climate. J Biogeogr 19:117–134

Rannie WF (1986) Summer air temperature and number of vascular species in arctic Canada. Arctic 39:133–137

Raynolds MK, Comiso JC, Walker DA, Verbyla D (2008a) Relationship between satellite-derived land surface temperatures, arctic vegetation types, and NDVI. Rem Sens Environ 112: 1884–1894

Raynolds MK, Walker DA, Comiso JC (2008b) Spatial patterns of land-surface temperature and NDVI, and their relation to vegetation distribution on the Yamal Peninsula, Russia. Poster presented at the Carbon Cycle and Ecosystems Joint Science Workshop, Adelphi, 1–2 May 2008. Abstract 365. http://cce.nasa.gov/cgi-bin/meeting_2008/mtg2008_ab_search.pl

Raynolds MK, Walker DA, Maier HA (2006) NDVI patterns and phytomass distribution in the circumpolar Arctic. Rem Sens Environ 102:271–281

Romanovsky VE, Osterkamp TE (2001) Permafrost: changes and impacts. In: Paepe R, Melnikov V, Overloop EV, Gorokhov VD (eds) Permafrost response on economic development. Environmental security and natural resources. Kluwer Academic Publisher, Dordrecht, pp 297–315

Stammler F (1998) Wo Unser Erdgas Herkommt. Pogrom 201:33–35

Stammler F (2005) Reindeer Nomads meet the market: culture, property and globalisation at the end of the land. Muenster, Litverlag (Halle Studies in the Anthropology of Eurasia) 6, 320

Stammler F, Forbes BC, and Participants of the Symposium on Oil and Gas Development in NAO and YNAO (2009) "Ilebts" declaration on coexistence of oil and gas activities and indigenous communities on Nenets and other territories in the Russian North, Arctic Centre, University of Lapland. Rovaniemi, 10–11 December 2007. http://www.arcticcentre.org/declaration

Stammler F, Wilson E (2006) Dialogue for development: an exploration of relations between oil and gas companies, communities and the state. Sibirica 5:1–42

Starobin P (2008) Send me to Siberia. Natl Geogr 213:60–85

Streletskaya ID, Leibman MO (2003) Cryogeochemical model of tabular ground ice and cryopegs formation at central Yamal, Russia. Proceedings of the International Conference on Permafrost, Zurich. A.A. Balkema Publishers, Netherlands, 1111–1115

Stroeve J, Holland MM, Meier W, Scambos T, Serreze M (2007) Arctic sea ice decline: Faster than forecast. Geophys Res Lett 34(L09501). doi:10.1029/2007GL029703

Tape K, Sturm M, Racine C (2006) The evidence for shrub expansion in Northern Alaska and the Pan-Arctic. Glob Chang Biol 12:686–702

Treshnikov AF (1985) Atlas of the Arctic. Administrator of Geodesy and Cartography of the Soviet Ministry, Moscow (in Russian)

Tucker CJ, Pinzon JE, Brown ME, Slayback D, Pak EW, Mahoney R, Vermote E, El Saleous N (2005) An extended AVHRR 8-km NDVI data set compatible with MODIS and SPOT vegetation NDVI data. Int J Rem Sens 26:4485–4598

Ukraintseva NG (1997) Willows tundra of Yamal as the indicator of salinity of superficial sediments. Results of basic research of Earth cryosphere in Arctic and Subarctic. Nauka Publisher, Novosibirsk, pp 182–187

Ukraintseva NG (1998) Distribution of shrub tundra on Yamal. Biogeography. RGO Publisher, Moscow, pp 46–53

Ukraintseva NG, Leibman MO (2000) Productivity of willow-shrub tundra in connection with landslide activity. Proceedings of the 30th arctic workshop programme and abstracts, INSTAAR, University of Colorado, Boulder, 16–18 Mar 2000, 150–152. http://instaar.colorado.edu/meetings/AW2000/AW30_Pro_Abstr.pdf

Ukraintseva NG, Leibman MO (2007) The effect of cryogenic landslides (active-layer detachments) on fertility of tundra soils on Yamal peninsula, Russia. Proceedings of the 1st North American landslide conference, Omnipress, Vail

Ukraintseva NG, Leibman MO, Streletskaya ID (2000) Peculiarities of landslide process in saline frozen deposits of central Yamal, Russia. In: Bromhead E, Dixon N, Ibsen LL (eds) Landslides. Proceedings of the 8th International Symposium on Landslides 3, Thomas Telford, London, 1495–1500

Ukraintseva NG, Leibman MO, Streletskaya ID, Yermokhina KA, Smetanin NN (2002) Monitoring of the landslide on saline frozen deposits in typical tundra subzone (Yamal, Bovanenkovo Gas-field area), Ecology of northern territories of Russia. Problems, prediction of situation, ways of development, solutions, vol 1, Arkhangelsk, 832–837

Ukraintseva NG, Streletskaya ID, Ermokhina KA, Yermakov SY (2003) Geochemical properties of plant-soil-permafrost system at landslide slopes, Yamal, Russia. Proceedings of the international conference on permafrost, Zurich, A.A.Balkema Publishers, Netherlands, 1149–1154

UNEP (2001) GLOBIO Global methodology for mapping human impacts on the biosphere: the Arctic 2050 scenario and global application. United Nations Environment Programme

Vilchek GE (1997) Arctic ecosystem stability and disturbance. In: Crawford RMM (ed) Disturbance and recovery in Arctic lands: an ecological perspective. Kluwer Academic Publishers, Dordrecht, pp 179–189

Walker DA (1997) Arctic Alaskan vegetation disturbance and recovery: a hierarchic approach to the issue of cumulative impacts. In: Crawford RMM (ed) Disturbance and recovery in Arctic lands: an ecological perspective. Kluwer Academic Publishers Publishers, Dordrecht, pp 457–479

Walker DA, Epstein HE, Leibman ME, Moskalenko NG, Kuss JP, Matyshak GV, Kaärlejarvi E, Barbour E (2008a) Data Report of the 2007 expedition to Nadym, Laborovaya and Vaskiny Dachi, Yamal Peninsula region, Russia. NASA Project No. NNG6GE00A, Alaska Geobotany Center, Institute of Arctic Biology, University of Alaska, Fairbanks. http://www.geobotany.uaf.edu/yamal/documents/yamal_2007_dr080211

Walker DA, Epstein HE, Romanovsky VE, Ping CL, Michaelson GJ, Daanen RP, Shur Y, Peterson RA, Krantz WB, Raynolds MK, Gould WA, Gonzalez G, Nickolsky DJ, Vonlanthen CM, Kade AN, Kuss P, Kelley AM, Munger CA, Tarnocai CT, Matveyeva NV, Daniëls FJA (2008b) Arctic patterned-ground ecosystems: a synthesis of field studies and models along a North American Arctic Transect. J Geophys Res-Biogeosci 113(G03S01). doi10.1029/2007JG000504

Walker DA, Leibman MO, Epstein HE, Forbes BC, Bhatt US, Raynolds MK, Comiso JC, Gubarkov AA, Khomutov AV, Jia GJ, Kaarlejärvi E, Kaplan JO, Kumpula T, Kuss P, Matyshak G, Moskalenko NG, Orekhov P, Romanovsky VE, Ukraientseva NK, Yu Q (2009) Spatial and temporal patterns of greenness on the Yamal Peninsula, Russia: interactions of ecological and social factors affecting the Arctic normalized vegetation index. Environ Res Lett 4:045004. doi:10.1088/1748-9326/4/4/045004

Walker DA, Raynolds MK, Daniëls FJA, Einarsson E, Elvebakk A, Gould WA, Katenin AE, Kholod SS, Markon CJ, Melnikov ES, Moskalenko NG, Talbot SS, Yurtsev BA (2005) The circumpolar arctic vegetation map. J Veg Sci 16(3):267–282

Walker DA, Webber PJ, Binnian EF, Everett KR, Lederer ND, Nordstrand EA, Walker MD (1987) Cumulative impacts of oil fields on Northern Alaskan landscapes. Science 238:757–761

Weller C, Thomson J, Morton P, Aplet G (2002) Fragmenting our lands: the ecological footprint from oil and gas development. The Wilderness Society, Seattle

Young SB (1971) The vascular flora of St. Lawrence Island with special reference to floristic zonation in the arctic regions. Contributions from the Gray Herbarium 201:11–115

Chapter 10
Interactions of Arctic Aerosols with Land-Cover and Land-Use Changes in Northern Eurasia and their Role in the Arctic Climate System

Irina N. Sokolik, Judith Curry, and Vladimir Radionov

Abstract Atmospheric aerosols have been hypothesized as playing an important role in significant climate and environmental changes that have been occurring in the Arctic. This Chapter concentrates on the role of Arctic aerosols in the energy balance and the hydrological cycle by considering several major aerosol types (sulfates, black carbon and dust) that originate in Northern Eurasia. Aerosols can affect the energy balance directly by scattering, absorbing, and emitting atmospheric radiation as well as by changing the surface albedo. Furthermore, aerosols perturb the radiative energy balance indirectly by affecting the properties, lifetime, and coverage of clouds. Aerosol-induced changes in clouds are also important in the hydrological cycle. An additional complexity arises from the potential connection of aerosols to feedbacks that involve the physical climate, ecological, and human components of the Arctic system. The abundances, chemical composition and spatiotemporal distributions of natural and anthropogenic aerosols, which are controlled by sources and ageing processes occurring during atmospheric transport, are the major factors governing the aerosol climate forcing. Over the past decades, the warming climate, socio-economic changes and changes in land cover and land use occurring in Northern Eurasia have been affecting sources and properties of atmospheric aerosols. These changes were likely to affect not only aerosol burden in the Russian Arctic but through the whole Arctic. Understanding how changes in land cover and land use have been affecting the abundances and distributions of natural and anthropogenic aerosols and how the aerosol-induced varying forcing has been affecting the Arctic climate system is of great importance to understand the overall response of the Arctic region to global warming associated with steadily increasing greenhouse gases.

I.N. Sokolik (✉)
School of Earth and Atmospheric Sciences, Georgia Institute of Technology, Atlanta, GA 30332-0340, USA
e-mail: isokolik@eas.gatech.edu

G. Gutman, A. Reissell (eds.), *Eurasian Arctic Land Cover and Land Use in a Changing Climate*, DOI 10.1007/978-90-481-9118-5_10,

10.1 Introduction

Dramatic changes occurring in the Arctic have received considerable attention in recent years. The consensus is that global warming caused by carbon dioxide (CO_2) and other greenhouse gases (GHGs) has been contributing to observed changes along with several other important natural and anthropogenic factors. The complex nature of climate forcing agents, their interactions, and feedbacks within the climate system pose a major challenge to understanding and quantifying the impact of individual agents, as well as to predicting their contributions to future changes in the Arctic. Recently, there has been an increasing interest in the role of atmospheric aerosols and whether or not they have been augmenting the GHG-induced warming of the Arctic. Although aerosols in the Arctic have been studied for nearly 3 decades, the magnitude of their impact upon the regional climate remains highly uncertain. This uncertainty is related to limited understanding of some major mechanisms involved, the inability of models to describe accurately many of the complex processes and feedbacks related to aerosols, as well as a paucity of observational data. This Chapter examines the impacts caused by aerosols that are thought to be of importance to the Arctic energy and water cycles. The main focus is on the role of sulfates, black carbon and wind-blown dust that originate in Northern Eurasia and their linkages with the land-cover and land-use changes that have been occurring in this region during past 50 years. We address the dynamics of aerosol sources (Section 10.2), long-term changes of aerosol characteristics observed in the Arctic (Section 10.3), and major processes and feedbacks through which aerosols affect the Arctic system (Section 10.4).

The natural Arctic environment has limited sources of atmospheric particulates and their gaseous precursors such as sulfur dioxide (SO_2), dimethylsulfide (DMS), and volatile organic compounds (VOCs). Natural aerosols include sulfates, which are formed through gas-to-particle conversion of SO_2 derived from oxidation of DMS, and sea-salt aerosols, both originating from ice-free ocean and sea-water. Also common are organic aerosols formed from biogenic emission of VOCs. Local sources also include volcanoes (from Iceland, Kamchatka, and Alaska) and wildfires, either natural or human-related. Open biomass fires produce several important types of aerosols, including organic carbon (OC) and black carbon (BC). In addition, crustal particles are generated locally during the snow-free season, but the majority of mineral aerosols are thought to be transported to the Arctic from the arid and semi-arid regions located in Asia and Northern Africa. Although natural aerosols are an important component of the functioning of the Arctic system, there is increasing interest in the impacts of air pollutants (or anthropogenic aerosols).

Prevalent intrusions of polluted air into the high Arctic – called Arctic haze – occur in winter and spring, with enhanced levels of sulfates, carbonaceous (OC and BC) and mineral dust mass loadings (Barrie 1986; Sokolik 1992; Koch and Hansen 2005; Quinn et al. 2007). Much of pollution in the high Arctic originates from mid-latitudes, although there are some local (north of about 70°) pollution sources from industrial cities like Norilsk and Nickel, emissions from local use of

fossil fuels, and emissions from the oil industry and shipping. Because of favorable transport pathways north of the winter Arctic front, Northern Eurasia sources have been identified as the major contributor to Arctic haze and also a primary source of dust aerosol, and hence this region is central to understanding the nature, variability and impacts of Arctic aerosols. The various changes that have been occurring in Northern Eurasia during the past 50 years, including land-use and land-cover changes, undoubtedly affected the abundance and properties of aerosols, and hence aerosol impacts not only across the Russian Arctic but also over the whole Arctic region and likely over the globe (see Section 10.2).

Unlike long-lived CO_2, aerosol particles have an average lifetime in the atmosphere from days to weeks, but exhibit a somewhat longer lifetime in the Arctic. Because of the physical, chemical, and thermodynamic characteristics of the Arctic atmosphere, aerosols transported to the high Arctic can accumulate during winter and spring, mainly because of slow dry and wet removal processes and extreme static stability of the lower troposphere. Marked annual cycle of Arctic aerosols with maximum concentrations during the Arctic haze season (late winter-earlier spring) is apparent from ground-based observations and supported by the atmospheric chemical transport models. Furthermore, frequent episodic intrusions of smoke from fires in Northern Eurasia and Canada occurring during the summer-fall period are thought to play an important role also. Overall, observations, albeit limited, are revealing the complex spatiotemporal distribution of Arctic aerosols and their long-term variability (see Section 10.3). This aerosol dynamics along with changes in the strength of aerosol sources are central to understanding the aerosol impact upon the Arctic system.

The impact of aerosols on climate and their involvement in local and global climate feedbacks proceeds through a number of complex and interconnected mechanisms that operate over a wide span of spatial and temporal scales (Curry 1995; Shindell 2007). Aerosol particles scatter and some (such as BC and dust) can absorb sunlight. At the same time, aerosols also act like greenhouse gases by absorbing and emitting longwave (LW) radiation, especially coarse size particles such as coarse dust (Sokolik 2003). Absorption of solar radiation by aerosols in the atmosphere is enhanced by highly reflective snow- and ice-covered surfaces in the Arctic. At the same time, deposition of light-absorbing aerosols on snow or ice can decrease surface albedo (Hansen and Nazarenko 2004). Thus, the shortwave (SW) component of the energy balance can be affected by light absorbing aerosols through the atmosphere and in the ice/snow surface. With respect to the LW component, the aerosol effect in the Arctic differs from other regions because of the cold atmospheric temperatures, frequent occurrences of temperature inversion, and low water vapor amount. The LW radiation plays a particularly important role in the energy balance in the Arctic because of prolonged polar nights with little or no sunlight. Overall, through direct interactions with SW and LW radiation, aerosol particles can affect the radiative balance at the top of the atmosphere-underlying surface system, energy balance at the surface, as well as within the atmosphere by providing a radiative heating (or cooling) in the aerosol-laden layers (Sokolik 2008).

Despite concentrated efforts to improve quantification of the overall direct radiative forcing of aerosols (e.g., IPCC 2007), this remains a challenging problem globally and particularly in the Arctic (see Section 10.4.1).

Furthermore, the direct radiative forcing is not the only mechanism by which aerosols affect the Earth's climate system. Aerosols can influence the microphysical and macrophysical properties of clouds and hence their impacts on the energy balance, precipitation, and the hydrological cycle (called the indirect aerosol effects). Depending on composition and size, aerosol particles can serve as cloud condensation nuclei (CCN) or ice-forming nuclei (IN). The sulfate species in the Arctic aerosol is a particularly efficient CCN. Enhanced CCN may increase cloud particle number concentrations but decreases droplet sizes. This results in higher reflectivity of SW radiation by liquid clouds, but at the same time cause higher infrared emissivity of clouds, thus having opposing tendencies in the cloud impact upon the energy balance. Enhanced CCN may also increase the cloud coverage and lifetime and suppress liquid precipitation, providing additional pathways in affecting the energy balance and the hydrological cycle (see Section 10.4).

In contrast to sulfates, insoluble aerosol particles such as BC and dust are not efficient CCN but can serve as ice-forming nuclei. Availability of IN in the Arctic is important because mid and lower tropospheric Arctic clouds can have supercooled water throughout the annual cycle. The low-level, mixed-phase clouds (that contain both liquid and ice phases) are believed to be the most common type in the Arctic, and have a large impact on the radiative budget (Curry et al. 1996). Modeling studies suggested that the mixed-phase clouds are very sensitive even to small changes in IN concentrations (Harrington and Olsson 2001). Simulations show that enhanced IN may transform a stratus cloud of large area coverage into a broken thin cloud system because of preferential growth of ice crystal at the expense of liquid drops that also lead to rapid ice precipitation (Prenni et al. 2007). Conversely, decreasing IN concentrations or deactivating IN by coating insoluble particle by sulfate (or other soluble aerosol species) increases the cloud lifetime. The indirect aerosol effects are thought to be the most climatically significant but pose a major challenge for climate models (see Section 10.4).

An additional complexity arises from the potential connection of aerosols to feedbacks that involve the physical climate, ecological, and human components of the Arctic system. By affecting radiation, clouds and surface albedo, aerosols are linked to the radiation-climate feedback processes such as snow/ice-albedo feedbacks, water vapor feedback and cloud-radiation feedbacks that all have been known for some time to be of importance for the Arctic climate (McGuire et al. 2006). The best estimate is that these feedbacks are positive (Curry et al. 1996), except the aerosol-dehydration feedback proposed by Blanchet and Girard (1995). Moreover, it has been suggested that the recent warming in the Arctic has triggered a broad spectrum of changes in the ecological and human systems of the region in which aerosol might play some role. Currently, the magnitude and even the sign of these feedbacks are associated with significant uncertainties, and some feedbacks are likely still unidentified.

10.2 Sources of Arctic Aerosols in Northern Eurasia and Their Dynamics

Growing evidence suggests that the warming climate, socio-economic changes, and changes in land cover and land use occurring in the Russian Arctic as well as over the entire Northern Eurasia region have been affecting sources of natural and anthropogenic aerosols over the past decades. These changes are believed to be responsible for the spatiotemporal variability of the chemical composition and burden of Arctic aerosols (see Section 10.3). Here we concentrate on the sources associated with sulfates, carbonaceous (especially BC) and mineral dust aerosols.

It is well recognized that pollution from various industrial processes and energy production cause significant environmental problems (Chapter 11, this volume). In relation to Arctic aerosols, emission of BC (also called soot) and SO_2 is of primary interest. The largest sources of SO_2 affecting the Arctic region are the industrial areas of Western and Central Siberia, particularly the non-ferrous smelters located in Norilsk in the Taymyr Peninsula and Nickel in the Kola Peninsula. Norilsk, being a single largest source of air pollutants, has large copper-nickel smelters that were established originally in the 1930s and then expanded in the early 1970s. The highest SO_2 emission from non-ferrous metallurgy was reported in 1982–1983, declining since then. This decline coincided with a decrease of SO_2 from energy production (e.g., electricity generation by power plants) related to overall slowdown of the economy in the former Soviet Union. The 1980s also saw a decline in SO_2 emissions due to more strict regulations on air quality in West European countries as well as the former Soviet Union. Many studies have attributed decreasing trends of Arctic haze since about 1982 that are apparent in observations taken within the Arctic region to declining SO_2 emissions (Quinn et al. 2007). However, the linkages are not straightforward and are likely to be affected by a number of interrelated factors (see Section 10.3).

The most recent report of Arctic Monitoring and Assessment Programme (AMAP 2006) confirmed significant reduction in sulfur emission from the non-ferrous metal smelters on the Kola Peninsula. There was a general decrease in SO_2 concentrations between 1990 and 2003 in Nikel, Monchegorsk, and Norilsk. However, interannual variability is very high (in Norilsk annual average concentrations can vary by a factor of two), making it impossible to detect clear trends in the SO_2 concentration. Non-ferrous metal production in Russia still remains the dominant source of sulfur emissions to the atmosphere within the Arctic. Other significant anthropogenic sources of sulfur emissions within or close to the Arctic include energy production plants and mining industries. The AMAP report also highlights the increasing level of nitrate aerosol during the Arctic haze season at Alert (Canada) and Barrow (Alaska). Sources of nitrogen emissions within the Arctic include transportation (particularly shipping), oil and gas extraction and refining activities. Detailed information on all of these sources is generally lacking.

Expected increase in oil- and gas-related activities in the Arctic is likely to result in increased pollutant emissions. It has been suggested that the Barents Sea region might be affected the most. At present, the main areas of oil and gas exploitation in

the Arctic include the North Slope of Alaska, the offshore areas in the Norwegian and Barents Sea, and the Yamalo-Nenets and Komi areas of Russia. Oil- and gas-related production involves emission of both SO_2 and NO_x. Emissions from shipping are another source of SO_2 and nitrogen oxides NO and $NO_2(NO_x)$ in the Arctic that is projected to increase in the next 10–15 years. In the Russian Arctic, shipping activities are concentrated mainly along the Northern Sea Route that connects the Barents Sea and the Bering Strait and serves ports at the major Russian rivers. There are also extensive shipping activities in the Canadian Arctic.

Emission sources outside the Arctic have also been experiencing significant changes in past decades. The collapse of the economy in the former Soviet Union is thought to lead to a decrease in emissions of carbonaceous aerosols. But these aerosols have various other sources. Broadly, sources are often sub-divided based on the type of consumed fuel: fossil fuel (oil and coal), biofuel (wood, agricultural waste, animal waste, and charcoal) and biomass (forest, grasslands, and scrublands). Emissions of BC as well as other particulates (and gases) during the burning process are highly variable and depend on many factors, including the type of fuel, amount of burned fuel, burning conditions, phase of burning (smoldering vs. flaming), among others. These factors also control the BC/OC emission ratio, which is important to understanding the overall effect of carbonaceous aerosols (with higher BC contributing to more warming). Unfortunately, large uncertainties associated with these factors and missing data render the assessment of BC emissions highly problematic (Bond et al. 2004; Lavoue et al. 2000; Streets et al. 2004).

A recent study by Bond et al. (2007) attempted to assess historical emissions of BC by reconstructing fossil fuel consumption and accounting for changes in technology on a national and sectoral basis. Figure 10.1 shows that North America and Europe dominated black carbon emissions in the early industrial era. The former Soviet Union was also a contributor, but emissions declined in the late twentieth century. Figure 10.1 also shows that emissions from East and Southeast Asia were increasing rapidly over the same time. Further decline in the future global BC emissions was predicted by Streets et al. (2004). Using the four IPCC scenarios (A1B, A2, B1, and B2, out to 2030 and 2050), they estimated a decline in global BC

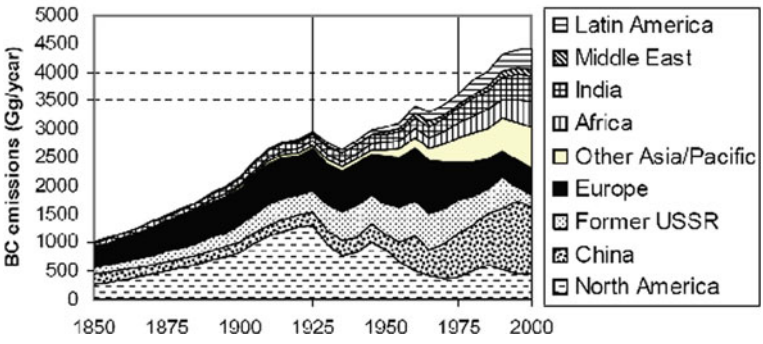

Fig. 10.1 Historical reconstruction of black carbon (BC) emissions (from Bond et al. 2007)

emissions from 8.0 Tg in 1996 to 5.3–7.3 Tg by 2030 and to 4.3–6.1 Tg by 2050. BC emissions in Russia are expected to decline also; however, East and Southeast Asia show increasing emissions in several scenarios. It is important to stress that the Streets et al. forecasts (2004) did not include potentially large and increasing contributions from natural wildfires.

It has been suggested that growing industrial emissions in East and Southeast Asia may be an important source of air pollutants in the Arctic (Koch and Hansen 2005). Based on US National Aeronautics and Space Administration (NASA) Goddard Institute for Space Studies (GISS) general circulation model results, Koch and Hansen (2005) argued that South Asia is currently a predominant source of BC in the Arctic region. This result is in conflict with commonly accepted view of Western Europe and Russia being the main sources of Arctic aerosols due to the large extent of preferential transport mechanisms (Eckhardt et al. 2003). Another possibility is that regional sources may have different contributions to BC concentrations at the surface and higher in the troposphere in the Arctic. Koch and Hansen (2005) suggested that Russia, Europe, and South Asia each contribute about 20–25% of BC to the low-altitude springtime Arctic haze, but in the Arctic upper troposphere/lower stratosphere during the spring, South Asia sources contribute 30–50% of BC. The dominant contribution of South Asia to BC in the Arctic continues to be debated (e.g., Stohl et al. 2007). A recent study by Shindell et al. (2008) provides some support for the findings of Koch and Hansen (2005). Based on the results of ten transport models and varying emission scenarios, Shindell et al. demonstrated that European emissions dominate Arctic pollutants at the surface, whereas emissions from Asian become progressively important with increasing altitude, and are dominant in the upper troposphere. In addition, they found a distinct seasonality of BC contributions from different sources. The largest contribution during boreal winter was associated with European emissions, while East Asian and North American emissions contributed the most during spring. The deposition of BC in the Arctic was dominated by the European emissions, except for Greenland where North America and Europe each contribute about 40% of total BC deposition with 20% from East Asia.

Unfortunately, Shindell et al. (2008) did not consider at all emissions from Russia, although they did highlight the importance of aerosol sources in this region, especially the role of open biomass burning. Many studies stressed that, to date, biomass burning in Northern Eurasia and Western Europe has been likely underestimated as a source of aerosol and air pollution for the Arctic, relative to emissions from fossil fuel combustion (Stohl et al. 2007; Law and Stohl 2007). One of the key problems is that emissions of BC in Northern Eurasia coming from open biomass burning that includes boreal forest, peatland, and agriculture fires that are difficult to quantify. This is a critical issue because recent studies have predicted more frequent and severe fires as the climate changes, implying increasing emissions in the future which is counter to the trends of decreasing emissions of sulfates and BC associated with fossil fuel burning. Boreal fires in Northern Eurasia are of particular importance to the Arctic because they consume large quantities of fuel and spread quickly, creating high energy release rates that are often sustained for long

burning periods (Soja et al. 2007). These emissions occur at high latitudes, mainly in the summer and earlier fall months, and exhibit large interannual variability. Most intensive boreal fires can result in convective plumes with strong vertical development that reach beyond the tropopause and favor long-range transport of smoke to the Arctic. Recent satellite observations and lidar measurements observed substantial amounts of forest fire smoke in the tropopause region and lower stratosphere at high latitudes and in the Arctic region (e.g., Fromm et al. 2000; Damoah et al. 2004; Kampe and Sokolik 2007). Figure 10.2 shows the transport of smoke from Russia to the Arctic observed by the GLI sensor onboard the Japanese ADEOS-II satellite in May, 2003. The smoke plume is clearly detected by associated higher aerosol particle concentrations. At the same time, this image helps to illustrate the limitations in measuring aerosols with passive remote sensing. Large black areas (with missing data) across the Arctic are apparent. Nevertheless, satellite remote sensing offers the best approach for obtaining global measurements of aerosols to characterize their transport to the Arctic. In particular in this case, a trans-Pacific pathway of the smoke plume is clearly detected. Satellite data reveal that this type

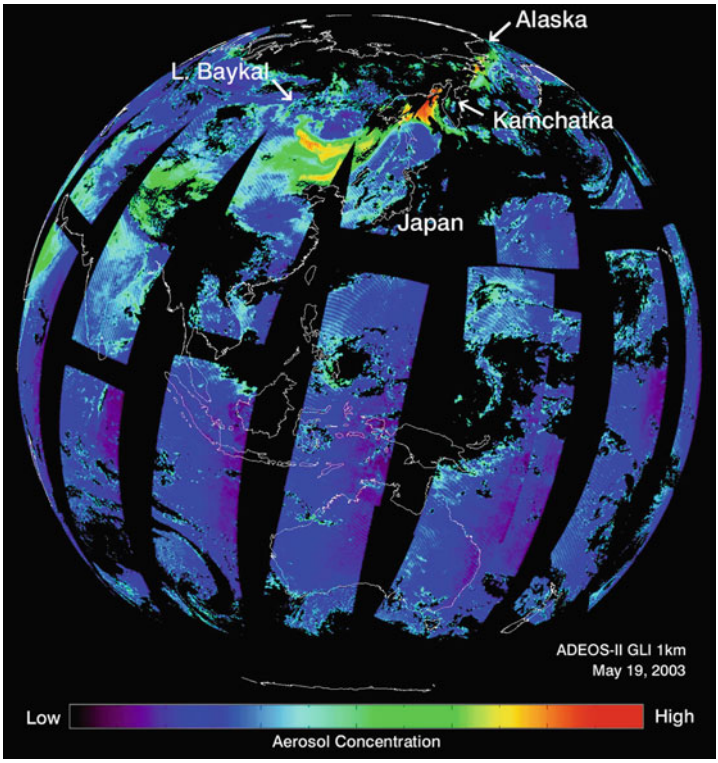

Fig. 10.2 Transport of Siberian wildfire smoke to the Arctic observed by the GLI sensor onboard the Japanese ADEOS-II satellite in May, 2003

of long-range transport is common for smoke events originating in Eastern and Far Eastern Siberia.

In addition to boreal fires in Siberia, peatland and agriculture fires are also important but highly variable sources of carbonaceous aerosols. Northern peatlands hold one third of the soil organic matter on Earth and the amount of carbon stored in peatlands per square meter is typically larger than that held in forested zones. Satellite observations reveal that smoke from peatland fires in Western Siberia can be transported as far as Canada and the High Arctic; however, frequency and the overall contribution of BC and OC to the Arctic remain to be quantified. In turn, agricultural fires were found to account for 8–11% of the annual global fire activity during 2001 and 2003, and their contribution was significantly higher on a regional basis (Korontzi et al. 2006). Russia was the largest contributor to agricultural burning globally producing 31–36% of all agricultural fires (Korontzi et al. 2006). One of the most severe air pollution events recorded at Ny-Alesund (Svalbard Archipelago, Norway) resulted from the transport of smoke from agriculture fires occurring in Belarus, the northern parts of Ukraine and Western Russia in April and May of 2006 (Stohl et al. 2007).

The progressive warming in the Russian Arctic is expected to cause greening of the tundra and likely more frequent fires in the future. Emissions from tundra fires (including scrubs and peatlands) can contribute to additional BC and OC concentrations in the Arctic but at an unknown rate. Because of the importance of carbonaceous aerosols to the arctic climate, a reliable past, present-day and future emission inventory is necessary for the application of regional atmospheric chemistry models and general circulation models. Establishing quantitative linkages between changes in land cover and land use and emissions of aerosols from burning processes in Northern Eurasia is clearly of great importance.

The changes in land cover and land use in Northern Eurasia, especially in the drylands, have also been affecting the sources of mineral dust. Many studies demonstrated that Asian dust can be transported as far as Alaska, Canadian Arctic and Greenland. Yet to date, there have been no comprehensive studies performed to establish the linkages between sources, transport and spatial distributions of mineral dust in the Arctic. Nevertheless, numerous individual episodes have been documented. Rahn et al. (1977) was the first study that reported the presence of Asian dust in the atmosphere of the Arctic from aircraft measurements. More recently, transport of dust from China and Mongolia to the Arctic was demonstrated with ground-based, aircraft and satellite observations. The Asian dust outbreaks to the Arctic seem to be more frequent during spring, coinciding with the highest frequency of dust storms in the source regions. In spring 2001, incursions of Asian dust were reported in Alaska (Cahill 2003) and northern Canada (McKendry et al. 2008). During spring 2002, Asian dust plumes were observed over the Arctic by multiple satellites. Figure 10.3 presents satellite SeaWiFS images that show the dust plume in the source regions in East Asia and later when Asian dust reached the Arctic. Increased aerosol optical depths and lidar measurements at Barrow, Alaska, in conjunction with trajectory analyses provided corroborating evidence for

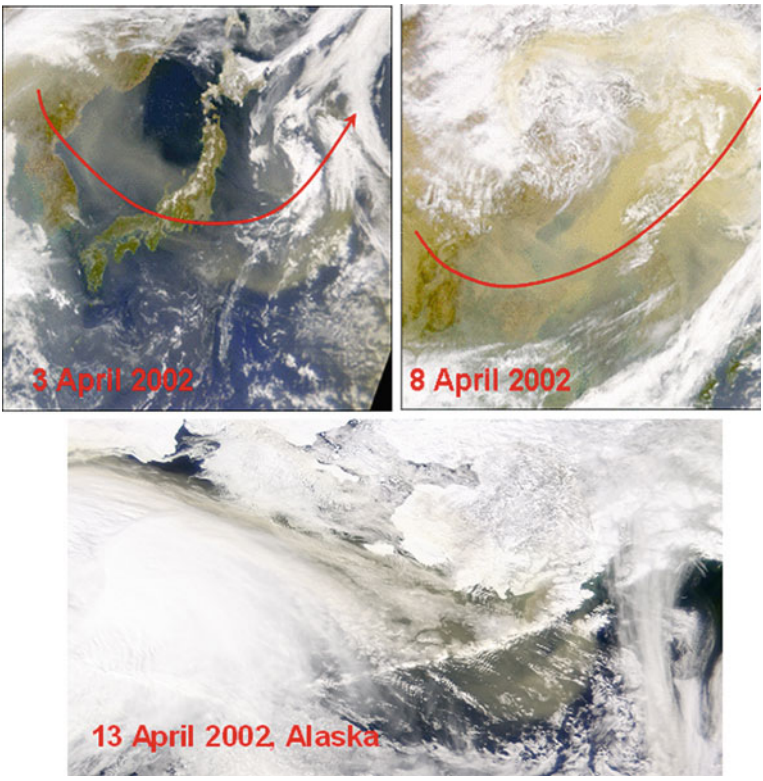

Fig. 10.3 NASA Sea-viewing Wide Field-of-view Sensor (SeaWiFS) satellite images of the Asian dust storm (*upper panels*) in the source region and (*lower panel*) in the Arctic. SeaWiFS view of Alaska (*upper right*) and the Bering Sea (*center*), collected on 13 April, 2002

the presence of Asian dust in Alaska during that time (Stone et al. 2007). Figure 10.4 shows the transport of Asian dust in spring 2007 as observed by NASA Ozone Monitoring Instrument (OMI) and Moderate Resolution Imaging Spectroradiometer (MODIS) satellite sensors (Sokolik et al. 2008). This and many past studies documented the trans-Pacific transport of Asian dust to the Northern America, but only a few studies explored the transport to and within the Arctic. Satellite observations reveal that Asian dust events affect Alaska, Canada, Greenland and the Bering/Chukchi/Beaufort Seas. These regions are experiencing the largest changes in temperature and clouds (see Section 10.4). Whether or not dust originating in East Asia affects the whole Arctic cannot be resolved with satellite passive remote sensing because of difficulties in detecting aerosols over snow- and ice-covered surfaces and the persistence of clouds in this region. In summary, numerous studies provide solid evidence that intrusions of Asian dust to the Arctic occur each year, although they are sporadic in nature. The dust is likely to be present in the spring season when dust sources in East Asia are the most active. Thus, it would appear that Asian dust has been contributing to the Arctic haze phenomenon all the time,

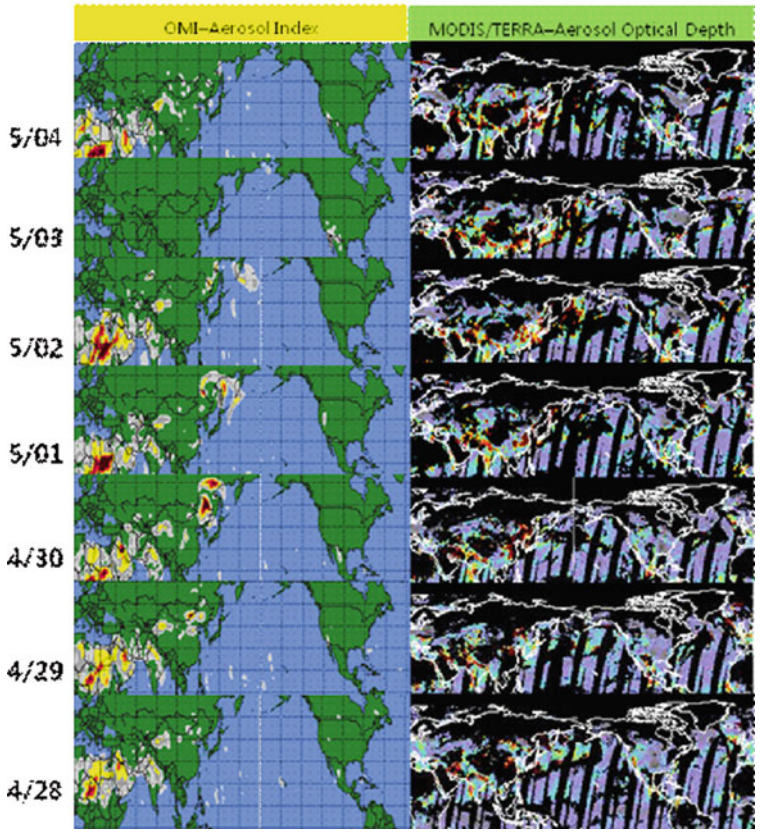

Fig. 10.4 Transport of Asian dust to the Arctic in spring 2007 reconstructed with OMI aerosol index and MODIS aerosol optical depth

but was largely misidentified because the focus was traditionally on sulfate aerosols or other air pollutants.

10.3 Characteristics of Arctic Aerosols, Their Variability and Linkages with Northern Eurasia

Long-term observations of aerosols in the Arctic reveal the complex variability of the aerosol burden, indicating that the nature of the impact of aerosols on the Arctic system differs from that of well-mixed, monotonically increasing CO_2. In addition to changes in sources discussed above, the variability of atmospheric circulation that controls transport of aerosols and air pollutants to the Arctic and varying aerosol removal and ageing processes play an important role in shaping the spatiotemporal distribution and properties of Arctic aerosols. Representation of these processes in regional and global climate models is subject to large uncertainties that translate in

Fig. 10.5 Location of stations performing aerosol chemical measurements in the Arctic (*blue* triangles) and Russian actinometric stations (*red* circles)

significant uncertainties in assessments of aerosol forcings on the Earth's climate, especially in the Arctic. Observations are critical to improve the models and to make estimations of aerosol impacts more realistic.

Unfortunately, long-term observations in the Arctic are extremely limited. Figure 10.5 shows the location of long-term ground-based monitoring stations across the region. There are only a few stations in the Arctic that conduct measurements of aerosol chemical composition (denoted by blue triangles). In the Russian Arctic, Janikoski (68°56′ N, 28°51′ E) is the only station that has provided long-term observations of sulfate and nitrate aerosols in the atmosphere (since 1979). A number of actimonetric stations (shown with red circles) in the Russian Arctic provided long-term observations of surface radiation and some meteorological variables. These radiation measurements allow for retrievals of aerosol optical depth (AOD); however, they do not provide direct information on aerosol composition. Aerosol optical depth is also measured at several other sites in the Arctic (see Section 10.3.2). The stations at Barrow and Alert conducted long-term measurements of light scattering and/or light absorption of aerosols near the surface. From the late 1970s, episodic observations of aerosols were also made at several sites across the Russian Arctic, including measurements of the particle size distribution and the spectral aerosol optical depth. Measurements of aerosol microphysical and chemical properties are also available from a few aircraft field experiments conducted in the Northern American and European Arctic. A number of expeditions onboard research vessels have been conducted that provided information on aerosol properties in the boundary layer (e.g., Shevchenko 2003).

10.3.1 Observed Long-Term Changes in Concentrations and Composition of Arctic Aerosols

The trends in sulfate, nitrate and BC measured in situ at ground-based stations in the Northern American and European Arctic were recently reviewed by Quinn et al. (2007). Here we briefly summarize some major features that help to visualize the region-specific nature of aerosol concentrations and their variability. In addition, we discuss measurements of crustal species that are representative of mineral dust.

Concentrations of sulfate aerosol have been measured at Alert, Canada since 1980, which is the longest record of sulfate in the Arctic. Analyses of monthly mean values for March and April show no clear trend in the 1980s and a decreasing trend since about 1991, although overall there is a decrease of about 60–70% between 1981 and 2003 (Sirois and Barrie 1999; Quinn et al. 2007). This decreasing trend was also observed at several other stations, including Zeppelin, Karasjok and Oulanda. Sulfate concentrations at these stations decreased by 30–60% since 1990. However, filter measurements at Barrow do not reveal any significant trend in sulfate concentrations (Quinn et al. 2007). Also, there are no significant trends at Svanvik and Janiskoski stations, but the overall decreasing tendency is apparent. Various differences in the recorded time serious of aerosol concentrations illustrate the regional specifics of the aerosol distribution across the Arctic, despite the overall decrease of industrial emission of SO_2 in Northern Eurasia and Europe (see Section 10.2).

Measurements of light scattering at Barrow have been conducted since 1977. Scattering depends on aerosol concentrations but is also affected by particle sizes and composition. Bodhaine and Dutton (1993) found a maximum in light scattering in 1982 followed by a factor of two decrease for March and April between 1982 and 1992. No decrease in other months was observed. Analyzing updated data through 2006, Quinn et al. (2007) reported a significant decreasing trend for March over the entire measurement period. However, if the time period from 1997 to 2006 is considered, then there seems to be an increasing tendency in light scattering. Apparently, decreasing trends in light scattering do not relate directly to changes in sulfate aerosols and SO_2 emissions. Nevertheless, there is general support for decreasing sulfate during the Arctic haze season in the 1990s that is consistent with decreasing sulfur emissions in Western Europe and Northern Eurasia.

Light absorption measurements that have been conducted at Barrow and Alert since 1988 and 1989, respectively, allow evaluation of the concentration of BC. These records indicate that BC concentrations have declined by 54% at Alert and 27% at Barrow from 1989 to 2003, but with some indication of a recent increase of BC concentrations (Sharma et al. 2006). Observations in conjunction with the back trajectory analysis suggested that Russian sources have the strongest influence on BC levels at Alert and Barrow. There is no convincing observational evidence to support the dominant role of Southeast Asian sources of BC as suggested by some modeling studies discussed in Section 10.2.

Available chemical measurements of crustal constituents (such as Al, Ca and Mg) conducted at Barrow and Alert do not show monotonic trends. Both locations show higher concentrations in winter and spring, indicating the seasonal variation of

mineral aerosol in the Arctic that is consistent with the long-range transport of Asian dust. These measurements reveal a clear seasonal cycle but also a strong interannual variability (Quinn et al. 2007). At Alert, the second maximum in the concentration of crustal constituents in observed in fall that is likely caused by local wind erosion (Sirois and Barrie 1999). The presence of dust in the marine boundary layer in the Russian Arctic during summer and fall was also reported from research vessel expeditions (Shevchenko 2003). The origin of this dust is likely from the coastal land through aeolian processes.

In summary, in situ ground-based measurements of chemical composition and optical characteristics reveal a well-defined seasonal cycle of aerosol species across the Arctic, although large interannual variability is also apparent. BC concentrations are highest during late winter and spring and have a minimum during summer. Anthropogenic sulfate concentration tends to peak slightly later in winter than black carbon, since sulfate formation depends upon photochemical processes that become active when the polar sun rises. Measurements of crustal constituents also show higher concentrations in winter and spring, indicating the presence of highest concentration of mineral aerosol during the Arctic haze season.

10.3.2 Seasonal Cycle and Trends in Aerosol Optical Depth

Measurements of atmospheric radiation that have been conducted at actinometric stations in the Russian Arctic since about the 1940s (see Fig. 10.5), provide a unique, long-term data set for examining the aerosol trends in terms of aerosol optical depth (AOD). Unfortunately, these stations stopped to operate in the early 1990s. AOD is one of the key optical characteristics of aerosols that control the magnitude of direct radiative forcing. Because AOD is proportional to the column-integrated aerosol amount, changes in AOD relate to changes in aerosol concentrations within the entire atmosphere, including high level volcanic aerosols when present. A summary of historical radiation observations in the Arctic over the past 30 years can be found in Tomasi et al. (2007). More recently, AOD is being routinely measured at many ground-based stations throughout the world as well as retrieved from satellite observations. Unfortunately, only few of these stations are located in the Arctic [e.g., Barrow (since 1977), several AERONET stations in Northern America, including a Canadian sunphotometer network called AEROCAN (since about 1994), and Ny Alesund (since 1991)]. Furthermore, satellite measurements do not permit retrievals of AOD over the bright surfaces (such as snow and ice), during the polar night, and in cloudy conditions. Therefore, observations of the spatial coverage of AOD in the Arctic remain limited.

Recently, active remote sensing instruments such as the Cloud-Aerosol Lidar and Infrared Pathfinder Satellite Observation (CALIPSO) satellite have been deployed which provide the capability to measure the vertical profiles of aerosols and clouds from lidar backscatter measurements (Winker et al. 2007). Figure 10.6 shows observations from the CALIPSO lidar of the Asian dust event (shown in Fig. 10.4) reaching the Northern American Arctic on 4 and 5 April 2007. The high-altitude

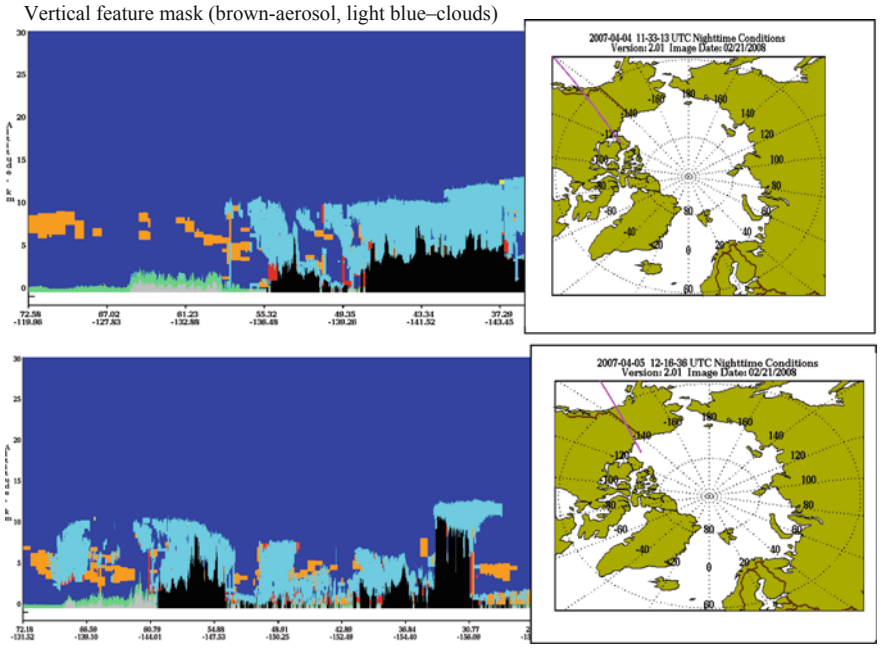

Fig. 10.6 Observations from the CALIPSO Lidar from 4 to 5 April 2007 showing layers of Asian dust (in *brown* color) acquired along the orbit tracks (shown in panels at the *right side*) that passed over the Northern American Arctic. *Blue* color indicates clouds

layers of Asian dust (shown in brown color) as well as dust mixed with clouds are apparent. The CALIPSO lidar, performing day and night measurements over multiple overpasses over the Arctic, has the high potential to provide new insights on the vertical distribution of aerosols and clouds, albeit limited by the CALIPSO mission lifetime.

Long-term observations have demonstrated that AODs exhibit a seasonal cycle with a springtime maximum caused by Arctic haze and summertime minimum across the entire Arctic. In spite of this, various differences from station to station and from year to year were found (Radionov and Marshunova 1992; Radionov et al. 1995). Figure 10.7shows the seasonal cycle of AODs at stations across the Russian Arctic. AODs are higher in spring in the western and central (Kara Sea – Laptev Sea) parts of the Eurasian Arctic compared to the eastern (East Siberian Sea – Chukchi Sea) part. Conversely in the summer (June–August), the eastern Russian Arctic experiences higher AODs than the western part. The higher AODs in the western and central Russian Arctic during spring months can be explained by the relative proximity to the sources of anthropogenic pollution located in Western and Central Siberia and Western Europe. The opposite tendency observed in the summer was explained by regional differences in atmospheric circulation (Shahgedanova and Lamakin 2005). The eastern Eurasian Arctic experiences more frequent high-pressure or low-pressure gradient systems with low wind speeds in

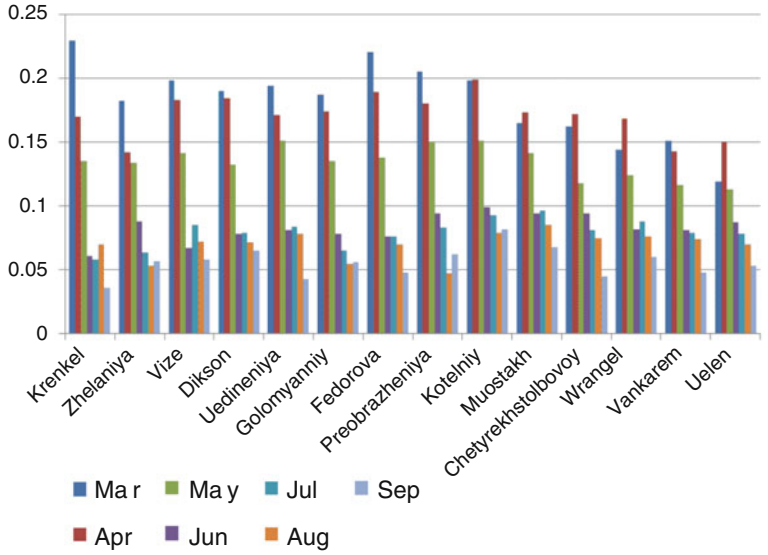

Fig. 10.7 Seasonal cycle of the multi-annual monthly mean values of AOD measured at the actinometric stations located in the Russian Arctic. Data and the retrieval procedure are described in Shahgedanova and Lamakin (2005)

summer, resulting in less efficient removal of aerosol from the atmosphere. Large day-to-day variability in AOD in the Barents Sea–Kara Sea–Laptev Sea region during all seasons was also attributed to strong variability in weather patterns and air mass trajectories (Shahgedanova and Lamakin 2005).

During the twentieth century, two large volcanic eruptions affected the aerosol optical depth globally through enhanced concentrations of stratospheric aerosols. A uniform increase in AOD over the entire Arctic was observed in 1983 after the El Chichon eruption in 1982 and in 1991–1993 after the Pinatubo eruption in 1991. It is common to exclude the 1982–1983 and 1991–1993 time periods in the analysis of trends in AOD related to tropospheric aerosols. After removing the volcanic contribution, a statistically significant positive trend in AOD was observed in the Kara Sea–Laptev Sea region of the Russian Arctic between the late 1950s and the early 1980s, predominantly in spring when pollution-derived aerosol dominates the Arctic atmosphere. However, no significant trends were found at stations in the eastern Russian Arctic, except the most eastern station Uelen on the Bering Strait coast. This station is located relatively close to Barrow, Alaska where measurements of AOD have been conducted since 1977. Both Uelen and Barrow show an increasing tendency in AODs until about 1982.

Since the early 1980s, a widespread decline in AOD was observed in the eastern Russian Arctic during spring, but the decrease was limited only to two sites in the western Russian Arctic (Dikson Island and Uedineniya Island). Because of the lack of spatially uniform trends in AODs in the spring during 1982–1999, Shahgedanova and Lamakin (2005) concluded that the post-1982 decline in

anthropogenic emissions in Europe and the former Soviet Union has had a limited effect on aerosol load in the Arctic while changes in general circulation played an important role. Examining the relationship between AODs and air mass types for the Dikson Island (western Russian Arctic) and Wrangel Inland (eastern Russian Arctic), they suggested that strong westerly and northerly flows result in low AOD values in the eastern Russian Arctic. By contrast, strong southerly flow associated with the passage of depressions results in high AOD in the western Russian Arctic. Their study found that high values of AOD in summer were associated with low pressure gradient or anticyclonic conditions. The frequency of this weather type has declined significantly since the early 1980s in the Kara Sea–Laptev Sea region. It has been suggested that this decline could partly explain the decline in summer AOD in this region. Although differences in meteorological and some climatic characteristics between the different parts of the Russian Arctic have been well recognized (Radionov et al. 2007), they do not offer a clear explanation of observed AOD trends.

Furthermore, the AOD trends observed in the Russian Arctic differ from other regions of the Arctic. Examination of trends through 2002 for Barrow revealed a continued decrease of AOD during March; however, for April there seems to be an increasing tendency between 1998 and 2002 (Quinn et al. 2007). Unlike the Barrow record, a weak positive trend in AOD of about 1% per year from 1991 to 1999 was reported by Herber et al. (2002) from measurements at the Koldewey station in Ny-Alesund, Spitzbergen. For summer months, Tomasi et al. (2007) reported a decreasing trend of –1.6% per year for the time period of 1977–2002 for Barrow, and for Ny-Alesund of about –2.2% per year between 1991 and 2006. Thus, different parts of the Arctic showed different trends in AOD during both spring and summer seasons.

The regional and seasonal variations of trends in aerosol optical characteristics in the Arctic are clearly complex. The sulfate concentration, aerosol light scattering, and absorption exhibit downward trends at some sites across the Arctic. Some locations also exhibit decreasing trends in AOD. These decreasing trends are largely attributed to emission reductions in the source regions. However, nitrate concentrations have been increasing over the past 2 decades. Existing decreasing trends in AODs during the summer are mainly controlled by natural aerosols. Yet the contribution of emissions from natural sources within the Arctic (volcanoes, marine algae, soil and forest fires) are very difficult to quantify and almost impossible to project. Transport of smoke from fires in Northern Eurasia and Northern America and dust from East Asia is highly variable, so the trends of these species in the Arctic remain unknown. Furthermore, there are some differences between long-term changes in aerosol surface concentrations and AOD. Radionov et al. (2007) demonstrated that the temperature inversion in the Arctic leads to decoupling of surface aerosols from layers aloft. The existence of vertically layered aerosol structure is supported by aircraft observations and lidar measurements (see Fig. 10.6). The complex spatiotemporal patterns of Arctic aerosols and a paucity of data render the assessment of the aerosol impact on the Arctic system particularly difficult.

10.4 Climate Forcings of Arctic Aerosols and Feedbacks

Assessment of the impact of aerosols on the Earth's climate remains one of the most challenging problems (IPCC 2007). The large uncertainty stems from the complex nature of interactions of aerosols with the different components of the Earth system that involve many interrelated processes and depend on the various physical and chemical properties of aerosol particles and their spatiotemporal distribution. The latter makes the assessment of aerosol impacts quite different compared to CO_2 whose contribution to the climate warming proceeds through a radiative perturbation of the Earth's energy balance, and concentrations of CO_2 are a major single quantity needed to predict the LW radiative forcing by CO_2. Unlike greenhouse gases, aerosol particles affect the climate system not only through interactions with atmospheric radiation but also by affecting directly the hydrological cycle and important biogeochemical cycles. The IPCC (2007) report has identified aerosols as a key climate forcing agent whose impact on climate change remains highly uncertain. Given the complexity of sources of Arctic aerosols and a paucity of observations, understanding how aerosols have been contributing to changes occurring in the Arctic region seems to be a very difficult task.

Many studies have attributed the observed post-1960 warming in the Arctic to changes in the atmospheric circulation pattern (e.g., Serreze et al. 2000), the greenhouse effect by CO_2 and other greenhouse gases, or their combination. The same factors were suggested to be responsible for a shift of precipitation in the Arctic. Assessments of twentieth-century precipitation (IPCC 2007) show the largest increase in precipitation in the Arctic region relative to any other latitudinal zone. However, the Arctic warming of the recent decades appears to have multiple causes. This warming has been strongest in winter and spring, when the impact of Arctic aerosols could be the largest. Given that much of Arctic aerosols are of anthropogenic origin and can cause significant impacts, aerosols are likely to exert an important anthropogenic forcing (not a component of the natural Arctic system) affecting climate change of the Arctic that is not due to natural climate variability. Below we explore the main mechanisms and feedbacks involving Arctic aerosols and implications to the energy balance and hydrological cycle in the Arctic.

10.4.1 Direct Radiative Forcing of Arctic Aerosols

By scattering and absorbing SW and LW radiation and emitting LW radiation, atmospheric aerosols can affect directly the energy balance. Of particular importance is the aerosol impact on the radiative energy balance at the top-of-the-atmosphere (called direct TOA radiative forcing), at the surface (called direct surface radiative forcing) and within the aerosol layers, by providing the additional radiative heating or cooling to the layers. Collectively, these mechanisms are referred to as the direct radiative forcing of aerosols. The contribution to the energy balance is determined by the net radiation which is the difference between the downward and upward radiative fluxes. It is common to represent radiative fluxes as a sum of direct and

diffuse fluxes. The presence of aerosols (or clouds) always decreases the direct radiation but the diffuse radiation can increase depending on the optical depth and the light absorption. The direct radiative impact of aerosols is determined by a set of optical characteristics including the AOD, single scattering albedo and asymmetry parameter (or scattering phase function). It also depends on the atmospheric conditions (especially, the temperature profile and concentrations of gases), the presence of Sun and its position, as well as conditions of the surface that control the surface reflectivity (albedo) in the shortwave and surface emissivity in the longwave. Coupling of the radiative impact of aerosols and the surface albedo is particularly important in the Arctic for a number of reasons (see Section 10.4.2). For instance, even the small amount of light absorptive aerosols (such as BC or dust) cause a positive TOA direct radiative forcing over bight surfaces such as snow and ice, while the same aerosol cause a negative forcing over surfaces with lower albedo such as dark water and snow-free tundra. In addition, the shortwave heating of the aerosol layers is greater over surfaces with higher albedo because of multiple reflection of light between the surface and the aerosol layers.

Much of our current understanding of the direct radiative impact of aerosols has been derived from model simulations. In particular, a large number of studies have used 1-D radiative transfer models to estimate the magnitude of the radiative effects of Arctic aerosols (e.g., MacCraken et al. 1986; Shaw and Stamnes 1980; Iziomon et al. 2006; Stone et al. 2008). Although information on the optical properties and their vertical distribution required in such modeling are limited for Arctic aerosols, these studies are broadly in agreement with observations and help to assess the magnitude of aerosol direct radiative forcing. These studies also help to determine the relative importance of different aerosol species constituting Arctic aerosols. For instance, a recent study by Stone et al. (2007) analyzed an incursion of Asian dust to Barrow, Alaska during spring 2002 (see Fig. 10.3). They utilized a suite of measurements to empirically determine the direct surface radiative forcing caused by dust in conjunction with the MODerate spectral resolution atmospheric TRANSsmittance (MODTRAN) radiative transfer code. As expected, they found that the presence of Asian dust in the Arctic atmosphere significantly decreases the SW radiation but increases the LW radiation reaching the surface, while heating occurs within the dust layer itself. For observed AOD of about 0.4 at the 500 nm wavelength and for a typical spring day at Barrow, solar heating within the layer was about 2 K per day with a net loss of the surface SW radiation of 12 W m^{-2} (for solar angle of 75°). Their findings imply that incursions of Asian dust will tend to cool the surface at high northern latitudes and heat the atmosphere, leading to increased stability of the lower atmosphere. Similar analyses were performed for the case study of smoke plumes (Stone et al. 2008). For snow-covered surfaces, their study reported a SW radiative forcing at the surface of 15 W m^{-2} and at the top of the atmosphere of -5 W m^{-2}. For the same aerosol optical depth (AOD=0.25 at the 500 nm), the respective forcings over the sea were -25 W m^{-2} at the surface and -10 W m^{-2} at the TOA. These values are in agreement with past studies. However, it is difficult to generalize implications of the aerosol impact found from the individual case studies, which were conducted at a local measurement site for a short (a few

days) time period, to the whole Arctic and to longer time scales that are needed for understanding climate change.

Unfortunately, no long-term measurements of the TOA forcing and heating/cooling rates have been conducted in the Arctic. However, long-term ground-based radiation measurements provide an opportunity to explore the role of Arctic aerosols in the surface energy balance at longer time scales. Given the long-term changes in AODs and aerosol composition in the Arctic (see Sections 10.2 and 10.3), one would expect to see associated changes in observed surface radiation. However, detecting an aerosol signal in radiation observations is not straightforward.

The historical radiation measurements from the Russian Arctic have been analyzed by a number of studies (Gavrilova 1963; Abakumova et al. 1996; Radionov et al. 2007). Abakumona et al. demonstrated a decreasing tendency in the time series of direct and total (direct plus diffuse) solar radiation in 60% of actinometric stations located in the former Soviet Union. However, the stations in the Russian Arctic did not show clear trends. The most recent analysis by Radionov et al. confirmed the previous finding that there are no significant trends in total solar radiation in the Russian Arctic during the past half-century, although some differences in radiation regimes in the western, eastern and central parts of the Russian Arctic were demonstrated. The absence of trends was explained by changes in clouds. However, analyses of cloud-free radiation measurements did not reveal significant trends either (Radionov et al. 2007).

On the contrary, distinct trends in radiation were reported for Northern American Arctic. Weston et al. (2007) analyzed trends in net and solar radiation measurements that have been conducted over the past half-century at Alert (82°30′ N, 62°20′ W) and Resolute Bay (74°42′ N, 94°50′ W), Canadian Arctic. They found that downward solar radiation decreased significantly at both sites. The decreasing trends of 2.25 and 2.50% per decade in solar radiation were observed at Alert (from 1964 to 2002) and Resolute Bay (from 1957 to 2003), respectively. Analyses of cloud-free radiation data indicated that observed trends are due to changes in atmospheric constituents (aerosols and gases). Cloud cover did not show any significant trends in any months of the year. Pinker et al. (2005) show a similar decrease in solar radiation at Barrow, Alaska, from 1983 to 2001 based on both satellite and ground-based measurements. However, both studies pointed out that there appears to be an increase in solar radiation in the most recent decade at both sites.

In contrast to decreasing solar radiation, Weston et al. (2007) reported a significant overall increase in net (SW plus LW) surface radiation of 26.7% and 17.9% per decade at Alert and Resolute Bay, respectively. Most changes were observed in the months of May and June when snowmelt occurs, while there were no strong changes in other months. Analyses of independent measurements of the surface albedo for Resolute Bay revealed a decreasing trend (in annual average values) and a strong inverse correlation between the surface albedo and net radiation. This was explained by earlier snowmelt and longer snow-free periods that resulted in lower (snow-free tundra) albedo during months when solar radiation is high and hence more solar radiation absorbed by the surface. Weston et al. also suggested that the increase

of net surface radiation was partly due to increasing LW component of the surface energy balance.

Overall, the records of surface radiation in the Arctic show that the long-term aerosol direct impact must be considered along with changes of the surface albedo, clouds, and gases in understanding variations of the arctic surface radiation budget. Even in cloud-free conditions, decreasing (increasing) AOD will not necessarily lead to an increase (decrease) of the net surface radiation since coincident changes in other atmospheric and surface conditions may compensate for the radiative effect of aerosols. Conversely, aerosols can modulate the effect of increasing greenhouse gases and warmer temperatures on the surface energy balance in the Arctic and hence snowmelt.

10.4.2 Arctic Aerosols and Surface Albedo Interactions

It has been long recognized that deposition of light absorbing aerosols such as BC and dust onto snow- and ice-covered surfaces can result in a reduction of the surface SW albedo. Clarke and Noone (1985) found that snow albedo is reduced by 1–3% in fresh snow and by another factor of three as the snow ages and the BC concentrations increases. A modeling study by Hansen and Nazarenko (2004) found that this decrease in the surface albedo in the Arctic resulted in a hemispheric positive radiative forcing of +0.3 W m^{-2} which may have had a substantial impact on the Northern Hemisphere climate in recent decades. It has been suggested that the climate forcing due to this albedo effect is relevant when compared with the effect of greenhouse gases. The efficacy of the albedo effect, measured as the effectivity in increasing the surface air temperature per unit of forcing, is twice as large as that of CO_2 forcing, and it may be even more effective in melting snow and ice. Unfortunately, these assessments are subject to large uncertainties because of limited measurements of BC in snow in the Arctic region. No studies have assessed the impact of dust deposition on snow surfaces. Loadings of dust in the Arctic might be larger than BC, given that both long-range transport and local erosion processes supply dust particles. The changes in snow cover due to the ongoing warming might lead to more exposed soil and hence promote the dust emission.

The changes in land cover, snow and sea-ice also have a profound effect on the direct radiative forcing of Arctic aerosols. Chapin et al. (2005) demonstrated a significant decrease in summer surface albedo due to terrestrial changes caused by high-latitude warming trends. Also, the retreat of sea-ice opens large water bodies with lower surface albedo relative to sea-ice. Decreases in the surface albedo will lead to more negative SW surface forcing of aerosols that counters the effect of greenhouse gas warming.

The retreat of sea-ice in the Arctic Ocean might also provide an additional source of dimethylsulfide (DMS), which is produced by marine phytoplankton and sea-ice algae that can lead to the production of sulfate aerosols. Open ocean also provides additional sea-salt aerosols. By reflecting solar radiation, these aerosols further contribute to the cooling of the surface. In addition, they are effective CCN and

promote the formation of clouds that in turn tend to cool the dark surfaces. Thus, if warming leads to higher production of DMS, sulfates and sea-salt, then there will be an additional mechanism (through clouds) leading to cooling. Gabric et al. (2005) demonstrated that a decrease in sea-ice extent of approximately 20% over the annual cycle (about 60% during the summer-autumn season) can lead to an 80% increase in DMS production by 2080. This increased production is estimated to have a cooling effect of between 5 and 13 W m^{-2} over the Arctic Ocean during the summer months (June–September), which would be a substantial negative feedback on the radiative balance of the Arctic.

10.4.3 Indirect Radiative Effects of Arctic Aerosols

More complicated and likely of greater climatic importance is the indirect effect of aerosols on the properties and radiative forcing of clouds. Given their large spatial and temporal coverage, Arctic clouds have a large impact on the radiative budget of the Arctic system, governing the transfer of both SW and LW radiation. The potential indirect effect in the Arctic is especially large because of the significant cloud radiative couplings with energetics and dynamics (Vavrus 2004). Furthermore, Arctic clouds play significant roles in the influential but not well understood ice–albedo and cloud–radiation feedback mechanisms (Curry et al. 1996).

Arctic aerosols have the potential to affect all properties of clouds relevant to their interactions with atmospheric radiation, as well as the hydrological cycle in the Arctic (see Section 10.4.4). Water soluble aerosols (e.g., sulfate, nitrate and sea-salt) act as cloud condensation nuclei. Increasing CCN concentration results in clouds with larger droplet concentrations and smaller droplet sizes relative to clouds forming under more pristine conditions. Clouds with larger droplet concentration and smaller droplet sizes reflect more solar radiation back to space (Garret et al. 2004). It has also been suggested that aerosols can increase the LW emissivity of Arctic liquid phase clouds (Lubin and Vogelmann 2006; Garret and Zhao 2006). Because Arctic clouds are often relatively thin and do not emit like a blackbody as thick water clouds usually do, their emissivity increases with the decreasing effective size of cloud droplets. This enhances the downwelling LW radiation fluxes, an effect opposed to the increasing cloud albedo effect on the solar radiation. In the Arctic, the LW emissivity effect is most important in winter and early spring, when Arctic haze aerosols are abundant, thin clouds persist, and the radiation balance is controlled chiefly by LW radiation because of the absence or small magnitude of solar radiation.

Furthermore, insoluble aerosol (e.g., dust and BC) may act as ice-forming nuclei. Increasing the concentration of IN could change the phase of clouds at temperatures below the freezing point from liquid to ice, resulting in decreased shortwave reflectivity and longwave emissivity of the clouds. However, aerosol-ice microphysical interactions, and their potential impact on the regional cloud cover, thermodynamics, and mesoscale dynamics in the Arctic, remain highly uncertain.

The impact of pollution on IN is hypothesized to be largely dependent upon the chemical composition. Borys (1989) suggested that a large sulfate component may deactivate existing IN. In contrast, frequent intrusions of smoke and Asian dust to the Arctic will supply more IN. A modeling study by Jiang et al. (2000) showed that an increase by only a factor of two in IN can transform a stable stratus cloud layer into a broken optically-thin cloud layer, significantly affecting the radiative budget. Thus, aerosol from pollution sources, biomass burning, and desert dust can modify the concentrations of both CCN and IN but in different ways, and hence varying chemical composition of Arctic aerosols is likely to be an important factor in perturbing cloud properties and their radiative impacts.

Indirect aerosol effects may differ significantly in the Arctic compared with other regions due to uniqueness of the surface and thermodynamic properties of the atmosphere. The Arctic is particularly susceptible to aerosol indirect effects, because the low aerosol number concentrations result in a large fraction of particles being activated during cloud formation. In the Arctic, low-level mixed-phase clouds tend to occur frequently throughout the year (Curry et al. 1996). These clouds may be especially sensitive to aerosol since they are unstable and tend to occur under weak synoptic forcing (Zuidema 2005). Indirect aerosol effects may be particularly important over the Arctic Ocean, since fairly small changes in the surface radiative fluxes may significantly impact the thickness and concentration of sea-ice over climatic timescales (Curry et al. 1996). These surface changes may, in turn, impact the aerosol and cloud microphysics, representing a potentially important feedback pathway. Understanding these interactions and feedbacks is critical to understanding the climate change occurring in the Arctic.

Although indirect aerosol effects on clouds have been well recognized, there have been no comprehensive studies conducted to investigate how varying Arctic aerosols have been affecting cloud properties in the Arctic over the past decades. Some recent studies that analyzed changes in clouds in this region mainly interpreted observed trends in terms of changes in atmospheric moisture and meteorological conditions. For instance, Wang and Key (2003) reported trends in satellite-derived cloud and surface properties from 1982 to 1999. They concluded that the Arctic has warmed and become cloudier in spring and summer but has cooled and become less cloudy in winter. The increase in spring cloud amount radiatively balances changes in surface temperature and albedo, but during summer, fall, and winter, cloud forcing has tended toward increased cooling. This implies that, if seasonal cloud amounts were not changing, surface warming would be even greater than that observed. Wang and Key suggested that strong correlations with the Arctic Oscillation indicate that the rise in surface temperature and changes in cloud amount are related to large-scale circulation rather than to local processes. Based on satellite and reanalysis data, another study reported a decrease in cloud cover in winter (December, January, February) over most of the Arctic Ocean from 1982 to 2000 (Liu et al. 2007). Concurrently, wintertime moisture convergence has decreased significantly over the Nansen Basin and parts of the Barents and Kara Seas (75–90°N, 45–90°E). Over this region, correlation coefficients between monthly anomalies in the satellite-derived cloud cover and moisture convergence in the cold season were large and statistically

significant. Liu et al. (2007) suggested that this reduction in moisture convergence results in a decrease in cloud formation due to weakening cyclone activity over this region. Reduced cloud amount over this area leads to decreased cloud cover over the entire central Arctic because less cloud is advected to other regions. The same mechanism has been observed over northeastern Russia and the Bering Strait area (65–75°N, 150–200°E) and is therefore an additional, and perhaps more important, control over cloud cover in the Chukchi/Beaufort Seas and the Laptev Sea region.

Neither of the above studies considered the effects of aerosols as a potential mechanism. As discussed in Section 10.3, the regions where the largest changes in clouds are observed have been affected the most by transported aerosols. Alternatively, decreasing cloudiness in winter might be explained through the aerosol indirect effect. Girard et al. (2005) hypothesized that a trend in aerosols characteristics is altering ice nucleation and resulting in less atmospheric water vapor and more precipitation cooling the surface. Furthermore, Shindell (2007) suggested that aerosols in the mid-latitudes can affect meridional transport of moisture and heat to the Arctic from lower latitudes. Approximately half the warming of the Arctic is being attributed to increased moisture and heat fluxes transported to the region (McGuire et al. 2006). Thus, not only Arctic aerosols themselves are of importance but also aerosols in the mid-latitudes and tropics might play an important role in modulating the Arctic climate (Shindell 2007). The contribution of this aerosol-involved teleconnection to the regional changes occurring in the Arctic region remains practically unknown.

Recently, regional and global climate models were used to assess the response of Arctic climate to aerosol direct and indirect radiative forcing. Quinn et al. (2008) reported an assessment of seasonally average radiative forcing of direct and indirect aerosol forcings in the Arctic (60–90°N) and compared them to forcing caused by ozone and methane. Their study used the NASA GISS general circulation model that was forced globally with aerosol composition changes. The direct radiative forcing was calculated as the change in "instantaneous" forcing by adding fossil fuel and biofuel emission to the baseline simulations (i.e., emissions from the present-day biomass burning). Thus, Quinn et al. (2008) neither reproduced the observed long-term changes in sulfate and BC in the Arctic, nor considered the dynamics of smoke and dust intrusions. The surface temperature response due to BC deposition on snow and ice surfaces was calculated with the US National Center for Atmospheric Research (NCAR) CAM3 model (Flanner et al. 2007). The indirect radiative forcing included the cloud albedo and cloud cover changes. The LW forcing by clouds was not computed by the model but was assigned to a value reported by Garrett and Zhao (2006) from observations. Comparing individual direct and indirect aerosol forcings, Quinn et al. (2008) suggested that direct radiative forcing caused by changes in sulfate+OC+BC concentrations resulted in a decrease in the surface temperature between –0.47 and –1.1°C depending on the season, whereas changes in cloud cover (i.e., indirect aerosol forcing) resulted in somewhat smaller decreases between –0.45 and –0.89°C. In contrast, the deposition of BC onto the ice/snow surfaces and aerosol-related changes in LW cloud forcing resulted in an increase of surface temperature of 0.5°C and 1–1.6°C, respectively. Thus to assess the overall aerosol effect

on the surface temperature in the Arctic, one must account for opposing tendency of individual forcings, which poses a difficult problem because of large uncertainties associated with the variability of the abundance and composition of aerosols in the Arctic.

Furthermore, Quinn et al. (2008) found an offset between the season of maximum forcing and maximum response in surface temperature. For instance, the largest direct radiative surface forcing of aerosols was calculated for the summer season but the largest changes in surface temperature were in the winter. This offset was interpreted by the influence of forcing in other regions on the changes in Arctic surface temperature. Another study specifically examined the response of the surface temperature, T_s, in the Arctic (68–90°N) to local forcing (due to Arctic aerosols) versus the remote forcing that caused by aerosols in the Northern Hemisphere but outside of the Arctic region (Shindell 2007). The Shindell's study, which was also based on the NASA GISS climate model, suggested that, except for the summer season, changes in T_s were not correlated with the local forcing but were driven by global or Northern Hemisphere forcings. This decoupling implies a greater role of anthropogenic aerosols in mid-latitudes in controlling the Arctic climate through altering large-scale transport of heat and moisture to the Arctic than was previously thought. If this would be the case, then controlling emissions of air pollutants in Europe, Northern Eurasia, and Northern America along with increasing frequency of wild fires and dust storms might lead to more warming in the Arctic.

10.4.4 Impacts of Aerosols on the Arctic System

Through direct (including the surface albedo effect) and indirect forcing discussed above as well as aerosol-induced feedbacks, Arctic aerosols can affect precipitation and the main components of the cryosphere (such as sea-ice and land snow cover) and hence play an important role in the Arctic climate system, including terrestrial ecosystems. Suggested mechanisms include aerosol-induced changes in clouds that affect precipitation, and aerosol-related changes in sea-ice and snow coverage.

In addition to increasing the SW cloud albedo, it has been hypothesized that enhanced aerosol concentrations increase the number concentration and decrease the size of cloud droplets, causing a reduction of rain formation and an increase of cloud lifetime (termed as the second indirect effect, Albrecht 1989). Despite the recent emphasis of observational and modeling studies on indirect aerosol effects, few studies have focused specifically on indirect aerosol effects in the Arctic. The consensus is that the availability of IN may be a critical factor in the persistence of weakly-forced arctic mixed-phase clouds and their precipitation efficiency (Harrington et al. 1999; Jiang et al. 2000; Morrison et al. 2005; Morrison and Pinto 2005). The general lack of in situ sources of IN and depletion of IN within cloud layers may play a key role in the longevity and evolution of these clouds. Morrison and Pinto (2005) found that increased concentration of IN led to decreased precipitation rates in arctic mixed-phase stratus due to rapid depletion of liquid water and subsequent changes in the heat and moisture budgets, while Lohmann (2002a, b)

found that increased IN led to rapid glaciation and more overall precipitation in a general circulation model. Lohmann et al. (2003) present evidence that increasing anthropogenic aerosols may actually increase precipitation in the Arctic by modifying droplet size, contrary to mid-latitude studies that show increased pollution may decrease snowfall by limiting riming (e.g., Borys et al. 2000, 2003).

A recent modeling study by Morrison et al. (2008) demonstrated that sensitivity of the springtime mixed-phase clouds to CCN and especially IN concentrations was dependent on the underlying surface conditions. Over the open ocean, which is a significant source of moisture and heat to the atmosphere, sensitivity to changes in both CCN and IN was relatively low because of large liquid water content of clouds, whereas over the snow-covered land clouds exhibited strong sensitivity to changes in CCN and IN. Nevertheless, Morrison et al. demonstrated that increasing the CCN concentration produced smaller cloud droplets, leading to decreased snowfall rate in the model. Two processes contributed to these changes: decreased riming efficiency of cloud ice and snow by droplets, and decreased droplet collision coalescence and hence production of supercooled drizzle. Increasing the IN concentration increased the precipitation rate. Overall, these studies suggest the importance of aerosols in modifying precipitation but also highlight uncertainties in our understanding of microphysical processes in cold clouds.

The Intergovernmental Panel on Climate Change (IPCC 2001, 2007) has consistently reported increasing precipitation in the twentieth century in northern high latitudes. The greatest increase appears to have occurred during the first half of the twentieth century. However, the time series are based on data from the synoptic station network, which is unevenly distributed and has undergone much change. Thus in addition to poor knowledge of Arctic aerosol-cloud interactions, delineating the aerosol impact on precipitation is difficult because of the large uncertainties in the distribution of precipitation throughout the Arctic.

Several studies explored the linkages between changes in clouds and the decrease in sea-ice extent. The past 50 years have seen a dramatic loss of Arctic sea- ice (see also Chapter 2, this volume), especially during late summer (Serreze et al. 2007). Francis et al. (2005) and Francis and Hunter (2006) suggested that variability in the summer-minimum ice-edge position is highly correlated with anomalies in the downward LW radiation flux from the atmosphere, especially after 1992 when the ice cover was thinner and thus more susceptible to anomalies in the surface energy balance. These studies also found that the ice-edge retreat is anticorrelated with anomalies in the incident solar radiation, suggesting that the observed increases in springtime cloudiness (Wang and Key 2003) cause increased emission of LW radiation to the surface that exceeds the increased reflection of incoming solar energy by the clouds. Francis and Hunter (2006) also found that in the Pacific sector, approximately half of the variance in ice-edge position attributable to downward LW radiation anomalies results from the increasing trend in LW forcing during the melt season. If these changes in cloudiness were caused by aerosols, at least partially, then aerosols contributed to the decrease of the sea-ice extent.

In addition to affecting the precipitation and sea-ice, aerosols can influence snowmelt and permafrost thawing through the direct and indirect radiative forcings.

Snow cover extent over the Arctic land areas has decreased by 10% in the past 20 years (Hasool et al. 2004), with the decrease greatest in spring (April/May). Increasing incidence of thaw/freeze in fall and winter leads to ice layer formation that in turn restricts access of land animals to food and nesting sites (see Chapters 8 and 9, on reindeer herding in this volume). The change in snow cover is leading to shifting vegetation zones, with substantial impact to the boreal forest. The increasing snow-free period is also leading to an increase in forest fires. Besides the impact to the arctic ecosystems, the longer melt season substantially disrupts surface transportation requiring the presence of ice roads and frozen tundra for oil and gas extraction and timber harvesting. There are two critical issues relevant for surface hydrology: the onset of the spring snow melt and the onset of the autumnal snow accumulation. A recent global climate simulation of the atmospheric transport and deposition of BC to Arctic snow performed by Flanner et al. (2007) showed that resulting perturbations to Arctic climate included shifting the peak in the snowmelt season to almost a month earlier in springtime, limited primarily by available sunlight. As a result of earlier snowmelt, the Arctic sea-ice underneath absorbed more solar radiation and melted earlier, with resulting Arctic-wide temperature increases of >2 K.

10.5 Conclusions

The dramatic changes that have been occurring in the Arctic system remain poorly explained due the complex nature of climate forcing agents and their interactions. Nevertheless, climate change in the Arctic may have profound implications for both fragile ecosystems and unique modes of human habitation in this region, as well as far-reaching consequences on the Earth's climate system. Modeling and observational studies have provided evidence that atmospheric aerosols are linked to major processes that affect the atmosphere, cryosphere, land and ocean, and hence have played at least some role in changes occurring in the Arctic in recent decades. However, accurate assessment of the climate impact of aerosols in the Arctic is difficult because of very complicated interactions and feedbacks involving aerosols. Paucity of aerosol data further complicates such assessments. Despite the complexity involved, improved assessments of aerosol impacts in the Arctic is of high priority because of the uncertainty and magnitude of the potential impacts caused by anthropogenic aerosols.

The Arctic haze phenomenon is a manifestation of long-range transported air pollutants originating in the mid-latitudes or within the Arctic. On average, the largest contributions are believed to come from northern Europe and Northern Eurasia, in particular the Russian Arctic, with largest industrial sources of air pollutants. Climatic, political and economical changes occurring in Northern Eurasia over the past decades have altered the amount and properties of a major component of the Arctic aerosols. In particular, declining concentrations of anthropogenic sulfate and black carbon have been attributed to changes in emissions in Northern Eurasia. However, observed long-term changes of aerosols in the Arctic are complex,

reflecting the interplay of various factors affecting the lifetime of aerosols and their transport to the Arctic.

Models and measurements have demonstrated that atmospheric aerosols can affect the Arctic radiation balance in a number of ways: directly by interacting with shortwave and longwave radiation, affecting the surface albedo, and indirectly by changing the properties of clouds. Individual mechanisms cause different tendencies contributing to either warming or cooling of the Arctic system that render assessments of the overall aerosol impact particularly difficult. Changing properties of clouds also have important impacts on Arctic hydrological processes, including snowfall and permafrost. The complicated feedbacks among the aerosols, clouds, radiation, sea ice, snow cover, and transport processes in the atmosphere and ocean add further complexity. The impact of future increases in pollutant emissions locally or in mid-latitudes could have complex effects on the Arctic climate.

A key question remains as to the overall role that anthropogenic aerosols and the associated feedbacks play in modulating the greenhouse warming in the Arctic as well as the global climate system. Improved understanding of the impact of Arctic aerosols on regional and global climate requires further research addressing the dynamics of aerosol sources, variability in transport to high latitudes due to changes in general circulation, as well as changes in other climatic characteristics that might be involved in aerosol-induced feedbacks. Our understanding of the relevant physical processes has been hampered by a lack of concurrent measurements of aerosols, clouds, radiation, snow and sea ice processes; isolated measurements of the individual components of this system cannot be used to elucidate the relevant physical processes or to validate model simulations.

Concentrated efforts during the International Polar Year are beginning provide new insights into aerosol-clouds-radiation interactions. Several large-scale, international field campaigns have recently been conducted in the Arctic aimed at better understanding of Arctic aerosols and their impacts. However, a long-term, well-coordinated observational system is needed to provide a new set of data to address the broad, interdisciplinary problems related to the Arctic system. Improvements in parameterizations of physical processes involving aerosol, clouds and precipitation in the models are also urgently needed.

References

Abakumova GM, Feigelson EM, Russak V, Stadnik VV (1996) Evaluation of long-term changes in radiation, cloudiness, and surface temperature on the territory of the Former Soviet Union. J. Clim 9:1319–1327

Albrech BA (1989) Aerosols, cloud microphysics, and fractional cloudiness. Science 245:1227–1230

AMAP (2006) AMAP assessment 2006: acidifying pollutants, Arctic haze, and acidification in the Arctic. Arctic Monitoring and Assessment Programme, Oslo

Barrie LA (1986) Arctic air pollution: an overview of our current knowledge. Atmos Environ 20:643–663

Biscaye PE, Grousset FE, Svensson AM, Bory A, Barrie L (2000) Eurasian air pollution reaches eastern North America. Science 290:2258–2259

Blanchet JP, Girard E (1995) Water-vapor temperature feedback in the formation of continental arctic air: implications for climate. Sci Total Environ 160/161:793–802

Bodhaine BA, Dutton EG (1993) A long-term decrease in Arctic haze at Barrow, Alaska. Geophys Res Lett 20(10): 947–950

Bond TC, Streets DG, Yarber KF, Nelson SM, Woo JH, Klimont Z (2004), A technology-based global inventory of black and organic carbon emissions from combustion. J Geophys Res 109(D14203). doi:10.1029/2003JD003697

Bond TC, Bhardwaj E, Dong R, Jogani R, Jung S, Roden C, Streets DG, Trautmann NM (2007) Historical emissions of black and organic carbon aerosol from energy-related combustion, 1850–2000. Glob Biogeochem Cycles 21(GB2018). doi:10.1029/2006GB002840

Borys RD (1989) Studies of ice nucleation by arctic aerosol on AGASP-II. J Atmos Chem 9: 169–185

Borys RD, Lowenthal DH, Mitchell DL (2000) The relationships among cloud micro- physics, chemistry, and precipitation rate in cold mountain cloud. Atmos Environ 34:2593–2602

Borys RD, Lowenthal DH, Cohn SA, Brown WOJ (2003) Mountaintop and radar measurements of anthropogenic aerosol effects on snow growth and snow rate. Geophys Res Lett 30. doi:10.1029/2002GL016855

Cahill CF (2003) Asian aerosol transport to Alaska during ACE-Asia. J Geophys Res 108(D23):8664. doi:10.1029/2002JD003271

Clarke AD, Noone KJ (1985) Soot in the Arctic snowpack: a cause for perturbation in radiative transfer. Atmos. Environ. 19:1053–2053

Chapin FS III, Sturm M, Serreze MC, McFadden JP, Key JR, Lloyd AH, McGuire AD, Rupp TS, Lynch AH, Schimel JP, Beringer J, Chapman WL, Epstein HE, Euskirchen ES, Hinzman LD, Jia G, Ping CL, Tape KD, Thompson CDC, Walker DA, Welker16 JM (2005) Role of land-surface changes in Arctic summer warming. Science 310(5748):657. doi:10.1126/science.1117368

Curry JA (1986) Interactions among turbulence, radiation, and microphysics in Arctic stratus clouds. J Atmos Sci 43:90–106

Curry JA (1995) Interactions among aerosols, clouds, and climate of the Arctic Ocean. Sci. Total Environ 160:777–791

Curry JA, Rossow WB, Schramm JL (1996) Overview of Arctic cloud and radiation properties. J Clim 9:1731–1764

Damoah R, Spichtinger N, Forster C, James P, Mattis I, Wandinger U, Beirle S, Stohl A (2004) Around the world in 17 days – hemispheric-scale transport of forest fire smoke from Russia in May 2003. Atmos Chem Phys 4:1311–1321

Eckhardt S, Stohl A, Beirle S, Spichtinger N, James P, Forster C, Junker C, Wagner T, Platt U, Jennings SG (2003) The North Atlantic Oscillation controls air pollution transport to the Arctic . Atmos Chem Phys 3:1769–1778

Flanner MG, Zender CS, JT Randerson JT, Rasch PJ (2007) Present day climate forcing and response from black carbon in snow. J Geophys Res 112(D11202). doi:10.1029/2006JD 008003

Francis JA, Hunter E, Key J, Wang X (2005) Clues to variability in Arctic minimum sea ice extent. Geophys Res Lett 32(L21501). doi:10.1029/2005GL024376

Francis JA, Hunter E (2006) New insight into the disappearing Arctic sea ice. Eos, Trans Am Geophys Union 87:509–524

Fromm M, Alfred J, Hoppel K, Hornstein J, Bevilacqua R, Shettle E, Servranckx R, Li Z, Stocks B (2000) Observations of boreal forest fire smoke in the stratosphere by POAM III, SAGE II, and lidar in 1998. Geophys Res Lett 27:1407–1410

Gabric AJ, Qu B, Matrai P, Hirst AC (2005) The simulated response of dimethylsulfide production in the Arctic Ocean to global warming. Tellus B 57(5):391–403. doi: 10.1111/j.1600-0889.2005.00163.x

Garrett TJ, Zhao C, Dong X, Mace GC, Hobbs PV (2004) Effects of varying aerosol regimes on low-level Arctic stratus. Geophys Res Lett 31(L17105). doi:10.1029/2004GL019928

Garrett TJ, Zhao C (2006) Increased arctic cloud longwave emissivity associated with pollution from mid-latitudes. Nature 440:787–789

Gavrilova MK (1963) Radiation Climate of the Arctic. Gidrometeoizdat, Leningrad, 225p

Girard E, Blanchet JP, Dubois Y (2005) Effects of arctic sulphuric acid aerosols on wintertime low-level atmospheric ice crystals, humidity and temperature at Alert, Nunavut. Atmos Res 73:131–148

Hansen J, Nazarenko L (2004) Soot climate forcing via snow and ice albedos. Proc Natl Acad Sci USA 101:423–428

Harrington JY, Reisen T, Cotton WR, Kreidenweis SM (1999) Cloud resolving simulations of Arctic stratus. Part II: Transition-season clouds. Atmos Res 51:45–75

Harrington JY, Olsson PQ (2001) On the potential influence of ice nuclei on surface-forced marine stratocumulus cloud dynamics. J Geophys Res 106:27473–27484

Hassol SJ, Berner J, Callaghan TV, Fox S, Furgal C, Hoel AH, Instanes A, Juday GP (2004) Impacts of a warming Arctic. Cambridge University Press, Cambridge, 140 p

Herber A, Thomason LW, Gernandt H, Leiterer U, Nagel D, Schulz K, Kaptur J, Albrecht T, Notholt J (2002) Continuous day and night aerosol optical depth observations in the Arctic between 1991 and 1999. J Geophys Res 107(D10):4097. doi:10.1029/2001JD000536

IPCC (2001) Radiative forcing of climate change. In: Climate change 2001, Cambridge University Press, New York

IPCC (2007) Climate change 2007: the physical science basis-summary for policy makers. Contribution of working group I to the fourth assessment report of the intergovernmental panel on climate change, Geneva

Iziomon MG, Lohmann U, Quinn PK (2006) Summertime pollution events in the Arctic and potential implications. J Geophys Res 111(D12206). doi:10.1029/2005JD006223

Jiang H, Cotton WR, Pinto JO, Curry JA, Weissbluth MJ (2000) Cloud resolving simulations of mixed-phase arctic stratus observed during BASE: sensitivity to concentration of ice crystals and large-scale heat and moisture advection. J Atmos Sci 57:2105–2117

Kampe TU, Sokolik IN (2007) Remote sensing retrievals of fine mode aerosol optical depth and impacts on its correlation with CO from biomass burning. Geophys Res Lett 34(L12806). doi:10.1029/2007GL029805

Koch D, J Hansen (2005) Distant origins of Arctic black carbon: a Goddard Institute for Space Studies ModelE experiment. J Geophys Res 110(D04204). doi:10.1029/2004JD005296

Korontzi S, McCarty J, Loboda T, Kumar S, Justice C (2006) Global distribution of agricultural fires in croplands from 3 years of Moderate Resolution Imaging Spectroradiometer (MODIS) data. Glob Biogeochem Cycles 20(GB2021). doi:10.1029/2005GB002529

Lavoue D, Liousse C, Cachier H, Stocks BJ, Goldammer JG (2000) Modeling of carbonaceous particles emitted by boreal and temperate wildfires at northern latitudes. J Geophys Res 105:26871–26890

Law KS, Stohl A (2007) Arctic air pollution: origins and impacts. Science 315:1537

Liu Y, Key JR, Francis JA, Wang X (2007) Possible causes of decreasing cloud cover in the Arctic winter, 1982–2000. Geophys Res Lett 34(L14705). doi:10.1029/2007GL030042

Lohmann U (2002a) Possible aerosol effects on ice clouds via contact nucleation. J Atmos Sci 59:647–656

Lohmann U (2002b) A glaciation indirect effect caused by soot aerosols. Geophys Res Lett 29. doi:10.1029/2001GL014357

Lohmann U, Zhang J, Pi J (2003) Sensitivity study of the effect of increased aerosol concentrations and snow crystal shapes on the snowfall rate in the Arctic. J Geophys Res 108. doi: 10.1029/2003 JD003377

Lubin D, Vogelman AM (2006) A climatologically significant aerosol longwave indirect effect in the Arctic. Nature 439:453–456

MacCraken MC, Cess RD, Potter GL (1986) Climatic effects of anthropogenic Arctic aerosols: an illustration of climatic feedback mechanisms with one-and two-dimensional climate models. J Geophys Res 91:14445–14450

McGuire AD, Chapin FS III, Walsh JE, Wirth C (2006) Integrated regional changes in Arctic climate feedbacks: implications for the global climate system. Ann Rev Environ Res 31:61–91

McKendry IG, McDonald A, Leaitch WR, van Donkelaar A, Zhang Q, Duck TJ, Martin RV (2008) Trans-Pacific dust events observed at Whistler, British Columbia during NTEX-B. Atmos Chem Phys 8:6297–6307

Morrison H, Shupe M, Pinto JO, Curry JA (2005) Possible roles of ice nucleation mode and ice nuclei depletion in the extended lifetime of arctic mixed phase clouds. Geophys Res Lett 32(L18801). doi:10.1029/2005GL023614

Morrison H, Pinto JO (2005) Mesoscale modeling of springtime Arctic mixed-phase stratiform clouds using a new two-moment bulk microphysics scheme. J Atmos Sci 62:3683–3704

Morrison H, Pinto JO, Curry JA, McFarquhar GM (2008) Sensitivity of modeled arctic mixed-phase stratocumulus to cloud condensation and ice nuclei over regionally varying surface conditions. J Geophys Res 113(D05203). doi:10.1029/2007JD008729

Pinker RT, Zhang B, Dutton EG (2005) Do satellites detect trends in surface solar radiation. Science 308:850–854

Prenni AJ, Harrington JY, Tjernström M, DeMott PJ, Avramov A, Long CN, Kreidenweis SM, Olsson PQ, Verlinde J (2007) Can ice-nucleating aerosols affect arctic seasonal climate? Bull Am Meteorol Soc 88:205–221. doi:10.1175/BAMS-88-4-541

Quinn PK, Shaw G, Andrews A, Dutton EG, Ruoho-Airola T, Gong SL (2007) Arctic haze: current trends and knowledge gaps. Tellus 59B:99–114

Quinn PK, Bates TS, Baum E, Doubleday N, Fiore AM, Flanner M, Fridlind A, Garrett TJ, Koch D, Menon S, Shindell D, Stohl A, Warren SG (2008) Short-lived pollutants in the Arctic: their climate impact and possible mitigation strategies. Atmos Chem Phys 8:1723–1735

Randerson JT, Liu H, Flanner MG, Chambers SD, Jin Y, Hess PG, Pfister G, Mack MC, Treseder KK, Welp LR, Chapin FS, Harden JW, Goulden ML, Lyons E, Neff JC, Schuur EAG, Zender CS (2006) The impact of boreal forest fire on climate warming. Science 314:1130. doi:10.1126/science.1132075

Radionov VF, Marshunova MS (1992) Long-term variations in the turbidity of the Arctic atmosphere in Russia. Atmos-Ocean 30(4):531–549

Radionov VF, Marshunova MS, Russina YN, Lubo-Lesnischenko KY, Pimanova YY (1995) Atmospheric aerosol turbidity over polar regions. Izvestiya, Atmos Ocean Phys 30:762–766

Radionov VF, Rusina YN, Sibir EE (2007) Particularities of long-term variability of total solar radiation and atmospheric transparency characteristics in the polar region. Prob Arct Antarct 76:131–136 (in Russian)

Rahn KA, Borys R, Shaw GE (1977) The Asian source of Arctic Haze bands. Nature 268:713–715

Serreze MC, Walsh JE, Chapman FS, Osterkamp T, Dyurgerov M, Romanovsky V, Oechel WC, Morison J, Zhang T, Barry RG (2000) Observational evidence of recent change in the northern high latitude environment. Clim Change 46:159–207

Serreze MC, Holland MM, Stroeve J (2007) Perspectives on the Arctic's shrinking sea-ice cover. Science 315:1533–1536

Sirois A, Barrie LA (1999) Arctic lower tropospheric aerosol trends and composition at Alert, Canada: 1980–1995. J Geophys Res 104 (D9):11599–11618

Shahgedanova M, Lamakin M (2005) Trends in aerosol optical depth in the Russian Arctic and their links with synoptic climatology. Sci Total Environ 341:133–148

Shaw GE, Stamnes K (1980) Arctic haze: perturbation of the Polar radiation budget. Ann NY Acad Sci 338:533–539

Sharma S, E Andrews, Barrie LA, Ogren JA, Lavoue D (2006) Variations and sources of the equivalent black carbon in the High Arctic revealed by long term observations at Alert and Barrow: 1989 – 2003. J Geophys Res 111(D14208). doi:10.1029/2005JD006581

Shevchenko V (2003) The influence of aerosols on the oceanic sedimentation and environmental conditions in the Arctic. Berichte zur Polar-und Meeresforschung 464:150 p

Shindell DT (2007) Locale and remote contributions to arctic warming. Geophys Res Lett 34 (L14704). doi:10.1029/2007GL030221

Shindell DT, Teich H, Chin M, Dentener F, Doherty RM, Faluvegi G, Fiore AM, Hess P, MacKenzie IA, Sanderson MG, Schultz MG, Schulz M, Stevenson DS, Textor C, Wild O, Bergmann DJ, Bian H, Cuvelier C, Duncan BN, Folberth G, Horowitz LW, Jonson J, Kaminski JW, Marmer E, Park R, Pringle KJ, Schroeder S, Szopa S, Takemura T, Zeng G, Keating TJ, Zuber A (2008) A multi-model assessment of pollution transport to the Arctic. Atmos Chem Phys Discuss 8:8385–8429

Soja AJ, Tchebakova NM, French NHF, Flannigan MD, Shugart HH, Stocks BJ, Sukhinin AI, Parfenova EI, Chapin FS III, Stackhouse W Jr (2007) Climate-induced boreal forest change: predictions versus current observations. Glob Planet Change 56:274–296

Sokolik IN (1992) Microphysical, optical and radiative properties of Arctic aerosols. Izvestiya. Atmos Ocean Phys 7:675–688

Sokolik IN (2003) Dust. In: Holton JP, Curry JA, Doyle J (eds) Encyclopedia of atmospheric sciences. Academic Press, London, pp 668–672

Sokolik IN (2008) Global radiation balance. In: Jorgensen E (ed) Encyclopedia of ecology. Elsevier, Oxford

Sokolik IN, Choi H, Darmenov A, Karabanov A (2008) Characterization of Arctic aerosol and its climate forcing with A-Train satellite constellation observations. Eos Trans Am Geophys Union 89(53)

Stohl A, Berg T, Burkhart JF, Forster C, Herber A, Lunder C, McMillan WW, Oltmans S, Shiobara M, Simpson D, Solberg S, Stebel K, Treffeisen R, Virkkunen K, Yttri KE (2007) Arctic smoke –record high air pollution levels in the European Arctic due to agricultural fires in Eastern Europe. Atmos Chem Phys **7**:511–534

Stone RS, Anderson GP, Andrews E, Dutton EG, Shettle EP, Berk A (2007) Incursions and radiative impact of Asian dust in northern Alaska. Geophys Res Lett 34(L14815). doi:10.1029/2007GL029878

Stone RS, Anderson GP, Shettle EP, Andrews E, Loukachine K, Dutton EG, Schaaf C, Roman MO III (2008) Radiative impact of boreal smoke in the Arctic: Observed and modeled. J Geophys Res 113(D14S16). doi:10.1029/2007JD009657

Streets DG, Bond TC, Lee T, Jang C (2004) On the future of carbonaceous aerosol emissionsIO. J Geophys Res 109(D24212). doi:10.1029/2004JD004902

Tomasi C, Vitale V, Lupi A, Di Carmine C, Campanelli M, Herber A, Treffeisen R, Stone RS, Andrews E, Sharma S, Radionov V, von Hoyningen-Huene W, Stebel K, Hansen GH, Myhre CI, Wehrli C, Aaltonen V, Lihavainen H, Virkkula A, Hillamo R, Ström J, Toledano C, Cachorro VE, Ortiz P, de Frutos AM, Blindheim S, Frioud M, Gausa M, Zielinski T, Petelski M, Yamanouchi T (2007) Aerosols in polar region: A historical overview based on optical depth and in situ observations. J Geophys Res 112(D16205). doi:10.1029/2007JD008432

Vavrus S (2004) The impact of cloud feedbacks on Arctic climate under greenhouse forcing. J Clim 17:603–615

Wang X, Key J (2003) Recent trends in Arctic surface, cloud, and radiation properties from space. Science 299(5613):1725–1728

Weston ST, Bailey WG, McArthur LJB, Hertzman O (2007) Interannual solar and net radiation trends in the Canadian Arctic. J Geophys Res 112(D10105). doi:10.1029/2006JD008000

Winker DM, Hunt WH, McGill MJ (2007) Initial performance assessment of CALIOP. Geophys Res Lett 34(L19803). doi:10.1029/2007GL030135

Zuidema P (2005) An Arctic springtime mixed-phase cloudy boundary layer observed during SHEBA Journal of the Atmospheric Sciences 62:160–176

Chapter 11
Interaction Between Environmental Pollution and Land-Cover/Land-Use Change in Arctic Areas

John Derome[†] **and Natalia Lukina**

Abstract Climate change in the Arctic is taking place within the context of a wide range of other changes and disturbances including environmental pollution. During the past two centuries climatic change in the region has been accompanied by the added complexity of anthropogenic pollutants. This chapter deals with the interactions between climate change and environmental pollution generated in the Arctic, as well as that originating from outside the region, and the effects of these interactions on changes in land cover and land use in the Arctic. The main sources of pollutants and their effects are discussed. Heavy metal, SO_2 and sulphate deposition originating from non-ferrous metal smelting and mining activities in the region are the main threat to the prevailing land cover. Increasing mercury and POP pollution in the Arctic poses a considerable threat to animal life in the region, and therefore also indirectly may have long-term effects on the land cover. Environmental pollution originating from oil and gas exploration and extraction activities in the Arctic is expected to increase considerably in the Eurasian Arctic. Forest fires also cause tremendous short- and long-term changes in the land cover in the Arctic. The chapter discusses how global warming may aggravate the effects of environmental pollution on land cover, and how pollutants may amplify climatic stress.

11.1 Introduction

Climate change in the Arctic is taking place within the context of a wide range of other changes and disturbances including environmental pollution. During the last period of major climatic change, i.e. during the Holocene (11,700 – ca. 2,000 BP), these natural changes were not accompanied by the added complexity of anthropogenic pollutants. However, over the past two millennia, and especially during the

N. Lukina (✉)
Centre for Forest Ecology and Productivity RAS, 117997, Moscow, Russia
e-mail: lukina@cepl.rssi.ru

John Derome is deceased.

G. Gutman, A. Reissell (eds.), *Eurasian Arctic Land Cover and Land Use in a Changing Climate*, DOI 10.1007/978-90-481-9118-5_11,

past two centuries, there has been a transient rise in the levels of virtually every contaminant in Arctic glacial ice emitted by human activities (Boutron et al. 1995; 1998; Gregor et al. 1995; Hong et al. 1994; Masclet et al. 2000; Rosman et al. 1997). Ice core drilling on Svalbard clearly shows that significant changes in atmospheric pollution within the Arctic have only occurred since the beginning of the industrial era (Isaksson et al. 2003). During the past 50 years, the north-western and central parts of Arctic Russia have been subjected to the impacts of the huge emissions sulphur dioxide (SO_2) and heavy metals, primarily nickel (Ni) and copper (Cu) from the non-ferrous metallurgical complexes on the Kola Peninsula and in Norilsk, north-western Siberia.

11.2 Sources of Pollution and the Effects of Pollution

There are a number of major pollution sources located in the Eurasian part of the Arctic, and pollution is also carried into the Arctic from a range of sources in North America, Europe (including European Russia), Siberia and the Far East (China, India, Japan etc.). Pollution has already caused considerable problems in parts of the Arctic, and heavy metals, SO_2 and sulphate and persistent organic pollutants (POPs) are of particular concern (AMAP 1998, 2004, 2005). There are considerable regional and local variations in the distribution and magnitude of pollutant levels within the region. Acidification caused by the deposition of acidifying compounds (mainly SO_2 and sulphate) is primarily a sub-regional problem, and is of major concern only in those areas relatively close to the pollution sources that have a sensitive geology (e.g. granitic soils with a low base saturation). The effects of acidic deposition on terrestrial ecosystems depend on the magnitude of the deposition load and on the capacity of the ecosystem (primarily the soil) to buffer and neutralize the load. The deposition of heavy metals from the metallurgical industry is a serious problem causing changes in land cover, primarily through destruction of the forest cover, in a number of relatively restricted parts of the region. The extensive mining activities in the region can have a serious effect on land cover through removal of the topsoil and the generation of dust, but this is usually only a relatively localized problem. POPs derived from both local and mid-latitudinal sources represent an ever-increasing problem in the Arctic, and in the future they may have an indirect, but marked, effect on terrestrial ecosystems and, subsequently, on land cover. Oil and gas are the most important non-renewable fossil fuels currently being exploited, and to some extent also processed, in the region. Exploration and extraction activities are expected to increase considerably, and environment pollution from these sources will almost certainly increase in the Eurasian Arctic. The transportation of oil and gas (via pipelines or by sea) out of the region also poses a considerable risk of pollution to terrestrial ecosystems. Anthropogenic sources of radionuclide emissions/discharges, with their associated radiological effects, are a relatively unknown factor in the region, but may have far-reaching impacts in the future, in particular. Forest fires, of natural but to an ever-increasing extent of human origin, have in recent years become a serious threat, and potentially can cause tremendous changes, even long-lasting ones, in land cover in the Arctic.

11.2.1 Acidifying Compounds

11.2.1.1 Sources

The main acidifying compounds in atmospheric deposition are sulphur dioxide (SO_2), sulphate (SO_4), nitrogen oxides (NO_x), and ammonia (NH_3). Sulphur dioxide emissions are mainly associated with point sources such as power plants, the pulp and paper industry, non-ferrous metal smelters, and oil and gas processing. There are also natural sources of these gaseous substances in the region, such as volcanoes that emit SO_2 in Kamchatka and Iceland, as well as marine algae. The frequency, duration and severity of forest fires in the boreal forest zone, which is a major source of SO_2 and sulphur aerosols within and adjacent to the Arctic region, appear to have increased in the late twentieth century (Stocks et al. 1998; Shvidenko and Nilsson 2000; Shvidenko and Goldhammer 2001; McGuire et al. 2002, 2004), and there are no reasons to assume that this increase will not continue in the future. Ammonia and NO_x emissions, derived from diffuse sources such as agriculture and vehicular traffic, are of only very localised concern in the Arctic.

The major anthropogenic sources of SO_2 emissions in the region are located in the Russian Arctic: the non-ferrous metal smelter complexes at Nikel, Monchegorsk, and Zapolyarnyy on the Kola Peninsula, and the even larger smelter complex at Norilsk in north-western Siberia. During the last couple of decades, however, SO_2 emissions from the sources on the Kola Peninsula have decreased to some extent: SO_2 emissions from the Pechenganickel (Zapolyarnyy/Nikel) and Severonickel (Monchegorsk) smelters decreased by a factor of 1.7 and 5 correspondingly, during the period 1990–2003 (Fig. 11.1). Total SO_2 emissions from the five regions in north-western Russia (the Murmansk Oblast, Republic of Karelia, Archangelsk Oblast, Nenets Autonomous Okrug and the Komi Republic) amounted to 240 (ca. 85% from the Kola smelters), 77, 89, 3.8, and 65 kt, respectively, in 2002 (AMAP 2006). Between 1990 and 2003 there has been a clear increase (as much as 2–3 times) in NO_x concentrations in Russian urban cities (Nikel, Norilsk, and Salekhard), clearly reflecting the sharp increase in the number of private vehicles in the Russian Arctic. Oil and gas production involves the emission of exhaust gases containing carbon dioxide (CO_2), nitrogen oxides (NO_x), sulphur oxides (SO_x) and volatile organic compounds (VOC). As energy consumption and air pollution are directly linked, any increase in oil- and gas-related activities is likely to result in increased emissions of greenhouse gases and acidifying compounds. Additional sources of acidifying gases include the pulp and paper industry in the Republic of Karelia and Archangelsk Oblast (Russia), the oil and gas industry in the Nenets Autonomous Okrug and Komi Republic (Russia), and the Snöhvit gasification complex in northern Norway (Arctic Oil and Gas 2007).

Shipping is apparently not currently a major contributor to the deposition of acidifying pollution in the Arctic (AMAP 2006). In the longer term, however, a significant increase in marine traffic, resulting from increases in oil transport (particularly in the Barents Sea) and a longer navigation season due to the reduced ice cover, will undoubtedly lead to more substantial emissions of acidifying pollutants

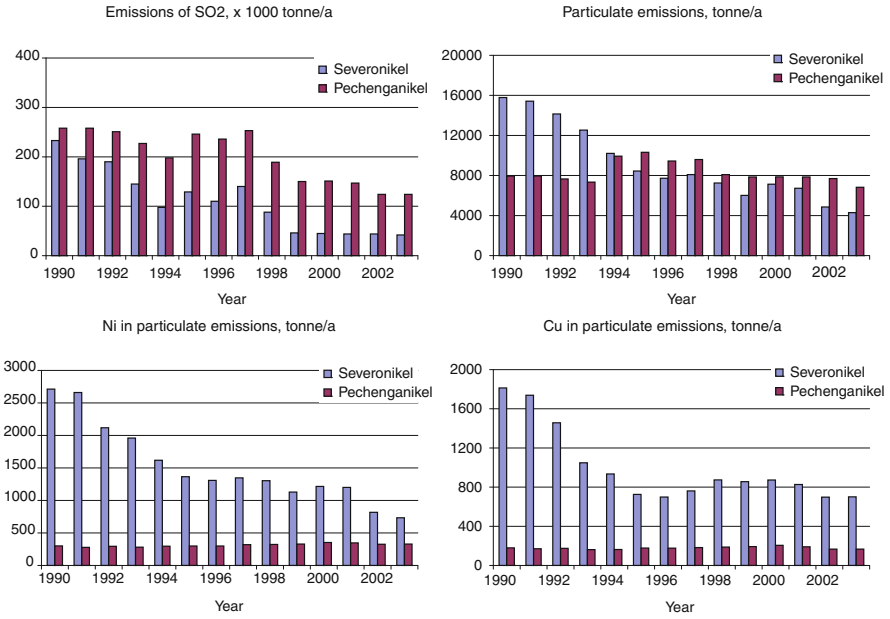

Fig. 11.1 Emissions from the two Cu-Ni smelter complexes on the Kola Peninsula, NW Russia. Source: Kola mining-metallurgy company, http://www.kolagmk.ru/rus/ecology

in the region. The most extensive shipping activities in the Arctic are in Russia, the Northern Sea Route (NSR) carrying the largest volume of traffic of any Arctic seaway.

11.2.1.2 Effects

The non-ferrous metal smelters in the region are primarily responsible for the direct and acidification-related effects on plants and soils in the Norilsk region, and north-western part of Russia and northern Fennoscandia. In Norilsk, the total area of barren and semi-barren land currently exceeds 400,000 ha (Kozlov and Zvereva 2007). At the beginning of the 1990s the total area on the Kola Peninsula, NW Russia, where the critical deposition of sulphur (0.3 g S m^{-2} g^{-1}) was exceeded was more than 90 000 km^2 (Tuovinen et al. 1993). The area of industrial barren and semi-barren land, caused by pollution from the Cu-Ni smelters on the Kola Peninsula, totalled 44,000 ha in Monchegorsk and 31,000 ha in Nikel (Kozlov and Zvereva 2007). There was visible damage to forest ecosystems over an area of 39,000 km^2 on the Kola Peninsula (Rigina and Kozlov 1998).

Strongly acidic precipitation is deposited only within a radius of about 30 km from the smelters. The lack of widespread soil acidification, despite the high SO_2 emissions, have been attributed to the simultaneous emission of alkaline fly ash from the power plants and the apatite fertilizer complex in Apatity, the relatively low rate of interception of acidifying compounds (SO_2) by the sparse tree, shrub and ground

layer vegetation, and the low rate of conversion of sulphur dioxide to sulphuric acid, especially during the dark winter (AMAP 2006).

There is relatively conflicting evidence about the effects of acidifying deposition, derived from the Cu-Ni smelters, on the acidity of the organic layer in coniferous ecosystems in Arctic areas (e.g., Lukina and Nikonov 1995, 1996; Derome et al. 1998). Unexpectedly, changes in soil acidity do not appear to be a direct result of the deposition of acidifying compounds, but rather to the destruction of the forest ecosystems in the area around the smelters. In the industrial barrens and extensively damaged, very low density forests close to the smelters, the dramatic decrease in the living plant cover and considerable reduction in the production of plant litter have resulted in a decrease in the acidity (i.e. pH increase) of the organic horizon. The deposition of alkaline dust from the smelters and power plants has also contributed to some extent to the reduction in acidity. In contrast, the mineral soil horizons in the forest ecosystems close to the Monchegorsk smelters are strongly acidified partly due to the low base cation content of the parent bedrock. In the Nikel area and Norilsk region, on the other hand, a high proportion of the parent bedrock consists of calcium-rich, alkaline mineral deposits.

The direct effects of SO_2 include visible leaf/needle damage, a decrease in the number of needle age classes in conifers (Kruychkov and Syroid 1979; Myking et al. 2008), and elevated sulphur concentrations in the needles of conifers (Manninen et al. 1998) and ground vegetation, including mosses (Äyräs et al. 1997; Isaeva et al. 2008). Changes in the plant community structure (species composition and coverage) also indicate indirect effects of SO_2/SO_4 deposition (Aarrestad et al. 2008). Lichen fields in northern Fennoscandia and the Kola Peninsula, as well as elsewhere in the Arctic, represent an important component of the vegetation cover in both tundra and coniferous forest ecosystems. Lichens, which obtain both water and nutrients from precipitation, are extremely susceptible to the harmful effects of exposure to both SO_2 and heavy metal deposition. Satellite imagery has clearly demonstrated major changes in the coverage of lichens in northern Fennoscandia and the Kola Peninsula, and strong correlations have been found between SO_2 emission levels from the smelter complex at Nikel and Zapoljarnyi and the lichen coverage in the region (Fig. 11.2) (Tömmervik 2008). Changes reported in invertebrate populations near Monchegorsk are due to habitat deterioration, and the changes in insect populations primarily to changes in host plant abundance and physiology, accompanied by a decline in some natural predators, and to changes in habitat structure (Kozlov and Whitworth 2002; AMAP 2006).

11.2.2 Heavy Metals

11.2.2.1 Sources of Pollution

Anthropogenic emissions of many heavy metals from sources within and outside the Arctic region are considerably greater than those from natural sources (AMAP 1998). There are three main anthropogenic sources of heavy metals to

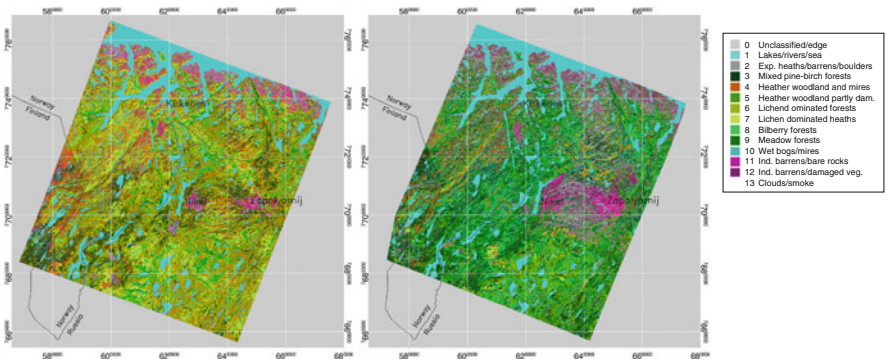

Fig. 11.2 Land-cover maps based on Landsat imagery of NE Norway and the NW part of the Kola Peninsula, Russia. The non-ferrous smelting plants are located in Nikel and Zapoljarnij. Damaged areas are shown in *red* to *violet* colour. Lichen-dominated forests and alpine heaths are *yellow* to *green*. The map shows the situation in 1973 and in 1999. Source: Tömmervik et al. (2003)

the atmosphere: fossil fuel combustion, non-ferrous metal production, and waste incineration. The first AMAP assessment reported that about two thirds of the heavy metals in winter air over the High Arctic is derived from sources outside the Arctic region proper, i.e., sources on the Kola Peninsula, and in the Norilsk region, the Pechora Basin, and the Urals (AMAP 2005). Emissions of heavy metals from the Severonikel smelter on the Kola Peninsula decreased considerably during the period 1990–2003 (see Fig. 11.1). The majority of the emissions produced in, or near, the region, are deposited relatively close to the emission sources. The deposition of some metals derived from sources in lower latitudes has decreased as a result of highly successful legislation, e.g. to reduce lead (Pb) emissions through the introduction of low-leaded and "unleaded" gasoline in Europe, the United States, and Canada (Fig. 11.3). Despite the decline in anthropogenic mercury (Hg) emissions,

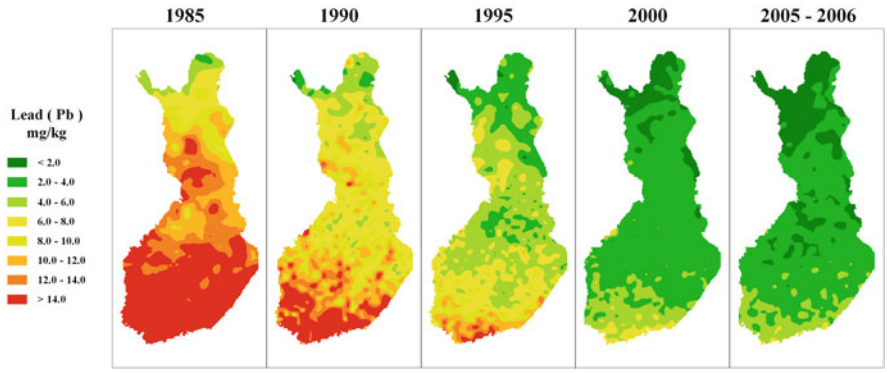

Fig. 11.3 Lead concentrations in forest mosses in Finland during the period 1985–2005/6. The survey was carried out as a part of the UN/ECE ICP Vegetation monitoring programme. Reproduced by permission of J. Piispanen, Finnish Forest Research Institute

at least in the period between the 1980s and the 1990s, the Arctic ecosystem appears to be increasingly exposed to Hg accumulation. Much of this Hg is most probably derived from sources in China, India, and other parts of the Far East. There is very little accurate information available about heavy metal emissions from natural sources, such as volcanic eruptions, soil dust, and sea salt aerosols. However, we do know that they can be considerable, although very often only of sporadic occurrence.

11.2.2.2 Effects

The heavy metals that are currently of the greatest toxicological concern in the Arctic biosphere as a whole are Hg and cadmium (Cd). The transformation of elemental Hg in the snowpack during polar sunrise suggests that the Arctic is a global sink for Hg (Lindberg et al. 2002). Lead is still a local concern in some areas due to the use of lead shot in waterfowl hunting. Heavy metals such as Ni and Cu, as well as iron (Fe) and cobalt (Co) associated with larger particles, and selenium (Se), tellurium (Te), arsenic (As), molybdenum (Mo), antimony (Sb), bismuth (Bi), Pb, vanadium (V), chromium (Cr), zinc (Zn) and thallium (Tl) derived from anthropogenic sources, either from the smelters themselves or from coal burning and, in the case of Pb, also from the use of leaded gasoline, do pose a serious threat to terrestrial ecosystems in some relatively restricted parts of the region (Kola Peninsula and Norilsk) (Lukina and Nikonov 1996; Kharuk et al. 1996; Derome et al. 1998; Steinnes et al. 2000; Nikonov et al. 2004). Although metals naturally occur in soils at extremely variable levels depending on the chemical composition of the bedrock, elevated levels derived from anthropogenic sources can have adverse effects on terrestrial ecosystems. Biological soil processes that are extremely important for the establishment, growth and reproduction of the vegetation cover (e.g. nitrogen mineralization and organic matter decomposition), may be indirectly affected by the adverse effects of elevated metal concentrations on soil micro-organisms and invertebrates (Fritze et al. 1989; Kozlov 1997). The vegetation may be altered through reduced growth, early senescence of leaves or, in extreme cases, death. Metal-induced changes in plant communities can also indirectly affect wildlife by reducing the availability of food or refuge, and directly through the toxic effects of metals on their metabolism, ultimately leading to their death. Biological effects directly attributable to heavy metal pollution in Arctic terrestrial ecosystems primarily occur around smelters and mining sites. In the case of smelters, however, it can be difficult to differentiate the direct effects of heavy metals from those caused by the high SO_2 emissions (AMAP 2005). Heavy metals can affect macronutrient availability (Derome and Lindroos 1998) and nutrient uptake by plants (Helmisaari et al. 1999). The main cause of forest decline and death in the vicinity of smelters is the direct toxic effect of SO_2 on trees and plants, combined with the inhibition of soil microbial activity and the death of mycorrhizae and fine roots resulting from the accumulation of toxic heavy metal levels in the soil. In addition, changes in the species diversity of saprophytic bacteria, algae, and fungi in the soil are thought to influence nutrient availability (Evdokimova 2000).

Heavy metals can retard litter decomposition processes in polluted areas where there are no visible signs of damage to the vegetation. Elevated levels of Cu are known to be toxic to fungi. In the vicinity of the Harjavalta Cu-Ni smelter in western Finland, for instance, Cu had the strongest inhibiting effect on fungal biomass (Fritze et al. 1989). Similar effects of heavy metals have been reported in the vicinity of the Monchegorsk Ni-Cu smelter on the Kola Peninsula (Nikonov et al. 2001). Adverse effects on microbial processes in forest soils have been reported at concentrations only a few times higher than the current background concentrations in Sweden: 3 times for Hg, 5 for Cd, and 10 times for Pb (Johansson et al. 2001).

Heavy metals, like POPs, are associated with several environmental risks to mammals, such as estrogenic effects, disruption of endocrine functioning, impairment of immune system functioning, functional and physiological effects on reproduction, and reduced survival and growth of offspring (AMAP 1998, 2005).

11.2.3 Persistent Organic Pollutants (POPs)

11.2.3.1 Sources of Pollution

There are sources of POPs within the Arctic that could be of local and regional significance. These include polychlorinated biphenyl (PCB) emissions from military bases, harbours, and landfills, as well as other toxic organic compounds [polychlorinated dibenzodioxin and dibenzofurans (PCDD/Fs) and polycyclic aromatic hydrocarbons (PAHs)] originating from the smelters located on the Kola Peninsula and in the Norilsk region. On a local scale, however, household heating in settlements, the burning of hydrocarbons for electricity and transport, and the incineration and open burning of household and industrial waste, contribute significantly to the input of organic pollutants such as PAHs. In several Arctic regions, mineral exploration, coal mining and heavy industry account for the highest input of persistent pollutants such as PAHs and PCBs. Current and former military bases in the Russian part of the Arctic, especially those with older radar equipment, have previously been identified as potential sources (AMAP 1998; AMAP 2004). Present levels of most POPs cannot be related to known potential sources within the Arctic, and can therefore only be explained by long-range transport from lower latitudes (AMAP 2004).

11.2.3.2 Effects

It is very difficult to link contaminant levels or biochemical indicators of effects to effects on Arctic animals at the individual or population level. Assessments are also complicated by the fact that the thresholds for the effects of many contaminants are not well documented, and very little is known about the effects of mixtures of contaminants (AMAP 2004). Effects that are of biological significance, primarily in mammals and birds, include their impact on resistance to infection, reproduction, and behaviour. Several species are known to be at risk to the effects

on neurobehaviour, reproduction, and their immune systems (polar bears, glaucous gulls, peregrine falcons). Knowledge gaps, such as a lack of understanding about the influence of confounding factors, indicate that other biomarkers studied in Arctic biota (thyroid hormones, vitamin A and cytochrome P450 activity) should be considered as indicators of increased exposure. It is not yet possible to conclude that any documented changes in these biomarkers imply increased risk. Biomarkers for POP effects measure changes at the cellular or individual level, and are warning signals. The results from biomarker studies in the Arctic have shown that there are associations between several biomarkers and concentrations of some POPs (AMAP 2004).

11.2.4 Oil and Gas Exploration and Extraction

11.2.4.1 Sources

Oil and gas are among the most important non-renewable resources of fossil fuel in the Arctic today. Commercial oil and gas activities started in the Arctic already in the 1920s. By the 1960s, large oil and gas reserves had been discovered in the Yamalo-Nenets Autonoumous Okrug and in the Nenets Autonoumous Okrug in Russia. At the present time, the main areas of oil and gas exploitation in the Eurasian Arctic include the offshore areas in the Norwegian and Barents Sea, and the Yamalo-Nenets and Komi regions of Russia. Extensive petroleum resources also exist elsewhere in the region, and oil and gas exploration activities are being actively pursued in the offshore areas west of Greenland, around the Faroe Islands, and in the Kara, Chukchi, and East Siberian Seas. The construction of long pipelines has been essential because these regions are remote from the potential markets (Arctic Oil and Gas 2007). In the 1970s and 1980s extensive pipelines systems were constructed in Russia. Today, the Arctic produces about one tenth of the world's oil and one quarter of its gas. Of these amounts, about 80% of the oil and 99% of the gas currently come from the Russian Arctic. In Russia, oil and gas production activities will increase in the Timan-Pechora and West Siberia provinces, and in the Kara and Barents Seas.

From the exploration phase to the final closure of a production field, oil and gas production involve emissions and discharges into the air, water and, through spills, onto the land. Emissions into the air include exhaust gases containing CO_2, NO_x, SO_x, methane (CH_4) and non-methane volatile organic compounds (nmVOC) from various types of combustion equipment and other sources including gas turbines, engines and boilers, and gas flaring and oil and gas burning in connection with well-testing and well-maintenance work (Arctic Oil and Gas 2007). Other sources of hydrocarbon gases (CH_4 and nmVOC) include gas ventilation, minor leaks, and diffuse emissions and the boiling down of hydrocarbon gases (primarily nmVOC) from the storage and loading of crude oil. Power generation, using natural gas and diesel oil as fuel, is the predominant reason for CO_2 and NO_x emissions, followed by gas flaring.

The main cause of SO_x emissions is the combustion of sulphur-containing hydrocarbons. These emissions may have considerable effects on the local climate, and they may cause acidification on nearby land areas. CH_4, which is a powerful greenhouse gas, is also released to the atmosphere during gas drilling, from leaky pipelines, and by venting and flaring activities on oil and gas rigs (AMAP 1998).

11.2.4.2 Effects

Hydrocarbons associated with oil and gas are known as petroleum hydrocarbons which are natural in origin and, unlike POPs, tend to be biodegradable. This class of compound comprises alkanes, cycloalkines, aromatics, and sulphur compounds. 80–90% of the petroleum hydrocarbons currently entering the arctic environment are thought to come from natural seeps. The toxicity of petroleum hydrocarbons to plants and animals depends on the size of the dose they are exposed to. Oil spills can kill a large number of animals by physically covering them in oil. Transport and spills from the general use of refined petroleum products also account for a significant part of the petroleum hydrocarbon pollution at the local level.

The greatest effect of oil and gas activities on the land cover and land use in the Arctic has been physical disturbance, i.e., the covering of land by gravel pads, roads, and airstrips. Oil and gas infrastructure can influence a large area. The greatest impact is most probably habitat fragmentation. In relation to climate change, the major change is the thawing of permafrost on land surfaces. Many arctic facilities today use permafrost as a "solid" foundation for buildings, pipelines, and roads, or for the containment of waste materials. Warming, either resulting from a change in climate or directly as a result of human activities, may partially melt permafrost, thereby harming existing facilities and releasing waste materials into the terrestrial environment (Arctic Oil and Gas 2007).

11.2.5 Fires

Fires are a major source of sulphur aerosols, black carbon, heavy metals and organic pollutants. It was realized only recently that boreal wildfire emissions affect the atmosphere at the hemispheric scale (Wotawa et al. 2001; Chapter 6, this volume). There are speculations that the deposition of black carbon originating from boreal forest fires could enhance the melting of arctic glaciers and sea ice (Kim et al. 2005). Between 0.5 and 1% of the boreal forests burn annually, with the highest rates in Siberia along the Yenisey River (McGuire et al. 2002). The fire frequency in Siberia is higher than that in Alaska and Canada (Shvidenko and Nilsson 2000; Shvidenko and Goldhammer 2001; McGuire et al. 2002). Over the last 50 years, around 2 million ha have burnt annually in Canada (Amiro et al. 2001) and about 250,000 ha annually in Alaska (Kasischke et al. 2003). In Russia, 0.5–5.5 million ha of forest burn annually in protected areas (2/3 of the area of the total growing stock), and about 80% of these areas are located in Siberia and the Far East. In unprotected areas of northern Siberia and the Far East, where forest fires are not registered or

controlled, the proportion of slash fires out of the total growing stock are as much as 2–3 times higher than the total area covered by aerial- and ground-based forest protection (Isaev and Korovin 2003).

11.3 Anthropogenic Pollution and Climate Change

11.3.1 Interactions Among Environmental Pollution, Climate Change, and Land-Cover/Land-Use Change

Environmental pollution, like other disturbances, may interact with climate change in ways that tend to enhance warming (positive feedbacks) and through effects that tend to mitigate warming (negative feedbacks). The major mechanisms (feedbacks) by which environmental pollution can contribute to climate change are changes in land cover (reflectivity of the surface) and changes in the amount of greenhouse gases emitted to the atmosphere from the land.

The first feedback mechanism involves the effect of environmental pollution on the reflectivity of snow and ice that cover much of the Arctic. As greenhouse gas concentrations rise and warm the lower atmosphere, the snow cover is formed later in the autumn and melts earlier in the spring. The deposition of black carbon (soot) on the snow/ice cover accelerates this trend (positive feedback). The formation of soot during the burning of flammable material (both fossil fuels and natural vegetation), and its subsequent deposition, results in a darker snow cover with a higher absorbance of solar energy and partial melting of the snow and ice. Complete melting of the snow and ice exposes the underlying land surface, which is of a much darker colour, with the result that even more solar energy is absorbed. This results in the generation of a self-enforcing cycle of amplification and acceleration, i.e. a warming trend (ACIA 2004).

It has been forecasted that a warming climate will result in a considerable increase in the area burnt annually in forest fires in Russian and Canadian boreal forests (Stocks et al. 1998). Furthermore, the frequency, severity, and duration of boreal forest fires are likely to increase and the pollution plumes produced by these summer fires are likely to extend over ever-increasing areas. In severe fire years, boreal forest fires may be the dominant source of black carbon (soot) in the Arctic (AMAP 2006). Soot in the atmosphere also increases solar absorption, further warming the region (Chapter 10, this volume). Both black carbon in atmospheric aerosols, and the black carbon that is deposited on snow and ice surfaces, are of major significance from the viewpoint of climate change (positive feedback). Increases in fire frequency have the potential to rapidly release large amounts of carbon (McGuire and Chapin 2003; Goulden et al. 1998), and these responses may more than offset the increases in carbon storage that might be arising from the slow expansion of boreal forest into tundra regions (McGuire and Hobbie 1997), or increased productivity due to elevated atmospheric CO_2 concentrations (McGuire et al. 1997).

Changes in the distribution and composition of the vegetation can result in the storage or loss of carbon (Chapters 5 and 6, this volume). Owing to an increase in the absorption of solar energy, it is projected that forests will expand northward into areas that are currently covered by tundra vegetation, which is much more reflective than forest, especially when covered by snow. The reduction in reflectivity will result in further warming while, on the other hand, the increased tree growth is expected to absorb more CO_2. Anthropogenic pollution is, in certain areas, likely to act as a barrier to the northwards expansion of forest. Industrial barrens and semi-barren land around the smelters can cover extremely large areas: from 30,000 to 400,000 ha in the vicinity of the Ni-Cu smelters in Nikel and Monchegorsk on the Kola Peninsula (Figs. 11.2 and 11.5) and Norilsk in NW Siberia, respectively. The reflectivity of these completely denuded land surfaces will be higher during the winter when they are covered by snow. On the other hand, if the snow and ice has a covering of soot and other dark particles, its reflectivity will decrease.

The restoration or natural re-vegetation of land impacted by air pollution will result in changes in the reflectivity of the surface and in carbon cycles (e.g. through the active uptake of CO_2 by photosynthesising plants) (Fig. 11.4).

The total area affected by Cu-Ni smelters in Russia is much greater than the area of barren and semi-barren land. In the beginning of the 1990s the area subjected to critical levels of sulphur and heavy metal in the Murmansk region covered more than 90,000 km^2(about 60% of the total area of the region). In the Norilsk region the affected area is considerably greater. Forest succession in these areas consists of the replacement of non-tolerant by more resistant species. Because the forests in the sub-Arctic have a relatively low canopy density, the cover of lichens and ground mosses is very important, not only with respect to carbon and nutrient cycling, but also for the reflectivity (albedo) properties of forest land. The moss cover also plays a very important role in water retention. Lichens and mosses are much more

Fig. 11.4 Successful restoration of the vegetation cover close to the Monchegorsk smelter, Kola Peninsula, Russia. (*left*) Industrial barren before planting in the immediate vicinity of the Cu-Ni smelter. (*right*) Planting with birch and sowing with a mixture of herbaceous seed in autumn 2003 on a substrate of semi-decomposed sawdust (600 t ha^{-1}), municipal sewage (300 t ha^{-1}), NPK fertilizer (175 kg ha^{-1} containing 25 kg ha^{-1} ammonium nitrate) and limestone (2 t ha^{-1}). Photographed in 2006. Reproduced by permission of L. Isaeva

sensitive to pollution than grasses and dwarf shrubs, and *Deschampsia flexuosa* and boreal dwarf shrubs usually replace lichens and mosses in forests subjected to air pollution (Lukina et al. 1993).

The frequency of fires in severely polluted areas dramatically increases owing to the presence of large amounts of combustible material (dead lichens, mosses and tree branches, dieback trees etc.). The combined effects of SO_2 and heavy metal pollution and fire in the Arctic result in the replacement of coniferous forests by deciduous (usually birch) forests with a completely different ground vegetation composition. The reflectivity surfaces of coniferous and deciduous forests are very different: the winter albedo of coniferous and deciduous stands is 0.11 and 0.21, respectively. During the summer the albedo of boreal vegetation is lower than that in winter, and deciduous forests have approximately twice the albedo of coniferous forest (Bets and Ball 1997; Sellers et al. 1997; Hall 1999, 2001). The heat fluxes of coniferous and deciduous forests are also different: the sensible heat fluxes in coniferous forests are 2–3 times higher than in deciduous, but the latent energy fluxes (evapo-transpiration) of deciduous forests are 1.5–1.8 times higher than those of coniferous ones (Baldocchi et al. 2000; Chapin et al. 2000).

Polluted areas are therefore characterized by mosaics of pollution- and fire-induced succession. Both the direct and indirect effects of pollutants and fires lead to changes in species composition, reflectivity surface, heat fluxes and biogeochemical cycles, including alterations in the mineralization rate, carbon to nitrogen ratio, nutrient availability and biomass production (Lukina et al. 2005; Lukina and Chernenkova 2008).

Elevated heavy metal concentrations in the soils have adverse effects on microbial processes and, indirectly, on ecosystem functioning. A reduction in microbial activity and fungal (in forest soil primarily ectomycorrhizal fungi) biomass results in increased accumulation of organic matter and a reduction in nutrient availability (Fritze et al. 2000; Nikonov et al. 2001; Johansson et al. 2001). The accumulation factors for Hg and Pb, especially in the topsoil of forests in south Sweden, already exceed the values shown to have adverse effects on soil biological processes and organisms in gradient studies close to local emission sources and in laboratory experiments (Johansson et al. 2001). If climate warming causes an increase in the rate of litter decomposition, then the elevated levels of heavy metals may inhibit decomposition processes and thereby counteract the effects of climate warming (negative feedback).

11.3.2 Global Warming May Aggravate the Effects of Pollutants, and Air Pollutants May Amplify Climatic Stress

Permafrost thawing is one expected consequence of climate warming (Chapter 7, this volume). The melting of permafrost will result in the release of many contaminants currently encapsulated in the soil. Permafrost underlies about 25% of the land area in the Northern Hemisphere, including large areas of Canada, Russia, China

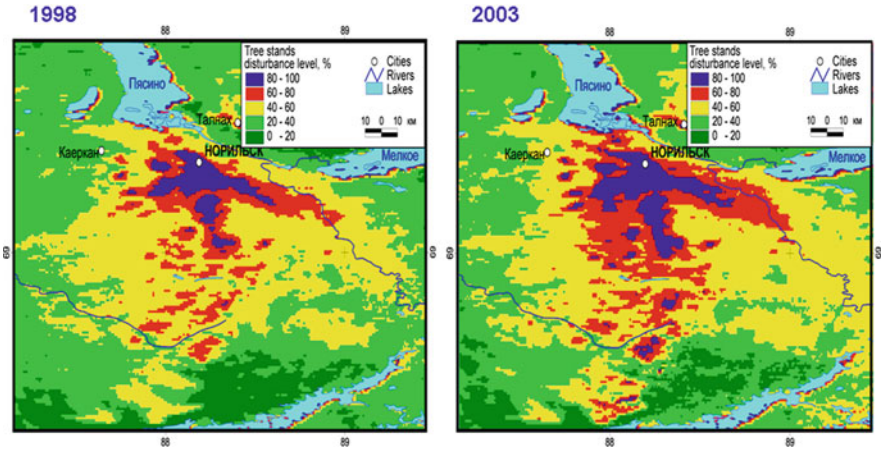

Fig. 11.5 Development of forest degradation during 1998–2003 in the Norilsk region, NW Siberia. SPOT Vegetation data. Reproduced by permission of S. Bartalev

and Alaska (ACIA 2004). Regions of discontinuous permafrost in large parts of northern Canada, Alaska and Russia are especially vulnerable to climate change. The Intergovernmental Panel on Climate Change (IPCC 2002) suggests that the permafrost area could be reduced by as much as 12–22% by 2100. An area of about 2 million ha of taiga-tundra forests are dead or severely damaged by pollution from the Norilsk smelters (Fig. 11.5). Much of this forest area overlies permafrost, and its melting will result in the release of considerable amounts of heavy metals accumulated in the permafrost.

Global change is likely to influence human activities in the Arctic and may encourage new activities that result in heavy metal and POP contamination. The increased risk of storm damage to coastal infrastructure (e.g., pipelines, mines, communities) could enhance the release of contaminants from erosion and flooding (AMAP 2003). Increases in shipping, tourism, commercial fishing, agriculture, industry, and oil exploration could introduce local and regional sources of contamination. Erosion, development, and commerce are likely to increase activities such as dredging, waste discharge, and sea disposal, adding to and remobilizing contaminants. Thus, under certain circumstances, warming may aggravate the effects of pollution.

The physiological changes induced by air pollutants may amplify climatic stress. These changes include reduced mass, depth and functioning of plant roots, and increased respiration and reduced water use efficiency of plants (McLaughlin and Percy 1999). Furthermore, the overall adverse effect of acidifying deposition and air pollutants on genetic diversity and hence biodiversity may also diminish the fitness of affected populations to cope with the further threat of global warming. This would be of particular consequence for systems recognized as being sensitive to both air pollution and global warming (Chapter 10, this volume).

11.3.3 Effect of Climate Change on Contaminant Pathways

Climate change and how and where the effects of pollution manifest themselves are closely interlinked in the Arctic. For instance, changes in the direction and magnitude of air currents will have a considerable effect on the pollution transport chain (Alcamo et al. 2002). Changes in temperature will affect which pollutants are deposited, where they are deposited and how they migrate between sea and land, and vice versa, and in which plants and animals the pollutants accumulate. The thawing of permafrost in certain areas will result in the release of pollutants that have been encapsulated in permafrost for years or even decades.

The most important message of the AMAP assessment on the influence of global change on contaminant pathways (AMAP 2003) is that "a contaminant's journey from its point of emission to its accumulation in an Arctic ecosystem is a conspiracy that cannot work without the compliance of many steps, all of which can be altered by global change".

The atmosphere may predominate initially as a transporting medium, but other slower moving media (e.g. water, soil) may gradually take over, especially if they constitute the largest pool of contaminants. Heavy metals and POPs are transported to the Arctic via long-range air and water pathways, and they accumulate in both food webs and in the soil.

All the factors that can influence the contaminant transport system, including temperature, wind speed and direction, precipitation as both rain and snow, ocean currents, ice cover (on lakes, rivers and the oceans), the magnitude of river flow, and the composition and functioning of terrestrial ecosystems especially, will most probably change. In the Arctic, the changes associated with the ice cover and precipitation patterns (the 0°C isotherm) (Chapter 2, this volume), and with temporary or permanent disturbances in the structure and functioning of ecosystem, have the greatest potential to alter contaminant pathways and exposure (AMAP 2003).

The interaction between airborne contaminants and terrestrial systems (forests, grasslands, tundra) will have an important impact on the overall fate and long-range transport of pollutants, especially of those semi-volatile chemicals that migrate between the gaseous and condensed states. Owing to their high organic matter content, terrestrial ecosystems (e.g. soils, with their cover of forest, grassland or tundra) act as pools for many POPs (Simonich and Hites 1994) and heavy metals.

The extent to which pollutants are associated with aerosols has a decisive effect on their transport via atmospheric pathways into the Arctic. In the Arctic region a considerable proportion of the pollutants are deposited as so-called dry deposition (i.e. aerosols and particles). Forests, especially those comprising coniferous trees, are highly efficient at intercepting dry deposition from the atmosphere in their foliage, thereby contributing to the formation of a long-term pool in forest soil (Wania and McLachlan 2001). Even a small change in climate (temperature) may alter the dynamics of this process and, through this, the cycling of pollutants. Terrestrial vegetation has an indirect impact on the accumulation and transformation of organic pollutants through its effect on the depth and extent of the snow cover and, subsequently, on soil temperature (Sturm et al. 2001).

Of the heavy metals, Hg appears to pose the greatest threat in the Arctic. Despite declining anthropogenic emissions in North America and Europe, a continuous increase is taking place in Hg levels in Arctic ecosystems. The reason for this is unclear: the pathway of Hg transport into the Arctic has still not been fully resolved, and the contribution of Far-Eastern anthropogenic emissions of Hg is poorly documented. The atmospheric transport of Hg and its deposition on surfaces in the Arctic (Hg depletion events) is a climate-sensitive process that may explain much of the susceptibility of the Arctic to Hg contamination (AMAP 2006). An increase in the occurrence and extent of wetlands, e.g. resulting from the melting of permafrost, may also provide an increasing source of Hg passing into the atmosphere and watercourses (AMAP 2005). Climate warming will probably enhance the conversion of Hg into the highly toxic methyl mercury (MeHg), resulting in increased biotic uptake. Climate change may instigate changes in the complexity of food webs, adding or removing specific trophic levels, or altering the age-distribution of animal and plant species. The effect of such changes on Hg levels may be comparable to, or even exceed, the effect of climate change on physical pathways (AMAP 2005).

Arctic haze is also closely linked to climate change, and it is widely understood to be a man-made phenomenon. The location of pollution sources and the transport pathways that result in the formation of arctic haze are still relatively unknown (see also Chapter 10, this volume). Much of the pollution appears to originate from sources in central Eurasia and the Far East (AMAP 2005).

11.3.4 Changes in Arctic Land Use Resulting from the Interaction Between Environmental Pollution and Climate Change

The presence of permafrost in the Arctic plays a key role in the interaction between environmental pollution and climate change. Recently it was realized that permafrost is not really a permanent phenomenon, but only multi-year frozen soil. The major change associated with climate warming is the thawing of permafrost on land (Chapter 7, this volume). As a result of permafrost thawing and degradation, landfills will be washed directly into the rivers or the ocean, and the increase in surface runoff will accelerate the leaching of pollutants into the groundwater. The disposal of waste substances in the sub-Arctic and Arctic has earlier occurred in the form of sewage lagoons, dump sites on the Distant Early Warning Line (a chain of defence radar stations, many now abandoned, along latitude 66°N in Canada, and also extending into Alaska and Greenland), solid refuse dumps in small Arctic communities, mine tailings, and oil drilling sumps (AMAP 2004).

The industrial and domestic waste dumped in the permafrost region in the Russian Arctic will also become a serious problem if the permafrost melts. The problem of radioactive waste is one of the most critical threats, and reports on future sites for radioactive waste repositories have suggested that the waste be disposed of in igneous bedrock, for instance on the Kola Peninsula, instead of in the permafrost in Novaya Zemlya (Melnikov 1999).

Many oil and gas facilities nowadays use permafrost as a solid foundation for buildings, pipelines, waste disposal and roads. Climate warming may degrade the permafrost, causing considerable damage to existing facilities, releasing waste materials and making future land development complicated and expensive (Arctic Oil and Gas 2007).

It is still unclear whether climate change will make the Arctic more attractive for human activities, but it is clear that any expansion in activities will most probably increase contamination by heavy metals, POPs, petroleum hydrocarbons etc.

Indigenous people throughout the Arctic maintain a strong connection to the environment through hunting, herding, fishing and the gathering of natural products. Climate warming will affect their access to food resources, as well as the quality and safety of these resources (ACIA 2004, also Chapter 9, this volume).

An increase in mean temperatures will accelerate mineralization and decomposition processes in the soil. This may result in increased mobility and availability of heavy metals and radionuclides, with subsequently higher concentrations in mushrooms, berries, reindeer meat, fish and birds. An increase in precipitation in the Arctic, resulting from global warming, may increase the deposition of pollutants, and associated leaching, even though there is an overall decrease in emissions. This will inevitably be reflected in increased accumulation of pollutants, including heavy metals and radionuclides, in traditional foodstuff. Higher pollutant availability will also be one consequence of their release from permafrost.

11.4 Conclusions

Climate change in the Arctic is taking place within the context of a wide range of other changes and disturbances including environmental pollution. Heavy metal, SO_2 and sulphate deposition originating from non-ferrous metal smelting and mining activities in the region are the main threat to the prevailing land cover. Increasing mercury and POP pollution in the Arctic poses a considerable threat to animal life in the region, and therefore may also have long-term, indirect effects on the land cover. Environmental pollution originating from oil and gas exploration and extraction activities in the Arctic is expected to increase considerably in the Eurasian Arctic. Forest fires also cause tremendous short- and long-term changes in the land cover in the Arctic. Global warming may aggravate the effects of environmental pollution on land cover, and the extent and mechanisms through which pollutants can amplify climatic stress.

References

Aarrestad P-A, Bakkestuen V, Gytarsky M, Hartikainen M, Karaban R, Korotkov V, Kuzmicheva V, Salemaa M, Vassilieva N (2008) Ground vegetation. In: Derome J, Myking T, Aarrestad P-A (eds) Current state of terrestrial ecosystems in the Joint Norwegian, Russian and Finnish border area in Northern Fennoscandia. Working Papers of the Finnish Forest Research Institute 85:1–98

ACIA (2004) Impacts of a warming Arctic. Arctic climate impact assessment overview report. In: Hassol SJ (ed). Cambridge University Press, Cambridge, 144 p

Alcamo J, Mayerhofer P, Guardans R, van Harmelen T, van Minnen J, Onigkeit J, Posch M, de Vries B (2002) An integrated assessment of regional air pollution and climate change in Europe: findings of the AIR-CLIM project. Environ Sci Policy 5:257–272

AMAP (1998) AMAP assessment report: Arctic pollution issues. Arctic monitoring and assessment programme (AMAP), Oslo

AMAP (2003) AMAP assessment 2002: the influence of global change on contaminant pathways to, within, and from the Arctic. Arctic monitoring and assessment programme (AMAP), Oslo

AMAP (2004) AMAP assessment 2002: persistent organic pollutants (POPs) in the Arctic. Arctic monitoring and assessment programme (AMAP), Oslo

AMAP (2005) AMAP assessment 2002: heavy metals in the Arctic. Arctic monitoring and assessment programme (AMAP), Oslo

AMAP (2006) AMAP assessment 2006: acidifying pollutants, arctic haze and acidification in the Arctic. Arctic monitoring and assessment programme (AMAP), Oslo

Amiro B, Todd J, Wotton B, Logan K, Flannigan M, Stocks B, Mason J, Martell D, Hirsch K (2001) Direct carbon emissions from Canadian forest fires, 1959–1999. Can J For Res 31:512–525

Arctic Oil and Gas 2007 (2007) Arctic monitoring and assessment programme (AMAP), Oslo

Äyräs M, Niskavaara H, Bogatyrev I, Chekushin V, Pavlov V, de Caritat P, Halleraker J, Finne T, Kashulina G, Reimann C (1997) Regional patterns of heavy metals (Co, Cr, Cu, Fe, Ni, Pb, V and Zn) and sulphur in terrestrial moss samples as indication of airborne pollution in a 188,000 km^2 area in northern Finland, Norway and Russia. J Geochem Explor 58:269–281

Baldocchi D, Kelliher F, Black T, Jarvis P (2000) Climate and vegetation controls on boreal zone energy exchange. Glob Change Biol 6:69–83

Bets A, Ball J (1997) Albedo over the boreal forest. J Geophys Res – Atmos 102:28901–28909

Boutron C, Candelone J-P, Hong S (1995) Greenland snow and ice cores: unique archives of large-scale pollution of the troposphere of the Northern Hemisphere by lead and other heavy metals. Sci Tot Environ 160/161:233–241

Boutron C, Vandal G, Fitzgerald W, Ferrari C (1998) A 40 year record of mercury in central Greenland snow. Geophys Res Lett 25:3315–3318

Chapin F, McGuire A, Randerson J, Pielke R, Baldocchi D, Hobbie S, Roulet N, Eugster W, Kasischke E, Rastetter E, Zimov S, Oechel W, Running S (2000) Feedbacks from arctic and boreal ecosystems to climate. Glob Change Biol 6:211–223

Derome J, Lindroos A-J (1998) Effects of heavy metal contamination on macronutrient availability and acidification parameters in forest soil in the vicinity of the Harjavalta Cu–Ni smelter, SW Finland. Environ Pollut 99:225–232

Derome J, Lindroos A-J, Niska K (1998) Effects of SO_2 and heavy metal emissions from the Kola Peninsula, NW Russia, on soil acidity parameters in NW Russia and Finnish Lapland. Scandinavian J For Res 13(4):421–428

Evdokimova GA (2000) The impact of heavy metals on the microbial diversity of podzolic soils in the Kola Peninsula. In: Innes J, Oleksyn J (eds) Forest dynamics in heavily polluted regions. Report of the International Union of Forest Reseach Organizations (IUFRO) Task Force on Environmental Change 1, CAB International, UK, 67–76

Fritze H, Niini S, Mikkola K, Mäkinen A (1989) Soil microbial effects of a Cu-Ni smelter in southwestern Finland. Biol Fertil Soils 8:87–94

Fritze H, Pennanen T, Haini J, Siira-Pietikainen A, Vanhala P (2000) Effects of heavy metals on soil mircoflora. In: Mälkönen E (ed) Forest condition in a changing environment – the Finnish case. Forestry Sciences 65, Kluwer Academic Publishers, Dordrecht, pp 260–265

Goulden M, Wofsy S, Harden J, Trumbore S, Crill P, Gower S, Fries T, Daube B, Fan, S-M, Sutton D, Bazzaz A, Munger J (1998) Sensitivity of boreal forest carbon balance to soil thaw. Science 279:214–217

Gregor D, Peters A, Teixeira C, Jones N, Spencer C (1995) The historical residue trend of PCBs in the Agassiz Ice Cap, Ellesmere Island, Canada. Sci Total Environ 160/161:117–126

Hall F (1999) Introduction to special section: BOREAS in 1999 Experimental and science perspective. J Geophys Res 104:27627–27639
Hall F (2001) Introduction to special section: BOREAS III experimental and science perspective. J Geophys Res 106:33511–33516
Helmisaari H-S, Makkonen K, Olsson M, Viksna A, Mälkönen E (1999) Fine root growth, mortality and heavy metal concentrations in limed and fertilized Pinus sylvestris (L.) stands in the vicinity of a Cu-Ni smelter in SW Finland. Plant Soil 209:193–200
Hong S, Candelone J-P, Patterson C, Boutron C (1994) Greenland ice evidence of hemispheric lead pollution two millennia ago by Greek and Roman civilizations. Science 265:1841–1843
IPCC (2002) The third assessment. Intergovernmental panel on climate change. http://www.ipcc.ch/
Isaev A, Korovin G (2003) Large-scale changes in the Eurasian boreal forests and methods for their assessment with using satellite information. Lesovedenie 2:3–9
Isaeva L, Poikolainen J, Myking T, Derome J, Sukharev T, Rautio P (2008) Element concentrations in plants. In: Derome J, Myking T, Aarrestad P-A (eds) Current state of terrestrial ecosystems in the Joint Norwegian, Russian and Finnish border area in Northern Fennoscandia. Working Papers of the Finnish Forest Research Institute 85:1–98
Isaksson E, Hermanson M, Hicks S, Igarashi M, Kamiyama K, Moore J, Motoyama H, Muir D, Pohjola V, Vaikmae R, van de Wal RSW, Watanabe O (2003) Ice cores from Svalbard – useful archives of past climate and pollution history. Phys Chem Earth 28:1217–1228
Johansson K, Bergback B, Tyler G (2001) Impact of atmospheric long range transport of lead, mercury and cadmium on the Swedish forest environment. Water Air Soil Pollut: Focus 1: 279–297
Kasischke E, Rupp T, Verbyla D (2003) Fire trends in the Alaskan boreal forest region. In: Chapin F III, Oswood M, van Cleve K, Viereck L, Verbyla D (eds) Alaska's changing boreal forest. Oxford Press, New York
Kharuk V, Winterberger K, Tzibulsky G, Yahimovich A, Moroz S (1996) Pollution induced damage of Norilsk valley forests. Ecologiya 6:424–430
Kim Y, Hatsushika H, Muskett R, Yamazaki K (2005) Possible effect of boreal wildfire soot on Arctic sea ice and Alaska glaciers. Atmospheric Environ 39:3513–3520
Kozlov M (1997) Pollution impact on insect biodiversity in boreal forests: evaluation of effects and perspectives of recovery. In: Crawford R (ed) Disturbance and recovery in Arctic Lands: an ecological perspective. Proceedings of the NATO advanced research workshop on disturbance and recovery of arctic terrestrial ecosystems, Rovaniemi. NATO ASI series. Partnership subseries 2. Environment 25. Kluwer Academic Publishers, Dordrecht
Kozlov M, Whitworth T (2002) Population densities and diversity of Calliphoridae (Diptera) around a nickel-copper smelter at Monchegorsk, Northwestern Russia. Entomologica Fennica 13:98–104
Kozlov M, Zvereva E (2007) Industrial barrens: extreme habitats created by non-ferrous metallurgy. Rev Environ Sci Biotechnol 6:233–259
Kruychkov V, Syroid N (1979) Changes of the Kola North ecosystems subjected to anthropogenic activity, III Symposium Biological Problems of the North, Apatity, 39–42
Lindberg S, Brooks S, Lin C-J, Scott K, Landis M, Stevens R, Goodsite M, Richter A (2002) The dynamic oxidation of gaseous mercury in the Arctic troposphere at polar sunrise. Environ Sci Technol 36:1245–1257
Lukina N, Chernenkova T (2008) Pollution-induced successions in the Kola peninsula forests. Russian J Ecol 4:1–9
Lukina N, Liseenko L, Belova E (1993) Pollution-induced changes in the vegetation cover of spruce and pine ecosystems in the Kola North region. In: Kozlov M, Haukioja E, Yarmishko V (eds) Proceedings of the international workshop on aerial pollution in Kola Peninsula, 14–16 April, St. Petersburg
Lukina N, Nikonov V (1995) Acidity of podzolic soils subjected to sulphur pollution near a Cu-Ni smelter at the KolaPeninsula. Water Air Soil Pollut 85:1057–1062

Lukina N, Nikonov V (1996) Biogeochemical cycles in the northern forest ecosystems subjected to air pollution, Part 1, 2. Kola Science Centre RAS, Apatity, 410 p

Lukina N, Sukhareva T, Isaeva L (2005) Pollution-induced digressions and demutation successions in northern taiga forests. Nauka, Moscow, 245 p

Manninen S, Huttunen S, Perämäki P (1998) Effect of ambient SO_2 levels on S fractions in Pinus sylvestris foliage growing in the subarctic. Scandinavian J For Res 13:306–316

Masclet P, Hoyau V, Jaffrezo J, Cachier H (2000) Polycyclic aromatic hydrocarbon deposition on the ice sheet of Greenland. Part 1: Superficial snow. Atmos Environ 34:3195–3207

McGuire A, Chapin FS III (2003) Climate feedbacks. In: Alaska's Changing Boreal Forest. Oxford University Press, New York

McGuire A, Hobbie J (1997) Global climate change and the equilibrium responses of carbon storage in arctic and subarctic regions. In: Modeling the Arctic system: a workshop report of the Arctic system science programe. Arctic Research Consortium of the US, Fairbanks, 53–54

McGuire A, Melillo J, Kicklighter D, Pan Y, Xiao X, Helfrich J, Moore B III, Vorosmarty C, Schloss A (1997) Equilibrium responses of global net primary production and carbon storage to doubled atmospheric carbon dioxide: Sensitivity to changes in vegetation nitrogen concentration. Glob Biogeochem Cycles 11:173–189

McGuire A, Wirth C, Apps M, Beringer J, Clein J, Epstein H, Kicklighter D, Bhatti J, Chapin F III, de Groot B, Efremov D, Eugster W, Fukuda M, Gower T, Hinzman L, Huntley B, Jia G, Kasischke E, Melillo J, Romanovsky V, Shvidenko A, Vaganov E, Walker D (2002) Environmental variation, vegetation distribution, carbon dynamics, and water/energy exchange at high latitudes. J Veg Sci 13:301–314

McGuire A, Apps M, Chapin FS III, Dagraville R, Flannigan M, Kasischke E, Kicklighter D, Kimball J, Kurz W, McRae D, McDonald K, Melilli J, Myneni R, Stocks B, Verbyla D, Zhuang Q (2004) Land cover disturbances and feedbacks to the climate system in Canada and Alaska. In: Gutman G, Janetos A, Justice C, Moran E, Mustard J, Rindfuss R, Skole D, Turner B II, Cochrane M (eds) Land Change Science. Observing, monitoring and understanding trajectories of change on the Earth surface. Kluwer Academic Publishers, Dordrecht, pp 139–163

McLaughlin S, Percy K (1999) Forest health in North America: some perspectives on potential roles of climate and air pollution. Water Air Soil Pollut 116:151–197

Melnikov N (1999) About building long-term repository for the solid radioactive wastes on Archipelago Novaya Zemlya. Kola Scientific Centre RAS, Apatity, 1–31

Myking T, Lindgren M, Gytarsky M, Karaban R, Kuzmicheva V (2008) Crown condition. In: Derome J, Myking T, Aarrestad P-A (eds) Current state of terrestrial ecosystems in the Joint Norwegian, Russian and Finnish border area in Northern Fennoscandia. Working Papers of the Finnish Forest Research Institute 85:1–98

Nikonov V, Lukina N, Polyanskaya L, Panikova A (2001) Distribution of microorganisms in the Al–Fe–humus podzols of natural and anthropogenically impacted boreal spruce forests. Microbiology 70(3):319–328

Nikonov V, Lukina N, Bezel V, Belsky E, Bespalova A, Golovchenko A, Gorbacheva T, Dobrovolskaya T, Dobrovolsky V, Zukert N, Isaeva L, Lapenis A, Maksimova I, Marfenina O, Panikova A, Pinsky D, Polanskaya L, Steinnes E, Utkin A, Frontasieva M, Tsibulsky V, Chernov I, Yatsenko-Khmelevskaya M (2004) Trace elements in boreal forests. In: Isaev AS (ed), Nauka, Moscow, pp 1–616

Rigina O, Kozlov M (1998) Pollution impact on sub-Arctic forests in the Kola peninsula, Russia. In: Impacts and amelioration of air pollution in heavily polluted regions. IUFRO, The Task Force on Environmental Change

Rosman K, Chisholm W, Hong S, Candelone J-P, Boutron C (1997) Lead from Carthaginian and Roman Spanish mines isotopically identified in Greenland ice dated from 600 BC to 300 A.D. Environ Sci Technol 31:3413–3416

Sellers P, Hall F, Kelly R, Black A, Baldocchi D, Berry J, Ryan M, Ranson K, Crill P, Lattenmaier D, Margolis H, Cihlar J, Newcomer J, Fitzjarrald D, Jarvis P, Gower S, Halliwell D, Williams D, Goodison B, Wickland D, Guertin F (1997) BOREAS in 1997 experiment overview, scientific results and future directions. J Geophys Res 102:28731–28769

Shvidenko A, Goldhammer J (2001) Fire situation in Russia. Int Fire News 23:49–65
Shvidenko A, Nilsson S (2000) Fire and carbon budget of Russian forests. In: Kasischke E, Stocks B (eds) Ecological studies 138 – fire, climate change and carbon cycling in the Boreal Forests. Springer, New York, pp 289–311
Simonich S, Hites R (1994) Importance of vegetation in removing polycyclic aromatic hydrocarbons from the atmosphere. Nature 370:49–51
Steinnes E, Lukina N, Nikonov V, Aamlid D, Royset O (2000) A gradient study of 34 elements in the vicinity of a copper-nickel smelter in the Kola Peninsula. Environ Monitor Assess 60:71–88
Stocks B, Fosberg M, Lynham T, Mearns L, Wotton B, Yang Q, Jin J-Z, Lawrence K, Hartley G, Mason J, McKenny D (1998) Climate change and forest fire potential in Russian and Canadian boreal forests. Clim Change 38:1–13
Sturm M, McFaden J, Liston G, Chapin I, Holmgren J, Walker M (2001) Snow-shrub interactions in Arctic tundra: a hypothesis with climatic implications. J Climate 14:336–344
Tömmervik H (2008) Satellite imagery. In: Derome J, Myking T, Aarrestad P-A (eds) Current state of terrestrial ecosystems in the Joint Norwegian, Russian and Finnish border area in Northern Fennoscandia. Working Papers of the Finnish Forest Research Institute 85:1–98
Tømmervik, H., Høgda, K.A, Solheim I (2003) Monitoring vegetation changes in Pasvik (Norway) and Pechenga in Kola Peninsula (Russia) using multi-temporal Landsat MSS/TM data. Rem Sens Environ 85:370–388
Tuovinen JP, Laurila T, Lattila H, Ryaboshapko A, Brukhanov P, Korolev S (1993) Impact of the sulphur dioxide sources in the Kola peninsula on air quality in Nothernmost Europe. Atmos Environ 27A:1379–1395
Wania F, McLachlan M (2001) Estimating the influence of forests on the overall fate of semivolatile organic compounds using a multimedia fate model. Environ Sci Technol 35:582–590
Wotawa G, Novelli P, Trainer M, Granier C (2001) Interannual variability of summertime CO concentrations in the Northern Hemisphere explained by boreal forest fires in North America and Russia. Geophys Res Lett 28:4575–4578

Chapter 12
Summary and Outstanding Scientific Challenges for Land-Cover and Land-Use Research in the Arctic Region

Garik Gutman and Chris O. Justice

Abstract This chapter summarizes the volume content focusing on NASA LCLUC Program contribution to the IPY program, which has been completed. The volume is compilation of results of the most recent US and European studies on land-cover and land-use changes and their interactions with biogeochemical and water cycles, atmospheric aerosol, and human and wildlife populations in the Northern Eurasian Arctic. Emphasis of global change research in this region has traditionally focused on the processes of the biophysical systems. The papers presented in this volume extend this research, primarily addressing land cover but also some of the human-environment interactions in this region. Outstanding scientific challenges are outlined as they were discussed in each chapter.

12.1 Introduction

The Arctic Climate Impact Assessment 2004 report (ACIA 2004) which was presented in testimony before the United States Senate on November 16, 2004, stated that the Arctic climate is warming rapidly and that much larger changes are projected to Arctic ecosystems, with worldwide implications. Since 2004, the observed warming trends have continued and records are being set. Near-surface warming in the Arctic has been twice the global average over the last decades (Graversen et al. 2008) and the Arctic sea-ice areal extent reached a record minimum in 2007 (Maslanik et al. 2007). The projected changes for the region include a shift of vegetation zones, which, in turn, will impact animal species' diversity, ranges, and distribution. The future of the iconic arctic animal species is in question (Courtland 2008). Socio-economic impacts include increasing exposure to storms for coastal communities and facilities, disruption of transportation, buildings, and other infrastructure due to permafrost thawing (ACIA 2004). Moreover, multiple stresses

G. Gutman (✉)
NASA Headquarters, 300, E. Street, SW Washington, DC 20546, USA
e-mail: ggutman@nasa.gov

G. Gutman, A. Reissell (eds.), *Eurasian Arctic Land Cover and Land Use in a Changing Climate*, DOI 10.1007/978-90-481-9118-5_12,

interact, causing impacts to humans and ecosystems, including major economic and cultural impacts on indigenous communities. Issues related to increased marine transportation and access to the Arctic's natural resources as a result of reduced sea ice, as well as security and safety concerns are also likely to arise (ACIA 2004). A growing awareness of the consequences of climate change and human activities in the Arctic region has prompted the United States to recently announce a new Arctic policy superseding its 1994 policy.

The current satellite data record is now of sufficient duration (over 30 years for the AVHRR and over 35 years for Landsat) to conduct meaningful analyses of the interannual variability in land-cover and land-use changes in the various regions of the world. This long-term data record has been enhanced over time with new sensors with improved monitoring capabilities (Townshend and Justice 2002). The contributions in this volume demonstrate the utility of satellite data for monitoring changes and trends over time, including the associations among vegetation productivity, surface temperature, sea ice concentrations, biogeochemical and water cycles, and air pollution under changing climate conditions, and their relation to wildlife and human population dynamics in the Arctic.

In this concluding chapter, based on lessons learned from these studies, we outline the outstanding scientific issues, which land-cover and land-use scientists need to address when studying arctic ecosystems, and we identify some future research directions.

12.2 Modeling and Analysis of Forest-Cover Changes

Recent modeling efforts indicate that substantial refinements in models are needed for vegetation distribution, tree migration, and tundra vegetation responses to climate warming, particularly to capture dispersal mechanisms, migration rates, and changes in biogeochemical cycling (Chapter 2, this volume). Continued collection and associated improvements to observations are also needed, not only to inform the models but also to calibrate and validate the outcomes of model simulations, under the wide range of conditions that are predicted to occur across the Arctic region in the next few decades. It is primarily through the combined use of field and satellite measurements that we will be able to capture the various feedbacks between terrestrial ecosystems and the physical climate system and better predict how those changes will be manifested, so that Arctic communities and resource managers can plan and adapt to the inevitable changes that will follow. The latter will require modeling with regional specificity and translation of the research results into information available for resource management.

In Northern Eurasia, lightning fires play a primary role in areas not subject to human exploitation. Where human activities are higher, the trend has been towards an increase in fire frequency (Kovacs et al. 2004), even though separating the climatic from the anthropogenic impacts is difficult. The resulting losses in forest cover have implications for modeling biogeochemical cycles and climate, forest management and nature conservation, all of which benefit from the quantification of forest-cover dynamics.

High rates of forest-cover loss bring into question the sustainability of high-latitude forests, given the long time periods required to reestablish forest cover (Chapter 3, this volume). More retrospective and prospective studies are required to bring greater understanding on long-term trends of forest cover within high-latitude forests.

12.3 Prospects for Using Satellite Data

In addition to the systematic, optical observations at coarse resolutions (e.g., AVHRR, SPOT VEGETATION and MODIS) and moderate resolutions (e.g., Landsat), a number of new sensors with global coverage are now available. Also, microwave data, such as for example, from RADARSAT can be used to analyze areas where high resolution is required and cloud cover or low illumination precludes the use of Landsat-like data (Chapter 4, this volume). Current Landsat-7 sensor problems, caused by the scan line corrector malfunction in 2003, make this option especially useful. For MISR on board the EOS Terra platform, frequent cloud cover and the infrequent coverage may limit its utility. The results described in this volume suggest that MODIS may be an appropriate tool for longer-term monitoring when Landsat data or other moderate resolution data are available for training purposes. The 500-m data sets provide useful information, but further work is needed to explore the effectiveness of using the two 250-m MODIS channels.

With the need to secure consistent long-term satellite data records to detect and monitor surface changes in remote Arctic regions and an increasing number of Earth observation satellite systems being put into service by the international community, attention should to be given to coordination of data acquisition (coverage), data interoperability, cross calibration and access. Efforts to generate preprocessed data sets to facilitate use by research and resources management communities, which are not primarily concerned with satellite data processing, are particularly helpful (Gutman et al. 2008).

Satellite imagery can help overcome the sparseness of in situ observations, and the role of satellite data sets will continue to grow. Remote sensing has proven extremely useful in monitoring changes in lake extent, glacier retreat, and soil freeze/thaw conditions (Stow et al. 2004; Kääb 2008). However, while satellite-derived snow-cover extent products show some degree of reliability, at present, high quality satellite-based methods for monitoring snow-water equivalent are still lacking (Chapter 7, this volume), and it is crucial that improved methods are developed.

In many cases trade-offs exist between spatial and temporal resolutions. For example, synthetic aperture radar sensors have sufficient spatial resolution to accurately capture the extent of lakes and wetlands; however, they have low temporal frequency, making it difficult to capture their seasonal evolution (Alsdorf et al. 2007). Meanwhile, passive microwave sensors provide daily overpasses but at low spatial resolution. Multi-sensor, blended data products may help solve this problem (Chapter 7, this volume).

12.4 Improved Land Surface Mapping for Characterizing the Carbon Budget

The current scenarios of climate change with the associated regional warming predict the expansion of larch forest northward to the Arctic coast, whereas the zone currently dominated by larch is being invaded by dark coniferous species (Siberian stone pine, spruce, and fir) advancing from the south and west (Rupp et al. 2001; Kharuk et al. 2005, 2006). Studies testing these predicted changes require an accurate mapping of vegetative cover and comparable data sets over time. Comparison of satellite-derived land-cover products for Arctic Eurasia, even at relatively coarse resolution, reveals significant differences in their representations of vegetation distribution (Chapter 5, in this volume). Thus, the choice of a specific land-cover product can have a major impact on the results of research projects in the region. This source of uncertainty is often overlooked and a strong case can be made for improved validation of the land cover products.

The differences in categorical maps are highest at borders between biomes and in parts of the region where significant presence of open canopies of woody plants (trees and shrubs) or herbaceous vegetation is expected. The geographic distribution of disagreement may reflect the limitation of coarse-resolution categorical maps to represent open vegetation covers and mixed or fragmented landscapes. Vegetation Continuous Field maps of dominant vegetation types are a promising alternative to categorical maps. The agreement among the compared maps is highest for tree-dominated vegetation, which is represented more consistently than other vegetation-cover types in the categorical maps, and is lowest for herbaceous vegetation. The differences in mapping can lead to substantially different estimates of the regional carbon balance, as a very different picture of the regional C balance emerges when changing the ratio of tree cover (an estimated C source) to shrub cover (C sink).

12.5 The Arctic: Carbon Source or Sink?

The simulation framework and subsequent analyses presented in this book allow for attribution of mechanisms responsible for the shift in carbon balance for this region of the world over the last 10 years (Chapter 6, this volume). The results show that the estimated positive effect on regional C balance from CO_2 fertilization was offset by negative responses to climate, such as disturbance and land-use change. The current trend toward warmer, drier conditions in the boreal forest may also be leading to an increase in the area burned (Kurz and Apps 1999; Stocks et al. 2000, 2003) and therefore a large, additional negative land-cover/land-use change effect. This correlated climate-fire effect in boreal forests appears to be the largest signal in the negative C-balance response of the Northern Eurasian region during the last 10-year time period. Model simulations suggest that a shift in terrestrial ecosystem C balance from a sink to a source may be occurring in the boreal forests of Northern Eurasia as a result of changes in climate and an increase in fire activity in recent

years. These modeling results do include several important sources of uncertainty, however, and it is critical to compare these results with those based on inversion models and ground inventory-based estimates.

The ability of the model to estimate C dynamics in earlier time periods and to simulate the stand age distribution of the boreal forest landscape is limited primarily by the length of the historical fire record. A full exploitation of the AVHRR satellite record for this region from 1982 to 2000 is needed, including use of the global 1-km data compilation initiated by IGBP-DIS available from 1992 (Teillet et al. 2000). Burned area products need to be generated from the available coarse-resolution data record and validated using international standards (Roy et al. 2005). The burned area products need to be continued with the current satellite systems and those planned for launch in the next few years (Townshend and Justice 2002).

In future simulations, it is important to also address insect disturbance, as the areas affected by insects are comparable to those burned (Kurz and Apps 1999; Werner et al. 2006). Quantifying such large areas is needed in order to reduce the uncertainty of estimates of contemporary C dynamics, especially with respect to the effects of land-cover/land-use change. It is, however, even more of a challenge to produce projections of C balance according to future scenarios. All of these issues are important to consider in view of a potential weakening, or disappearance, of the terrestrial C sink in high-latitude ecosystems, creating a positive feedback to climate change by effectively accelerating the build-up of CO_2 in the atmosphere.

12.6 Characterizing the Water Cycle

The hydrologic effects of land cover change are intertwined with the effects of climate change over last 50 years (Chapter 7, this volume). The existing observations are too sparse or cover too short a time period to allow us to unravel these interactions entirely. Not only are the measurements of hydrologic variables, such as precipitation, river discharge, and soil moisture, sparse in the harsh climate of the Arctic, but also their spatial distributions are skewed towards the warmer parts of the domain, where population density is highest. While remote sensing can expand the extent of monitoring efforts, it will always have limits in terms of resolution and sub-surface penetration. For sub-surface processes, large-scale hydrologic models should be used utilizing assimilation of remotely sensed data. However, integration of glacier dynamics in most large-scale hydrologic models presents challenges. Improvements in these models depend on better in situ and remotely sensed observations.

To fully understand the hydrologic cycle of Northern Eurasia and to predict how it might respond to future changes in climate and land cover, it will be necessary to combine in situ and remotely-sensed observations, modeling, and process studies into a more coherent analysis system. Future observation missions should be designed from a systems perspective that specifically anticipates the merging of in situ and satellite data and their use in large-scale models, and prioritizes development of these components accordingly.

12.7 Human Dimensions: Land Management

The human dimensions aspects are often overlooked when climate change is studied in the Arctic. Yet the human population of this region and their associated livelihoods will be impacted and will need to adapt (ACIA 2004). Based on the analysis of the present situation of local Arctic ethnic groups and their land use, including reindeer herding, it is imperative that governments and the associated management, and policy- and decision-makers incorporate traditional local and scientific knowledge in future planning (Chapter 8, this volume). Analysis of the current situation indicates that reindeer herders are trying to develop preventative measures against pasture loss and damage from multiple external stresses pressures, be it climate change or new local industrial projects, through collaborative planning incorporating indigenous knowledge and science. Specially designed systems, such as the EALÁT/Reindeer Mapper Information System (http://arcticportal.org/en/icr/ealat) can assist in the ongoing analyses of trends as well as detection of emerging events and conditions that affect humans, agriculture, and the environment, in order to enhance early warning and management of responses and adaptation to external stresses. Such systems should be able to provide reindeer herders with an efficient tool for managing the real-time movements and migrations of their herds. By providing real-time local, satellite or other environmental data (e.g., ice melt in lakes and rivers, weather events) such systems will enable improved efficiency in linking different members of the herder settlements or communities and making real-time adjustments to herd movements, to avoid problems such as changing weather/climate conditions, freeze-thaw "lock-out" problems, or to take advantage of availability of better pasturelands along migration routes. The system is being designed to allow users to input their own data into the system for analysis in addition to the data provided by the system itself. More effort is needed to create the information infrastructure within the Eurasian indigenous community and to build the capabilities necessary to adapt successfully to major changes taking place across Northern Eurasia.

12.8 Landscape Effects Under Multiple Stresses

New tools are needed for the various stakeholders in the Arctic to envision the cumulative effects of multiple stresses (Chapter 9, this volume). Direct impacts of industrial activities are currently local and limited in extent, but this is changing rapidly as extensive oil and gas fields are developed and land- and sea-transportation corridors are developed for transportation to markets. Indirect impacts of this development, such as those from off-road vehicles, are much more extensive, but probably not as long-lasting as the direct impacts. Industrial infrastructure development (mainly roads and pipelines) is creating serious barriers to animal migration corridors, fragmenting their habitats (Nellemann et al. 2003) and limiting the areas of summer pasture. Herders currently view the threats from industrial development to be much greater than threats from climate change. Land withdrawals by industry,

increasing local populations, and larger reindeer herds are putting increasing pressure on the rangelands. However, the locals have an overall positive view of gas development because of increased local economic and social advantages (AMAP 2007).

The actual effects of climate change on vegetation are currently hard to document on the ground level because of the lack of baseline data and long-term ground observations and the difficulty of excluding reindeer grazing in these studies. Ground-based baseline studies are urgently needed to enable the documentation of future changes in plant species composition, biomass, active layer depths and soils properties.

There is a high potential for extensive landscape alterations where there are unstable sandy soils or extremely ice-rich, near-surface permafrost on slopes. If exposed by natural or anthropogenic causes, ice-rich permafrost is highly susceptible to catastrophic failures. For example, over large areas of the Yamal Peninsula, landslides have transformed the zonal sedge, dwarf-shrub tundra to the low-shrub tundra that is typically found on disturbed sites in this subzone (Chapter 9, this volume).

Vegetation-change models, such as the ones used in the Walker et al. study in this volume, help predict the changes that will occur to the vegetation from the combined influence of climate change, industrial development, and changes in reindeer foraging impact. Additional modeling efforts are needed to predict the locations and densities of road and pipeline networks. In addition, more wide-ranging assessments that include air and water quality, and biodiversity of terrestrial and aquatic organisms are needed. Comprehensive assessments and integrated models that can anticipate numerous various development scenarios and draw on other international experiences are needed to plan for the cumulative effects of resource development, climate change, and demographic changes.

12.9 Atmospheric Effects

Modeling and observational studies have provided evidence that atmospheric aerosols are linked to major processes that affect the atmosphere, cryosphere, land and ocean, and hence have played at least some role in changes occurring in the Arctic in recent decades (Chapter 10, this volume). However, accurate assessment of the climate impact of aerosols in the Arctic is very difficult because of complicated interactions and feedbacks involving aerosols. A paucity of aerosol data further complicates such assessments. Despite the complexity, improved assessments of aerosol impacts in the Arctic is of high priority because the uncertainty and magnitude of the potential impacts caused by anthropogenic aerosols.

The Arctic haze phenomenon is a manifestation of long-range transported air pollutants originating in the mid-latitudes or within the Arctic (Quinn et al. 2006). Observed long-term changes of aerosols in the Arctic are complex, reflecting the interplay of various factors that affect the lifetime of aerosols and their transport to the Arctic.

A key question remains as to the overall role that anthropogenic aerosols and the associated feedbacks play in modulating the greenhouse warming in the Arctic, as well as the global climate system. Improved understanding of the impacts of Arctic aerosols on regional and global climate requires further research, addressing the dynamics of aerosol sources, variability in transport to high latitudes due to changes in general circulation, as well as changes in other climatic characteristics that might be involved in aerosol-induced feedbacks. Our understanding of the relevant physical processes has been hampered by a lack of concurrent measurements of aerosols, clouds, radiation, snow and sea ice processes. Isolated measurements of the individual components of this system cannot be used to elucidate the relevant physical processes or to validate model simulations.

The International Polar Year (IPY, http://www.ipy.org) provides new important insights into aerosol-clouds-radiation interactions. Several large-scale, international field campaigns are being conducted, aimed at better understanding Arctic aerosols and their impacts. However, a long-term, well-coordinated observational system is needed to provide new sets of data to address the broad, inter-disciplinary problems related to the Arctic system. Improvements in parameterizations of physical processes involving aerosol, clouds and precipitation in the models are urgently needed.

12.10 Polluting the Arctic

Climate change in the Arctic is taking place within the context of a range of other changes and disturbances, including environmental pollution. Many oil and gas facilities nowadays use permafrost as a solid foundation for buildings, pipelines, waste disposal and roads. Environmental pollution originating from oil and gas exploration and extraction activities in the Arctic is expected to increase considerably in the Eurasian Arctic, based on the projected expansion in oil and gas activities in the region (AMAP 2007). Climate warming may degrade the permafrost, causing considerable damage to existing facilities, releasing waste materials and making future land development complicated and expensive (Chapter 11, this volume). Indigenous people throughout the Arctic maintain a strong connection to the environment through hunting, herding, fishing and the gathering of natural products. Climate warming will affect their access to food resources, as well as the quality and safety of these resources. Traditional ways of life will be challenged as oil and gas activities increase in the region.

It is still unclear whether climate change will make the Arctic more attractive for human activities, but it is clear that any expansion in human activities will most probably increase contamination by heavy metals, persistent organic pollutants, and petroleum hydrocarbons (Chapter 11, this volume). Heavy metal, SO_2 and sulphate deposition originating from non-ferrous metal smelting and mining activities in the region pose a serious threat to the prevailing land cover. Increasing mercury pollution in the Arctic adversely impacts animal life in the region, and, therefore, may also have long-term, indirect effects on the land cover.

Global warming may aggravate the effects of environmental pollution on land cover and the extent and mechanisms through which pollutants can amplify climatic stress (Chapter 11, this volume). An increase in mean temperatures will accelerate mineralization and decomposition processes in the soil. This may result in increased mobility and availability of heavy metals and radionuclides, with subsequently higher concentrations in mushrooms, berries, reindeer meat, fish and birds. An increase in precipitation in the Arctic, resulting from global warming, may increase the deposition of pollutants, and associated leaching, even though there is an overall decrease in emissions. This will inevitably be reflected in increased accumulation of pollutants, including heavy metals and radionuclides, in traditional foodstuff.

12.11 Conclusions

This volume is a NASA LCLUC Program contribution to the IPY program, which has been completed. Its goal was to summarize results of the most recent US and European studies on land-cover and land-use changes and their interactions with biogeochemical and water cycles, atmospheric aerosol, and human and wildlife populations in the Northern Eurasian Arctic. Emphasis of global change research in this region has traditionally focused on the processes of the biophysical systems. With the Arctic exhibiting some of the earliest signs of global warming, the impacts of climate change being felt by the indigenous populations living in coastal areas and the promise of increased economic development, research on land use and ecosystems is gaining more attention. Research on land-use change requires a stronger role of social scientists familiar with the region. To enable the science to proceed, there is also a need for continued observation and monitoring of the region. An expanded program of satellite and in situ observations is needed to provide the data to better understand the processes and to quantify the changes. International cooperation, which is a characteristic of the NASA LCLUC program, will be needed to secure the necessary observations and continue the exchange of data, and a better understanding of this important and rapidly changing region.

References

ACIA (2004) Impacts of a warming arctic. Arctic climate impact assessment Overview Report. In: Hassol SJ (ed) Cambridge University Press, Cambridge, 144p

Alsdorf DE, Rodríguez E, Lettenmaier DP (2007) Measuring surface water from space. Rev Geophys 45(RG2002). doi:10.1029/2006RG000197

Arctic Monitoring and Assessment Programme (AMAP) (2007) Arctic oil and gas 2007. Oslo, 40 p

Courtland R (2008) Polar bear numbers set to fall. Nat News 453:432–433

Graversen RG, Mauritsen T, Tjernström M, Källén E, Svensson G (2008) Vertical structure of recent Arctic warming. Nature 541:53–56

Gutman G, Byrnes R, Masek J, Covington S, Justice C, Franks S, Headley R (2008) Towards monitoring land cover and land use changes at a global scale: the global land survey 2005. Photogramm Eng Rem Sens 74(1):6–10

Kääb A (2008) Remote sensing of permafrost-related problems and hazards. Permafr Perigl Process 19(2):107–136

Kharuk VI, Dvinskaya ML, Ranson KJ, Im ST (2005) Expansion of evergreen conifers to the Larch-Dominated zone and climatic trends. Russian J Ecol 36(3):164–170

Kharuk VI, Ranson KJ, Im ST, Naurzbaev MM (2006) Forest-tundra Larch forest and climatic trends. Russian J Ecol 37(5):291–298

Kovacs K, Ranson KJ, Sun G, Kharuk VI (2004) The relationship of the Terra MODIS fire product and anthropogenic features in the central Siberian landscape. Earth Interact 8:1–25

Kurz WA, Apps MJ (1999) A 70-year retrospective analysis of carbon fluxes in the Canadian forest sector. Ecol Appl 9:526–547

Maslanik JA, Fowler C, Stroeve J, Drobot S, Zwally J, Yi D, Emery W (2007) A younger, thinner Arctic ice cover: increased potential for rapid, extensive sea-ice loss. Geophys Res Lett 34(L24501). doi:10.1029/2007GL032043

Nellemann C, Vistnes I, Jordhøy P, Strand O, Newton A (2003) Progressive impact of piecemeal infrastructure development on wild reindeer. Biol Conserv 113:307–317

Quinn P, Andrews B, Dutton E, Shaw G, Ruoho-Airola T (2006) Arctic haze. In: Forsius M, Nyman M (eds) AMAP assessment 2006: acidifying pollutants, arctic haze, and acidification in the Arctic. Arctic Monitoring and Assessment Programme (AMAP), Oslo, pp 31–40

Roy DP, Frost PGH, Justice CO, Landmann T, Le Roux JL, Gumbo K, Makungwa S, Dunham K, Du Toit R, Mhwandagara K, Zacarias A, Tacheba B, Dube O, Pereira JMC, Mushove P, Morisette JT, Santhana Vannan CK, Davies D (2005) The Southern Africa Fire Network (SAFNet) regional burned area product validation protocol. Int J Rem Sens 26:4265–4292

Rupp TS, Chapin FS III, Starfield AM (2001) modeling the influence of topographic barriers on treeline advance at the forest-tundra ecotone in Northwestern Alaska. Clim Change 48:399–416

Stocks BJ, Fosberg MA, Wotten MB, Lynham TJ, Ryan KC (2000) Climate change and forest fire activity in North American Boreal Forests. In: Kasischke ES, Stocks BJ (eds) Fire, climate change, and carbon cycling in the boreal forest. Ecological Studies Series, Springer, New York, pp 368–376

Stocks BJ, Mason JA, Todd JB, Bosch EM, Wotton BM, Amiro BD, Flannigan MD, Hirsch HG, Logan KA, Martell DL, Skinner WR (2003) Large forest fires in Canada 1959–1997. J Geophys Res 108(D1):8149. doi:10.1029/2001JD000484

Stow DA, Hope A, McGuire D, Verbyla D, Gamon J, Huemmrich F, Houston S, Racine C, Sturm M, Tape K, Hinzman L, Yoshikawa K, Tweedie C, Noyle B, Silapaswan C, Douglas D, Griffith B, Jia G, Epstein H, Walker D, Daeschner S, Petersen A, Zhou L, Myneni R (2004) Remote sensing of vegetation and land-cover change in Arctic Tundra Ecosystems. Rem Sens Environ 89(3):281–308

Teillet PM, El Saleous N, Hansen MC, Eidenshink JC, Justice CO, Townshend JRG (2000) An evaluation of the global 1-km AVHRR land data set. Int J Rem Sens 21:1987–2021

Townshend JRG, Justice CO (2002) Towards operational monitoring of terrestrial systems by moderate-resolution remote sensing. Rem Sens Environ 83(1–2):351–359

Werner RA, Raffa KF, Illman BL (2006) Insect and pathogen dynamics in the Alaskan boreal forest. In: Chapin FS III, Oswood MW, Van Cleve K, Viereck LA, Verbyla DL (eds) Alaska's changing boreal forest. Oxford University Press, New York, pp 133–146

Index

G. Gutman, A. Reissell (eds.), *Eurasian Arctic Land Cover and Land Use in a Changing Climate*, DOI 10.1007/978-90-481-9118-5,

S